WOODHEAD PUBLISHING
IN MECHANICAL ENGINEERING

HCCI and CAI engines for the automotive industry

Edited by Hua Zhao

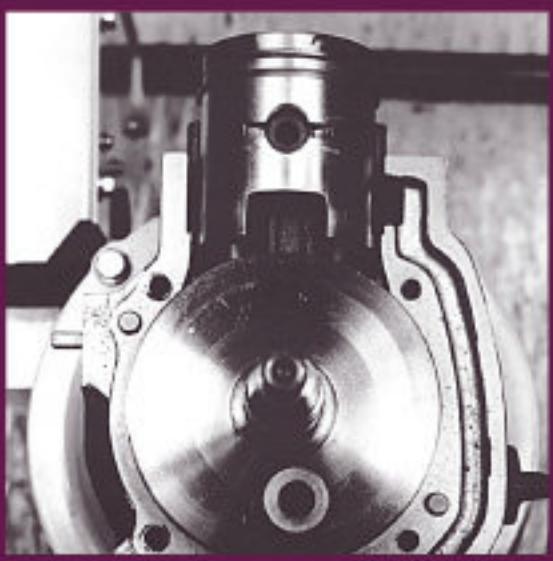

CRC

WP

HCCI and CAI engines for the automotive industry

www.TechnicalBooksPDF.com

Related titles:

The science and technology of materials in automotive engines
(ISBN 978-1-85573-742-6)
This authoritative book provides an introductory text on the science and technology of materials used in automotive engines. It focuses on reciprocating engines, both four- and two-stroke, with particular emphasis on their characteristics and the types of materials used in their construction. The book considers the engine in terms of each specific part: the cylinder, piston, camshaft, valves, crankshaft, connecting rod and catalytic converter. The materials used in automotive engines are required to fulfil a multitude of functions, resulting in a subtle balance between material properties, essential design and high performance characteristics. The intention here is to describe the metallurgy, surface modification, wear resistance, and chemical composition of these materials. It also includes supplementary notes that support the core text. The book is essential reading for engineers and designers of engines, as well as lecturers and graduate students in the fields of combustion engineering, machine design and materials science looking for a concise, expert analysis of automotive materials.

The automotive industry and the environment
(ISBN 978-1-85573-713-6)
The future of car manufacturing may be very different to the current practice of large-scale, large-assembly plant construction methods based on economies of scale and the marketing of new vehicles with ever increasing complexity and value-added options. A sustainable future is envisaged in this ground-breaking study, which concentrates on the recent research into alternative production methods with an emphasis on life-cycle management, recyclability and manufacture tailored to the customer's individual specifications.

IPDS 2006 Integrated Powertrain and Driveline Systems 2006
(ISBN 978-1-84569-197-4)
The holistic view of powertrain development that includes engine, transmission and driveline is now well accepted. Current trends indicate an increasing range of engines and transmissions in the future with, consequently, a greater diversity of combinations. Coupled with the increasing introduction of hybrid vehicles, the scope for research, novel developments and new products is clear. This volume presents some of the latest developments in a collection of papers from the Institution of Mechanical Engineers' Conference *Integrated Powertrain and Driveline Systems 2006 (IPDS 2006)* organised by the IMechE Automobile Division. Main themes include transmissions; concept to market evolution; powertrain integration; and engine integration. Novel concepts relating, for example, to continuously variable transmissions (CVTs) and hybridisation are discussed, as well as approaches to modelling and simulation.

Details of these books and a complete list of Woodhead's titles can be obtained by:

- visiting our website at www.woodheadpublishing.com
- contacting Customer Services (e-mail: sales@woodhead-publishing.com; fax: +44 (0) 1223 893694; tel.: +44 (0) 1223 891358, ext. 130; address: Woodhead Publishing Limited, Abington Hall, Abington, Cambridge CB21 6AH, England)

www.TechnicalBooksPDF.com

HCCI and CAI engines for the automotive industry

Edited by CH.NAGENDRA

WOODHEAD PUBLISHING LIMITED
Cambridge England
CRC Press
oca Raton Boston New York Washington, DC

www.TechnicalBooksPDF.com

Published by Woodhead Publishing Limited, Abington Hall, Abington,
Cambridge CB21 6AH, England
www.woodheadpublishing.com

Published in North America by CRC Press LLC, 6000 Broken Sound Parkway, NW,
Boca Raton, FL 33487, USA

First published 2007, Woodhead Publishing Limited and CRC Press LLC
© 2007, Woodhead Publishing Limited except for Chapter 9 which is © 2007,
Shell Global Solutions
The authors have asserted their moral rights.

This book contains information obtained from authentic and highly regarded sources. Reprinted material is quoted with permission, and sources are indicated. Reasonable efforts have been made to publish reliable data and information, but the authors and the publishers cannot assume responsibility for the validity of all materials. Neither the authors nor the publishers, nor anyone else associated with this publication, shall be liable for any loss, damage or liability directly or indirectly caused or alleged to be caused by this book.

Neither this book nor any part may be reproduced or transmitted in any form or by any means, electronic or mechanical, including photocopying, microfilming and recording, or by any information storage or retrieval system, without permission in writing from Woodhead Publishing Limited.

The consent of Woodhead Publishing Limited does not extend to copying for general distribution, for promotion, for creating new works, or for resale. Specific permission must be obtained in writing from Woodhead Publishing Limited for such copying.

Trademark notice: Product or corporate names may be trademarks or registered trademarks, and are used only for identification and explanation, without intent to infringe.

British Library Cataloguing in Publication Data
A catalogue record for this book is available from the British Library.

Library of Congress Cataloging in Publication Data
A catalog record for this book is available from the Library of Congress.

Woodhead Publishing ISBN 978-1-84569-128-8 (book)
Woodhead Publishing ISBN 978-1-84569-354-1 (e-book)
CRC Press ISBN 978-1-4200-4459-1
CRC Press order number WP4459

The publishers' policy is to use permanent paper from mills that operate a sustainable forestry policy, and which has been manufactured from pulp which is processed using acid-free and elementary chlorine-free practices. Furthermore, the publishers ensure that the text paper and cover board used have met acceptable environmental accreditation standards.

Project managed by Macfarlane Production Services, Dunstable, Bedfordshire, England
(e-mail: macfarl@aol.com)
Typeset by Replika Press Pvt Ltd, India
Printed by TJ International Limited, Padstow, Cornwall, England

www.TechnicalBooksPDF.com

Contents

Contributor contact details *xiii*

Preface xvii

Part I Overview

1 Motivation, Definition, and History of HCCI/CAI engines 3

H Zhao, Brunel University West London, UK

1.1 Introduction 3
1.2 Current automotive engines and technologies 5
1.3 Historical background of HCCI/CAI type combustion engines 6
1.4 Principle of HCCI/CAI combustion engines 10
1.5 Definition of HCCI and CAI combustion engines 15
1.6 Summary 16
1.7 References 16

Part II Gasoline HCCI/CAI combustion engines

2 Overview of CAI/HCCI gasoline engines 21

H Zhao, Brunel University West London, UK

2.1 Introduction 21
2.2 Fundamentals of CAI/HCCI gasoline engines 21
2.3 Effects of use of exhaust gases as diluents 29
2.4 Approaches to CAI/HCCI operation in gasoline engines 35
2.5 Summary 40
2.6 References 40

3 Two-stroke CAI engines 43

P Duret, IFP, France

3.1 Introduction 43

www.TechnicalBooksPDF.com

3.2 Principles of the two-stroke CAI combustion 46
3.3 How to control the two-stroke CAI combustion 56
3.4 The potential application of the two-stroke CAI combustion 67
3.5 Future trends 72
3.6 Sources of further information and advice 74
3.7 References 75

4 Four-stroke gasoline HCCI engines with thermal management 77
J YANG, USA
4.1 Introduction 77
4.2 The optimized kinetic process (OKP) HCCI engine 79
4.3 Strengths and weaknesses 91
4.4 Future trends 97
4.5 Sources of further information and advice 99
4.6 References 101

5 Four-stroke CAI engines with residual gas trapping 103
H ZHAO, Brunel University West London, UK
5.1 Introduction 103
5.2 Principle of CAI operation with residual gas trapping 103
5.3 CAI operation in a four-stroke port fuel injection (PFI) gasoline engine 107
5.4 Effect of direct injection on CAI combustion in the four-stroke gasoline engine 115
5.5 Effect of spark ignition on CAI combustion in the four-stroke gasoline engine 129
5.6 Summary 132
5.7 References 134

6 Four-stroke CAI engines with internal exhaust gas recirculation (EGR) 136
A FÜRHAPTER, AVL List GmbH, Austria
6.1 Introduction 136
6.2 Principle of CAI with internal EGR 137
6.3 Engine concepts and layout 141
6.4 Thermodynamic results and analysis of CAI with internal EGR 146
6.5 Transient operation with CAI and internal EGR 155
6.6 Future trends 162

www.TechnicalBooksPDF.com

6.7 Sources of further information and advice 162
6.8 References 163

7 HCCI control 164

P Tunestål and B Johansson, Lund University, Sweden

7.1 Introduction 164
7.2 Control means 165
7.3 Combustion timing sensors 171
7.4 Methods 174
7.5 Summary and future trends 182
7.6 References 182

8 CAI control and CAI/SI switching 185

N Milovanovic, Delphi Diesel Systems Limited, UK and J Turner, Lotus Engineering, UK

8.1 Introduction about requirements for the control of the CAI engine 185
8.2 Problems in controlling the CAI engine 185
8.3 Transition between operating modes (CAI-SI-CAI) 188
8.4 The 'mixed mode' CAI-SI engine in operation: presentation and discussion of the experimental results obtained 192
8.5 Summary 202
8.6 References 203

9 Fuel effects in CAI gasoline engines 206

G T Kalghatgi, Shell Global Solutions, UK

9.1 Introduction 206
9.2 Practical transport fuels 207
9.3 Auto-ignition quality of fuels 210
9.4 The octane index and the *K* value 217
9.5 The auto-ignition requirement of an HCCI engine and fuel effects in combustion phasing 222
9.6 Combustion limits 224
9.7 *IMEP* and indicated efficiency 226
9.8 Other approaches to characterising fuel performance in HCCI engines 228
9.9 Fuel requirements of HCCI engines 230
9.10 Summary 233
9.11 References 234
9.12 List of notations 236
Appendix – HCCI predictor 237

www.TechnicalBooksPDF.com

Part III Diesel HCCI combustion engines

10 Overview of HCCI diesel engines 241

J V Pastor, J M Luján, S Molina and J M García, CMT-Motores Térmicos, Spain

10.1 Introduction 241
10.2 Conventional diesel combustion 242
10.3 Fundamentals of HCCI combustion 247
10.4 Overview of diesel HCCI engines 252
10.5 Summary 261
10.6 References 263

11 HCCI combustion with early and multiple injections in the heavy-duty diesel engine 267

Y Aoyagi, New ACE, Japan

11.1 Introduction 267
11.2 Experimental apparatus 268
11.3 Early injection HCCI (PREDIC) by low cetane fuel 271
11.4 Multiple injections HCCI by low cetane fuel (two-stage combustion, MULDIC) 274
11.5 HCCI for normal cetane fuel 277
11.6 Summary 285
11.7 Acknowledgements 286
11.8 References 286
11.9 Nomenclature 288

12 Narrow angle direct injection (NADI™) concept for HCCI diesel combustion 289

B Gatellier, IFP, France

12.1 Introduction 289
12.2 The NADI™ concept overview 290
12.3 First results and limitations 292
12.4 Development of the concept 296
12.5 Evaluation of the concept in a multi-cylinder engine 307
12.6 Future trends 318
12.7 References 320

13 Low-temperature and premixed combustion concept with late injection 322

S Kimura, Nissan Motor Company, Japan

13.1 Introduction 322
13.2 Basic concept of low-temperature and premixed combustion 323

www.TechnicalBooksPDF.com

13.3 Characteristics of combustion and exhaust emissions with modulated kinetics (MK) combustion 324
13.4 Second generation of MK combustion 330
13.5 Emission performance improvement of second generation of MK combustion 334
13.6 Future trends 337
13.7 References 340

14 HCCI fuel requirements 342
T W Ryan III, SWRI, USA
14.1 Introduction 342
14.2 Background 342
14.3 Diesel fuel HCCI 345
14.4 HCCI fuel ignition quality 350
14.5 Gasoline HCCI 354
14.6 HCCI fuel specification 358
14.7 Fundamental fuel factors 360
14.8 Future trends 361
14.9 References 362

Part IV HCCI/CAI combustion engines with alternative fuels

15 Natural gas HCCI engines 365
N Iida, Keio University, Japan
15.1 CNG HCCI engine experiment and calculation conditions 365
15.2 CNG composition 366
15.3 Influence of equivalence ratio 369
15.4 Auto-ignition timing and combustion duration 371
15.5 Auto-ignition temperature and auto-ignition pressure 372
15.6 Exhaust emission, maximum cycle temperature and combustion efficiency 374
15.7 Influence of n-butane on auto-ignition and combustion in methane/n-butane/air mixtures 376
15.8 Summary of naturally aspirated natural gas HCCI engine 383
15.9 Supercharged natural gas HCCI engine setup and experiments 383
15.10 Performance and exhaust gas characteristics at a compression ratio of 17 385
15.11 Performance and emission characteristics at a compression ratio of 21 388
15.12 Potential of natural gas turbocharged HCCI engines 389
15.13 Summary 391
15.14 References 392

www.TechnicalBooksPDF.com

16 HCCI engines with other fuels 393

N Iida, Keio University, Japan

16.1 Characterization of DME 393
16.2 DME HCCI engine 394
16.3 DME chemical reaction model 394
16.4 Combustion completeness in the DME HCCI engine 396
16.5 Combustion control system for a small DME HCCI engine 408
16.6 Method of combining DME and other fuels 421
16.7 Reducing pressure rise rate by introducing 'unmixed-ness' of DME/air mixture 423
16.8 Summary 425
16.9 References 429

Part V Advanced modeling and experimental techniques

17 Auto-ignition and chemical kinetic mechanisms of HCCI combustion 433

C K Westbrook and W J Pitz, Lawrence Livermore National Laboratory, USA and H J Curran, National University of Ireland, Galway

17.1 Introduction 433
17.2 Kinetics of auto-ignition 434
17.3 Reaction types 435
17.4 Temperature regimes of auto-ignition 437
17.5 Illustrations of auto-ignition in the rapid compression machine 445
17.6 Kinetic models for HCCI ignition 451
17.7 Summary 453
17.8 References 453

18 Overview of modeling techniques and their applications to HCCI/CAI engines 456

S M Aceves, D L Flowers, R W Dibble and A Babajimopoulos, Lawrence Livermore National Laboratory, USA

18.1 Introduction 456
18.2 Fundamentals of HCCI ignition and combustion 457
18.3 The chemistry of HCCI 458
18.4 Prediction of ignition in HCCI engines 462
18.5 Detailed calculation of HCCI combustion and emissions 465
18.6 Prediction of operating range 468
18.7 Summary and future trends 470
18.8 References 471

www.TechnicalBooksPDF.com

19 Overview of advanced optical techniques and their applications to HCCI/CAI engines 475

M Richter, Lund University, Sweden

19.1 Introduction 475
19.2 Diagnostic approaches 476
19.3 Spectroscopic environment 481
19.4 Chemiluminescence imaging 482
19.5 Laser induced fluorescence 484
19.6 Thermographic phosphors 498
19.7 Future trends 500
19.8 References 502

Part VI Future directions for CAI/HCCI engines

20 Outlook and future directions in HCCI/CAI engines 507

H Zhao, Brunel University West London, UK

Index *510*

www.TechnicalBooksPDF.com

www.TechnicalBooksPDF.com

Contributor contact details

(* = main contact)

Editor

Professor H. Zhao
School of Engineering and Design
Brunel University West London
Uxbridge
Middlesex, UB8 3PH
UK

E-mail: Hua.Zhao@brunel.ac.uk

Chapters 1, 2, 5 and 20

H. Zhao
School of Engineering and Design
Brunel University West London
Uxbridge
Middlesex, UB8 3PH
UK

E-mail: Hua.Zhao@brunel.ac.uk

Chapter 3

P. Duret
IFP
228-232 avenue Napoléon
Bonaparte
92852 Rueil-Malmaison Cedex
France

E-mail: pierre.duret@ifp.fr

Chapter 4

J. Yang
582 Terrace Court
Canton, MI 48188
USA

E-mail: jayyang5@yahoo.com

Chapter 6

A. Fürhapter
AVL List GmbH
Hans-List-Platz 1
A-8020 Graz
Austria

E-mail: alois.fuerhapter@avl.com

Chapter 7

Per Tunestål
Lund University
Faculty of Engineering
Dept. of Energy Sciences/
Combustion Engines
PO Box 118
221 00 Lund
Sweden

E-mail: per.tunestal@vok.lth.se

www.TechnicalBooksPDF.com

Chapter 8

N. Milovanovic*
Combustion, NVH and Fuel
Department Manager
Delphi Diesel Systems
Courteney Road
Hoath Way
Gillingham ME8 ORU

J. Turner
Chief Engineer
Powertrain Advanced Concept
Lotus Engineering
Hethel
Norwich, NR14 8EZ
UK

E-mail:
Nebojsa.Milovanovic@delphi.com
jturner@lotuscars.co.uk

Chapter 9

G. T. Kalghatgi
Shell Global Solutions, UK
Cheshire Innovation Park
PO Box 1
Chester, CH1 3SH
UK

E-mail: gautam.kalghatgi@shell.com

Chapter 10

J. V. Pastor*, J. M. Luján,
S. Molina and J. M. García
CMT-Motores Térmicos
Universidad Politécnica de Valencia
Camino de Vera, s/n
46022 Valencia
Spain

E-mail: jpastor@mot.upv.es
jlujan@mot.upv.es
samolina@mot.upv.es
jgarciao@mot.upv.es

Chapter 11

Y. Aoyagi
Representative and Managing
Director
Research Department
New ACE. Institute Co., Ltd.
2530 Karima, Tsukuba-shi,
Ibaraki Pref.,
305-0822
Japan

E-mail: aoyagi@nace.jp

Chapter 12

Bertrand Gatellier
IFP
1 et 4, avenue de Bois-Préau
92852 Rueil-Malmaison Cedex
France

E-mail: bertrand.gatellierfp.fr

Chapter 13

Shuji Kimura
Nissan Motor Co., Ltd.,
1 Natsushima-cho, Yokosuka-shi
Kanagawa 237-8523
Japan

E-mail: shu-kimura@mail.nissan.co.jp

www.TechnicalBooksPDF.com

Chapter 14

Thomas W. Ryan III
Institute Engineer
Southwest Research Institute
P.O. Drawer 28510
San Antonio
Texas 78228-0510
USA

E-mail: tryan@swri.org

Chapters 15 and 16

N. Iida
System Design Engineering Dept
Keio University
3-14-1 Hiyoshi
Kohoku-ku
Yokohama 223-8522
Japan

E-mail: Iida@sd.keio.ac.jp

Chapter 17

C. K. Westbrook* and W. J. Pitz
Lawrence Livermore National
Laboratory
7000 East Avenue
L-644
Livermore, CA 94551
USA

E-mail: westbrook1@llnl.gov

H. J. Curran
Chemistry Department
NUI Galway
University Rd
Galway
Ireland

E-mail: Henry.Curran@nuigalway.ie

Chapter 18

S. Aceves
Lawrence Livermore National
Laboratory
7000 East Avenue
L-644
Livermore, CA 94551
USA

E-mail: saceves@LLNL.gov

Chapter 19

M. Richter
Dept. of Physics
Div. of Combustion Physics
PO Box 118
S-22100 Lund
Sweden

E-mail: mattias.richter@forbrf.lth.se

www.TechnicalBooksPDF.com

www.TechnicalBooksPDF.com

Preface

Controlled Auto-Ignition (CAI) and Homogeneous Charge Compression Ignition (HCCI) combustion are radically different from the conventional spark ignition (SI) combustion in a gasoline engine and compression ignition (CI) diffusion combustion in a diesel engine. The combination of a diluted and premixed fuel and air mixture with multiple ignition sites throughout the combustion chamber eliminates the high combustion temperature zones and prevents the production of soot particles, hence producing ultra-low NOx and particulate emissions. The use of lean, or more often diluted, air/fuel mixture with recycled burned gases permits unthrottled operation of a CAI/HCCI gasoline engine, thus yielding higher engine efficiency and better fuel economy than SI combustion. Therefore, CAI/HCCI combustion represents for the first time a combustion technology that can simultaneously reduce both NOx and particulate emissions from a diesel engine and has the capability of achieving simultaneous reduction in fuel consumption and NOx emissions from a gasoline engine.

Based on these promises, the interest in CAI/HCCI combustion exploded at the turn of the new millennium and has since grown so much that the HCCI session has consistently been the largest session in the world's largest annual gathering of automotive engineers, the annual SAE Congress in Detroit, for the last five years. Each year, scores of papers are published at a number of international conferences and in various journals. It would be a daunting task to read every publication in this field. In addition, it presents a particular challenge for someone to plan working in this field or for someone to make a management decision on CAI/HCCI technology. In the meantime, the research and development efforts in this field over the last ten years have reached a stage that not only has better understanding of the underlying physical and chemical process in CAI/HCCI combustion been achieved but also several dominant and promising means have emerged for the adoption of CAI/HCCI combustion in automotive applications. It is therefore timely that the large volume of technical information should be made available in an organised way so that the description of the fundamental processes, insights

www.TechnicalBooksPDF.com

on technical issues, and identification of future research and development can be found between one set of covers.

Following the introduction and history of CAI/HCCI engines in Part I, the main body of the book is organised in six parts: Part II on the CAI/HCCI gasoline engines, Part III on diesel fuelled HCCI engines, Part IV on HCCI engines with alternative fuels, Part V on latest developments in kinetics, and analytical and experimental techniques for CAI/HCCI combustion research. Part VI concludes the book with a brief discussion of future directions of CAI/HCCI engines.

In Part II, a detailed description of CAI/HCCI combustion in the gasoline engine is provided in Chapter 2. Chapter 3 presents an interesting account of the discovery of this alternative and originally unwanted combustion mode in two-stroke gasoline engines in the 1970s and its subsequent turnabout on improving two-stroke engines' performance and emissions. Chapter 3 also serves as an introduction to the residual gas trapping method that was subsequently adopted to achieve CAI combustion in the four-stroke gasoline engine. Chapters 4 to 6 present and discuss three most promising approaches to achieve CAI/HCCI combustion in the four-stroke gasoline engine. As CAI/HCCI combustion does not have a direct means of controlling its combustion process, closed loop control is necessary to achieve optimised CAI/HCCI engine operation. Chapter 7 introduces the sensors and control techniques and their applications for closed loop control of the CAI/HCCI engine. Chapter 8 presents approaches to achieve switching between the alternative combustion mode and the conventional SI mode, which would be necessary to cover the whole operational range of a gasoline engine. Part II concludes in Chapter 9 with a discussion on the fuel properties that are relevant to the CAI/HCCI gasoline engine.

Part III starts with an overview on the HCCI combustion in direct injection diesel engines in Chapter 10. A main challenge in achieving diesel HCCI combustion is to obtain a sufficiently premixed air and fuel mixture before the start of ignition. Due to the high pressure injection employed for fast atomisation, wall wetting will occur with the very early fuel injection that is desirable for premixed charge operation. Therefore, alternative solutions have to be found. Chapter 11 provides a description of the progress made in the research on premixed type HCCI combustion in heavy duty diesel engines at New ACE institute over the last decade. The wall wetting was initially avoided by the use of two side-mounted injectors, but later work focused on the use of optimisation of fuel injection strategy and high exhaust gas recirculation (EGR). Whilst at IFP, the wall wetting problem has been resolved by the adoption of a narrow cone angle fuel injector, as discussed in Chapter 12, together with information on the radically different piston bowl design and different injection strategies suited for high and low load operations. Chapter 13 presents Nissan's HCCI diesel combustion concept, MK, a HCCI

www.TechnicalBooksPDF.com

combustion technology that has been employed in production engines for several years. Late injection is employed to avoid the wall wetting. Together with high EGR and high swirl, HCCI type diesel combustion has been achieved at part-load operations in light-duty diesel engines. Part III ends in Chapter 14 with an overview on fuel properties and their influence on HCCI combustion.

Part IV focuses on HCCI engines with gaseous fuels. Due to its abundant supply, natural gas is considered as a viable alternative fuel for automotive applications. Its ignition and combustion characteristics in HCCI combustion are discussed in Chapter 15. The other gaseous fuel considered is dimethyl ether (DME), which can be produced from biomass as well as from coal or natural gas. Chapter 16 presents the results of an analytical study of DME HCCI combustion and then gives a detailed description of a prototype DME HCCI engine.

Part V is concerned with the fundamentals of CAI/HCCI combustion. In Chapter 17, the kinetic aspects of CAI/HCCI combustion are reviewed. Detailed discussion is given regarding hydrocarbon oxidation chemistry and autoignition processes leading to HCCI combustion. This is followed by an overview on various HCCI engine modelling approaches with differing computational complexity in Chapter 18. Finally, the advanced laser diagnostic techniques for in-cylinder air/fuel distribution, autoignition, and combustion in CAI/HCCI engines are presented in Chapter 19 with some excellent images taken from HCCI combustion engines. The final part of the book explores the current trends in the future development of CAI/HCCI engines.

This book has been written by the leading researchers in this field, who have contributed with the intention of providing a systematic description and personal insights on detailed technical issues in their field of expertise. It would serve as an excellent base for anyone who is interested in the field. The references listed at the end of each chapter will also provide a convenient way for someone who needs to have ready access to the most relevant literature.

I am delighted to have taken on such an enjoyable task, during which I have had the pleasure of corresponding with the contributing authors, whom I thank for agreeing to undertake the work and for sticking to the agreed publication schedule. I would also like to thank Sheril Leich and Ian Borthwick of Woodhead Publishing for initiating the project and their professional support in preparing this book.

Hua Zhao
Brunel University, West London
2007

www.TechnicalBooksPDF.com

www.TechnicalBooksPDF.com

Part I

Overview

www.TechnicalBooksPDF.com

www.TechnicalBooksPDF.com

1

Motivation, definition and history of HCCI/CAI engines

H ZHAO, Brunel University West London, UK

1.1 Introduction

Since their introduction around a century ago, IC engines have played a key role, both socially and economically, in shaping of the modern world. Their suitability as an automotive power plant, coupled with a lack of practical alternatives, means road transport in its present form could not exist without them. However, in recent decades, serious concerns have been raised with regard to the environmental impact of the gaseous and particulate emissions arising from operation of these engines. As a result, ever tightening legislation, that restricts the levels of pollutants that may be emitted from vehicles, has been introduced by governments around the world. In addition, concerns about the world's finite oil reserves and, more recently, by CO_2 emissions brought about climate change has lead, particularly in Europe, to heavy taxation of road transport, mainly via on duty on fuel. These two factors have lead to massive pressure on vehicle manufacturers to research, develop and produce ever cleaner and more fuel-efficient vehicles. Though there are technologies that could theoretically provide more environmentally sound alternatives to the IC engine, such as fuel cells, practicality, cost, efficiency and power density issues will prevent them displacing IC in the near future.

Over the last 30 years, levels of NOx, CO and VOC emissions from vehicles have been dramatically reduced and this has largely been achieved by the use of exhaust gas after-treatment systems, such as the catalytic converter. This has been motivated by a continually tightening band of legislation related to emission of these pollutants that has been enforced in the United States (USA), Japan and Europe (EU). Table 1.1 shows the permitted emission levels for the EU and California Air Resources Board.

EU emissions legislation demands that all vehicles comply with the particular standard that is in force at that time they are manufactured. The permitted emission levels are given on a specific basis and are the maximum permitted over a standard drive cycle, intended to be representative of a typical vehicle journey. Legislation from CARB is included in Table 1.1 because it is currently

www.TechnicalBooksPDF.com

Table 1.1 Current and future EU and CARB legislated emission levels for passenger cars [1, 2]

Euro Standard	Year	Engine type	CO (g/km)	HC/NMOG (g/km)	NOx (g/km)	HC+NOx (g/km)	PM (g/km)
Euro III	2001	SI	2.3	0.2	0.15	–	–
		CI	0.64	–	0.5	0.56	0.05
Euro IV	2005	SI	1.00	0.1	0.08	–	–
		CI	0.5	–	0.25	0.3	0.025
Euro V	2008	SI	–	0.05	0.08	–	0.0025
		CI	–	0.05	0.08	–	0.0025
CARB (LEV II)			2	0.033	0.04	–	–
TLEV			–	–	–	–	–
LEV	2004–10		4.2	0.056	0.07	–	0.01
ULEV			2.1	0.034	0.07	–	0.01
SULEV			1	0.006	0.02	–	–

(CARB) for passenger cars [1, 2].

the most stringent in the world. The US legislation is significantly different from the EU standards in that it operates a 'fleet-averaged' system, where the average emissions output from the total sales of a manufacturer's product range must be within the prescribed limits. In this way, a manufacturer can, for example, use sales of SULEVS to offset the higher emissions from TLEVS to keep within the required limits. In addition, differences in the test drive cycle and the measurement method of VOC's make direct comparison of the 'Euro' and CARB standards impossible. Johnson [3] has shown, through normalisation of the US and European standards, that the levels of uHC permitted by the US LEV II and EURO IV standards are roughly similar. However, he also concluded that the US standard permits approximately half the amount of NOx emissions, which was likely to seriously limit the penetration of HSDI Diesel and GDI engines into this market until adequate exhaust gas after-treatment systems are developed.

In addition to standards concerned with limiting local pollution, government policy is used to reduce global climate change by attempting to limit vehicle CO_2 emissions. In the UK and much of Europe this takes the form of heavy taxation of fuel, discounts on Road Fund Duty for small capacity vehicles and, most recently, the introduction of a sliding scale of 'company car tax' that heavily penalises the operation of vehicles with high CO_2 emissions. As part of this, CO_2 emission levels for all new passenger cars and LGVs must be published. Driven by this strong desire to reduce CO_2 emissions, a voluntary agreement has been reached between many of the major European car manufacturers to reduce their fleet average fuel consumption from the current 160g/km to 120g/km by the year 2012, equivalent to a 25% reduction. In the

www.TechnicalBooksPDF.com

US, legislation was introduced in the 1970s that required manufacturers to achieve certain levels of fleet average fuel consumption for passenger cars and light trucks, though the motivation for this was based largely on concerns regarding the supply of oil, rather than the consequences of high CO_2 emissions.

1.2 Current automotive engines and technologies

The ultimate target of emissions legislation is to push technology to the point where a practical, affordable zero emissions vehicle (ZEV) with acceptable performance becomes a reality. Although the technology exists to produce true ZEVs, powered by a fuel cell that consumes hydrogen produced from water by electricity generated from renewable sources, it is highly unlikely that the resulting vehicle would even come close to meeting any of the other criteria listed above in the short and medium terms. For this reason, the bulk of vehicle research and development resources are still being applied to the IC engine.

Weiss *et al*. [4] used the 'well to wheels efficiency' concept to quantify the total 'energy cost' and subsequent environmental impact of different vehicle technologies. The study attempted to assess and compare current and emerging technologies, with developments projected to 2020. In each case, the total energy cost was evaluated, including vehicle production, fuel processing and running costs. They concluded that, in terms of energy consumption per unit distance travelled, diesel/electric and gasoline/electric hybrids offered the best solution. Fuel cell vehicles, that use a reformer to produce their hydrogen fuel from gasoline, were found to be least energy efficient. The added problems of poor range and performance suffered with today's batteries, plus the major problems that must be solved before the introduction of a hydrogen supply infrastructure, also added weight to the conclusion that IC engines will be the dominant means of powering transport for the foreseeable future. Since this report, both Honda and Toyota have introduced gasoline/electric hybrids onto the world-wide market. As the technology inevitably decreases in price and consumers become more aware of the need to reduce fossil fuel use, their popularity can be expected to increase.

While hybrid vehicles may prove to be a stepping-stone to a ZEV, recent developments in traditional SI gasoline and CI diesel engine technology have allowed large improvements in emission and fuel consumption to be made. In terms of emissions, the adoption of the 3-way catalytic converter in SI gasoline engines has allowed engine-out emissions of CO, uHC and NOx to be reduced by over 90%. But, in order to maintain these conversion efficiencies, this unit, can only be used with an engine operating within a few percent of stoichiometry [5]. Such a requirement for continuous stoichiometric operation prevents the engine from operating with a lean AFR

www.TechnicalBooksPDF.com

at part load, leading to a small but significant increase in overall fuel consumption.

However, high speed direct injection (HSDI) diesel engines, and stratified charge gasoline direct injection (GDI) engines permit lean combustion by allowing fuel flow rate (and hence load), to be varied independently of airflow. These approaches can therefore achieve significant reductions in fuel consumption, particularly at part load. However, their operation away from stoichiometry prevents the effective use of traditional exhaust after-treatments for reducing NOx emissions. Though the technology to achieve NOx reduction from lean burn engines is available [6], it is currently very expensive and will require either ultra-low super fuel in the case of NOx storage catalyst or on-board system and infrastructure of Urea supply for a DeNOx catalyst. Another problem with diesel engines is their tendency to produce high levels of particulate matter (PM). The emissions legislation beyond EU V and US Tier 2 demands levels of PM control that can only be achieved with the use of particulate filters within the exhaust. Furthermore, both lean-burn NOx after-treatment and PM filter will each incur a fuel consumption penalty of 3–4%.

Over the last decade, an alternative combustion technology, commonly known as homogeneous charge compression ignition (HCCI) or controlled auto-ignition (CAI) combustion, has emerged that has the potential to achieve efficiencies in excess of GDI units and approaching those of current CI engines, but with levels of raw NOx emissions up to two levels of magnitude lower than either, and with virtually no smoke emissions. Their abilities offer the potential to meet current and future emissions legislation, without the need for expensive, complex and inefficient exhaust gas after-treatment systems.

While the potential benefits of this new combustion technology are significant, this combustion mode faces its own set of challenges, such as difficulty in controlling the combustion phasing, a restricted operating range, and high hydrocarbon emissions. Over the last decade, efforts have been made with not only better understanding of the physical and chemical processes involved in this combustion mode but also technical solutions for practical applications which have led to the incorporation of this new combustion mode in certain production DI diesel engines.

1.3 Historical background of HCCI/CAI type combustion engines

1.3.1 Introduction

Amongst the numerous research papers published over the last decade, the homogeneous charge compression ignition (HCCI) or controlled auto-ignition

www.TechnicalBooksPDF.com

(CAI) combustion has often been considered a new combustion process in reciprocating internal combustion engines. However, it has been around perhaps as long as the spark ignition (SI) combustion in gasoline engine and compression ignition (CI) combustion in diesel engines. In the case of diesel engines, the hot-bulb 2-stroke or 4-stroke oil engines or diesel engines were patented and developed over 100 years ago [7], wherein kerosene, or raw oil was injected onto the surface of a heated chamber (hot-bulb), which was separated from the main cylinder volume, very early in the compression stroke, giving plenty of time for fuel to vaporise and mix with air. During the start-up, the hot-bulb was heated on the outside by a torch or a burner. Once the engine had started, the hot-bulb was kept hot by the burned gases within. The bulb was so hot that the injected fuel vaporised immediately when it got in contact with the surface. Later design placed injection through the connecting passage between the hot-bulb and the main chamber so that a more homogeneous mixture could be formed, resulting in auto-ignited homogeneous charge combustion.

In the case of gasoline engines, the auto-ignited homogeneous charge combustion had been observed and was found responsible for the 'after-run'/'run-on' phenomenon that many drivers had experienced with their carburettor gasoline engines in the sixties and seventies, when a spark ignition engine continued to run after the ignition was turned off. The same type of combustion was also found to be the cause of 'dieseling' or hot starting problems encountered in the early high compression gasoline engines. In fact, the most recognised original work on HCCI/CAI by Onishi *et al.* [8] and Noguchi *et al.* [9] was motivated by their desire to control the irregular combustion caused by the auto-ignition of cylinder charge to obtain stable lean-burn combustion in the conventional ported 2-stroke gasoline engine.

1.3.2 Controlled auto-ignition gasoline engines

Although it is generally accepted that the first systematic investigation on the new combustion process was carried out by Onishi [8] and Noguchi [9] in 1979, the theoretical and practical roots of the HCCI/CAI combustion concepts are attributed to the pioneering work carried out by the Russian scientist Nikolai Semenov and his colleagues in the field of ignition in the 1930s. Having established his chemical or chain theory of ignition, Semenov sought to exploit a chemical-kinetics controlled combustion process for IC engines, in order to overcome the limitations imposed by the physical-dominating processes of SI and CI engines. By subjecting entire cylinder charge to the thermodynamic and chemical conditions similar to those of cool flames of hydrocarbon air mixtures, a more uniform heat release process should be reached. This led to the first 'controlled-combustion' engine utilising the LAG (Avalanche Activated Combustion), developed by Semenov and

www.TechnicalBooksPDF.com

Gussak *et al*. in the 1970s [10]. This system employed a lean intake charge to limit the rate of heat release, supplemented by a partially burned mixture at high temperature discharged from a separate prechamber. As this rich mixture traversed into the main combustion chamber, it was extinguished and became thoroughly mixed with the main charge, providing active species and thermal energy for more homogeneous combustion.

Following the pioneering work by Onishi and Noguchi, research and development on 2-stroke gasoline engines has culminated in the introduction, by Honda, of the first production CAI automotive engine, the 2-stroke ARC 250 motorbike engine [11]. With this unit, which uses the thermal energy of residual gases to promote CAI, Honda claims to reduce fuel consumption by up to 29% while simultaneously halving uHC emissions.

The apparent potential of this type of combustion process to reduce emissions and fuel consumption, coupled with serious shortfalls of the ported 2-stroke engine as an automotive power unit, led to an investigation into the application of the new combustion process to a 4-stroke single cylinder engine by Najt and Foster in 1983 [12]. The work was later extended by Thring to examine the effect of external EGR and air/fuel ratio on the engine's performance [13]. In this work, Thring introduced the terminology homogeneous charge compression ignition (HCCI) that has since been adopted by many others to describe this type of combustion process both in gasoline and diesel engines. In 1992, Stockinger *et al*. [14] showed for the first time that a four-cylinder gasoline engine could be operated with auto-ignition within a very limited speed and load range by means of higher compression ratio and pre-heating the intake air.

The largest gasoline engine with auto-ignition combustion in the late 1990s was demonstrated by Olsson *et al*. [15]. The engine was based on a 12-litre six-cylinder diesel engine. By employing combinations of isooctane and heptane through a closed loop control, as well as turbo-charging, high-compression ratio, and intake air heating, auto-ignition combustion was achieved over a large speed and load range.

While the above work demonstrated the feasibility and potential of CAI in 4-stroke gasoline engines, they do not represent a practical implementation of the auto-ignition combustion concept in a production engine. In order to develop a production viable gasoline auto-ignition combustion engine for automotive applications, it is necessary to operate without external charge heating or extremely high compression ratios, or special fuel blends.

Perhaps the most significant progress in the adoption of CAI to 4-stroke gasoline engines took place in Europe around the year 2000. Following the principle of auto-ignition combustion in 2-stroke gasoline engines, three independent studies showed that the CAI combustion could be achieved in 4-stroke gasoline engines over a range of speed and load by early closure of the exhaust valve(s) or negative valve overlap [16–19]. At Lotus and Volvo

www.TechnicalBooksPDF.com

Cars, the negative valve overlap method was realised by employing fully flexible variable valve actuation systems. Meanwhile, IFP and Brunel University demonstrated that CAI combustion could be readily achieved in a production four-cylinder engine over a reasonable speed and load range with only the use of modified camshafts.

Over the last few years, the residual gas trapping and exhaust gas re-breathing [20] for initiating and controlling CAI has proved to be increasingly popular with researchers, since it appears to offer the best chance of incorporating CAI combustion operation in a production gasoline engine in the short to medium term, requires no radical (expensive) changes to vehicle or engine architecture.

1.3.3 HCCI diesel engines

As mentioned in the introduction, some of the very early 2-stroke and 4-stroke diesel engines had been operated with compression ignition of premixed air and fuel mixtures through early injection onto the hot surface of a heated chamber. However, the best, but little known, example of homogeneous charge compression ignition diesel engines ever developed is the 2-stroke diesel model airplane engine developed since the 1940s by a small British company called Progress Aero Works (PAW). The fuel is a special blend of kerosene, oil, ether, and an ignition improver and it is fed into the engine's intake through a carburettor so that a premixed air/fuel mixture is formed in the cylinder. In order to get the engine firing, it is necessary to screw in the compression screw on the top of the engine to set the engine to a higher compression ratio. After the engine has started, it is necessary to unscrew the compression to achieve maximum power output. These little PAW engines produce power from 0.06 bhp to 1.2 bhp at speeds from 10,000 rpm to over 20,000 rpm and are readily available from the manufacturers.

However, it was not until the mid-1990s that systematic investigation had began of the potential for diesel fuelled HCCI engines for automotive applications, due to the need for substantial reductions in both NOx and PM emissions. The research and development of HCCI diesel engines had been pursued along three main technical routes, depending on the mixture preparation process involved. The first approach involves injecting the fuel into the intake air, upstream of the intake valve, similar to a conventional port-fuel-injection (PFI) SI engine. This method has been used in the past for diesel fumigation wherein diesel or often other more volatile fuels are injected in the manifold together with direct injection of diesel into the cylinder. Most recently, research on this premixed HCCI diesel combustion has been mostly performed to demonstrate the strong potential of HCCI to substantially reduce NOx and smoke emissions as well as to understand the fundamental characteristics of HCCI diesel combustion [21]. However, this approach is

www.TechnicalBooksPDF.com

unlikely to be developed into a practical solution due to poor vaporisation of the diesel fuel, high fuel consumption, and high uHCs.

With the advent of fully flexible high-pressure electronic fuel injection systems, in particular the common rail (CR) fuel injection system, direct fuel injection into the cylinder well before TDC has been the most popular approach to achieve HCCI combustion in diesel engines [22–24]. By injecting all or part of the fuel early in the compression stroke, the higher cylinder temperature and densities can facilitate the fuel vaporisation and promote its subsequent mixing with air. In addition, the flexibility of fuel injection timing and multiple injections can be employed to control and optimise the combustion phasing. However, the most successful HCCI diesel system in production to date is achieved through the employment of the late injection after TDC developed by the Nissan Motor Company [25]. Known as MK (Modulated Kinetics), this combustion process has been used at part load and low to medium speeds in their production diesel engines since 1998. Further enlargement of HCCI combustion operation was achieved in their second-generation system in 2001 to include the entire range of the Japanese 10–15 mode test.

One of the difficulties with very early injection is the cylinder wall wetting due to over penetration of the fuel, which leads to increased uHCs and CO emissions as well as the washout of lubricants on the cylinder wall. Although the cylinder wall wetting can be prevented by employing the injection nozzle of a smaller cone angle [26], a variable geometry nozzle would be necessary if conventional diesel combustion is to be restored for higher load operations. With the advancement in the high pressure CR fuel injection system, multiple injections have been investigated as a means to achieve near homogeneous charge combustion in a diesel engine without the cylinder wall wetting due to the reduced penetration depth of each fuel injection [27, 28]. In fact, multiple injection, up to five injections, has now been incorporated in the production engines [29].

Although it has been demonstrated recently that HCCI diesel combustion can be obtained at more than 15 bar BMEP [30], hybrid HCCI/diesel combustion operation will remain to be the approach for production car engines in the short and medium terms. For medium and heavy duty truck applications, significant advances are required to extend HCCI combustion to high load operations which constitute the majority of their driving cycle.

1.4 Principle of HCCI/CAI combustion engines

1.4.1 Principle and combustion characteristics of HCCI/CAI engines

Plate 1 (between pages 268 and 269) illustrates the salient features of the SI engine, CI engine, and the CAI/HCCI engine. Similar to a conventional

www.TechnicalBooksPDF.com

SI engine, in a HCCI/CAI engine the fuel and air are mixed together either in the intake system or in the cylinder with direct injection. The premixed fuel and air mixture is then compressed. Towards the end of the compression stroke, combustion is initiated by auto-ignition in a similar way to the conventional CI engine. The temperature of the charge at the beginning of the compression stroke has to be increased to reach auto-ignition conditions at the end of the compression stroke. This can be done by heating the intake air or by keeping part of the hot combustion products in the cylinder. Both strategies result in a higher gas temperature throughout the compression process, which in turn speeds up the chemical reactions that lead to the start of combustion of homogeneously mixed fuel and air mixtures. Although the start of main heat release usually occurs when the temperature reaches a value of 1050–1100K for gasoline or less than 800K for diesel, many hydrocarbon components in gasoline and diesel undergo low temperature oxidation reactions accompanied by a heat release that can account for up to 10% of the total energy released. The contribution of the low temperature energy release to obtaining auto-ignition and heat release rate from the HCCI/CAI combustion depends not only on the unique chemical kinetics of the fuel used and the dilution strategy, but also on the thermal conditions or the temperature-pressure history that the mixture goes through during compression. In an idealised HCCI/CAI engine, the auto-ignition and combustion will take place simultaneously throughout the combustion chamber, resulting in a rapid rate of heat release. In order to prevent the runaway heat release rate associated with the simultaneous burning of mixtures, HCCI/CAI engines have to run on lean or/and diluted fuel and air mixtures with burned gases.

The heat release characteristics of the HCCI/CAI combustion can be compared with those of SI and CI combustion using Fig. 1.1. In the case of SI combustion, a thin reaction zone or flame front separates the cylinder charge into burned and unburned regions and the heat release is confined to the reaction zone. The cumulative heat released in a SI engine is therefore the sum of the heat released by a certain mass, dm_i, in the reaction zone and it can be expressed as

$$Q = \int_0^N q \cdot dm_i$$

where q is the heating value per unit mass of fuel and air mixture, N is the number of reaction zones.

In an idealised HCCI/CAI combustion process, combustion reactions take place simultaneously in the cylinder and all the mixture participates in the heat release process at any instant of the combustion process. The cumulative heat release in such an engine is therefore the sum of the heat released from each combustion reaction, dq_i, of the complete mixture in the cylinder, m, i.e.

www.TechnicalBooksPDF.com

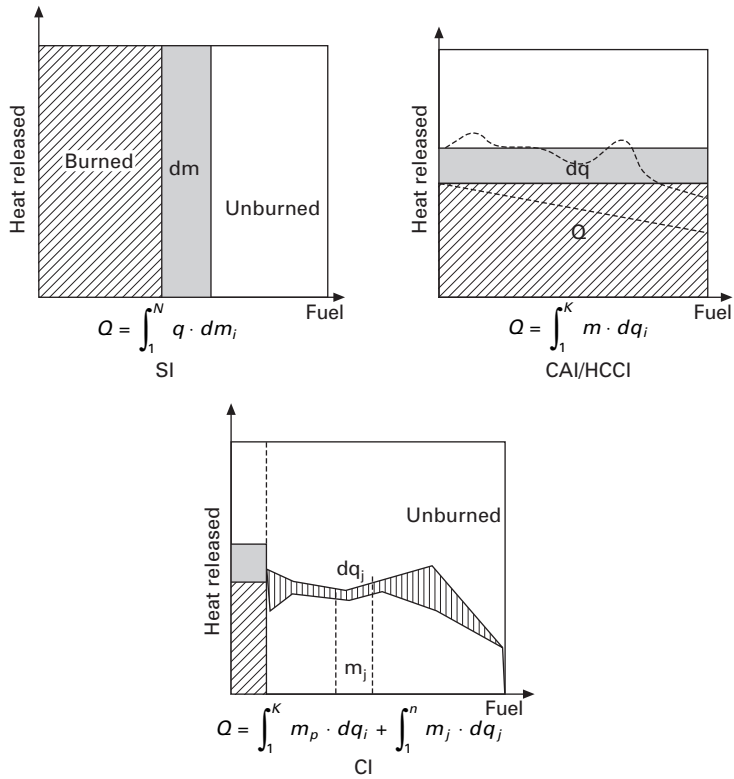

1.1 Heat release characteristics of SI, CAI/HCCI and CI combustion.

$$Q = \int_1^K m \cdot dq_i$$

where K is the total number of heat release reactions, and q_i is the heat released from the ith heat release reaction involving per unit mass of fuel and air mixture. Whereas the entire heating value of each minute parcel of mixture must be released during the finite duration spend in the reaction zone in a SI engine, heat release takes place uniformly across the entire charge in an idealised HCCI/CAI combustion. However, in practice, due to inhomogeneities in the mixture composition and temperature distributions in a real engine, the heat release process will not be uniform throughout the mixture. Faster heat release can take place in the less diluted mixture and/or high temperature region, resulting in a non-uniform heat release pattern as indicated by the dashed lines.

In comparison, combustion in a diesel engine is more complicated. In a typical direct injection diesel engine, soon after the start of fuel injection a small amount of mixture is involved in the premixed charge compression

www.TechnicalBooksPDF.com

ignition combustion process similar to HCCI/CAI, but most of the heat is released during the mixing controlled diffusion combustion process. The cumulative heat released may be expressed as a sum of the two processes:

$$Q = \int_1^K m_p \cdot dq_i + \int_1^n m_j \cdot dq_j$$

where the first part of the expression represents the premixed burning phase and the second is the diffusion burning, during which the heating value of each mixture varies according to the local mixture strength. In the above equation, m_p is the amount of premixed mixture taking part in the premixed burning phase, m_j and dq_j are the mass and heating value of each parcel being burned during diffusion burning.

Since the ideal HCCI/CAI process in IC engines involves the simultaneous reactive envelopment of entire intake charges, it allows a much more uniform and repeatable burning of fuel to proceed with respect to that of CI and SI engines, resulting in very low cycle-to-cycle variations in the engine's output as will be shown in Chapter 2.

1.4.2 Performance and emission characteristics of conventional combustion and HCCI/CAI combustion

SI engines rely on a minute electric plasma discharge to ignite a premixed near-stoichiometric air/fuel mixture within the cylinder, resulting in a singular advancing flame front, with distinct burned, burning, and unburned regions present. As the flame propagates within the cylinder, mixture that burns earlier is compressed to higher temperatures after combustion, as the cylinder pressure continues to rise. As a result, the temperatures of a gas element burned just after spark discharge can reach over 2500K. Nitric Oxide (NO) forms throughout the high temperature burned gases behind the flame through chemical reactions involving nitrogen and oxygen atoms and molecules. The higher the burned gas temperature, the higher the rate of formation of NO. As the burned gases cool during the expansion stroke, the reactions involving NO freeze, and leave NO far in excess of their equilibrium levels at exhaust conditions. As a result, a large amount of NO is emitted from the SI engine. As the SI combustion process involves the burning of premixed near-stoichiometric mixtures, SI engines are virtually free from soot emissions. However, the need to keep the air/fuel ratio near stoichiometric throughout the engine operating range warrants the use of a throttle valve to regulate the amount of air according to the fuelling requirement of the engine, resulting in significant pumping losses and hence poor engine efficiency at part-load operations that constitute majority of a typical passenger car driving cycle.

www.TechnicalBooksPDF.com

CI engines differ significantly in their operation from SI engines. Fuels of adequate cetane value are directly injected at high pressure later in the compression stroke, and the combustion is then initiated by auto-ignition after the ignition temperature has been reached. The rate at which fuel can mix with air limits the overall rate of combustion in CI engines, as the associated chemical reactions occur much faster than the mixing process. During the premixed phase of diesel combustion immediately following the ignition delay, near-stoichiometric air/fuel mixture burns due to spontaneous ignition and flame propagation, resulting in a rapid pressure rise and a region of high temperature burned gas. During the mixing controlled combustion phase after the premixed burn period, both lean and rich burning mixtures take part in the combustion process as mixing between already burned gases, air, and fuel occurs. Mixture which burns early in the combustion process is compressed to a higher temperature, increasing the NO formation rate, as combustion process proceeds and cylinder pressure rises. As CI engines always operate with an overall lean mixture, the formation of NO is noticeably less than in SI engines. But the overall leaner mixture tends to freeze the NO chemistry earlier, due to the faster drop in gas temperature as the high temperature gas mixes with cooler air during the expansion stroke, leading to much less decomposition of the NO in the CI engine than in the SI engine. Overall CI engines emit a lower but still significant amount of NO emissions. Furthermore, the high temperature combustion of fuel-rich mixture during the mixing controlled combustion process leads to the formation of soot in these regions and the subsequent emission of particulate matters. Unlike SI engines, the output of a naturally aspirated CI engine is principally controlled by fuelling at constant air supply, dispensing with the need for an intake throttle. In order to achieve auto-ignition, CI engines are designed to operate at higher compression ratios than SI engines. As a result, CI engines boast higher engine efficiency than SI engines.

In contrast, the new combustion mode is the process in which a premixed and highly diluted or lean air/fuel mixture is auto-ignited and burned simultaneously across the combustion chamber. As the burning takes place simultaneously, the compression effect on the burned gases is absent and hence the maximum localised high combustion temperature region is removed. More importantly, the overall combustion temperature is significantly reduced by the presence of excess air or diluents (exhaust gases recycled or trapped within the cylinder). As the peak combustion temperature can be kept below 1800K, above which the rate of NO formation increases exponentially, the new combustion process produces ultra-low NO emissions. Furthermore, the burning of premixed lean mixtures forms virtually no soot. For a HCCI/CAI engine, the load can be altered by fuelling at constant airflow or by altering the amount of exhaust gases going into the cylinder, dispensing with the need for an intake throttle and hence the associated pumping losses at part

www.TechnicalBooksPDF.com

load. The engine efficiency will therefore be higher than SI engines and can be similar to that of CI engines. Therefore, this new combustion technology has the potential to provide diesel-like engine efficiency and very low engine-out emissions, which may allow emissions compliance to occur without relying on lean after-treatment systems.

However, the lean-burn or high-dilution combustion process can cause the temperature to drop too low to have complete combustion. It has been shown that the main source of uHC emissions are of crevice emissions as in a SI engine below certain air/fuel ratio (AFR), above which the uHC emissions increase linearly with AFR as partial burning takes place [33]. Further increase in AFR will lead to misfire in the engine. While CO emissions from HCCI/CAI engines are normally higher than their equivalent of diesel engines, substantial reduction in CO emissions from CAI gasoline engines has been reported when residual gas trapping was used to initiate CAI combustion [17–19].

1.5 Definition of HCCI and CAI combustion engines

Over the last two decades, numerous names have been assigned to the new combustion process, including ATAC (Active Thermo-Atmospheric Combustion) [8], TS (Toyota-Soken) [9], ARC (Active Radical Combustion) [11] in conventional 2-stroke engines, CIHC (Compression-Ignited Homogeneous Charge) [12], Homogeneous Charge Compression Ignition (HCCI) [13], CAI (Controlled Auto-Ignition) [16–19], UNIBUS (Uniform Bulky Combustion System) [23], PREDIC (PREmixed lean Diesel Combustion) [24], MK (Modulated Kinetics) [25], PCCI (Premixed Charge Compression Ignition) [31], OKP (Optimised Kinetic Process) [32], etc. Close examination of these names and the rationales behind them shows that all names contain the description of two fundamental characteristics of the new combustion process: (1) premixed fuel and air mixture, and (2) auto-ignited combustion.

As will be discussed later, charge stratification is often present, in particular between the recycled or trapped burned gases and the air/fuel mixture, and it can sometimes be used to alter the auto-ignition and its subsequent heat release rate of such a combustion process in a gasoline engine. Furthermore, it should be noted that auto-ignition of the air/fuel mixture is not only caused by compression but also by heating externally or internally. In the case of diesel engines, compression leads directly to auto-ignition due to its higher compression ratio and low ignition temperature of diesel fuel. In contrast, intake charge heating or convective heat transfer from the hot burned gases is necessary to trigger the auto-ignition process of high octane fuels, such as gasoline and natural gas. It is therefore more appropriate to refer to the ignition process as auto-ignition, particularly for gasoline engines, rather

www.TechnicalBooksPDF.com

than compression ignition. It is also compatible with the classical classification of internal combustion engines (SI and CI) according to their ignition process.

Therefore, it is considered that CAI can be a more appropriate description of the underlying processes involved in this new combustion process and it will be used as the acronym for the auto-ignited combustion process in a gasoline engine. This notion has recently been endorsed by the ECO-Engine Network of Excellence (an engine research network comprising over 20 research institutions, universities, and automotive companies in Europe) for their joint educational activities. Since HCCI has been adopted by many researchers in their previous publications, it will be used in some chapters in Part III at the discretion of contributing authors. However, HCCI will be the only terminology used to represent the new combustion process in diesel and other CI engines in this book.

1.6 Summary

With increasingly stringent emission legislation and demand for significant reduction in CO_2 emission, research and development of cleaner and more efficient combustion engines has been intensified. HCCI/CAI combustion has emerged as an effective and viable technology that has the potential of simultaneously reducing pollutant emissions and fuel consumptions from internal combustion engines. The ideal HCCI/CAI process in IC engines involves the simultaneous reactive envelopment of entire intake charges in the cylinder. To achieve HCCI/CAI combustion in IC engines, temperatures must be sufficient to initiate and support the auto-ignition and the subsequent heat release reactions, yet a means must exist to prevent runaway energy release conditions. Significant research and development efforts are needed for HCCI/CAI combustion engines to be adopted for automotive applications and they are the subject of the following chapters in the rest of this book.

1.7 References

1. Euro III-V legislated emissions levels, Vehicle Certification Agency (VCA), obtained from http://www.carfueldata.org.uk/ June 2004.
2. 'California Exhaust Emissions Standards and Test Procedures for 2004 and Subsequent Model Passenger Cars. Light Duty Trucks and Medium Duty Vehicles, California Environmental Protection Agency Air Resources Board' (CARB), June 2004.
3. Johnson, T. V., 'Mobile Emissions Control technologies in review, International Conference on 21st Century Emissions Technology', IMechE Conference Transactions 2000-2, ISBN 186058 322 9, 2000.
4. Weiss, M., Heywood, J., *et al*., 'On the Road in 2020: A Life Cycle Analysis of New Automobile Technologies', MIT Energy Laboratory Report EL00-003, MIT, Cambridge, MA. 2000.
5. Stone, R., 'Introduction to internal combustion engines', third edition, p. 171, Macmillan Press, ISBN 0-333-86058 322 9, 2000.

www.TechnicalBooksPDF.com

6. Searles, R.A., 'Emission catalyst technology – challenges and opportunities in the 21st century.' International conference on 21st century emissions technology, IMechE, Conference Transactions 2000-2, ISBN 1 86058 322 9, 2000.
7. Erlandsson, O., 'Early Swedish hot-bulb engines – efficiency and performance compared to contemporary gasoline and diesel engines', SAE Paper 2002-01-0115, 2002.
8. Onishi, S., Hong Jo, S., Shoda, K., Do Jo, P., and Kato, S., 'Active thermo-atmosphere combustion (ATAC) – A new combustion process for internal combustion engines', SAE paper 790507, 1979.
9. Noguchi, M., Tanaka, Y., Tanaka, T., and Takeuchi, Y., 'A study on gasoline engine combustion by observation of intermediate reactive products during combustion', SAE paper 790840, 1979.
10. Gussak, L. A. *et al*., 'The application of lag-process in prechamber engines', SAE Paper 750890, 1975.
11. 'Honda readies activated radical combustion two-stroke engine for production motorcycle', *Automotive Engineer*, pp. 90–92, SAE publications, January 1997.
12. Najt, P. M., and Foster, D. E., 'Compression-ignited homogeneous charge combustion', SAE paper 830264, 1983.
13. Thring, R. H., 'Homogeneous-charge compression – ignition engines', SAE paper 892068, 1989.
14. Stockinger, V., Schapertons, H., and Kuhlmann, U., 'Investigations on a gasoline engine working with self-ignition by compression', *MTZ* vol. 53, pp 80–85, 1992.
15. Olsson, J., and Johansson, B., 'Closed loop control of an HCCI engine', SAE paper 2001-01-1031, 2001.
16. Lavy, J., Dabadie, J., Angelberger, C., Duret, P. (IFP), Willand, J., Juretzka, A., Schaflien, J. (Daimler Chrysler), Ma, T. (Ford), Lendress, Y., Satre, A. (PSA Peugeot Citroen), Shultz, C., Kramer, H. (PCI – Heidelberg University), Zhao, H., Damiano, L. (Brunel University), 'Innovative ultra-low NOx controlled auto-ignition combustion process for gasoline engines: the 4-SPACE project', SAE paper 2000-01-1837, 2000.
17. Zhao, H., Li, J., Ma, T., and Ladommatos, N., 'Performance and analysis of a 4-stroke multi-cylinder gasoline engine with CAI combustion', SAE paper 2002-01-0420, 2001.
18. Koopmans, L., and Denbratt, I., 'A four-stroke camless engine, operated in homogeneous charge compression ignition mode with a commercial gasoline', SAE paper 2001-01-3610, 2001.
19. Law, D., *et al*., 'Controlled combustion in an IC-engine with a fully variable valve train', SAE paper 2000-01-0251, 2000.
20. Fürhapter, A. *et al*., 'CAI – Controlled Auto Ignition – the Best Solution for the Fuel Consumption – Versus Emission Trade-Off?', SAE 2003-01-0754, 2003.
21. Ryan III, T.W., and Callahan, T.J., 'Homogeneous charge compression ignition of diesel fuel', SAE paper 961160, 1996.
22. Walter, B., and Gatellier, B., 'Development of the high power NADI concept using dual mode diesel combustion to achieve zero NOx and particulate emissions', SAE Paper 2002-01-1744, 2002.
23. Yanagihara, H., Satou, Y., and Mizuta, J., 'A simultaneous reduction of NOx and soot in diesel engines under a new combustion system (Uniform Bulky Combustion System – UNIBUS)', 17th Int. Vienna Motor Symposium, 1996.
24. Nishijima, Y., Asaumi, Y., and Aoygi, Y., 'Premixed Lean Diesel Combustion (PREDIC) using Impingement Spray System', SAE Paper 2001-01-1892, 2001.

www.TechnicalBooksPDF.com

25. Kimura, S., *et al*., 'New Combustion Concept for Ultra-clean and High Efficiency Small DI Diesel Engines', SAE Paper 1999-01-3681, 1999.
26. Walter, B., and Gatellier, B., 'Development of the High Power NADI Concept Using Dual Mode Diesel Combustion to Achieve Zero NOx and Particulate Emissions', SAE Paper 2002-01-1744, 2002.
27. Su, W.H., Lin, T., Zhao, H., and Pei, Y.Q., 'Research and Development of an Advanced Combustion System for the Direct Injection Diesel Engine', *Proc. Instn. Mech. Engrs Part D*, Vol. 219, pp. 241–252, 2005.
28. Buchwald, R., Brauer, M., Blechstein A., Sommer, A., and Kahrstedt J., 'Adaption of injection system parameters to homogeneous diesel combustion', SAE Paper 2004-01-0936, 2004.
29. BMW Group, 'Recent developments in BMW's diesel technology, DOE DEER conference, Aug. 2003.
30. Duffy, K. *et al.*, 'Diesel HCCI results at Caterpillar', DOE DEER conference, Aug., 2003.
31. Aoyama, T. *et al*., 'An experimental study on premixed-charge compression ignition gasoline engine', SAE Paper 960081, 1996.
32. Yang, J., Culp, T., and Kenny, T., 'Development of a Gasoline Engine System using HCCI Technology – the Concept and the Test Results', SAE Paper 2002-01-2832, 2002.
33. Kaiser E.W., Yang J., Culp, T., Xu N., and Maricq, C., 'Homogenous Charge Compression Ignition Engine-out Emissions – does flame propagation occur in homogeneous compression ignition?', *Int. J. of Engines Research*, Vol. 3, No. 4, pp 184–295, 2003.

www.TechnicalBooksPDF.com

Part II

Gasoline HCCI/CAI combustion engines

www.TechnicalBooksPDF.com

www.TechnicalBooksPDF.com

2

Overview of CAI/HCCI gasoline engines

H ZHAO, Brunel University West London, UK

2.1 Introduction

Homogeneous charge compression ignition (HCCI) or controlled auto-ignition (CAI) combustion, when applied to a gasoline engine, offers the potential for a noticeable improvement in fuel economy and dramatic reductions in NOx emissions as compared to the spark ignition operation. Indeed, it has been demonstrated that a CAI gasoline engine can achieve fuel economy levels comparable to those of a diesel engine, while producing engine-out NOx emissions that are as low as tail-pipe NOx emissions from a conventional SI engine equipped with a three-way catalyst.

In this chapter, the general characteristics of CAI operated gasoline engines will first be described, from which it will become apparent that high levels of dilution are essential for CAI operation. As perhaps the most effective dilution gas, the effects of exhaust gas on CAI operation will be analysed in Section 2.3. The most significant challenges associated with this combustion mode in a gasoline engine are the initiation of auto-ignition and the control of the ensuing heat release process. Different approaches to achieve controlled auto-ignition and combustion of a premixed fuel/air will be reviewed and will serve as an introduction to the other chapters in Part II, where details of each approach will be discussed.

2.2 Fundamentals of CAI/HCCI gasoline engines

Although CAI combustion in gasoline engines has been explored for over 20 years, there are still some fundamental questions that remain to be answered. CAI combustion is achieved by controlling the temperature, pressure and composition of the air/fuel mixture so that auto-ignited combustion can start at the right time and will proceed without causing a runaway heat release rate. There is no direct control over the ignition timing as in a SI or CI engine. As a result, the initial and boundary conditions as well as internal fluid flow will have a much greater effect on this combustion mode than the

www.TechnicalBooksPDF.com

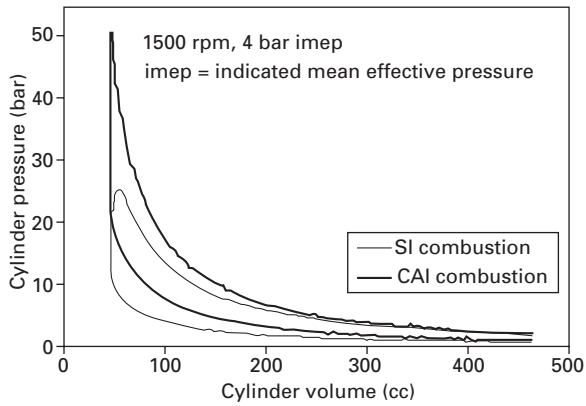

2.1 In-cylinder pressure traces of CAI and SI operation at the same operating condition.

SI and CI combustions. Furthermore, chemical kinetics plays a critical role in the better understanding and control of the auto-ignition process and ensuring heat release involved in this combustion mode. A large number of studies have been carried out to provide better understanding of these issues by means of advanced experimental and computational techniques. In this section, the general characteristics of CAI gasoline engines will be presented and discussed.

In an ideal case, CAI/HCCI combustion can be described as controlled autoignition of a premixed fuel/air mixture and involves the simultaneous reactive envelopment of the entire fuel/air mixture without a flame front. As shown in Plate 2 (between pages 268 and 269), the initiation of combustion always occurs at multiple sites in the premixed fuel/air mixture. The heat release process is much faster than the conventional SI combustion and is more closely described by a constant volume heat addition process, as shown in Fig. 2.1. This combustion mode also results in a more uniform and repeatable heat release in comparison with that of SI operation, as illustrated by the close resemblance of the mass fraction burned curves of 100 CAI combustion cycles in Plate 3 (between pages 268 and 269)

2.2.1 Region of CAI operation

Figure 2.2 shows a typical CAI region attainable for a gasoline engine [1]. These results were obtained from a single cylinder research engine operating at the following conditions.

Engine speed:	1500 rpm
Airflow:	WOT
Inlet charge temperature:	320 ± 1°C

www.TechnicalBooksPDF.com

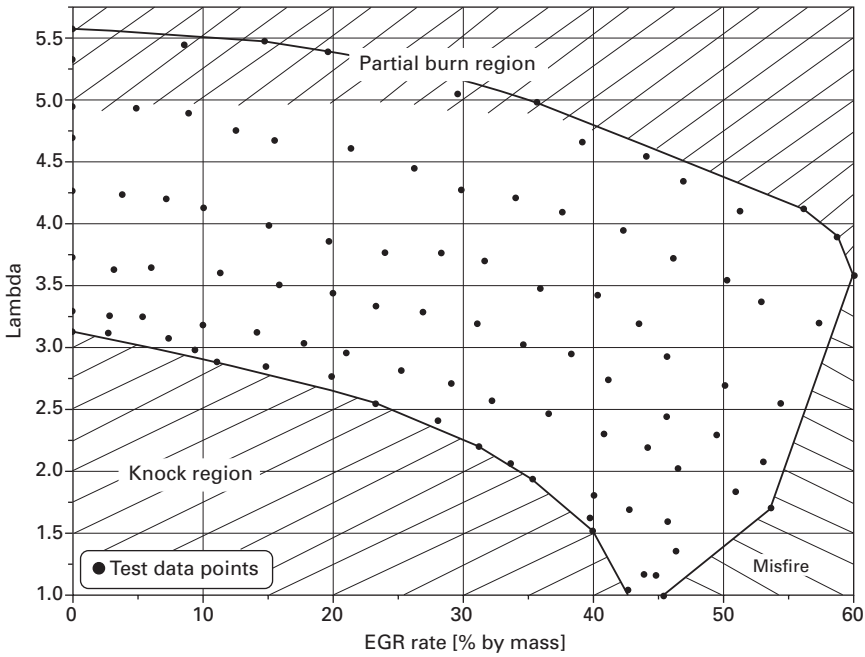

2.2 Boundary regions for CAI operation for unleaded gasoline.

Coolant temperature	80 ± 0.2°C
Oil temperature	55 ± 1°C
Compression ratio	11.5

In order to achieve CAI operation, the inlet charge temperature was raised to 320°C by an air heater. Exhaust gas re-circulating took place well before the air heater for homogeneous mixed air and EGR and was cooled sufficiently before entry to the inlet manifold to allow the inlet charge temperature to be controlled accurately by the heater irrespective of EGR rate. Fuel was delivered to the intake port at a pressure of 2.7 bar using a Bosch port injector.

The horizontal axis in Fig. 2.2 represents the total gravimetric percentage of EGR in the cylinder, and the vertical axis represents the overall A/F ratio of the cylinder charge. The attainable CAI region is limited by three boundaries:

1. misfire
2. partial burn
3. knock limit.

The first boundary defines the misfire region. At higher EGR rates, the CO_2 and H_2O content of the intake charge is raised significantly, causing the occasional failure of ignition. Higher EGR rates are obtainable as lambda is increased because there is increasingly more O_2 and less CO_2 and H_2O

www.TechnicalBooksPDF.com

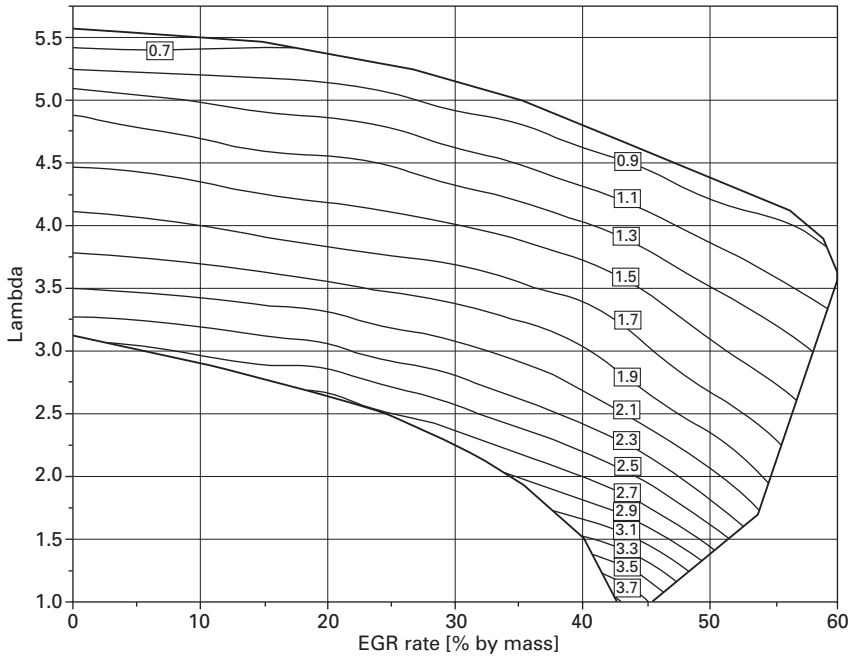

2.3 Indicated mean effective pressure (imep) values (bar) in the CAI operational range.

content in the intake charge, leading to more stable ignition and subsequent combustion.

As fuel flow-rate is decreased (lambda increase), the net heat-release is also decreased. The resulting gradual lowering of average combustion temperature leads to more unburned charge, characterised by high CO and unburned HC emissions, and by an increase in cycle-to-cycle variations.

Knocking combustion occurs at the lower boundary (high-load) of the region. At the knock boundary, if no EGR is used, the richest lambda attainable is approximately 3.15. As EGR is increased, the knock limit is brought closer to lambda 1.0, with 43% EGR.

Figure 2.3 shows the imep map for the gasoline CAI region. As expected, the imep decreases linearly with the A/F ratios as the fuelling is decreased at constant air flow rate. The highest imep of 3.8 bar occurs at lambda 1.0, EGR rate 43% at the knock limit while the lowest imep cannot be clearly defined as it will depend upon the acceptable levels of uHC and CO emissions, specific fuel consumption, and cyclic variation.

2.2.2 Unburned hydrocarbon (uHC) and CO emissions

Figures 2.4 and Fig. 2.5 show the specific unburned hydrocarbon emission and CO emission, respectively. Other studies by Kaiser *et al*. [2] and by Dec

www.TechnicalBooksPDF.com

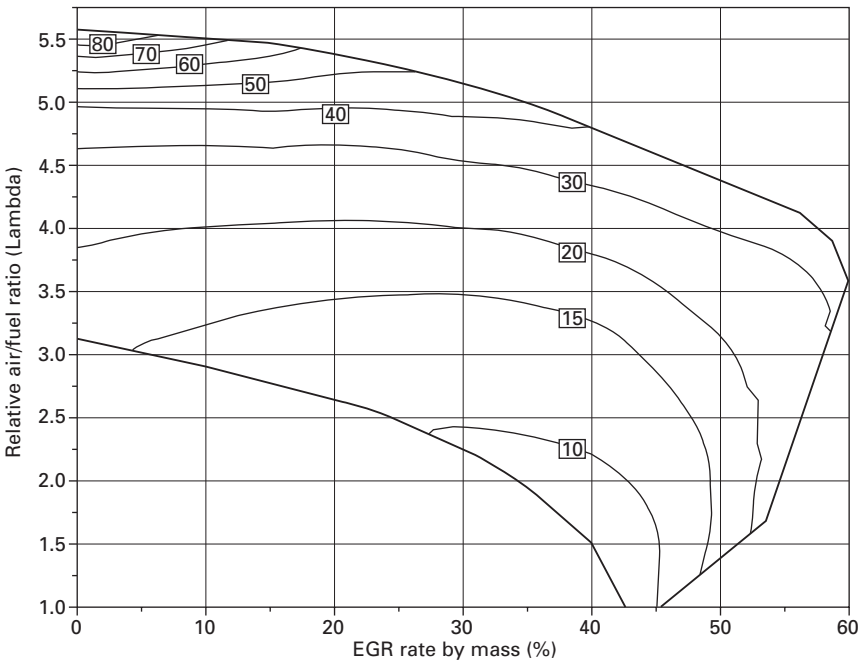

2.4 Indicated specific uHC emissions (g/kW.h) from CAI combustion.

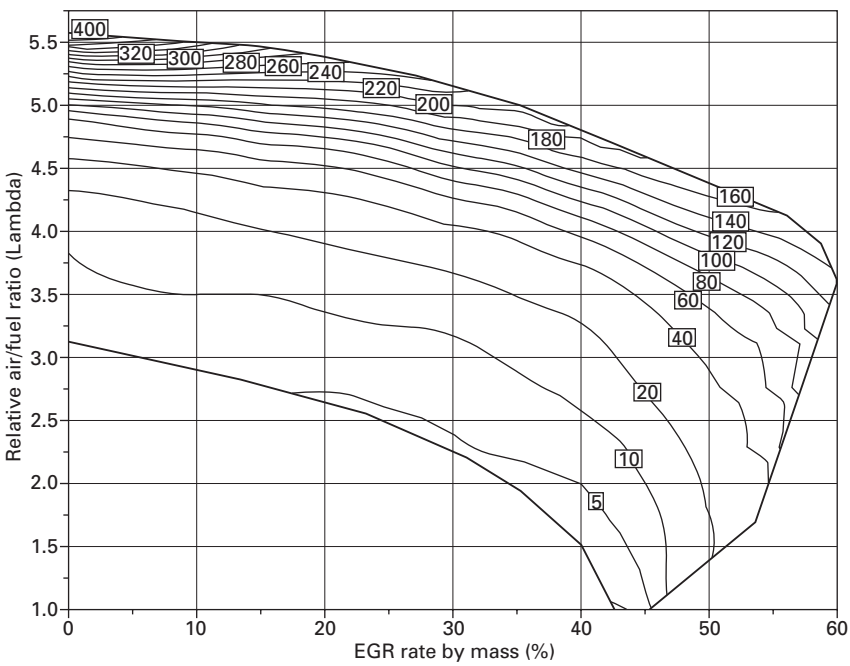

2.5 Indicated specific CO emissions, (g/kW.h) from CAI combustion.

www.TechnicalBooksPDF.com

and Sjoberg [3] also showed similar trends. Both uHC and CO emissions increase as the relative air/fuel ratio (lambda) is increased (reduction in load), due to the fact that total heat release and average combustion temperature are reduced as the load (fuel rate) is reduced. As a result, fuel/air mixtures are subject to low combustion and post-oxidation temperature and less complete oxidation of uHC and CO to CO_2. In addition, it is noted that an obvious break occurs in the CO emissions map, and to a lesser extent in the uHC emissions map, around the iso-line at $\lambda = 4.5$ without EGR, above which the iso-lines become increasingly closely distributed. As the conversion from CO to CO_2 requires a minimum temperature of 1400–1500K, below which the bulk of CO cannot be oxidised to CO_2, it is therefore not surprising to find that the peak combustion temperature calculated from the measured in-cylinder pressure traces in this region drops to 1400K.

Comparable uHC emissions for SI operation under these conditions are approximately 5 g/kW.h. uHC emissions for CAI combustion exceed this value over the entire region. This represents one of the major drawbacks of CAI combustion. In contrast, for the engine operation region close to the knock boundary, comparable CO emissions for SI operation under these engine-operating conditions are approximately 20 g/kW.h, much higher than CAI combustion. At the highest load point of operation in this region (lambda 1.0, EGR rate 43%), CO emissions are minimised at approximately 2 g/kW.h, offering substantial reductions compared to SI operation.

Whilst the air/fuel ratio has a large effect on uHC and CO emissions, the effect of EGR is small in most regions other than those of very high EGR concentrations.

2.2.3 NOx Emissions

A SI engine running at 1500 rpm and a load of 2–3 bar imep produces approximately 6 g/kW.h NOx. Figure 2.6 shows the NOx emissions map generated for gasoline CAI combustion under these conditions. As expected, NOx emissions are highest as the conditions approach the knock limit of the region, increasing further as lambda is decreased to 1.0. Heat release rates are highest in the region of the knock boundary, and combustion temperatures increase with EGR rate along that boundary, resulting in NOx emissions peaking with load at 0.35 g/kW.h. This represents a 94% reduction in emissions compared to SI operation.

Trends also show an increase in NOx emissions at low EGR rates and high lambda (top-left corner region of Fig. 2.6). This effect is attributable to extremely poor combustion efficiency in this region, as specific emissions are highly dependent on the relative difference between fuel consumption and power output.

www.TechnicalBooksPDF.com

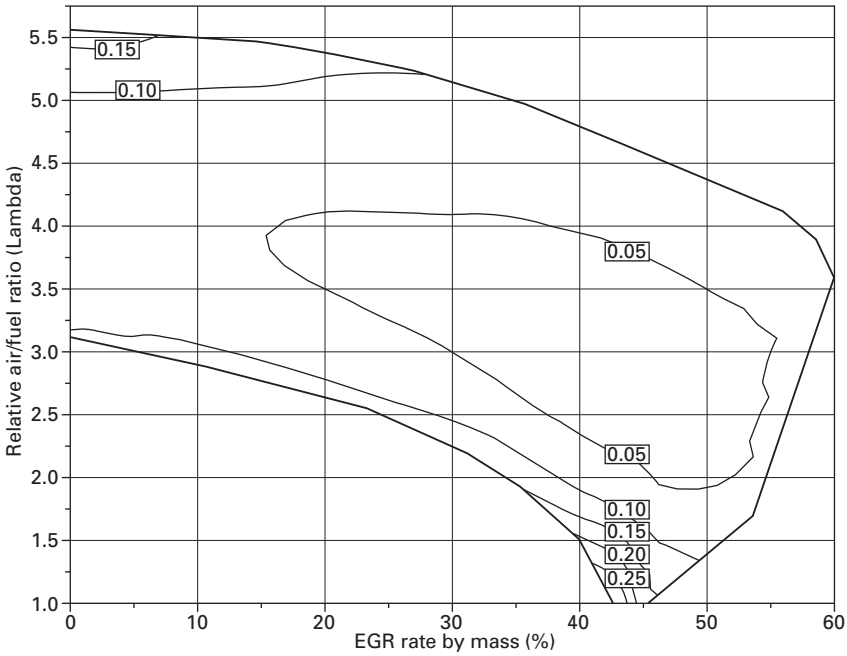

2.6 Indicated specific NOx emissions (g/kW.h) from CAI combustion.

2.2.4 Combustion characteristics

The combustion characteristics of CAI combustion are described here in terms of the start of combustion and combustion duration. The CAI combustion is considered to start as the crank angle at which 10% of the charge mass has burned. Although lower values (1%, 5%) of mass fraction burned could have been used, it has found that there is often a small quantity of heat released over an extended and variable period of crank angles prior to the start of the main combustion process. It was often difficult to obtain consistent measurements of the timings for such a small amount of heat released. Figure 2.7 shows the timing map for gasoline CAI combustion under these conditions. Trends indicate that timing is affected more by EGR dilution than by air dilution at low to moderate EGR rates (0–40%). At EGR rates beyond 40%, timing increasingly becomes dependent on lambda.

It is also found that the percentage of knocking cycles is independent of ignition timing but strongly affected by the fuel rate. That is, as fuel rate is increased for constant EGR rate at the knock boundary, ignition timing remains constant despite heavier knocking combustion. This is different from SI combustion, where ignition timing is one of the most important variables that determines whether engine knock occurs.

Figure 2.8 shows the combustion duration map. For low to moderate EGR

www.TechnicalBooksPDF.com

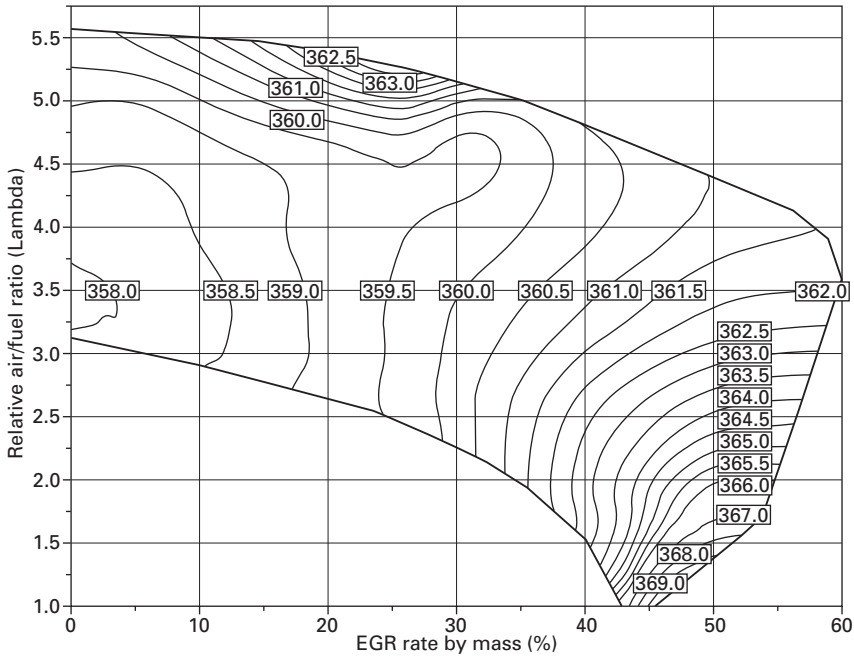

2.7 Start of CAI combustion (10% burn crank angle), (°CA, TDC = 360).

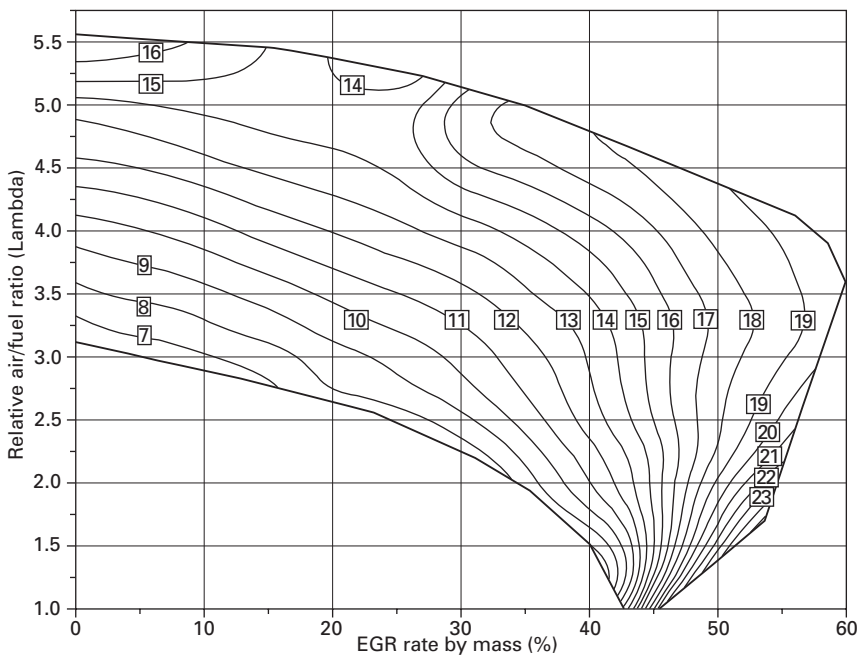

2.8 CAI combustion duration (10–90% burn), (°CA).

www.TechnicalBooksPDF.com

rates (up to 30%), combustion duration is dependent mainly on lambda, more than EGR rate. At moderate EGR rates (40–50%), duration becomes independent of A/F ratio. In this region and close to lambda 1.0, duration is increased significantly with small increases in EGR rate, similar to the way ignition timings are affected. In the region above 50% EGR rate, EGR clearly has a more detrimental affect to combustion phasing than air dilution. It would appear that the main effects of EGR on the CAI combustion could be caused by its higher specific heat that leads to a lower compression temperature, and/or by its dilution effect that tends to slow the reactions leading to auto-ignition and subsequent combustion. In order to determine which of the two effects is dominant, separate analytical studies have been carried out and their results will be presented in the next section.

2.3 Effects of use of exhaust gases as diluents

In order to achieve CAI/HCCI combustion, high intake charge temperatures and a copious amount of charge dilution must be present. In-cylinder gas temperature must be sufficiently high to initiate and sustain the chemical reactions leading to auto-ignition processes. Substantial charge dilution is necessary to control runaway rates of the heat releasing reactions. Both of these requirements can be realised by recycling and/or trapping the burnt gases within the cylinder.

The presence of the recycled or trapped burnt gases has a number of effects on the CAI combustion and emission processes within the cylinder. Firstly, if hot burnt gases are mixed with cooler inlet mixture of fuel and air, the temperature of the intake charge increases owing to the heating effect of the hot burnt gases. This is often the case for CAI combustion with high octane fuels, such as gasoline and alcohols. In this paper, this will be referred to as ***the charge heating effect***. Secondly, the introduction or retention of burnt gases in the cylinder replaces some of the inlet air and hence causes a substantial reduction in the oxygen concentration. The reduction of air/oxygen due to the presence of burnt gases is called ***the dilution effect***. Thirdly, the total heat capacity of the in-cylinder charge will be higher with burnt gases, mainly owing to the higher specific heat capacity values of carbon dioxide (CO_2) and water vapour (H_2O). This rise in the heat capacity of the cylinder charge is responsible for ***the heat capacity effect*** of the burnt gases. Finally, combustion products present in the burnt gases can participate in the chemical reactions leading to auto-ignition and subsequent combustion. This potential effect is classified as ***the chemical effect***. It should be noted that the chemical effects of active species or partially oxidised hydrocarbons are not included here and it would be an area that needs further research using more sophisticated models.

In order to examine the individual effects on CAI combustion of the

www.TechnicalBooksPDF.com

burned gases recycled or trapped within the cylinder, a single zone engine simulation model with detailed chemical kinetics was used to model the auto-ignition process and the subsequent combustion process under similar operating conditions in the same single cylinder engine described in the previous section. All calculations were carried out for a fixed amount of fuel (isooctane 12.4 mg/cycle, 2.3 imep) at 1500 rpm and 12:1 compression ratio. Individual effects of the recycled burnt gases on the start of auto-ignition, the combustion duration, and the heat release rate were investigated through a series of analytical studies [4].

2.3.1 Effects of cooled burned gases on CAI combustion

The first series of studies were carried out for homogeneously mixed fuel/air mixture and burned gases at the same temperature, i.e., there is no heating effect by the cooled burned gases. In practice, this can be achieved by passing the EGR gases through an EGR cooler before they are mixed with fresh charge in the cylinder. The results for cooled burned gases are shown in Fig. 2.9 to Fig. 2.11, where burnt gases of the same temperature as air at 600K are used in replacement of part of the air in the cylinder. It is noted that although auto-ignition could be achieved at an EGR level up to 70% (Fig. 2.10), incomplete combustion started to appear after about 60% EGR at the current operating condition. Hence, results in Fig. 2.10 and Fig. 2.11 are limited to 60%. Beyond 70% EGR, auto-ignition could not take place. It can be seen that the overall effect of cooled exhaust gases on the CAI combustion process is to retard the AI timing, to lengthen the combustion duration, and to reduce the $(dp/dt)_{max}$ value. Since the overall effect of the cooled burned gases

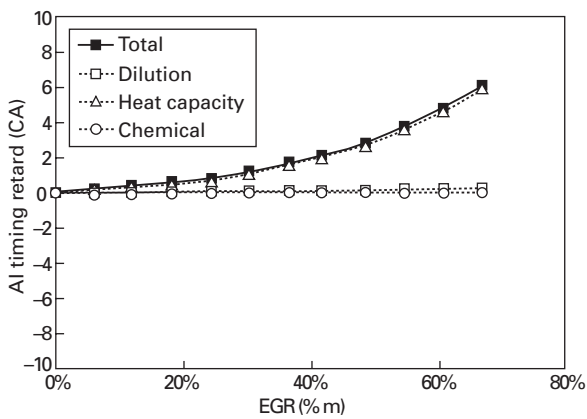

2.9 Individual effects of isothermal EGR on ignition timing.

www.TechnicalBooksPDF.com

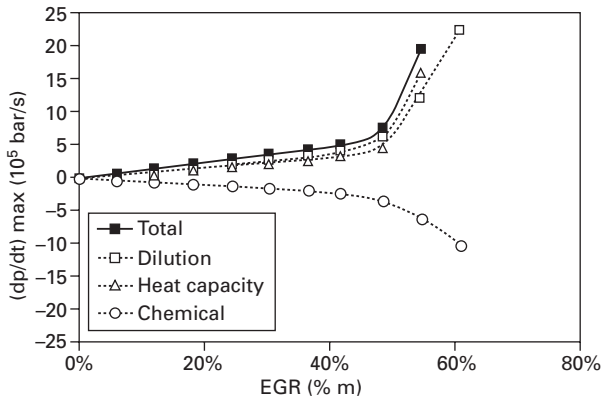

2.10 Individual effects of isothermal EGR on the combustion duration.

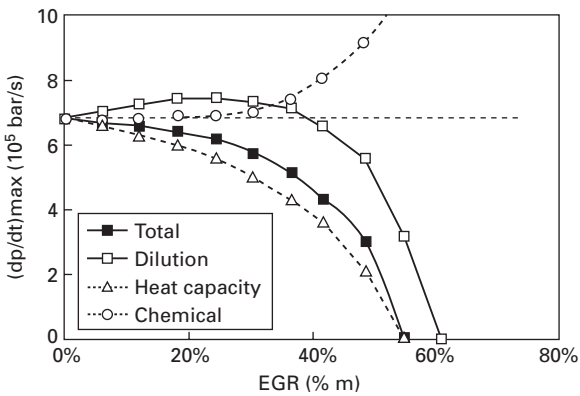

2.11 Individual effects of isothermal EGR on the maximum rate of pressure rise.

includes the dilution, heat capacity, and chemical effects of the recycled burnt gases, further analysis has been carried out to clarify each individual effect on the CAI combustion process.

Effect on the AI timing

The individual contributions of the dilution, heat capacity, and chemical effects of cooled burnt gases on the start of CAI combustion are summarised in Fig. 2.9. It can be seen that the heat capacity effect is the dominant factor for the retarded AI timing with EGR. This can be understood by considering the effect of burnt gases on the end-of-the-compression temperature: the

www.TechnicalBooksPDF.com

replacement of some O_2 by H_2O and CO_2 in the recycled burnt gases reduces the ratio of specific heats (γ value) of the cylinder charge. For a constant number of moles of mixture at the same initial pressure and temperature, the mixture will be compressed to a lower temperature at the end of the compression stroke owing to the lower γ value. Because of the strong temperature dependence of auto-ignition chemistry, the start of HCCI combustion is delayed to a later time when the compression temperature has reached the auto-ignition temperature.

In comparison, the chemical and dilution effects of cooled burned gases hardly affect the start of CAI combustion. The absence of the chemical effect can be explained by the fact that the dissociation of H_2O and CO_2 cannot take place at low temperatures before the start of combustion. Although some O_2 has been replaced with burnt gases (the dilution effect), the mixture remains lean and hence there is always sufficient oxygen for oxidation reactions to take place.

Effect on combustion duration

Figure 2.10 summarises the contributions of each individual effect of cooled burnt gases on the combustion duration as well as the overall effect of isothermal EGR. It shows that the combustion duration increases linearly with the burnt gases concentration up to 50%. A slight increase in burnt gases above 50% results in a much more rapid rise in the combustion duration. Incomplete combustion appears when 60% or more EGR is used. Figure 2.10 shows that dilution and heat capacity effects have similar influence in slowing down the combustion process, due to the reduced oxygen availability (the dilution effect) and lower combustion temperature caused by the presence of higher heat capacity gases of CO_2 and H_2O. Surprisingly, the chemical effect of CO_2 and H_2O tends to decrease the combustion duration.

Effect on the rate of pressure rise

Figure 2.11 illustrates the individual contributions on the maximum rate of the pressure rise $(dp/dt)_{max}$ that is often used as a measure of combustion generated noise. It can be seen that the presence of cooled burned gases reduces the heat release rate. Perhaps the most interesting feature of Fig. 2.11 is that most of the reduction in $(dp/dt)_{max}$ is caused by the heat capacity effect. In fact, the heat capacity effect is solely responsible for the reduction in $(dp/dt)_{max}$ when the concentration of the burnt gases is less than 50%. The dilution effect becomes noticeable only at very high EGR concentrations. Similarly, the chemical effect becomes significant only with very high burnt gas concentrations.

www.TechnicalBooksPDF.com

2.3.2 Effects of hot burned gases on CAI combustion

In practice, hot burned gases are preferred in most cases in order to increase cylinder charge temperature without external heating source. In order to study the effect of hot burned gases, the initial temperature of the fuel/air mixture was assumed at 400K and the burned gases temperature was 800K. At the start of each simulation, hot exhaust gases and fuel/air mixture were assumed completely mixed and the intake charge temperature was then calculated assuming isentropic mixing. Figure 2.12 shows the effect of hot burned gases on the total charge temperature and the relative air/fuel ratio of the cylinder charge. As expected, the initial charge temperature of the total in-cylinder charge was increased owing to the heating effect of hot burned gases, and the relative air fuel ratio λ was reduced as burned gases replaced some of the air. Here the range of the burned gas concentration was limited by misfire at low concentration due to insufficient heating for auto-ignition to start and at high concentration by incomplete combustion due to too much dilution.

It should be noted that the overall effect of hot burned gases includes the charge heating effect and all the other effects of cooled burned gases discussed previously. Figure 2.13 shows both the overall effect and charge heating effect of hot burned gases. The primary (bottom) *x*-axis and secondary (top) *x*-axis shows the percentage of EGR and the resulting charge temperature, respectively, when the overall effect of EGR was studied. The first feature of these results shown in Fig. 2.13 is that the overall effect of hot burned gases is to bring forward the start of combustion throughout the CAI combustion range. In comparison, the charge heating effect on ignition timing is more pronounced than the overall effect of hot EGR. The difference between the

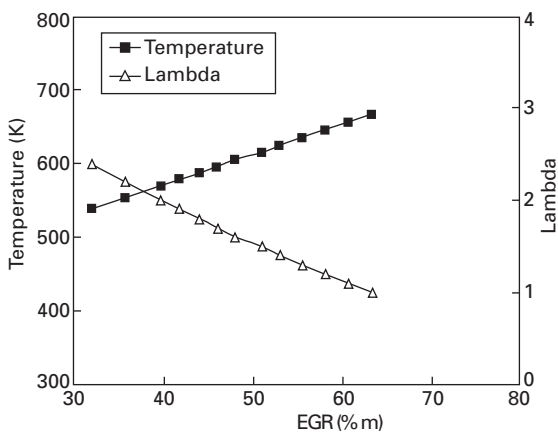

2.12 Lambda and initial charge temperature as a function of hot EGR.

www.TechnicalBooksPDF.com

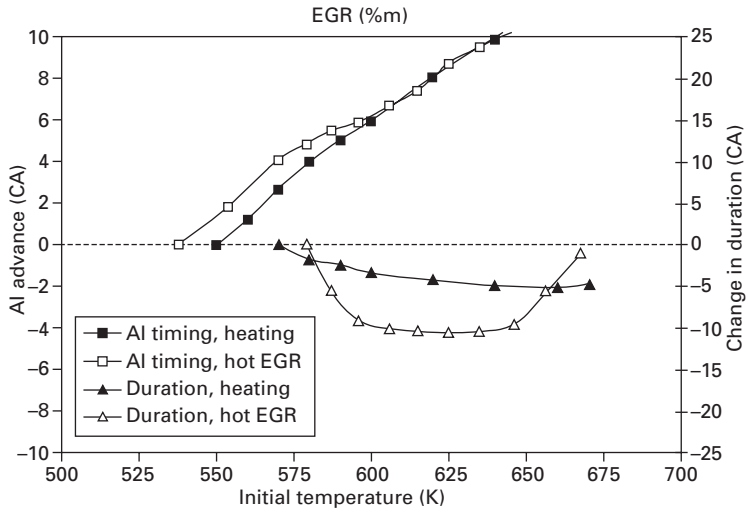

2.13 Overall and charge heating effects of hot EGR on AI timing and combustion duration.

charge heating and the overall effect is readily explained by the opposite effect of the higher heat capacity of burned gases, as shown in Fig. 2.9.

Figure 2.13 also shows that the combustion duration decreases linearly with intake temperature when only charge heating effect is present. However, the overall effect of hot burned gases on combustion duration is not linear. The presence of hot burned gases initially causes the CAI combustion process to accelerate. Further increase in the concentration of hot burned gas has little effect on the combustion duration in the middle region. The combustion duration then starts to rise when the concentration of burned gases approaches 60%. The trend shown in Fig. 2.13 of the combustion duration with hot EGR can be explained as follows. To the left of the minimum combustion duration region, the auto-ignition is retarded to near TDC so that HCCI combustion takes place in the expansion stroke at a lower pressure and temperature, hence slower burning. To the right of the minimum combustion duration region, the dilution and heat capacity effects become dominant in slowing down the combustion process, leading to increased combustion duration.

2.3.3 Effects of burned gases on CAI combustion and their implications

Both experiments and analytical studies have shown that the overall effect of hot burned gases is to advance the start of CAI combustion due to their charge heating effect. However, the cooled burned gases retard the auto-ignition process as the compression temperature is reduced by large heat

www.TechnicalBooksPDF.com

capacity gases. Ignition is dominated by the charge heating effect but the combustion duration is dominated by the dilution and heat capacity effect. The maximum rate of heat release is equally affected by the charge heating effect and by the combined dilution and heat capacity effect.

The above results have significant implications on how the burned gases should be used in CAI engines. For high-octane fuels, like gasoline, alcohols, natural gas, etc., it will be advantageous to retain burned gases at as high temperature as possible to promote auto-ignition of fuel/air mixture, particularly at low load operations. Whilst for more ignitable fuels, such as diesel and DME, cooled burned gas would be preferred in order to increase the ignition delay period to obtain premixed fuel/air mixture. It will also be true that cooler burned gases would help to minimise the runaway heat release rate for both high-octane fuels and more ignitable fuels, so that CAI can be achieved at higher load as shown by Cairns *et al*. [5].

2.4 Approaches to CAI/HCCI operation in gasoline engines

2.4.1 Approaches to CAI gasoline engines

The most successful outcome of CAI/HCCI research is demonstrated by the early work done on conventional ported 2-stroke engines, as demonstrated by the ATAC portable generator by Nippon Clean Engine Technology [6] and the limited production Honda ARC 250 motorbike engine [7]. Despite the apparent appeal of this engine, the problems associated with the conventional ported 2-stroke engine render it unsuitable for mainstream automotive applications.

In view of the apparent potential of CAI to reduce emissions and fuel consumption and the serious shortfalls of the 2-stroke ported engine as an automotive power unit, emphasis over the last decade has been placed on how to achieve the CAI combustion mode in 4-stroke gasoline engines. Several approaches have been suggested and explored over the last several years.

The most obvious approach to achieve auto-ignited combustion in a 4-stroke gasoline engine is by intake charge heating, as first adopted by Najt and Foster [8]. In this study, high intake air temperature was used to initiate CAI combustion, while a highly diluted charge was employed to control the subsequent heat release rate. In practice, the intake charge heating can be achieved by making use of the waste heat rejected from the engine coolant or exhaust through heat exchangers and switching valves as discussed in Chapter 4 and references within.

Another means that has been successfully used to achieve CAI combustion is to increase the compression ratio to the point where the required temperature

www.TechnicalBooksPDF.com

and pressure for auto-ignition are achieved mainly through compression [9]. However, in order to operate the engine in both SI and CAI combustion, a variable compression ratio (VCR) mechanism will be needed [10].

Variation in fuel blend has also been used by Olsson and Johansson [11] to achieve CAI combustion. This method, together with supercharging and intake air heating, used combinations of isoctane and heptane to achieve CAI combustion over a large speed and load range. A similar approach was also adopted by Kaimai *et al.* [12] by blending DME into methane to extend CAI operation and reduce emissions. Such work has demonstrated its potential as a method of achieving CAI in future production engines but it will be limited by the current lack of infrastructure to supply the required fuels as well as the complexity and cost of a dual fuel system.

The most successful and practical approach to CAI combustion in a gasoline engine is through the use of large amounts of burned gases by trapping them within the cylinder [13–16] or through internal recirculation [17, 18], as their thermal energy will heat the charge to reach auto-ignition temperature and help to tame the heat release rate as already discussed in the previous section.

This approach enables the CAI combustion at standard compression ratio without the need for external heating. There are two principal strategies for obtaining CAI combustion through the use of burned gases:

(i) The first approach involves the residual gas trapping by early closure of the exhaust valve(s) and is often referred as the residual gas trapping method. Significant amounts of burned gases are kept within the cylinder after the early closure of the exhaust valves during the exhaust stroke. In order to prevent the trapped burned gases from flowing into the intake manifold, the intake valves open well after the TDC. Hence, this approach is sometimes known as the negative valve overlap strategy and will be the subject of Chapter 5.

(ii) The second approach involves the recirculation of exhaust gases after they have left the cylinder. Recirculation of exhaust gases can be realised by the so-called internal EGR method through positive valve overlap but additional air heating or increased compression ratio is also needed to achieve auto-ignited combustion as will be discussed in Chapter 4. A more effective way to promote auto-ignited combustion is through the re-breathing method whereby the exhaust gas in the exhaust manifold is sucked back into the cylinder through the secondary opening of the exhaust valve(s) of small duration or through the extended opening of the exhaust valve(s) into the intake stroke. Chapter 6 will present detailed results obtained through the re-breathing method.

In comparison with the negative valve lap approach, the re-breathing method is characterised with a lower charge temperature as some heat will be lost

www.TechnicalBooksPDF.com

through the exhaust gas exchange process, and hence it may be more appropriate to higher load CAI operations. The higher charge temperature obtainable from the residual gas trapping method can be advantageous to extend CAI combustion to low load operation, it can lead to too advanced ignition and hence very fast rate of pressure rise at high load operations.

Over the last few years, the use of exhaust gas re-breathing and trapping to initiate and control CAI has proved to be increasingly popular with researchers since it appears to offer the best chance of producing a feasible production CAI/SI hybrid unit in the short to medium term. In addition, the method is likely to prove popular with motor manufacturers since it should be relatively cheap to implement and, apart from the addition of a new valve train and control system, requires no radical (expensive) changes to vehicle or engine architecture.

2.4.2 Challenges facing CAI/HCCI combustion in the gasoline engine

Although CAI combustion in a gasoline engine can be achieved using the methods described above, it presents several hurdles and challenges which need to be overcome before commercial application can be considered.

The first is to control the phasing and rate of combustion for best fuel economy and lowest pollutant emissions. Unlike SI combustion, CAI/HCCI combustion is achieved by controlling the temperature, pressure and composition of the in-cylinder mixture through the following parameters:

- EGR or residual rate
- air/fuel ratio
- compression ratio (CR)
- inlet mixture temperature
- inlet manifold pressure
- fuel properties or fuel blends
- injection timing of a DI gasoline engine
- coolant temperature.

Variable valve actuation allows fast and individual cylinder-based direct control over EGR/residual gases and effective CR, so that mixture temperature and composition can be altered for indirect control of combustion phasing. Fast thermal management based approach intends to control directly the mixture temperature and hence the combustion phasing. The employment of lean mixture has been found to be beneficial to slow down the heat release rate but air charging would be needed to provide the extra air required. Perhaps, a more interesting recent development in combustion phasing control is the use of direct injection and appropriate injection strategies. Several studies have shown that direct fuel injection can be used to influence

www.TechnicalBooksPDF.com

the CAI combustion by altering not only the local fuel distribution but more importantly the in-cylinder temperature history through early low temperature heat release and charge cooling [19–23]. In addition, direct injection strategy can also have a direct influence on the region of CAI operation. This will be discussed further in Chapter 5.

Another major hurdle blocking progression to commercial production of CAI/HCCI engines is the limited operating boundary compared with traditional SI operation. Knocking or violent combustion at high load and partial-burn or misfire at low load are the two main limiting regions in CAI/HCCI combustion in the gasoline engine. Boosting has been shown to extend the high load region of CAI operation when it is combined with leaner mixture [24]. In the case of residual gas trapping method, the use of cooled EGR has been shown to extend the upper boundary of CAI operation by retarding the start of CAI combustion [5]. Another interesting and potentially very effective way to lift the CAI combustion to the high load region is through the use of two-stroke operation in two-stroke/four-stroke switching engines, since for the same imep, the two-stroke CAI operation will produce twice the torque of the four-stroke operation [25].

Perhaps of equal importance is the ability of CAI combustion to be operated at lower load conditions. Recent studies have shown that spark ignition can assist CAI/HCCI combustion towards lower load operations by providing more favourable in-cylinder conditions for auto-ignition to take place [26]. The presence of spark also allowed lower compression ratio or lower inlet air temperature to be used for CAI operation [27]. In some studies, spark assisted CAI combustion has been found to facilitate the transition between SI and CAI combustion when it occurs at the boundary between the two combustion modes with internal EGR/residual gas operated CAI [18, 25, 28], whilst spark discharge was found to cause greater cyclic variations between mode transfer from HCCI to SI with thermally activated HCCI operation using high compression ratio and fast thermal management [27]. More recently, Urushihara *et al*. [29] extended the spark assisted CAI concept to SI and CAI hybrid combustion by igniting a stratified charge near the spark plug first so that the pressure rise associated with the early heat release from the SI combustion caused the premixed and diluted mixture to auto-ignite and burns. As a result, the maximum imep value could be increased but it was accompanied with higher NOx emissions than pure CAI operation.

There are also other techniques that can be used to expand both the high load and low load regions of CAI operation. One such method is through regulating coolant water temperature. Milovanovic *et al.* [30] has shown that with reducing coolant temperature to 65°C, the upper limit can be extended up to 14% while with increasing the coolant temperature the lower limit can be extended up to 28% for a single-cylinder engine operating in CAI through the negative valve overlap approach. In addition, thermal or/and charge

www.TechnicalBooksPDF.com

stratification has been investigated as a means to expand the region of CAI operation. Aroonsrisopon *et al*. [31] demonstrated that stratified charge could be used to provide more stable CAI combustion at the lean limit through the use of a PFI injector for premixed charge and an DI injector for stratified charge. Through modelling and some controlled experimental studies, Sjöberg *et al*. [32] showed that the potential for extending the high-load limit by adjusting thermal stratification was very large. It was stated that with appropriate thermal stratification 16 bar gross imep could be realised with a relatively slow rate of pressure rise with moderate combustion retard.

2.4.3 CAI/SI hybrid operation for automotive vehicle applications

Regardless of the means employed to achieve CAI combustion, the attainable operating range is often greatly reduced from that of an equivalent engine operating in the SI or CI mode. If the heat energy required for auto-ignition is introduced into the charge by intake air heating or increased compression ratio, over lean mixtures or copious amounts of dilution with exhaust gas must be used to limit the heat release rates. If the heat energy is supplied by IEGR, then space must be allotted for the requisite quantity of exhaust gas, which conveniently also provides the required charge dilution. In both cases, the amount of fuel that can be burned in any cycle is drastically reduced when compared to SI and CI engines, limiting maximum torque output.

As a result, CAI/SI hybrid operation would need to be implemented in the 4-stroke gasoline engine in order to cover the complete load and speed range of the engine, such that SI combustion could be used for very low load and high load operations whilst the CAI/HCCI combustion can be employed at low to mid-range loads. This would allow the emission and fuel consumption improvements with CAI/HCCI combustion at part-load operations while maintaining the full load engine performance using SI combustion. The CAI/SI hybrid operation would require the transition from SI to CAI and vice versa to be realised depending on the engine demand. Recent studies have shown that with the proper setting of the control parameters mode changes can be achieved without great difficulty [33–35]. Chapter 8 will present one such example on the transition between SI/CAI operations using two different valve train setups.

2.4.4 Controlling CAI/HCCI combustion

As CAI/HCCI combustion cannot be directly controlled using spark ignition in a gasoline engine, the phasing and combustion rate will depend on the thermal and chemical state of the in-cylinder mixture. In addition, a system has to be implemented that could take account of transient operation and

www.TechnicalBooksPDF.com

select the right operational mode, i.e., SI or CAI/HCCI without the interaction by the driver, if such a combustion system is to be implemented in real world applications. In particular, there is a much higher risk of misfire in CAI operation, which will have a much more severe consequence on the engine's performance and emissions than SI combustion. It is apparent that a control system with closed-loop combustion control will be needed for CAI operation. Initial studies were focused on feedback systems [36] and they are being extended into feed-forward and model based controllers [18, 37, 38]. Chapter 7 will present more detailed discussion on closed-loop combustion control techniques and their implementations.

2.5 Summary

In this chapter it has shown that application of CAI/HCCI combustion to the gasoline engine can produce ultra-low NOx emissions and significantly improved fuel economy over the conventional SI combustion. Through analytical studies, the effects of exhaust gases on CAI/HCCI combustion have been clarified. Major approaches to achieve CAI/HCCI combustion in gasoline engines have been introduced. It has been shown that in order to implement CAI/HCCI combustion for automotive applications, the CAI/HCCI operational range needs to be enlarged and the real-time closed-loop control and switching between SI and HCCI combustion are also necessary. In the following chapters, detailed discussions will be presented for the topics introduced in this chapter.

2.6 References

1. Oakley, A., Zhao, H., Ma, T., and Ladommatos, N., 'Experimental studies on controlled auto-ignition (CAI) combustion of gasoline in a 4-stroke engine', SAE paper 2001-01-1030, 2001.
2. Kaiser E.W., Yang J., Culp, T., Xu N., and Maricq, C., 'Homogeneous Charge Compression Ignition Engine-out Emissions – does flame propagation occur in homogeneous compression ignition?', *Int. J. of Engines Research*, Vol. 3, No. 4, pp. 184–295, 2003.
3. Dec, J.E., and Sjoberg, M.A., 'Parametric Study of HCCI Combustion – the Sources of Emissions at Low Loads and the Effects of GDI Fuel Injection', SAE Paper 2003-01-0752, 2003.
4. Zhao, H., Peng, Z., and Ladommatos, N., 'Understanding of Controlled Auto-Ignition Combustion in a Four-Stroke Gasoline Engine', *Proc. of Instn. Mech. Engrs*, Part D., Vol. 215, pp. 1297–1310, 2001.
5. Cairns, A., and Blaxill H., 'The effects of combined internal and external exhaust gas recirculation on gasoline controlled auto-ignition', SAE paper 2005-01-0133, 2005.
6. Onishi, S., Hong Jo Souk, Shoda, K., Do Jo, P., and Kato, S., 'Active thermo-atmosphere combustion (ATAC) – A new combustion process for internal combustion engines', SAE paper 790507, 1979.

www.TechnicalBooksPDF.com

7. Ishibashi, Y., and Asai, M., 'Improving the exhaust emissions of two-stroke engines by applying the activated radical combustion', SAE paper 960742, 1996.
8. Najt, P.M. and Foster, D.E., 'Compression-ignited homogeneous charge combustion', SAE paper 830264, 1983.
9. Christensen, M., Hultqvist, A., and Johansson, B., 'Demonstrating the multi fuel capability of a homogeneous charge compression ignition engine with variable compression ratio,' SAE paper 1999-01-3679, 1999.
10. Haraldsson, G., Hyvonen, J., Tunestal, P., and Johansson, B., 'HCCI combusion phasing in a multi-cylinder engine using variable compression ratio', SAE Paper 2002-01-2858, 2002.
11. Olsson, J., and Johansson, B., 'Closed loop control of an HCCI engine', SAE paper 2001-01-1031, 2001.
12. Kaimai, T., *et al*. 'Effect of a hybrid fuel system with diesel and premixed DME/methane charge on exhaust emissions in a small DI diesel engine', SAE paper 1999-01-1509.
13. Lavy, J., Dabadie, J.C., Angelberger, C., Duret, P., Willand, J., Juretzka, A., Schaflein, J., Ma, T., Lendresse, Y., Satre, A., Schulz, C., Kramer, H., Zhao, H., and Damiano, L., 'Innovative Ultra-low NOx controlled auto-ignition combustion process for gasoline engines: the 4-SPACE project', SAE paper 2000-01-1873, 2000.
14. Law, D., *et al*., 'Controlled combustion in an IC-engine with a fully variable valve train', SAE paper 2000-01-0251, 2000.
15. Li J., Zhao, H., and Ladommatos, N., 'Research and development of controlled auto-ignition (CAI) combustion in a four-stroke multi-cylinder gasoline engine', SAE paper 2001-01-3608, 2001.
16. Koopmans, L., and Denbratt, I., 'A four stroke camless engine, operated in homogeneous charge compression ignition mode with a commercial gasoline', SAE paper 2001-01-3610, 2001.
17. Kahaaina, N., Simon, A.J., Caton, P.A., *et al*., 'Use of dynamic valving to achieve residual-affected combustion', SAE paper 2001-01-0549, 2001.
18. Fuerhapter, A., Piock, W.F., and Fraidl G.K., 'CSI – Controlled Auto Ignition – the best Solution for the Fuel Consumption – Versus Emission Trade-Off?', SAE paper 2003-01-0754, 2003.
19. Marriott, C., and Reitz, R., 'Experimental Investigation of direct injection-gasoline for premixed compression ignited combustion phasing control', SAE 2002-01-0418, 2002.
20. Urushihara, T., Hiraya, K., Kakuhou, A., and Itoh, T., 'Expansion of HCCI Operating Region by the Combination of Direct Fuel Injection, Negative Valve Overlap and Internal Fuel Reformation', SAE Paper 2003-01-0749, 2003.
21. Standing, R., Kalian, N., Ma, T., and Zhao, H., 'Effects of injection timing and valve timings on CAI operation in a multi-cylinder DI gasoline engine', SAE paper 2005-01-0132, 2005.
22. Li, Y., Zhao H., Bruzos N., Ma T., and Leach B., 'Effect of Injection Timing on Mixture and CAI Combustion in a GDI Engine with an Air-Assisted Injector', SAE Paper 2006-01-0206, SAE Special Publication SP-2005, *Homogeneous Charge Compression Ignition (HCCI) Combustion 2006* ISBN Number: 0-7680-1740-8, 2006.
23. Cao, L., Zhao, H., Jiang. X., and Kalin, N., 'Investigation into the Effect of Injection Timing on Stoichiometric and Lean CAI operations in a 4-Stroke GDI Engine', SAE Paper 2006-01-0417, SAE Special Publication SP-2005, *Homogeneous Charge*

www.TechnicalBooksPDF.com

Compression Ignition (HCCI) Combustion 2006 ISBN Number: 0-7680-1740-8, 2006.
24. Christensen, M., Johansson, B., Amneus, P., and Mauss, F., 'Supercharged homogeneous charge compression ignition', SAE paper 980787, 1998.
25. Osbourne, R.J., Li, G., Sapsford, S.M., Stokes, J., Lake, T.H., and Heikal, M.R., 'Evaluation of HCCI for Future Gasoline Powertrains', SAE Paper 2003-01-0750, 2003.
26. Kalian, N., Standing, R., and Zhao, H., 'Effects of Ignition Timing on CAI Combustion in a Multi-Cylinder DI Gasoline Engine', SAE Paper 2005-01-3720, SAE 2005 Powertrain and Fluid Systems Conference, 2005.
27. Hyvonen, J., (Fiat-GM Powertrain Sweden) Haraldson, G., and Johansson, B., (Division of Combustion Engines, Lund Institute of Technology) 'Operating Conditions Using Spark Assisted HCCI Combustion during Combustion Mode Transfer to SI in a Multi-Cylinder VCR-HCCI Engine', SAE Paper 2005-01-0109, 2005.
28. Kalian, N., 'Investigation of CAI and SI combustion in a 4-cylinder Direct Injection Gasoline Engine', PhD thesis, Sept., 2006.
29. Urushihara, T., Yamaguchi, K., Yoshizawa, K., and Itoh, T., 'A study of a Gasoline-Fuelled Compression Ignition Engine–Expansion of HCCI Operation range Using SI Combustion as a Trigger of Compression Ignition', SAE 2005-01-0180, 2005.
30. Milovanovic, M., Blundell, D., Pearson, R., Turner, J., (Lotus Engineers), Chen, R., (Department of Aeronautical and Automotive Engineering, Loughborough University), 'Enlarging the Operational Range of a Gasoline HCCI Engine by Controlling the Coolant Temperature', SAE Paper 2005-01-0157, 2005.
31. Aroonsrisopon, T., Werner, P., Waldman, J.O., Sohm, V., Foster, D.E., Morikawa, T., and Lida, M., 'Expanding the HCCI Operation with the Charge Stratification', SAE Paper 2004-01-1756, 2004.
32. Sjöberg M., Dec J., and Cernansky, N.P, (Mechanical Engineering Department, Drexel University) 'Potential of Thermal Stratification and Combustion Retard for Reducing Pressure-Rise Rates in HCCI Engines, Based on Multi-Zone Modeling and Experiments', 2005-01-0113, 2005.
33. Koopman, L., Strom, H., Lundgren, S., Backland, O., (Volvo Car Corporation) Denbratt, I., (Chalmers University of Technology) 'Demonstrating a SI-HCCI-SI mode change on a Volvo 5-Cylinder Electronic Valve Control Engine', SAE Paper 2003-01-0753, 2003.
34. Sun, R., Thomas, R., and Gray, C.L. Jr., 'An HCCI Engine: Power Plant for a Hybrid Vehicle', SAE Paper 2004-01-0933, 2004.
35. Milovanovic, N., Blundell, D., Gedge, S., and Turner, J., 'SI-HCCI-SI Mode Transition at Different Engine Operating Conditions', 2005-01-0156, 2005.
36. Haraldsson, G., Tunestal, P., Johansson, B., and Hyvonen, J., 'HCCI closed-loop combustion control using fast thermal management', SAE Paper 2004-01-0943, 2004.
37. Gerdes, J.C., Shaver, G.M., Ravi, N., and Roelle, M., 'Controlling HCCI with Physically-based models', SAE Homogenous Charge Compression Ignition (HCCI) Symposium 2005, Lund.
38. Herrmann, H.-O., Herweg, R., Karl, G., Pfau, M., and Stelter, M. Der Einsatz der Benzindirekteinspritzung in Ottomotoren mit homogen-kompressionsgezündeter Verbrennung Direkteinspritzung im *Ottomotor V*, Haus der Technik, Essen 2005.

www.TechnicalBooksPDF.com

3

Two-stroke CAI engines

P DURET, IFP, France

3.1 Introduction

3.1.1 The CAI story started with two-stroke engines

Significant research work was performed from the end of the 1960s to the end of the 1970s in order to solve one of the main problems of the two-stroke engine which was the unstable, irregular and incomplete part load combustion responsible for excessive emissions of unburned hydrocarbons. Souk Hong Jo and his colleagues of the Nippon Clean Engine (NiCE) performed a lot of research work during this period to study the part load lean two-stroke combustion (Souk Hong Jo, 1973). They discovered that the irregularities of the combustion and the auto-ignition which were considered as the weak points of the two-stroke engine could be effectively controlled. This period was successfully concluded by the innovative pioneering work he published with his colleague Onishi who managed to get a part load stable two-stroke combustion process for lean mixtures in which ignition occurs without spark assistance (Onishi, 1979). Remarkable improvements in stability, fuel efficiency, exhaust emissions, noise and vibration were reported. Onishi and his NiCE colleagues called this new combustion process occurring without flame front 'ATAC' for 'Active Thermo-Atmosphere Combustion'. The first NiCE electric generator using an ATAC two-stroke engine was then commercialised in Japan from this period during a few years as shown in Fig. 3.1.

During the same year, 1979, another Japanese paper (Noguchi, 1979) concerning two-stroke auto-ignition was published. Noguchi and his colleagues named this auto-ignition the TS (Toyota-Soken) combustion process. They also found that such combustion occurred similarly without flame front while showing excellent efficiency and emissions figures. They tried to better understand the combustion chemistry of the TS combustion. They were the first to suggest that active radicals in residual gases could play an important role in the auto-ignition process.

www.TechnicalBooksPDF.com

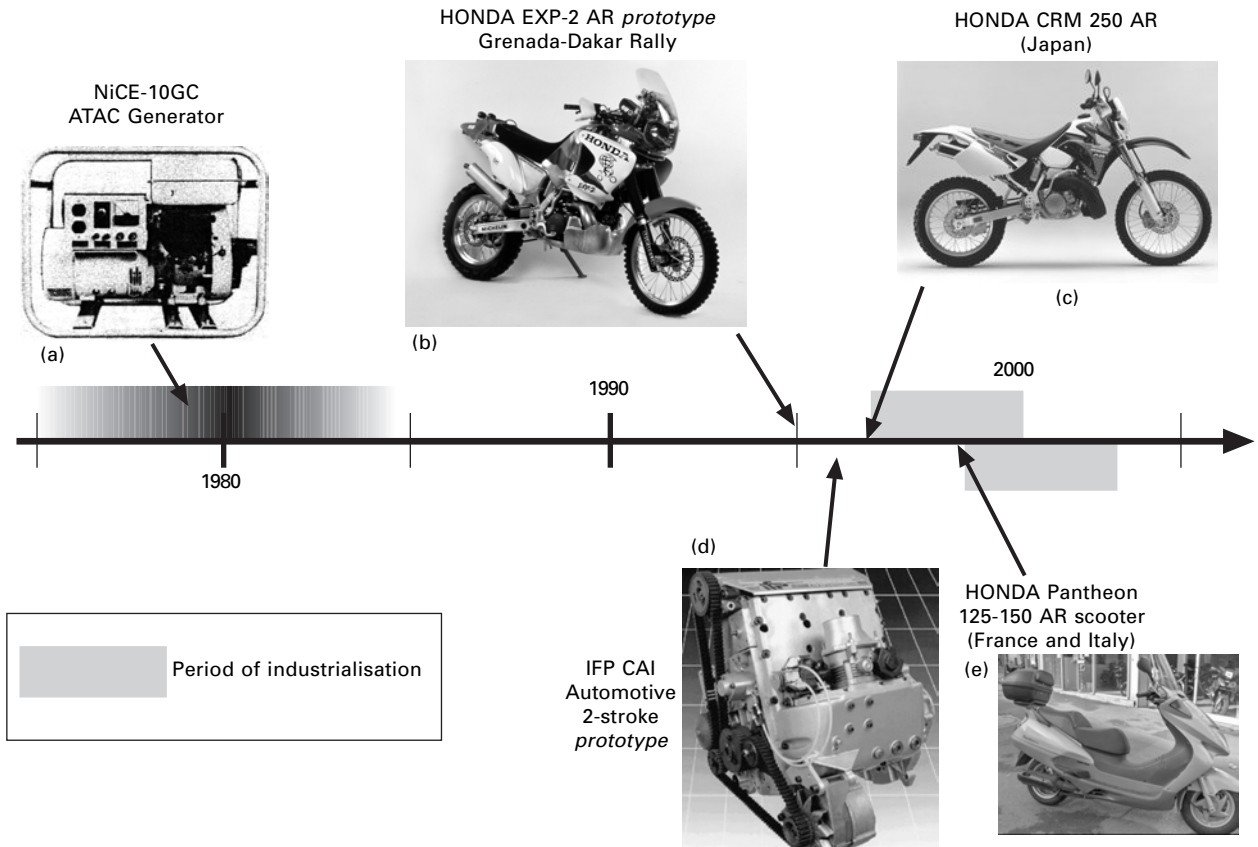

3.1 History of production and most advanced prototype CAI 2-stroke engines.

www.TechnicalBooksPDF.com

During the second half of the 1980s, several research works were undertaken worldwide to try to develop direct injection (DI) two-stroke engines for automotive application. The French research laboratory IFP (Institut Français du Pétrole) was one of the major players deeply involved in this development of DI two-stroke engines, in particular its innovative IAPAC air assisted direct fuel injection technology (Duret, 1988). To further improve the part load emissions of its IAPAC engine, Duret tried to apply Onishi's pioneering work to DI two-stroke engines. For this purpose, he investigated the idea of using a butterfly exhaust throttling valve as previously shown by Tsuchiya in a carburetted engine (Tsuchiya, 1980). The first application of ATAC auto-ignition with direct fuel injection engine was then described in 1990 (Duret, 1990). CFD calculations showed that mixing between the residual gas and fresh intake air may be reduced by precisely regulating the introduction of the intake flow through the use of an exhaust control valve.

This research work was further developed until the mid-1990s (Duret, 1992a and 1993) and the interest of using transfer port throttling (the transfer duct in a two-stroke engine is the duct in which the fresh charge is transferred from the pump crankcase to the combustion chamber through a port on the wall of the cylinder) to even better control the degree of mixing between the fresh charge and the hot and reactive residual gas was demonstrated. The first automotive two-stroke direct injection engine prototype using this transfer port throttling technique for running in controlled auto-ignition (CAI) was presented in 1996 (Duret, 1996) as shown by Fig. 3.1. Thanks to the advantage of combining direct injection with CAI, this engine was easily able to meet the European emissions standards valid up to the year 2000 without NOx after-treatment and with more than 20% fuel economy improvement compared to its four-stroke counterpart of equivalent power output.

In parallel to this automotive research work, Ishibashi investigated the possibility of using the auto-ignition in two-stroke motorcycle engines. He demonstrated that with an appropriate charge control exhaust valve (combining variable exhaust port timing with exhaust throttling) it was possible to control the amount of active residual gases in the combustion chamber as well as in cylinder pressure before compression (Ishibashi, 1993). He names this combustion process AR combustion (which stands for 'Activated Radicals' combustion). As shown by Fig. 3.1, two Honda EXP-2 400cc AR prototypes were prepared for the 1995 Grenada-Dakar rally and performed very well compared to the four-stroke motorcycles, thanks in particular to their high fuel economy. This work was further developed (Asai, 1995 and Ishibashi, 1996) up to the first industrial application of AR combustion in production in a Japanese motorcycle model in 1996 and in an European scooter model in 1998 (Fig. 3.1).

www.TechnicalBooksPDF.com

3.2 Principles of the two-stroke CAI combustion

3.2.1 The specific and particular combustion modes of two-stroke engines

Figure 3.2 shows the various combustion modes that can be encountered in a typical two-stroke SI engine. There is a misfiring area in the lightest load lowest speed region (especially around idle). In these conditions the amount of residual gases is so high (more than 80%) that the mixture cannot be ignited every cycle. One or more cycles are necessary to scavenge the residual

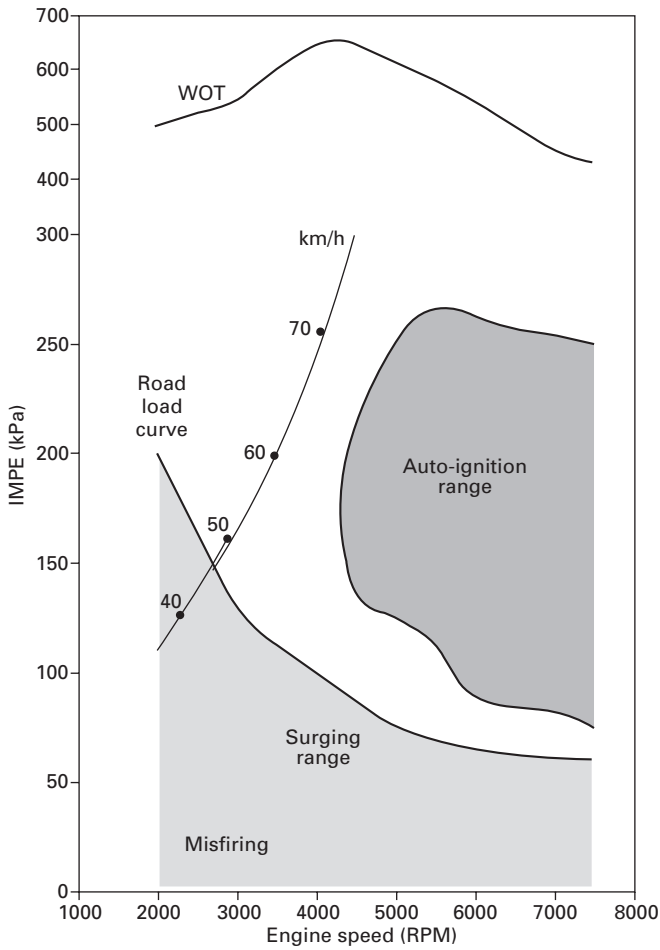

3.2 Surging and auto-ignition ranges in a typical two-stroke motorcycle engine (adapted from Tsuchiya, 1983).

www.TechnicalBooksPDF.com

gases enough and to reduce their concentration to a level allowing a correct spark ignition of the mixture. When the load increases slightly from idle, the amount of residual gases progressively decreases but not enough and partial misfiring or incomplete combustion remain responsible for engine surging operation. If we continue to increase the engine load, we arrive in the white area of the engine operating range represented in Fig. 3.2. The amount of residual gases has been further decreased and has reached a level where complete spark ignition combustion can be achieved every cycle. We can also see on the same figure that when the engine speed increases and the load remains low, the engine can enter in an uncontrolled auto-ignition range. Most of the two-stroke engines always present such low load high speed auto-ignition range but it is not well known because the typical engines generally never operate in this area (as shown by the road load curve represented in Fig. 3.2). The main progress and innovation brought by the Onishi work was to understand the interest of this auto-ignition range and to try to move it to the lower speed range in order to solve the major two-stroke engine problem of misfiring and poor combustion.

In Fig. 3.3, the effect of the typical two-stroke incomplete combustion on the engine fuel consumption can be clearly seen. This figure represents the BSFC (brake specific fuel consumption) of a two-stroke engine versus engine load. The full line is the actual BSFC and the dotted line the theoretical BSFC that could be achieved without misfiring at low load and without fuel short-circuiting at higher load. This figure illustrates what significant benefit in BSFC (dashed area) can be obtained if the incomplete part load combustion

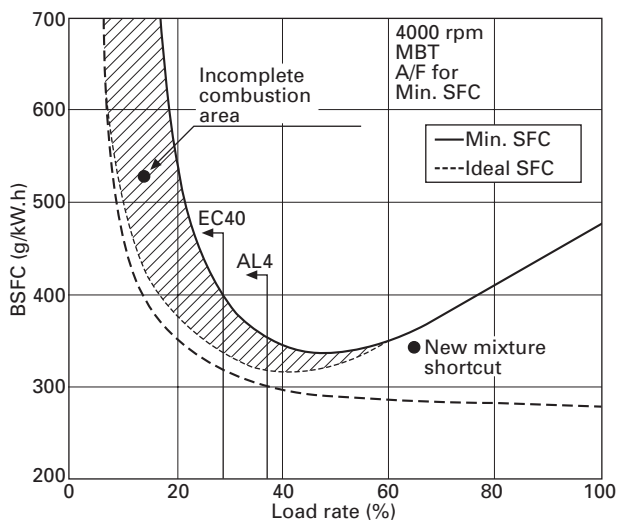

3.3 Actual and ideal brake specific fuel consumption versus 2-stroke engine load (Ishibashi, 1993).

www.TechnicalBooksPDF.com

problem of the two-stroke engine can be solved. If we can reach the theoretical light load BSFC curve, fuel consumption can even become much lower than those of the four-stroke counterpart thanks to the lower two-stroke pumping and friction losses. This figure really demonstrates all the interest of the Onishi, Noguchi and Tsuchiya pioneering works. In finding how to benefit from the inherent uncontrolled auto-ignition high speed low load combustion process to the low speed range, these Japanese researchers greatly contributed to the increase of the scientific knowledge in this field. They opened new research perspectives to all the researchers who have since been involved in the further investigation into this new combustion process as we will see in the following sections.

3.2.2 The basic principles of CAI combustion and the in-cylinder conditions for CAI

Figure 3.4 is a simple visual way of illustrating the main differences between spark ignition (SI) and ATAC auto-ignition. In the case of the conventional spark ignition, the figure shows that the people picking along a line represent

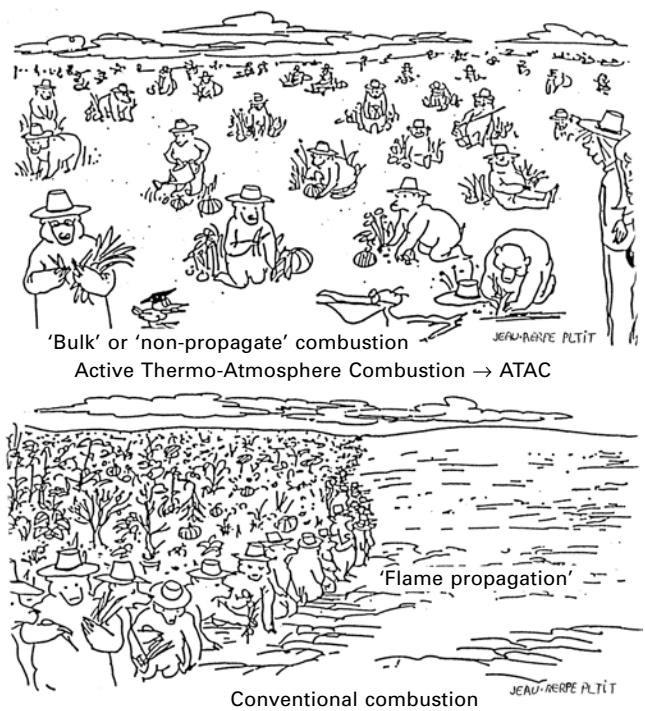

3.4 A 'simplified' way of illustrating the ATAC/SI combustion process difference.

www.TechnicalBooksPDF.com

the flame front separating the part where all the crops have been picked from the part not picked. In the case of ATAC, people do not need to move. They can pick around them. This visual representation allows easy understanding the main differences between both combustion processes. In the case of SI, there is a strong activity along the 'flame front' line corresponding to a strong energy release generating high temperatures and high emissions of nitrogen oxides (NOx). In the case of ATAC, the figure helps to imagine that on each site of combustion, the energy release is locally much lower with therefore much lower increase of local temperature and NOx emissions. Nevertheless, since local picking occurs simultaneously in all the 'combustion' area, the overall activity and therefore 'heat release' can be globally as fast as with the SI combustion.

The Fig. 3.5 shows ideal representations of both SI and ATAC/CAI combustion processes. In the case of SI, it is the flame front that separates the burnt gases from the fresh unburnt gases and its velocity controls the combustion heat release. In the case of CAI, the combustion reactions take place with multiple auto-ignition sites. Even if the combustion locally can progress slowly, since it occurs spontaneously and simultaneously at several locations within the combustion chamber, the overall heat release can be as fast or even faster than with the flame front controlled SI without generating the typically high combustion temperatures of the flame front. This could contribute to explain the CAI low NOx emissions advantage that will be described in the following section.

Figure 3.6 shows the relationship between the average charge temperature at the beginning of compression and the quantity of fresh charge and residual gas (Onishi, 1979). To get stable ATAC, high average charge temperature is necessary for auto-ignition. At very light load, the average charge temperature drops due to the low amount of energy released per engine cycle and becomes too low to produce stable ATAC. As the load increases, the charge temperature initially increases making ATAC possible. However, higher engine loads require more fresh charge, reducing the amount of residual gas and thus the

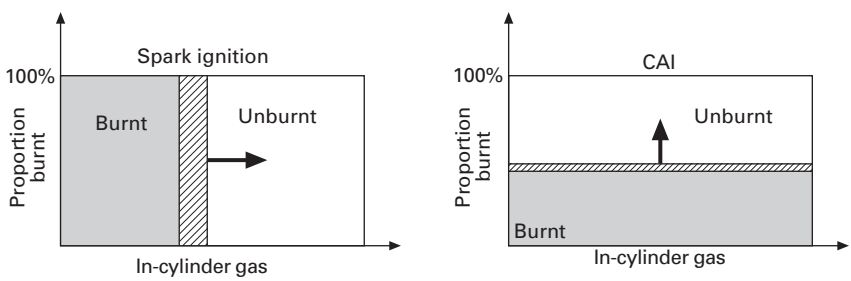

3.5 Ideal models of spark-ignition and controlled auto-ignition combustion (Wang, 2006, adapted from Onishi, 1979).

www.TechnicalBooksPDF.com

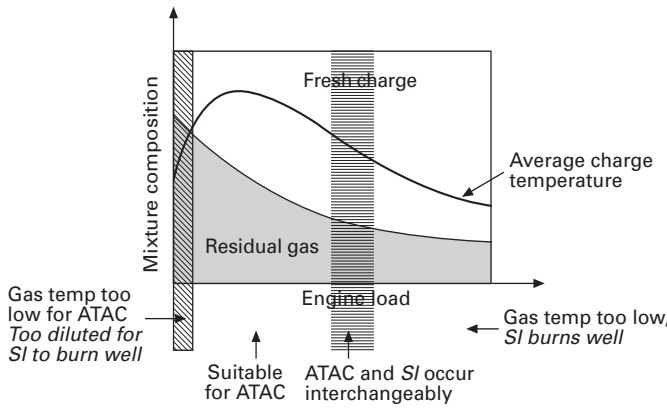

3.6 ATAC/SI combustion regions according to engine conditions (Wang, 2006, adapted from Onishi, 1979).

average charge temperature. This decreases the likelihood of auto-ignition, and after a transition in which both SI and ATAC occur interchangeably, the average charge temperature becomes too low to maintain the ATAC combustion.

To summarise this section, it has been shown that CAI combustion can be achieved in a two-stroke engine thanks to its inherent high amount of residual gases. The range of CAI operation is nevertheless limited to the part loads where the high residual gas rate results in high overall charge temperatures. We will see in the following sections that some additional devices such as, for example, transfer or exhaust port throttling allow achievement of a wider operating load range without increasing the residual gas rate and the overall charge temperature.

3.2.3 Advantages and benefits of CAI/SI

Improved combustion stability

Figure 3.7 shows a comparison between SI and CAI combustion stability at a light load operating point (about 2 bar IMEP). With SI combustion, a lot of fluctuations of the maximum in-cylinder pressure can be observed in correlation with corresponding IMEP fluctuations. This deterioration of the combustion comes from cycles with poor or incomplete combustion followed by cycles with higher IMEP.

Improved pollutant emissions and fuel efficiency

This deterioration of the combustion quality results in both high unburned hydrocarbon (HC) emissions and high fuel consumption as shown respectively

www.TechnicalBooksPDF.com

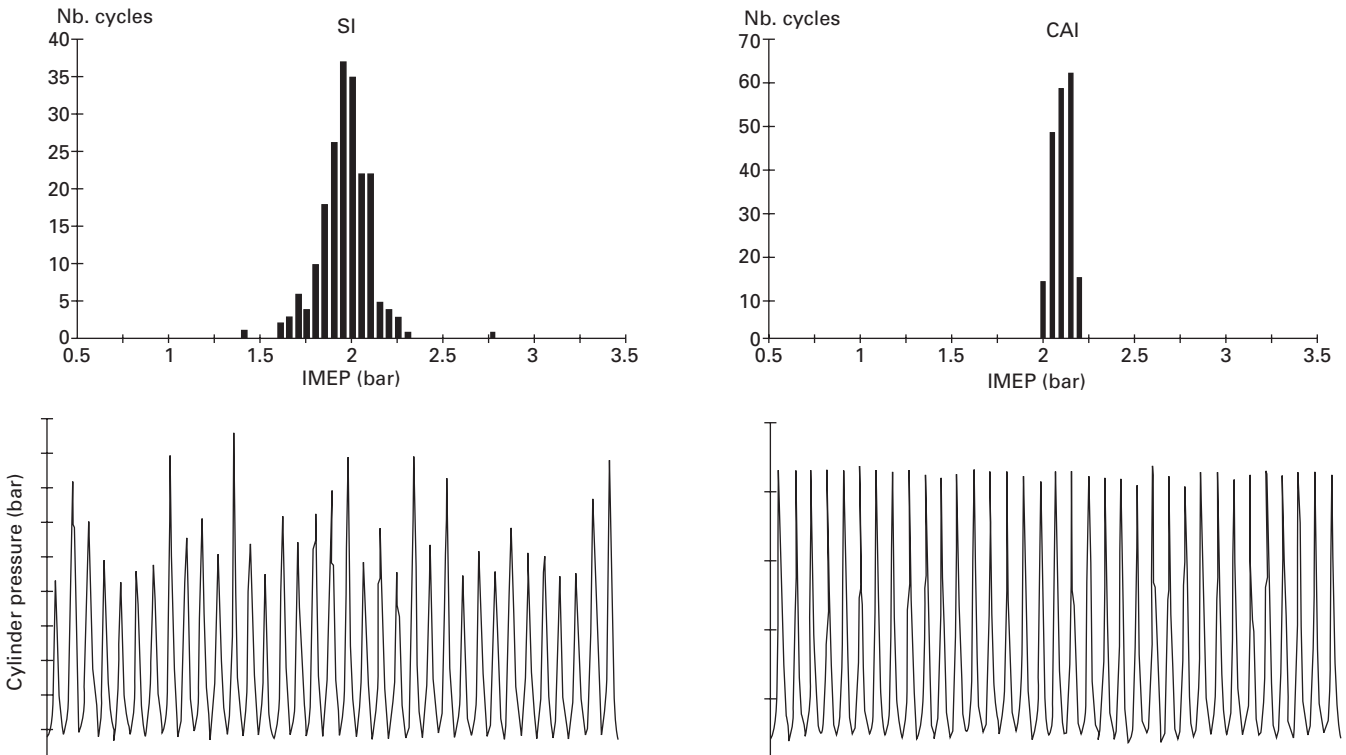

3.7 Compared in-cylinder pressure traces and IMEP distribution between SI and CAI combustion (Habert, 1993).

www.TechnicalBooksPDF.com

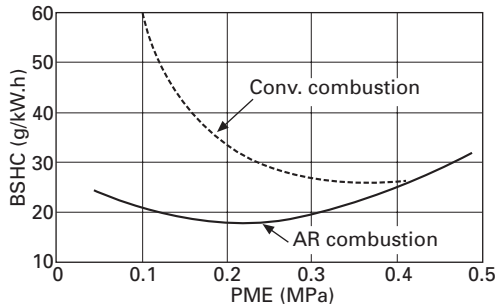

3.8 Benefits of CAI/AR combustion (obtained by the AR exhaust control valve) on 2-stroke engine brake specific HC emissions – 4000 rpm (Ishibashi, 1993).

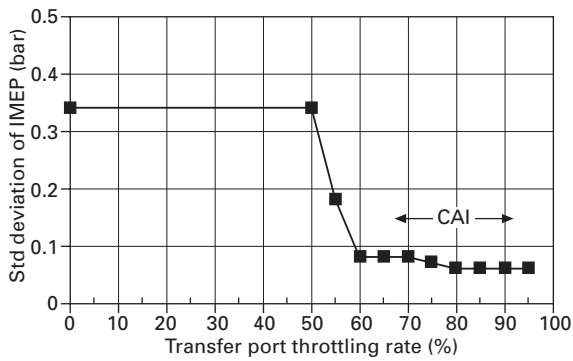

3.9 Effect of CAI (obtained by transfer port throttling) on 2-stroke engine stability – 1.2 bar BMEP @ 2000 rpm (Duret, 1996).

by Fig. 3.8 and Fig. 3.3. On the contrary, a remarkably stable cycle to cycle combustion can be achieved with CAI as shown by the in-cylinder peak pressure as well as by the IMEP distribution (Fig. 3.7). Thanks to CAI, the incomplete or poor combustion disappear and the theoretical ideal specific fuel consumption (SFC) curve of Fig. 3.3 can then be approached. For the same reason, the HC emissions can be significantly improved as shown by Fig. 3.8 (Ishibashi, 1993). In this figure, the HC emissions are reduced for engine loads below 4 bar BMEP and the reduction is maximum when the engine load goes down to 1 bar BMEP.

Similar advantages when CAI is combined with DI

In all the results presented in Figs 3.9, 3.10, 3.11 and 3.12 CAI is obtained by transfer throttling on a direct injection (DI) two-stroke engine. All the figures show that for this light load operating point (1.2 bar BMEP @ 2000

www.TechnicalBooksPDF.com

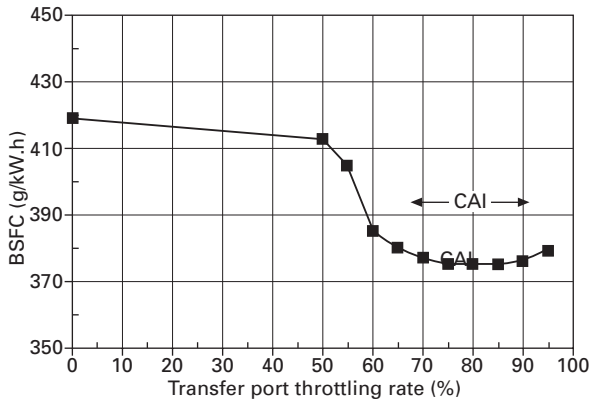

3.10 Effect of CAI (obtained by transfer port throttling) on 2-stroke engine brake specific fuel consumption – 1.2 bar BMEP @ 2000 rpm (Duret, 1996).

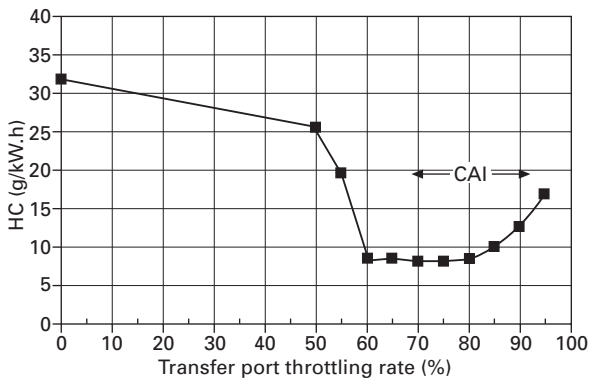

3.11 Effect of CAI (obtained by transfer port throttling) on DI 2-stroke engine brake specific HC emissions – 1.2 bar BMEP @ 2000 rpm (Duret, 1996).

rpm), the combustion becomes very stable above 60% of transfer throttling. The standard deviation of IMEP representative of the cyclic fluctuations of the combustion drops drastically to remarkably low values between 0.06 and 0.08 bar. A similar significant benefit is obtained in BSFC which is reduced from about 420 g/kWh to a minimum of 375 g/kWh. The improvement in HC emissions is even more spectacular since the already rather low level of HC obtained with direct injection (32 g/kWh) is divided by a factor of 4 for the best transfer throttling settings (between 60 and 80% throttling rate) reaching a level similar to four-stroke engine HC emissions. At this light load operating point, the NOx emissions are already remarkably low without CAI thanks to the two-stroke engine's inherent advantages of mainly the

www.TechnicalBooksPDF.com

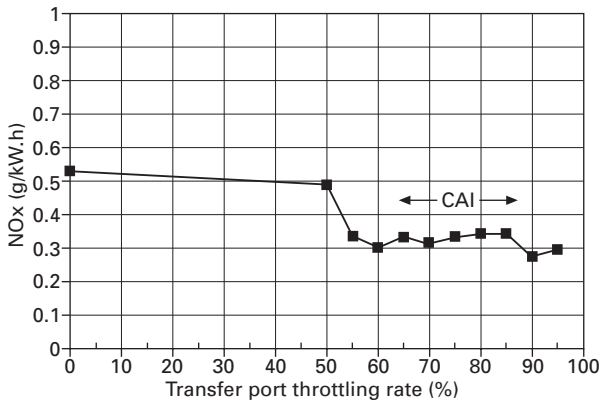

3.12 Effect of CAI (obtained by transfer port throttling) on DI 2-stroke engine brake specific NOx emissions – 1.2 bar BMEP @ 2000 rpm (Duret, 1996).

high dilution by internal EGR and the low IMEP per cycle because of a combustion frequency every cycle (Duret, 1990). Nevertheless it is interesting to remark that running in CAI doesn't increase the NOx. A tendency towards reduction is even observed. This explains why in Section 3.4.3, the potential of CAI-DI two-stroke engine for ultra low NOx and high efficiency automotive application will be discussed.

3.2.4 Drawbacks and difficulties

The light load limit of CAI range (irregular combustion and misfiring)

As shown by Fig. 3.6 there is a low load limit for the CAI combustion. When the load becomes too low, the amount of energy released per combustion cycle is too low to maintain a sufficiently high level of temperature of the internal EGR. To extend the CAI range to the lowest loads needs, therefore, to try to minimise as much as possible the mixing between the internal EGR and the fresh mixture while keeping the in-cylinder pressure at the beginning of the compression as high as possible. In this sense, the engine speed has a major effect. When the engine speed increases, the time for mixing between the fresh charge and the internal EGR decreases. This clearly explains why it is rather easy to reach very light loads CAI at medium to high engine speeds while it is much more difficult for engine speeds lower than 2000 rpm and especially at idle. Several solutions are possible to overcome (at least partly) this difficulty and will be described in the following section of this chapter. Among them, two solutions described in Section 3.3.2 are identified as the most effective as we will also see in Section 3.3.1. The transfer throttling is probably the most efficient to minimise the internal mixing and

www.TechnicalBooksPDF.com

increase the EGR stratification (Duret, 1996) and the exhaust throttling is more efficient to combine this stratification effect with an increase of the in-cylinder pressure (Ishibashi, 1993). Using these solutions, it is generally possible in the best engine configurations to reach light load auto-ignition below 2000 rpm for engine loads as low as 0.5 bar BMEP (see Fig. 3.24 in Section 3.4.3). Below such loads, it is difficult to maintain the CAI auto-ignition. Poor combustion and misfiring start to occur. It is a shame because to reach idle in CAI combustion would probably solve all the part load emissions problems of the two-stroke engines. This is the reason why a lot of researchers have worked in the direction of extending the CAI range up to idle. Nevertheless, from what is known in the scientific knowledge, idle operation in CAI has probably never been obtained until now. Even if in theory it seems feasible, it would probably require a combination of solutions such as both transfer and exhaust throttling combined with higher engine compression ratio and perhaps a more appropriate fuel formulation.

The high load limit (too strong uncontrolled combustion)

When the engine load increases in CAI operation, the combustion starts progressively earlier and earlier. Even if the engine can continue to run in auto-ignition, the heat release rate becomes very high with more than 50% of the mass fraction burnt before TDC. In these conditions, the combustion noise becomes very strong like severe knock and the NOx emissions quickly rise. There is no interest in keeping the auto-ignition mode (which is no longer 'controlled' as the CAI 'controlled auto-ignition' name would suggest!) and it is generally better to switch to the SI combustion mode. The next paragraph will show that this high load mode switch between CAI and SI can be rather easily managed in a two-stroke engine.

The management of the transition between SI and CAI combustion modes

From the previous explanations, it is clear that two types of combustion mode transition have to be distinguished, firstly the transition between irregular SI to stable CAI at light load and secondly the transition between CAI to higher load conventional SI. To simplify the engine management system, the spark ignition is generally maintained for all engine speeds and loads even if it has no effect inside the CAI range. As explained by Ishibashi, the transition between auto-ignition combustion to higher load conventional SI is easily and naturally achieved without any jump in engine torque. The main requirement is to make the transition range as short as possible to avoid the occurrence of combustion cycles with strong too early and noisy auto-ignition. To achieve this, when the load increases, the control valve (for example, the exhaust throttling or the transfer throttling valve) has to move quickly from

www.TechnicalBooksPDF.com

the throttled position to the fully open position without staying in an intermediate partially throttled position. On the other hand, the transition from CAI to the light load less regular SI combustion is more difficult. In this light load transition area, and for the same intake air delivery ratio (same intake throttle position), the engine gives more torque in auto-ignition than in spark ignition. To smooth this transition it is then necessary to use an additional countermeasure allowing delivery of more intake air in SI than in CAI. In the case of the AR motorcycle engine (with an exhaust control valve) Ishibashi used the solution of an additional air by-pass valve in the intake throttle body. This by-pass valve was maintained closed in AR combustion and open in light load SI to compensate for the drop in torque. In the case of the IAPAC-CAI automotive engine, Duret and Venturi adopted the solution of reopening the transfer throttling valve in light load SI (Duret, 1996). Obviously to definitively solve this difficulty, the best solution would be to have an engine able to run in auto-ignition up to idle!

3.3 How to control the two-stroke CAI combustion

In spark ignition mode the combustion can be rather easily directly controlled by the spark advance. In the case of CAI combustion, there are a lot of relevant control parameters with, in addition, complex interactions between some parameters. In this section we will see in the first part what are the main control parameters and in the second part what are the associated two-stroke engine devices and technologies which allow these parameters to actually be managed.

3.3.1 The relevant control parameters of the 2-stroke CAI combustion

Prior to examining in more detail the main relevant two-stroke CAI control parameters, it is important to define what has to be controlled: the combustion timing and the combustion heat release rate. A correctly controlled CAI combustion should have the best combustion timing for the highest combustion efficiency. In addition it is also necessary to rightly control the reaction speed of the combustion. Too fast combustions with high heat release rate have to be avoided because they generate high combustion noise, excessive gradient of cylinder pressure increase and high NOx emissions.

The key parameters: internal EGR and mixing/stratification between fresh charge/EGR

From the experiments done and the results achieved by several authors (Onishi, 1979; Noguchi, 1979; Duret, 1990, 1993; Lavy, 2000a), the internal EGR

www.TechnicalBooksPDF.com

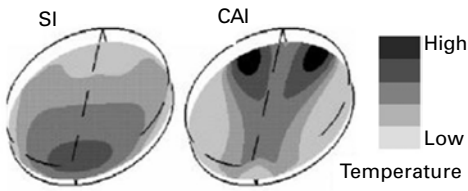

3.13 Comparison of in-cylinder temperature fields at 10 deg. CA BTDC in SI and CAI combustion (Lavy, 2000a).

can be considered as probably the major parameter for the control of the two-stroke CAI combustion. Inherently in a two-stroke engine, there is a high amount of internal EGR at part load. But if this EGR is well mixed with the fresh charge as is the case in a conventional two-stroke engine, especially at low engine speed, it has almost no effect on the combustion. What is efficient for getting CAI is to limit as much as possible the mixing of this internal EGR with the fresh mixture. In such cases, it is possible to achieve a temperature gradient within the charge for the same overall amount of in-cylinder EGR, which is to say, the same in-cylinder heat content. The overall charge is then composed of zones of higher fresh charge concentrations/lower gas temperature and zones with higher internal EGR charge concentrations/higher gas temperatures. Our understanding is that these zones or pockets of both high temperature and more reactive gases are responsible for initiating and generating the auto-ignition process. Figure 3.13 presents the in-cylinder temperature fields obtained by 3-D computation in SI and CAI modes. In the CAI case, transfer throttling is used to regulate the scavenging process in order to increase the fresh charge/residual gases stratification level, thus inducing higher local temperature as shown by the calculations. 3-D computation of a DI two-stroke engine with exhaust throttling has shown similar results (Habchi, 1993).

An indirect effect of the engine speed

The engine speed is an indirect CAI control parameter. It has an indirect effect on the mixing/stratification between the fresh charge and the EGR. As shown by Fig. 3.14, when the engine speed increases, the CAI combustion starts earlier and earlier and also becomes faster and faster. A consistent explanation for this phenomenon is to consider that the time for mixing between the internal EGR and the fresh charge is shorter and shorter when the engine speed increases. Therefore the internal stratification and the temperature gradient inside the trapped charge increase when the engine speed increases. This has the final consequence of advancing and accelerating the CAI combustion.

www.TechnicalBooksPDF.com

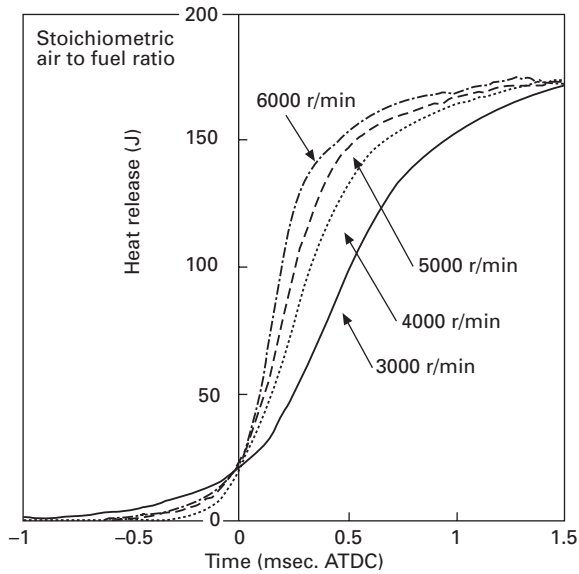

3.14 Effect of the engine speed on the heat release (in milliseconds) in CAI-AR combustion conditions (Ishibashi, 2001).

The control of in-cylinder flow velocities for smooth fresh charge introduction

In a conventional two-stroke engine at light engine load, a small amount of fresh charge is discharged into the cylinder from the crankcase in a few degrees crank angle at the beginning of the transfer ports opening. As a result, already mentioned by Onishi (Onishi, 1979), because of its high velocity, the air flowing into the cylinder tends to be dispersed and diluted in residual burned gas which is not conductive to the charge stratification required for CAI. On the contrary, when an exhaust throttling valve is used, for example, it has the indirect effect of slowing down the introduction of the fresh charge. Even if almost the same amount of fresh mixture is discharged in the cylinder, in this case the discharge happens here more slowly using all the available time of the scavenging period (on average 110 to 120 degrees crank angle from transfer ports opening to transfer ports closing). To introduce the same amount of fresh mixture in a much longer time means that the charge is introduced more smoothly at significantly lower velocities. This helps to prevent the dilution of the fresh inlet mixture in the residual gases which is favourable for getting CAI. By studying the in-cylinder and crankcase instantaneous pressure traces, it has been demonstrated experimentally that the CAI combustion is optimised when the fresh mixture introduction stops precisely at the end of the transfer ports opening (Duret, 1990; Ishibashi, 1993). According to this criterion it is possible to say that CAI is a fluid dynamically controlled combustion process (Duret,1993). The same

www.TechnicalBooksPDF.com

phenomenon is not limited to the case where CAI is obtained by exhaust throttling but can also be observed with transfer port throttling or with elongated transfer ducts.

The effect of the in-cylinder pressure

We have seen how the local charge temperatures can have a major effect on auto-ignition. In addition to that, it is also important to mention that for the same local temperature conditions, auto-ignition will occur earlier and faster with higher in-cylinder pressure and conversely the auto-ignition will be delayed and can even disappear with lower in-cylinder pressure. The easiest solution for controlling the in-cylinder pressure is to do it through the compression ratio (CR). A high compression ratio will then be favourable to extend the CAI range to the low speed low loads. Habert has shown for example, in his experiments that increasing the CR from 8 to 9 of the ATAC engine of the NiCE generator can reduce the engine speed and load of the low speed low load CAI limit by more than 500 rpm and about 0.4 bar IMEP (Habert, 1993). Nevertheless, the choice of the highest compression ratio favourable for CAI is always limited by the fact that the same engine also has to be able to run in spark ignition at full load without knock. Considering that, Ishibashi has shown an interesting approach of controlling the in-cylinder pressure at part load by its exhaust charge control valve (Ishibashi, 1993). Figure 3.15 shows the interesting results he found. These results were obtained in engine conditions where both SI and AR-CAI combustions could take place. The figure presents the gas exchange pressures (in-cylinder and crankcase pressures during scavenging), the in-cylinder pressure during combustion and the mass fraction burnt for three cases of EOR (Exhaust Opening rate = 75%, 55% and 25%). In the case (a) at EOR = 75%, the cylinder pressure at exhaust port closure (P_{EC}) is 24 kPa and the conventional SI combustion occurs. In conditions (b) at EOR = 55%, the P_{EC} is 55 kPa and AR-CAI combustion occurs. In both cases (a) and (b), the approximate beginning of the combustion designated as crank angle at 10% mass fraction burnt is almost identical. In the case (c) at EOR = 25%, P_{EC} is 90 kPa and AR-CAI combustion also takes place, but its ignition timing becomes too early and the combustion finishes before TDC. This shows that the in-cylinder pressure at exhaust port closing (resulting from the degree of opening of an exhaust control valve) is an effective parameter to control the combustion timing of the AR-CAI combustion.

A significant effect of the air/fuel ratio

The air/fuel ratio also has a direct effect on the timing of the CAI combustion as shown by Fig. 3.16. In this figure, the exhaust air/fuel ratio varies from

www.TechnicalBooksPDF.com

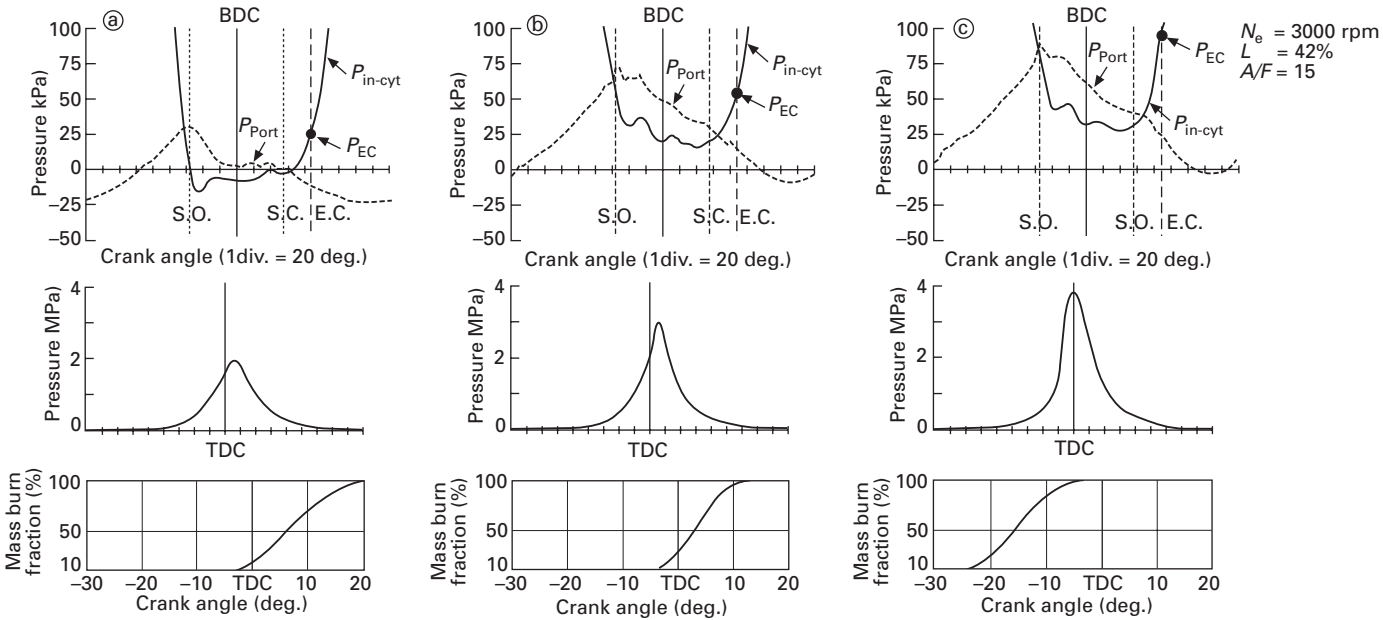

Symbol		ⓐ	ⓑ	ⓒ
Exhaust opening rate	(%)	75	55	25
Pressure, exhaust close	(kPa)	24	55	90
Combustion		Conv.	AR	AR
10% combustion	(° ATDC)	–2	–4	–24
95% combustion	(° ATDC)	18	12	–4
Specific heat ratio	(K)	1.32	1.31	1.31
Crank angle Max. pressure	(° ATDC)	14	10	–2
PMI	(MPa)	0.36	0.41	0.31

3.15 Influence of exhaust throttling and in-cylinder pressure at exhaust port closing on the CAI/AR combustion (Ishibashi, 1993).

www.TechnicalBooksPDF.com

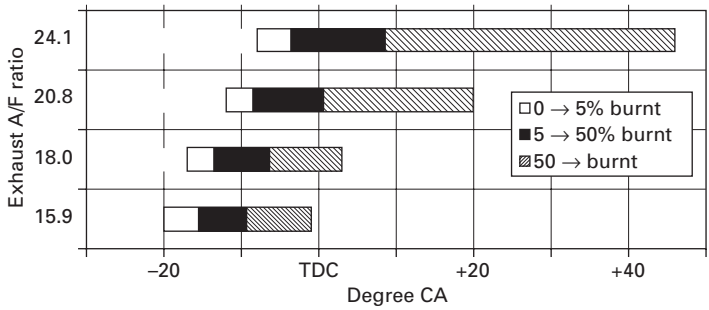

3.16 Effect of the air/fuel ratio on the CAI combustion timing and duration (Duret, 2000).

15.9 to 24.1. The figure shows that when the mixture is rather rich (in this example a direct injection two-stroke engine is used which means that due to the scavenging air losses, the measured exhaust AFR of about 16 corresponds approximately to an in-cylinder trapped AFR of about 14 i.e. close to stoichiometry), the auto-ignition starts too early and 95% of the charge burns before TDC in about 20 degrees CA. In this case the amount of air charge is minimised for a given quantity of fuel. The quantity of hot internal EGR is therefore maximised since the overall trapped mass changes very little with variation in the exhaust air/fuel ratio.

As the mixture becomes leaner, the air dilution increases which proportionally decreases the dilution by the hot internal EGR. It explains why, as shown by the figure, the start of combustion is progressively delayed and the combustion becomes smoother with a longer duration and more ideal phasing. This example clearly shows the influence of the air/fuel ratio in the control of the two-stroke CAI combustion timing and heat release.

The low sensitivity to the air-fuel mixture preparation

The CAI combustion can be obtained with numerous fuel supply systems and air-fuel mixture preparation devices. These include the following systems (listed most homogeneous to the least homogeneous):

- a carburetted homogeneous air-fuel mixture with the example of the ATAC combustion engine of the NiCE generator
- a rather homogeneous premixed air-fuel charge obtained by intake manifold fuel injection with the example of the Honda EXP-2 motorcycle AR combustion engine (Honda, 1995)
- a rather homogeneous directly injected air-fuel mixture obtained by air assisted direct fuel injection with the example of the IAPAC-CAI automotive two-stroke engine
- a rather heterogeneous air-fuel mixture obtained by liquid direct fuel injection.

www.TechnicalBooksPDF.com

In this last case, it is possible to vary the heterogeneity of the mixture by changing the fuel injection timing. Petit compared the effect of two direct fuel injection timings on the CAI combustion process: an early injection timing (200 deg CA before TDC) which produces a reasonably homogeneous mixture and a late injection timing (80 deg CA before TDC) which produces a more stratified air-fuel mixture (Petit, 1993). The speciated HC emissions analysis that he performed showed that early injection timing results in high HC emissions mainly from fuel short-circuiting and that late injection timing results in very low HC emissions with almost negligible unburned fuel components. The combustion timing and heat release rate were, however, very similar for the two injection timings. The difference observed between the two timings is therefore mainly related to the fuel short-circuiting phenomenon and not related to the combustion process itself. It was possible to conclude from this study that two-stroke CAI combustion is reasonably insensitive to the direct fuel injection timing and more generally to the air-fuel mixture preparation.

The effect of the overall temperature (intake charge, coolant)

Heating the intake charge increases the overall gas temperature and has the effect of advancing the CAI combustion timing and therefore of extending the CAI combustion range in the low load low speed region. Similarly, the CAI combustion is also sensitive to the engine liquid cooling temperature which indirectly affects the overall gas temperature. Figure 3.17 shows that, for example, from 50°C to 90°C engine coolant temperature, the CAI low load limit can be reduced by about 0.5 bar BMEP while the CAI low speed limit can be reduced by 300 rpm at low engine speed and up to more than

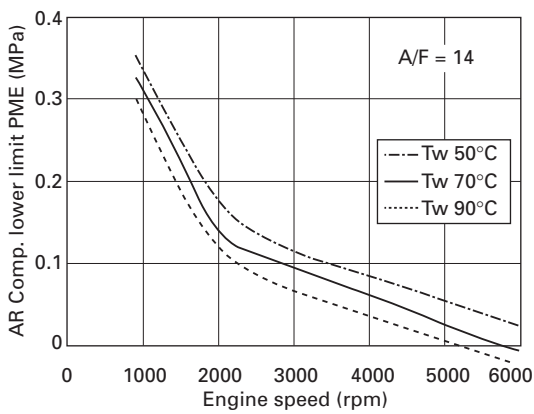

3.17 Influence of the engine liquid cooling temperature on the CAI/AR combustion lower load limit (Ishibashi, 1993).

www.TechnicalBooksPDF.com

1000 rpm at medium to high engine speed. Another thermal possibility of extending the CAI low speed low load limit is to use an insulated ceramics engine (Iida, 1994).

The sensitivity to the fuel formulation

Several researchers have studied the effect of the fuel formulation on two-stroke CAI combustion. Amongst them, Iida was one of the first to show that running an ATAC-CAI two-stroke engine with methanol allows significant widening of the auto-ignition range (Iida, 1994). More recently, Jeuland tried to find some correlations between the octane number of several fuels (research octane number RON and motor octane number MON) and their effect on the auto-ignition range. Surprisingly he found almost no correlation between either the RON or MON and the CAI range (Jeuland, 2003 and Lavy, 2000a). These results were consistent with the Iida result showing that a high octane fuel such as methanol could help to get CAI combustion on a wide operating range. We can then conclude that the fuel formulation can be a very effective control parameter of CAI combustion. Nevertheless, a lot of further research work would be necessary to fully understand the effects of fuel formulation before being able to use this control parameter for practical engine operation.

3.3.2 The associated technologies and control devices for the control of two-stroke CAI combustion

Among the possible control parameters described in the previous section, the in-cylinder gas temperature effect obtained by stratifying hot internal EGR (the EGR and fresh charge mixture/stratification being controlled by the in-cylinder flow velocities) and the in-cylinder pressure are the most relevant for practical application mainly because of their immediate response time in transient operation (which, for example, is not the case of intake air heating). Most of the technologies that have been developed and applied to obtain CAI combustion on two-stroke engines were based on the control of these two internal temperature and pressure effects. For this purpose, three main technologies and associated control devices have been demonstrated to be particularly effective and efficient: the elongated transfer duct, exhaust throttling and transfer throttling.

Elongated transfer duct

The elongated transfer duct was the first solution discovered by Onishi and his colleagues at NiCE . Figure 3.18 shows a cross-section of the 98 cc ATAC two-stroke engine of the NiCE generator commercialised in Japan.

www.TechnicalBooksPDF.com

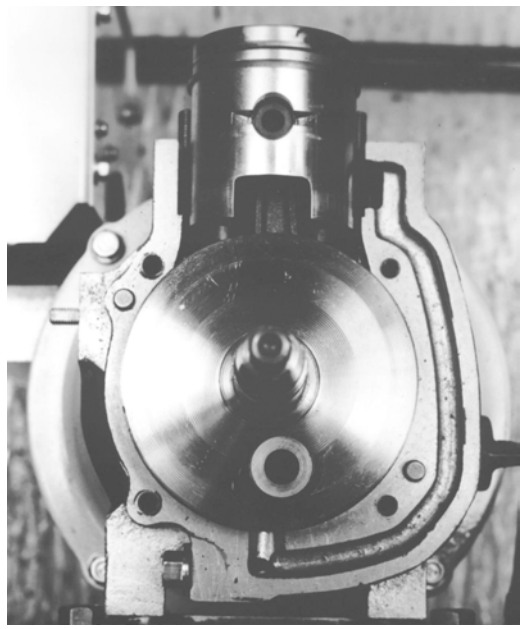

3.18 Cross-section of the 2-stroke NiCE-10GC engine with elongated transfer duct for ATAC combustion (source IFP).

A very long transfer duct can be seen starting from the bottom of the crankcase and reaching the transfer port after a duct length probably around five times longer than in a conventional two-stroke engine. This technology is very efficient to reduce the velocity of the fresh charge introduction. Its smooth delivery minimises internal mixing and then allows ATAC combustion. The main drawback of this solution is that the transfer duct length is not variable. With this technology, the ATAC-NiCE engine presented very good ATAC characteristics in terms of operating range and emissions performance. Nevertheless it suffered from very poor engine performance in terms of torque and power, the elongated transfer duct not being adapted for full load SI operation.

Transfer duct throttling

Even if Onishi didn't disclose any experimental development and results with transfer duct throttling, he applied for several patents on this subject (Onishi, 1984). The interest of the transfer throttling solution is its flexibility and fast response time. It allows the same engine to be able to run in part load CAI (with the transfer ducts throttled) and also in high load SI. Several technological solutions have been proposed for loop scavenged two-stroke engines. Figure 3.19 shows one example proposed by an Onishi patent. The

www.TechnicalBooksPDF.com

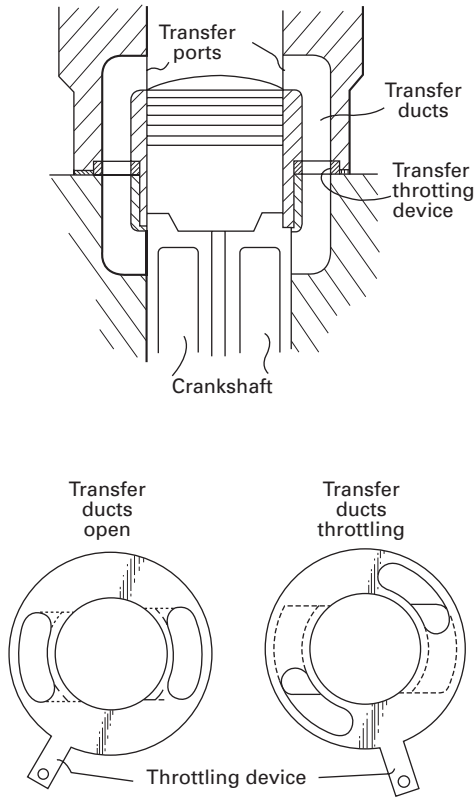

3.19 Principle of transfer port throttling arrangement in a loop scavenged 2-stroke engine (adapted from Onishi, 1984).

main drawback of all the solutions of transfer throttling in a loop scavenged engine is the space necessary around the cylinder. This solution is therefore possibly applicable in a single-cylinder engine where the space is less limited but it is not viable for a multi-cylinder engine. It would require a long distance between cylinder to cylinder axis with the consequence of a very long cylinder block. This is not compatible with the design constraints regarding the control of the cylinder block distortion as well as regarding the engine implementation in a vehicle. On the other hand, in the case of cross scavenged engine, the so called 'cross scavenging' is obtained by a special engine design. The specificity of this design is to use a deflector piston and to have all the transfer ports in front of the deflector. In such cases all the transfer ducts are located on only one side of the cylinder block. Their section can therefore be easily controlled by a rather simple throttling device (Duret, 1991 and 1992b). Therefore the cross scavenged configuration is particularly well adapted to be combined with transfer duct throttling, especially in a multi-cylinder engine. These two technologies have been chosen on the

www.TechnicalBooksPDF.com

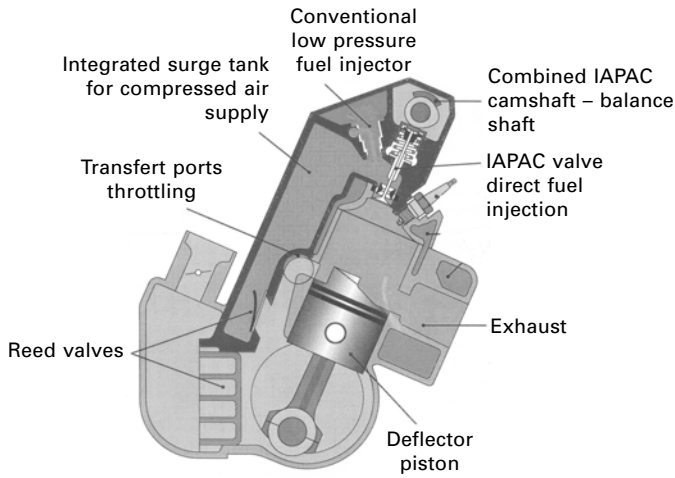

3.20 Transfer ports throttling adaptation in a cross scavenged 3-cylinder 2-stroke engine developed for automotive application (Duret, 1996).

CAI-IAPAC automotive 3-cylinder two-stroke engine represented in Fig. 3.20. The results presented in the following section will show how this combination was particularly effective in achieving a wide range of low emissions high efficiency CAI operation.

Exhaust port throttling

As with transfer throttling, Onishi applied for patents on exhaust throttling as a solution to get the auto-ignition as shown by Fig. 3.21. Tsuchiya was probably the first to describe a practical and efficient application on a two-stroke motorcycle engine (Tsuchiya, 1980). The results he presented allow the assumption that his engine was running in auto-ignition when the exhaust was throttled even if he didn't explicitly mention auto-ignition. The same idea was then used in the IFP direct injection loop scavenged engine (Duret, 1990) and later by Ishibashi who developed with his colleague Asai a special exhaust throttling valve allowing simultaneous varying of the exhaust port timing and the exhaust port opening area. This special exhaust throttling valve named ARC (for Activated Radicals Combustion) exhaust control valve is shown in Fig. 3.22. It is used to control both the internal EGR stratification and the in-cylinder pressure at exhaust port closing.

Combination of transfer and exhaust throttling

Such a combination is probably the most effective to obtain a wide range of CAI operation. A demonstration has been done more recently on a 2000 cc

www.TechnicalBooksPDF.com

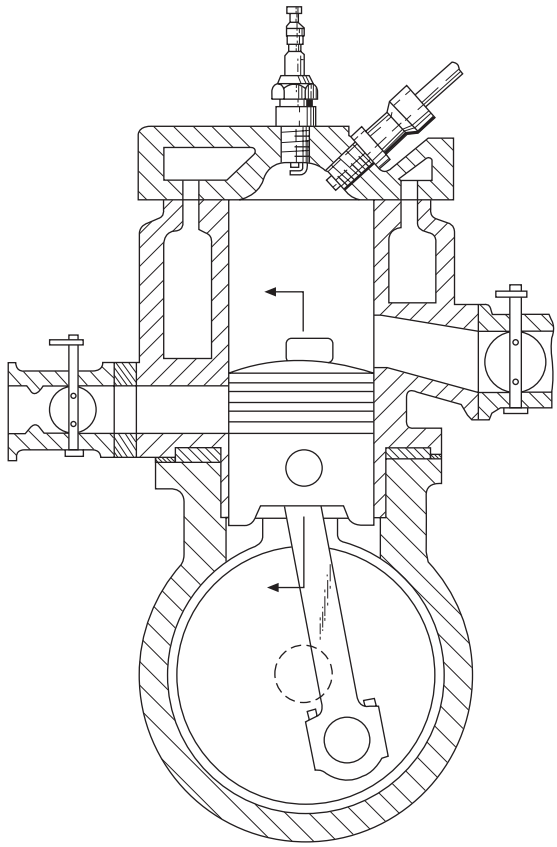

3.21 Example of exhaust throttling arrangement (Onishi, 1984).

DI two-stroke engine combining transfer throttling with a variable exhaust control valve and designed for automotive application (Duret, 2000). CAI was obtained at a remarkably low engine speed and load. Nevertheless, the engine design and its control were considered too complex to justify the additional benefits in terms of emissions and fuel economy.

3.4 The potential application of the two-stroke CAI combustion

As shown by Fig. 3.1, three types of application of CAI two-stroke engines have mainly been investigated and some of them industrially produced.

3.4.1 Small generators

At the end of the 1970s, Onishi and his colleagues of the NiCE company were the first to design and develop a two-stroke engine running in ATAC-

www.TechnicalBooksPDF.com

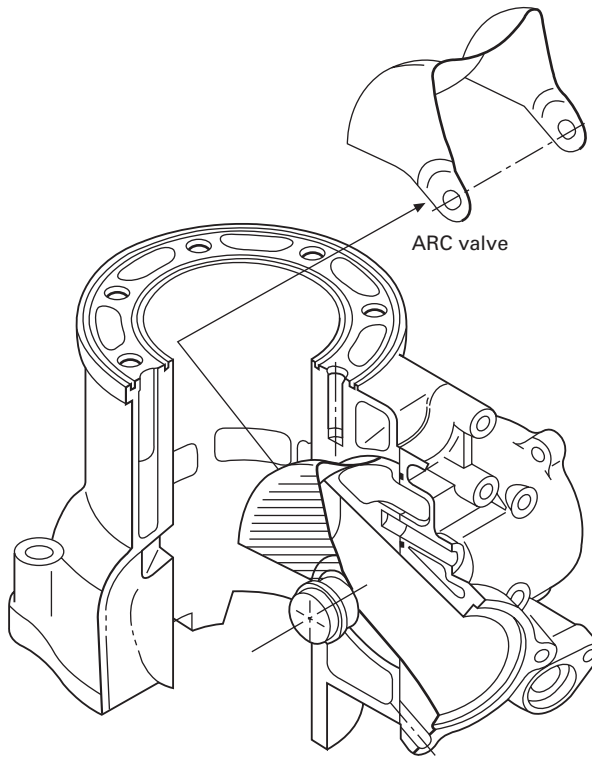

3.22 Example of exhaust valve controlling the effective opening area of the port (Asai, 1995).

CAI combustion that had been industrially produced (Onishi, 1979). This engine was a 98 cc forced air-cooled single-cylinder two-stroke engine. It was used in a generator named NiCE-10GC that was commercialised in Japan. The technology chosen on this engine to get the ATAC combustion was the elongated transfer duct as shown in Fig. 3.18. This choice limited its rated power to a moderate level of 2.2 horsepower at 3600 rpm. This was nevertheless considered sufficient for a small portable generator, since this ATAC two-stroke engine replaced a 144 cc four-stroke of nearly the same power output.

3.4.2 Two-wheeler engines incl. high performance motorcycles

At the beginning of the 1990s, Ishibashi and his colleagues from Honda developed a two-wheeler application of what they called the 'AR combustion'. Ishibashi started his research work on a 246 cc engine. After successful preliminary results that he published in 1993, Honda demonstrated the interest

www.TechnicalBooksPDF.com

and the practicability of the AR combustion for industrial application during the 1995 Grenada-Dakar Rally (Honda, 1995). Honda engaged two prototype motorcycles named EXP-2 (for experimental two-stroke engine) which were equipped with an AR single-cylinder two-stroke engine of 400 cc. It was the first time after 14 years that motorcycles with two-stroke engines participated in the Paris–Dakar Rally. These two EXP-2 motorcycles competed with motorcycles equipped with higher power and higher displacement (generally 700 cc) four-stroke engines giving a motorcycle maximum speed of 180 km/h instead of 160 km/h for the EXP-2.

Nevertheless the EXP-2 motorcycles demonstrated very good overall performance, especially during the sections of the rally where motorcycle lightweight, driveability and high fuel economy were required. One of these two motorcycles even finished in fifth place with a semi-professional driver. This was the first official demonstration of the potential of AR combustion. After that, pushed by Ishibashi progress in the control of the AR combustion, Honda introduced in production the first AR combustion 250 cc motorcycle in 1997 in Japan. It was equipped with the AR Combustion Exhaust Control Valve as described before and shown in Fig. 3.22. This was followed by the first AR combustion two-wheeler produced for the European market, the Honda Pantheon AR 125 scooter sold in France and the AR 125 and 150 cc sold in Italy from 1999. These less sophisticated engines were equipped with an exhaust throttling butterfly valve to get the AR combustion. Both the AR 250 motorcycle and the AR Pantheon scooter demonstrated very good emissions results meeting the current legislation in Japan and in Europe. Nevertheless, the production stopped in 2001 for the motorcycle and in 2003 for the scooter mainly because their engines used a carburettor, a technology with little future given the more and more stringent emissions standards.

This explains why more recent Ishibashi work has been focused on high performance motorcycle two-stroke engines combining both AR combustion and an innovative air assisted direct fuel injection technology named PDI (which stands for Pneumatic Direct Injection) (Ishibashi 2000, 2001 and 2005). The choice to focus on high performance engines is to target an ultra low emission engine that can achieve power output that cannot be reached by equivalent four-stroke engines. With this downsizing strategy, a smaller displacement PDI-AR two-stroke engine can achieve significantly better fuel economy than a four-stroke engine of similar performance. This strategy is clearly illustrated in Fig. 3.23 that compares the fuel economy of a 250 cc PDI-AR two-stroke (20 kW @ 6500–7000 rpm), to a 385 cc four-stroke named ‘Original’ in the figure with the same power output (20 kW @ 7500–8000 rpm) and a 250 cc four-stroke (about 13 kW @ 7000 rpm). The figure shows 68% improvement in fuel economy in favour of the PDI-AR two-stroke compared to the larger displacement ‘Original’ four-stroke of same power output. However, when the same displacement is used for the four-

www.TechnicalBooksPDF.com

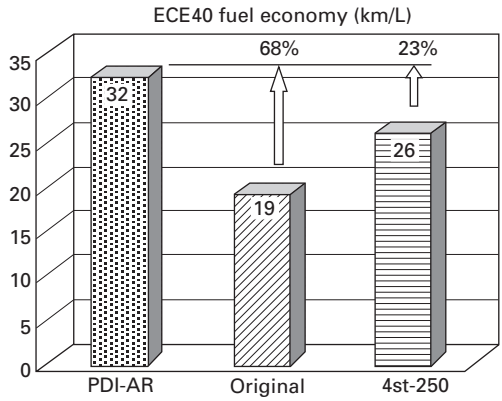

3.23 Improved fuel economy with 2-stroke PDI-AR 250 cc engine compared to 4-stroke original and 4-stroke 250 cc scooter engines (Ishibashi, 2005).

Table 3.1 Main characteristics of the CAI-IAPAC automotive two-stroke concept engine

Displacement	1230 cc
Bore	85.7 mm
Stroke	71.1 mm
Connecting rod length	108 mm
Geometric compression ratio	9.5
Scavenging type	Cross scavenging
CAI control system	Transfer throttling
Direct fuel injection system	IAPAC air assisted

stroke, the two-stroke fuel economy advantage is reduced to only 23% but the two vehicles are not comparable in terms of power output (35% less for the four-stroke).

3.4.3 Automotive engines: the first demonstration of the CAI ultra low NOx potential for passenger car applications

For an automotive application the two-stroke engine has to be multi-cylinder, which means that to get the CAI combustion the exhaust throttling technology can preferably be used. Transfer throttling technology can also be used at the condition of choosing a cross scavenged two-stroke engine design. This was the choice made by IFP which was involved in the early 1990s in the development of a CAI–IAPAC direct injected two-stroke concept engine for automotive applications. Table 3.1 presents the main characteristics of this engine already presented in a simplified cross section in Fig. 3.20.

www.TechnicalBooksPDF.com

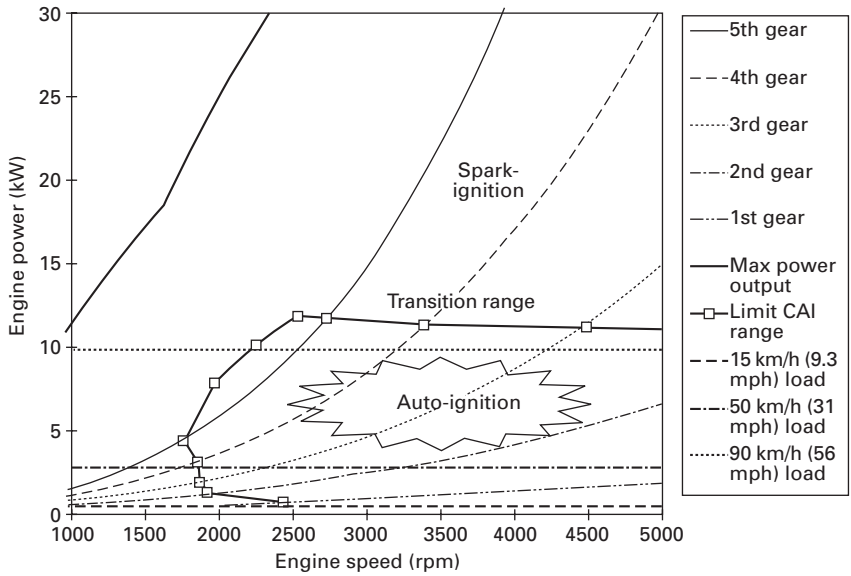

3.24 CAI operating range (spark ignition cut off) of the IAPAC 2-stroke automotive concept engine (Duret, 1996).

Thanks to the effectiveness of the transfer throttling system (especially when combined with the IAPAC air assisted direct fuel injection), this engine offered a remarkably wide CAI operating range as shown by Fig. 3.24. This CAI range has been precisely measured with the vehicle in the chassis dynamometer. The figure shows as a function of the engine speed the maximum power output curve, the road load curves for the five vehicle gears, the limit of the auto-ignition (CAI range) and finally the power required to drive the vehicle at three stabilised speeds (15, 50 and 90 km/h). For each gear ratio, the vehicle was first driven up to be inside the CAI range. The ignition was then cut off, and the vehicle speed was progressively decreased and similarly increased in order to find both the lower and upper vehicle speeds possible without spark ignition. Figure 3.24 shows for example that the vehicle was able to run without spark from about 15 km/h in first gear and in fourth gear from about 50 km/h up to 95 km/h.

Thanks to its rather wide CAI range this engine was able to really take all the benefits of the CAI combustion process especially in terms of pollutant emissions and fuel economy. It was able in 1996 to meet the Euro 2 emissions legislation with a safety margin of 32% in total HC+NOx and with extremely low CO value (70 times lower than the legislation). It also gave more than 20% improvement in both fuel economy and low engine speed maximum torque compared to the equivalent 1360 cc four-stroke engine of same power output. These results were obtained without exhaust after-treatment device

www.TechnicalBooksPDF.com

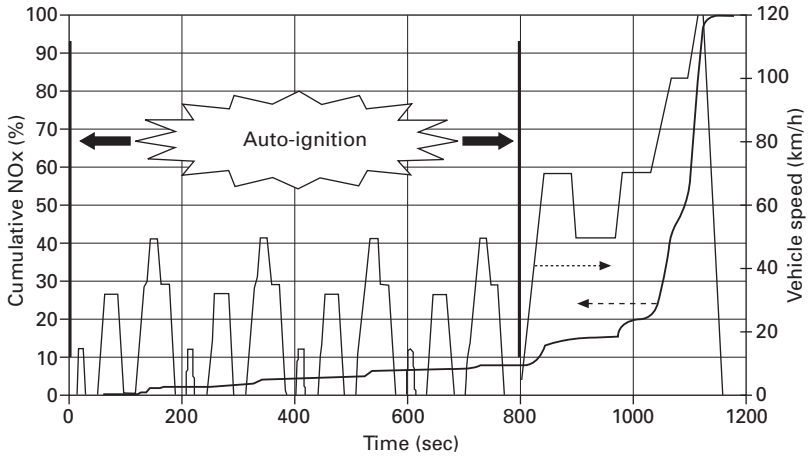

3.25 Cumulative NOx emissions on the MVEG cycle – IAPAC/CAI automotive 2-stroke concept engine (Duret, 1996).

other than oxidation catalyst for the control of the CO (0.03 g/km) and HC (0.07 g/km) emissions. Concerning NOx emissions, it is interesting to see in Fig. 3.25 that only less than 10% of the total NOx (0.27 g/km) were emitted during the first 800 seconds corresponding to the urban section of the driving cycle. During this extremely low NOx section (average NOx emissions below 0.07 g/km without after-treatment!) the engine was always running in CAI combustion mode (except at idle). This really shows the potential of the CAI combustion for ultra low NOx emissions.

3.5 Future trends

3.5.1 The future of two-stroke engines: what role for CAI?

The impressive and very encouraging results presented in Fig. 3.23 show that with the two-stroke downsizing strategy combining CAI combustion and direct fuel injection proposed by Ishibashi, it would be possible to produce probably the cleanest and most efficient internal combustion engines for motorcycles even compared to the best four-stroke counterpart. Nevertheless, this strategy has to face the pressure of the lobby of the four-stroke engine manufacturers. Even if it is therefore difficult to anticipate what will be the future of the two-stroke engine, we can assume that if there will be a future it will most probably combine new fuel introduction technologies (direct injection) with auto-ignition combustion process such as CAI, AR, ATAC, etc.

For the automotive application the situation is even more complex. After

www.TechnicalBooksPDF.com

a worldwide effervescence in the development of two-stroke engines for automotive at the end of the 1980s and beginning of the 1990s, the interest of the car manufacturers decreased rapidly. The main reason was that they finally consider as too risky to move to the two-stroke technology (with, for example, dry sump crankcase, roller bearings, etc.) in which their know-how and expertise were rather limited. What could nevertheless happen in the future is that with the progressive introduction of fully flexible technologies (such as variable valve actuation and multiple direct fuel injections) it will probably be possible to run the future automotive four-stroke engine in the two-stroke cycle frequency mode during a limited range of speed and load, especially if it presents some advantages in terms of fuel economy and emissions. The example of the recent results shown in Fig. 3.23 allows us to be reasonably optimistic. We could hope that in the future there will, perhaps, exist flexible multi-stroke automotive engines combining a four-stroke design especially for medium to high load SI operation with the possibility to run in CAI two-stroke mode in some areas of the light load range especially for its advantages of high fuel economy and low CO_2 emissions.

3.5.2 From two-stroke to four-stroke CAI combustion: how to transfer the two-stroke CAI knowledge to the development of four-stroke automotive CAI engines?

The previous CAI two-stroke automotive example achieving ultra low NOx emissions without after-treatment opens the idea of trying to transfer this CAI technology to the automotive four-stroke engine. This was the main purpose of the European funded precursor project '4-SPACE' (Lavy, 2000b and 2001) in which the understanding of the two-stroke internal conditions to get auto-ignition was studied in detail both by experiments and by simulation. Based on the results of this initial step of work it has been possible to reproduce firstly by simulation and then by experiments the internal conditions existing in a CAI two-stroke engine. This work was at the origin of a new step in the four-stroke auto-ignition without requiring intake air heating or increased compression ratio.

During the 1990s all the research work done on gasoline DI two-stroke engines finally led to the introduction of this direct injection technology in the first production automotive DI four-stroke engines.

Similarly we can conclude that at least a great success and great merit of all the fascinating and innovative two-stroke CAI research and development work is that it has opened the scope for applying this combustion process to the four-stroke automotive engine as we will see in the next chapter of this book.

www.TechnicalBooksPDF.com

3.6 Sources of further information and advice

In addition to the relevant references listed in Section 3.7, the following key books are recommended to consult for those interested by the two-stroke engine combustion:

- *Two-Stroke Cycle Spark-Ignition Engines*, Progress in Technology Series N°26 (PT-26), published in 1982 by the Society of Automotive Engineers. This book includes a selection of two-stroke engine papers through 1980. It covers well the two major problems of the two-stroke engine (fuel short-circuiting and poor combustion or misfiring at part load) and discusses several solutions. It includes in particular the Onishi (1979) and the Tsuchiya (1980) reference papers for CAI.
- *Advances in Two-Stroke Cycle Engine Technology*, PT-33, edited by Gordon P. Blair, published in 1989 by the Society of Automotive Engineers. This book includes a selection of two-stroke engine papers from 1981 to 1988. It covers a period with a lot of worldwide research work focused on the development of clean and efficient two-stroke engines, especially direct injected two-stroke engines. It includes in particular the Tsuchiya (1983) reference paper.
- *The Basic Design of Two-Stroke Engines*, by Gordon P. Blair, published in 1990 by the Society of Automotive Engineers.
  This is a reference book for the basics of two-stroke engines especially regarding the design characteristics and the typical two-stroke scavenging process.
- *A New Generation of Two-Stroke Engines for the Future*?, edited by Pierre Duret (pierre.duret@ifp.fr), Proceedings of the IFP International Seminar, 1993, Editions Technip, France.
  This book includes the papers of an IFP International Seminar specially focused on new generation two-stroke engines, which means mainly the controlled auto-ignition and the direct injection two-stroke engines. It includes, in particular, the Ishibashi (1993) and the Duret (1993) reference papers on CAI as well as the Habchi (1993) and the Petit (1993) papers.
- *The Two-Stroke Cycle Engine – Its Development, Operation and Design*, by John B. Heywood and Eran Sher, Combustion: An International Series, published in 1999 by the Society of Automotive Engineers.
  This book covers all significant progress made done during the 1980s and 1990s in terms of emissions reduction and fuel efficiency improvements for the two-stroke engine. It includes several sections dealing with the new combustion strategies such as direct injection, auto-ignition and combined CAI and DI.
- *A New Generation of Engine Combustion Processes for the Future?*, edited by Pierre Duret, Proceedings of the IFP International Congress, 2001, Editions Technip, France. This book includes the papers of an IFP

www.TechnicalBooksPDF.com

International Congress fully dedicated to new engine combustion processes like gasoline CAI and diesel HCCI. It includes, in particular, the Ishibashi (2001) and Lavy (2001) reference papers.

3.7 References

Asai M, Kurosaki T and Okada K (1995), 'Analysis on Fuel Economy Improvement and Exhaust Emission Reduction in a Two-Stroke Engine by Using an Exhaust Valve', Milwaukee, SAE 951764.

Duret P (1991), 'Moteur à deux temps multicylindre à injection pneumatique et à restriction de débit dans ses conduits de transfert', French Patent no. 2 663 081.

Duret P (1992a), 'The Key Points for the Development of Automotive Two-Stroke Engine', London, Fisita paper 925021, IME C 389/278.

Duret P (1992b), 'Two-Stroke Engine with Pneumatic Fuel Injection and Flow Restriction in at least one transfer passage way', US Patent no. 5090363.

Duret P and Moreau JF (1990), 'Reduction of Pollutant Emissions of the IAPAC Two-Stroke Engine with Compressed Air Assisted Fuel Injection', Detroit, SAE 900801.

Duret P and Venturi S (1996), 'Automotive Calibration of the IAPAC Fluid Dynamically Controlled Two-Stroke Combustion Process', Detroit, SAE 960363.

Duret P, Ecomard A and Audinet M (1988), 'A New Two-Stroke Engine with Compressed Air Assisted Fuel Injection for High Efficiency Low Emissions Applications', Detroit, SAE 880176.

Duret P, Venturi S and Carey C (1993), 'The IAPAC Fluid Dynamically Controlled Automotive Two-Stroke Combustion Process', in Duret P, *A New Generation of Two-Stroke Engines for the Future?*, IFP International Seminar, Rueil-Malmaison, Editions Technip.

Duret P, Dabadie JC, Lavy J, Allen J, Blundell D, Oscarsson J, Emanuelsson G, Perotti M, Kenny R and Cunningham G (2000), 'The Air Assisted Direct Injection ELEVATE Automotive Engine Combustion System', Paris, SAE 2000-01-1899.

Habchi C, Baritaud T, Monnier G and Keribin P (1993), '3D Modelling of Direct Injecteed Two-Stroke Engine', in Duret P, *A New Generation of Two-Stroke Engines for the Future?*, IFP International Seminar, Rueil-Malmaison, Editions Technip.

Habert P. (1993), 'Experimental Analysis of the ATAC Operating Characteristics of the NiCE 98 cc 2-Stroke Engine', Study Report (in French), IFP.

Honda (1995), 'Projet EXP-2 Cycle 2 Temps Experimental', Press release Grenada-Dakar Rally, February.

Iida N (1994), 'Combustion Analysis of Methanol-Fueled Active Thermo-Atmosphere Combustion (ATAC) Engine Using a Spectroscopic Observation', Detroit, SAE 940684.

Ishibashi Y (2000), 'Basic Understanding of Activated Radical Combustion and its Two-Stroke Engine Application and Benefits', Paris, SAE 2000-01-1836.

Ishibashi Y. (2005), 'Experimental Studies on the Auto-Ignition Combustion for the Petrol Engines', SAE HCCI Symposium, Lund, Sweden, September 2005.

Ishibashi Y and Asai M (1996), 'Improving the Exhaust Emissions of Two-Stroke Engine by Applying the Activated Radical Combustion', Detroit, SAE 960742.

Ishibashi Y and Tsushima Y (1993), 'A Trial for Stabilizing Combustion in Two-Stroke Engines at Part Throttle Operation', in Duret P, *A New Generation of Two-Stroke Engines for the Future?*, IFP International Seminar, Rueil-Malmaison, Editions Technip.

Ishibashi Y, Nishida K and Asai M (2001), 'Activated Radical Combustion in High Speed

www.TechnicalBooksPDF.com

High Power Pneumatic Direct Injection Two Stroke Engine', in Duret P, *A New Generation of Engine Combustion Processes for the Future?*, IFP International Seminar, Rueil-Malmaison, France, Editions Technip.

Jeuland N, Montagne X and Duret P (2003), 'Engine and Fuel Related Issues of Gasoline CAI (Controlled Auto-Ignition) Combustion', Yokohama (Japan), SAE 2003-01-1856.

Lavy J, Angelberger C, Guibert P and Mokhtari S (2000a), 'Towards a Better Understanding of Controlled Auto-Ignition (CAI™) Combustion Process from 2-Stroke Engine Results Analyses', Pisa (Italy), SAE 2000-01-1859.

Lavy J, Dabadie JC, Angelberger C, Duret P, Juretzka A, Schäflein J, Ma T, Lendresse, Satre A, Schulz C, Krämer H, Zhao H and Damiano L (2000b), 'Innovative Ultra-low NOx Controlled Auto-Ignition Combustion Process for Gasoline Engines: the 4-SPACE Project', SAE 2000-01-1837.

Lavy J, Dabadie JC, Duret P, Angelberger C, Le Coz JF and Cherel J (2001), 'Controlled Auto-Ignition (CAI): A New Highly Efficient and Near Zero NOx Emissions Combustion Process for Gasoline Engine Application', in Duret P, *A New Generation of Engine Combustion Processes for the Future?*, IFP International Seminar, Rueil-Malmaison, France, Editions Technip.

Noguchi M, Tanaka Y, Tanaka T and Takeuchi Y (1979), 'A Study on Gasoline Engine Combustion by Observation of Intermediate Reactive Products during Combustion', Detroit, SAE 790840.

Onishi S and Souk Hong Jo (1984), '2-Stroke Internal Combustion Engine and an Ignition-Combustion Method of an Internal Combustion Engine', US Patent 4 445 468.

Onishi S, Souk Hong Jo, Shoda K, Pan Do Jo and Kato S (1979), 'Active Thermo-Atmosphere Combustion (ATAC) – A New Combustion Process for Internal Combustion Engines', Detroit, SAE 790501.

Petit A, Lavy J, Monnier G and Montagne X (1993), 'Speciated Hydrocarbon Analysis: A Helpful Tool for Two-Stroke Engine Development', in Duret P, *A New Generation of Two-Stroke Engines for the Future?*, IFP International Seminar, Rueil-Malmaison, Editions Technip.

Souk Hong Jo, Pan Do Jo, Gomi T, Onishi S (1973), 'Development of a Low-Emission and High Performance 2-Stroke Gasoline Engine (NICE)', Detroit, SAE 730463.

Tsuchiya K, Hirano S, Okamura M, and Gotoh T (1980), 'Emission Control of Two-Stroke Motorcycle Engines by the Butterfly Exhaust Valve', Detroit, SAE 800973.

Tsuchiya K, Nagai, Y and Gotoh T (1983), 'A Study of Irregular Combustion in 2-Stroke Cycle Gasoline Engines', Detroit, SAE 830091.

Wang D. (2006), 'Overview – New Combustion Systems', in the Courses Proceedings of the 'Advanced Engine Combustion' ECO-Engines Summer School, IFP School, Rueil-Malmaison, France, July.

www.TechnicalBooksPDF.com

4

Four-stroke gasoline HCCI engines with thermal management

J YANG, USA

4.1 Introduction

4.1.1 Autoignition in 4-stroke HCCI engines

Combustion in HCCI engines is characterized by autoignition of a homogeneous mixture when reaching autoignition temperature. Raising mixture temperature to autoignition temperature in a 4-stroke HCCI engine is more difficult than in a 2-stroke HCCI engine. This is because thermal level in a 4-stroke engine is usually lower than that of a 2-stroke engine. A 2-stroke engine generates more combustion heat compared to 4-stroke engines because of its doubled firing rate. Residual gas fraction in a 2-stroke engine is larger than that in a conventional 4-stroke engine owing to the less efficient gas exchange process. The burned gases in a 2-stroke engine mix quickly with fresh charge, and then the mixture is immediately compressed. Thus the combustion-generated active radicals in the residuals in a 2-stroke engine may affect the fresh charge and promote autoignition. In contrast, active radicals in the residuals in a 4-stroke engine are more likely to be terminated during a long time period of expansion, exhaust, intake and the early portion of compression strokes. Therefore, to develop a 4-stroke HCCI engine, providing adequate thermal energy to the mixture to achieve autoignition temperature is a key task.

4.1.2 Available thermal energy sources in an engine

Raising mixture temperature to autoignition temperature requires thermal energy. Available thermal energy sources in an engine include the compression heat, thermal energy in the retained and recycled burned gases, thermal energy in the exhaust gases and coolant, thermal energy in the walls of combustion chamber and intake ports, and combustion heat of pilot fuel that is burned prior to the compression stroke if direct fuel injection is employed.

Compression heat comes from energy transfer from mechanical energy of

www.TechnicalBooksPDF.com

piston movement to thermal energy in in-cylinder gases. Compression heat is utilized in all of the HCCI engines to cause autoignition because piston engines rely on cyclic variations of the combustion chamber volume to transfer fuel chemical energy to mechanical energy. Heat release in a piston engine always occurs at high cylinder pressure. Compression heat increases with engine compression ratio. However, if an HCCI engine adopts HCCI-SI dual mode approach, effective compression ratio of the engine during SI mode operation is limited to about 10:1 to avoid engine knock.

Thermal energy in the burned gases can be utilized to increase mixture temperature by mixing a portion of the burned gas with fresh charge. In all of the piston engines, there is always a portion of the burned gases staying in the cylinder as residuals due to inefficiency of gas exchange. Residual gas fraction can be increased using unconventional valve timings, such as negative valve overlap. More burned gases can be retained in the cylinder using internal or external exhaust gas recirculation (EGR). Internal EGR relies on valve timing strategies to suck a portion of the exhaust gases back into the cylinder. External EGR requires a recirculation pipe for a portion of the burned gases to flow from the exhaust port to the intake port and then enter the cylinder.

Thermal energy in tail-pipe exhaust gases and coolant can also be utilized to heat the intake air through heat exchangers. For an engine on vehicle, loads and speeds vary. Approaches have to be developed to adjust the inlet air temperature promptly achieving fast thermal management.

Under warmed-up condition, walls of engine combustion chamber and intake ports are always hotter than intake air. The hot walls heat the intake charge through heat transfer. It is seldom to adjust the wall temperature to control HCCI combustion. Wall temperature cannot be changed quickly due to thermal inertia. The range of wall temperature variation is also small, limiting its effect on HCCI combustion timing control. Under warmed-up conditions, engine parts' temperatures are constrained within a certain range by operation requirements and materials of the parts.

Finally, charge temperature can be increased using pilot fuel that is burned prior to the compression stroke. Early combustion, however, reduces engine thermal efficiency because the released chemical energy from pilot fuel at low cylinder pressure cannot be transferred to mechanical energy.

4.1.3 Utilization of available thermal energy sources

There are different ways to utilize available thermal energy sources in an engine to cause autoignition. Table 4.1 lists the available thermal energy sources and four typical HCCI engine systems. CAI (Willand *et al*. 1998) and CSI (Fuerhapter *et al*. 2003) engines rely on thermal energy in the retained burned gases with a conventional compression ratio. OKP engine

www.TechnicalBooksPDF.com

Table 4.1 List of available thermal energy sources in an engine and utilization of these energy sources by different gasoline HCCI systems

Gasoline HCCI engine systems:	CAI	CSI	OKP	VCR-HCCI
Compression heat, CR=	~10:1	~10:1	~15:1	up to ~20:1
Residuals (not include EGR)	increased	normal	increased	normal
Internal EGR	not use	use	not use	not use
Exhaust gases	not use	not use	use	use
Coolant	not use	not use	use	not use
Hot walls of chamber and port	use	use	use	use
Fuel burned before compression	may use	not use	not use	not use

(Yang *et al*. 2002) utilizes almost all of the available thermal energy sources, including those in exhaust gases and coolant, compression heat with a higher compression ratio of about 15:1, and retained residuals. The original VCR-HCCI engine uses higher compression ratio up to 20:1 (Christensen *et al*. 1999). Its later version also utilizes thermal energy in the exhaust gases though a heat exchanger (Hyvonene *et al*. 2003). Different HCCI engine systems have different engine layouts, employ different hardware and adopt different combustion timing control strategies.

This chapter discusses those gasoline HCCI engine systems that are characterized by utilizing thermal energy in the exhaust gases and coolant to heat the intake air with fast thermal management. The discussion starts with the optimized kinetic process (OKP) engine, followed by brief discussions of other engine systems.

4.2 The optimized kinetic process (OKP) HCCI engine

4.2.1 OKP engine system concept

OKP engine is a 4-stroke HCCI-SI dual-mode gasoline engine (Yang *et al*. 2002). For mixture autoignition, the engine utilizes waste thermal energy contained in the exhaust gases and coolant to heat the intake air, and retains more hot residuals. Its compression ratio is increased to about 15:1. Thus, almost all of the available thermal energy sources in an engine are utilized for mixture autoignition. Combustion timing control of the OKP engine in HCCI mode relies on fast thermal management of the inlet air temperature.

To utilize thermal energy in exhaust gases and coolant, two heat exchangers are employed to heat the intake air, as shown in Fig. 4.1. One intake air stream flows initially through a coolant-air heat exchanger and then through an exhaust gas-air heat exchanger. Another intake air stream bypasses the

www.TechnicalBooksPDF.com

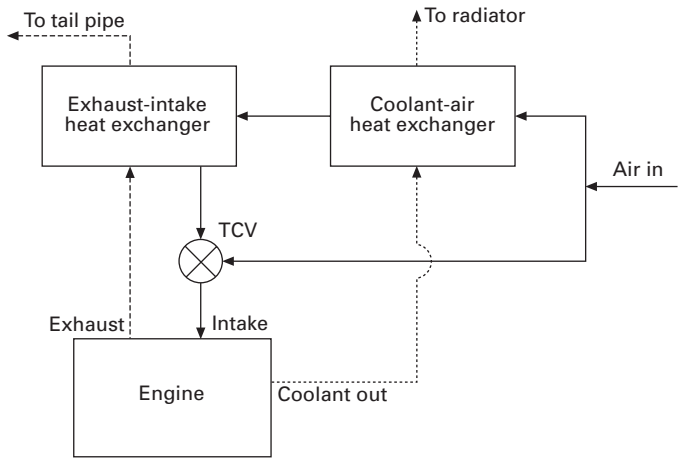

4.1 Schematic of a fast thermal management system using heat exchangers and flow-rate control.

heat exchangers, remains unheated. Both air streams can enter the cylinder. Average temperature of the intake air depends on the ratio of mass flow rates of the two airstreams. The ratio of the two flow rates is controlled by a temperature control valve (TCV), as shown in Fig. 4.1. Alternatively, two throttles can be installed in the hot and cold passages, respectively, to control the flows. Another approach is to flow the two air streams into the cylinder independently through different intake valves. In all of the three cases, controlling the ratio of the heated and unheated flow rates allows a quick adjustment of the intake air temperature for HCCI combustion timing control, achieving fast thermal management.

At high loads or during cold start, the OKP engine operates in SI mode. To avoid engine knock, effective compression ratio in SI mode is reduced from 15:1 to about 10:1, and the engine operates using Atkinson cycle. Residual gas fraction in SI mode is also reduced to a normal level for spark ignition and flame propagation. To adjust both the effective compression ratio and the residual gas fraction, a variable valve timing (VVT) device is employed. One type of such VVT device is variable cam timing (VCT). Valve lift curves in HCCI and SI modes using VCT are shown in the upper part of Fig. 4.2. The use of VCT with an extended intake event length allows the engine to operate in SI mode with a retarded intake valve close timing and conventional valve overlap. Thus, effective compression ratio and residual gas fraction are reduced to the levels of a conventional SI engine. Another type of VVT device is cam profile switching (CPS). Valve lift curves in HCCI and SI modes using CPS are shown in the lower part of Fig. 4.2. The use of CPS can achieve the same targets of VCT. In HCCI mode, negative valve overlap is used to retain more hot residuals instead of using an extended

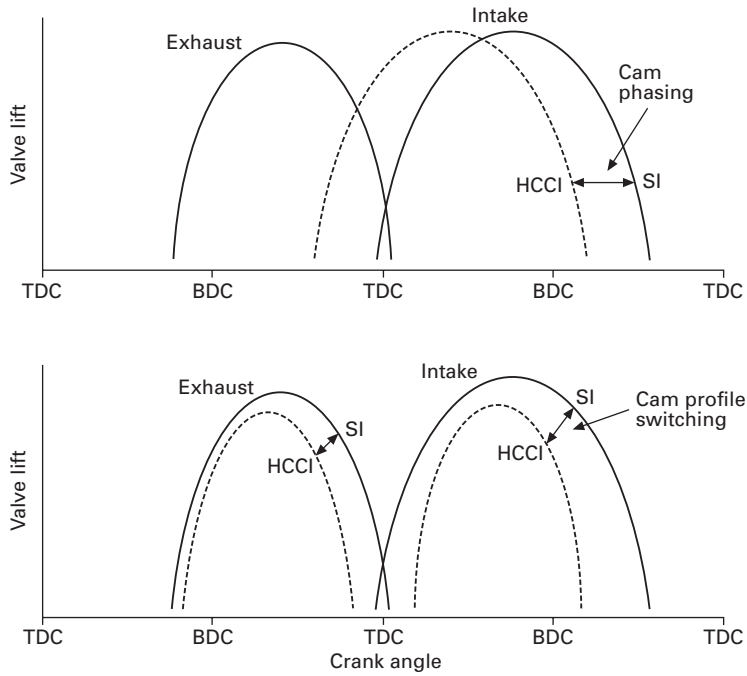

4.2 Schematic of two sets of valve lift curves, the upper set using cam phasing and the lower set using cam profile switching.

valve overlap. Using CPS has an advantage over using VCT. A CPS device can change the valve timing within one cycle hence can meet the need of combustion mode transition. In contrast, the phase change speed of a VCT device can be an issue for mode transition.

Another way to operate in SI mode is to employ a variable compression ratio (VCR) mechanism to reduce engine geometric compression ratio without retarding the intake valve close timing. But, a VVT device is still needed to control residual gas fraction. In SI mode, thermal efficiency of the engine using VCR is at the same level of a conventional PFI engine.

When operating with Atkinson cycle using a retarded intake valve close timing, volumetric efficiency of the OKP engine is decreased. To compensate for the loss in volumetric efficiency, inlet pressure at high loads is boosted. An intercooler is used to reduce the boosted intake air temperature. If a VCR mechanism is employed to reduce geometric compression ratio in SI mode, boosting the inlet pressure is no longer necessary since volumetric efficiency is not decreased.

The proposed OKP approaches allow the HCCI engine to operate with a high thermal efficiency and a wide operating range. Advantages of the OKP engine system are analyzed in detail in Section 4.3.

4.2.2 Test results

Single-cylinder OKP engine

The OKP engine concept has been evaluated through dynamometer tests with a single-cylinder engine (Yang *et al*. 2002). The engine has a bore of 89 mm, a stroke of 105.8 mm, and a compression ratio of 15.1:1. It has a pent-roof combustion chamber with two intake valves and two exhaust valves. A gasoline DI injector is mounted under the intake ports. Intake valve event length was extended from about 240 to 300 crank-angle degrees (CAD). To increase the valve overlap in HCCI mode, intake valve open (IVO) was timed at 62 CAD before TDC. Exhaust valve event length was 240 CAD. Two electric heaters were used during the test to simulate the heat exchangers.

Operating range

The engine was tested over a fairly broad range of operating conditions. Figure 4.3 shows the test data points in both HCCI and SI modes. In HCCI mode, the engine was tested from 750 rpm to 4750 rpm, and from light loads to 5.5 bar of Net indicated Mean Effective Pressure (NMEP). The capability to operate over a fairly broad range of operating conditions in HCCI mode is a major advantage of the OKP concept. It allows better utilization of the

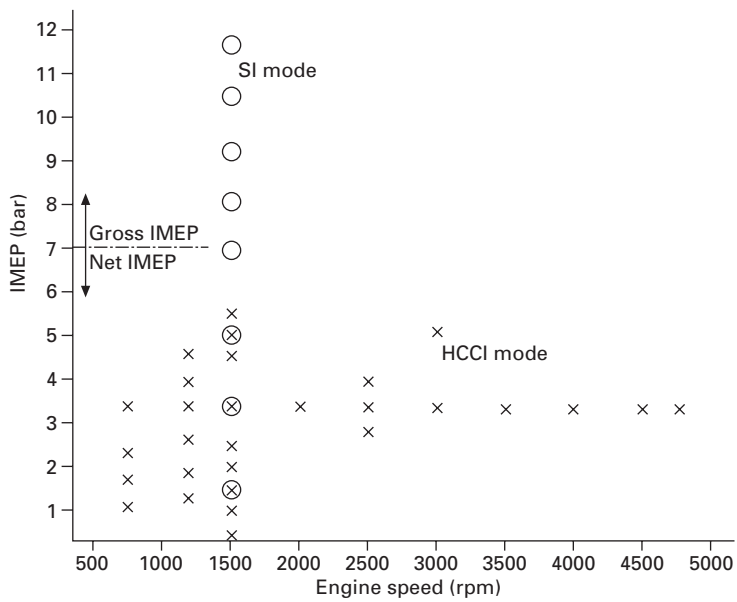

4.3 The map of data points of single-cylinder OKP engine tests in HCCI mode and in SI mode.

benefit of HCCI combustion to improve vehicle fuel economy over regulatory drive cycles. The reasons for the broad operating range will be analyzed in Section 4.3.

The OKP engine was also tested in SI mode using valve timings for SI operations, as shown in Fig. 4.2. Without boost, the engine was operated up to 7 bar NMEP. With boosting the inlet pressure to 1.5 bar, the engine was operated up to 11.7 bar of Gross indicated Mean Effective Pressure (GMEP) at 1500 rpm, as shown in Fig. 4.3. The OKP engine delivered a peak torque comparable to a conventional gasoline engine with the same displacement.

Thermal efficiency

The single-cylinder OKP engine in HCCI mode demonstrated high thermal efficiencies. Figure 4.4 compares the Net indicated Specific Fuel Consumptions (NSFC) of the OKP engine, a prototype stratified-charge direct-injection spark-ignition (SC-DISI) engine and two port-fuel-injection (PFI) engines at different loads and 1500 rpm. For all of the engines, GMEP was determined by the difference in measured torques at fired and motored operations. Then, NMEP was determined from GMEP and engine pumping loss, which was measured using a pressure transducer. At a typical light-load operating condition of 1500 rpm and 3.3 bar NMEP (equivalent to 2.62 bar BMEP), OKP engine

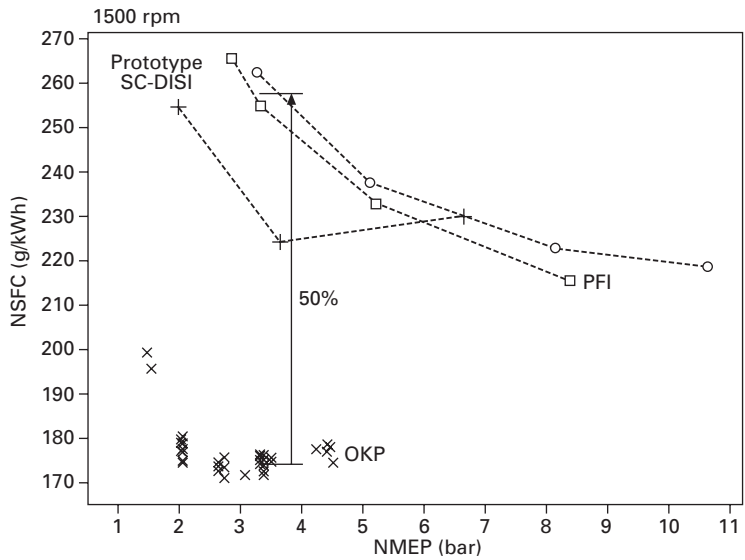

4.4 Comparison of net ISFC of the single-cylinder OKP engine in HCCI mode, a prototype stratified-charge DISI engine and two production PFI engines.

improved thermal efficiency by 50% over conventional PFI engines, and by 30% over the prototype SC-DISI engine. The high thermal efficiency of the OKP engine in HCCI mode is another advantage of the OKP concept, which will be analyzed in the next section. The high thermal efficiency and the wide operating range in HCCI mode allow the OKP engine to significantly improve vehicle fuel economy over regulatory drive cycles.

In SI mode, part-load thermal efficiency of the OKP engine was improved due to the high expansion ratio and reduced pumping losses using the Atkinson cycle. At 5 bar NMEP, thermal efficiency of the engine was improved by 7% over PFI engines.

Emissions in HCCI mode

NOx emissions of the OKP engine in HCCI mode were dramatically reduced, as shown in Fig. 4.5. Below 4 bar NMEP, the Net indicated Specific NOx emissions (NSNOx) of the OKP engine were below 0.1 g/kWh, which were only 1% or 2% of that of PFI and SC-DISI engines. The extremely low NOx emissions of the OKP and other HCCI engines resulted from the low combustion gas temperature of a lean (or diluted) mixture. It is known that removing NOx from the exhaust gases of a lean-combustion engine is difficult. The extremely low NOx emissions of the HCCI engines can facilitate the

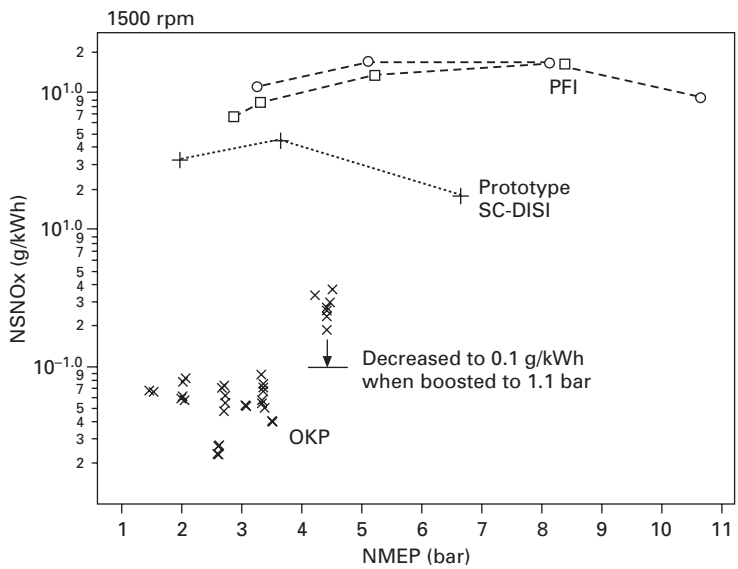

4.5 Comparison of NOx emissions of the single-cylinder OKP engine in HCCI mode, a prototype stratified-charge DISI engine and two production PFI engines.

design of engine aftertreatment systems to meet the stringent emission regulations.

When NMEP increased to 4.5 bars, NOx emissions increased significantly. This was because dilution of the mixture became inadequate at higher loads with the increase in fuel mass per cycle. The richer mixture resulted in higher burned gas temperature beyond 1800~1900K, which is the threshold for NO formation. To suppress NO formation, the mixture can be further diluted by increasing the inlet pressure, i.e. adding more air to the mixture. During the tests, NOx emissions at a load of 4.5 bar NMEP were suppressed from about 0.3 g/kWh to 0.1 g/kWh when the inlet pressure increased from 1.0 bar to 1.1 bar.

Hydrocarbon (HC) emission indexes of the OKP engine in HCCI mode were between those of PFI and SC-DISI engines, as shown in Fig. 4.6. Although the correlation of HC index versus loads of the OKP engine was similar to that of the SC-DISI engine, the mechanism of HC emissions in OKP engine, at least at higher loads, is presumably closer to that in PFI engines, i.e. owing to crevice loading of HC (Kaiser *et al*. 2002, 2005). HC emissions of the OKP engine were higher than that of PFI engines, because the OKP engine had a higher compression ratio and a larger crevice volume compared with conventional PFI engines. The larger crevice volume of the single-cylinder OKP engine resulted from a design constraint owing to the use of a DISI cylinder head. For a production OKP engine, this design

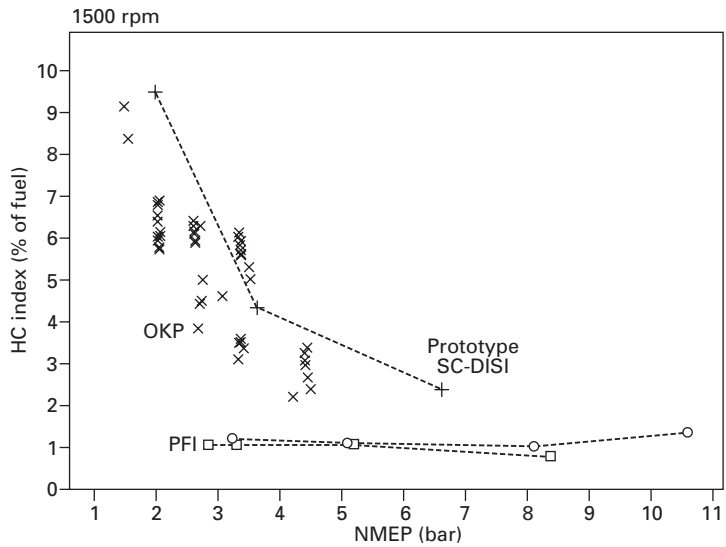

4.6 Comparison of HC emissions of the single-cylinder OKP engine in HCCI mode, a prototype stratified-charge DISI engine and two production PFI engines.

constraint can be removed. But the effect of higher compression ratio of the OKP engine on HC emissions cannot be eliminated.

When load decreased, HC emissions of the OKP engine increased quickly, although they were still lower than that of SC-DISI engines. This was presumably because crevice loading of HC with a very lean mixture has a bigger effect on HC emissions than that with a stoichiometric mixture. The burned gas temperature of a very lean mixture can be too low for the crevice hydrocarbons to be oxidized during the expansion stroke. The lower gas temperature is not favorable for HC oxidation in the exhaust ports. Furthermore, the low combustion gas temperature of a very lean mixture can result in incompletion of the combustion process, similar to that occuring in the fuel-leaner region in SC-DISI engines.

Carbon monoxide (CO) emission indexes of the OKP engine in HCCI mode are shown in Fig. 4.7. At higher loads, CO emissions of the OKP engine were much lower than that of SC-DISI and PFI engines. This was because in a homogeneous lean mixture there was almost no region which is richer than stoichiometric to produce CO emissions. When load is decreased, however, CO emissions increased rapidly. This rapid increase resulted from the quenching of the CO oxidation process in the lean mixture as the gas temperature dropped below 1500 K (Jun *et al.* 2003). At light loads, incompletion of the CO and HC oxidation processes resulted in a significant decrease in combustion efficiency.

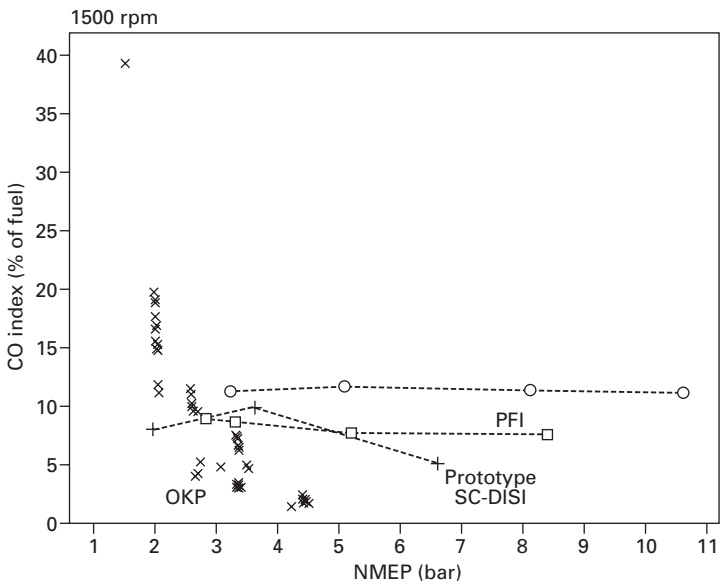

4.7 Comparison of CO emissions of the single-cylinder OKP engine in HCCI mode, a prototype stratified-charge DISI engine and two production PFI engines.

4.2.3 Expanding HCCI operating range

The HCCI operating range is constrained by engine performance/control issues and emissions (Yang, 2005). The major constraints to the HCCI operation range are shown schematically in Fig. 4.8. Because the HCCI operating range affects the improvement in vehicle fuel economy over drive cycles using HCCI technology, expanding the HCCI operating range is a critical target for HCCI engine development.

Methods to expand the lower boundary

The lower boundary of HCCI operating range is constrained by a sharp increase in CO emissions with decrease in combustion efficiency and by the increase in cycle-by-cycle variations that lead to misfire. As discussed earlier, a sharp increase in CO emissions of the OKP engine at light loads resulted from the decrease in the burned gas temperature below a threshold of 1500 K. To improve CO emissions and combustion efficiency at light loads, the burned gas temperature should be increased. One control method to increase the burned gas temperature is to advance the combustion timing so that gases during combustion tend to be compressed. Advancing combustion timing requires more thermal energy for the mixture to achieve autoignition temperature at an earlier time. Another control method is the use of a stratified charge, which reduces local air-fuel ratio in the fuel-richer zone. Richer

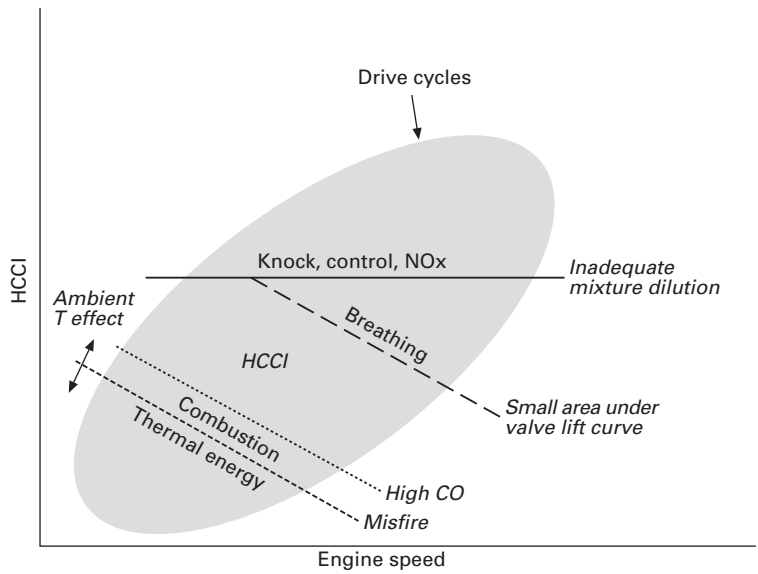

4.8 The constraints to the HCCI operating range.

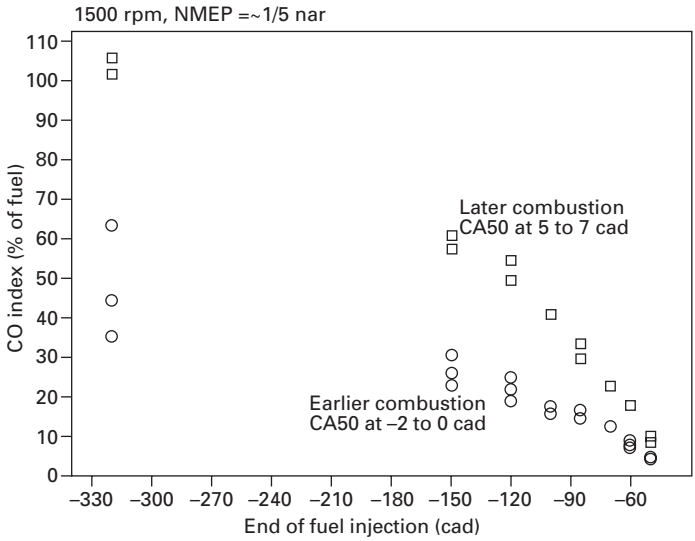

4.9 The effects of fuel injection timing and combustion timing on CO emissions.

mixture has a higher burned gas temperature. Charge stratification can be realized by retarding the fuel injection timing if the engine employs direct fuel injection.

Figure 4.9 shows the effects of charge stratification and combustion timing, in terms of crank angle of 50% heat release (CA50), on CO emissions. When combustion timing is advanced and fuel injection timing is retarded, CO emission indexes were significantly reduced (Yang *et al*. 2006). However, excessively retarding the fuel injection timing beyond –110 CAD after TDC resulted in a rapid increase in NOx emissions since mixture in the fuel-richer region became too rich that the burned gas temperatures were beyond the 1800~1900K threshold of NO formation.

There are two other control methods to reduce CO emissions at light loads, including the decrease in inlet pressure by throttling, and the increase in residual gas fraction (Yang 2005). Decreasing inlet pressure reduces gas mass in the cylinder, resulting in an increase in burned gas temperature. Increasing residual gas fraction results in a lower exhaust gas mass flow rate, resulting in lower CO emissions (Yang *et al*. 2006).

During the tests, cycle-by-cycle variations increased with the decrease in load when maintaining the same combustion timing CA50. At the same light load, cycle-by-cycle variations decreased with the advance of combustion timing. The single-cylinder OKP engine has operated steadily at an air-fuel ratio of 270:1 (Yang *et al*. 2002). As indicated earlier, advancing combustion timing requires more thermal energy to heat the mixture.

Methods to expand the upper boundary

The upper boundary of the HCCI operating range is constrained by the intolerable combustion roughness or knock, the reduced window of combustion timing control, and the increase in NOx emissions when load increases. These problems result from inadequate dilution of the mixture at higher loads due to the increase in fuel mass per cycle. A less diluted mixture releases more heat per mixture mass during combustion, resulting in higher combustion gas temperature. The higher gas temperature, in turn, increases heat release rate and promotes knock (Yelvington *et al*. 2004). Because of the higher heat release rate at high loads, HCCI combustion timing is more sensitive to the variations in mixture temperature. Thus the temperature window becomes smaller, and HCCI combustion timing control becomes more difficult (Yang 2005). A less diluted mixture also results in a higher burned gas temperature, resulting in the increase in NOx emissions.

Because inadequate mixture dilution constrains the upper boundary of HCCI operating range, increasing dilution of the mixture can push the upper boundary to higher loads. An effective way to dilute the mixture is the boost of inlet pressure while maintaining fuel mass per cycle unchanged. Figure 4.10 shows the effect of inlet pressure and residual gas fraction on the slope of the correlation of combustion timings CA50 versus inlet temperatures. Boosting the inlet pressure from 1.0 to 1.3 bar significantly reduced the

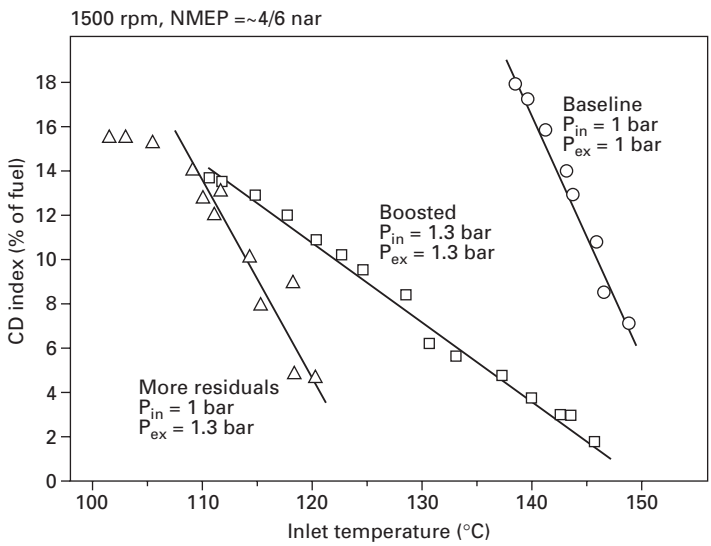

4.10 Sensitivity of combustion timing to the variation of inlet temperature at different inlet pressures and different residual gas fractions.

sensitivity of combustion timing to the variations in inlet temperature, as shown by the flatter correlations in Fig. 4.10. As a result, the intake air temperature can vary over a larger range when combustion timing is controlled within the same window. In other words, the controllability of HCCI combustion timing was improved. Boosting the inlet pressure to dilute the mixture can also suppress NOx emissions (Fig. 4.5) and heat release rate (Yang 2005).

For the case of increased residual gas fraction (Fig. 4.10), sensitivity of CA50 to the variations in inlet temperature was almost unchanged. The correlation moved leftward since a larger residual gas fraction requires a lower inlet temperature to achieve the same mixture temperature.

Boosting the inlet pressure can operate an HCCI engine at higher load. An HCCI engine has operated at 16 bar Brake Mean Effective Pressure (BMEP) with a boosted inlet pressure of 3.2 bar (Olsson *et al.* 2001). However, the maximum cylinder pressure at that load reached 200 bar, which requires a strong engine structure. A stronger engine structure not only increases engine weight, but also results in higher mechanical friction losses. If a light gasoline engine structure is used, the intake pressure and the maximum load in HCCI mode are constrained. That is why many HCCI engines adopt a dual combustion mode approach.

The upper boundary of HCCI operating range can also be expanded by retarding the HCCI combustion timing (Sjoberg *et al.* 2004). When combustion timing is retarded, the volume of combustion chamber during the combustion process tends to expand, reducing the in-cylinder gas temperature and chemical reaction rate. Thus, combustion roughness and knocking tendency are reduced (Yang 2005). Excessively retarding the combustion timing increases cycle-by-cycle variations and eventually leads to misfire. This is because the released heat and the radicals, which are generated during the low-temperature reactions, may not be adequate to proceed to high-temperature reactions in the mixture if gas temperature drops too quickly owing to expansion of the combustion chamber volume. Therefore, the usage of retarding HCCI combustion timing is constrained.

Thermal stratification in the cylinder can reduce the overall heat release rate at high loads. Mixture in the relatively hot region starts chemical reaction earlier than that in the relatively cold region. Due to the difference in chemical reaction timings, the overall heat release rate is decreased. To create thermal stratification in the cylinder, Iwashiro *et al.* (2002) employed water injection into the cylinder to form a cold region. Sjoberg *et al.* (2004) reduced engine coolant temperature to 50°C to enhance gas-wall heat transfer that results in a thicker thermal boundary in the combustion chamber. Both tests have successfully demonstrated a reduction in the overall heat release rate. But these approaches have disadvantages. Using water injection needs to resolve an issue of corrosion. Lower coolant temperature results in higher heat transfer losses. A better way to create thermal stratification is the introduction of

intake airs at different temperatures into the cylinder through different intake valves. An OKP engine can use this approach with a special intake system design.

4.3 Strengths and weakness

4.3.1 High thermal efficiency

A gasoline HCCI engine is more complicated and more expensive than a conventional SI engine. Therefore, application of a gasoline HCCI engine on vehicle is justified if thermal efficiency can be significantly improved. Different HCCI approaches result in different thermal efficiencies. To understand the potential of HCCI technology in improving vehicle fuel economy, the major factors that affect engine part-load thermal efficiency are analyzed. These factors and different engine systems, including conventional SI engines, diesel engines (CI), stratified-charge (SC) DISI engines, and a few typical HCCI engines, are listed in Table 4.2. A two-grade score system is used to rank these engine systems.

Engine compression ratio, pumping loss and gas specific heat ratio, which are listed in Table 4.2, are three major factors that differentiate a diesel engine from a conventional SI engine in thermal efficiency. A gasoline SI engine is constrained by combustion knock. Hence its compression ratio is limited to about 10:1. Spark ignition and flame propagation require an air-fuel ratio below 20:1. The use of a 3-way catalyst to control tail-pipe emissions requires a stoichiometric mixture. Thus an SI engine at part loads is throttled, resulting in engine pumping losses. The constrained air-fuel ratio also limits gas specific heat ratio, reducing engine part-load thermal efficiency.

The first three factors also affect thermal efficiency of other engine systems. A stratified-charge DISI engine uses an overall lean mixture at part loads. Its air-fuel ratio can be increased up to 45:1. Hence gas specific heat ratio is increased, and pumping loss is reduced. But, compression ratio of the SC-

Table 4.2 List of the factors that affect engine part-load efficiency and evaluation of different engine systems with two-grade scores

Engine systems:	SI	CI	SC-DISI	CAI	OKP	VCR-HCCI
Compression ratio	B	A	B	B	A	A
Pumping loss	B	A	A–	A–	A	A
Specific heat ratio	B	A	A–	B	A	A
Heat transfer	B	B–	B	A	A	A–
Gas dissociation	B	B	B	A	A	A
Combustion timing	A	A–	B	A–	A	A
Mechanical friction	A	B	A	A	A	A–

Notes: Score A is better than score B.

DISI engine remains essentially unchanged at about 10:1. Thermal efficiency of a SC-DISI engine therefore is still lower than that of a diesel engine. A CAI engine (Willand *et al*. 1998) retains more hot residuals at part loads to operate in HCCI mode without throttling the intake flow. Although there are minor pumping losses associated with charge compression during the negative valve overlap period, total pumping loss of the CAI engine is reduced. CAI engines use a compression ratio of conventional SI engines and a nearly stoichiometric mixture. Therefore, from the viewpoint of the three major factors, thermal efficiency of a CAI engine is between PFI and diesel engines. CSI engine (Fuerhapter *et al*. 2003) has a similar compression ratio and a similar air-fuel ratio of a CAI engine. Hence the two engines have similar thermal efficiencies. In contrast, OKP (Yang *et al*. 2002) and VCR-HCCI engines (Hyvoenen *et al*. 2003) use higher compression ratios and lean mixtures without throttling. Air fuel ratio of the engines can be increased to about 75:1, limited only by CO emissions. Therefore, from the viewpoint of the three major factors of Table 4.2, OKP and VCR-HCCI engines have a similar high indicated thermal efficiency of diesel engines at part loads.

Next two factors in Table 4.2 that affect engine thermal efficiency include heat transfer losses and gas dissociation at high temperature. All of the HCCI engines use highly diluted mixture that results in lower combustion gas temperature, usually below 1800~1900 K. Thus, the losses due to heat transfer and gas dissociation in all of the HCCI engine systems are reduced. Heat transfer losses of the VCR-HCCI engine are higher than other HCCI engines owing to its higher compression ratio.

Combustion-timing affects engine thermal efficiency through its effect on combustion timing losses and heat transfer losses. In most of the engine systems, combustion timing can be controlled over a wide range, except for the SC-DISI engines. In wall-guided SC-DISI engines, combustion timing is constrained by the processes of fuel-air mixing and mixture formation, requiring early combustion (Yang and Kenney 2002). In spray-guided SC-DISI engines, combustion timing is less constrained, but completion of the combustion process in the fuel-leaner region is still a concern. For a modern diesel engine, combustion timing is constrained by emission concerns and therefore is often not optimized for the highest thermal efficiency. For CAI engines, adoption of pilot injection during the negative valve overlap period results in combustion timing losses because heat release at low cylinder pressure can do little mechanical work. Combustion timing of other HCCI engines is not constrained except near the boundaries of HCCI operating range, as discussed earlier.

Mechanical friction reduces engine brake thermal efficiency. Engine mechanical friction losses depend mainly on the peak cylinder pressure. Higher peak cylinder pressure requires a stronger engine structure with larger bearing diameters and more piston rings, resulting in higher friction losses.

Higher cylinder pressure also increases the forces between piston and cylinder liner, and between crankshaft and bearings, resulting in higher friction losses. Diesel engines usually have a peak cylinder pressure higher than that of other engines, and therefore have more mechanical friction losses. A VCR-HCCI engine may also have a higher peak cylinder pressure and more friction losses, depending on system design.

From the analysis, it can be seen that the OKP engine is always in the better category for all of the factors that affect engine part-load thermal efficiency. Therefore, the OKP concept allows the engine to approach the technical upper limit of part-load thermal efficiency of an internal combustion engine. The VCR-HCCI engine has a similar indicated thermal efficiency of an OKP engine, but its brake thermal efficiency can be lower than that of an OKP engine due to higher mechanical friction losses.

4.3.2 Wide HCCI operating range

Improvement in vehicle fuel economy using an HCCI engine depends on not only engine thermal efficiency in HCCI mode, but also HCCI operating range. The major constraints to HCCI operating range have been shown earlier in Fig. 4.8. Different HCCI approaches result in different operating ranges. This section compares different HCCI engine systems for their capability to operate over a wide range.

Upper boundary of HCCI operating range

The upper boundary of HCCI operating range is constrained by intolerable combustion roughness or knock, the reduced window for combustion timing control and the increase in NOx emissions when load increases. These constraints result from inadequate dilution of the mixture when load increases.

To evaluate different HCCI engine systems, control methods and approaches for operation at higher loads are listed in Table 4.3. A two-grade score system is used to rank different engine systems. Boosting the inlet pressure

Table 4.3 List of approaches for high-load HCCI operation and evaluation of different HCCI engine systems with two-grade scores

Gasoline HCCI engine systems:	CAI	CSI	OKP	VCR-HCCI
Boosted intake pressure	A	B	A	A
High valve lift and event length	B	A	A	A
Retarded combustion timing	A	A	A	A
High CR for low charge T	B	B	A	A+
Temperature stratification	B	A	A	B

Notes: Score A is better than score B.

to dilute the mixture, in principle, can be applied in all of the HCCI engines. The CSI engine, however, also requires increasing the exhaust backpressure since its exhaust valves re-open during the intake stroke. Valve lift and event length for almost all of the HCCI engines can be the same as those of conventional engines except for CAI. The negative valve overlap of a CAI engine leads to a shorter valve event length and a smaller valve lift, deteriorating engine breathing. Retarding HCCI combustion timing can be applied in all of the HCCI engines to reduce heat release rate. Engine geometric compression ratio of the OKP and VCR-HCCI engines are increased to about 15:1 and 20:1, respectively, to provide more compression heat for mixture autoignition. Thus the required charge temperature prior to compression is reduced, leading to a higher gas density. A simple simulation predicted that the retained gas mass increases 17% when compression ratio increases from 10:1 to 15:1 (Yang 2005). In contrast, compression ratio of CAI and CSI engines is similar to that of SI engines, about 10:1, because CAI and CSI engines adopt no approach to operate in SI mode with a higher geometric compression ratio. Finally, thermal stratification can be realized in OKP and CSI engines through intake or exhaust system design to reduce the overall heat release rate. The OKP engine can induce the heated and unheated intake airs into the cylinder through different intake valves. The CSI engine can re-breath the exhaust gases through one of two exhaust valves. In contrast, CAI and VCR-HCCI can only reduce coolant temperature or inject water into the cylinder to realize thermal stratification.

In evaluating the control methods and approaches to operate at higher loads, the OKP engine is always in the better category. The OKP and VCR-HCCI engines can operate at higher loads in HCCI mode compared to CAI and CSI engines.

Lower boundary of HCCI operating range

The lower boundary of HCCI operating range is constrained by the increase in cycle-by-cycle variations, which eventually lead to misfire, and by a sharp increase in CO emissions with decrease in combustion efficiency (Yang 2005). These constraints result from the excessive dilution of the mixture when load decreases.

As discussed earlier, control methods can be used in all of the gasoline HCCI engines to operate at light loads, including advancing combustion timing, intake flow throttling, increasing EGR and charge stratification if using direct fuel injection. However, the capabilities of different HCCI engines to provide adequate thermal energy at light loads to advance HCCI combustion timing are different.

Thermal energy at light loads can be an issue for operation in HCCI mode. At light loads, the demand on thermal energy for mixture autoignition

increases because heat transfer losses increase due to the decreased wall temperature. Meanwhile, available thermal energy to heat the mixture reduces due to the reduced combustion heat and the lower combustion gas temperature. The lack of adequate thermal energy for mixture autoignition results in retardation of combustion timing, increase in cycle-by-cycle variations and misfire. This situation becomes more serious at lower ambient temperature and at lower engine speed. Lower inlet air temperature requires more thermal energy for the mixture to reach autoignition temperature. Lower engine speed results in higher heat transfer losses per cycle. The lack of thermal energy for autoignition constrained the lower boundary of HCCI operating range as shown in Fig. 4.8.

To evaluate different gasoline HCCI engine systems, available thermal energy sources in an engine and utilization of these energy sources by different HCCI engines are shown in Table 4.4. Again, a two-grade score system is used in ranking these systems. Compression heat plays an important role for mixture autoignition in all of the HCCI engines. Both OKP and VCR-HCCI engines use a higher compression ratio, hence more compression heat, for mixture autoignition. Thermal energy in residuals or EGR also plays an important role in mixture autoignition in all of the HCCI engines. CAI and CSI engines significantly increase the residual gas fraction for mixture autoignition. An OKP engine also retains more burned gases although its residual gas fraction is smaller than those of CAI and CSI engines. Residual gas fraction in a VCR-HCCI engine is at the same level of a conventional engine. Thermal energy in the tail-pipe exhaust gases is utilized in OKP and VCR-HCCI engine systems through a heat exchanger. Thermal energy in the coolant is utilized in the OKP engine system. Early combustion prior to the compression stroke can be applied in a CAI engine with pilot fuel injection to heat the mixture. This approach may also be applied in OKP engines if negative valve overlap is used (see lower part of Fig. 4.2).

In summary, the OKP engine is almost always in the better category. Therefore, OKP approach has a higher potential to operate at light loads than

Table 4.4 List of major thermal energy sources for light-load HCCI operation and evaluation of different HCCI engine systems in using the energy sources with two-grade scores

Gasoline HCCI engine systems:	CAI	CSI	OKP	VCR-HCCI
Compression heat	B	B	A	A+
Residuals gas fraction and EGR	A	A	A–	B
Exhaust gases	B	B	A	A
Coolant	B	B	A	B
Fuel burned before compression	A	B	B+	B

Notes: Score A is better than score B.

other HCCI engine systems except the VCR-HCCI engine. The VCR-HCCI engine, in theory, can have a very high compression ratio to achieve autoignition temperature at light loads without utilizing other thermal energy sources.

4.3.3 Other advantages

The OKP engine system has more advantages. The use of OKP approaches facilitates the control of HCCI combustion during transient operations and improves engine cold start and warm-up. In addition, an OKP engine system uses only conventional hardware.

The capability of quick adjustment of HCCI combustion timing is required for an HCCI engine or vehicle. While different HCCI engine systems use different ways to adjust combustion timing, the capability of quick adjustment depends on the response of the control devices. The OKP system uses flow-control valves, which have a fast response. Other HCCI engines may use control devices that are heavier and require a larger force to act. For example, changing the compression ratio using VCR requires a large force to act against the cylinder pressure. Changing the camshaft phase using VCT requires a large force to act against the valve springs. Hence response time of these devices can be an issue.

An HCCI engine on a vehicle sometimes operates at idle or at negative loads depending on drive conditions. Under such conditions, it is difficult to operate in HCCI mode, as explained earlier. The OKP engine utilizes thermal inertia to help operation in HCCI mode when load temporarily decreases to idle. Owing to thermal inertia, temperature of the heat exchanger decreases slowly. Thus, the intake air temperature at idle can remain high for a while to continue HCCI operation until the heat exchangers are cooled down. During transient operations, the slow variation in heat exchanger temperature helps HCCI control. This is because, at different loads, the required inlet temperatures for controlling the combustion timing are close to each other. The slow variation in heat-exchanger temperature helps to maintain the inlet temperature and to control the combustion timing during transient operations.

Combustion mode transition of a dual-mode HCCI engine requires compensation for the changes in residuals temperature. For the first HCCI cycle, the residuals are from previous SI combustion cycle and hotter than that of the following HCCI cycles. For an OKP engine, there is another phenomenon during mode transition. Because variation in inlet air temperature requires time, inlet air temperature for the first HCCI cycle can be lower than that for the following HCCI cycles. The two trends in an OKP engine can partially compensate for each other at the first HCCI cycle, facilitating mode transition control.

The OKP approaches can help engine cold start and warm-up. Under those conditions, effective compression ratio of the OKP engine can be

increased without knock. The higher compression ratio results in an increase in compression heat that promotes fuel vaporization and combustion efficiency. In addition, the intake air during engine warm-up can flow through the heat exchanger. Thus the engine can be warmed up faster utilizing thermal energy in exhaust gases.

Finally, the OKP engine system uses only conventional hardware, such as heat exchangers, airflow control valves, intake air pressure booster and CPS devices. It does not require a camless valvetrain or a VCR mechanism. The conventional hardware is reliable, and the increased engine system cost is limited.

4.3.4 Concerns

OKP engine system is more complicated than CAI and CSI engine systems because it employs more hardware. Owing to the complexity of the OKP engine system, development of engine control is more difficult. An OKP engine is also more expensive than an SI, CAI or CSI engine, although it is less expensive than a modern diesel engine and probably less expensive than a VCR-HCCI engine. Due to the use of heat exchangers, the size of the OKP engine system is larger than that of a conventional PFI engine with the same displacement. Packaging the OKP engine system is therefore more difficult.

4.4 Future trends

The scope of HCCI research is expanding beyond the original concepts of 'homogeneous charge' and 'compression ignition'. Instead of using a homogeneous charge, there is a trend of using more stratified charge when operating near the boundaries of HCCI operating range. Instead of using compression ignition, there is a trend of using a spark to assist autoignition.

As discussed earlier, charge stratification results in higher combustion gas temperature in the relatively richer zone. Thus, at light loads, CO emissions and combustion efficiency can be improved. Charge stratification near the upper boundary of HCCI operating range was also tested (Marriot *et al.* 2002). Since relatively richer mixture burns earlier and faster than the relatively leaner mixture, the overall heat release rate can be reduced. However, charge stratification at high loads results in higher NOx emissions.

Spark assisted autoignition has also been investigated. In 2002, the effect of ignition timing of a pulsed flame jet (PFJ) igniter on the autoignition timing had been successfully demonstrated in a rapid compression machine (Murase *et al.* 2002). Later, electric sparks were used to ignite relatively richer mixture in a stratified charge to trigger autoignition of surrounding leaner mixture (Urushihara *et al.* 2005). In another test, electric sparks were used to assist HCCI combustion during combustion mode transition (Hyvonen

et al. 2005). Both tests were at high loads. At light loads, it was also claimed that a spark played a role in controlling HCCI combustion (Xie *et al*. 2005). Tests by others, however, showed little effect of sparks on HCCI combustion. For example, in a study using PRF80 fuel with excess air ratio lambda between 2.7 and 3.2, the effect of sparks on HCCI combustion was weak (Weinrotter *et al*. 2005).

A spark can assist mixture autoignition only under certain conditions. It is known that an SI engine misfires when air-fuel ratio is beyond 22:1. In a leaner mixture, less heat is released in the spark plug gap, and the burned gas temperature can be too low to cause combustion of surrounding mixture. A way to ignite a lean mixture using a spark is to elevate the mixture temperature. Thus the burned gases in the spark plug gap have a higher temperature, and the required thermal energy to ignite surrounding lean mixture is reduced. The capability for a spark to assist autoignition in an HCCI engine depends on both the degree of mixture dilution and the mixture temperature.

Figure 4.11 shows schematically the ranges of mixture temperature for HCCI and spark assisted combustion. The solid line is the lower boundary of mixture temperature for autoignition without spark assistance. Above this line is the range of mixture temperature for HCCI combustion. As load increases, HCCI combustion timing is more sensitive to the variations in mixture temperature. The window of required inlet air temperature becomes smaller. Below the solid line is a triangle region in which an electric spark

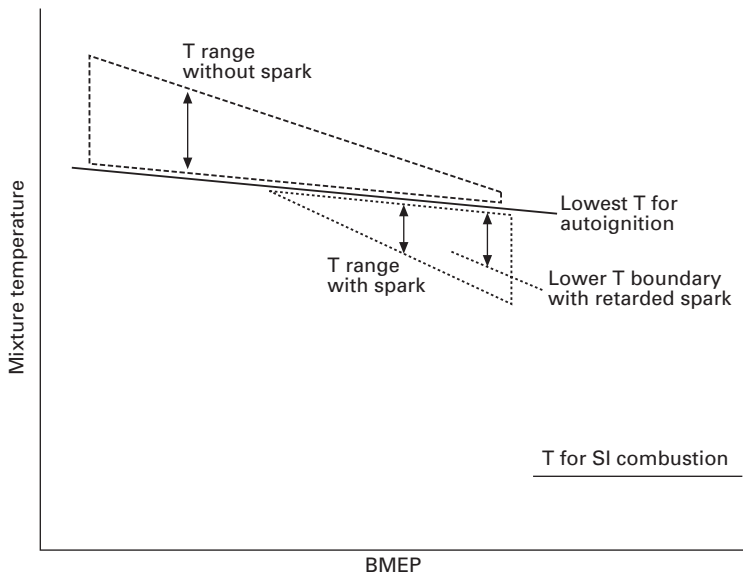

4.11 Schematic of mixture temperature range at different loads with and without using a spark to assist autoignition.

can assist autoignition. The temperature range of spark assisted HCCI increases at higher loads since the mixture becomes richer. A richer mixture requires less elevation of mixture temperature for spark assisted autoignition. Therefore, near the upper boundary of HCCI operating range, using an electric spark can expand the temperature window to improve HCCI combustion timing control. A spark can also assist to retard the HCCI combustion timing to reduce combustion roughness. With the assistance of a spark, autoignition may be trigged at a later time after TDC when the mixture starts to expand. When combustion is retarded, it is more difficult to auto-ignite the mixture. Thus the lower boundary of mixture temperature for the spark assisted HCCI moves up.

Figure 4.11 can also be used to explain why not all of the tests demonstrated the expected effect of sparks on HCCI combustion. Below the solid line, a spark plays a critical role in assisting autoignition in the combustion chamber. Above the solid line, an electric spark is less important.

4.5 Sources of further information and advice

4.5.1 Other HCCI engines using thermal management

In 1992, a gasoline HCCI engine study was published using thermal management (Stockinger *et al.* 1992). As shown schematically in Fig. 4.12, thermal energy in the burned gases was utilized to increase fresh charge

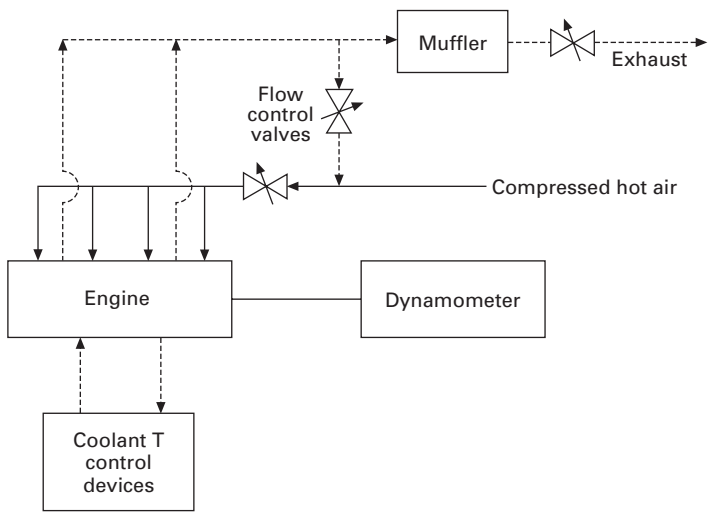

4.12 Schematic of an HCCI engine system controlling EGR and coolant temperature to realize thermal management (Stockinger *et al.* 1992).

temperature by recycling a portion of the exhaust gases (EGR). The amount of recycled exhaust gases was controlled by flow-control valves. Hence mixture temperature was controlled, achieving fast thermal management. The engine system also employed a coolant temperature control device for slow thermal management. An air compressor was employed to further dilute the mixture and provide compression heat to the intake air. That study is probably the first effort towards a practical gasoline HCCI engine system using fast thermal management.

Another gasoline HCCI engine system using fast thermal management was published in 2003. That engine system is based on an original VCR-HCCI engine using VCR to control compression heat and HCCI combustion timing (Christensen *et al*. 1999). Later, Hyvonen *et al*. (2003) modified the intake and exhaust systems of the VCR-HCCI engine utilizing thermal energy in the exhaust gases to heat the intake air through a heat exchanger. Intake air temperature was controlled by mixing the heated and un-heated intake airstreams using flow-control valves. Thus, the modified VCR-HCCI engine employed fast thermal management. Comparisons between the VCR-HCCI engine and other engines are shown in Tables 4.1 to 4.4.

4.5.2 Advice

There is little time before all of the fossil fuel in the earth is exhausted by human beings. For the past one hundred years, lots of the petroleum fuel has been burned out by inefficient gasoline engines. Engine researchers have the obligation to significantly improve thermal efficiency. There is a good opportunity to achieve this target using HCCI technology with modern control technologies.

HCCI is just another combustion concept. An engine that operates in HCCI combustion mode does not mean that thermal efficiency of the engine is improved. Vehicle fuel economy depends on both engine thermal efficiency in HCCI mode and the HCCI operating range. Using different approaches, engine thermal efficiency and HCCI operating range can be significantly different.

To achieve the goal of a significant improvement in vehicle fuel economy, the direction of HCCI research is critical. Engine developers should aim at the HCCI engines that can approach the technical upper limit of thermal efficiency of an internal combustion engine with a wide HCCI operating range. Because an HCCI engine will cost more than a conventional PFI engine, using an HCCI engine on a vehicle may not be practical unless thermal efficiency of the engine can be significantly improved. Fundamental researchers should investigate the phenomena in those HCCI engines that have a high thermal efficiency and a wide HCCI operating range. The practical value of fundamental research depends on whether or not the results can help to develop practically valuable HCCI engines.

4.6 References

Christensen, M., Hultqvist, A., and Johansson, B. (1999), 'Demonstrating the multi fuel capability of a homogeneous charge compression ignition engine with variable compression ratio,' SAE paper 1999-01-3679.

Fuerhapter, A., Piock, W., and Fraidl, G. (2003), 'CSI – controlled autoignition – the best solution for the fuel consumption – versus emission trade-off?' SAE paper 2003-01-0754.

Hyvoenen, J., Haraldsson, G., and Johnansson, B. (2003), 'Operating range in a multi-cylinder HCCI engine using variable compression ratio,' SAE paper 2003-01-1829.

Hyvoenen, J., Haraldsson, G., and Johnansson, B. (2005), 'Operating conditions using spark assisted HCCI combustion during combustion mode transition to SI in a multi-cylinder VCR-HCCI engine,' SAE paper 2005-01-0109.

Iwashiro, Y., Tsurushima, T., Nishijima, Y., Asaumi, Y., and Aoyagi, Y. (2002), 'Fuel consumption improvement and operation range expansion in HCCI by direct water injection,' SAE paper 2002-01-0105.

Jun, D., Ishii, K., and Iida, N. (2003), 'Combustion analysis of natural gas in a four-stroke HCCI engine using experiment and elementary reactions calculation,' SAE paper 2003-01-1089.

Kaiser, E., Yang, J., Culp, T., Xu, N., and Maricq, M. (2002), 'Homogeneous charge compression ignition engine-out emissions – does flame propagation occur in homogeneous charge compression ignition?' *Int. J. Engine Research*, 3, 4.

Kaiser, E., Maricq, M., Xu, N., and Yang, J. (2005), 'Detailed hydrocarbon species and particulate emissions from a HCCI Engine as a Function of Air-Fuel Ratio,' SAE paper 2005-01-3749.

Marriot, C., and Reitz, R. (2002), 'Experimental investigation of direct injection-gasoline for premixed compression ignited combustion phasing control,' SAE paper 2002-01-0418.

Murase, E., and Hanada, K. (2002), 'Control of the start of HCCI combustion by pulsed flame jet,' SAE paper 2002-01-2867.

Olsson, J., Tunestal, P., Haraldsson, G., and Johansson, B. (2001), 'A turbo charged dual fuel HCCI engine,' SAE paper 2001-01-1896.

Sjoberg, M., Dec, J., Babajimopoulos, A., and Assanis, D. (2004), 'Comparing enhanced natural thermal stratification against retarded combustion phasing for smoothing of HCCI heat-release rates,' SAE paper 2004-01-2994.

Stockinger, V., Schäpertöns, H., and Kuhlmann, P. (1992), 'Versuche an einem gemischansaugenden Verbrennungsmotor mit Selbstzündung,' MTZ 53.

Urushihara, T., Yamaguchi, K., Yoshizawa, K., and Itoh, T. (2005), 'A study of a gasoline-fueled compression ignition engine – expansion of HCCI operation range using SI combustion as a trigger of compression ignition,' SAE paper 2005-01-0180.

Weinrotter, M., Wintner, E., Iskra, K., Neger, T., Olofsson, J., Seyfried, H., Alden, M., Lackner, M., Winter, F., Vressner, A., Hultqvist, A., and Johansson, B. (2005), 'Optical diagnostics of laser-induced and spark plug-assisted HCCI combustion,' SAE paper 2005-01-0129.

Willand, J., Nieberding, R., Vent, G., and Enderle, C. (1998), 'The knocking syndrome – Its cure and its potential,' SAE paper 982483.

Xie, H., Yang, L., Qin, J., Gao, R., Zhu, H., He, B., and Zhao, H. (2005), 'The effect of spark ignition on the CAI combustion operation,' SAE paper 2005-01-3738.

Yang, J. (2005), 'Expanding the operating range of homogeneous charge compression

ignition-spark ignition dual-mode engines in the homogeneous charge compression ignition mode,' *Int. J. Engine Res*. Vol. 6.

Yang, J. and Kenney, T. (2002), 'Some concept of DISI engine for high fuel efficiency and low emissions,' SAE paper 2002-01-2747.

Yang, J., and Kenney, T. (2006), 'Robustness and performance near the boundary of HCCI operating regime of a single-cylinder OKP engine,' SAE paper 2006-01-1082.

Yang, J., Culp, T., and Kenney, T. (2002), 'Development of a gasoline engine system using HCCI technology – the concept and the test results,' SAE paper 2002-01-2832.

Yelvington, P., Rallo, M., Liput, S., Tester, J., Green, W., and Yang, J. (2004), 'Prediction of performance maps for homogeneous-charge compression-ignition engines,' *Combust. Sci. and Tech*., 176, 1243–1282.

5

Four-stroke CAI engines with residual gas trapping

H Z H A O, Brunel University West London, UK

5.1 Introduction

In Chapter 2, various approaches to achieve controlled auto-ignition (CAI) or homogeneous charge compression ignition (HCCI) have been discussed, among which the residual gas trapping method has been presented as one of the most effective and practical approaches for four-stroke gasoline engines. In this chapter, the principle of residual gas trapping and its operational characteristics will be described in detail in Section 5.2. This will be followed by a presentation of results obtained from a production type 4-cylinder port fuel injection (PFI) gasoline engine in Section 5.3. The effects of direct fuel injection on engine performance and CAI combustion are then discussed in Section 5.4. In Section 5.5, the introduction of spark discharge on CAI combustion and its implications for the highly exhaust gas diluted combustion system are discussed.

5.2 Principle of CAI operation with residual gas trapping

The principle of CAI operation with residual gas trapping is to initiate CAI combustion and to control the subsequent heat release rate by trapping large and variable amounts of residual gases in the cylinder. The burned gases from the previous cycle are trapped in the cylinder by closing the exhaust valves relatively early. As shown in Fig. 5.1, the trapped burned gases or residuals are then compressed during the final stage of the exhaust stroke. As the piston subsequently descends on the induction stroke, the inlet valves are opened late so that a fresh mixture of fuel and air in a PFI engine or only fresh air in a DI engine is drawn into the cylinder that has already been partially filled with the trapped residuals. The cold fresh charge mixes with the hot residual gases and gains the thermal energy from the residual gases. Shortly afterwards the intake valves are closed and the in-cylinder charge is compressed by the ascending piston, resulting in auto-ignition of the air/fuel

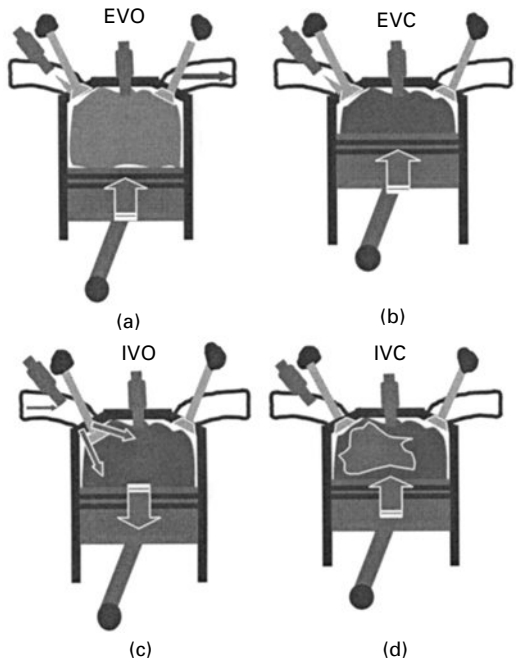

5.1 Principle of the residual gas trapping method.

mixture and the subsequent combustion around TDC. As shown in Fig. 5.2(a), in addition to the normal pressure peak near TDC during the combustion process, there is a secondary pressure peak at the other TDC position as the trapped residuals are compressed and then expand. As a consequence, the opening of the intake valves should be delayed accordingly to prevent unwanted backflow of the residual gases into the intake port.

Figure 5.3 shows the valve lift curves for normal SI operations and CAI operations. Ideally, the exhaust valves should be opened as normal towards the end of the expansion stroke for maximum work output and then will be closed earlier to trap burned gases within the cylinder; and the intake valves should be closed as normal while their opening is advanced, as indicated by the dotted valve lift curves. In order to achieve the ideal valve lift curves for CAI operation, a fully flexible variable valve actuation or camless system is required. Although it is possible to achieve fully flexible variable valve actuation using electro-magnetic controlled valves [1] or electro-hydraulic actuated valves [2], their complexity and cost will limit them to laboratory uses for the near future. Due to their excellent reliability and durability as well as relatively low loss, mechanical camshafts will still be the only practical solutions for mass produced engines. Therefore, a solution suitable for current gasoline engines must be sought and is found by employing reduced camshaft lifts. As shown in Fig. 5.3, when a low lift cam profile is used, both the

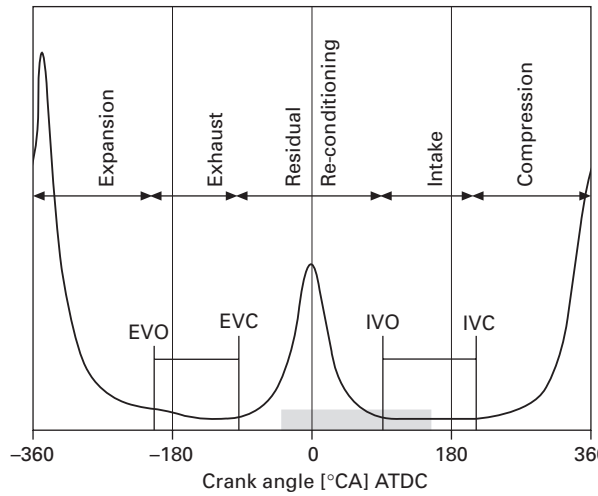

(a) In-cylinder pressure diagram with residual gas trapping

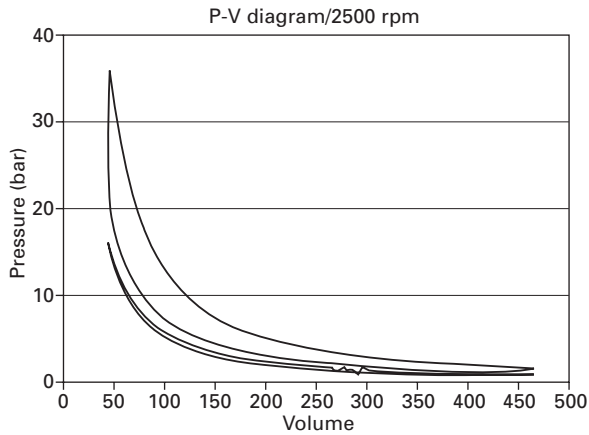

(b) P-V diagram with residual gas trapping

5.2 Pressure diagrams of CAI operation with residual gas trapping.

exhaust valves' and intake valves' opening durations will be reduced substantially, causing a substantial amount of burned gases to be trapped within the cylinder and limited fresh charge to flow into the cylinder. In combination with variable cam timing (VCT) devices, the opening/closing positions of both intake and exhaust valves can be altered relative to each other, but always with a negative valve overlap, hence the residual gas trapping method is also known as the negative valve overlap approach.

Unlike spark ignition operation, the engine load is controlled primarily by the exhaust camshaft phasing. As the load is decreased, the exhaust valve

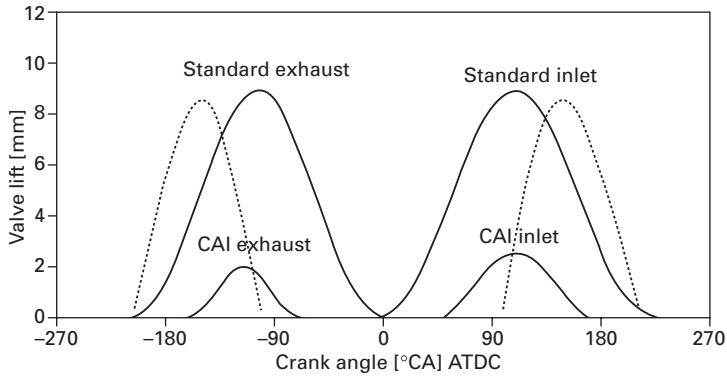

5.3 Valve lifts and durations.

closure (EVC) is advanced so that more burned gases are trapped, and the intake valve opening (IVO) is retarded accordingly to avoid backflows of residuals into the intake ports. The larger amount of residuals trapped will lead to less fresh charge being admitted into the cylinder and hence less fuel being burned. Conversely, retarded EVC will lead to reduced amount of residuals and hence more fresh charge to be flowed into the cylinder for greater work output. It is important to note that such operations are carried out with wide open throttle and hence there are no pumping losses associated with a partly closed throttle as in the SI operation.

However, there is a drawback with the negative valve overlap approach. As the residual gases are recompressed and expanded, heat loss would take place from the hot residuals to the cylinder walls. As a result, a small pumping loop is produced as demonstrated by the experimental P-V diagram shown in Fig. 5.2 (b).

Furthermore, the use of a mechanical variable camshaft system does not allow independent control of valve opening and closure. As a consequence, any change in EVC is always accompanied by a corresponding change in EVO (exhaust valve opening); similarly IVC (inlet valve closure) is affected by IVO. Therefore, advancing EVC for low load operation is compromised with lower expansion work due to early EVO. In the meantime, retarded IVO required for low operation leads to lower effective compression ratio as intake valves closes later in the compression stroke. Both reduced expansion work and lower compression ratio could offset the fuel economy gains associated with the non-throttled operation. For the high load CAI operation, as EVC retards towards TDC, the effective compression ratio becomes higher as the intake valves open and close earlier, increasing the engine's tendency to violent or knocking combustion.

Finally, the phasing of IVO relative to EVC may be used to control the mixing of fresh and residual gases and, to a certain extent, the final charge

temperature and ignition timing. If the intake valves are opened early, when the cylinder pressure is higher than the intake manifold pressure, backflow of the trapped residual gases into the manifold will occur. However, as the piston moves downward the backflow gas, along with fresh charge air, will be pulled back into the cylinder. Some heat from the backflow gas will be lost to the manifold walls. This is termed early backflow. If the intake valves are opened late, when the cylinder pressure has fallen below the manifold pressure, there will be no backflow at IVO. However, the late IVO will result in a late IVC, causing some of the in-cylinder gas to be expelled into the intake manifold as the piston begins to rise. This gas will then dwell in the manifold until it is returned to the cylinder at IVO of the next cycle and is termed late backflow. It is quite likely that during the intake and early compression strokes some degree of horizontal stratification will be present in the cylinder, with the fresh charge sitting above the residual gas, particularly around the intake valves. For this reason it is likely that the majority of the gas expelled in this manner will be the newly inducted air and as a result little heat will be lost from the residual gases. Indeed, a small amount of heat may be absorbed by the expelled fresh air, resulting in a slight increase in the overall charge temperature on its return to the cylinder.

5.3 CAI operation in a four-stroke port fuel injection (PFI) gasoline engine

5.3.1 Performance and combustion characteristics

In this section, the operation and engine performance results will be presented for the first 4-cylinder production type PFI gasoline engine operating with CAI combustion. Furthermore, in order to understand better the CAI combustion process, the in-cylinder process governing the CAI combustion process will be analysed.

The engine used was a Ford 1.7 Litre Zetec SE 16-valve four-cylinder port-fuel injection gasoline engine [3]. The sequential fuel injection strategy was adopted to ensure that the same mixture preparation event was applied to each of the four cylinders. The intake and exhaust camshafts were equipped with two independent VCT systems. Other than a pair of special camshafts of reduced lift, the engine was essentially the same as the production engine and the compression ratio was kept at 10.3. The fuel used was the standard unleaded gasoline of RON 95.

During the tests the throttle was kept at wide open and the air flow was changed by varying the cam timings, which could be continuously changed by up to 40 degrees crank angle. Intake and exhaust cam timings for minimum residual fractions were chosen to start the engine with spark ignition combustion. After a couple of minutes, CAI combustion started to appear in

some of the cycles while SI combustion occurred in other cycles. CAI combustion took over completely once the coolant temperature had reached 60°C. When the engine was running with stable CAI combustion, changing the spark timing had little effect on combustion. All experiments were carried out when the coolant reached 90°C or over in order to minimise the effects of coolant temperature. Although the engine could be operated with slightly lean or rich mixtures [3], only results at lambda 1 are presented here.

Figure 5.4 shows the speed and load range within which CAI combustion was achieved in the engine. Though the engine could be operated with CAI at lower speeds than 1000 rpm, it was considered untypical for a real engine to operate at such low speed (other than at idle) and hence not fully investigated. In addition, CAI combustion could also be obtained at higher engine speed than 3500 rpm, but only in a tiny load range. At a given speed, the load was varied by changing the cam timings. At each speed there was a minimum BMEP, which was limited by misfire. At these conditions a lot of residual gases were retained but the exhaust gas temperature was too low, and the mixture failed to auto-ignite. At higher speeds, the lower limit was shifted to lower load as the exhaust gas temperature increased at higher speeds.

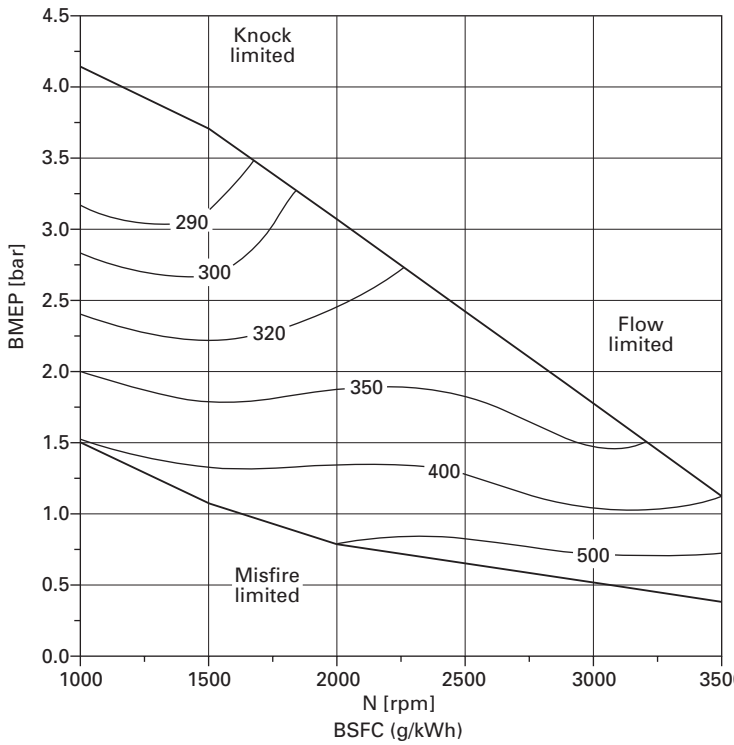

5.4 CAI operation range with residual gas trapping.

The maximum BMEP values at each speed were mainly limited by the restricted airflow due to the reduced valve lifts of camshafts used. As speed increased, there was less time for the gas exchange process and hence more residuals were trapped in the cylinders and less fresh charge was inducted, resulting in lower maximum BMEP values. At 3500 rpm the CAI operation ranged from 0.4 to 1.1 bar BMEP. However, knocking combustion was observed between 1000 rpm and 1500 rpm, as indicated by rapid rate of pressure rise and pressure oscillation. Here the knocking combustion was detected by measuring the amplitude of pressure signal after it has passed a bandpass filter with a frequency range between 5 and 15 kHZ. A knocking cycle was characterised by a peak amplitude of 0.5 bar or higher, and if more than 20% of the cycles were knocking, knocking combustion was deemed to have occurred at this operating condition.

The engine output during the CAI combustion operation was varied by controlling the amount of residuals in the cylinder by adjusting the valve phasing. As shown in Fig. 5.5, there was a linear correlation between the residual fraction and engine's output, independent of the engine speed. The higher the residual fraction was, the lower the torque became. As the engine was operated at WOT, the mass in the cylinder was more or less the same and only the mixture concentration changed. The more residuals were trapped, the less air/fuel mixture the engine could breathe in, and hence the lower torque could be generated.

Figure 5.6 shows variation of the maximum rate of pressure rise with residuals or load. In most cases, the maximum rate of pressure rise decreased with residuals or increased with load, so was the peak cylinder pressure. The rate of maximum pressure rise varied between 1 and 7 bar/CA. There were three points at 1000 rpm at which the maximum pressure rise rate exceeded 8 bar/CA. Such a rate of pressure rise would have been associated with knocking combustion in a normal SI gasoline engine. However, in most

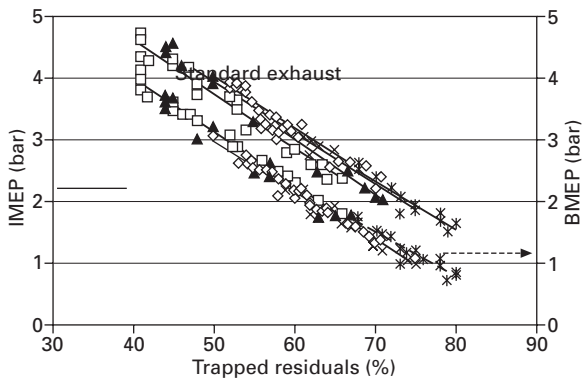

5.5 Relationship between residual fractions and engine output.

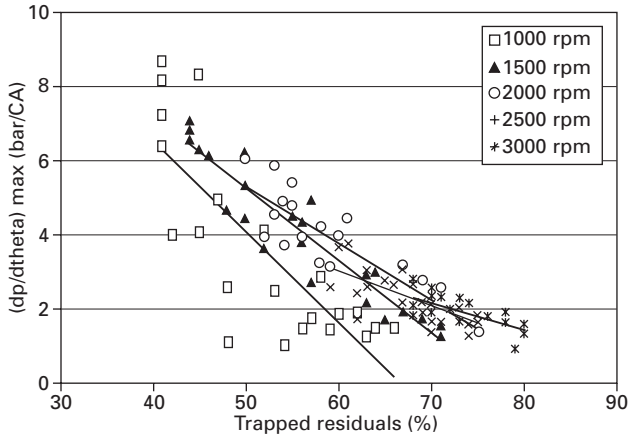

5.6 Effect of residual fractions on the maximum rate of pressure rise.

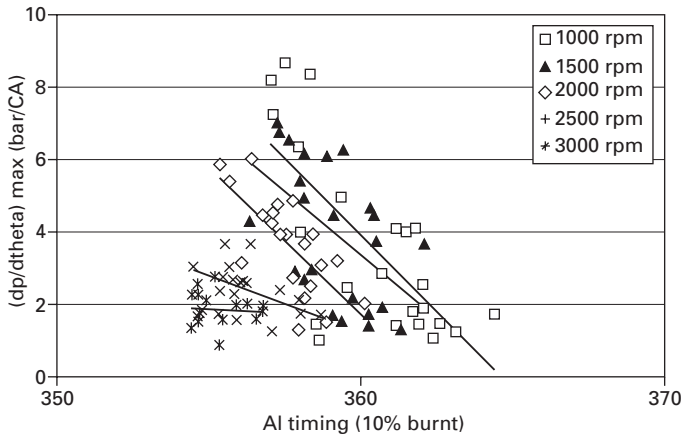

5.7 Relationship between start of combustion and the maximum rate of pressure rise.

cases, neither any distinctive knocking noise was present nor were the characteristic pressure fluctuations shown in the in-cylinder pressure traces during these tests. At these conditions, the NOx emissions were more than 2.5 g/kWh due to increased combustion temperature caused by the rapid pressure rise. In addition it is noted that the maximum rate of pressure rise could vary significantly at the same load point but different inlet valve timings. For example, at 1000 rpm and about 41% residuals, the maximum rates of pressure rise from two different cycles were 6.3 to 8.7 bar/CA, respectively.

The effect of residual fractions on the maximum rate of pressure rise shown may be better understood by looking at Fig. 5.7, where the maximum

rate of pressure rise is plotted against the crank angle at which 10% fuel had been burnt. It is apparent that results in Fig. 5.6 were to a great extent the result of changing combustion phasing, going from low load (high residual fraction) to high load (low residual fraction). Advanced combustion timing led to higher peak cylinder pressure and faster pressure rise. Hence, one effective way to moderate the rapid heat release rate at high load operation is to somehow retard the combustion phasing, such as the use of cooled EGR [4], lean-boosted intake [5], or lower effective compression ratio. Finally, it is also noted that there were additional changes in the maximum rate of pressure rise even at the same combustion timing, which were caused by the different combinations of intake and exhaust valve timings.

In order to assess the characteristics of CAI combustion, the in-cylinder pressure has been used to derive the fuel mass fraction burned as a function of crank angle. Figure 5.8 shows the crank angles at which 10% and 90% of fuel had been burnt, respectively. The auto-ignition started between 355 and 364 deg. CA, depending upon speed and load. Generally, at higher loads, the residuals' temperatures were higher and the auto-ignition started earlier. At higher engine speeds, the residuals' temperature prior to ignition was higher, hence the ignition started earlier as well. Further calculations have shown that temperature at the start of main combustion was about 1070 ± 50K throughout the CAI operational range and it increased slightly to 1150K at very high residual concentrations. As shown in Fig. 5.9, the combustion duration varied from 5 to 14 CA degrees, mainly dependent on load. The speed effect was not apparent, except for 1000 rpm at which combustion was slower and took about 3 CA degrees longer than the other speeds, probably because of higher heat losses at this speed.

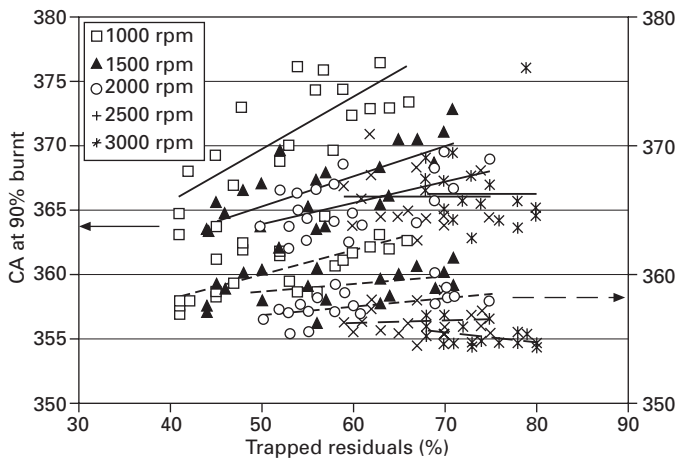

5.8 Effect of residual fractions on the start and finish of CAI combustion.

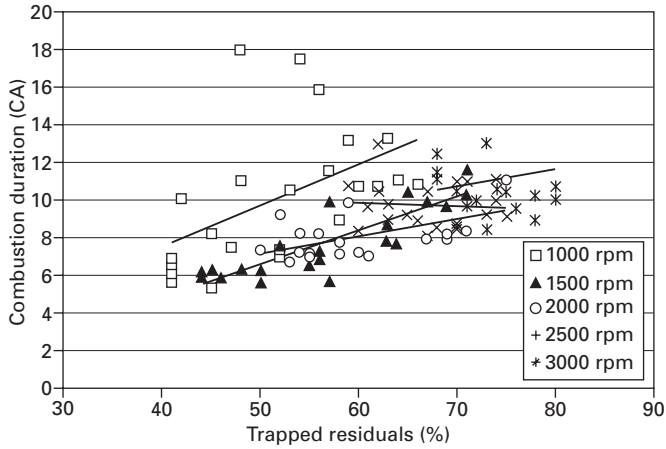

5.9 Effect of residual fractions on CAI combustion duration.

The above analyses show that the CAI combustion process was closely related to engine load. At higher loads, CAI combustion started earlier and burned faster, and the combustion temperature, exhaust temperature, peak pressure and maximum pressure rise were higher. The effect of speed seemed to be moderate. Higher speeds resulted in less heat losses, higher temperatures and earlier ignition.

5.3.2 Fuel consumption and emission characteristics

Figures 5.10 to 5.13 compare the fuel consumption and emission results of the CAI combustion mode and SI mode from the same engine. The SI engine operation was run with standard camshafts and the brake specific emissions before the catalyst were considered. Within the whole CAI range of speed and load, there were marked improvements in BSFC ranging from several percent at medium load to more than 30% at low load as shown in Fig. 5.10. The improvement in BSFC primarily came from the absence of pumping losses of throttling at part load. Figure 5.11 illustrates the effectiveness of CAI combustion in reducing the NOx emissions. Throughout the speed and load range, the NOx emission was reduced by up to 99%. Figure 5.12 shows that the unburned hydrocarbons were much higher from CAI combustion than that from SI combustion with port-fuel injection, but they were on a par with those from the stratified charge direct injection gasoline engine. In addition, Fig. 5.13 shows that the CAI combustion with residual gas trapping produced much less CO emissions than the SI engine, which was confirmed by other studies using the residual gas trapping method [1, 2]. The reduction in CO emissions is likely caused by the recycling of burned gases and their

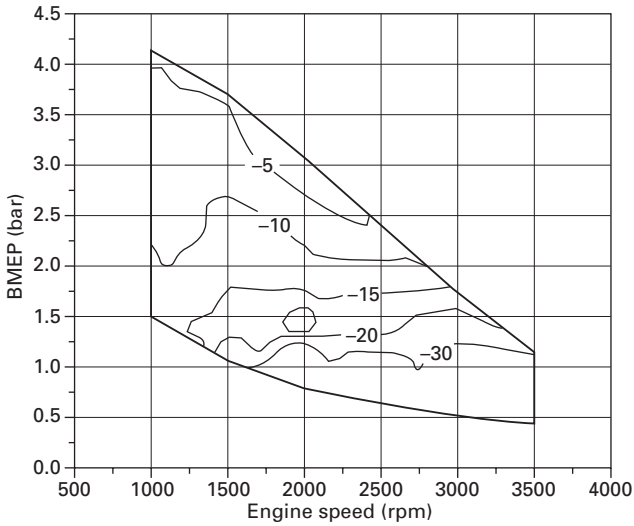

5.10 Changes in BSFC (%) with CAI combustion relative to SI.

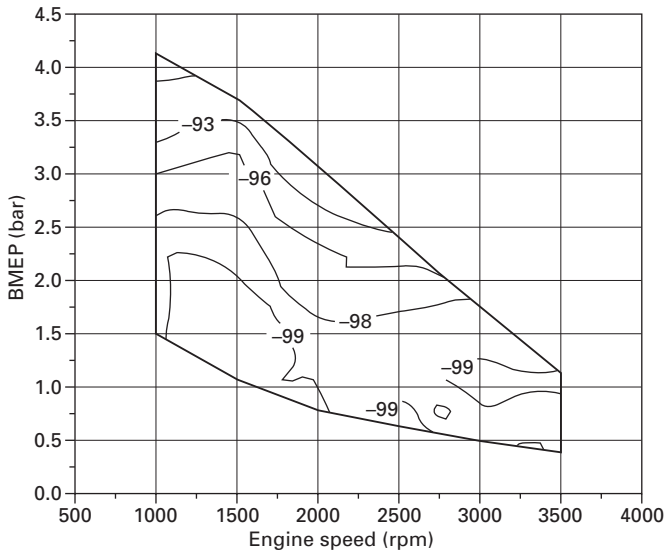

5.11 Changes in BSNOx emissions (%) with CAI combustion relative to SI.

subsequent conversion into CO_2 in the next cycle. It should be noted that CAI/HCCI combustion in the 4-stroke gasoline engine had been always associated with higher CO emissions than the SI combustion until the residual gas trapping method was employed.

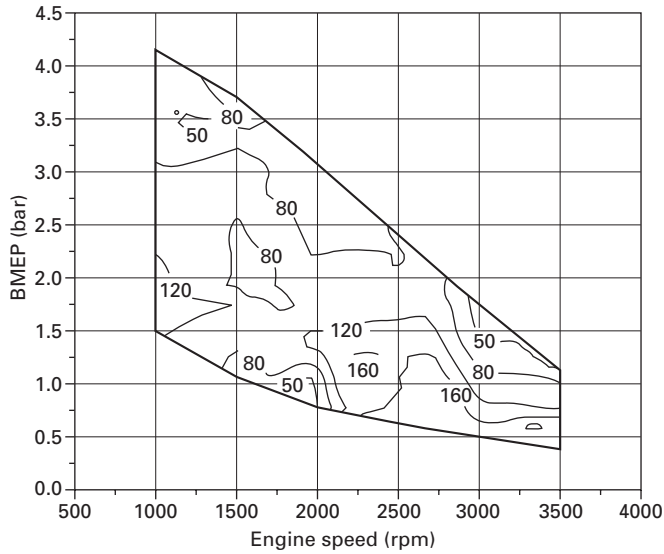

5.12 Changes in BSHCs emissions (%) with CAI combustion relative to SI.

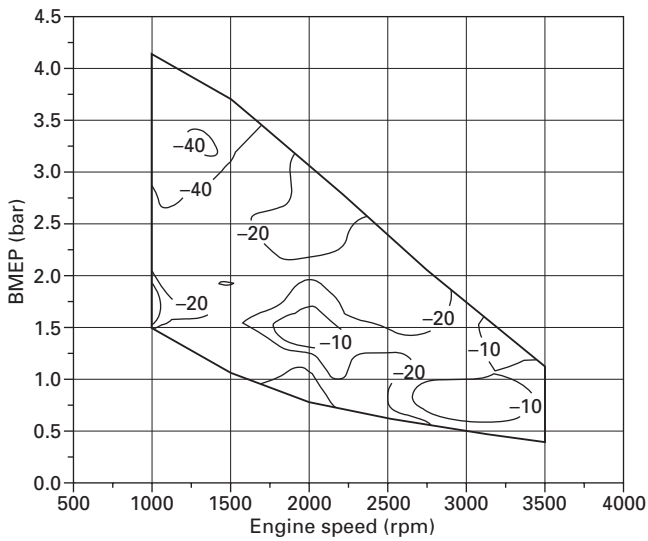

5.13 Changes in BSCO emissions (%) with CAI combustion relative to SI.

5.3.3 Extended CAI operation through combined variable valve lift and variable valve timing

The use of fixed lift camshafts allows a production type 4-stroke gasoline engine to achieve CAI operation with minimum modification, but the significantly reduced valve lift optimised for low speed operation leads to choked flow at higher engine speeds as shown in Fig. 5.4. In order to overcome such a limitation, combined continuous variable lift and timing devices have since been applied to 4-stroke gasoline engines by the author and his co-workers at the State Key Laboratory of Engines in Tianjin University [6] and by Ricardo UK Ltd [7]. Both engines are equipped with variable valve lift and timing devices on the intake and exhaust camshafts, based on the BMW's Valvetronic and Vanos systems in mass production. The introduction of continuously variable valve lift mechanism results not only in enlarged CAI operation at high engine speeds [7] but also provides a more flexible means of controlling the transition between SI and CAI operations throughout the engine's operational range [6].

5.4 Effect of direct injection on CAI combustion in the four-stroke gasoline engine

The above results have shown that CAI combustion can be achieved in a production type 4-cylinder gasoline engine with only modification to the camshafts. During the CAI operation, engine output is principally controlled by the EVC timing. As the engine load or speed increases, combustion starts earlier and burns faster, leading to too rapid a rate of heat release and very high peak cylinder pressure as well as higher fuel consumption. At the low load region, the very retarded combustion causes large cyclic variation and even partial burn. Therefore, it will be desirable and necessary to find other means capable of more independent control over the combustion phasing from the engine load, in order to improve the CAI combustion and its operational range. Research done at the author's laboratory [8–10] and others [11–13] has shown that direct fuel injection into the cylinder can be used as one of the most effective means of controlling the combustion phasing for optimised engine performance and emissions. This section will present some of the main findings from such studies.

As shown in Fig. 5.2(a), there are three significant phases occurring sequentially in the CAI engine cycle with negative valve overlap, namely, residuals trapping, residuals conditioning and CAI combustion. Each phase has an effect on the following, with the end-of-cycle conditions feeding back to the first phase in order to sustain the CAI operation continuously. The ***residual trapping phase*** is controlled primarily by the exhaust valve closing timing (variable early EVC) and the trapped residuals temperature.

Once trapped, the mass of the residuals is fixed for the subsequent cycle, but its temperature and pressure are variable during the ***residuals conditioning phase*** according to re-compression and re-expansion and further heat subtraction and heat addition if fuel can be injected directly into the residuals during that period. At the end of the residuals conditioning phase which also marks the beginning the intake period (variable late IVO), the released temperature and pressure of the residuals will affect the intake air flow, the charge dilution (residuals/total volume ratio) and the combustible charge temperature, while direct fuel injection during the intake and compression periods will affect the charge homogeneity or stratification as well as charge temperature and quantity, leading up to the ***CAI combustion phase*** which is characterised by the CAI ignition timing, heat release rate, IMEP, ISFC and exhaust emissions. The final exhaust gas temperature after CAI is then fed back to the next cycle to initiate the next residuals trapping phase.

The above analysis indicate that fuel injection timing can be grouped into three categories: (i) early injections during the negative valve overlap period, in which fuel is injected into the hot residual gas in the cylinder for the purpose of reforming the fuel or initiating the minor combustion if possible, and improving ignitability; (ii) mid-injections during the intake stroke and early compression stroke to create a homogeneous mixture of different charge temperature or quantity; (iii) late injections during the late compression stroke for charge/thermal stratification.

5.4.1 Early injections during the negative valve overlap period

The experimental results from a 4-cylinder DI gasoline engine are shown in Figs. 5.14 and 5.15 and Plates 5 and 6 (between pages 268 and 269) [10]. The engine has a displacement volume of 1.6 litres and a compression ratio of 11.5. A high pressure swirl injector mounted below and between the two intake valves was operated at an injection pressure of 100 bar. Both intake and exhaust camshafts were equipped with VVT devices and their cam lobes were machined to produce maximum valve lifts around 2 mm. As shown in Fig. 5.14, the early fuel injection had different effects on the pumping losses during the CAI engine cycle. For the stoichiometric mixture, the pumping losses due to re-compression and re-expansion decreased monotonically as the start of fuel injection was retarded from recompression to re-expansion before it levelled off after IVO. In comparison, for the lean fuel air mixture, the pumping work first increases to a peak as the injection timing was retarded towards TDC during the recompression stroke and then started to decrease as the injection takes place in the re-expansion process before it levelled off after IVO. Plate 5 (between pages 268 and 269) shows that the pressure traces became unsymmetrical about TDC of negative valve overlap

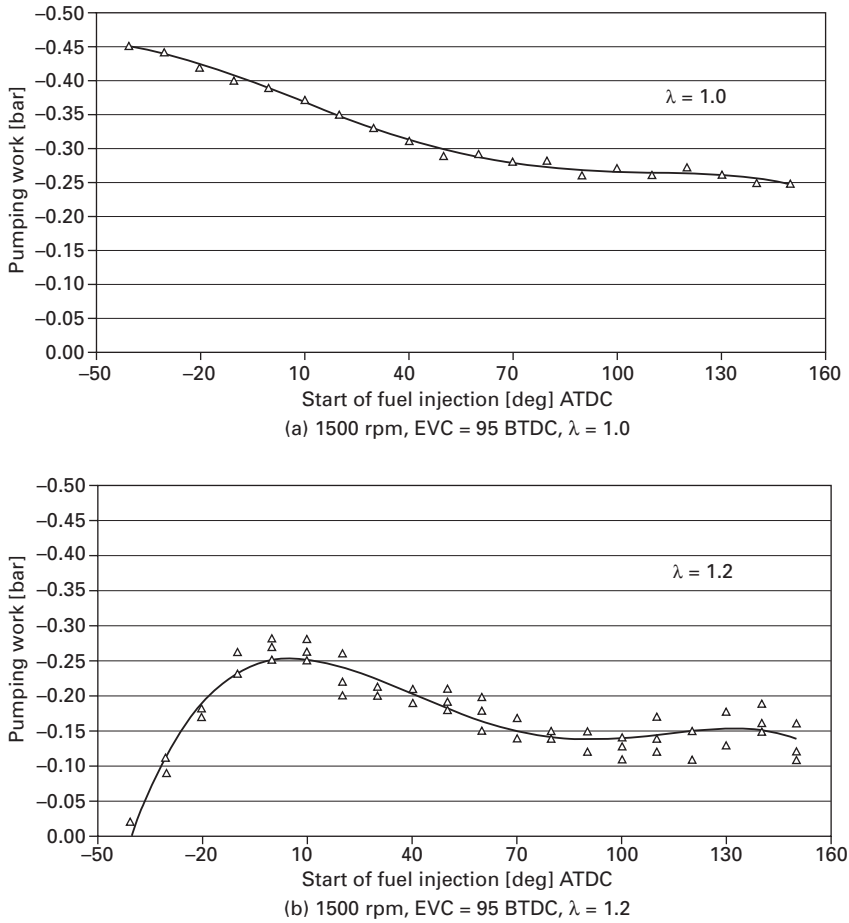

5.14 Effect of fuel injection timings on the pumping work.

as early injection took place during the recompression process; for the stoichiometric mixture the expansion pressure became lower as the injection was more advanced, and for the lean burn mixture opposite occurred, i.e., higher expansion pressure was observed with earlier injections. The corresponding heat release profiles in Plate 6 (between pages 268 and 269) indicate that some negative heat release occurred shortly after the injection starts, because of the charge cooling effect of fuel evaporation for both mixtures. However, positive heat release was also seen to occur afterwards when early injection into lean burn mixture takes place.

Figure 5.15(a) shows the effect of fuel injection timings on the main combustion process. It can be seen that the earlier the fuel injection took place during the negative valve overlap period, the more advanced the start of main combustion when the engine operated with a lean fuel air mixture.

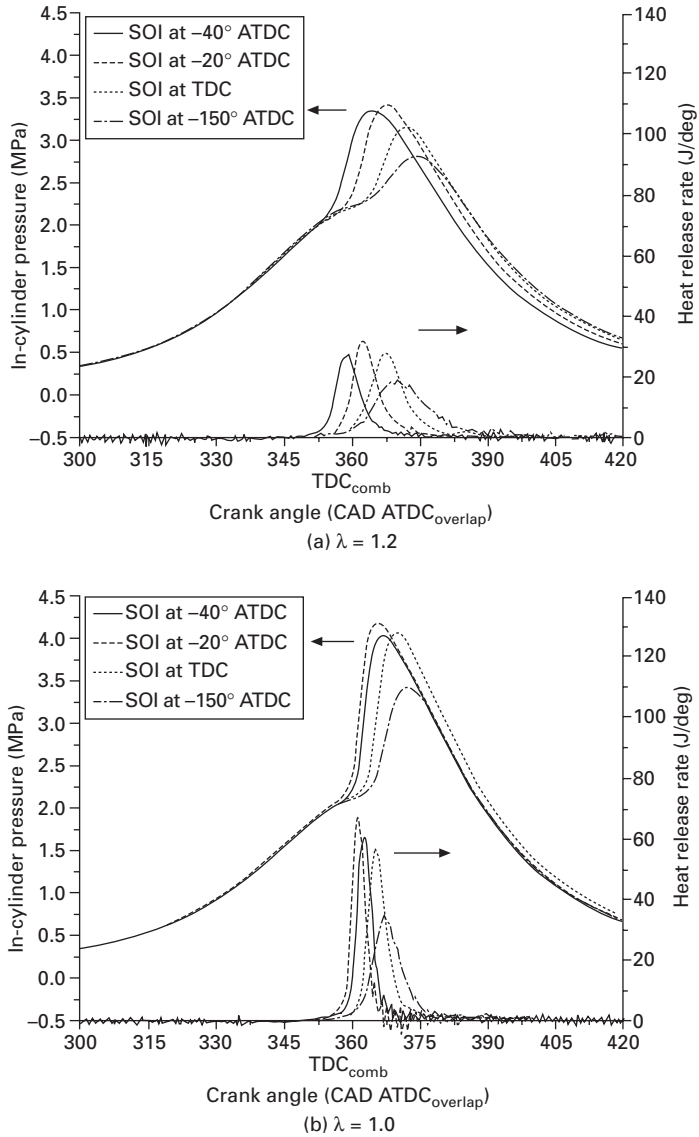

5.15 In-cylinder pressure and heat release profiles with various injection timings for lean and stoichiometric mixtures.

However, in the case of stoichiometric mixture shown in Fig. 5.15(b), fuel injection at 20 BTDC during the recompression phase led to the earliest combustion, followed by 40 BTDC and TDC injections. Delayed injection into the intake stroke resulted in the most retarded combustion and the lowest peak pressure in both stoichiometric and lean mixtures. In addition,

it can be seen that the early injections into lean burned mixtures led to more advanced combustion than for stoichiometric mixtures.

In order to understand better the underlying mechanisms, detailed analysis has been carried out on the physical and chemical processes taking place within the cylinder by means of 3-dimensional full cycle engine simulation [14]. The simulation programme is based on the KIVA3v with improvements in turbulence, the gas/wall heat transfer, spray atomisation, ignition and combustion and it takes into account the gas exchange processes that are crucial to the residual gas trapping method. The Shell ignition model is chosen and has been modified to simulate the auto-ignition process in low temperature combustion. For the high temperature combustion, a characteristic time combustion model is used. The transition from auto-ignition to the main combustion process is based on the local cell temperature: when the temperature of a cell exceeds 1080K, high temperature combustion model is activated for such a cell. The simulation programme was validated against engine experiments before it was applied to study CAI combustions. Plate 7 (between pages 268 and 269) shows the spatial distributions of charge temperature, equivalence ratio, local heat release rate at $TDC_{overlap}$ with early injections during the negative valve overlap period. These results show that heat release does occur when fuel is injected into a lean burn mixture ($\lambda = 1.2$) and it starts at the boundary of the fuel rich zone, where high temperature and oxygen availability favour the exothermic reactions. The temperature evolution and the early heat release associated with minor combustion during the negative valve overlap period are given in Fig. 5.16. It is noted that the case with injection at –40° $ATDC_{overlap}$ leads to more heat release than the other three injections. Approximately 3% of the total fuel energy is released during the negative valve overlap period with injection at –40° $ATDC_{overlap}$, as compared with 1.5%, 2.6% and 0.5% with injections at –75°, –20° $ATDC_{overlap}$ and $TDC_{overlap}$ respectively. The amount of heat released during the negative valve overlap is limited by the oxygen available as well as local charge temperature. As shown in Fig. 5.16, injection at –75° $ATDC_{overlap}$ lowers the charge temperature during the negative valve overlap so much that the heat release is largely limited by charge temperature. By comparison, lower charge temperature in the re-expansion process due to charge cooling effect and downward piston motion contribute to less heat released with injections at –20° $ATDC_{overlap}$ and $TDC_{overlap}$ than that with injection at –40° $ATDC_{overlap}$.

The corresponding pressure and heat release rate profiles for the main combustion process are given in Fig. 5.17. As it shows, the highest peak pressure and earliest combustion phasing are seen with injection at –40° $ATDC_{overlap}$, which also has the largest amount of early heat release during the negative valve overlap period. This indicates that the early heat release from the endothermic reactions during the negative valve overlap period is

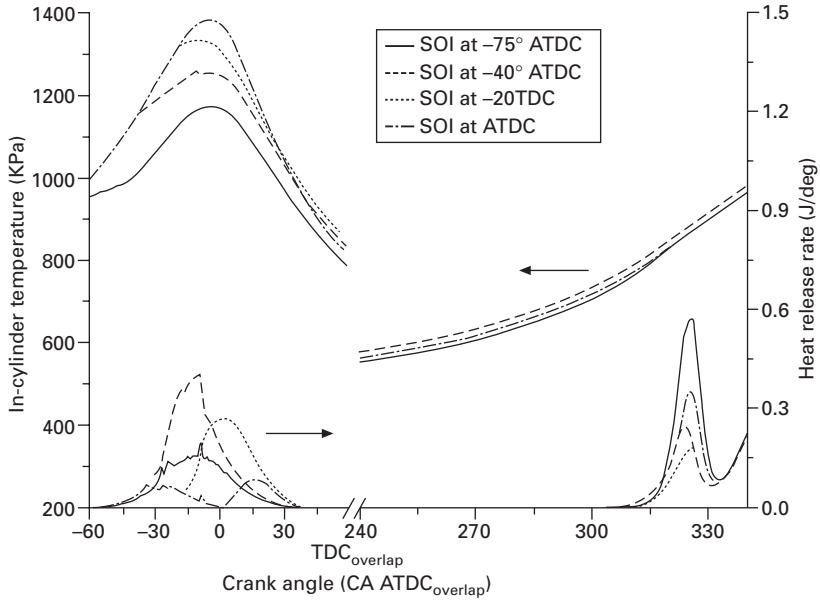

5.16 Temperature profiles and heat release curves during the negative valve overlap period and compression stroke at λ = 1.2.

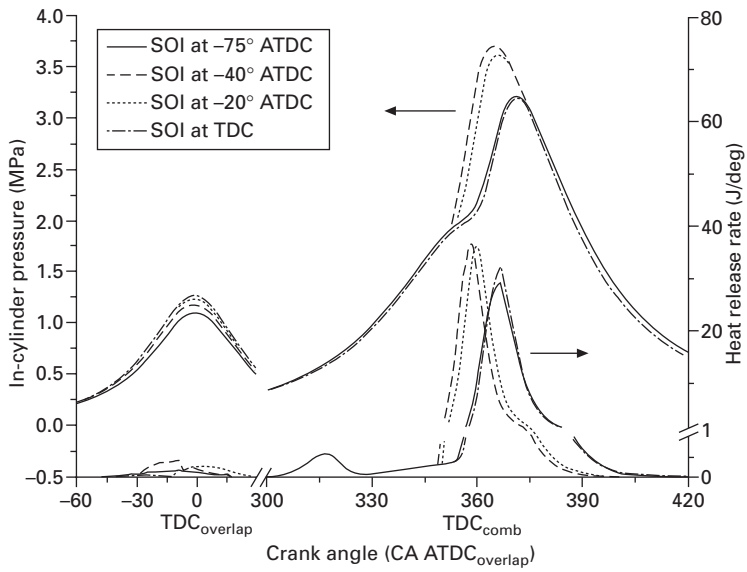

5.17 In-cylinder pressure and heat release rate profiles throughout the cycle at λ = 1.2.

primarily responsible for the earlier start of main combustion, due to elevated charge temperatures during the intake and compression strokes shown in Fig. 5.16.

For injections at –75° $ATDC_{overlap}$ and $TDC_{overlap}$, the thermal or charge heating effect becomes less significant due to a relatively small heat released during the negative valve overlap period. However, the first stage ignition due to low temperature heat release, which was observed in the experimental studies [3, 9, 10], occurs at 320° $ATDC_{overlap}$ prior to the start of main combustion, and it is more pronounced than that seen with –40° injection timing, despite its slightly lower charge temperature during the intake and early part of compression strokes, as shown in Fig. 5.16 and Fig. 5.17. This can be explained by referring to Fig. 5.18, which shows the traces of radical R and labile intermediate species Q, defined as products of low temperature auto-ignition chemistry in the Shell auto-ignition model [15]. As can be seen, large amounts of intermediate species Q formed during the negative valve overlap period with injection at –75° $ATDC_{overlap}$ can promote quick build-up of branching agent B, which leads to higher heat release during the first-stage of ignition as seen in Fig. 5.16.

The main combustion characteristics for injections during the negative valve overlap period are summarised in Table 5.1. The value of net IMEP is closely related to combustion phasing and pumping loss. Both too early combustion phasing and higher pumping losses contribute to lower IMEP values with injections at –40° and –20° $ATDC_{overlap}$, as compared with the injection at –75° $ATDC_{overlap}$. Comparing the cases with injections at –75° $ATDC_{overlap}$ and $TDC_{overlap}$, the combustion phasings of those two injection cases are quite similar, however the higher pumping losses result in lower IMEP with injection at $TDC_{overlap}$.

5.4.2 Mid and late injections during the intake and compression strokes

Using the same three dimensional full cycle engine simulation programme, the effect and underlying mechanism of mid and late injections on CAI combustion were examined. Figure 5.19 shows the pressure and heat release rate varying with injection timings. Comparing the two injections during the intake stroke, the start of combustion is slightly retarded with later injection timing (SOI at 150° $ATDC_{overlap}$), leading to lower peak pressure. Table 5.2 shows that there is little difference in the compression temperature between the two injections during the intake stroke. The delayed start of combustion with later injection is therefore likely related to the time available for fuel to mix with air and subsequent low temperature chemical reactions. However, the combustion phasing is advanced, as the injection is retarded further into the compression stroke (SOI at 218° $ATDC_{overlap}$). This is more likely due to

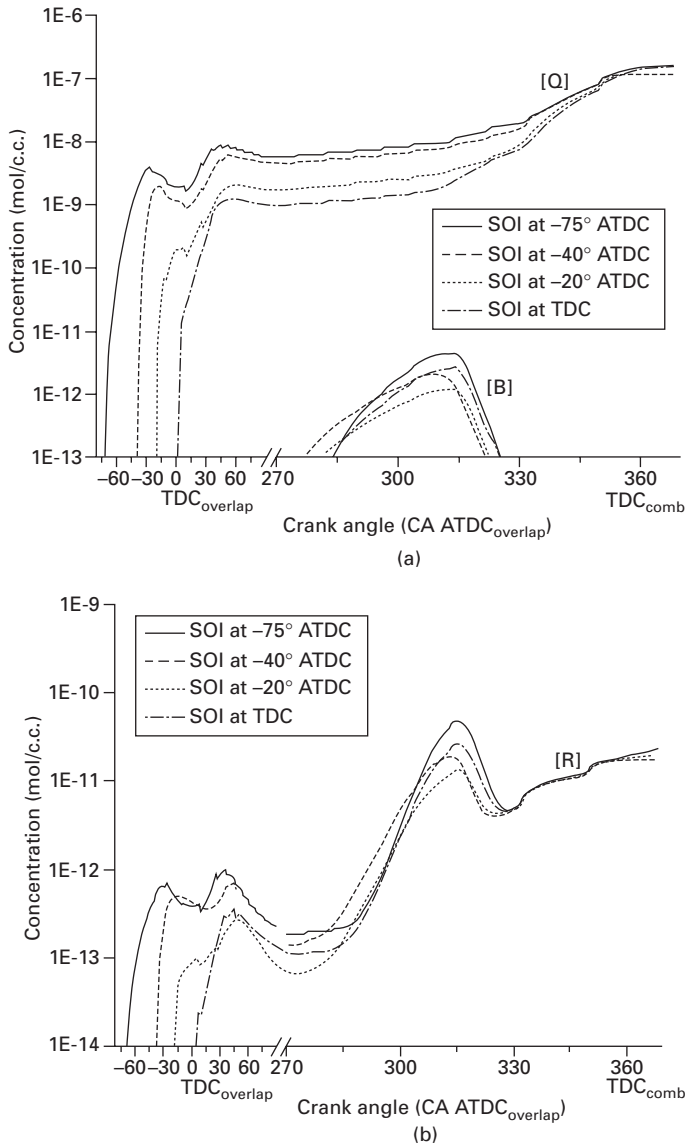

5.18 Temporal profiles of radical R and intermediate species Q and branching agent B-throughout the cycle with early injections.

the in-cylinder mixture stratification. A study of the scatter plot of equivalence ratio and temperature distributions in Fig. 5.20 reveals that the mixture stratification increases as the injection is retarded. The most stratified mixture charge can be seen with the late injection in the compression stroke, due to the shorter time interval between the end of injection and the ignition point.

Table 5.1 Effect of early fuel injection timings on CAI combustion at 1500 rpm and $\lambda = 1.2$

	SOI at –75 ATDC	SOI at –40 ATDC	SOI at –20 ATDC	SOI at TDC
10% MFB [°CA]	360.0	353.4	354.8	360.8
50% MFB [°CA]	366.6	358.5	360.2	366.8
90% MFB [°CA]	376.0	367.0	368.0	375.5
10–50% MFB [°CA]	6.6	5.1	5.4	6.0
50–90% MFB [°CA]	9.4	8.5	7.8	8.7
10–90% MFB [°CA]	16.0	13.6	13.2	14.7
Pmax [MPa]	3.21	3.71	3.62	3.19
Tmax [K]	1880	2012	1987	1895
Net IMEP [MPa]	0.311	0.287	0.291	0.305
ISFC [g/kW·h]	248	269	265	253
Comb. efficiency	0.95	0.95	0.94	0.94
ISNOx [g/kg·fuel]	0.083	0.892	0.653	0.239

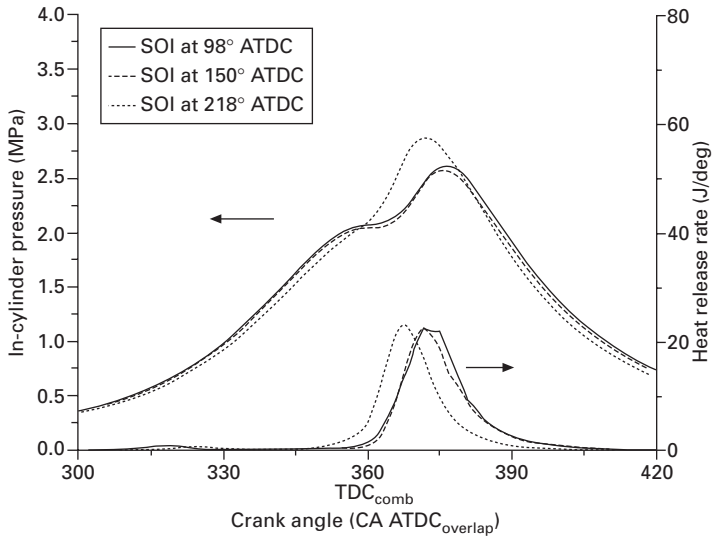

5.19 Pressure and heat release rate profiles with mid and late injections.

In order to investigate the effect of fuel stratification, a further analysis is carried out on the distributions of equivalence ratio, charge temperature and local heat release rate. As indicated in Plate 8 (between pages 268 and 269), at 350° CA ATDC$_{overlap}$, the presence of more fuel rich pockets with injection at 218° ATDC$_{overlap}$ (10° BTDC in the compression stroke) gives out more heat than that of homogeneous charge with injection at 98° ATDC$_{overlap}$, resulting in earlier start of combustion with late injection at the compression

Table 5.2 Effect of mid and later fuel injection timings on CAI combustion at 1500 rpm and λ = 1.2

	SOI at 98 ATDC	SOI at 150 ATDC	SOI at 218 ATDC
10% MFB [°CA]	364.8	365.2	360.3
50% MFB [°CA]	373.6	373.3	368.3
90% MFB [°CA]	386.0	387.8	379.0
10–50% MFB [°CA]	8.8	8.1	8.0
50–90% MFB [°CA]	12.4	14.5	10.7
10–90% MFB [°CA]	21.2	22.6	18.7
Pmax [MPa]	2.61	2.57	2.86
Tmax [K]	1746	1707	1763
Net IMEP [MPa]	0.304	0.292	0.279
ISFC [g/kW·h]	254	264	276
Comb. efficiency	0.93	0.90	0.85
ISNOx [g/kg·fuel]	0.0232	0.0383	0.0542
Temp. at 340° ATDC [K]	967	965	957

stroke. However, the presence of over-lean and over-rich mixtures due to late injection in the compression stroke decreases the combustion efficiency and hence lower IMEP value, as also shown in Table 5.2.

Based on the above studies, the mechanisms of combustion phasing control by injection timing in a lean-burn CAI DI gasoline engine can be summarised as shown in Fig. 5.21. The factors include the thermal/chemical effects caused by early injection during the negative valve overlap period, or charge cooling effect by injection during the intake stroke, or fuel stratification effect by late injection at the compression stroke. Heat release or thermal effect associated with injection during the negative valve overlap period has a dominant effect on advancing the start of main combustion. The chemical effect is secondary and its presence promotes the first stage of ignition during the compression stroke. However, injection during the negative valve overlap period can also slow down the main combustion process, if the in-cylinder temperature during the recompression process is reduced significantly due to charge cooling effect and hence less or no heat release reactions can take place during the recompression and re-expansion. The late injection during the compression stroke can lead to an advanced combustion due to charge stratification, whilst the injection during the intake stroke slows down the start of main combustion by charge cooling effects.

5.4.3 Effect of split fuel injections

In the previous section, injection timing in the single fuel injection strategy has been shown to have a large effect on combustion characteristics. In order to optimise combustion phasing and engine-out emissions, split fuel injection

is investigated using the full engine simulation programme. The proportion of fuel injected in each of the two injections is varied from 10%, 15%, 25%, 50% and 75%, while the start of the first and second injections are fixed at –75° and 98° $ATDC_{overlap}$, respectively. The total amount of fuel in each

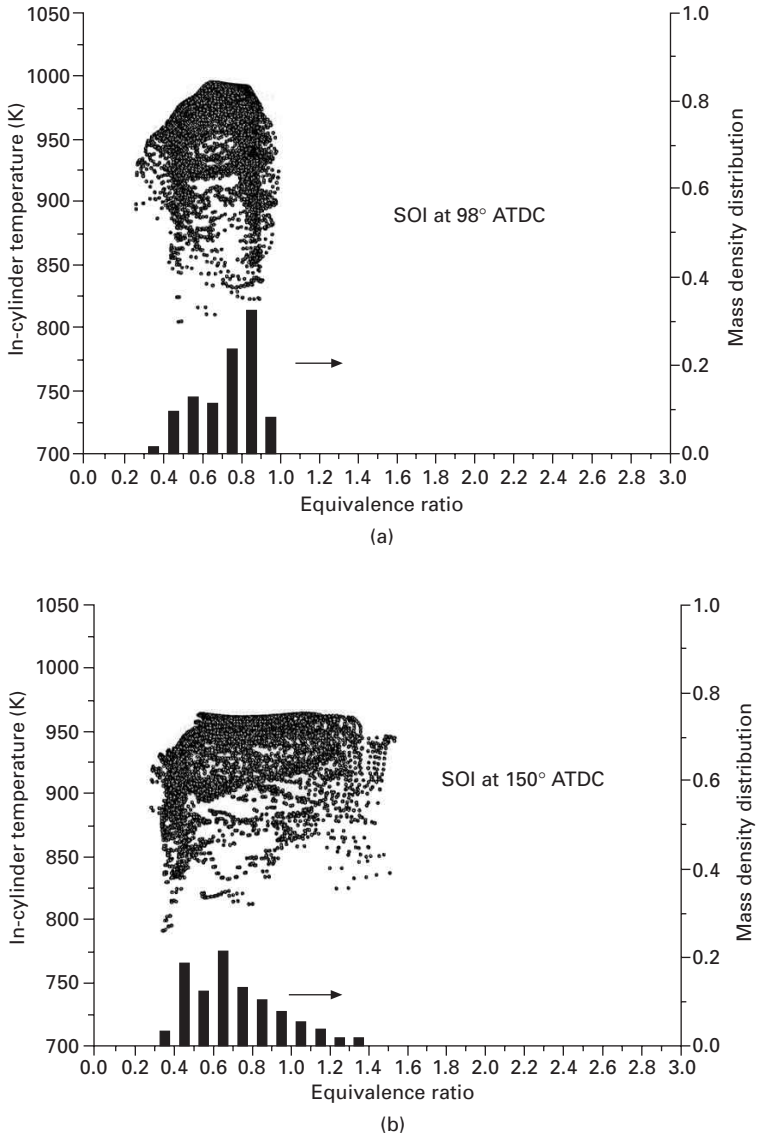

5.20 Statistical analysis of in-cylinder temperature and fuel distributions at 20°CA BTDC with mid and later fuel injections.

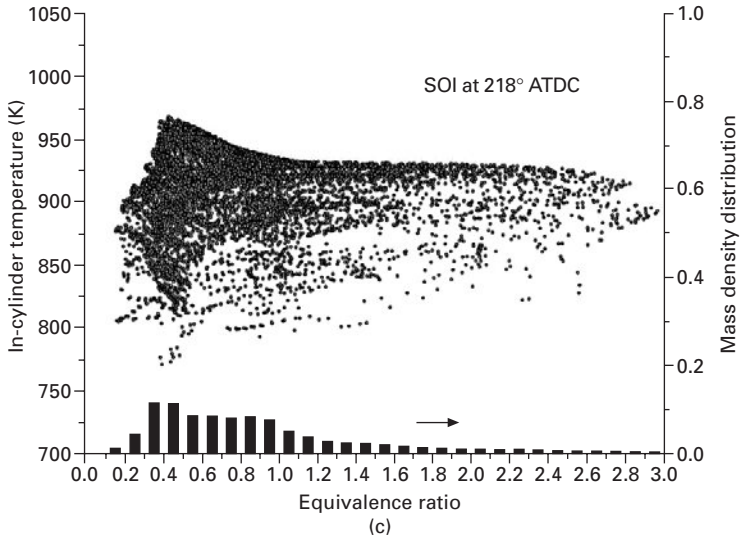

5.20 Continued

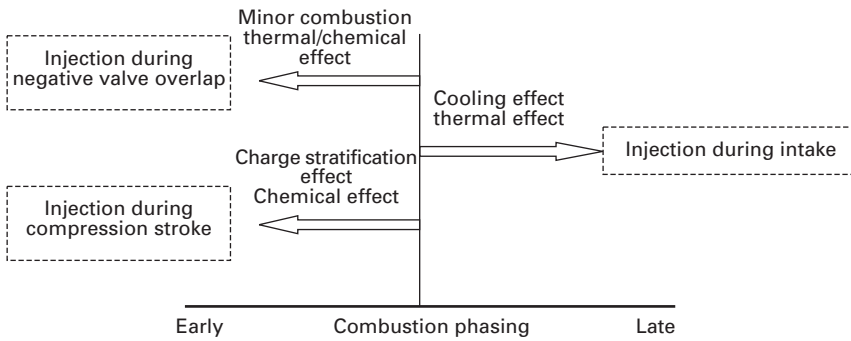

5.21 Summary of single fuel injection timing on combustion phasing.

engine cycle is kept constant (9 mg), with an overall equivalence ratio around 0.8 and at 1500 rpm.

The heat release curves during the negative valve overlap period with variable split injection ratios are given in Fig. 5.22. It is noted that the early heat release during the negative valve overlap period remains almost constant when less than 25% of fuel is injected in the first injection. When the amount of fuel injected in the first injection is increased to 50% or more the early heat release during the negative valve overlap period is reduced. This could be explained by referring to the corresponding temperature during the negative valve overlap period as shown in Table 5.3. It can be seen that the increased portion of fuel injected during the recompression process leads to significant

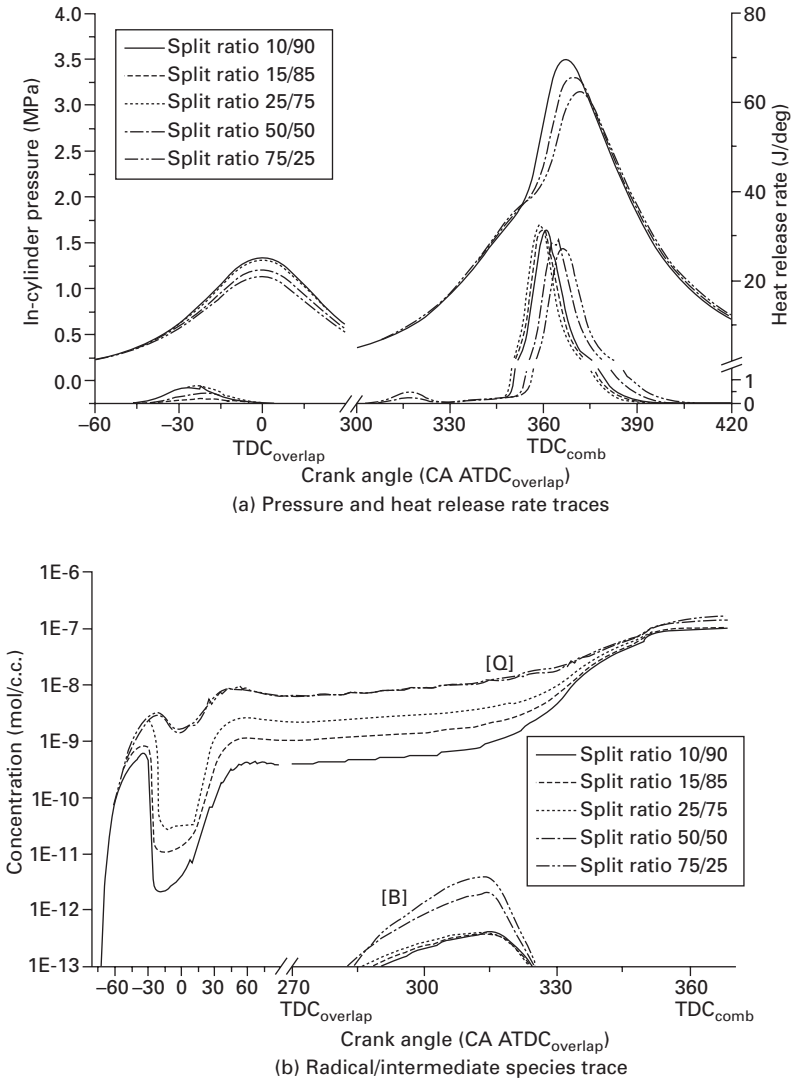

5.22 Effect of split fuel injections on auto-ignition reactions and CAI combustion.

reduction in temperature, due to fuel evaporation, resulting in smaller early heat release associated with minor combustion during the negative valve overlap period shown in Fig. 5.22(a). On the other hand, more fuel injected during the negative valve overlap promotes the build-up of radical and intermediate species, which leads to higher first stage heat release at 320° ATDC$_{overlap}$ with 50/50 and 75/25 split injections as shown in Fig. 5.22(b). In addition, it is noted that earlier start of main combustion for the first three

Table 5.3 Effect of split fuel injections on CAI combustion at 1500 rpm and λ = 1.2

	Inject. ratio 10/90	Inject. ratio 15/85	Inject. ratio 25/75	Inject. ratio 50/50	Inject. ratio 75/25
Early heat release/total	0.055	0.056	0.060	0.036	0.021
Temp. at $TDC_{overlap}$ [K]	1452	1443	1413	1298	1218
10% MFB [°CA]	355.5	354.5	353.5	358.3	360.4
50% MFB [°CA]	361.5	360.5	359.4	364.8	367.1
90% MFB [°CA]	372.1	371.0	369.1	375.0	377.4
10–50% MFB [°CA]	6.0	6.0	5.9	6.5	6.7
50–90% MFB [°CA]	10.6	10.5	9.7	10.2	10.3
10–90% MFB [°CA]	16.6	16.5	15.6	16.7	17.0
Pmax [MPa]	3.50	3.55	3.61	3.31	3.15
Tmax [K]	1965	1979	2000	1912	1866
PMEP [MPa]	–0.0160	–0.0145	–0.0133	–0.0241	–0.0329
Net IMEP [MPa]	0.313	0.310	0.309	0.314	0.311
ISFC [g/kW·h]	247	249	250	246	248
Comb. efficiency	0.96	0.96	0.96	0.96	0.96
ISNOx [g/kg·fuel]	0.312	0.365	0.452	0.146	0.080

cases is caused by the greater amount of heat released during the negative valve overlap period and the subsequent higher charge temperature. This indicates that the thermal effect due to early injection during the negative valve overlap period seems to play a predominant role in determining the combustion phasing. Furthermore, comparing 10/90, 15/85 and 25/75 split injections, the earlier start of main combustion with 25/75 split injection is attributed to the higher level of radical and intermediate species present prior to the main combustion shown in Fig. 5.22(b), since a similar amount of heat has been released during the negative valve overlap period as shown in Table 5.3 and Fig. 5.22(a).

Table 5.3 shows the main combustion characteristics and engine performance with different split injection strategies. It is noted that the highest amount of heat release during the negative valve overlap period is obtained with 25/75 split injection, which leads to the most advanced crank angle of 10% MFB or the start of main combustion, the shortest combustion duration and the highest peak cylinder temperature, and hence the highest NOx emissions. As also shown in Table 5.3, the pumping loss is at its lowest value with 25/75 split injection. This can be explained by the opposing effects of charge cooling and heat release on the pumping work during the negative valve overlap period. As more fuel is injected into the negative valve overlap period, the charge cooling effect lowers the charge temperature, and hence inhibits the fuel reforming and heat release process as shown in Fig. 5.22(a), but more importantly the greater charge cooling effect due to the increased first fuel injection causes the cylinder pressure to drop more during the re-

expansion stage, and hence higher PMEP. Whilst smaller amounts of fuel injection experience earlier and more heat release during the re-compression stage, which results in larger re-compression work than the re-expansion work during the negative valve overlap, leading to higher PMEP. Although the 25/75 split injection has the lowest PMEP, it has the lowest IMEP or highest ISFC. This is due to that fact that ignition and combustion are too advanced (with the crank angle of 50% MFB just before TDC_{comb}). The best ISFC is obtained with 10/90 or 50/50 split injections, whilst 90/10 split injection results in the lowest NOx emission. These results demonstrate that split injection strategy could be used to achieve different optimisation results as required.

In parallel to the analytical studies described here, experimental studies on single cylinder engines with an air assisted injector [16] and high pressure swirl injector [13] have been carried out and similar trends have been noted. Furthermore, the split injection strategy has been used in the closed loop control over the engine output during the switching process between CAI/SI combustion in a four-cylinder DI gasoline engine with switching tappets [17].

5.5 Effect of spark ignition on CAI combustion in the four-stroke gasoline engine

When CAI combustion was achieved in the 4-cylinder PFI gasoline engine [3], it was found that the engine could operate stably with the spark disabled and the spark had little effect on CAI combustion within the range of CAI operation. Subsequent studies on single and multi-cylinder direct injection gasoline engines [8–10] have also shown that the presence of spark discharge hardly affected CAI engine operation when the engine was operating well within the CAI operational range. However, as attempts were made to extend the low load limit of CAI combustion, the effect of spark discharge became noticeable and in some cases the presence of spark was crucial to get CAI combustion going. This section will present some of the results on spark assisted CAI combustion.

The same 4-cylinder 1.6 litre prototype DI gasoline engine as described in Section 5.4.1 was used and made to operate with CAI combustion using the negative valve overlap approach [18]. As shown in Fig. 5.23, for the chosen EVC and IVO timings the presence and timing of spark discharge caused significant changes to the IMEP values for all the injection timings investigated. In general, the introduction of spark led to higher engine output and better fuel consumption at the same load. For each injection timing, there was an optimal spark timing for maximum engine output in the spark assisted CAI operation mode. Such spark timing is equivalent to the MBT timing for SI combustion. As shown in Fig. 5.24(a), as the spark timing was advanced, the

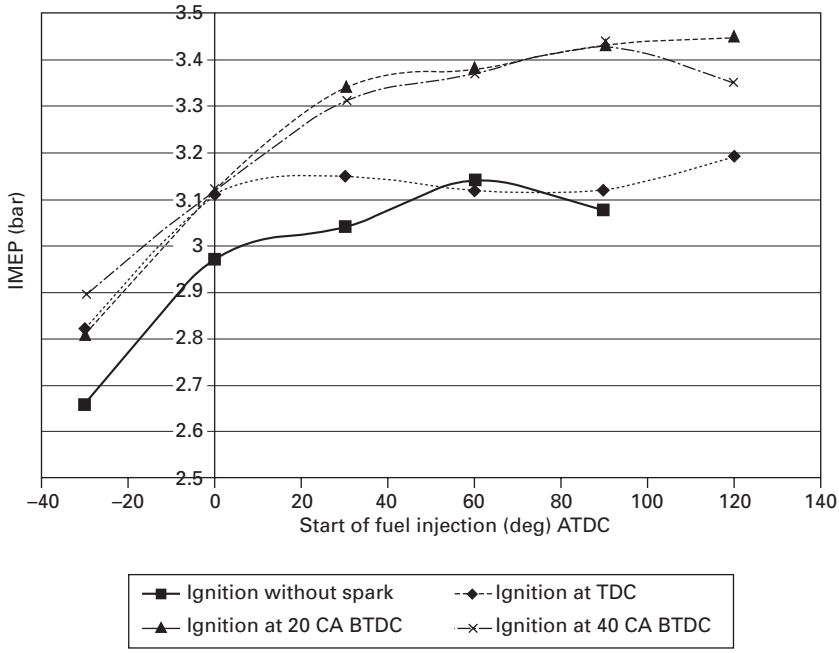

5.23 Effect of spark ignition on CAI engine output at 1500 rpm and $\lambda = 1.2$.

start of combustion consequentially advanced towards TDC. For this particular case, the maximum IMEP was reached with a spark timing of 20 CA BTDC. As the spark ignition was advanced to 40 CA BTDC, the IMEP dropped to a lower value due to early combustion.

In addition, it is noticed that the effect of spark was more pronounced with later injection at 90 CA ATDC (Fig. 5.24(b)) than the early injection at 30 CA ATDC (Fig. 5.24(a)). There are two likely reasons. Firstly, the later injection tends to render a stratified charge and hence more ignitable combustible charge near the spark plug for initial flame propagation. Secondly, there is less time available for the mixing of fuel/air/hot residual gas to take place and hence fewer opportunities for auto-ignition reactions to progress.

Heat release analysis shown in Table 5.4 also reveals that the presence of spark has a more pronounced effect on the 50–90% burn duration rather than the earlier stage. The 50–90% mass fraction burned (MFB) stage has the characteristics of typical CAI operation with very fast heat release rate as the auto-ignition combustion takes place simultaneously across the unburned mixture. Table 5.4 also shows that the spark assisted CAI leads to significant reduction in the COV imep value as combustion becomes more stable and repeatable.

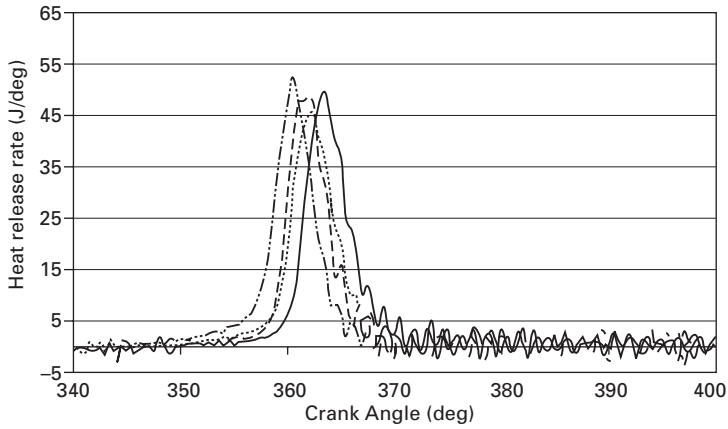

(a) Heat release rate curves for SOI at 30° $ATDC_{overlap}$

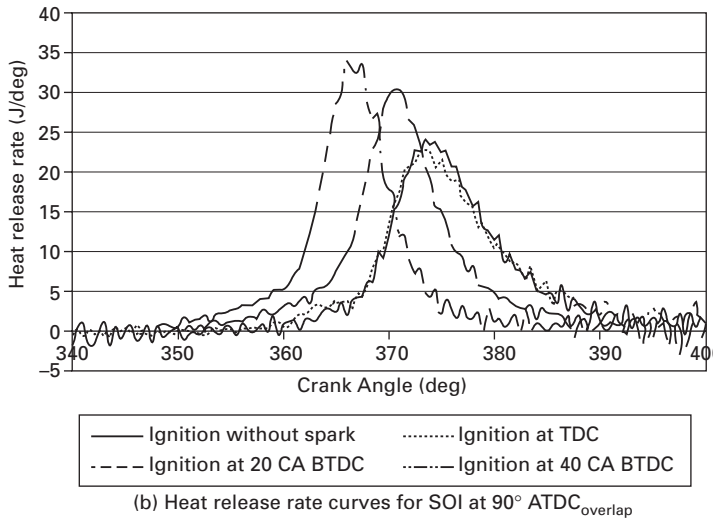

(b) Heat release rate curves for SOI at 90° $ATDC_{overlap}$

5.24 Effect of spark ignition on CAI engine output at 1500 rpm and λ = 1.2.

As shown in Fig. 5.25(a) and (b), spark assisted CAI had a favourable effect on reducing uHC and CO emissions. With the introduction of spark ignition, combustion now took place closer to TDC at higher temperature and pressure and was more stable, leading to more complete burning of CO and uHCs but higher NOx emissions as shown in Fig. 5.25(c).

Finally, it is worthwhile to consider the spark assisted CAI region in relation to the SI and CAI regions for an engine operating with negative valve overlap. As shown in Plate 9 (between pages 268 and 269), all three combustion modes could be accomplished with the residual gas trapping method using the same set of low lift camshafts. SI combustion occurred on

Table 5.4 Effect of spark ignition on CAI combustion and engine performance at 1500 rpm, λ = 1.2 and SOI@60°CA BTDC

Combustion and performance parameters	CAI	SI @ TDC	SI @ 20°CA BTDC	SI @ 40°CA BTDC
10% mass burned (CA)	368.0	366.6	363.7	359.9
50% mass burned (CA)	375.4	376.1	370.7	366.1
90% mass burned (CA)	394.1	390.3	381.9	378.0
10–50% burn duration (CA)	7.4	9.5	7	6.2
50–90% burn duration (CA)	18.7	14.2	11.2	11.9
10–90% burn duration (CA)	26.1	23.8	18.2	18.1
Peak pressure (MPa)	26.4	24.8	32.3	37.2
Location of peak pressure	379	378.5	374.5	370
NET IMEP (MPa)	3.14	3.12	3.38	3.37
T_{exh} (K)	413	425	384	384
Trapped residuals (%)	44.91	43.27	45.86	46.42
Temperature at IVC (K)	436	452	445	440
ISFC (g/kWh)	301.2	299	285.7	282.6
COV (%)	3.51	9.06	1.736	1.17

the left-hand side of the map where EVC timings were most retarded and in-cylinder burned gas fractions were lowest, whilst CAI combustion happened on the opposite side where the highest in-cylinder burned gas fractions were obtained due to the most advanced EVC timings. Spark assisted CAI was located in the boundary region between SI and CAI combustion where in-cylinder charge was too diluted for SI combustion and the charge temperature was too low for self-ignition to occur near TDC.

Currently, traditional SI and newly emerging CAI combustion have shown limitations in their operating range with regards EGR tolerance as well as load, see Fig. 5.26, such that a step change is required to switch between the operating modes with the current technologies. Therefore, the enlargement of CAI operational range and increased EGR tolerance in SI mode would be required in order to take advantage the full potential of CAI operation and to provide less frequent and, more importantly, a smooth transition between SI and CAI operations by closing the SI/CAI transitional gap and by identifying a suitable transitional mode between the two operations. The results shown in Plate 8 (between pages 268 and 269) indicate that spark assisted CAI combustion could be used as a method of achieving smooth transition between SI and CAI operations.

5.6 Summary

CAI combustion has been realised in both single cylinder research engines and multi-cylinder production type PFI and DI gasoline engines using the negative valve overlap approach. It is achieved by trapping copious amount

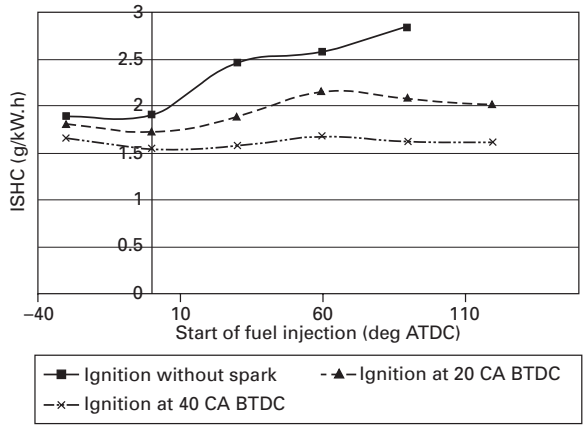

(a) uHC emissions

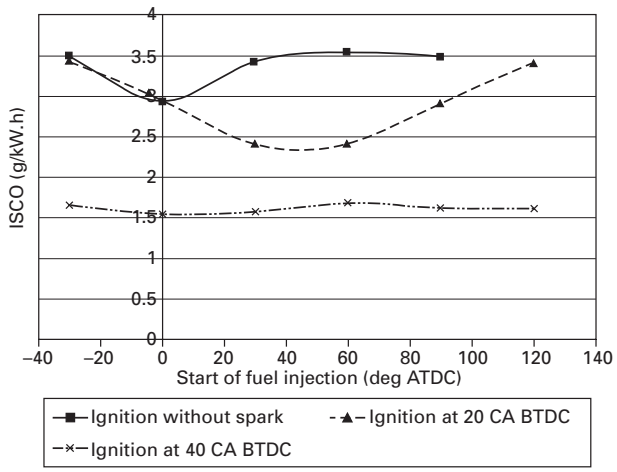

(b) CO emissions

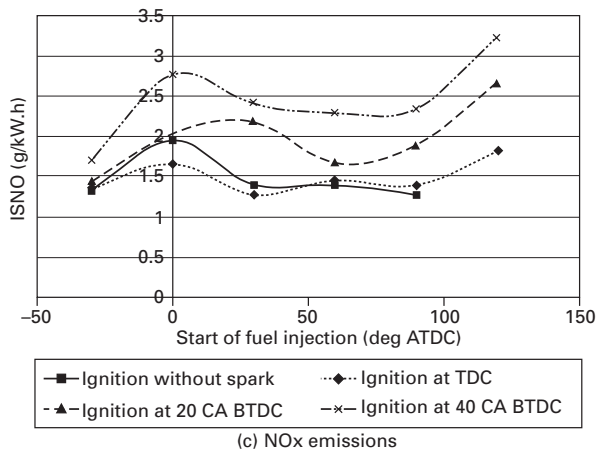

(c) NOx emissions

5.25 Effect of spark ignition on CAI engine emissions at 1500 rpm and λ = 1.2.

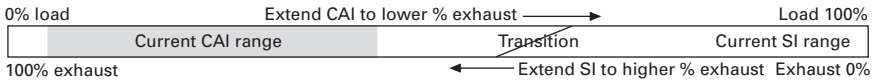

5.26 Engine tolerance to in-cylinder exhaust gas concentration.

of burned gases in the cylinder through closing the exhaust valves early. Such engines are characterised with superior fuel economy due to the lack of throttling loss and extremely low NOx emissions. The only modification required is the camshafts on the engine and hence it is a simple and effective technology that can be readily adapted to production engines. However, the range of CAI operation needs to be significantly extended not only to the high load region but also the low load region to take advantage the fuel economy and low emission benefits across the vehicle driving modes. In addition, additional and more independent control over CAI output and combustion phasing are required for optimised performance and emissions. One such technology reported in this chapter is direct fuel injection. It has shown that fuel injection timing and split injections can be used as an effective means to control CAI combustion. In addition, it offers better control over the switching process between SI and CAI combustion. Finally, it has been shown that CAI combustion could be assisted with the presence of spark discharge for better engine performance and fuel economy. Such spark assisted CAI combustion is found to lie in the boundary regions between spark ignited flame propagation combustion and multiple auto-ignition dominant combustion and it could be used to bridge the gap between the conventional SI combustion with moderate exhaust gas dilution and CAI combustion at very high exhaust gas dilution, opening up the possibility of engine load control through variable exhaust dilutions throughout its load range for simultaneous reduction in fuel consumption and vehicle exhaust emissions.

5.7 References

1. Koopmans, L., and Denbratt, I., 'A four stroke camless engine, operated in homogeneous charge compression ignition mode with a commercial gasoline', SAE paper 2001-01-3610, 2001.
2. Law, D., *et al*., 'Controlled combustion in an IC-engine with a fully variable valve train', SAE paper 2000-01-0251, 2000.
3. Li, J., Zhao, H., and Ladommatos, N., 'Research and development of controlled auto-ignition (CAI) combustion in a four-stroke multi-cylinder gasoline engine', SAE paper 2001-01-3608, 2001.
4. Cairns, A., and Blaxill, H., 'The effects of combined internal and external exhaust gas recirculation on gasoline controlled autoignition', SAE 2005-01-0133, 2005.
5. Cairns, A., and Blaxill, H., 'Lean boost and exhaust recirculation for high load controlled autoignition', SAE 2005-01-3744, 2005.
6. Hui Xie, S. Hou, Yan Zhang, Jing Qin, and Hua Zhao, 'Simulation study on control

strategy of gasoline CAI Engine operation based on a 4-variable valve actuating system-4VVAS', SAE Paper 2006-01-1083, 2006.
7. Stokes, J., Lake, T., Murphy, R., Osborne, R., Patterson, J., and Seabrook, J., 'Gasoline Engine Operation with Twin Mechanical Variable Lift (Tmvl) Valvetrain-Stage 1: Si and Cai Combustion with Port Fuel Injection', SAE Paper 2005-01-0752, 2005.
8. Leach, B., Zhao, H., Li, Y., Ma, T., 'Control of CAI combustion through injection timing in a GDI engine with an air-assited injector', SAE Paper 2005-01-0134, 2005.
9. Li, Y., Zhao H., Bruzos N., Ma T., and Leach B., 'Effect of Injection Timing on Mixture and CAI Combustion in a GDI Engine with an Air-Assisted Injector', SAE Paper 2006-01-0206, SAE Special Publication SP-2005, 2006.
10. Standing, R., Kalian, N., Ma, T., Zhao, H., 'Effects of injection timing and valve timings on CAI operation in a multi-cylinder DI gasoline engine', SAE paper 2005-01-0132, 2005.
11. Marriott, C., and Reitz, R., 'Experimental Investigation of direct injection-gasoline for premixed compression ignited combustion phasing control', SAE 2002-01-0418, 2002.
12. Sjoberg, M., Edling, L., Eliassen, T., Magnusson, L., and Angstrom, H., 'GDI HCCI: Effects of injection timing and air swirl on fuel stratification, combustion and emission formation', SAE Paper 2002-01-0106, 2002.
13. Urushihara, T., Hiraya, K., Kakuhou, A., and Itoh, T., 'Expansion of HCCI Operating Region by the Combination of Direct Fuel Injection, Negative Valve Overlap and Internal Fuel Reformation', SAE Paper 2003-01-0749, 2003.
14. Cao, L, Zhao, H., Jiang. X, Kalin, N., 'Investigation into the Effect of Injection Timing on Stoichiometric and Lean CAI operations in a 4-Stroke GDI Engine', SAE Paper 2006-01-0417, 2006.
15. Halstead, M., Prothero, A., and Quinn, C.P., 'The Autoignition of Hydro-Carbon Fuels at High Temperatures and Pressures – Fitting of a Mathematical Model', *Combustion and Flame*, 30, pp. 45–60, 1977.
16. Li, Y., Zhao H., Bruzos N., and Leach B., 'Control of CAI combustion by injection in a DI engine', Paper submitted to *Proc. IMechE*, Part D, 2006.
17. Herrmann, H.-O., Herweg, R., Karl, G., Pfau, M., and Stelter, M., 'Der Einsatz der Benzindirekteinspritzung in Ottomotoren mit homogen-kompressionsgezündeter Verbrennung Direkteinspritzung im Ottomotor V', Haus der Technik, Essen 2005.
18. Kalian, N., *Investigation of CAI and SI combustion in a 4-cylinder Direct Injection Gasoline Engine*, PhD thesis, Brunel University, Sept., 2006.

6

Four-stroke CAI engines with internal exhaust gas recirculation (EGR)

A FÜRHAPTER, AVL List GmbH, Austria

6.1 Introduction

In order to find a simple and precisely controllable method to bring a homogeneous cylinder charge to its auto-ignition conditions without external energy supply, the use of internal residual gas as driving force for charge temperature management has been investigated. This chapter concentrates on the internal residual gas delivery via changed valve timing compared to conventional spark ignited gasoline engines. In contrast to the residual trapping method, the re-breathing method tries to minimise pumping losses by making a standard exhausting stroke and sucking back the exhaust gas within the intake stroke, whereas the trapping method keeps the residual gas in the cylinder by a residual gas compression within the gas exchange cycle. The timing of the hot EGR (exhaust gas re-circulation) back-flow and the way this re-breathing is realised for practical use in an internal combustion engine can be achieved by different methods and operation strategies. The principal advantages and disadvantages of the different methods are more or less the same.

A practical example carried out on a 4-cylinder engine with a modified valve train system will be discussed and the pros and cons of this type of auto-ignition control will be shown. Absolute values shown in this chapter have to be seen in relation to the base engine that was taken for these investigations. All comparisons are based on measurements done on the same engine with fixed valve train and homogeneous stoichiometric spark ignition combustion. The whole investigation was done under the restriction of using standard European premium gasoline with a RON (Research Octane Number) of 95.

Special concern was taken regarding transient capability and the mode transition from auto-ignition to spark ignition operation and vice versa.

6.2 Principle of CAI with internal EGR

6.2.1 Characterisation of the re-breathing method by comparison with the trapping method

Compared to the standard valve timing of a gasoline engine, the two most efficient methods to catch a large amount of internal EGR by changed valve timing are residual gas compression, also known as residual gas trapping, and exhaust gas re-breathing. These two different strategies are shown as timing diagrams in Fig. 6.1 and compared to a standard valve timing diagram. The overlapping phase, where intake and exhaust valves are open at the same time, is hatched, and also the phase where most of internal EGR is introduced is highlighted as internal EGR supply phase.

The trapping method (or residual gas compression) operates with shorter opening durations of exhaust and intake valves, resulting in an early exhaust valve closing combined with late intake valve opening. The timing controls the amount of residual gas trapped and with the intake closing event the virtual compression ratio can be adjusted to a maximum depending on geometric compression ratio and pressure waves in the intake system.

The re-breathing method shown in the diagram operates with a second opening of at least one exhaust valve in the late intake phase. Duration and end of this second exhaust opening defines the amount of residual gas in the cylinder and the virtual compression ratio. The shorter intake valve opening leads to a well defined separation of fresh air delivery and exhaust gas delivery within the induction stroke.

One part of the efficiency improvement with HCCI combustion systems results from the possibility to avoid pumping losses by more or less dethrottled operation. Therefore the question has to be answered, which method for the internal EGR supply offers the better gas exchange efficiency. An experiment

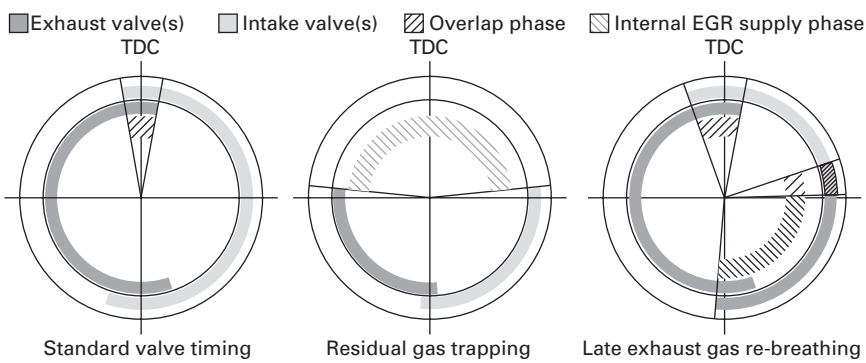

6.1 Valve timing diagrams for different operation strategies.

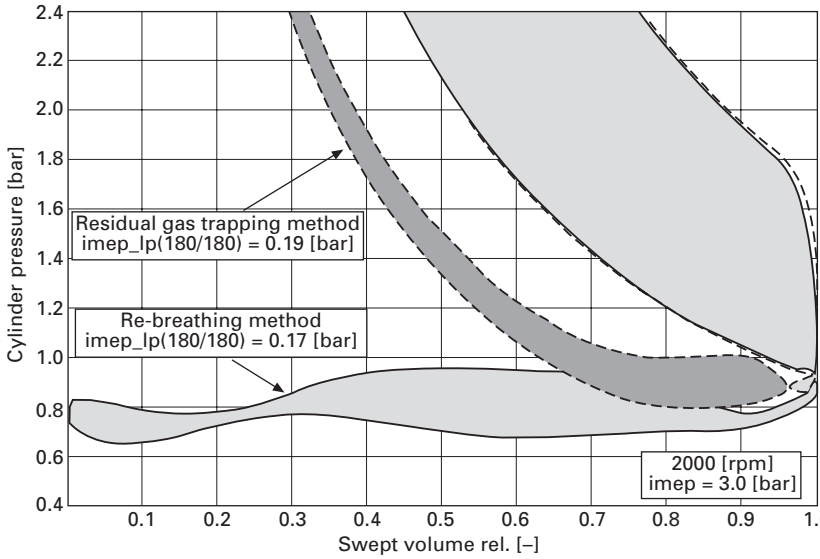

6.2 P-V diagram for different methods of residual gas supply.

at 2000 rpm and 3 bar imep shows the p-V diagram of the two methods discussed above, Fig. 6.2.

The losses for the trapping method in the gas exchange phase are thermal losses through the cylinder wall and blow-by losses in the residual gas compression phase, whereas the losses for the re-breathing method are caused by the gas flow and gas dynamics in the intake and exhaust system. The absolute value for the two variants are nearly equal for this load point. For lower load there are some benefits for the trapping method, at higher load the re-breathing method shows slightly lower overall pumping losses.

6.2.2 Comparison of different re-breathing methods

Let us focus now on methods with burned gas re-breathing, which keep the hot residual gas on a low pressure level in the gas exchange phase. In principle there are three different strategies for the re-breathing of burned gas, common to all approaches is to store the needed exhaust gas in the ports and peripheral piping for the next engine cycle. Again the primary question is, which strategy is the most efficient with respect to charge temperature rise (for safe HCCI combustion) and gas exchange losses (for optimal efficiency). A second aspect is the system stability and controllability. In all three methods shown in this chapter, the exhaust gas control is managed by a second lift of either an intake valve or an exhaust valve. Again the timing diagrams help to understand the principle of the effects in the gas exchange phase, Fig. 6.3.

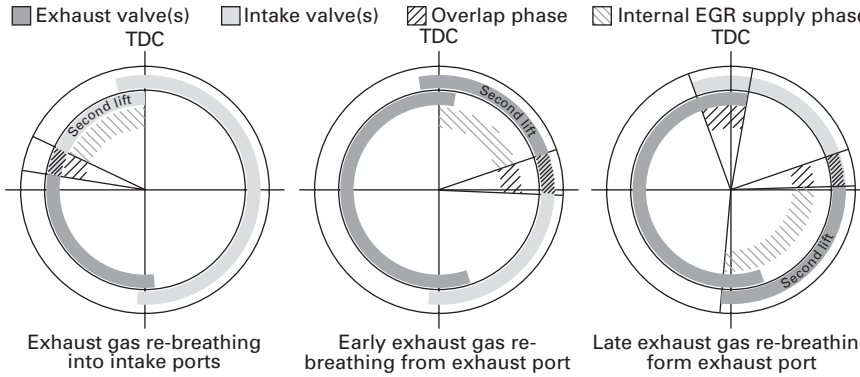

6.3 Different methods of exhaust gas re-breathing.

Table 6.1 Qualitative evaluation of different internal EGR supply methods

	PL	T comp	P comp	Dilution	CR control
(Method 1) Backflow intake	O	O	O	O	O
(Method 2) Early re-breathing	O	+	O	O	O
(Method 3) Late re-breathing	O	++	+(+)	O(+)	+

PL	pumping losses
T comp	temperature at start of compression
P comp	in cylinder pressure at start of compression
Dilution	charge dilution
CR control	control of the virtual compression ratio

The first method operates by blowing back the burned gas into at least one intake port by early opening of at least one intake valve (as indicated by the second lift in the diagram). The opening timing and duration defines the amount of residual gas for the following cycle. In the suction stroke the burned gas plus fresh air is delivered to the cylinder.

The second method uses a second opening of at least one exhaust valve in the early phase of the intake stroke. The burned gas is sucked directly from the exhaust port into the cylinder and mixed with fresh air from the intake side. The EGR rate is controlled mainly by the duration of the second exhaust valve lift.

In the third method the second exhaust valve lift takes place at the end of the intake phase after the fresh air is delivered to the cylinder. The burned gas comes directly from the exhaust port. Again the amount of internal EGR is controlled by the opening duration of the second exhaust valve lift.

To evaluate the advantages and disadvantages of the three methods described above, Table 6.1 compares their pumping losses, temperature and pressure of the cylinder charge at the beginning of the compression stroke, overall

dilution and the controllability of the real compression ratio. The comparison was done under the assumption of same fresh air content in the cylinder and a typical pressure difference between exhaust- and intake-system with a few mbar higher pressure in the exhaust system.

The following observations are noted:

- Regarding pumping losses all three types show more or less the same potential.
- Big differences can be seen regarding the temperature at the end of the intake stroke before the compression phase. Method 1 stores the hot burned gas in the relatively cool intake ports where the exhaust gas has plenty of time to cool down, before it is delivered back to the combustion chamber. Also method 2 with the EGR back-flow at the beginning of the intake stroke enables a significant cool-down in the cylinder, before the compression phase starts. Only method 3 stores the hot burned gas as long as possible in the hot exhaust system before it is delivered back into the cylinder shortly before compression starts.
- Regarding the charge pressure before compression, method 3 also shows a significant advantage, because for this strategy the exhaust system back-pressure defines the in-cylinder charge pressure, and this pressure is always somewhat higher than the intake system pressure. As an option it can be thought about a flap in the exhaust system to raise the feed pressure for the exhaust gas back-flow. This shows advantages regarding EGR rate, pressure and temperature at the start of compression, but it has disadvantages in pumping losses by higher back pressure also in the exhaust stroke. A modified strategy using this method is also known as exhaust blow down supercharging.[1]
- The overall dilution, means overall charge-mass relative to the stoichiometric charge differs not too much between the three discussed methods, because the benefit in charge pressure from method 3 is more or less compensated by the higher EGR temperature and so lower density.
- For combustion control, method 3 offers some benefits due to the fact that both main control parameters, EGR mass and real compression ratio, are controlled by the same valve-lift event, namely the second exhaust lift, using the same actuator.

In conclusion, the internal EGR supply method with re-breathing via a second exhaust valve opening in the late intake phase represents the most favourable operation strategy to ensure a stable auto-ignition operation. This is even more the case when a partly variable valve train with reduced flexibility is used, as it is discussed in the following section.

6.3 Engine concepts and layout

6.3.1 Approaches to CAI combustion with internal EGR

All methods using internal EGR for CAI operation need some flexibility in the valve train system. Cam phasing technology combined with two-stage valve lift profile switching devices represents a relatively simple solution. Fully variable mechanical valve train systems and fully flexible electro-hydraulic or electro-magnetic valve train systems are concepts with the highest degree of flexibility. These systems offer the possibility to use all different methods, residual gas trapping as well as the different re-breathing methods mentioned above.

D. Law[2] shows the difference in high pressure cycle between trapping method and re-breathing with a fully flexible valve train called AVT (active valve train). The AVT from Lotus Engineering represents a purely hydraulic system with predefined valve lift curves. It can be operated as residual gas trapping or re-breathing engine. Also the different re-breathing methods can be investigated. This valve train concept, like all other camless systems, is actually designed for research use mainly on single cylinder engines. Series production of such a system is not planned before 2010.

The AVL-CSI[3] valve train represents a combined mechanical and electro-hydraulic solution, where the components with the highest degree of flexibility are specially designed and optimised for the EGR re-breathing method with a second exhaust valve lift. The base layout of the valve train is a standard cam driven valve actuation. A conversion for mass production could be realised with comparably less production risk.

Electro-magnetic valve actuation systems[4] are in a pure research status and regarding flexibility they are not competitive to hydraulic systems in the moment. In principle, this valve train concept is capable of operating auto-ignition combustion using all different EGR supply methods. A decision for the overall valve train concept has to be made with respect to the overall engine design, the demands from the combustion side and production costs combined with technology and reliability risks.

6.3.2 EGR re-breathing with a combined mechanical electro-hydraulic valve train

Focusing the exhaust gas re-breathing method with late EGR back-flow (re-breathing method 3 as described in the previous section) this section shows an approach designed and patented by AVL which represents a combined mechanically and hydraulically driven valve train. For the 4-cylinder demonstrator, a 2.0 litre engine, the valve train system was optimised to the mentioned AVL-CSI system, covering exactly the flexibility demands of the CAI combustion.

Table 6.2 Base engine characterisation

Base engine type	OPEL 2.0 l 16V, 4 inline
Bore × Stroke	86 × 86 mm
Conrod length	143 mm
Displacement	1998 cm^3
Compression ratio	1 : 12.2
Injection System	BOSCH – Gasoline direct injection
Fuel	Premium gasoline RON 95

The engine is equipped with gasoline direct injection, the cylinder head concept is based on the belt driven tappet valve train in production. Table 6.2 shows the base values of the 2.0 litre engine.

The mechanical part covers the standard functionality of a valve train system and consists of two camshafts, one standard camshaft with fixed valve timing for the exhaust valves in the exhaust stroke, and one camshaft for the intake valves equipped with a continuously cam phasing device and two-stage valve lift shifting mechanism from INA. The second exhaust valve opening for the EGR re-breathing phase is done by an electro-hydraulic device with optimised functionality at one exhaust valve per cylinder and represents an add-on solution to the cam driven valve train system. Whenever the cam is on its base circle this hydraulic lift can be activated with full flexibility in start and duration of the valve event. The parameters for the re-breathing exhaust valve event can be set for each cylinder individually. This offers maximum freedom for combustion control in auto-ignition mode.

In Fig. 6.4 an overview of the valve train system of this 4-cylinder engine is shown with all its components. On the intake side a cam phaser and switchable tappets, both in series production, offer enough flexibility, the main components of the electro-hydraulic valve actuation (EHVA) system for one exhaust valve per cylinder are a small hydraulic pump with about 50 bar oil pressure, a high pressure oil rail with integrated 3/2-way solenoid valves for each cylinder and the actuator itself integrated into the tappets. Figure 6.5 shows a schematic diagram of the oil circuit and its implementation into the standard engine oil circuit. The high pressure oil pump is controlled by the ECU and it is only switched on via an electro-magnetic clutch when the oil pressure for the EHVA system is needed. The pressure in the high pressure oil rail is also controlled by the ECU. Four 3/2-way solenoid valves distribute the high pressure to the actuators for each cylinder individually. The oil back-flow from the actuator is transported via a low pressure rail back to the inlet of the high pressure pump. So it is more or less a separate oil circuit in which only the leakage, mainly at the actuator, is compensated by oil from the standard engine oil circuit.

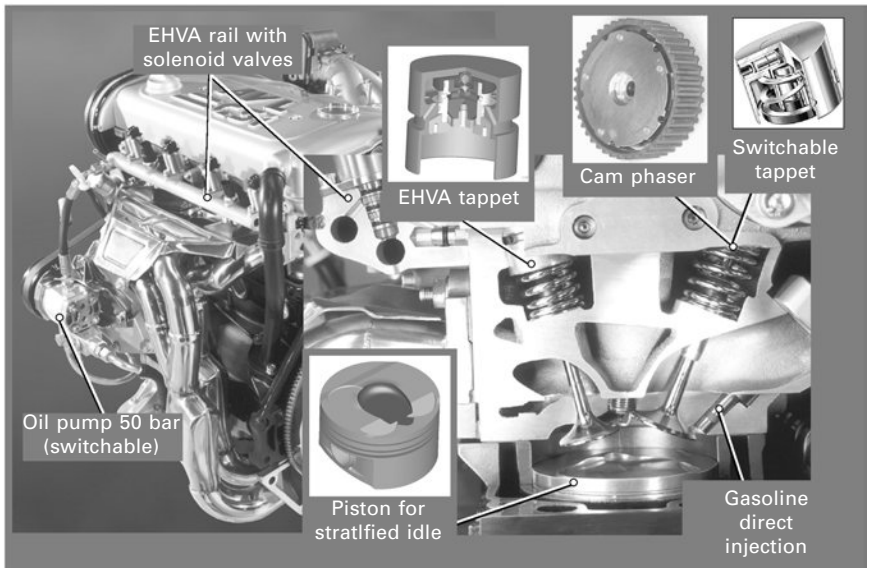

6.4 Valve train system configuration CSI engine.

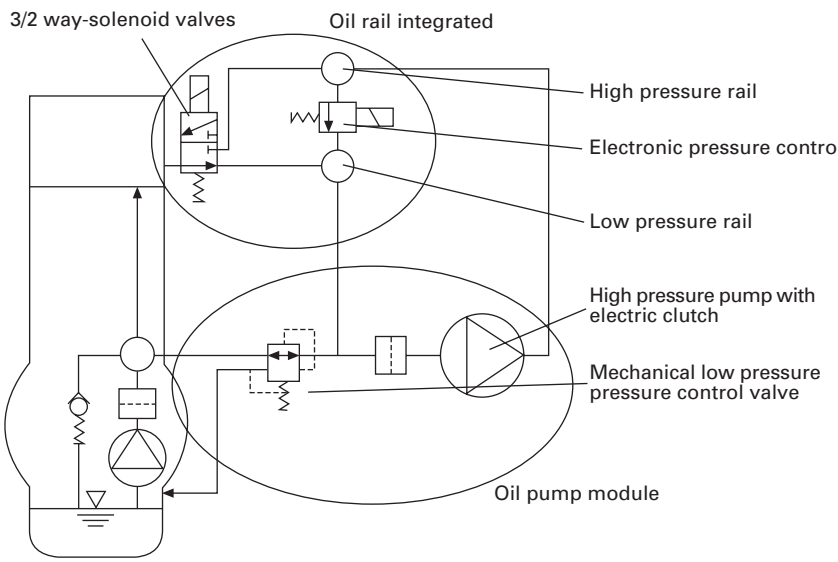

6.5 Schematic of EHVA oil circuit.

The technical details of the EHVA system can be found in previous publications.[5,6] However, a short description of the system and its functionality is given here in order to understand the detailed combustion processes involved.

The main features of the system, implemented on one exhaust valve of each cylinder, can be characterised as follows:

- fully flexible regarding the second opening timing of the exhaust valve
- fixed valve lift (mechanically adjusted)
- fully flexible in length of the second exhaust opening event
- all parameters of the second exhaust opening controlled individually for each cylinder.

In Fig. 6.6 a typical valve lift event with this hydraulic actuator is shown. As can be seen it has a reduced valve lift (in the actual design about 3 mm) big enough to provide the flow area for exhaust gas re-breathing. Advanced damping measures at the end of the opening and closing ramp were developed to ensure sufficient reliability of the EHVA prototype. The combination of the standard mechanically driven exhaust lift and the hydraulically actuated re-breathing lift is shown in Fig. 6.7 for the exhaust valve equipped with the EHVA.

6.3.3 Operation strategies with a combined mechanical electro-hydraulic valve train

Together with the purely mechanical valve lift switching on the intake valves, the overall system offers a lot of different operation modes. Figure 6.8 explains these valve timing strategies by means of a speed/load map of the engine and the fitting valve timing diagrams. The exact limit-curves for each operation area depend on the overall layout. The actual approach represents a well balanced compromise between CAI capability and standard spark ignited operation at high engine load. In naturally aspirated CAI operation NOx formation and maximum cylinder pressure rise are physical borders when approaching higher loads – this will be discussed in the following sections.

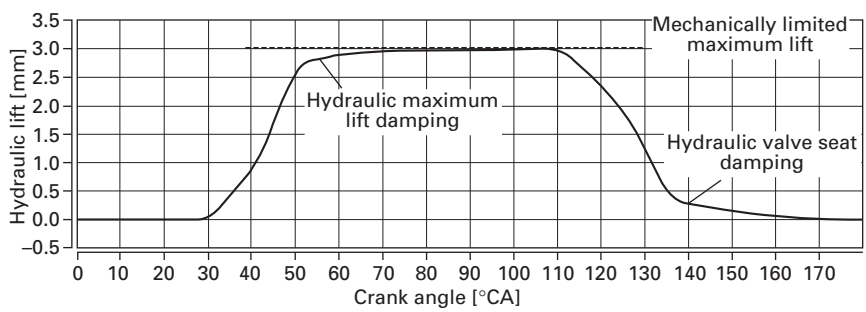

6.6 Valve lift curve with EHVA system.

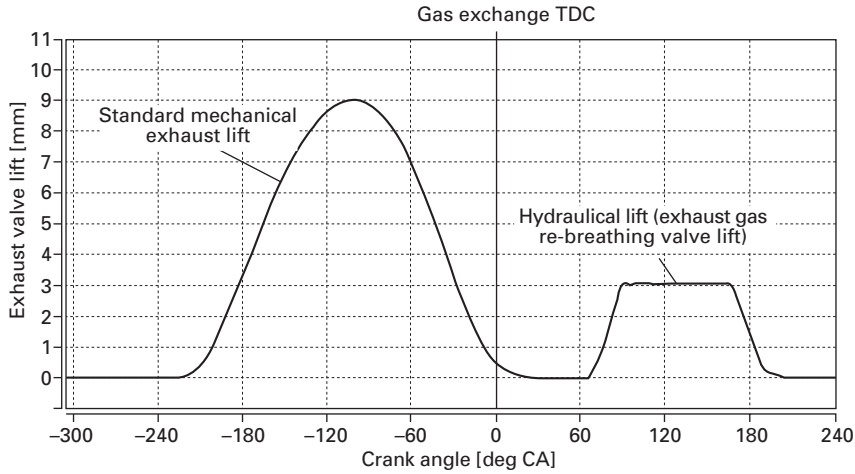

6.7 Combination of mechanical and electro-hydraulic valve actuation.

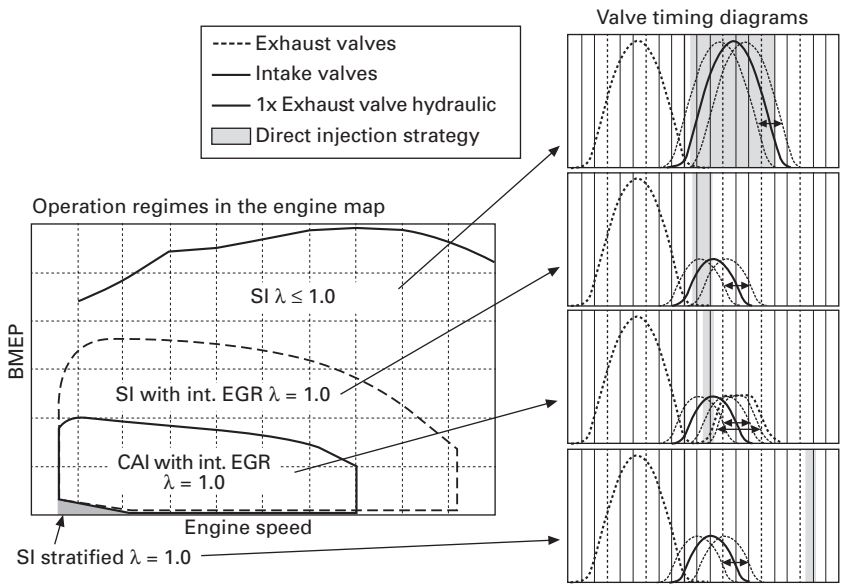

6.8 Operation modes with the AVLCSI prototype engine.

Explanation of the different operation modes

The whole engine map can be operated in spark ignited homogeneous stoichiometric operation like a conventional spark ignition engine. This is a must for real-life engine operation to ensure cold start and warm up when auto-ignition operation is not possible and to cover the high load region outside the HCCI operation area.

The second regime represents a homogeneous spark ignited stoichiometric operation using valve lift switching and cam phasing on the intake side. This operation mode has reduced pumping losses and increased internal EGR, both improve fuel consumption in spark ignited operation and help to optimise overall system performance.

The CAI mode, which is of primary interest, uses the second exhaust lift via the EHVA. The speed/load area is limited mainly by cylinder pressure rise, a rate of pressure rise of 4 bar per degree crank angle was found to be an acceptable limit for combustion noise. Due to reduced dilution, the NOx emissions also rise rapidly when crossing a certain load. In practice this limitation correlates well with the limitation by the rate of cylinder pressure rise.

As an option a stratified mode is also possible. This charge stratification with spark ignition operation makes sense only at lowest load and speed region, where an auto-ignition operation with internal EGR becomes useable due to combustion stability.

It should be mentioned that this variety of operation strategies and valve train flexibility has to be managed by the engine control unit. Therefore a rapid prototyping ECU was used where new functionalities can be implemented with relatively less effort. The ECU has to handle the additional hardware such as the four EHVA actuators and the oil pressure control as well as the extended operation with different combustion modes and the switching strategies from one mode to the other in fully transient operation.

6.4 Thermodynamic results and analysis of CAI with internal EGR

6.4.1 Basic investigations on a single cylinder research engine

As usual, basic investigation has been done on a single cylinder research engine. This single cylinder engine is derived from the 4-cylinder engine enabling the same operation strategies as the full engine. Figure 6.9 shows the amount of internal EGR together with the air/fuel ratio for the CAI operation range based on the results of the single cylinder research engine with late exhaust gas re-breathing. The values represent the measurements using optimised parameters for best combustion stability and lowest fuel consumption.

Charge temperature at the start of compression around BDC (bottom dead centre) resulting from the mixture with hot internal EGR is printed in the map Fig. 6.10. The results represent a recalculation of measured data with 1D-engine process simulation software. The following compression of the charge leads to a mixture temperature of 900–1100 K at start of combustion.

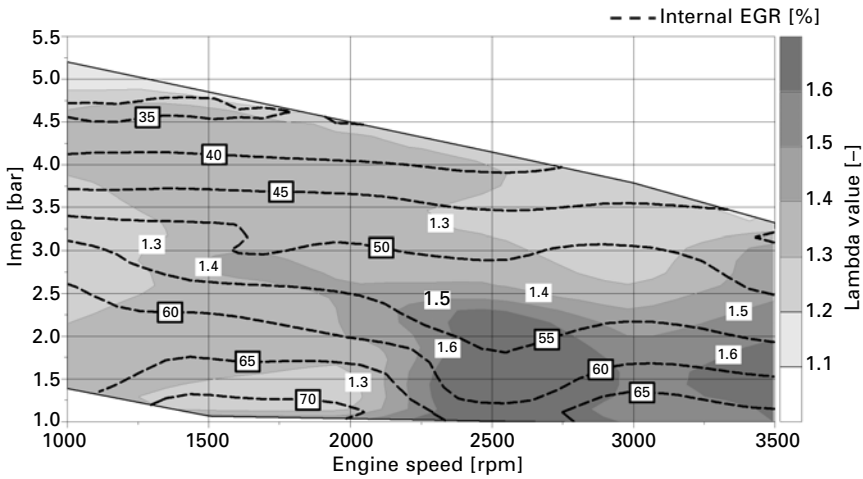

6.9 Lambda and internal EGR for CAI operation.

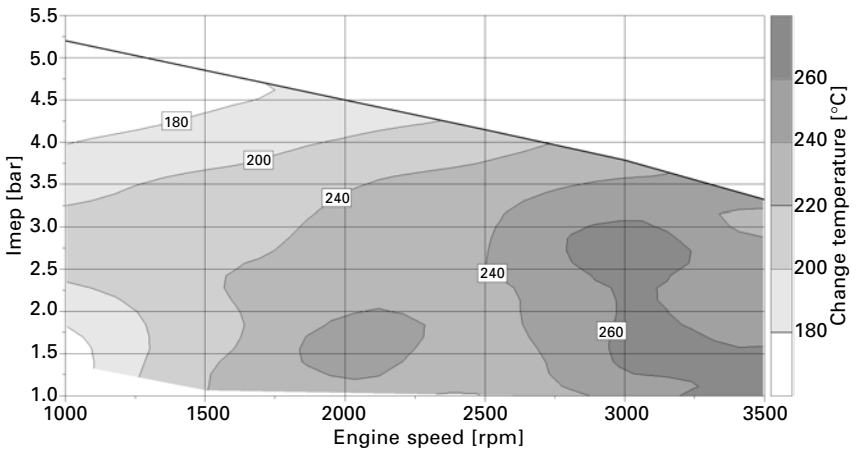

6.10 Charge temperature at start of compression.

Higher charge temperatures appear at higher engine speed and at lower engine load. The explanation for the speed dependency can be found in the ignition delay, which is primarily a function of time, because it is a process caused by relatively slow chemical reactions. At higher engine speed the pre-reactions have to start earlier on a crank angle basis to reach the self-ignition conditions near TDC. The combination of air excess and EGR rate represents the overall charge dilution and it is also called G/F ratio (gas/fuel ratio).[1] A value for the charge dilution can be found by calculating the ratio between the total in-cylinder charge mass, consisting of fresh air mass plus internal EGR mass, and the theoretical stoichiometric air mass as given by

$$\lambda_{\text{dilution}} = \frac{\dot{m}_{\text{air}} + \dot{m}_{\text{EGR}}}{\dot{m}_{\text{fuel}} * L_{\text{St}}} \qquad 6.1$$

The charge dilution value varies from 2 to 3.5 within the CAI/HCCI operation range, see Fig. 6.11. The high dilution values are responsible for the ultra low NOx emissions. The temperature rise from the combustion and so the in-cylinder peak temperature in the combustion process is kept below a certain limit of about 1800K–1900K, although the charge has to be hotter at the end of the compression stroke than that with spark ignited operation to initiate the self-ignition process. Down to a dilution of about 3 the NOx emission stays below 10 ppm, then NOx emission rises rapidly to a value of about 170 ppm at a dilution value of 2, see Fig. 6.12. Depending mainly on the combustion phasing and so the charge peak temperature there is a scatter band for the NOx emission. Also the homogeneity of the charge and so the local in-cylinder temperature affects local NOx formation.

6.4.2 Investigation of the 4-cylinder engine

For the 4-cylinder demonstrator the AVL-CSI valve train was adapted as described in Section 6.3. The target was to transfer the combustion system from the single cylinder to the 4-cylinder engine. This section will give an overview on the tests performed and results achieved with this engine type and this specific valve train concept. The statements and conclusion of this investigation are generally valid, even when the absolute values cannot be transferred directly to an engine with another valve train concept for internal EGR re-breathing. Nevertheless, the results to be presented will give an impression about the potential regarding fuel consumption and emissions, and show the relevant considerations regarding combustion control and stability.

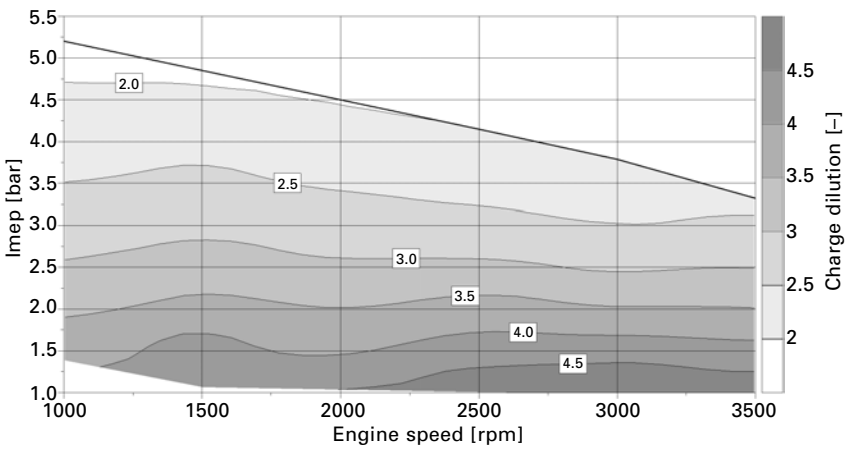

6.11 Charge dilution ratio in the CAI operation regime.

Parameter optimisation was done to identify the stationary optimum regarding fuel consumption and emissions. The complexity of CAI combustion systems makes it necessary to do a screening in a multi-parameter space. New methodologies help to minimise the effort and to generate a more global view on the interactions of parameters. The knowledge about the response of the combustion system when changing a parameter is a requirement to control the system, especially in a highly dynamic environment like a powertrain for use in a vehicle. The variety of influencing parameters can be seen in Table 6.3, based on the AVL-CSI system layout.

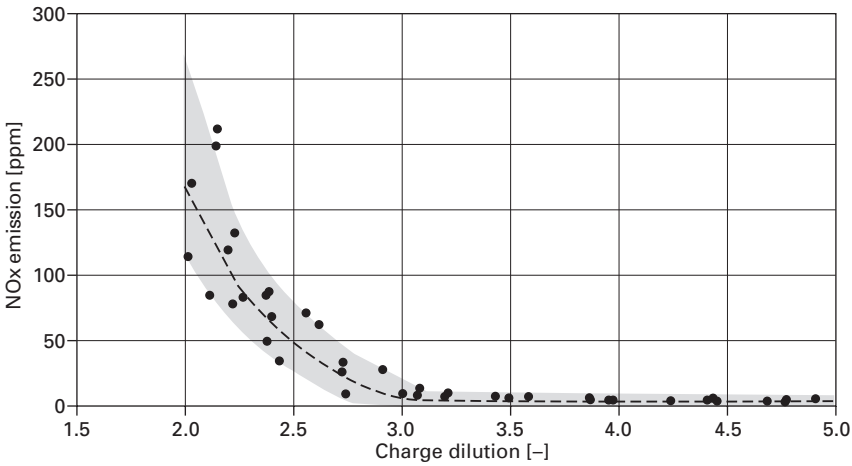

6.12 NOx emission versus dilution.

Table 6.3 Main parameters influencing CAI combustion with internal EGR

Parameter	Controlled by	Combustion influence	Main effect on
Injection timing (SOI)	ECU	Homogenisation	Emission
Intake valve timing (IVO)	ECU	Air mass, pumping losses	Fuel consumption
2nd exhaust value opening (EVO)	ECU	Internal EGR rate	Combustion stability
2nd exhaust value closing (EVC)	ECU	Virtual compression ratio	Emission, stability
Fuel pressure (FUP)	ECU	Homogenisation	Emission
Manifold pressure (MAP)	ECU	Air mass, pumping losses	Fuel consumption
Engine temperature (ENT)	Ambient	EGR demand	Combustion stability
Intake air temperature (IAT)	Ambient	EGR demand	Combustion stability
Exhaust gas temperature (EXT)	Combustion	EGR temperature	Combustion stability

A very common method for this highly sophisticated approach is the use of DoE (design of experiments), which represents in few words a model-based description of a complex multi-parameter system based on a specially selected set of measurements. The mathematical description of the models is kept as simple as possible and mostly limited to models of second order for the parameters.[7,8] Figure 6.13 represents two pictures of the result of such a DoE screening with five parameters. The parameters SOI, IVO, EVO, EVC and MAP were varied, for the response parameter the combustion phasing was analysed, the crank angle value for 50% mass fraction burned was evaluated. On top of the figure the valve lift diagram is plotted to understand the variation parameters of the valve train system. The two 3D-plots represent the sensitivity of the combustion to the timing of the re-breathing exhaust valve lift, characterised by EVO and EVC. The value for SOI and MAP are fixed for these result plots, for the IVO two different positions are shown. On the left-side late intake valve opening, means less valve overlap at gas exchange TDC is shown, whereas on the right side the same situation with early IVO, which means big valve overlap at gas exchange TDC, is evaluated. It is obvious that combustion is quite sensitive to a change of EVO with late IVO whereas with early IVO this sensitivity significantly reduced. Two aspects now have to be considered: for stationary operation the sensitivity should be small to make the combustion system robust, but to control the combustion a precisely controllable parameter with higher sensitivity has to be used to get predictable behaviour of the system. In other words, if EVO is taken for combustion control, the valve overlap has to be small to ensure good control characteristics.

Under such constraints and considering the control demands, local optimisations were done for a limited number of operation points. The results can be seen in the following engine maps representing fuel consumption and emissions. It has to be mentioned that in the maps the area outside the CAI operation range is also plotted, although there the engine runs at homogeneous stoichiometric spark ignited operation with early intake valve closing. The CSI valve train system allows this operation mode, see Section 6.3.3, which is beneficial for fuel consumption reduction when the engine is not operating in the autoignition mode. The figures should give a more global view on the potential of the overall system. The first map, Fig. 6.14, shows the lambda-value together with the internally re-breathed EGR in CAI mode for the 4-cylinder engine.

The necessary dilution and EGR rate is quite similar to that of the single cylinder engine, discussed in Section 6.4.1. Figures 6.15 and 6.16 represent the relative improvement regarding fuel consumption and NOx emission compared to a purely spark ignited operation without usage of the flexibility

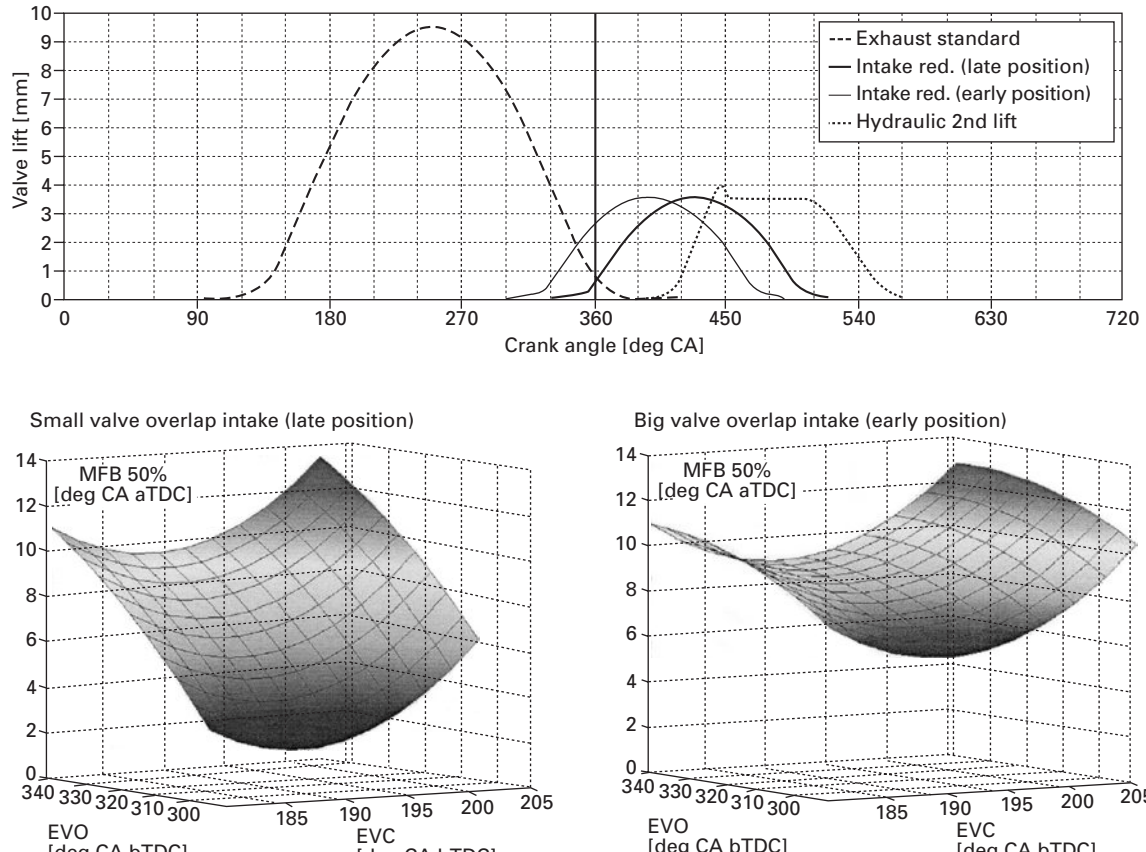

6.13 Combustion sensitivity.

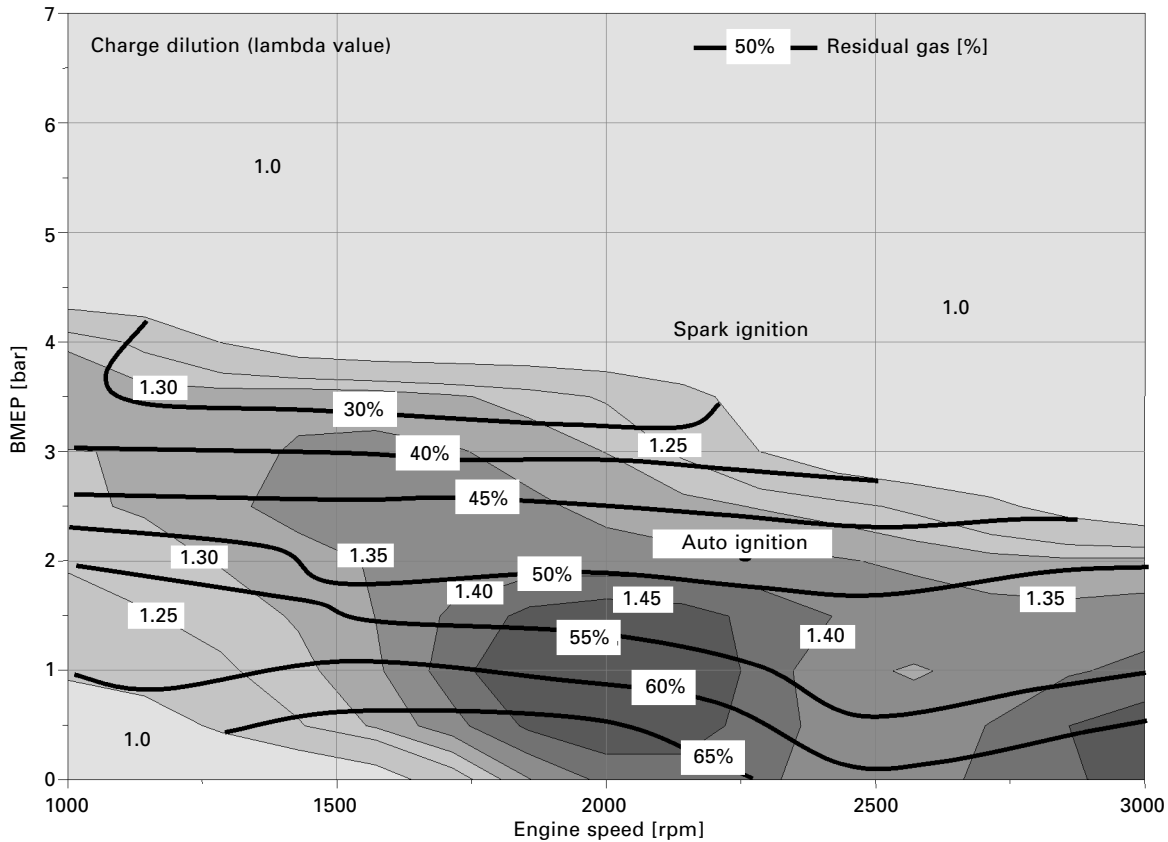

6.14 Charge dilution by internal EGR and air at CAI operation.

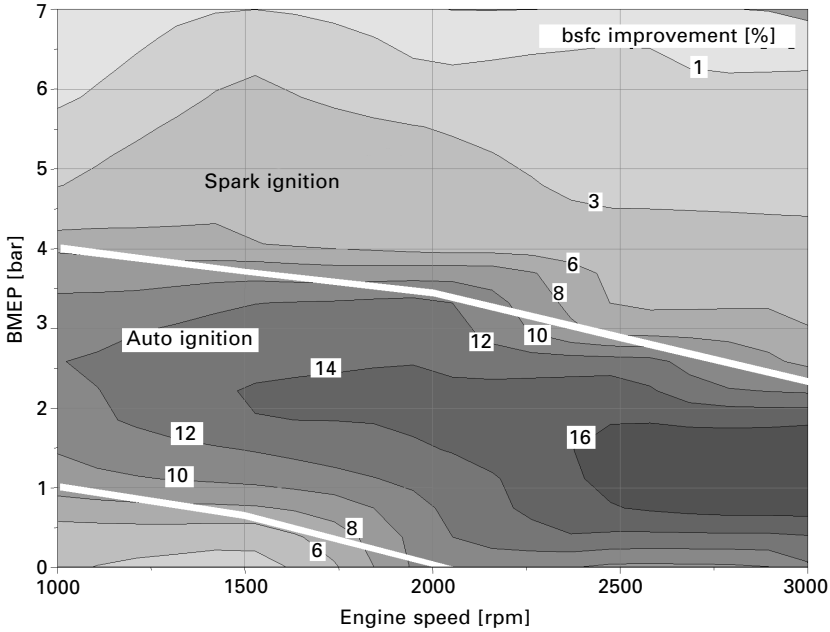

6.15 bsfc improvement with CSI engine.

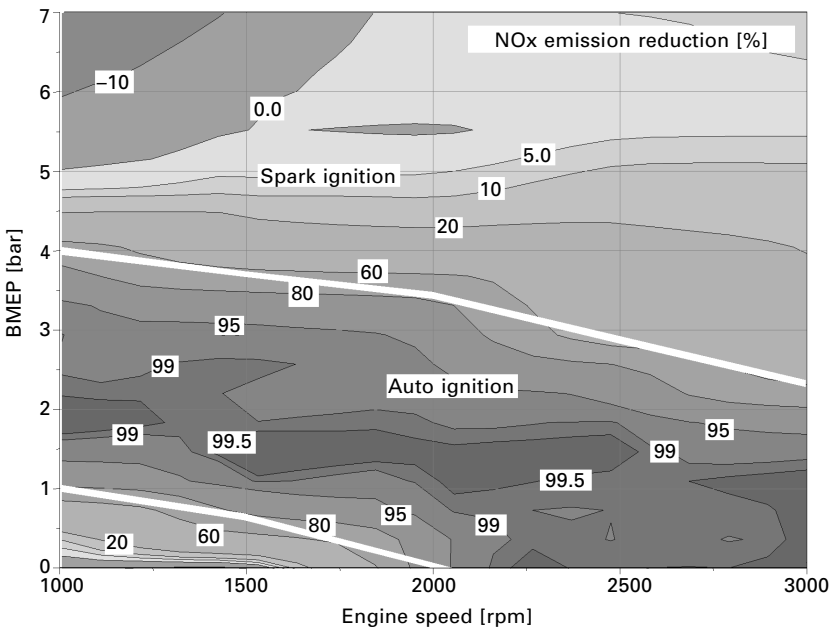

6.16 NOx emission reduction with CSI engine.

given by the valvetrain. The auto-ignition operation range is highlighted by the operation borders, at high load the limitation is caused by the maximum cylinder pressure rise and/or NOx emission, whereas at lowest load and speed, misfiring prohibits CAI mode.

For the emissions the 80% NOx reduction line marks more or less the operation limit. Within the sufficiently diluted area NOx engine out emissions are reduced to 0.5 to 5% of the values with homogeneous stoichiometric spark ignited combustion.

6.4.3 Energy balance analysis of CAI combustion with internal EGR

Based on the experiments and results discussed in Section 6.4.2 an energy balance analysis is done for the different combustion modes in this chapter. The CAI combustion is compared to stoichiometric spark ignited combustion with fixed valve timing and a stoichiometric spark ignited combustion using cam phasing and the valve lift shifting device on the intake side of the AVL-CSI valve train. The evaluation is done for a fixed amount of fuel, which means a constant input of chemical energy to the system. Directly measurable values are set in relation to the introduced chemical energy. These measurement values are the pumping losses (imep_lp) and the indicated mean effective pressure (imep) from the indication measurement system, the chemical exhaust energy from the exhaust gas analysis and the exhaust gas enthalpy from the exhaust gas temperature and mass flow measurement. The distribution of the energy left is comparatively difficult to evaluate, but it contains all thermal losses through water and oil as well as convection to the air.

Under these constraints Fig. 6.17 compares the energy balance for the three combustion systems; for the SI-combustion 36.6% gross indicated efficiency (based on the work done in the compression and expansion stroke only) can be evaluated, in the exhaust gas 21.1% can be found as thermal energy and 4.8% as unburned chemical components. Only a slightly high pressure cycle improvement is seen with the stoichiometric operation with early intake closing, a spark ignited combustion mode using the so called SI-Miller cycle. That means the relation between the different losses remains the same. A significant difference can be seen with CAI combustion. It shows significantly lower losses through the exhaust gas. The larger part, namely 2.8%, of the introduced energy can be found as improvement of the high pressure efficiency leading to a 39.4% efficiency at this part load point, the rest is transferred to thermal losses through the cooling water. That is not really surprising because of the fact that the CAI combustion operates at a much higher pressure level and apart from the combustion process itself the temperature level is also higher especially in the compression phase.

Figure 6.18 shows the energy balance with a more detailed view of the

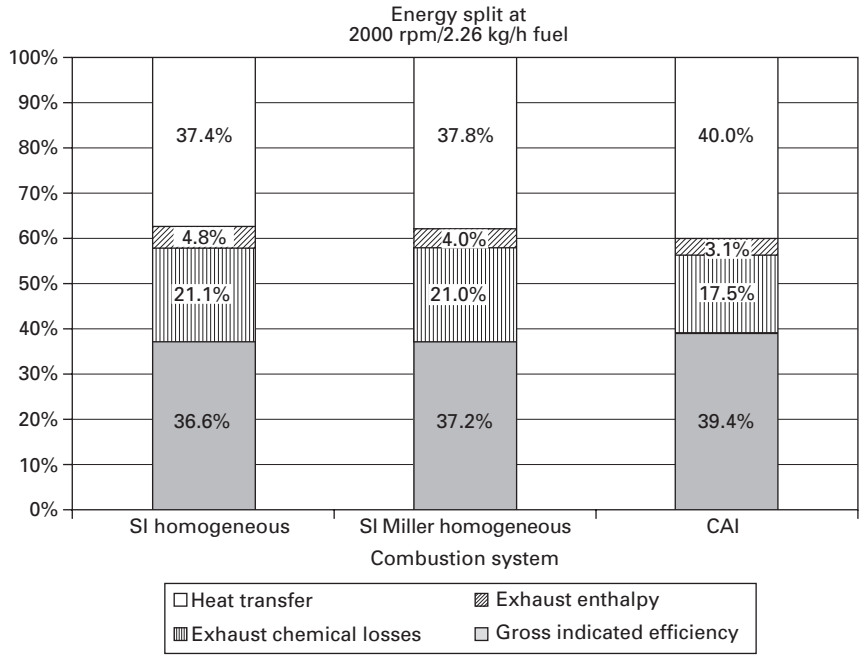

6.17 Energy split of different combustion modes.

high pressure cycle, split into gas exchange losses and indicated efficiency. Here the dethrottling effect of the early intake valve closing (Miller cycle) can be seen directly, this leads to a net indicated efficiency of 31.6% (based on the work done throughout the 4-stroke cycle). For CAI combustion the pumping losses can be reduced from 7.8% to 1.9% of the introduced energy, which leads to 37.5% net indicated efficiency, representing an improvement of about 30% compared to stoichiometric operation. The overall improvement of the net indicated efficiency with CAI combustion compared to spark ignited stoichiometric combustion has its origin mainly in reduced pumping losses (about 68%) and secondly in better high pressure efficiency (32% of the whole improvement). Exhaust enthalpy and losses due to unburned components are significantly reduced by the high internal exhaust gas recirculation rates.

6.5 Transient operation with CAI and internal EGR

6.5.1 Combustion control using internal EGR for CAI

A key challenge with CAI combustion is the combustion control, which is discussed in more detail in Chapter 8 of this book. Nevertheless, the peculiarities that occur using internal EGR and the re-breathing method should be mentioned

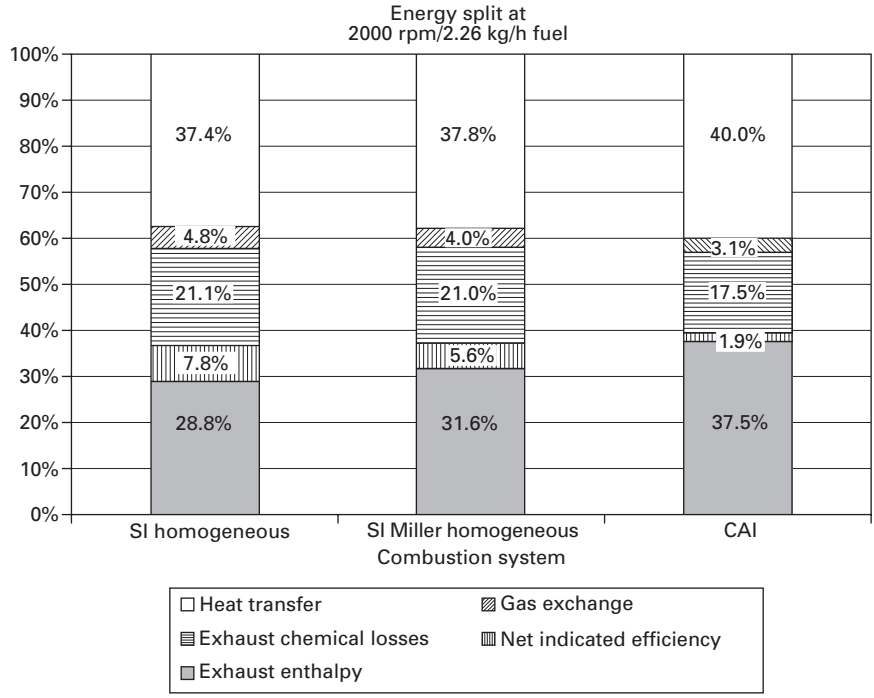

6.18 Energy split with pumping losses.

at this point. The re-breathing method uses the exhaust gas from the previous engine cycle to heat the charge, therefore the charge composition and temperature depend strongly on the previous cycle. Also the operation conditions of the engine and the actual ambient condition have a strong impact on the behaviour. For example, the CAI combustion will behave differently if the engine has been operated at idle conditions for a longer time, or if a full load phase has just passed. The history of load distribution and so the actual component temperatures have a significant impact on the actual behaviour.

The CSI 4-cylinder engine has the possibility to control the combustion in each cylinder individually and on a cycle-by-cycle basis, due to the fact that the re-breathing actuator is controlled like an injection valve that introduces EGR instead of fuel. The strategy that is used for this engine is based on a closed loop combustion control with a cylinder pressure sensor used as feedback, combined with a physically based model that is capable of predicting the CAI combustion behaviour and taking into consideration the load history of the engine. One of the most critical operation conditions is the switching from standard spark ignited operation to auto-ignition operation, because it is an unsteady state. The closed loop combustion control is not able to handle

this mode-switch because it has to measure and evaluate some combustion-events in CAI for the feedback signal first, before making the necessary parameter corrections. This means that the closed loop controller can be activated at the earliest after a certain number of engine cycles in CAI mode. The prediction of the combustion phasing without any feedback by the model-based switching algorithm has to be as accurate as possible. Figure 6.19 shows a block diagram of the switching algorithm that has been developed to overcome the difficulty associated with closed loop control. It is initialised at every changeover from SI to CAI mode, and it represents a functionality that is based on the stationary optimised parameters stored in maps in the ECU. A model-based part calculates correction parameters depending on engine temperature, load history and cycle number after switching. The outcome is a characteristic curve over time for the closing timing (parameter EVC) of the re-breathing exhaust valve lift. Due to the fact that the exhaust gas is much hotter in SI mode than in CAI mode, especially for the first few cycles, the internal EGR mass has to be reduced significantly. To ensure correct combustion phasing for the subsequent engine cycles as well, the internal EGR has to be increased, on a cycle-by-cycle basis, to the steady state CAI conditions.

In Fig. 6.20 the recorded measurement of a switching event from SI to CAI mode is shown, the dark curves represent a switching process with

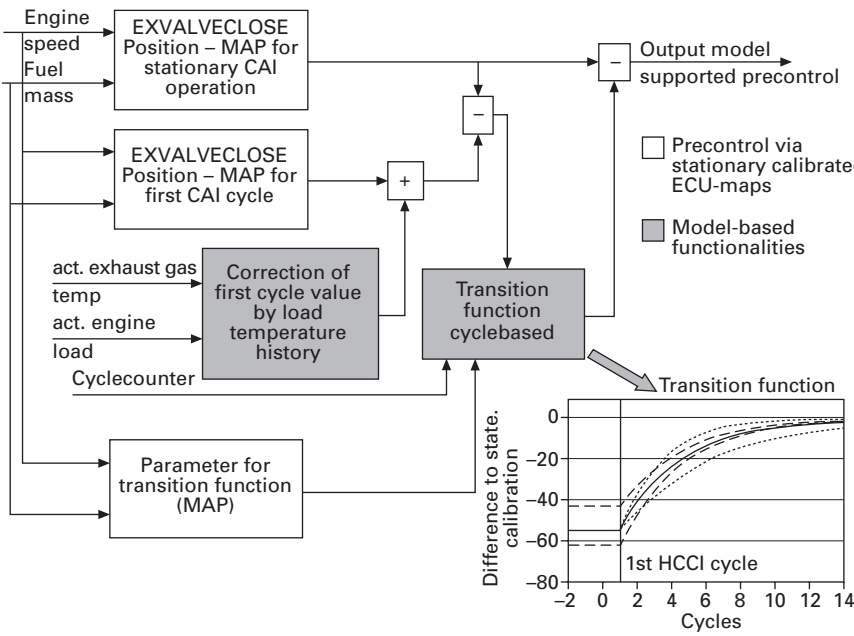

6.19 Switching algorithm used in CSI engine.

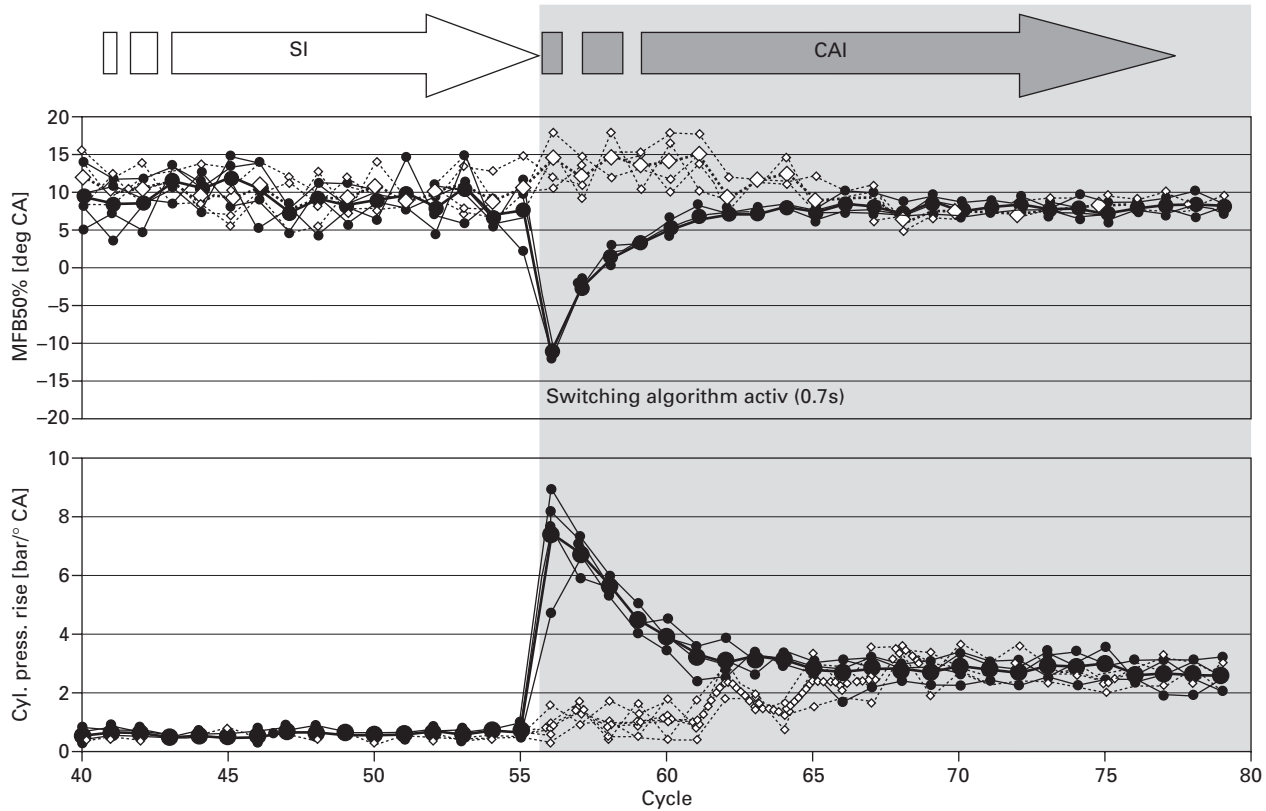

6.20 Switching between SI and CAI.

deactivated algorithm, which means that the ECU uses the stationary calibrated parameters also for the first few cycles in CAI operation. This leads to dramatically advanced combustion and a maximum cylinder pressure rise of more than 8 bar per degree crank angle. This is not acceptable regarding combustion noise and component stress. The light grey curves represent the changeover phase with activated switching algorithm using the cycle synchronous internal EGR control. A smooth combustion mode change can be reached without significantly higher cylinder pressure rise or combustion instability.

6.5.2 Real driving transient operation of the 4-cylinder engine

In general the real world conditions for a powertrain in vehicles vary greatly. Also the dynamics demanded by a driver can be seen as disturbance of the stationary engine run. But at least the engine has to cope with these boundary conditions. Ambient changes are always relatively slow processes compared to an engine cycle. These changes can easily be balanced by a closed loop controller and adaptation functionality. More critical are the speed and especially load changes according to the driver demand. A load change from low part load to full load has to be performed within a few 100 ms which means within fewer than five engine cycles. An engine such as the discussed CSI prototype has to show and prove the capability to follow these highly dynamic demands in CAI combustion and it has to perform combustion mode changes within this time. Therefore the engine was tested on a highly dynamic test bed performing the European driving cycle as is necessary for emission legislation, all transients including gear shifting are simulated. This driving cycle has an urban part (UDC) and an extra urban part (EUDC) with vehicle speeds up to 120 km/h. The test cycle duration is 20 minutes and the driving distance within this time is 11.8 km. The test bed automation system simulates the vehicle mass and the road resistance in a way that the engine is operated in the same speed and load regime as on a real chassis dyno test.

Figure 6.21 shows the speed and load range of the driving cycle plotted into the engine map. The intensity scale of the map represents the consumed fuel mass and not the operating time for each load point. The different operation modes are highlighted by their operation borderlines. In the European driving cycle the 70 km/h-point in 5th gear is one of the most important for the overall performance in the test, also the 100 km/h in 5th gear and idling have significant influence on the overall fuel consumption. The 100 km/h-point, the 120 km/h-point as well as idle and a lot of the accelerations are outside the CAI operation range. On the one hand, it is apparent that the fuel consumption in the spark ignited operation at these operating points has

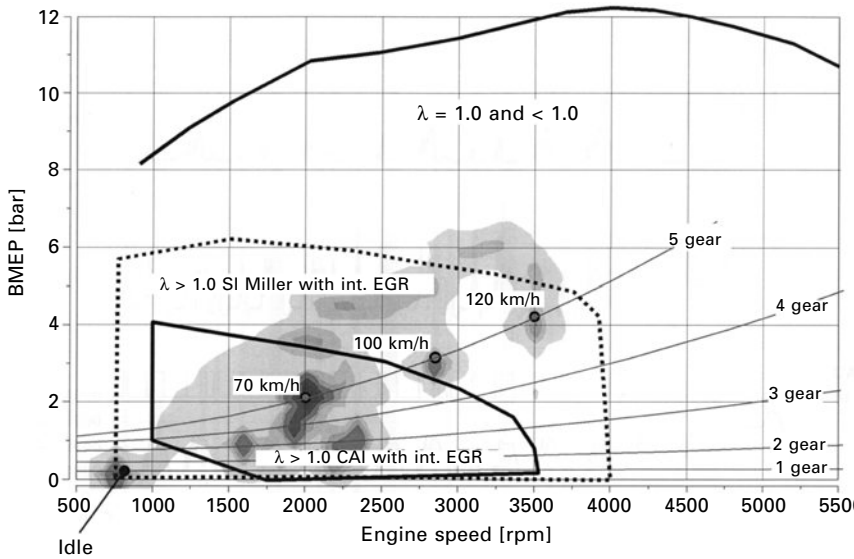

6.21 Load regime in European driving cycle.

significant impact on the overall fuel consumption. On the other hand, frequent changes between the different combustion modes can be expected.

The interesting question is now, how much of the stationary potential regarding fuel consumption can be transferred to a real driving cycle, and how it looks like regarding emissions using a simple 3-way catalyst technology, which means that the NOx from the lean CAI operation is not reduced by aftertreatment. To answer these questions the actual fuel consumption and the actual emissions together with A/F ratio and air mass from the ECU were recorded for the whole cycle. After synchronisation of the signals by a synchronisation mark, the mass-flow for the different exhaust components was evaluated.

Figure 6.22 shows the recorded NOx and HC emissions and the vehicle speed over the whole test cycle. The phases in HCCI operation with nearly zero engine-out NOx emissions can be easily identified. The bar graph, Fig. 6.23 represents the cumulated engine-out emissions on the left side and the emissions after catalyst on the right. The amount of engine-out NOx emitted in lean conditions is equivalent to the tail pipe emissions, whereas in stoichiometric operation a more than 98% conversion rate is usual. For the HC emissions, the relation between engine-out emissions and tail pipe emissions does not differ significantly from that of a full stoichiometric operation. The absolute emission values are good to meet the actual EURO 4 emission legislation limits without an expensive lean aftertreatment system. For the real driving fuel consumption, Fig. 6.24 shows the comparison between stoichiometric operation with fixed valve timing and the full flexibility including

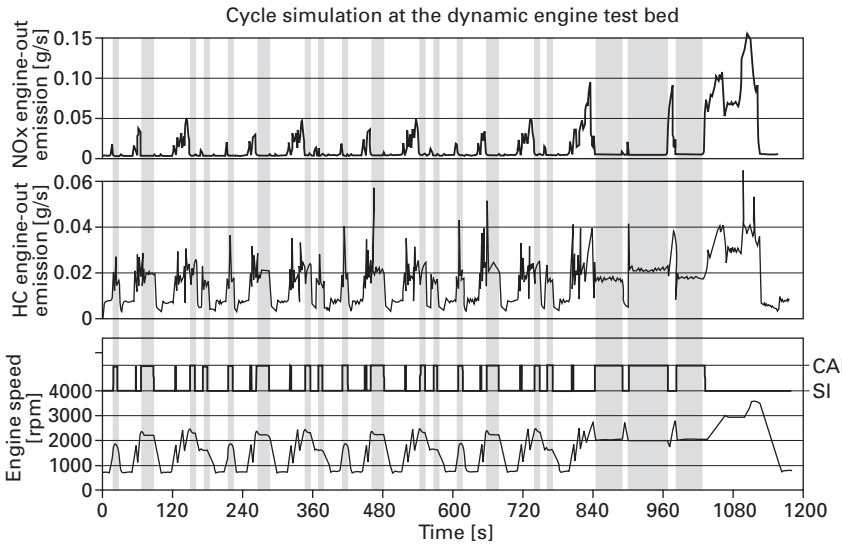

6.22 NOx and HC emission in the NEDC cycle.

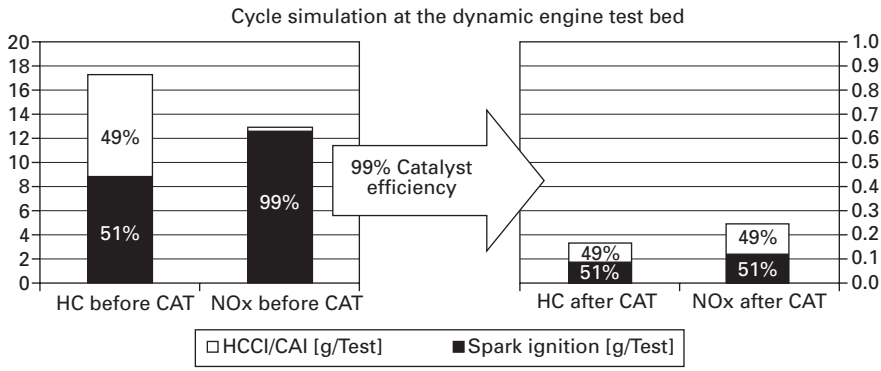

6.23 Cumulative emissions engine-out and tail pipe in hot NEDC.

CAI operation. To also get a value for the fuel consumption in the CAI operation phases the whole driving cycle was evaluated in 1-second steps and then sorted by the measured A/F ratio for this time step. The curves in Fig. 6.24 represent the cumulated fuel consumption over lambda-value. A clear isolation of the stoichiometric and the lean operation can be done. For the driving cycle with CAI operation 41% of the consumed fuel can be assigned to the lean auto-ignition operation. The overall fuel consumption shows a 10.1% benefit for the CSI engine with CAI operation in the described engine configuration.

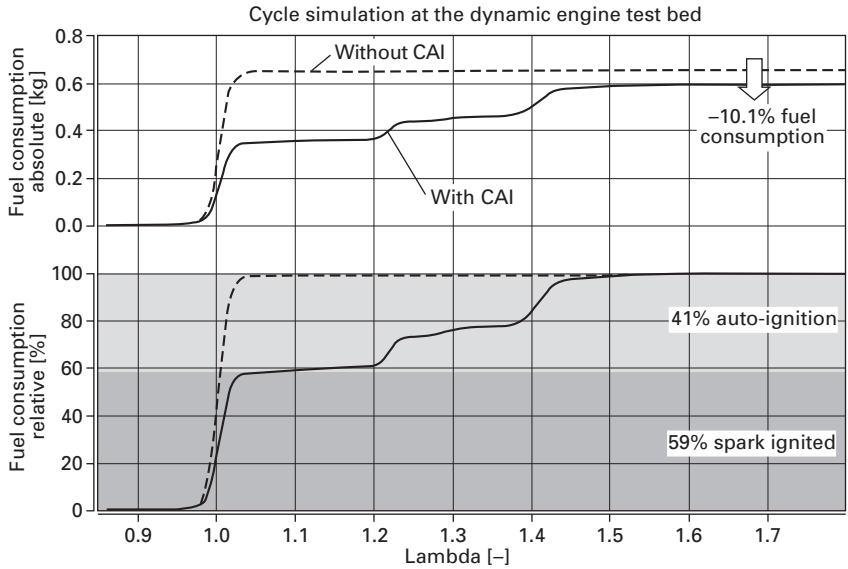

6.24 Fuel consumption with and without CAI operation.

6.6 Future trends

The clear challenge for the future of homogeneous auto-ignition for vehicle powertrains is to find a hardware configuration that is cost-efficient, which means that the benefit regarding fuel consumption and so CO_2 emission reduction is bigger than the on-costs of the system that allows the necessary flexibility regarding EGR supply. In this chapter, different possibilities for the re-breathing method with internal EGR have been discussed and one special design was analysed in more detail, showing the actual potential.

A logical evolution of the presented AVL solution is, for example, the changeover from a tappet valve train to a finger-follower valve train, as in modern engine concepts. This offers a significant improvement potential regarding power consumption of the hydraulically driven re-breathing exhaust valve (EHVA system). The measured 10.1% fuel consumption reduction the European driving cycle will be improved to a value of 12.8% with such a redesigned and friction optimised system. As already mentioned frequently in this chapter the overall system has to be optimised to give CAI combustion a chance to be applied to combustion engines for vehicle use.

6.7 Sources of further information and advice

As CAI or HCCI with internal EGR is a part load combustion system there is the necessity to design an engine concept for multi-mode operation, which

means that conventional spark ignited combustion must be possible without significant disadvantages for use in a powertrain. As often, the overall concept has to represent the best compromise. The presented CSI engine concept tries to merge CAI operation and conventional combustion.

From the emission side CAI combustion represents the only solution for vehicle use that enables a lean engine operation without the necessity of a lean exhaust gas aftertreatment. The NOx emission is directly connected to the charge dilution and so to a physically given limitation for the CAI operation range. Some new ideas also with exhaust gas re-breathing, using, for example, supercharging by exhaust blow down is described in a paper of Koichi Hatamura,[1] can offer solutions to enhance the dilution and extend the operation area towards higher loads, without crossing the NOx formation borderline, but maybe with some disadvantages regarding fuel consumption and cost efficiency of the system.

6.8 References

1. JSAE 20055211, A Study on HCCI (Homogeneous Charge Compression Ignition) Gasoline Engine Supercharged by Exhaust Blow Down Pressure, Koichi Hatamura, Japan.
2. SAE 2001-01-0251, Controlled Combustion in an IC-Engine with a Fully Variable Valve Train, D. Law, *et. al*., Lotus Engineering Ltd.
3. Patent Application EP 1 296 043 A2, A. Fürhapter, AVL List GmbH.
4. SAE 2003-01-0032, Controlled Autoignition Combustion Process with an Electro Mechanical Valve Train, P. Wolters, *et. al.*, FEV Motorentechnik GmbH.
5. SAE 2003-01-0754, CSI – Controlled Auto Ignition – the Best Solution for the Fuel Consumption – Versus Emission Trade-Off?, A. Fürhapter, *et. al*., AVL List GmbH.
6. SAE 2004-01-0551, The new AVL CSI Engine – HCCI Operation on a Multi Cylinder Gasoline Engine, A. Fürhapter, *et. al*., AVL List GmbH.
7. SAE 2003-01-1053, Optimization of New Advanced Combustion Systems Using Real-Time Combustion Control, R. Leithgoeb, *et. al*., AVL List GmbH.
8. SAE 2002-01-0708, Automated Model-Based GDI Engine Calibration Adaptive Online Doe Approach, H. Stuhler, Robert Bosch GmbH, K. Gschweitl, AVL List GmbH, *et. al*.

7

HCCI control

P TUNESTÅL and B JOHANSSON,
Lund University, Sweden

7.1 Introduction

As mentioned previously, one of the greatest challenges with HCCI is the absence of direct control of the ignition timing. Compression ignition of a nearly homogeneous mixture of fuel and air takes place when the conditions are right in terms of temperature and pressure for the particular mixture of fuel and air. Combustion that occurs too early in the cycle causes excessive cylinder pressure and temperature. This increases nitric oxide (NOx) emissions and fuel consumption and, in severe cases, engine damage can result. If the combustion is too late it will be quenched before completion during the expansion stroke, causing increased fuel consumption as well as hydrocarbon (HC) and carbon monoxide (CO) emissions. The worst case of 'too late combustion' is a complete misfire that, if repeated, can cause engine stall. Another possibility is that the engine enters a vicious circle with one misfiring cycle followed by a cycle with very strong combustion due to the fuel-rich residuals, followed by another misfire and so on. Thus, there is a crank angle window where combustion has to take place.

A further complication is that the HCCI ignition process is very sensitive and on the brink of instability. In fact, some HCCI operating points are unstable. This means that it is impossible to map an HCCI engine reliably. Small changes in, for example, intake temperature or coolant temperature, will have a large impact on the combustion timing. Thus, closed-loop combustion control is necessary to guarantee correct combustion timing.

The necessity of closed-loop combustion control for the very operation of the HCCI engine distinguishes it from the Diesel and the spark ignition (SI) engines. These engines can run quite well without any closed-loop control even though modern regulations concerning exhaust emissions cannot be accommodated without it.

7.1.1 The combustion timing control problem

The combustion timing control problem consists of measuring the combustion timing with some sensor and using this measurement to adjust some input variable to control the combustion in order to approach the desired combustion timing. Ideally there is one sensor and one actuator per cylinder in which case each cylinder can be treated as an individual control problem, see Fig. 7.1.

Combustion in a reciprocating internal combustion engine can be characterized by the rate of heat release as a function of crank angle. The combustion timing should be a consistent measure of where in the cycle this heat release takes place. It is tempting to use a simple measure such as, e.g., the crank angle of peak pressure. The strong coupling between pressure and volume from the ideal gas law, however, causes the pressure maximum to gravitate towards top dead centre (TDC), the crank angle at which the combustion chamber volume is minimal. This makes the crank angle of peak pressure very inaccurate as a combustion timing measure, particularly if the combustion timing is early. A very consistent measure of combustion timing is the crank angle of 50% accumulated heat release (CA50), see Fig. 7.2. At or near CA50 the rate of heat release reaches its maximum and thus the difference in crank angle between, e.g. CA40 and CA60, is very small. At CA10 the rate of heat release is much lower and the potential crank angle error of a misdetection is thus much larger.

7.2 Control means

As mentioned above, HCCI combustion is very sensitive to almost everything, which means that there are many possibilities for actuation. Anything that controls the temperature during the compression stroke, the dilution level or the auto-ignition properties of the fuel has potential as an HCCI combustion timing actuator.

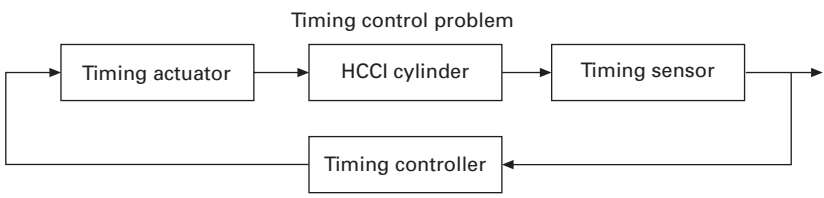

7.1 Combustion timing control problem. The controller adjusts some input variable based on combustion timing measurements in order to maintain the desired combustion timing.

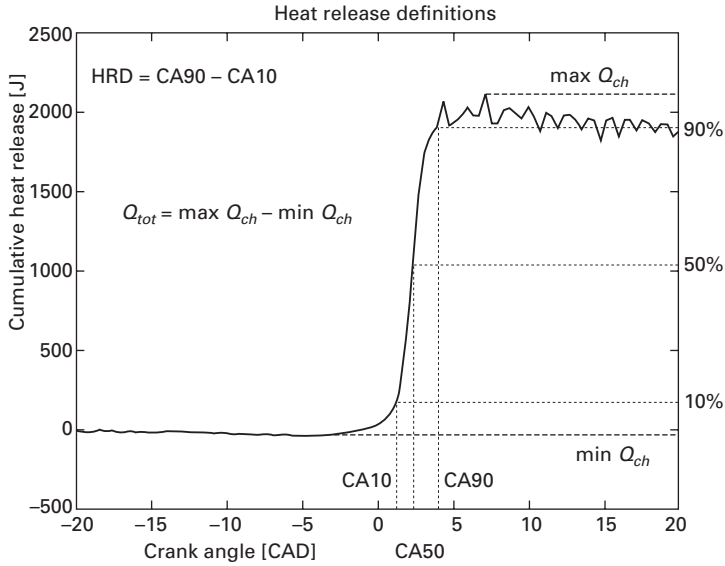

7.2 Illustration of accumulated net heat release and various parameters that can be extracted from it.

7.2.1 Variable valve actuation

Variable valve actuation, VVA, provides a very fast means of affecting the breathing of the engine. VVA exists in many flavors with different degrees of freedom. There are systems that merely provide cam phasing on the intake cam shaft. Other systems provide cam profile switching, CPS, or combinations of cam phasing and CPS. Finally there are systems that provide fully variable valve timing as well as lift.

For HCCI control purposes there are two major methodologies; *residual gas control* and *effective compression ratio control*.

Residual gas control using VVA

VVA can be used to control the initial charge temperature by retaining residual gas or rebreathing hot exhaust gas through the exhaust valve. Combustion control by retained residual gas is often called controlled auto-ignition, CAI. Figure 7.3 shows how residual gas can be retained using a negative valve overlap, NVO. Normally combustion engines have a (positive) valve overlap in order to maximize the volumetric efficiency. With NVO, the exhaust valve closes early and the intake valve opens late resulting in a recompression of retained residual gas at the gas exchange TDC. Increasing the NVO results in more residual gas and thus earlier combustion and vice versa.

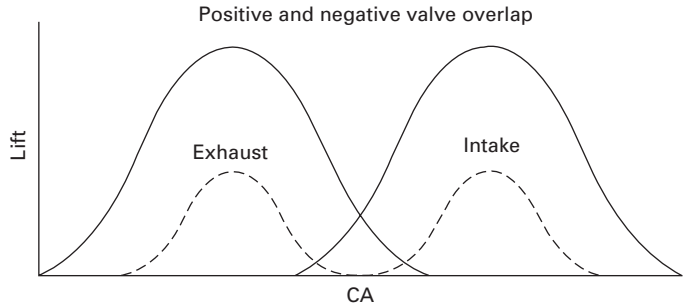

7.3 Illustration of NVO strategy (dashed) as opposed to the normal positive valve overlap strategy (solid).

The NVO approach is attractive since many production engines have VVA capability that allows CPS and cam phasing. Normally VVA implies equal valve timing on all cylinders, though, which means that there is no support for individual cylinder control. Another limitation with this approach is that the possible operating region is narrow. The high load limit is dictated by the lack of dilution necessary to achieve high load. High load is achieved by retaining as little residuals as possible, thus minimizing the charge temperature and phasing the combustion as late as possible. At maximum load this is not sufficient to keep a reasonable combustion phasing however. The lack of dilution makes the combustion chemistry extremely fast and advances combustion far into the compression stroke with very high pressure derivative and low efficiency as consequences. Low load requires a lot of residuals to maintain a high enough charge temperature for ignition. At low engine speeds it is impossible to maintain a high enough temperature for ignition unless the load is higher than approximately 1.5 bar brake mean effective pressure (BMEP). The situation can be somewhat improved if direct fuel injection is available. With fuel injection during the negative valve overlap some pre-reactions can occur during the recompression which results in a more reactive charge and earlier combustion.

A strategy closely related to NVO is the exhaust rebreathe strategy, see Fig. 7.4, in which the exhaust valve is reopened during the intake stroke in order to reinduct some of the exhaust gas back into the combustion chamber. The ratio between the ‘normal’ exhaust valve opening and the rebreathe opening determines how much hot exhaust is reinducted and thus the combustion phasing. This kind of valve control most likely requires a VVA system with more degrees of freedom than a standard cam switching/cam phasing system. A less demanding solution is to keep the exhaust valve open throughout the beginning of the intake stroke and use the exhaust valve closing angle to control the amount of reinducted exhaust gas as indicated in Shaver *et al*. (2006).

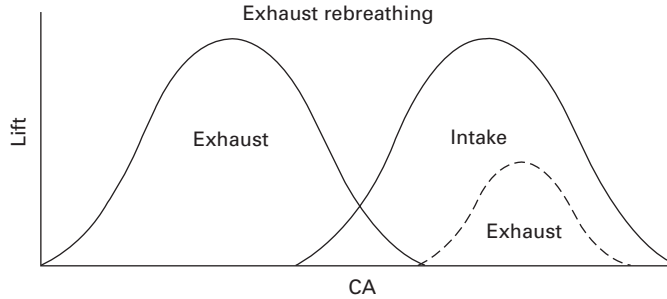

7.4 Illustration of the exhaust rebreathe strategy with which the exhaust valve is reopened (dashed line) during the intake stroke in order to reinduct hot exhaust gas into the combustion chamber.

Effective compression ratio control using VVA

Another way to control the charge temperature is by advancing or retarding the intake valve closing, IVC, angle. This will reduce the effective compression ratio of the engine, which is easy to understand in the case of retarded IVC. The compression process begins when the piston has already started moving towards TDC. In the case of advanced IVC it is somewhat more complicated. What happens is that IVC occurs during the expansion stroke before the piston has reached the bottom dead centre (BDC) where the combustion chamber volume is maximal. This means that the charge, which is essentially at intake pressure when the intake valve closes, is first expanded until BDC and then compressed again to intake pressure before any additional compression takes place. The difference between 'ideal' and early/late IVC is illustrated in Fig. 7.5. In Fig. 7.6 the combustion timing response to early and late IVC can be seen respectively.

A disadvantage with controlling the effective compression ratio using VVA is that it also reduces the effective displacement volume, see Example 7.1. During a load increase the increased fuel concentration as well as the subsequent increase in cylinder wall temperature will have an advancing effect on the combustion timing. This can be counteracted by a reduction of the effective compression ratio. The reduction of the effective displacement volume will, however, cause an undesired reduction of the air/fuel ratio and eventually limit the maximum load of the engine.

Example 7.1 (Early/late intake valve closing). An automotive engine cylinder has a displacement volume of 0.5 l and a compression ratio of 11. Find the effective compression ratio and the effective displacement volume if the intake valve is closed when the combustion chamber volume is 90% of the maximum volume.

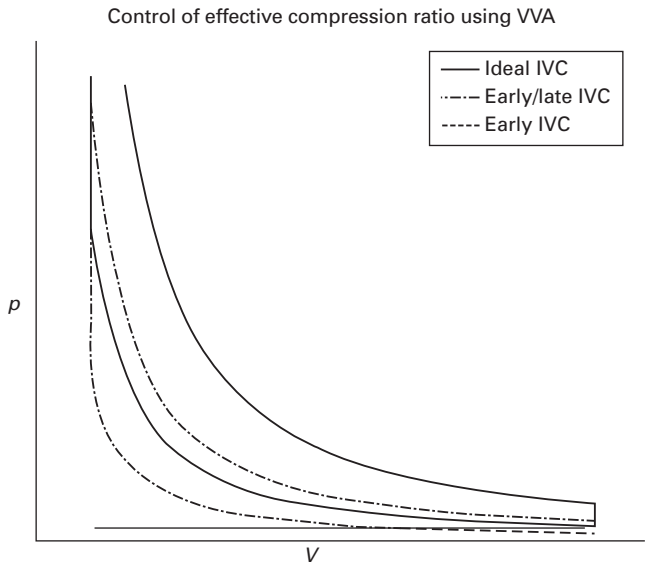

7.5 Reduction of effective compression ratio using late or early IVC. The dash-dotted line represents a reduction of the effective compression ratio by 40% using early or late IVC. The dashed line represents the expansion and compression that takes place around gas exchange TDC with early IVC. The solid line represents ideal IVC.

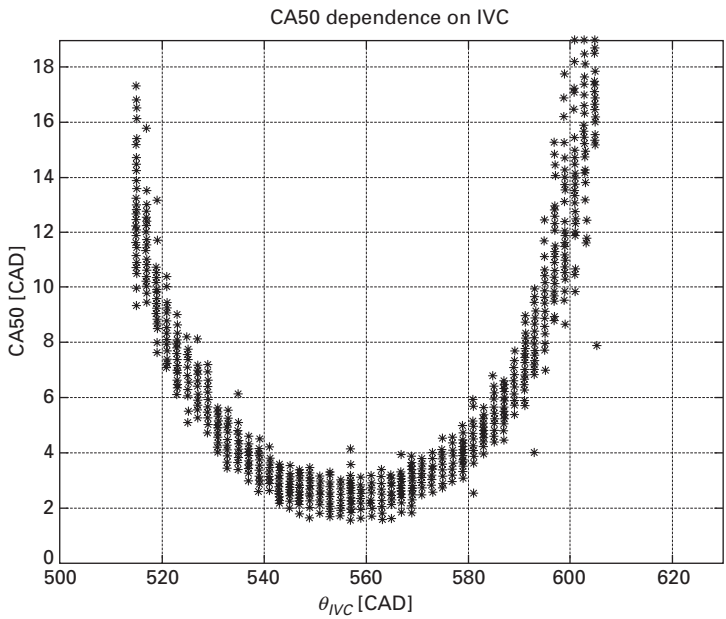

7.6 Combustion timing as a function of IVC angle, θ_{IVC}. Adapted from (Strandh *et al.*, 2005).

Solution:
Start by computing the clearance and maximum volumes.

$$V_d = 0.5\,1$$
$$r_c = 11$$

$$\begin{cases} V_{\max} = V_c + V_d \\ \dfrac{V_{\max}}{V_c} = r_c \end{cases} \Rightarrow \begin{cases} V_{\max} = \dfrac{r_c}{r_c - 1} V_d = \dfrac{11}{11 - 1} \cdot 0.51 = 0.550\,1 \\ V_c = \dfrac{V_d}{r_c - 1} = \dfrac{0.51}{11 - 1} = 0.050\,01 \end{cases}$$

Compute the volume when the intake valve closes.

$$V_{IVC} = 0.9 \cdot V_{\max} = 0.9 \cdot 0.550\,1 = 0.495\,1$$

The effective compression ratio is then given as the ratio between V_{IVC} and V_c.

$$r_{c,eff} = \frac{V_{IVC}}{V_c} = \frac{0.495}{0.0550} = 9.9$$

which is 90% of the geometric compression ratio. The effective displacement volume is given as the difference between V_{IVC} and V_c

$$V_{d,eff} = V_{IVC} - V_c = 0.495 - 0.0500\,1 = 0.445\,1$$

which is 89% of the geometric displacement volume. □

7.2.2 Fast thermal management to control intake temperature

Intake temperature control is usually thought of as too slow for closed loop control of transient HCCI combustion. The most direct implementation of intake temperature control is an electric heating element in the intake air path and then the thermal inertia of the heating element itself causes a time constant of the order of seconds which is indeed too slow for closed loop control of transient HCCI combustion. A more sophisticated solution is fast thermal management (FTM), introduced in Haraldsson *et al*. (2004), which makes use of two temperature sources; one *hot* and one *cold*. With this solution the thermal inertias of the temperature sources are turned into advantages instead, since it actually helps maintain the control authority even when a lot of cooling or heating is temporarily needed.

With FTM, the intake air is formed as a mix of air from the cold source and the hot source. Two inversely coordinated throttles select the correct ratio of hot and cold airflow in order to obtain the appropriate intake air temperature. An even more sophisticated solution involves cylinder individual air temperature control. In this case there is one common hot throttle and

then one individual cold throttle for each cylinder. This kind of system is studied in Haraldsson *et al*. (2005).

7.2.3 Dual fuel control

Auto-ignition takes place essentially when the charge has reached the ignition temperature of the fuel. Since the ignition temperature varies quite significantly with the fuel composition, see Fig. 7.7, it is possible to control the combustion timing using the fuel composition.

The most obvious solution is to put a double port-injection system on an engine and inject a fuel with a low ignition temperature with one set of injectors and a fuel with a high ignition temperature with the second set of injectors. By varying the ratio of injection between the two fuels it is then possible to dynamically control the ignition temperature of the fuel over a wide range. Such a setup allows cylinder individual control of combustion timing over a wide range of operating conditions.

7.3 Combustion timing sensors

In order to perform closed-loop control of the combustion timing it is necessary to measure the combustion timing. Theoretically this is possible to do both inside and outside the combustion chamber. Cylinder pressure and ion current sensors are located inside the combustion chamber. An optical sensor requires

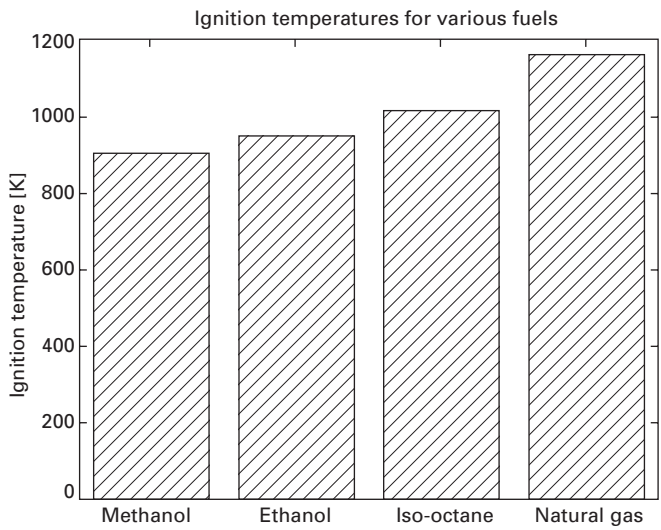

7.7 Experimentally determined ignition temperature for various fuels. Ignition temperature determined at $\lambda = 3$ with HCCI combustion. Data taken from (Christensen, 2002).

an optical window into the combustion chamber whereas knock sensors and crank shaft sensors rely on effects that the combustion has on external engine parts.

7.3.1 Cylinder pressure

The pressure inside the combustion chamber provides information about the thermodynamic state of the charge. Using the first law of thermodynamics and some simplifying assumptions it is possible to extract information about the rate at which combustion is taking place. This is done with a net heat release analysis by integrating [7.1],

$$\frac{dQ_{hr}}{d\alpha} = \frac{1}{\gamma - 1} V \frac{dp}{d\alpha} + \frac{\gamma}{\gamma - 1} p \frac{dV}{d\alpha} \qquad 7.1$$

where γ is the specific heat ratio, p is the pressure inside the combustion chamber and V is the instantaneous combustion chamber volume. The resulting Q_{hr} looks as in Fig. 7.2. The only tunable parameter in [7.1] is γ and normally 1.3 is a suitable value. It is sufficient to integrate the heat release equation between 30 crank angle degrees (CAD) before TDC and 40 CAD after TDC. This crank angle interval will cover the entire combustion event for all HCCI operating conditions. The crank angle resolution needed depends on how accurately the combustion timing has to be controlled but a rule of thumb is to sample the cylinder pressure at least once per CAD.

Extracting combustion timing information from the net heat release is a fairly simple procedure. As mentioned above, CA50 is normally used as a measure of combustion timing due to its robustness. CA50 is found according to:

1. Find the minimum, min (Q_{hr}), and maximum, max (Q_{hr}) of the net heat release;
2. Calculate the halfway heat release $\overline{Q_{hr}}$ where half the combustion has taken place

$$\overline{Q_{hr}} = \frac{\min(Q_{hr}) + \max(Q_{hr})}{2}$$

3. Find the crank angle where the net heat release is equal to $\overline{Q_{hr}}$.

The crank angle obtained in step 3 is CA50.

7.3.2 Ion current

Ion current sensing is an attractive method for in-cylinder measurement of combustion timing since it is very inexpensive. A suitable sensing element is a normal spark plug, which makes the method particularly suitable for applications where mode switching between SI and HCCI combustion is intended.

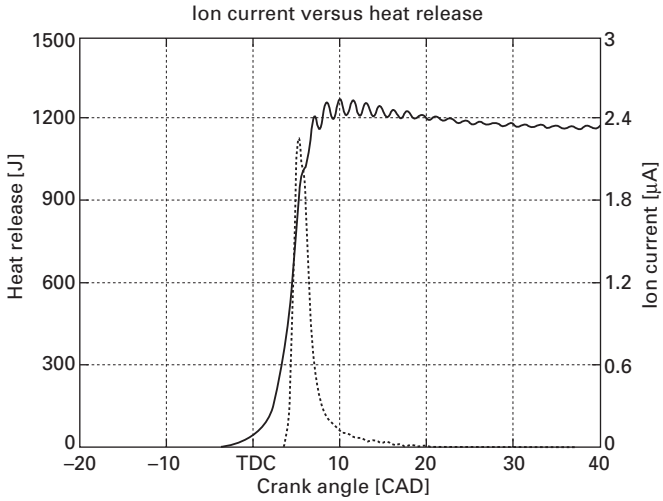

7.8 Ion current (·····) and accumulated heat release (———). The rising flank of the ion current signal coincides with the rising flank of the accumulated heat release. Adapted from (Strandh *et al.,* 2003).

Figure 7.8 shows an ion current and pressure-based accumulated heat release from a single HCCI combustion cycle and indicates that the rising flank of the ion current signal coincides with the rising flank of the accumulated heat release. Ion current feedback has been successfully applied (Strandh *et al*., 2003) for closed-loop HCCI control.

7.3.3 Optical sensing

The chemical reactions during HCCI combustion give rise to spontaneous light emission, chemiluminescence. If an optical window is installed into the combustion chamber, this light information can be used for combustion timing measurement. Fouling of the window will likely pose a challenge to any practical attempt to apply this method.

7.3.4 Crank shaft torque fluctuations

The gas pressure from combustion acting on the piston top is transferred through the connecting rod and crank throw to the crank shaft. This means that some information from the combustion is available in the form of torque fluctuations on the crank shaft. A complicating factor is that, for an engine without offset, the gas force has no lever when the piston is at TDC. Thus, there is no turning torque on the crank shaft resulting from the pressure. There is, however, a bending force, but it is much more difficult to measure. A further complication is that the torque on the crank shaft, is also affected

by the load (e.g., road load) put on the engine. This, together with the torsional dynamics of the crank shaft, makes it a challenging task to extract combustion timing information from crank shaft torque measurements. In Larsson and Andersson (2005), crank shaft torque measurements have been used to estimate the mass fraction burned profile for an SI engine.

7.3.5 Engine speed fluctuations

The engine speed is essentially the time-integral of the net crank shaft torque. With net crank shaft torque is here meant the crank shaft torque in excess of what is needed to maintain a constant engine speed. Thus, by differentiating the engine speed it should be possible to obtain the crank shaft torque fluctuations, which are more directly linked to the cylinder pressure. Obviously, it is, however, even more challenging to extract the cylinder pressure information from this integrated signal, since the low frequency information tends to drown the more interesting high-frequency information. Reconstruction of crank shaft torque and cylinder pressure based on measurement of engine speed fluctuation has been performed (Lee *et al*., 2001).

7.4 Methods

Many different control methods have been attempted for HCCI control, both model-based and empirical. Model-based control methods can rely on either physically based models or black-box models derived from experiments.

7.4.1 Physically based auto-ignition models

Three main types of low-order physically based auto-ignition models suitable for control purposes have been attempted; the *knock integral model*, the *integrated Arrhenius rate threshold model* and the *Shell autoignition model* with increasing level of complexity.

The knock integral model relies on an Arrhenius correlation for the ignition delay, τ.

$$\tau = Ap^{-n}\, e^{B/T}$$

T and p represent gas temperature and pressure respectively and A, n and B are positive constants. The inverse of the ignition delay is then integrated with respect to time and the model indicates start of combustion (SOC) when the integral reaches one.

$$\int_{t_{IVC}}^{t_{SOC}} \frac{1}{\tau(s)} ds = 1$$

The integration is evaluated from IVC, t_{IVC}. The time when combustion starts is denoted t_{SOC}. The simplicity makes the knock integral method very suitable for closed loop combustion control and an example of its use can be found in (Agrell *et al*., 2003). It does, however, have its drawbacks, e.g. the effect of equivalence ratio is not modeled. In principle this means that a separate set of model parameters has to be estimated for each equivalence ratio.

The Arrhenius rate threshold model is closely related to the knock integral model but explicitly models the dependence on fuel and oxygen concentration. This means that the dependence on equivalence ratio, intake pressure and exhaust gas recirculation (EGR) can be predicted without explicit mapping. The inverse of the ignition delay is modeled using the standard Arrhenius rate expression including the dependence on reactant concentrations.

$$\frac{1}{\tau} = Ae^{E_a/(R_u T)}[C_a H_b]^x [O_2]^y$$

The inverse of the ignition delay is then integrated with respect to time and combustion is predicted to start when the integral reaches a certain threshold.

$$\int_{t_{IVC}}^{t_{SOC}} \frac{1}{\tau(s)}\, ds = K_{th}$$

C_aH_b represents the hydrocarbon fuel and the model parameters A, E_a, R_u, x and y all have to be experimentally determined for this specific fuel. An example of the use of the Arrhenius rate threshold model for HCCI control can be found in Shaver *et al*. (2004).

The Shell autoignition model is suggested for HCCI control (Bengtsson, 2004). This model takes another step towards the full chemical kinetics that describes ideal HCCI combustion. It features a full combustion mechanism with initiating, branching, propagating and terminating reactions. In order to make it computationally inexpensive the species have been lumped into one hydrocarbon fuel, one radical, one intermediate and one chain branching agent. In total, this means four species and eight reactions. Despite its limited size compared to the full mechanisms, which even for simple model fuels feature thousands of reactions, it was found to be somewhat too computationally expensive for use in closed-loop control. It is, however, validated against engine experiments and found to perform somewhat better than the simpler knock integral and Arrhenius rate threshold models.

7.4.2 System identification of black-box HCCI combustion timing models

As there is a lack of accurate physically based HCCI heat release models, system identification can be applied to estimate parameter values for unknown

parameters in parametric system models aimed at predicting, e.g. CA50 based on measurable quantities. The two system identification methods that have been applied for HCCI control purposes are: *Sensitivity estimation from stationary maps* and *PRBS excitation for identification of state space models*. A pseudo-random binary sequence (PRBS) is a binary sequence of numbers with statistical properties closely resembling white noise and hence with very rich spectral content.

Sensitivity estimation from stationary map

The simplest kind of black box system identification that can be made is to estimate the sensitivity of CA50 to changes in the control variable as a function of operating point. In Olsson *et al*. (2001a) the sensitivity of CA50 to changes in fuel octane number was modeled as a product of five single-variable functions of engine speed, intake temperature, fuel mass, octane number and combustion timing respectively.

$$S = f_n(n) \cdot f_{T_i}(T_i) \cdot f_{m_f}(m_f) \cdot f_O(O) \cdot f_{CA50}(CA50)$$

where

$$S = \frac{d(CA50)}{dO}$$

Figure 7.9 shows how the sensitivity model corresponds to measured sensitivity over a wide range of operating conditions.

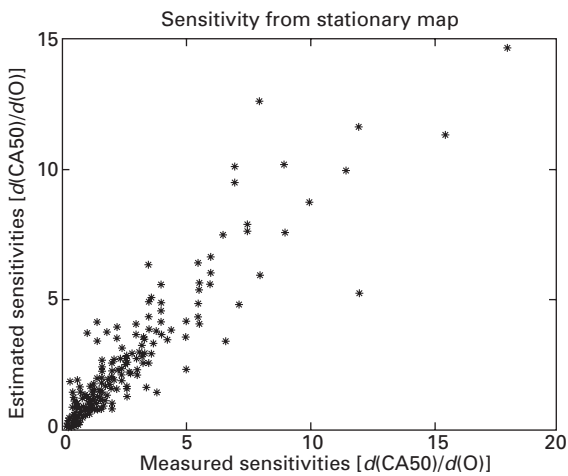

7.9 Modeled sensitivity versus measured sensitivity of CA50 to changes in fuel octane number. Adapted from (Olsson *et al.*, 2001a).

PRBS excitation for identification of state space models

Accurate high-bandwidth feedback control design requires a dynamic model of the system to be controlled. This cannot be obtained from the kind of sensitivity mapping experiments described in the previous section. The simplest kind of dynamic systems are the linear time-invariant, LTI, systems described by:

$$\begin{cases} x_{k+1} = Ax_k + Bu_k \\ y_k = Cx_k + Du_k \end{cases}$$

where x_k is the state vector, u_k the input vector, y_k the output vector and k represents the sample (cycle) number. The sizes of the parameter matrices A, B, C and D depend on the order of the system and the number of inputs and outputs.

An LTI system description of an HCCI engine cylinder can be obtained by exciting the inputs with PRBS, and performing system identification on the recorded input-output data. A system identification method that has been successfully applied in, e.g. Pfeiffer *et al.* (2004) and Bengtsson *et al.* (2006) is the subspace method, developed by Verhaegen (1994). Figure 7.10 shows the result of such a system identification experiment where the dynamic

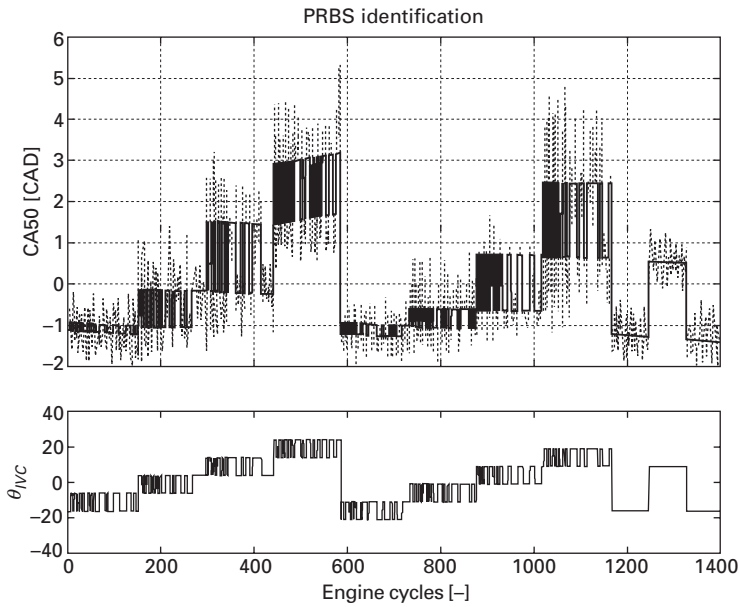

7.10 System identification using PRBS excitation of IVC angle (lower plot). The upper plot shows measured combustion timing (gray) and output from identified second order linear model (black). Adapted from (Strandh *et al.*, 2005).

response of CA50 to a PRBS excitation of the intake valve closing angle has been identified.

7.4.3 Control

Various means for combustion feedback and control have been presented above and many of them have been used in experimental studies. In the following, results and experience from some of these studies will be presented.

Dual fuel control

Dual fuel control was the first published method for closed-loop HCCI control, in Olsson *et al*. (2001a). In this study a six-cylinder heavy duty engine was equipped with dual port fuel injection systems that allowed cylinder individual injection of two different fuels. The primary reference fuels iso-octane and n-heptane with octane numbers 100 and zero respectively were used in order to cover a wide range of auto-ignition characteristics. CA50 based on cylinder pressure was used as combustion feedback. Gain scheduled cylinder-individual controllers with proportional, integral and derivative (PID) action were used for combustion phasing control. Figure 7.11 shows the response to a step change in the combustion phasing reference. The controllers respond to the reference change by gradually increasing the octane rating of the injected

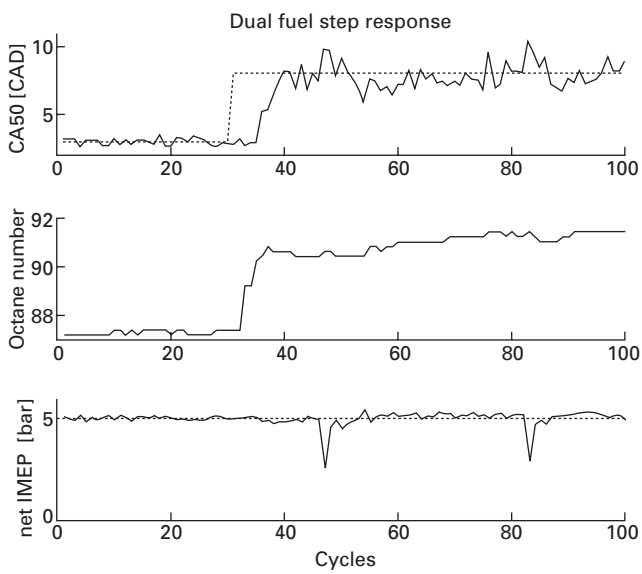

7.11 Response to a step change in the combustion timing reference. Adapted from (Olsson *et al.*, 2001a).

fuel, i.e. increasing the amount of iso-octane and decreasing the amount of n-heptane. This makes the fuel mix more resistant to auto-ignition and thus retards the combustion.

The automatic combustion timing control enables operation at load points that were impossible with manual control. In Olsson *et al*. (2001b) a turbocharged dual fuel setup with ethanol and n-heptane was used to produce 16 bar BMEP with HCCI combustion.

Residual gas control using VVA

Residual gas control using VVA has been used for closed-loop HCCI control, e.g. in Agrell *et al*. (2003). A fully variable electromechanical valve actuation system is used on a heavy-duty single-cylinder engine to control the valve lift profiles. When an advancement of combustion is needed, a suitable negative valve overlap is applied. Retarded combustion at higher load was achieved by reducing the effective compression ratio using late intake valve closing.

Control of effective compression ratio using VVA

In Strandh *et al*. (2005) cylinder individual control of combustion phasing is achieved using variable IVC angle. Figure 7.12 shows the response to a

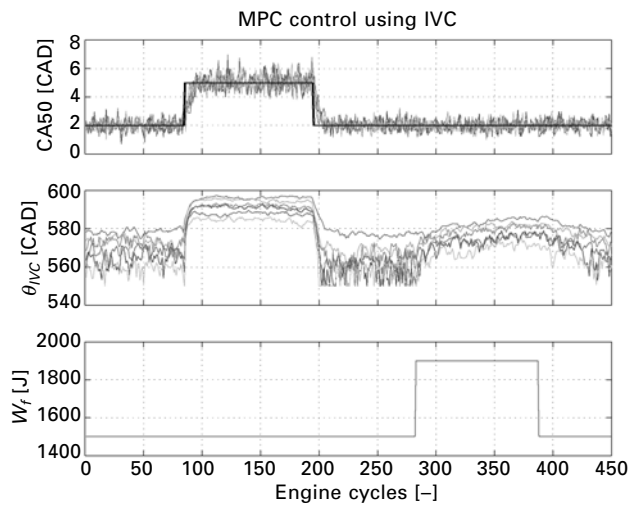

7.12 MPC control of combustion timing using variable late IVC. Response to positive and negative step changes of combustion timing reference and positive and negative step changes of fuel amount per cycle, W_f. Adapted from (Strandh *et al.*, 2005).

positive followed by a negative step change in combustion timing reference and subsequently a positive followed by a negative step change in the load. The control method employed is model predictive control (MPC) which is essentially online optimization of the control input in order to achieve the lowest possible combustion timing error over a specified time horizon. MPC can also take constraints into account such as saturation of the input. In the presented case there is, e.g., a limited crank angle interval available for the intake valve closing which is handled as a constraint in the optimization procedure.

Variable compression ratio

There are not many engines equipped with true variable compression ratio (VCR) which, of course, limits the number of studies with closed-loop HCCI control based on VCR. The SAAB variable compression concept, which was initially designed for downsized SI operation, has, however, been utilized for HCCI control in Haraldsson *et al*. (2002, 2003); Hyvönen *et al*. (2003). In Hyvönen *et al*. (2003) it was concluded that the operating range for HCCI could be extended using preheated air and a high, but variable, compression ratio compared to the standard CAI approach of low compression ratio and high residual gas fraction using NVO.

Most VCR concepts, including the SAAB concept, do not allow cylinder-individual compression ratio control. This means that some other, cylinder-individual, control input is needed to balance the combustion timing between the cylinders.

Fast thermal management

HCCI control using FTM has been reported in Haraldsson *et al*. (2004, 2005). FTM does not provide the true cycle-to-cycle control that some VVA systems do but, as can be seen in Fig. 7.13, it can come fairly close. An interesting effect that can be seen in the figure is that the throttle positions, controlling the intake air temperature, are not constant even when the combustion timing is kept constant. Particularly after changing to retarded combustion, the intake air temperature has to be gradually increased in order to keep the combustion timing constant. This is because the cylinder walls cool down with retarded combustion and thus the intake air temperature has to be increased to compensate.

Mode switching between SI and HCCI

Although high loads have been achieved with HCCI, it is primarily seen as a part load alternative to SI and Diesel combustion. This means that mode

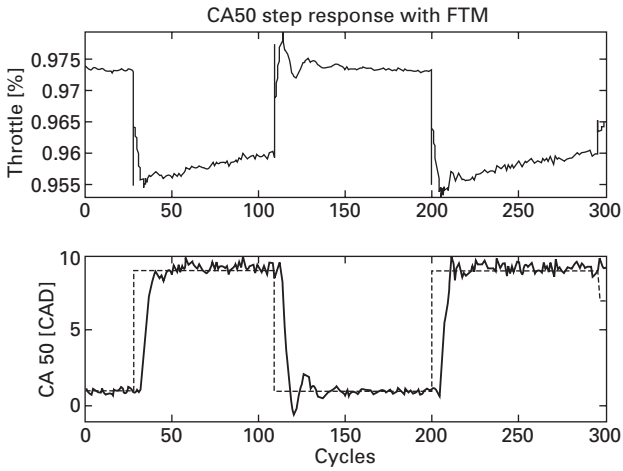

7.13 Positive and negative step changes of desired CA50 with closed-loop HCCI control based on FTM. Upper plot shows the duty cycle for the hot throttle. Lower plot shows desired CA50 (- - -) and measured CA50 (——). 2 bar BMEP at 2000 rpm. Adapted from (Haraldsson *et al.*, 2004).

switching between the different combustion modes has to be considered. In an automotive engine it is necessary to ensure mode transitions that are not considered awkward by the driver of the vehicle. In essence this means that the output torque from the engine should be constant throughout a mode change. The change in sound characterics of the engine should also not be too drastic when switching between combustion modes.

One of the first mode switching studies between SI and HCCI combustion was reported in Koopmans *et al*. (2003) where a fully variable electromechanical valve actuation system was used to switch between positive and negative valve overlap for SI and HCCI combustion respectively. During SI operation late IVC is used instead of a throttle to limit the captured air mass. When switching to HCCI, the exhaust valve closing angle is advanced and the intake valve opening angle is retarded in order to produce NVO. In order to prevent over-advanced HCCI combustion immediately following the mode transition, the IVC angle is retarded to reduce the effective compression ratio.

In Fuerhapter *et al*. (2004) a model-based approach was taken. A collapsable hydraulic lifter on the exhaust valve allowed control of the exhaust valve closing angle and thus the amount of retained residuals. The exhaust valve closing angle was controlled based on the temperature history of the engine and the exhaust in order to ensure HCCI combustion with the correct timing throughout the mode switch. The change in efficiency was also taken into account when controlling the fuel injection in order to keep the torque constant.

7.5 Summary and future trends

HCCI control is a rapidly evolving field of research and development. The curse of HCCI, that the combustion timing is affected by almost everything, is to some extent the blessing of HCCI control, since it means that there are many different possibilities to control the combustion timing. Many of these have been explored in a research setting but only some of them will make their way into production. VVA of some flavor is definitely one of them, since the technology already exists in many production SI engines. VCR is also a possible candidate, since it is the next natural step towards more flexible combustion engines. FTM, particularly cylinder-individual, is probably less likely, since it requires extensive plumbing as well as additional actuators and a heat exchanger. Dual fuel is only likely if the second fuel is used in such small quantities that it can be refilled with maintenance intervals. It would also have to be one central injector, since a full set of extra injectors would be too expensive and difficult to fit.

There are fewer viable options for measuring the outcome of the combustion event. Cylinder pressure offers perfect performance but the cost and reliability issues have limited the pressure sensing to research engines. However, the recent development in pressure sensing technology is likely to accelerate the adoption of pressure sensing in production engines in the near future. Ion current offers acceptable performance, except at very lean conditions, to an acceptable cost. All other alternatives are less likely to perform reliably.

The trend of HCCI research is towards the borderline of the conventional SI and Diesel combustion modes where spark timing and injection timing have a certain influence on the combustion timing. In the Diesel-HCCI case there is also the possibility of split injection and/or rate shaping, and with extremely fast combustion feedback and injection hardware, there may be a possibility of controlling the combustion as it happens. There is ongoing work on hardware implementation of heat release computation, which would offer a virtually instantaneous heat release trace as the combustion evolves.

The trend of HCCI control algorithms is towards more model-based control. Kinetic models of HCCI combustion are combined with one-dimensional engine simulation to provide a very accurate prediction of combustion timing. These models are, however, far too computationally demanding for use in closed-loop control and thus model reduction in order to extract the essence of the combustion behavior with a less complex model is necessary. Another possibility is to implement the models, or specific time-consuming parts, in hardware in order to reduce the computational time.

7.6 References

Agrell F, Ångström H-E, Eriksson B, Wikander J and Linderyd J (2003), *Integrated simulation and engine test of closed loop HCCI control by aid of variable valve timings*, SAE Technical Paper 2003-01-0748.

Bengtsson J (2004), C*losed-loop control of HCCI engine dynamics*, PhD thesis, Lund University, Faculty of Engineering.

Bengtsson J, Strandh P, Johansson R, Tunestål P and Johansson B (2006), 'Hybrid control of homogeneous charge compression ignition (HCCI) engine dynamics', *Int J Control*, 79(5): 422–448.

Christensen M (2002), *HCCI combustion*, PhD thesis, Lund University, Faculty of Engineering, 2002.

Fuerhapter A, Unger E, Piock W F and Fraidl G K (2004), 'The new AVL CSI engine – HCCI operation on a multi cylinder gasoline engine', *SAE Transactions*, 113(3) 337–348.

Haraldsson G, Tunestål P, Johansson B and Hyvönen J (2002), 'HCCI combustion phasing in a multi cylinder engine using variable compression ratio', *SAE Transactions*, 111(3): 2654–2663.

Haraldsson G, Tunestål P, Johansson B and Hyvönen J (2003), 'HCCI combustion phasing with closed-loop combustion control using variable compression ratio in a multi-cylinder engine', *SAE Transactions*, 112(4): 1233–1245.

Haraldsson G, Hyvönen J, Tunestål P and Johansson B (2004), 'HCCI closed-loop combustion control using fast thermal management', *SAE Transactions*, 113(3): 599–610.

Haraldsson G, Tunestål P, Johansson B and Hyvönen J (2005), *Transient control of a multi cylinder HCCI engine during a drive cycle*, SAE Technical Paper 2005-01-0153.

Hyvönen J, Haraldsson G and Johansson B (2003), 'Operating range in a multi-cylinder HCCI engine using variable compression ratio', *SAE Transactions*, 112(4): 1222–1232.

Koopmans L, Denbratt I, Ström H, Lundgren S and Backlund O (2003), *Demonstrating a SI-HCCI-SI mode change on a Volvo 5-cylinder electronic valve control engine*, SAE Technical Paper 2003-01-0753.

Larsson S and Andersson I (2005), 'An experimental evaluation of torque sensor-based feedback control of combustion phasing in an SI engine', *SAE Transactions*, 114(3): 143–151.

Lee B, Rizzoni G, Guesennec Y, Soliman A, Cavalletti M and Waters J (2001), 'Engine control using torque estimation', *SAE Transactions*, 110(3): 869–881.

Olsson J-O, Tunestål P and Johansson B (2001a), 'Closed-loop control of an HCCI engine', *SAE Transactions*, 110(3): 1076–1085.

Olsson J-O, Tunestål P, Haraldsson G and Johansson B (2001b), *A turbocharged dual-fuel HCCI engine*, *SAE* Technical Paper 2001-01-1896.

Pfeiffer R, Haraldsson G, Olsson J-O, Tunestål P, Johansson R and Johansson B (2004), 'System identification and LQG control of variable-compression HCCI engine dynamics', *Proceedings of the 2004 IEEE International Conference on Control Applications Taipei*, pp. 1442–1447.

Shaver G M, Gerdes J C and Roelle M J (2004), 'Physics-based closed-loop control of phasing, peak pressure and work output in HCCI engines utilizing variable valve actuation', *Proceedings of the American Control Conference*, pp. 150–155.

Shaver G M, Roelle M J and Gerdes J C (2006), 'Modeling cycle-to-cycle dynamics and mode transition in hcci engines with variable valve actuation', *Control Engineering Practice*, 14(3): 213–222.

Strandh P, Christensen M, Bengtsson J, Johansson R, Vressner A, Tunestål P and Johansson B (2003), *Ion current sensing for HCCI combustion feedback*, SAE Technical Paper 2003-01-3216.

Strandh P, Bengtsson J, Johansson R, Tunestål P and Johansson B (2005), *Variable valve actuation for timing control of a homogeneous charge compression ignition engine*, SAE Technical Paper 2005-01-0147.

Verhaegen M (1994), 'Identification of the deterministic part of MIMO state space models', *Automatica*, 30: 61–74.

8

CAI control and CAI/SI switching

N MILOVANOVIC, Delphi Diesel Systems Limited, UK
and J TURNER, Lotus Engineering, UK

8.1 Introduction about requirements for the control of CAI engine

The CAI engine experiences problems with cold start, running at idle and high loads that together with controlling the combustion over the entire speed/load range limit its practical application. A solution to overcome these problems is to operate the engine in 'mixed mode', where the engine operates in CAI mode at low, medium and cruising loads and switches to spark ignition (SI) mode at a cold start, idle and higher loads. The transition between these modes, during changes in engine load and speed, will play a crucial role. The valve train and engine management system (EMS) must provide a fast and smooth transition between these two very different combustion modes keeping all relevant engine and combustion parameters in an acceptable range.

The aim of this chapter is to discuss possible solutions of controlling CAI 'mixed mode' operations (CAI-SI) and transition between these modes and requirements needed for implementation in commercial engines. Test results obtained on a single cylinder 'mixed mode' engine (CAI-SI) are presented and discussed. This chapter is organised such that problems in controlling the CAI engine are presented first followed by the requirements for 'mixed mode' CAI-SI engines and transition between these modes, presentation and discussion of the test results obtained, before finishing with conclusions.

8.2 Problems in controlling the CAI engine

The control of a CAI engine is one of the challenges which has to be solved for commercially viable applications. CAI combustion is controlled by the charge temperature, composition and pressure and therefore prevents the use of direct controlling mechanisms such as is the case in spark ignited gasoline combustion and injection timed diesel combustion. Using a large amount of trapped residual gas (TRG) or re-circulated exhaust gas (EGR) is seen as one

of the ways to achieve and control CAI in a certain operating range. By varying the amount of TRG in the fresh air/fuel mixture, obtained by early exhaust valve closure coupled with late intake valve opening, i.e. 'negative valve overlap' (Fig. 8.1), the charge mixture temperature and composition can be controlled and hence the auto ignition timing and heat release rate [1–5]. This method is termed *recompression*. Another method which can provide CAI control in a certain operating range, consists of re-introducing EGR into the cylinder, from the exhaust manifold during the intake stroke by having both inlet and exhaust valves opened simultaneously (Fig. 8.2). This method requires a second exhaust event and is termed *re-breathing* [4, 6, 7].

There are also other methods for initiating and controlling CAI combustion, such as preheating the intake air [8, 9], variable compression ratio [10], using dual fuels (gasoline/diesel, gasoline/dimethyl ether, etc.) [8, 11, 12], or using plasma jet [13] and laser induction [14]. These methods provide control of CAI in a certain operating range and are mainly used for research rather than for commercial engine applications.

The above-mentioned controlling methods, however, cannot solve problems with cold start, running at idle and high loads. The operating range in terms of engine load and speed, for a naturally aspirated CAI gasoline engine, is restricted by misfire at low load and by a high rate of pressure rise (knock) or misfire at high load. As a consequence, the possible area for CAI operation, in naturally aspirated port-fuelled SI engines, is fairly restricted (Fig. 8.3). A

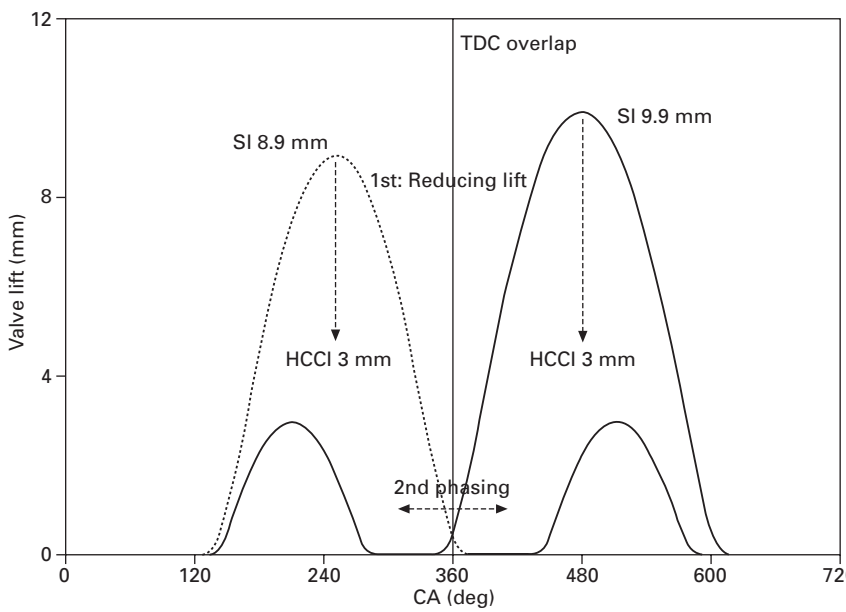

8.1 Recompression method.

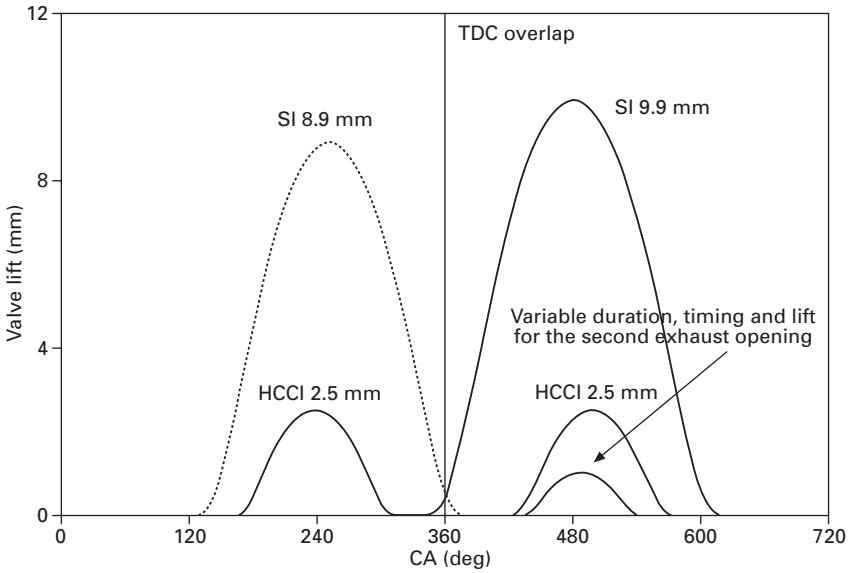

8.2 Re-breathing method.

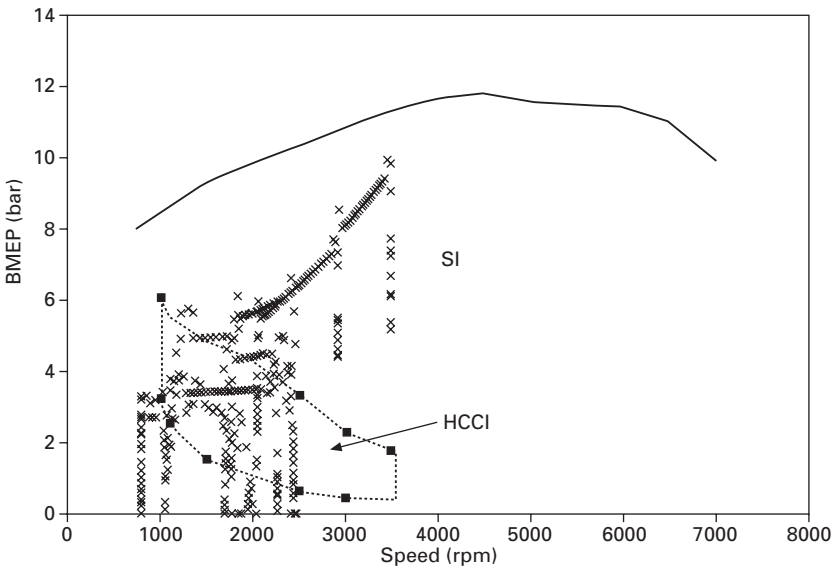

8.3 Possible regions for CAI and SI operations for a naturally aspirated port-fuelled 1.8L engine.

major problem in applying CAI for commercial use is to expand the operating range in order to cover all or most of the New European Driving Cycle (NEDC) in Europe or FTP-75 (in USA) and Japan 10-15 drive cycles.

Some of the above mentioned disadvantages might be reduced or eliminated by operating the CAI engine in a 'mixed mode' (i.e. in CAI-SI) where the engine operates in CAI mode at low, medium and cruising loads and speeds and in conventional spark ignition (SI) mode at cold start, idle and high loads and speeds. This concept has so far been implemented in a two-stroke gasoline engine [15–17] and in a CI medium duty diesel engine [18, 19]. It is now apparent that the 'mixed mode' engine concept will be the first step in the development of a commercial fully operational CAI gasoline or CAI diesel engine.

In typical use such an engine will have frequent changes in engine load and speeds and therefore frequent transitions between CAI and SI operations. To perform mode transitions smoothly without compromising engine driveability and pollutant emissions and to control the CAI combustion itself, controlling and transition strategies have to be derived. These will be discussed in the following sections.

8.3 Transition between operating modes (CAI-SI-CAI)

Enabling frequent transitions between CAI and SI modes, during changes in engine speeds and loads, in a 'mixed mode' engine, will play a crucial role. The valve train and engine management system (EMS) must provide a fast and smooth transition between these two very different combustion modes, keeping all relevant engine and combustion parameters within an acceptable range. These demand significant variation in valve events (timing, duration and lift), with the engine needing to be able to switch from one mode to another from one cycle to the next. To accommodate such a demand, the valve train has to provide profile switching from the SI valve profile to CAI valve profile or vice versa, within the next cycle, which consequently leads to a necessity for a variable valve train (VVT) system, with as high a degree of flexibility as possible.

8.3.1 Valve train requirements in a 'mixed mode' CAI-SI engine

Various mechanical VVT systems that provide different degrees of flexibility for the valve timing, duration and lift currently exist at the market, such as VarioCam Plus [20], Valvetronic [21], Oscillating Cam, Mechanically Variable Valve Train [4], and many more. All of these mechanical systems are, however, limited in flexibility of individual valve and individual cylinder control due

to the mechanical constraint of the camshaft, and hence the engine can only be optimised at specific operating conditions (steady-state conditions). In order to allow optimisation under all operating conditions (including transient and dynamic ones), an individual valve and cylinder control is required, hence a camless valve train system would be the optimal choice from the control point of view. Camless VVT systems such as electro-magnetic and electro-hydraulic types offer considerably higher degrees of flexibility in comparison to mechanical VVT systems, and can also be driven independently of the crankshaft. Due to complexity in production and control issues these system are yet not available commercially; however, electro-magnetic systems developed by Honda [22] and Valeo [23] and an electro-hydraulic one developed jointly by Eaton and Lotus (Production Active Valve Train – Pro AVT™) are currently testing/running on research engines and are planned to be brought to market in the near future.

In order to choose an adequate valve train system for a future 'mixed mode' CAI-SI engine various factors have to be considered such as flexibility, complexity, benefits and cost, the latter likely being the most influential one for future commercial applications. With all of these in mind it was decided to test experimentally two different VVT systems:

- The low cost option but with restricted flexibility and individual cylinder control – based around cam profile switching (CPS) system with camshaft phasing devices – 'CPS-P'
- The electro-hydraulic fully variable valve train (Pro AVT™) as a counterpart system with a maximum degree of flexibility and individual cylinder control; however, with a drawback of its control complexity and additional increased cost.

8.3.2 Cam profile switching and phasing device VVT system

To achieve two different valve lift modes and to phase them afterwards a cam profile switching (CPS) mechanism with the camshaft phasing devices is applied. The basic components of the simulated direct acting CPS mechanism are inner and outer co-axial bucket tappets and three cam lobes per engine valve (Figs 8.4 and 8.5).

The inner tappet operates directly onto the engine valve via a hydraulic lash adjuster and is controlled by the central cam lobe. The outer tappet is driven by the outer identical pair of cam profiles and has its own set of lost motion springs within the tappet to absorb lost motion and to ensure it remains in correct contact with its cams at all times. To achieve profile switching (from the outer one to inner cam profile) the valves within a chosen cylinder are switched, by releasing the locking pins and allowing the

8.4 Co-axial bucket tappet and three-lobe camshaft (INA tappet) [20].

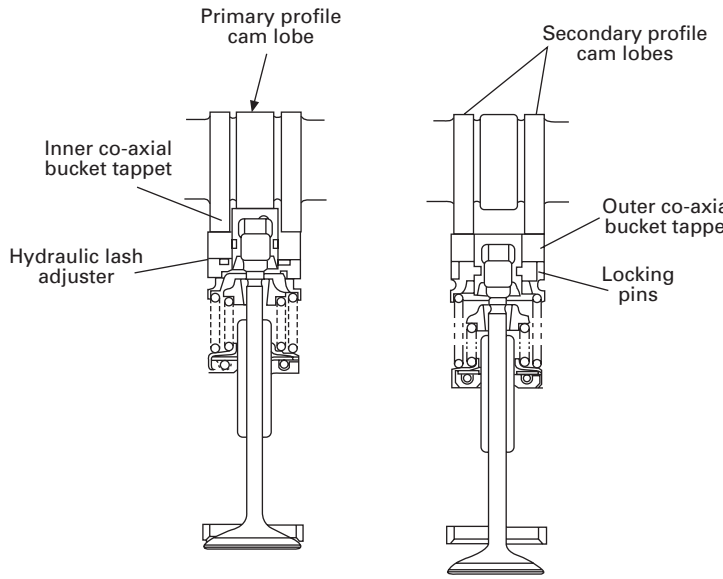

8.5 Cross section through co-axial bucket tappet in two operating conditions.

inner and outer tappets to slide relative to each other. This now means the engine valve is controlled purely by the inner tappet and if the inner cam (lobe) has been manufactured with a small/zero lift relative to the outer cam (lobe) the engine valve will be lifted with a small/zero lift (Fig. 8.5). During normal engine operation the locking pins are held in the locked position by engine oil pressure. When a profile switch is required to the lower lift value,

the oil pressure supplied to the tappets is reduced to a lower level by the use of a simple pressure modulating solenoid valve, thus allowing a light spring to move the locking pins to the unlocked position.

Extensive development and durability testing has shown that tappet switching between low lift and long lift can easily be achieved within one engine cycle up to engine speeds of 5000 rpm even at low engine temperatures [20]. This very rapid switching ability allows the switching of tappets to be synchronised to the engine cycle, even with multi-cylinder engines. More detailed explanation about this CPS switching mechanism and cam phasers can be found in [20].

For a valve timing variation (valve profile phasing) a geared camshaft adjuster/phaser is used [Fig. 8.6]. The system includes an axial plunger which is activated by the oil pressure via a switch valve. The plunger moves the outside stator relative to the inner rotor.

The CPS and phaser system has so far been used commercially in various Porsche models and Subaru X-6 and other applications [20].

8.3.3 Research grade AVT™ system

The system consists of a hydraulic piston attached to the engine poppet valve, which moves inside a hydraulic cylinder. Movement of the piston, and thus the engine poppet valve, is controlled by flow of hydraulic fluid either above or below the piston (Fig. 8.7).

8.6 Camshaft adjuster/phaser [20].

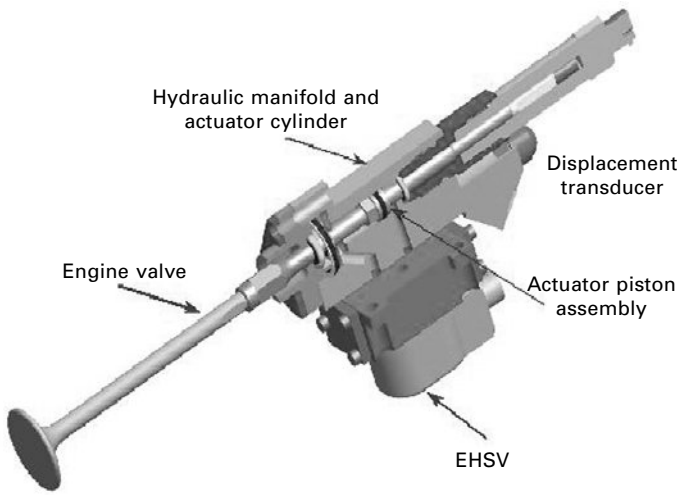

8.7 Sectioned model of research AVT™ system.

Hydraulic flow control is the function of the high-speed servo valve. Operating at approximately 400 Hz, the servo valve allows controlled valve velocities up to engine speeds of 4000 rpm maintaining 'soft-touchdown' capabilities. The research AVT system has full control over valve timing, lift and velocity including the precision valve closing deemed necessary for complete control of the engine valves. The system is capable of controlling each individual valve separately and can operate different profiles on different valves. The system is also capable of opening and closing valves more than once per engine cycle, and is limited only by hydraulic fluid delivery in terms of valve velocity and hence operating strategy. Valve profiles are easily generated (polynomial, triangular or trapezoidal) and up to 256 individual profiles can be stored in a useable array. This allows for dynamic changing of any stored profile within the operating array, with the demanded profile change occurring at TDC firing of the next cycle. More details about the research AVT system can be found in [5].

8.4 The 'mixed mode' CAI-SI engine in operation: presentation and discussion of the experimental results obtained

8.4.1 Experimental apparatus and set up

Engine

The engine employed in this research was a single-cylinder, 4-stroke research engine based on General Motors 'Family 1' 1.8 litre architecture. In Fig. 8.8 a photograph of the engine is shown.

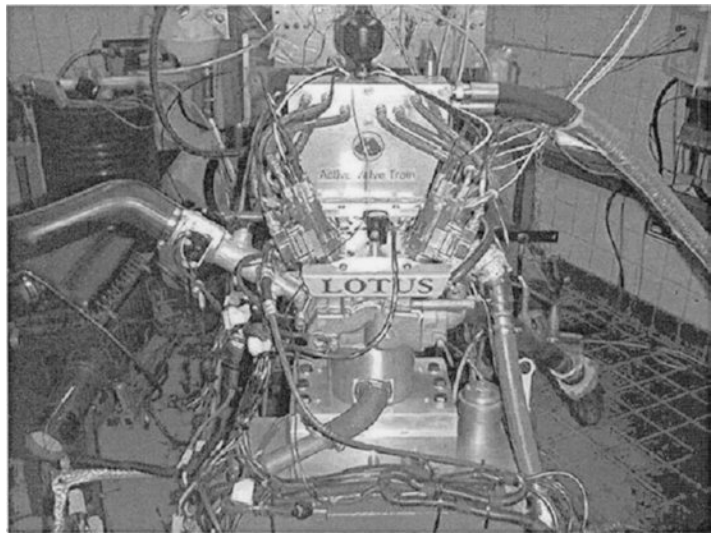

8.8 Single-cylinder research engine with the research AVT™ system.

Table 8.1 Single-cylinder engine specification

Bore	80.5 mm
Stroke	88.2 mm
Swept volume	450 cm^3
Compression ratio	10.5
Number of valves per cylinder	4
Valve control	Electro-hydraulic research AVT system
Fuel injection	Port fuelled
Fuel	Standard gasoline (95 RON)
Equivalence air/fuel ratio	Stoichiometric
Intake temperature	25°C
Inlet pressure	Naturally aspirated
TRG	Up to 80% (by volume)

The major engine specifications and test conditions are shown in Table 8.1. The detail description of the engine can be found in [4, 5].

The research AVT™ system is fitted to allow the variable valve timing strategy to be used. The engine was connected to a Froude AG30 30 kW eddy-current dynamometer. A redline ACAP data acquisition system from DSP Technologies Inc. was used together with Horiba MEXA 7100 DEGR heated line emission analyser. The fuel was port injected and the engine management system was a conventional Lotus production engine controller.

Valve profiles used for CAI and SI mode

The valve profiles (inlet and exhaust) for CAI and SI combustion mode are presented in Figs 8.9 and 8.10.

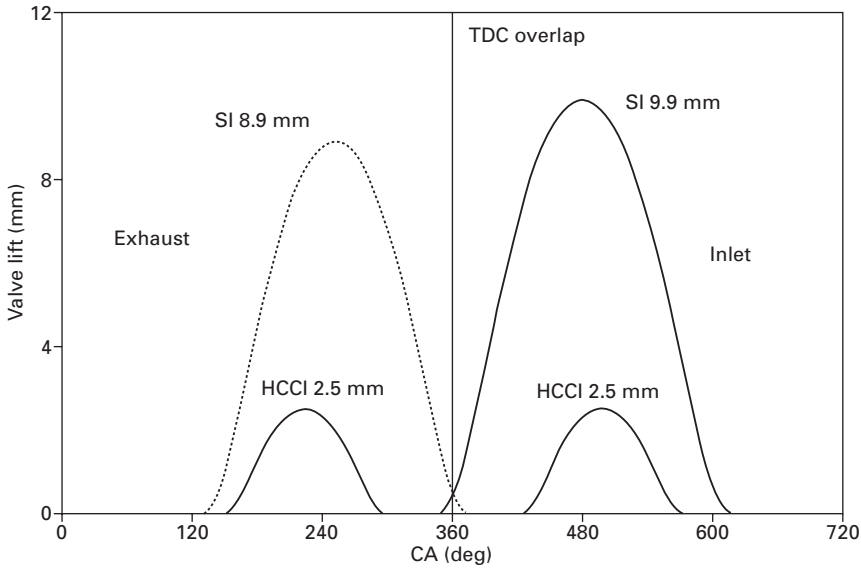

8.9 Valve profiles used for the SI and CAI combustion mode with the simulated CPS and phaser system.

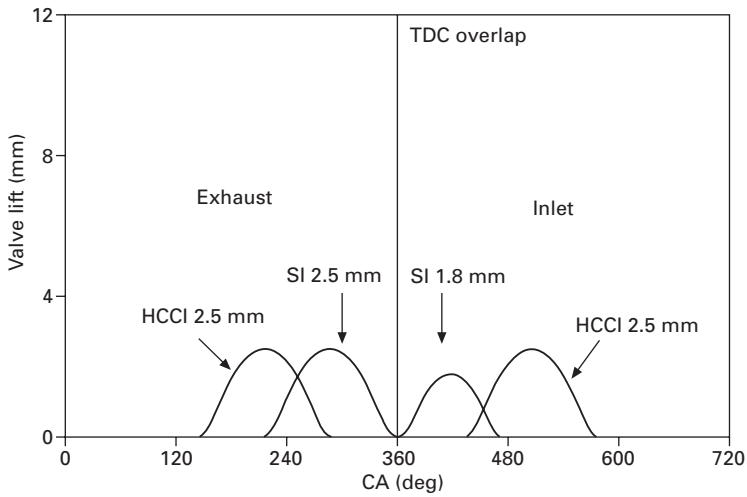

8.10 Valve profile used for the SI and CAI combustion mode with the fully variable AVT™ system.

With both systems (CPS-P and fully variable research AVT system) the same profiles are used for CAI mode (Figs 8.9 and 8.10). On the other hand, different profiles are used for SI mode, since using the CPS and phaser system the engine is throttled in SI mode (the throttle half open – 50%) and WOT in CAI mode, whilst using the research AVT system the engine operated at WOT in both SI and CAI modes. This is enabled by the flexibility of the AVT system which allows control of the load, in SI mode, by optimising the inlet and exhaust valve profiles, hence overruling the requirement for using a throttle. The CAI profiles are optimised for medium engine load (IMEPgross ~ 5 bar) at 2000 rpm, whilst the profiles for SI combustion are optimised for the maximum load of the production engine.

Cold start and mode transition

The research engine is started in SI mode and when the coolant temperature and oil sump temperature reach 90°C the mode transition can be performed. The profile transition from SI to CAI and vice versa should occur within one engine cycle, and therefore the mode transition could also occur within that engine cycle. With both valve train systems studied the transition is performed within one engine cycle (see Figs 8.9 and 8.10).

The research grade AVT™ system is used for mode transition in all experiments and hence to mimic the CPS-P and Pro AVT strategies. The reason for this decision is the flexibility of the Lotus AVT research system which facilitates very rapid valve strategy development and testing whilst minimising engine down-time.

8.4.2 Results and discussion

The results obtained using the simulated CPS and phaser system and Pro AVT system are presented and compared. The experimental investigation is focused mainly on the influence of these systems regarding the transition smoothness (engine torque, power, combustion stability and maximum rate of pressure rise-MRPR) necessary for the mode switch to go unnoticed by the driver.* The pollutant emissions (NOx and THC emissions) are also monitored since they are important in meeting emissions legislation. All tests are run with stoichiometric AFR, naturally aspirated, intake air conditioned by the test cell to 25°C and with spark timing at 30° BTDC for the SI mode and at TDC firing for the CAI mode. During a mode transition, the throttle

*It is worth noting that established criteria to quantify the smoothness of transition between combustion modes currently do not exist, but change in the engine torque is widely used (i.e. the transition is assumed smooth if the change in torque does not exceed ~1–2% of its total value).

angle, spark timing and fuel injection pulse are all adjusted to suit the engine operational mode with all experiments performed with closed loop fuelling control.

Mode transition using the simulated CPS-P VVT system

An example of mode transition from SI to CAI to SI, using the simulated CPS and phasers VVT setup, captured over 500 cycles, is presented in Fig. 8.11. To investigate transition points in more detail a cycle-by-cycle analysis of the cylinder pressure (Cylinder Cy1) and intake manifold pressure (Pressure_MAP) is performed. The results obtained for the SI-CAI transition are presented in Fig. 8.12 and for the CAI-SI transition in Fig. 8.13.

It can be seen (Fig. 8.12) that the transition from SI (66th cycle) to CAI (67th cycle) occurs within one engine cycle as enabled by the valve profile switching. During this cycle, the profiles are changed and phased accordingly. The throttle position and spark timing are also changed at the same cycle with the valve profiles. The fuelling rate, in the first CAI cycle, is reduced by 35% in response to decrease in the intake airflow rate and thus to prevent a rich mixture. The SI combustion mode is characterised with one pressure peak, while the CAI combustion has two peaks, one at the end of compression (caused by fuel auto ignition/combustion) and the other at the end of the exhaust stroke (caused by the recompression of the trapped exhaust gases).

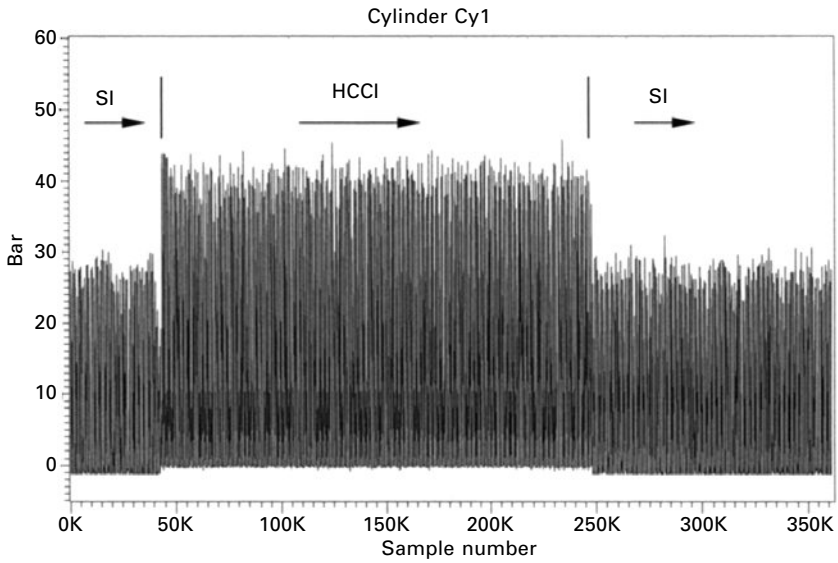

8.11 SI-CAI-SI mode transition during 500 consecutive engine cycles using the simulated CPS-P VVT system (IMEPgross = 4.3 bar at 2000 rpm).

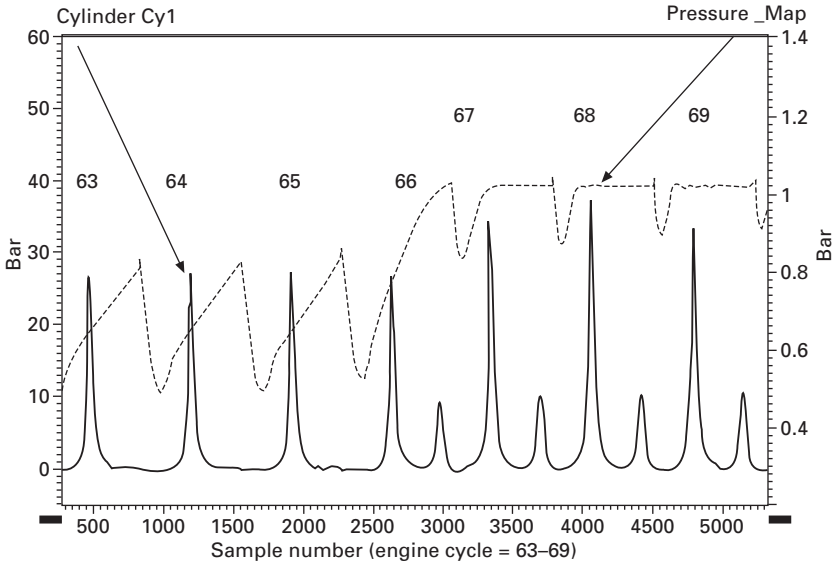

8.12 SI-CAI mode transition using the simulated CPS-P VVT system (IMEPgross = 4.3 bar at 2000 rpm).

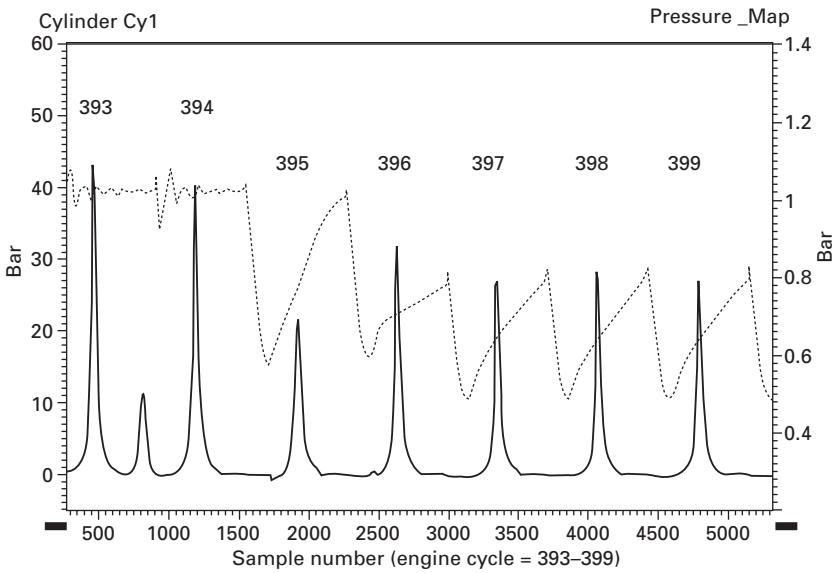

8.13 CAI-SI mode transition using the simulated CPS-P VVT system (IMEPgross = 4.3 bar at 2000 rpm).

The throttle angle position from half open to wide open takes a few more cycles (5–6) to finally stabilise.

When the transition from CAI to SI is performed, a weak combustion occurred at the first SI cycle (395th) but the next one (396th cycle) proceeded well (Fig. 8.12). The spark timing is moved at the same cycle when the valve profile switch occurred. The fuelling rate, in the first two SI cycles, is increased by 20% (due to the globally lean mixture). During the transition from CAI to SI, a large amount of trapped exhaust gas flows out from the cylinder immediately after the change, since the valve profile change takes place. The slow closing speed of the throttle results in a relatively high intake manifold pressure (carried over from the CAI mode, due to its WOT operation); this is sustained during the transition to SI mode. This high intake manifold pressure enhances the cylinder charging in the first SI mode cycle and therefore increases the airflow rate at the intake valves. Increased airflow rate and a lower combustion chamber temperature (inherited from the CAI combustion mode) causes the first SI cycle to burn more slowly than the stabilised rate. To prevent such behaviour, which can be more pronounced at a higher engine speed, synchronisation of the throttle movement, valve profile switching and phasing and fuelling rate has to be further refined. Investigation of this is currently ongoing and results will be published elsewhere.

The changes in engine torque, *air-to-fuel ratio* (AFR), NOx and THC emissions obtained during the SI-CAI-SI transition with CPSP system are presented in Fig. 8.14. These values are plotted against time. The emission

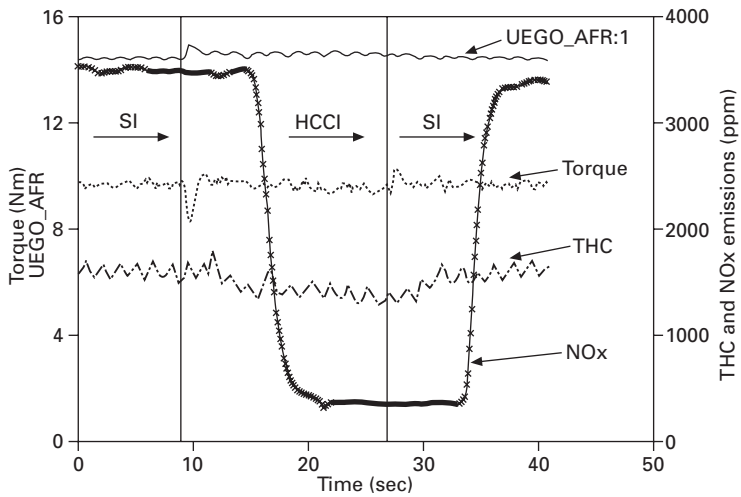

8.14 Changes in engine torque, AFR, NOx and THC emissions during the SI-CAI-SI transition with the simulated CPS-P VVT system (IMEPgross = 4.3 bar at 2000 rpm).

curves are phased later relative to the torque and AFR curves (~ 3 sec), due to the delayed sample time of the analyser.

It can be seen in Fig. 8.14 that during the transition from SI to CAI there is a noticeable increase in AFR as a consequence of airflow disturbances caused during the stabilisation of the throttle angle position at WOT. Consequently the engine torque decreases before it stabilises at the steady state value. The NOx emission significantly decreases, as expected, due to much lower combustion temperature in the CAI mode, while the small decrease in THC emission is a result of more complete fuel oxidation in the boundary layers and bulk gas (due to a higher level of energy available from trapped residual gas – TRG).

During the transition from CAI to SI there is a no visible change in AFR but a slight increase in the engine torque, which is most probably a consequence of inadequate fuelling rate in the second SI cycle (396th) after transition (Fig. 8.13). The NOx emission increases considerably due to higher combustion temperatures resulting from the reduced TRG levels associated with SI combustion, whilst the THC emission increases slightly as a result of incomplete fuel oxidation.

The measured location of peak pressure (LPP) values, in SI and CAI modes, is largely at a level acceptable for stable combustion and noise vibration and harshness – NVH (~ 13°ATDC). The maximum rate of pressure rise (MRPR) value obtained in SI mode is ~ 1.5 bar/°CA, whilst in CAI mode ~ 4 bar/°CA with peaks in transition cycles of ~ 8 bar/°CA. The increased MRPR value is a consequence of higher rate of heat release and faster combustion speed associated with CAI mode. The overall transition quality regarding changes in torque, AFR ratio, LPP and MRPR along with changes in pollutant emissions (THC and NOx) using the simulated CPS and phaser system can be considered good. However, a step change in engine torque, observed during CAI to SI transition, is unacceptable for a commercial engine and the smoothness of this transition has to be improved further. The transition process simulating the CPS and phaser VTT system depends strongly on the synchronisation between the throttle angle, profile switching, fuelling rate and ignition, and therefore to meet these demands a new ECU has to be made. Future refinements, as mentioned above, may then yield an acceptable switch using this specification of valve train.

Mode transition using the fully variable VVT system-AVT system

The cylinder pressure trace recorded during the SI to CAI to SI mode transition, using the AVT™ system, over 500 cycles, is presented in Fig. 8.15. Detailed cycle-by-cycle analysis of changes of cylinder pressure trace (Cylinder Cy1) and intake manifold pressure (Pressure_MAP) during mode transition are presented in Figs 8.16 and 8.17.

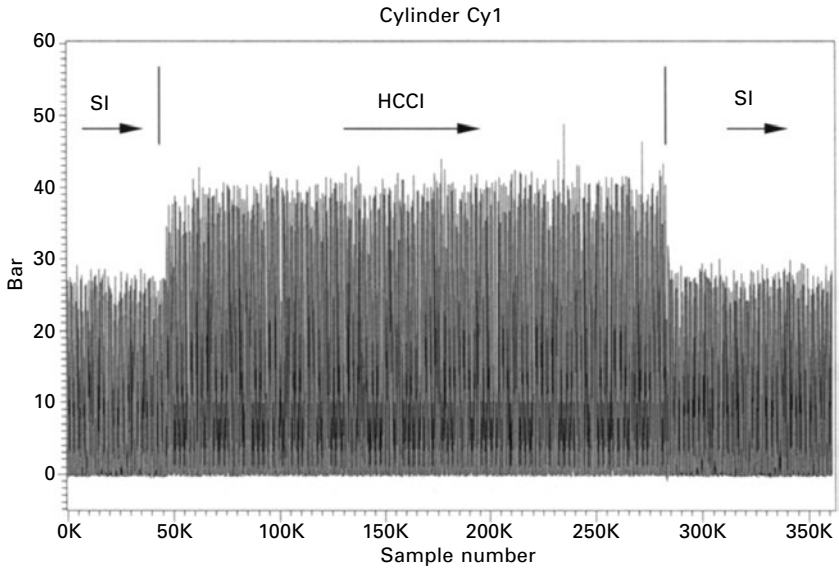

8.15 SI-CAI-SI mode transition during 500 consecutive engine cycles using the AVT™ system (IMEPgross = 4.3 bar at 2000 rpm).

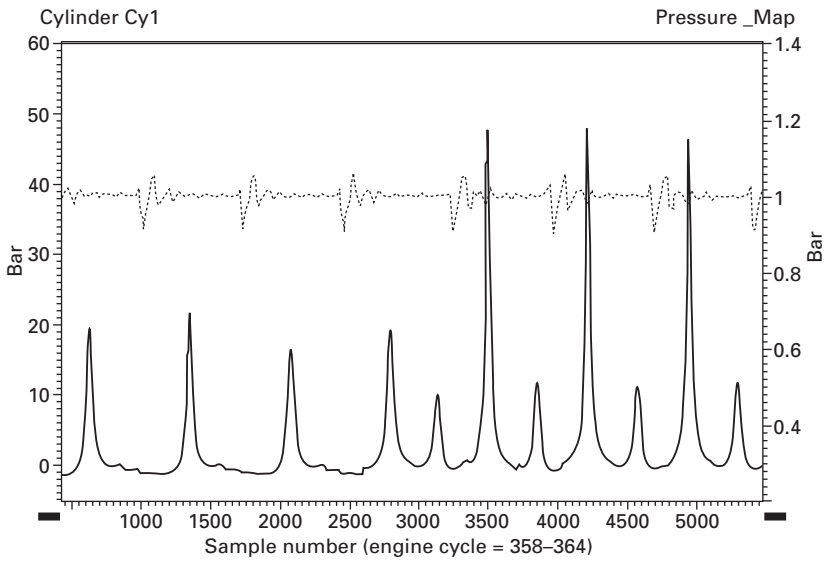

8.16 SI-CAI mode transition using the AVT™ system (IMEPgross = 4.3 bar at 2000 rpm).

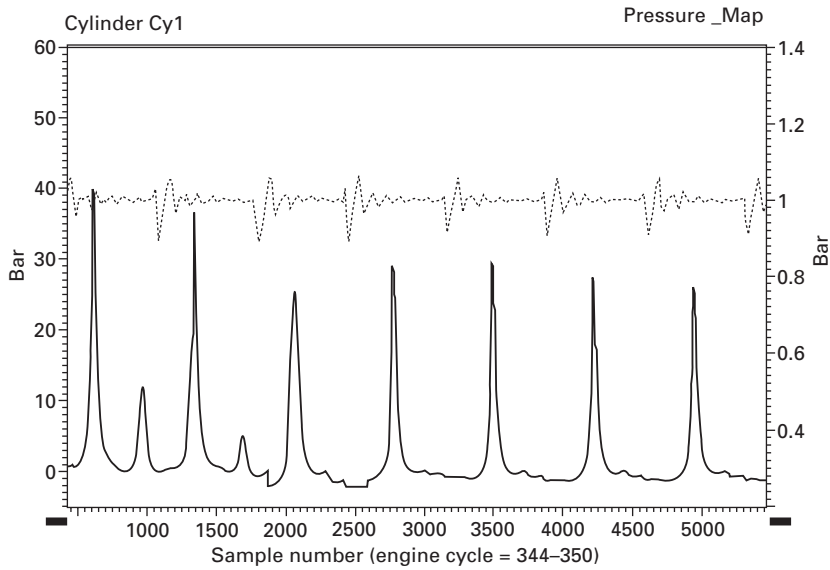

8.17 CAI-SI mode transition using the AVT™ system (IMEPgross = 4.3 bar at 2000 rpm).

It can be seen that during transitions from SI to CAI and vice-versa there is no discernible change in the intake manifold pressure since the engine operates WOT. Therefore, disturbances in airflow caused by the throttle movement are avoided and hence the CAI-SI transition is smoother compared with the CAI-SI transition with CPS-P system, i.e. without a weak combustion in the first SI cycle (Figs 8.13 and 8.17). The valve profile controls the amount of air supplied to and exhaust gases expelled from the cylinder and therefore the charge composition and the quality of SI and CAI combustion switching.

The changes in engine torque, AFR, NOx and THC emissions during the SI-CAI-SI transition with the AVT™ system are presented in Fig. 8.18. It can be seen that there are no noticeable peaks or troughs in engine torque. From this it is apparent that, in the transition process with the AVT system, the valve profile change plays a crucial role in the transition smoothness. The NOx emission shows the usual behaviour during mode transitions, i.e. it decreases in the CAI mode and increases in the SI mode, whilst THC emission remains unchanged. The LPP values in SI and CAI modes are ~ 13°ATDC, whilst the MRPR value in SI mode is ~1.5 bar/°CA and in CAI mode is slightly higher ~4 bar/°CA with peaks of ~6 bar/°CA in transition points.

The overall transition quality regarding changes in torque, AFR ratio, LPP and MRPR along with changes in pollutant emissions (THC and NOx)

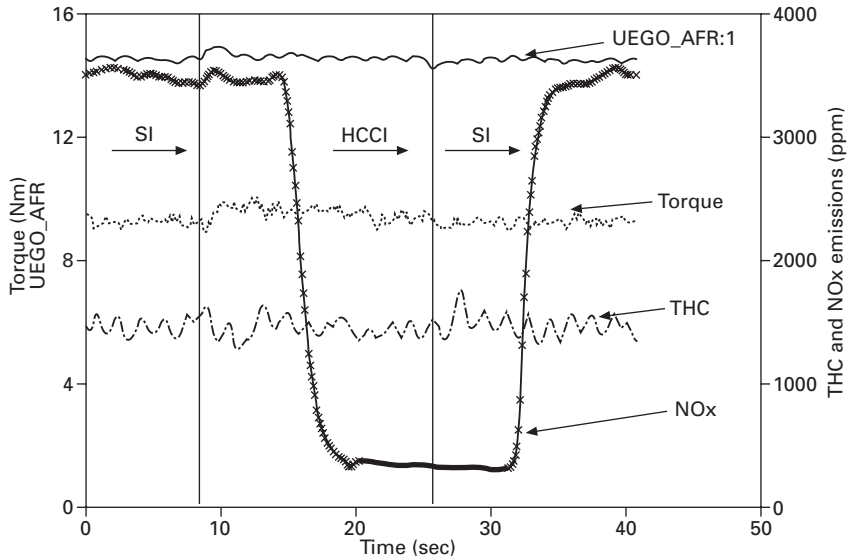

8.18 Changes in the engine torque, AFR, NOx and THC emissions during the SI-CAI-SI transition with the AVT™ system (IMEPgross = 4.3 bar at 2000 rpm).

using the AVT system can be considered very good since there was no weak combustion or step change in engine torque, and is hence better than that obtained with the CPS-P VVT system.

Since the mode transition with the AVT system depends mainly on valve profile changing (engine operates WOT in both modes) there is no need for a completely new ECU and the existing one can easily be adapted because valve motion is controlled by the AVT system. Moreover, AVT enables a 'mixed mode' CAI-SI engine to operate without a throttle and thus with reduced pumping losses and hence an improved fuel consumption in all modes of operation. A wider range of CAI operation can also be expected [24].

The drawback of using the AVT™ system for the SI-CAI-SI mode transitions is that it is still being developed for mass production and therefore its true cost and durability are yet to be established.

8.5 Summary

For commercial applications of CAI to production engines, problems with cold start, running at idle and high loads together with controlling the combustion over the entire speed/load range need to be resolved. A possible solution to overcome these problems, by operating the CAI engine in 'mixed mode' switching between CAI and SI, was presented and discussed. From

the experimental results obtained on the single cylinder 'mixed mode' CAI-SI engine using two different VVT systems (cam profile switching and phasing device – (CPS-P) system and fully variable electro-hydraulic – Pro AVT system the following observations and conclusions are drawn:

- In such an engine CAI combustion can be initiated and controlled in a certain range by trapping residual gas inside the cylinder – *the recompression method* or by re-introducing the exhaust gas during the intake stroke – *the re-breathing method*. The former method was used in the experiments reported in the present work.
- In any 'mixed mode' CAI-SI engine, the transition between these combustion modes, during changes in engine load and speed, plays a crucial role, and hence the valve train and engine management system (EMS) have to provide a seamless operation, whilst keeping all relevant engine and combustion parameters in an acceptable range.
- The VVT train system was to be as flexible as possible, preferably the fully variable.
- The mode transition can be performed in one engine cycle with CPS-P system providing acceptable engine driveability and pollutant emissions. There is, however, a problem with the synchronisation of the valve profile switching and throttle response, which can cause an unacceptable step change in torque and therefore a new ECU is required.
- With the use of the Pro AVT system the mode transition can be also performed in one engine cycle but by operating at WOT in both modes, SI and CAI, the pumping losses were reduced, hence the fuel consumption. The mode transition was performed with improved engine driveability compared to that obtained with CPS-P system, since transition depended only on valve profile switching, because the engine operated with WOT. In the case of using Pro AVT system the existing ECU can be used with valve control being a supplementary part of the AVT system.

8.6 References

1. Koopmans, L. and Denbratt, I., A Four-Stroke Camless Engine, Operated in Homogeneous Charge Compression Ignition Mode with Commercial Gasoline, SAE Paper 2001-01-3610, 2001.
2. Urata, Y., Awasaka, M., Takanashi, J., Kakinuma, T., Hakozaki, T. and Umemoto, A., A Study of Gasoline-fuelled HCCI Engine Equipped with an Electromagnetic Valve Train, SAE Paper 2004-01-1898, 2004.
3. Law, D., Allen, J., Kemp, D., Kirpatrick, G. and Copland. T., Controlled Combustion in an IC-Engine with a Fully Variable Valve Train, SAE Paper 2001-01-0251, 2001.
4. Turner J., Blundell D., Bassett M., Pearson R. and Chen R., The Impact on Engine of Controlled Auto Ignition versus Spark Ignition with two Methods of Load Control. Proceedings of the Global Powertrain Conference (GPC), Michigan, USA, 2002.
5. Milovanovic N., Chen R. and Turner J., Influence of the Variable Valve Timing on

the Gas Exchange Process in a Controlled Auto Ignition (HCCI) Engine. Proceedings of the IMECHE Part D: *Journal of Automobile Engineering,* Vol. 218, No. 5, pg. 567–583, 2004.
6. Fuerhapter, A., Unger, E., Piock, W. and Fraidl, G., The New AVL CSI Engine – HCCI Operation on a Multicylinder Gasoline Engine, SAE Paper 2004-01-0551, 2004.
7. Lang, O., Salber, W., Hahn, J., Pischinger, S., Hortmann, K, and Bucker, C., Thermodynamic and Mechanical Approach Towards a Variable Valve Train for the Controlled Auto Ignition Combustion Process, SAE Paper 2005-01-0762, 2005.
8. Christensen M., Einewall P. and Johansson B., Homogeneous Charge Compression Ignition (HCCI) Using Iso-octane, Ethanol and Natural Gas-A Comparison with Spark Ignition Operation, SAE Paper 972874, 1997.
9. Matthews, J., Sanstoso, H. and Chend, W., Load Control for an HCCI Engine, SAE Paper 2005-01-0150, 2005.
10. Haraldsson, G., Hyvonen, J.,Tunestal, P. and Johansson, B., HCCI Combustion Phasing in a Multi Cylinder Engine Using Variable Compression Ratio, SAE Paper 2002-01-2858, 2002.
11. Christensen M. and Johansson B., Influence of Mixture Quality on Homogeneous Charge Compression Ignition, SAE Paper 982454, 1998.
12. Iida, N. and Igarashi, T., Auto-Ignition and Combustion of N-Butane and DME/Air Mixtures in a Homogeneous Charge Compression Ignition Engine, SAE Paper 2000-01-1832, 2001.
13. Murase, E. and Hanada, K., Control of the Start of HCCI Combustion By Pulsed Flame Jet, SAE Paper 2002-01-2867, 2002.
14. Weinrotter, M., Wintner, E., Iskra, K., Neger, T., Olofsson, J., Seyfried, H., Alden, M., Lackner, M., Winter, F., Vressner, A., Hultqvist, A. and Johansson, B., Optical Diagnostics of Laser-Induced and Spark Plug Assisted HCCI Combustion, SAE Paper 2005-01-0129, 2005.
15. Asai, M., Kurosaki, T. and Okada, K., Analysis on Fuel Economy Improvement and Exhaust Emission Reduction in a Two-Stroke Engine by Using and Exhaust Valve, SAE Paper 951764, 1995.
16. Ishibashi Y., Isomura S., Kudo O. and Tsushima Y., Improving the Exhaust Emissions of Two-Stroke Engines by Applying the Activated Radical Combustion. SAE Paper 960742, 1996.
17. Blundell D., Turner J., Duret P., Lavy J., Oscarsson J., Emanuelsson G., Bengtsson J., Hammarstrom T., Perotti M., Kenny R. and Cunningham G., Design and Evaluation of the ELEVATE two-stroke automotive engine. SAE Paper 2003-01-0403, 2003.
18. Yanagihara, H., Satou, Y., and Mizuta J., A Simultaneous Reduction of NOx and Soot Diesel Engines under a New Combustion System (Uniform Bulky Combustion System–UNIBUS), 17th Int. Vienna Motor Symposium, 1996.
19. Kimura S., Aoki O., Ogawa H., Muranaka S. and Enomoto Y., New Combustion Concept for Ultra-Clean and High-Efficiency Small DI Diesel Engines. SAE Paper 1999-01-3681, 1999.
20. Brustle C. and Schwarzenthal D., VarioCam Plus – A Highlight of the Porsche 911 Turbo Engine. SAE Paper 2001-01-0245, 2001.
21. Schausberger C., Bachmann P., Borgmann K., Hofmann R. and Liebl J., The new BMW Otto Engine Generation. Proceedings Aachener Kolloquium Fahrzeug und Motorentechnik, Germany, 2001.
22. Sugimoto C., Sakai H., Umemoto A., Shimizu Y. and Ozawa H., Study on Variable

Valve Timing System Using Electromagnetic Mechanism. SAE Paper 2004-01-1869, 2004.
23. Valeo's press release about a new VVT system, 2005.
24. Cairns, A. and Blaxill, H., The Effects of Combined Internal and External Exhaust Gas Recirculation on Gasoline Controlled Auto-Ignition, SAE Paper 2005-01-0133, 2005.

9

Fuel effects in CAI gasoline engines

G T KALGHATGI, Shell Global Solutions, UK

9.1 Introduction

In Homogeneous Charge Compression Ignition (HCCI) engines fuel and air are premixed as in a Spark-Ignition (SI) engine but heat release occurs by auto-ignition as in a Compression Ignition (CI) engine. It is marked by the absence of a narrow flame front and is controlled by chemical ignition kinetics that is dominated by decomposition of H_2O_2 (Westbrook, 2000) and reaction between OH and fuel (Peters *et al*., 2002). Indeed even in CI engines, where auto-ignition occurs when the mixture is quite fuel rich as the fuel and air mix (Dec, 1997), it is determined by the same chemical kinetic mechanisms (Westbrook, 2000). Auto-ignition depends on the pressure and temperature history of the unburnt fuel/air mixture and also on the auto-ignition quality of the fuel and this can vary very widely across different fuels. In SI engines, fuels need to be resistant to auto-ignition whereas in conventional CI engines fuels should auto-ignite readily. In HCCI engines the required auto-ignition quality of the fuel varies widely depending on the engine design and operating conditions as discussed later.

Combustion phasing or the timing of heat release is critical in HCCI engines and needs to occur in a narrow crank angle window near top dead centre (TDC) in order to run the engine with acceptable levels of stability and pressure rise rate (Kalghatgi and Head, 2006). Engine design and operational parameters affect auto-ignition and can be used to control combustion phasing with a given fuel. For instance, the temperature at the start of compression could be altered by heating the intake charge or by retaining hot exhaust gases in the cylinder by using negative valve overlap (NVO); initial pressure can be increased by turbo-charging or supercharging. Auto-ignition is also affected critically by engine speed, which determines the time available – increasing engine speed reduces the chances of auto-ignition. Similarly making the mixture leaner or increasing the exhaust gas recirculation (EGR) level reduces the likelihood of auto-ignition. The compression ratio of the engine determines the final pressure and temperature

attained by the mixture. Indeed HCCI engines can be run on almost any fuel if appropriate conditions are chosen. Of course the fuel needs to be volatile enough for it to be sufficiently well mixed with air; however, it should be remembered that the mixture in HCCI combustion is never truly homogeneous (Hultqvist *et al*., 2002). This can be achieved with even relatively involatile fuels such as practical diesel fuels with appropriate injection and mixture preparation strategies. Thus the challenge is to understand the auto-ignition behaviour of fuels in the context of the wide range of physical conditions that might be encountered.

There have been many studies where different fuels of different chemical composition have been used in the same HCCI engine. Some examples are: Aroonsrisopon *et al*. (2002), Jeuland *et al*. (2003), Risberg *et al*. (2003, 2005), Kalghatgi and Head (2006), Kitano *et al*. (2003), Koopmans *et al*. (2004), Montagne and Duret (2002), Oakley *et al*. (2001), Ryan and Matheaus (2002), Shibata and Urushihara (2006). All these studies show that, as expected, different fuels have different combustion phasing in most cases but this difference is small in some operating conditions (Koopmans *et al*., 2004; Kalghatgi and Head, 2004; Shibata and Urushihara, 2006). In most cases combustion phasing does not correlate with conventional measures of fuel auto-ignition quality such as Research and Motor octane numbers, *RON* and *MON* (e.g., Jeuland *et al*., 2003; Ryan and Matheus, 2002). However HCCI engines can also be run at such engine operating conditions that combustion phasing correlates with *RON* (Risberg *et al*., 2003) or *MON* (Kalghatgi and Head, 2004). There is a need for a general framework within which the auto-ignition of a wide range of fuels exposed to a wide range of physical environments can be understood.

In this chapter we first discuss the difference between gasoline and diesel fuels and consider the different approaches to defining the auto-ignition quality of practical fuels. We will then discuss the effect of gasoline auto-ignition quality on HCCI engine operation and finally discuss the fuel requirements of HCCI engines. In this context we will also discuss some other approaches that have been suggested to assess the suitability of a fuel for HCCI combustion.

9.2 Practical transport fuels

Liquid fuels have very high volumetric energy density at normal temperatures and pressures – from 32 to 36 MJ per litre; they are also easy and safe to handle and transport. Hence practical transport fuels are usually liquid fuels, though gases are also used in niche applications. Practical fuels are primarily made in refineries, starting with crude oil and blending the products of several refinery processes. A description of refinery and other processes used for making fuel components can be found in Owen and Coley (1995)

and a brief summary of the main processes emphasising the type of molecules produced is also given by Kalghatgi (2005). Crude oil, which contains thousands of different hydrocarbons, is first separated into different boiling range fractions by distillation. Up to 2% of the crude can be dissolved gases, which are released when the temperature is raised above ambient temperature – these constitute Liquid Petroleum Gas, LPG. The light fraction resulting from distillation and boiling roughly in the gasoline range from ~20°C to ~160°C is often termed 'naphtha'. The middle distillates form the kerosene/gas oil range and span the diesel boiling range of ~160°C to ~380°C. Depending on the crude, between 40% and 60% of its weight can be 'residue' with boiling points above ~380°C. Further processing of these streams is always necessary in order to convert heavier, low-value fractions into lighter fractions that can be used as fuel components. Auto-ignition quality is related to the molecular structure of the fuel (Heywood, 1988). Most of the complex refinery processing is aimed at making the streams from the initial distillation more resistant to auto-ignition, i.e. to increasing their anti-knock quality by changing their molecular structure.

In addition to components derived from crude oil, components derived from natural gas or plant material (bio fuels) are also used in practical fuels. In many parts of the world, governments are actively promoting the use of bio fuels. For instance the EU directive number 2003/30/EC aims to replace, by 31 December 2010, 5.75% by energy content, of all petrol and diesel used in the EU by bio-fuels.

- *Oxygenates* – alcohols such as ethanol and esters such as methyl tertiary butyl ether (MTBE) are used as gasoline components. Esters which are very prone to auto-ignition and usually made from vegetable oils, e.g. rape-seed methyl ester (RME), are used as diesel components.
- *Gas to liquid (GTL) fuels* – The Fischer-Tropsch process is used to produce paraffinic hydrocarbons from synthesis gas – a mixture of carbon monoxide and hydrogen – which in turn, can be produced from natural gas, coal or from biomass. New industrial processes using natural gas, like the Shell middle distillate synthesis (SMDS) process, produce paraffinic products with high carbon numbers which are very prone to auto-ignition and hence are good diesel components.

Gasolines are blended to the required auto-ignition quality using the products of the processes described above. The finished gasoline has to meet many other specifications, such as those on composition and volatility. Diesel fuels, unlike gasolines, must auto-ignite easily and hence are blended from components in the middle distillate range mostly not used for gasolines. In addition to their auto-ignition quality, diesel fuels have also got to meet other specifications, such as those on density and cold flow properties – long chain paraffins in diesel fuels are prone to come out of solution as waxes at low

Table 9.1 Some properties of a typical gasoline and a typical diesel fuel in Europe

Property	Gasoline	Diesel
RON*	95.4	
MON*	85.6	
Cetane number*		52
Energy content (to gas) MJ/kg	43.5	43.1
Density @ 15° C, kg/litre	0.738	0.833
Initial boiling point, IBP °C	28	168
Final boiling point, FBP °C	198.5	348
Normal paraffins, %v	10.8	
Iso paraffins, % v	43.4	
Total paraffins, % v	54.2	43
Naphthenes, % v	2.9	29
Olefins, % v	8.6	
Aromatics, %v	33.6	27
Average molecular formula		
C	6.64	15.4
H	12.11	32.4
AFR, stoichiometric air/fuel ratio	14.53	14.93

* See Section 9.3.

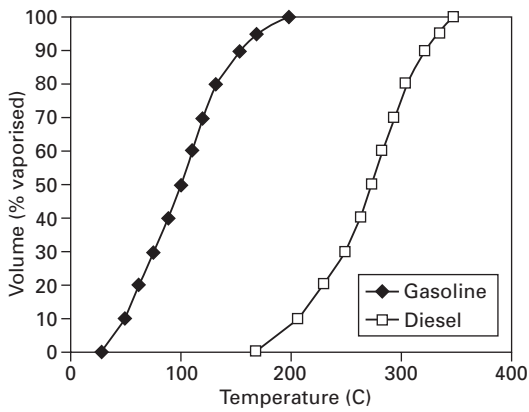

9.1 Volatility characteristics of a typical gasoline and a typical diesel fuel in Europe.

temperatures and block fuel lines and filters. Table 9.1 lists some properties of a typical gasoline and a diesel fuel in Europe. Figure 9.1 shows the distillation characteristics of such fuels; this is usually determined by using the standard ASTM D 86 test (ASTM, 2005). Gas chromatography (GC) reveals up to 150 compounds with carbon numbers of 2 to 12 in gasolines. In diesel fuels hydrocarbons with carbon numbers of 7 to 30 can be identified. In gasolines, iso-pentane and iso-octane are the most prominent paraffins

found, while toluene and xylenes often make up over half the aromatics. Thus practical fuels are complex mixtures of paraffins, aromatic hydrocarbons and olefins. They might also contain oxygenates.

9.3 Auto-ignition quality of fuels

Much that appears in this section was also discussed in Kalghatgi (2005).

9.3.1 Chemical kinetic modelling of auto-ignition

Auto-ignition can be studied at a fundamental level by modelling the kinetics of the chemical reactions involved as the pressure and temperature of the mixture change. Comprehensive chemical models of auto-ignition aim to use all relevant chemical reactions. The number of such reactions increases very rapidly as the size and the complexity of the fuel molecule increase. Westbrook and Dryer (1984), Warnatz (1984) and co-workers have built reaction mechanisms consisting of thousands of reactions for combustion chemistry, starting with simple fuels and then moving on to larger molecules. However, 'comprehensive' schemes cannot be perfectly accurate because of the uncertainties in the reaction rate constants and their temperature and pressure dependences (Bradley and Morley, 1997; Simmie, 2003). Thus comprehensive models include all available, though imperfect, chemical knowledge. They have to be calibrated using experimental data and can be used to interpolate and extrapolate chemical behaviour. Many practical applications use reduced or simplified chemical models which attempt to select the reactions of critical importance for the particular application (Griffiths, 1995; Bradley and Morley, 1997). Such models inevitably have a limited representation of real chemistry. However, for a given fuel and a given application they can be tuned by comparison with experiments. Then they can be used to predict auto-ignition phenomenon such as knock at other experimental conditions.

Unfortunately chemical reaction mechanisms applicable to auto-ignition in IC engines have only been developed for a very few pure compounds – mostly paraffins of low carbon numbers (Simmie, 2003). Another difficulty is that while the auto-ignition of a pure component is governed by the reactivity of the products of reaction, in a mixture it is the initial rate of radical reaction that is significant (Leppard, 1992). Thus even if the auto-ignition chemistry of two pure fuels is fully understood, it is not a simple matter to develop the auto-ignition chemistry of mixtures of the two fuels. Chemical kinetic schemes have been developed for mixtures of isooctane and n-heptane, known as primary reference fuels (PRF) but those for other relevant mixtures such as aromatics or olefins and paraffins are only just appearing (Andrae *et al.*, 2005). Indeed it is highly unlikely that the auto-ignition chemistry of a

practical fuel containing hundreds of different components could be modelled completely and reliably in the near future. However surrogate fuels with four or five components of different molecular structure could be reasonable substitutes for practical fuels – the models for such surrogate fuels are being developed (Naik *et al*., 2005). These models for non-PRF fuels are in a very early stage of development and would only be applicable to the particular simple mixtures used. They have not been fully calibrated and cannot be used to predict the auto-ignition of other mixtures with other components quantitatively. Their main role is likely to be in explaining experimental observations and in extending our understanding of auto-ignition chemistry. Thus auto-ignition in internal combustion engines using practical fuels cannot be fully described in terms of fundamental chemical kinetics at the moment.

9.3.2 Ignition delay and the Livengood-Wu integral

Many auto-ignition studies are conducted using a shock tube or a Rapid Compression Machine (RCM). In these devices the fuel/air mixture is compressed rapidly and held at a 'constant' pressure and temperature. Chemical reactions start and after some time, auto-ignition, marked by rapid heat release, occurs. The time between the end of compression and auto-ignition is known as the induction time or ignition delay, τ. The lower the value of τ, the more reactive the mixture, in terms of auto-ignition. Quite often ignition takes place in two stages, with a smaller earlier heat release associated with low temperature reactions (Heywood, 1988).

The ignition delay changes with temperature and pressure. Chemical kinetic models of auto-ignition are often calibrated using measured values of ignition delay. In IC engines the pressure and temperature of the fuel/air mixture both increase from the start of compression and at each point during the cycle the mixture will have a different value of τ. It is then assumed that auto-ignition occurs when the following condition is satisfied.

$$I = \int (1/\tau) \cdot dt = 1 \qquad 9.1$$

This approach was first suggested by Livengood and Wu (1955) and is now commonly used in knock studies (Heywood, 1988) as well as HCCI studies (Bradley *et al*., 2004). Ignition delays have been measured for several fuels at different temperatures and pressures relevant to IC engines by several groups (Cizeki and Adomeit, 1993; Fieweger *et al*., 1997, Davidson *et al*., 2004, Gauthier *et al*., 2004). An example of the complex variation of τ with temperature, T, is shown in Fig. 9.2 where ignition delay has been plotted against 1000/T for n-heptane (squares) and a gasoline of (*RON* + *MON*)/2 of 87 (triangles) at 20 bar (open symbols) and 55 bar (closed symbols). The data has been taken from Figures 11, 12 and 13 in Gauthier *et al*. (2004).

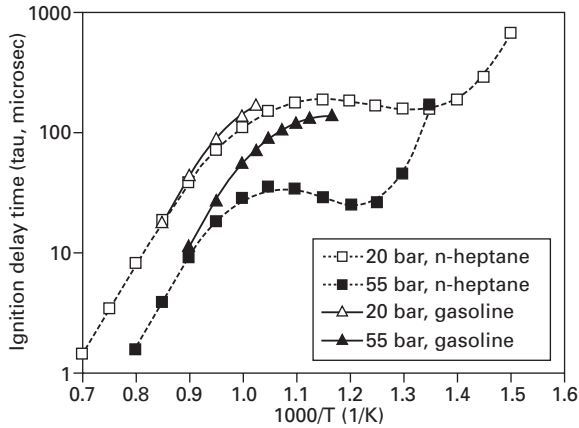

9.2 Ignition delay times plotted against 1000/T for n-heptane and a gasoline of (*RON* + *MON*)/2 of 87. The data come from Figs. 11, 12 and 13 in Gauthier *et al.* (2004).

Clearly, an increase in pressure causes a decrease in τ as the mixture becomes more reactive. In general τ can be expressed as

$$\tau = f(T)P^{-n} \tag{9.2}$$

A value of 1.7 for the pressure exponent, n is suggested by Douaud and Eyzat for PRF (1978) whereas Hirst and Kirsch (1980) suggest that for toluene/*n*-heptane mixtures, toluene reference fuels, TRF, n ~1.3. In general compared to paraffins, n is lower for aromatic and olefinic fuels. In other words, they become more resistant to auto-ignition, the value of τ decreases more slowly, when the pressure is increased for a given temperature (Gauthier *et al.*, 2004; Cowell and Lefebvre, 1986). This can be seen in Fig. 9.2 – the ignition delay for both fuels is very similar, for temperatures greater than 975 K at 20 bar but at 55 bar, the gasoline has very much higher ignition delays than n-heptane for a given temperature. It also appears that n is different in different temperature regimes for a given fuel (Davidson *et al.*, 2004). It is common practice (Heywood, 1988) to approximate the dependence of τ on T by an Arrhenius type expression and write Equation 9.2 as

$$\tau = AP^{-n}\exp\left(\frac{B}{T}\right) \tag{9.3}$$

The constants A, n and B are different for different fuels.

However Fig. 9.2 shows that such an expression is too simple – an Arrhenius relationship would be represented by a straight line. In fact, for a better description of τ through the entire pressure and temperature regime, Yates *et al.* (2005) have used three different equations of the form of Equation 9.3. Indeed for paraffins, over a middle range of temperatures, τ can actually

increase – reaction rates decrease – with increasing temperature (Leppard, 1990). Thus in Fig. 9.2, for n-heptane, ignition delay decreases with increasing temperature between 740 K and 870 K at 20 bar and between 830 K and 950 K at 55 bar. This phenomenon is described as the negative-temperature coefficient (NTC) behaviour. The heat release often observed before the main heat release in auto-ignition experiments (two-stage auto-ignition) is associated with the NTC region and called the first-stage heat release. It is common to describe the chemistry in the NTC region as 'low-temperature' chemistry in contrast to the auto-ignition chemistry leading up to the final heat release. During auto-ignition in SI and HCCI engines, the fuel/air mixture traverses the NTC region to varying degrees depending on engine design and operating conditions. The first-stage heat release from low-temperature chemistry is not simply a function of the fuel but depends on the pressure and temperature history of the fuel/air mixture and hence, in engine experiments, on the inlet pressure and temperature. Thus the first-stage heat release was significant for different PRF and non-PRF fuels in HCCI experiments at high inlet pressures and low inlet temperatures but was insignificant for the same fuels at higher inlet temperatures and lower inlet pressures (Kalghatgi *et al*., 2003, Risberg *et al*., 2003). The differences in the dependence of this chemistry on T and P are very important in explaining the differences in auto-ignition between different fuels.

In an engine consider moving from one operating point to another during compression – an initial condition of 20 bar and 700 K (inlet temperature of ~60°C, inlet pressure 1 bar abs) to 55 bar. The temperature will increase to ~ 910 K. For n-heptane this increase in temperature, if the pressure were held constant at 20 bar, will lead to very little change in ignition delay (open squares in Fig. 9.2 above). However the ignition delay will be over six times lower because of the increase in pressure. There is a danger of missing such effects of pressure if we focus too much on single curves such as those shown above. Also non-paraffinic fuels have much lower pressure exponents for the ignition delay compared to PRF fuels – as pressure increases, the ignition delay decreases much less, the fuels become more resistant to auto-ignition compared to PRF fuels. This is the primary reason why they behave so differently from PRF fuels in engines – e.g., the same gasoline could match a very wide range of PRF fuels for auto-ignition depending on the pressure and temperature history of the mixture.

Not surprisingly the ignition delay at a particular pressure and temperature is very poor at predicting auto-ignition when the pressure and the temperature change with time as in internal combustion (IC) engines (Griffiths *et al*., 1997). Thus, based on ignition delay measurements at 20 bar in the temperature range between 980 K and 1200 K in Fig. 9.2, one might be led to believe that n-heptane and gasoline have very similar auto-ignition properties but in most cases in IC engines – whether in knocking SI engines or in HCCI

engines – these fuels are very different from each other. τ as a function of T and P over the entire relevant range needs to be known for a fuel in order to estimate the Livengood-Wu integral in Equation 9.2. Such information simply does not exist for practical fuels but has only recently become available for a few model or surrogate fuels (Gauthier *et al*., 2004). An empirical approach to describe the auto-ignition behaviour of practical fuels is unavoidable because neither the chemical kinetic modelling approach, nor one based on using ignition delay is possible.

9.3.3 Empirical approaches to defining auto-ignition quality of fuels

The auto-ignition, anti-knock or octane quality of fuels for SI engines has been traditionally described by the Research and Motor octane numbers, *RON* and *MON*. The tests are done in a standardised, Co-operative Fuel Research (CFR) engine to a closely specified methodology. There are two distinct standard test methods. One, defined by the ASTM D 2699 test (ASTM, 2005), is run at an engine speed of 600 rpm and an intake temperature of 52°C and gives the *RON*. The other, defined by the ASTM D 2700 test (ASTM, 2005) known as the Motor method is run at 900 rpm and an intake temperature of 149 °C and gives the *MON*. In each test, the engine compression ratio is increased until the engine just knocks on the fuel being tested. The test is repeated under the same engine conditions with different proportions of iso-octane in a mixture with n-heptane, PRF. The octane number is the volume percent of iso-octane in the PRF. Thus a blend of 95% of iso-octane and 5% of n-heptane by volume is assigned the octane number of 95 [PRF 95] in both *RON* and *MON* scales. A fuel is rated by comparing its knocking behaviour with PRF in the *RON* and *MON* tests.

Thus a fuel matching the European specifications of 95 *RON* and 85 *MON*, ULG 95, will knock like a PRF 95, in the *RON* test and like a PRF 85, in the *MON* test. The difference between *RON* and *MON* is known as the sensitivity, S. By definition, PRF have zero sensitivity while most practical fuels have $S > 0$. *RON* and *MON* are amongst the most important fuel properties and critically affect the manufacture and marketing of transport fuels. Practical fuels for SI engines have *RON* ranging from 90 to 100 with sensitivity in the range of 7 to 12; the most common fuels in Europe have *RON* ~ 95 and *MON* ~ 85.

Diesel fuels are significantly more prone to auto-ignition. Moreover the *RON* and *MON* tests cannot be run on practical diesel fuels, which are also much less volatile than gasoline-like fuels. The auto-ignition quality of diesel fuels is determined by the cetane number, *CN*. It is measured for a given fuel by comparing its ignition characteristics with reference fuels in a CFR cetane engine using the standard ASTM D 613 test method (ASTM, 2005). The

reference fuels are made by blending normal cetane, n-hexadecane, which is defined to have a *CN* of 100 and heptamethyl nonane, a highly branched paraffin which is assigned a *CN* of 15. The *CN* of a reference fuel with *X*% volume normal cetane is given by

$$CN = X + 0.15(100 - X) \tag{9.4}$$

The fuel being tested is assigned the *CN* of the reference fuel with the same ignition quality in the cetane test.

More recently, a laboratory test method has been developed to measure the auto-ignition quality of diesel fuels – ASTM test method D 6890. This test is also referred to as the ignition quality test, IQT (Ryan and Matheaus, 2002). In this test, a small specimen of test fuel is injected into a heated, temperature-controlled constant volume chamber that has been previously filled with compressed air. The charge pressure and temperature are respectively, 21.37 ± 0.07 bar and 545 ± 30°C. The ignition delay, *ID* is measured as the time between the start of fuel injection and the start of significant heat release; an average of 32 firings is taken. The derived cetane number, *DCN* is related to *ID* by the following formula (ASTM, 2005)

$$DCN = 83.99\ (ID - 1.512)^{(-0.658)} + 3.547 \tag{9.5}$$

The repeatability and reproducibility of IQT measurements are better than those obtained in the cetane engine test. It is to be noted here that *ID* is different from the ignition delay discussed in Section 9.3.2 because the fuel and air are not pre-mixed in the IQT. Practical diesel fuels have cetane numbers ranging from 40 to 60.

The various measures of auto-ignition quality, discussed above, correlate well with each other. Cetane numbers were measured for PRFs and toluene/n-heptane mixtures using the ASTM D613 (engine) method – Fig. 9.3 shows measured *CN* plotted against *RON*. Thus,

$$CN = 54.6 - 0.42\ RON \tag{9.6}$$

Hence n-heptane has a *CN* of around 54 and iso-octane, a *CN* of about 12.5. Similar data are given by Ryan and Matheaus (2002). For practical fuels, in general below a *RON* of about 60, auto-ignition quality should be specified by its cetane number. Figure 9.4 shows the ignition delay, *ID*, in the IQT test plotted against *CN* and *RON* using Equations 9.5 and 9.6. Obviously *ID* increases as *RON* increases or *CN* decreases. Ignition delay, τ, was measured for different fuels in a rapid compression machine, in a pre-mixed fuel/air mixture compressed to 800 K and 40 bar by Tanaka *et al*. (2003) – their Figure 13 shows τ plotted against *RON*. For fuels of the same chemistry, such as PRFs, there is a good correlation between τ and *RON*, and τ increases with *RON* non-linearly, with the increase being sharper in the *RON* range of 80–100, than for *ID* shown in Fig. 9.4 above. However, for comparable

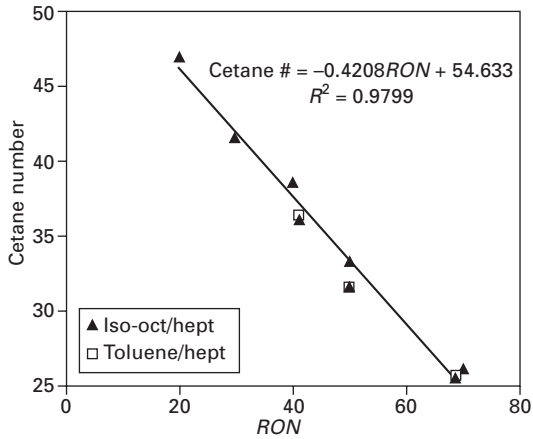

9.3 Measured cetane number vs research octane number (*RON*) for PRF and toluene/n-heptane mixtures.

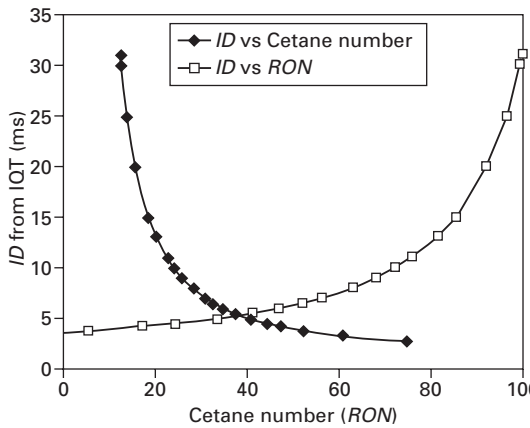

9.4 Ignition delay, *ID* from IQT vs cetane number or *RON* using Equations 9.5 and 9.6.

RON, there is a wide variation in τ for fuels of different chemistries. As discussed in Section 9.3.2 above, τ measured at just one pressure and temperature cannot predict *RON* in the range of practical gasoline fuels, and hence the fuel auto-ignition quality in IC engines. It is re-emphasised that *ID* from IQT is not strictly comparable to τ, which is measured in pre-mixed systems. Nevertheless, where comparison is possible, good correlation exists between these different empirical measures of auto-ignition propensity.

In general, definition of auto-ignition quality is simpler for practical diesel fuels than for gasoline fuels. For instance, if two diesel fuels of cetane numbers *CN*1 and *CN*2 are mixed in the ratio by volume of y and $(1 - y)$

respectively, the cetane number of the blend, *CN*mix can be predicted by the linear formula,

$$CN\text{mix} = yCN1 + (1 - y)CN2 \quad 9.7$$

However, *RON* or *MON* of a mixture of fuels of different molecular structure cannot be usually predicted by linear functions like Equation 9.7 (Bradley and Morley, 1997; Leppard, 1992). The auto-ignition quality of a diesel fuel can be adequately described by a single quantity measured at one experimental condition, such as the cetane number or the ignition delay in the IQT. Thus in HCCI tests, combustion phasing of fuels in the diesel auto-ignition range correlated very well with their cetane numbers for fuels of different chemical composition (Risberg *et al.*, 2005). However, as we will see below, for practical gasoline fuels even two measures, such as *RON* and *MON* established at different operating conditions are not sufficient to describe auto-ignition quality at all conditions. This is almost certainly because, in the range of practical diesel fuels, *CN* between 40 and 60, ignition delay times are much lower than for gasoline fuels and the difference in the structure of the fuel molecules becomes less relevant when the fuels are so prone to auto-ignition. It might also be because the reference fuels used in the cetane test are closer to practical diesel fuels than are the PRF fuels to practical gasolines.

We define gasoline-like fuels as those fuels with $RON > \sim 60$, $CN < \sim 30$ and concentrate on such fuels in the rest of this chapter.

9.4 The octane index and the *K* value

Typical average pressure signals from an HCCI engine are shown in Fig. 9.5a for two fuels of comparable *RON* used in Kalghatgi and Head (2006) – the engine was running at 1200 rpm with inlet pressure (P_{in}) of 2 bar abs. and inlet temperature (T_{in}) of 80°C and the normalised air fuel ratio (λ) of 4.0. The heat release rates calculated from the pressure curves are shown in Fig. 9.5b. Fuel F releases heat earlier than Fuel A even though it has a higher *MON* and hence in the normal course of things could be expected to be more resistant to auto-ignition. From individual cycles, the crank angle at which 50% of the total heat release occurs is calculated and is averaged over a hundred cycles to get the mean (*CA50*). This parameter is taken as the measure of the auto-ignition quality of the fuel – the larger the value of *CA50*, the more the resistance to auto-ignition. There is little or no correlation between *CA50* and *RON* or *MON* for different fuels at this condition as can be seen from Figs 9.6a and 9.6b but we can find a regression equation such that

$$CA50 = a\ RON + b\ MON + c \quad 9.8$$

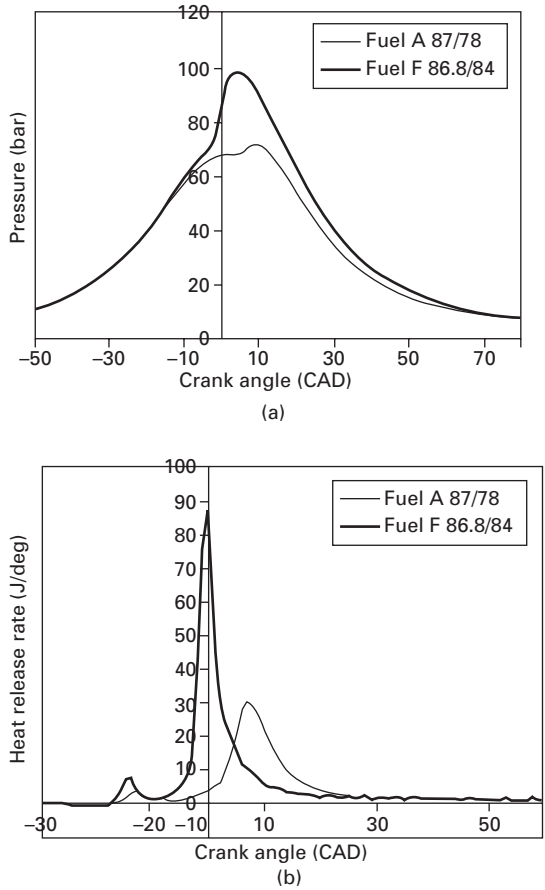

9.5 Average pressure and derived heat release parameters for fuels A and F. 1200 rpm, P_{in} = 2 bar abs., T_{in} = 80°C and λ = 4. (a) Pressure vs crank angle, (b) Heat release rate vs crank angle.

The octane index, *OI* is then defined with *RON* and *MON* and the coefficients from the linear regression.

$$OI = (1 - K)RON + KMON = RON - KS \tag{9.9}$$

$$K = \frac{b}{a + b} \tag{9.10}$$

Equation 9.8 can then be rewritten with the octane index.

$$CA50 = c + (a + b)OI \tag{9.11}$$

The value of K is found to be –1.48 after this analysis is done for the data shown in Figs 9.6a, 9.6b and 9.6c shows that there is a reasonable correlation between *CA50* and *OI* with this value for *K*.

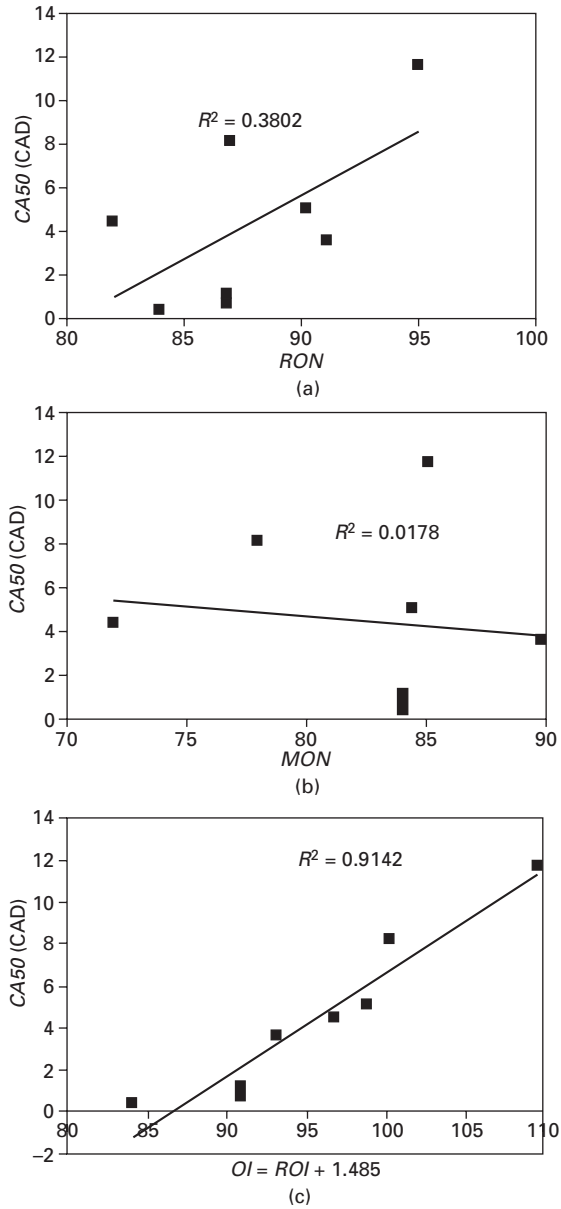

9.6 The crank angle at which 50% of total heat release occurs (average of 100 measurements), *CA50*, for different fuels plotted against *RON*, *MON* and octane index, *OI*; *K* is –1.48. Operating conditions as in Fig. 9.5. Data from experiments listed in Kalghatgi and Head (2006). (a) *CA50* vs *RON*; (b) *CA50* vs *MON* (c) *CA50* vs octane index, *OI*.

OI is the octane number of the equivalent PRF at the relevant test condition. By definition, for the *RON* test conditions, $K = 0$ and for the *MON* test conditions, $K = 1$. For a PRF, $S = 0$ but for a fuel which is not a PRF, *RON* > *MON*, and *OI* depends on the value of *K* as well as its *RON* and *MON*. Thus *S* can be taken to be a measure of the difference in chemistry between the non-PRF fuel and the PRF fuel as one moves from the *RON* to the *MON* test conditions while *K* is a measure of the difference of the particular operating condition from the *RON* test condition. The value of *K* varies with engine operating conditions and hence the same practical fuel will have different *OI* and will match different PRF for auto-ignition qualities at different operating conditions.

The value of *K* was measured over a wide range of engine operating conditions in two very different engines in some recent studies (Kalghatgi *et al*., 2003; Risberg *et al*., 2003 and 2004; Kalghatgi and Head, 2004 and 2006). Figure 9.7 shows examples of different compression temperature (*T*) vs pressure (*P*) curves at which the engines were run; different curves are obtained by varying the intake pressure and temperature. Apart from these parameters, mixture strength and speed are held constant while different fuels are tested as in Fig. 9.6. Temperature increases with pressure during compression and chemical reactions and heat release start at different stages during compression depending on the auto-ignition quality of the fuel. The value of *K* can vary widely and depends on the polytrope defining the operating

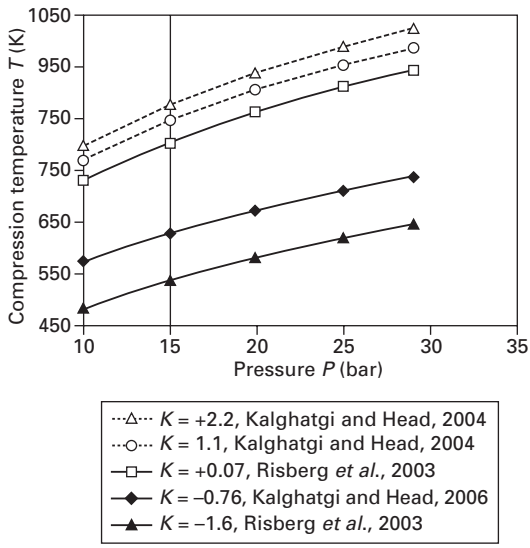

9.7 Compression temperature vs pressure at different operating conditions. The lower the temperature at a given pressure during compression, the lower the value of *K*.

condition. We can take the temperature at a pressure of 15 bar (T_{comp15}), as a parameter that can be used to define the operating polytrope. The value of K decreases as T_{comp15} decreases and can be negative or be greater than one – see Fig. 9.8. For $\lambda < 3.5$, K also appears to depend on λ, increasing with decreasing λ (Risberg *et al.*, 2003). For K, the following equations are suggested by Kalghatgi (2005).

for $T_{comp15} > 825$ K

$$K = 0.0426(T_{comp15}) - 35.2 \qquad 9.12a$$

Here T_{comp15} is expressed in degrees Kelvin.

For $T_{comp15} < 825$ K,

$$K = 0.0056(T_{comp15}) - 4.68 \qquad 9.12b$$

or

$$K = 0.00497\ T_{comp15} - 0.135\lambda - 3.67 \qquad 9.12c$$

Thus a sensitive fuel will have the same *CA50* as a PRF of the same *RON* with the pressure/temperature history when $K = 0$. However, if the engine is run with a lower T_{comp15} say by boosting the inlet, the sensitive fuel will become more resistant to auto-ignition. Its *OI* will be higher than its *RON*, the K value will be negative; its auto-ignition behaviour will be like a PRF with an octane number higher than its *RON*. On the other hand, if T_{comp15} is increased, the sensitive fuel will become more prone to auto-ignition compared to the PRF, its *OI* will be lower than its *RON* and K will be greater than zero.

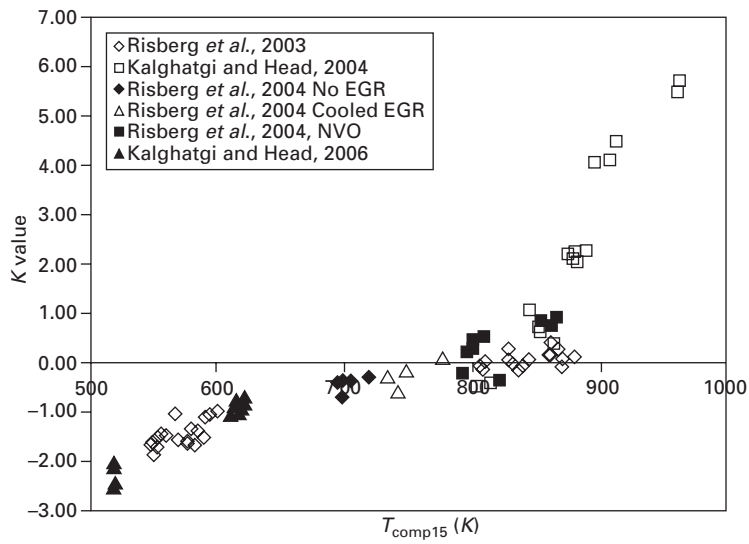

9.8 K vs T_{comp15}.

Thus in general, if the pressure is increased for a given temperature (T_{comp15} is reduced), non-PRF fuels become more resistant to auto-ignition (K decreases). This is in line with the observation that n, in Equation 9.3, is higher for paraffinic fuels compared to non-paraffinic (sensitive) fuels.

9.5 The auto-ignition requirement of an HCCI engine and fuel effects in combustion phasing

At each operating condition, there is also a fuel with $OI = OI_0$ such that heat release is centred at TDC, $CA50 = 0$. OI_0 can be considered to be the engine's requirement. We re-write Equation 9.11 as

$$CA50 = (a + b)[OI - OI_0] \tag{9.13}$$

OI_0 is found from the regression coefficients in Equation 9.8. OI_0 as well as the slope $(a + b)$ in Equation 9.13 were measured for the cases where K was measured. OI_0, which also varies widely in HCCI engines, could be empirically related to in-cylinder pressure and temperature and engine speed and mixture strength. It can be reasonably predicted from Equation 9.14 (Kalghatgi, 2005) for the two engines over the conditions tested.

$$OI_0 = 59 + 0.015T_{maxcomp}\ (\text{K}) + 0.663P_{maxcomp}\ (\text{bar abs}) - 2.6\lambda^* - 0.0123\ N\ (\text{rpm}) \tag{9.14}$$

$$\lambda^* = (1 + EGR_f)\ \lambda \tag{9.15}$$

where λ is the normalised air/fuel ratio (EGR_f) is the exhaust gas recirculation (EGR) mass fraction. EGR_f is assumed to be zero when the only exhaust gases present in the mixture come from residuals left in the cylinder at the end of the exhaust stroke as in the current results. In Risberg *et al*. (2004) the effect of EGR on HCCI combustion was studied and in many of those cases, EGR_f was not zero. OI_0 is dimensionless, $T_{maxcomp}$ and $P_{maxcomp}$ are the compression temperature and pressure at TDC expressed in degree Kelvin and bar (absolute) respectively. They depend on the conditions at the start of compression and the compression ratio and are calculated without including any heat release. N is the engine speed in rpm. Figure 9.9 shows that there is reasonable agreement between the measured value of OI_0 and the value predicted by Equation 9.14 even though the results are from two very different engines over a very wide range of operating conditions. If the fuel conversion efficiency is reasonably constant, higher load is achieved by having a higher fuel mass in the cylinder. This can be achieved by turbo-charging the engine and/or richening the mixture. This will increase $P_{maxcomp}$ and reduce λ^* in Equation 9.14. Thus at high loads, OI_0 will be large.

The third factor determining combustion phasing in HCCI engines is

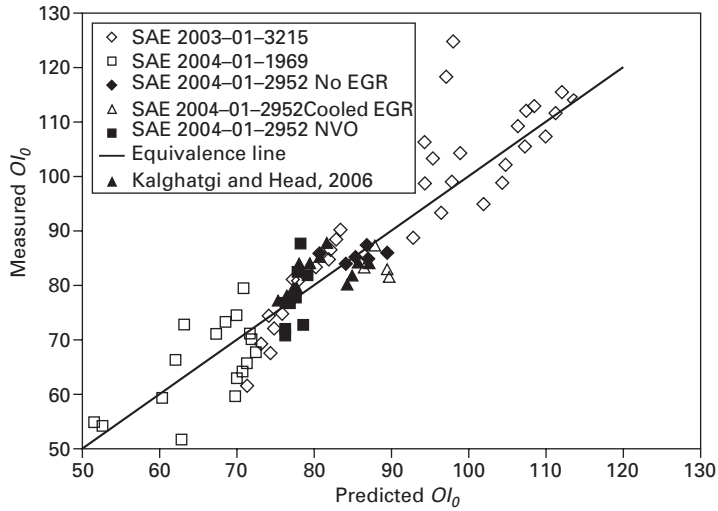

9.9 Measured OI_0 vs OI_0 predicted by Equation 9.14.

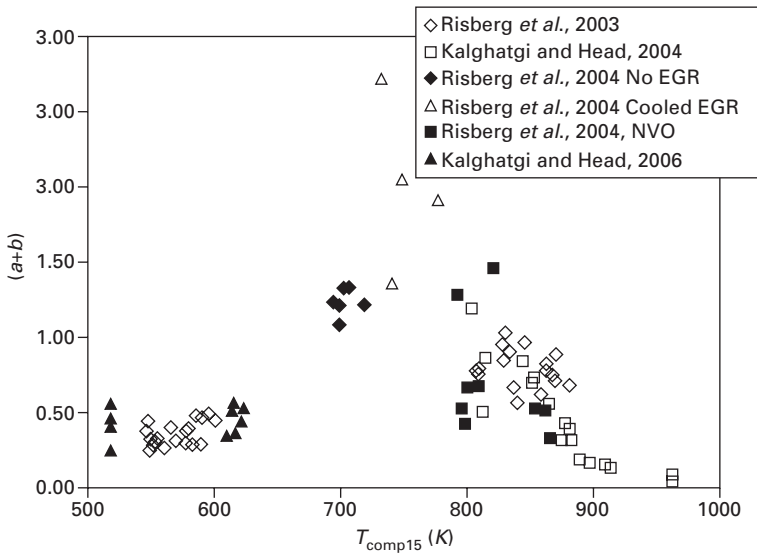

9.10 $(a + b)$ vs T_{comp15}.

$(a + b)$ in Equation 9.13, the sensitivity of *CA50* to changes in *OI* or OI_0. It is found that $(a + b)$ also depends on T_{comp15} – Fig. 9.10. Moreover, at high and low values of T_{comp15}, $(a + b)$ is small so that *CA50* does not differ much for different fuels. This is found to be the case reagardless of whether the temperature is increased by heating the intake charge (Kalghatgi and Head,

2004; Shibata and Urushihara, 2006) or by retaining a lot of internal EGR (Koopmans *et al*., 2004; Risberg *et al*., 2004). With high initial temperatures, ignition delay times for different fuels will be similar even at low pressures; during compression, temperatures will remain high and ignition delay times will continue to be comparable for different fuels (e.g., Fig. 9.2). As a result the Livengood-Wu condition (Equation 9.1) will be satisfied at the same point in the engine cycle and combustion phasing will be comparable for different fuels. Figure 9.10 suggests that combustion phasing becomes less sensitive to *OI* also at low values of T_{comp15}, which in practice, are obtained by increasing the inlet pressure.

Thus, for a fuel with known *RON* and *MON*, if T_{comp15} and other parameters in Equation 9.14 can be determined, *CA50* can be estimated using Equations 9.11–9.14 and Fig. 9.10 (see also Appendix). There are some fuels, particularly simple mixtures and particularly at high temperatures (Kalghatgi and Head, 2004; Risberg *et al*., 2004), whose auto-ignition quality is not predicted by their octane index. Also, small amounts of NO, which might be present in EGR gases, can have a large effect on *CA50* (Risberg, *et al*., 2006). Such anomalies simply highlight the need to understand these phenomena at a more fundamental level.

9.6 Combustion limits

There are two operating limits that are relevant to HCCI engine operation – the so-called 'knock limit' when the pressure rise rate is unacceptably high and the 'instability limit' or the 'misfire limit' when the cyclic variation is unacceptably high. Indeed the cause of excessive cyclic variation might be the failure of auto-ignition in some cycles. If the available fuel auto-ignition quality, *OI*, is greater than OI_0 *CA50* will occur after TDC; auto-ignition will fail to occur if *OI* is increased beyond OI_0 above a limit. Similarly if $OI < OI_0$, *CA50* will occur before TDC and the maximum heat release rate will increase as *OI* is reduced – auto-ignition will become more 'intense' and noise will increase. The knock limit is where the noise is deemed to be unacceptable. The noise can be related to the maximum pressure rise rate – Eng (2002), Jeuland *et al*. (2003).

In general, the pressure rise rate is related to the heat release rate through the energy equation. Ignoring heat losses, the pressure, P can be related to the volume, V and the net heat release, Q by Equation 9.16 (Stone, 1999); θ is the crank angle and γ is the ratio of specific heats.

$$\frac{dP}{d\theta} = \left[\frac{(\gamma - 1)}{V}\frac{dQ}{d\theta}\right] - \left[\gamma\frac{P}{V}\frac{dV}{d\theta}\right] \qquad 9.16$$

Kalghatgi and Head (2006) have studied the effect of fuel and engine parameters on the average value of maximum ($dP/d\theta$) over a hundred cycles

(*MPRR*) and the coefficient of variation (*COV*) of the indicated mean effective pressure (*IMEP*). They found that *MPRR* increases with Φ and P_{in} and decreases with increasing *CA50* and fuel sensitivity, *S*, if each of the parameters is varied while holding the others constant; here Φ is the equivalence ratio ($\Phi = 1/\lambda$) and P_{in} is the inlet pressure. Figure 9.11 summarises how *MPRR* depended on these various parameters in the tests in Kalghatgi and Head (2006). The results in Fig. 9.11 have been separated into three classes depending on the *COV* of *IMEP*. Thus the fuel auto-ignition quality affects *MPRR* through both *CA50*, which also depends on engine operating conditions as discussed in the previous section, and the sensitivity *S*.

In Fig. 9.12a *COV* of *IMEP* has been plotted against $Y = 1.55CA50 – 52\,\Phi$ from the tests described in Kalghatgi and Head (2006); *Y* was identified as the relevant parameter by regression analysis. *COV* of *IMEP* increases sharply for $Y > 0$. In Fig. 9.12b, the cumulative percentage of occurrence has been plotted against *COV* of *IMEP* with different criteria for *Y*. Thus in Fig. 9.12b, for $Y < 0$ (filled triangles), *COV* of *IMEP* will be less than 10% in about 80% of the cases. On the other hand, if $Y > 0$ (open triangles), *COV* of *IMEP* will be less than 10% in only about 12% of the cases. Thus *Y* can be used to discriminate between conditions of high and low cyclic variation; for reasonably low cyclic variation we should have $Y < 0$. Thus the fuel auto-ignition quality affects cyclic variation, again through *CA50*. Exhaust gas recirculation (EGR) reduces *MPRR* (Zhao *et al*., 2001) and also affects other aspects of auto-ignition – this is an area that requires further study.

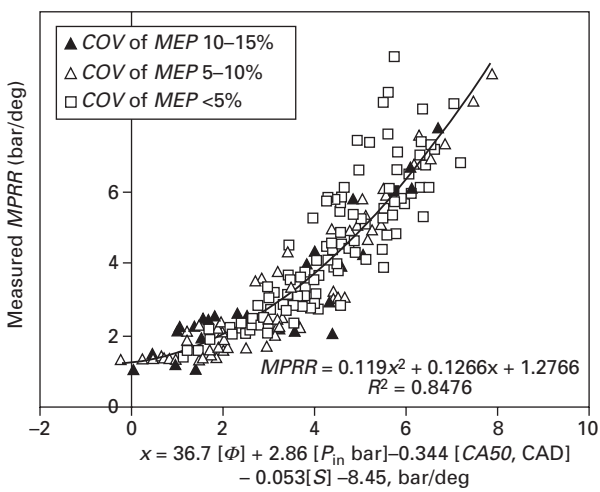

9.11 Dependence of measured mean maximum pressure rise rate on different engine and fuel parameters in Kalghatgi and Head (2006).

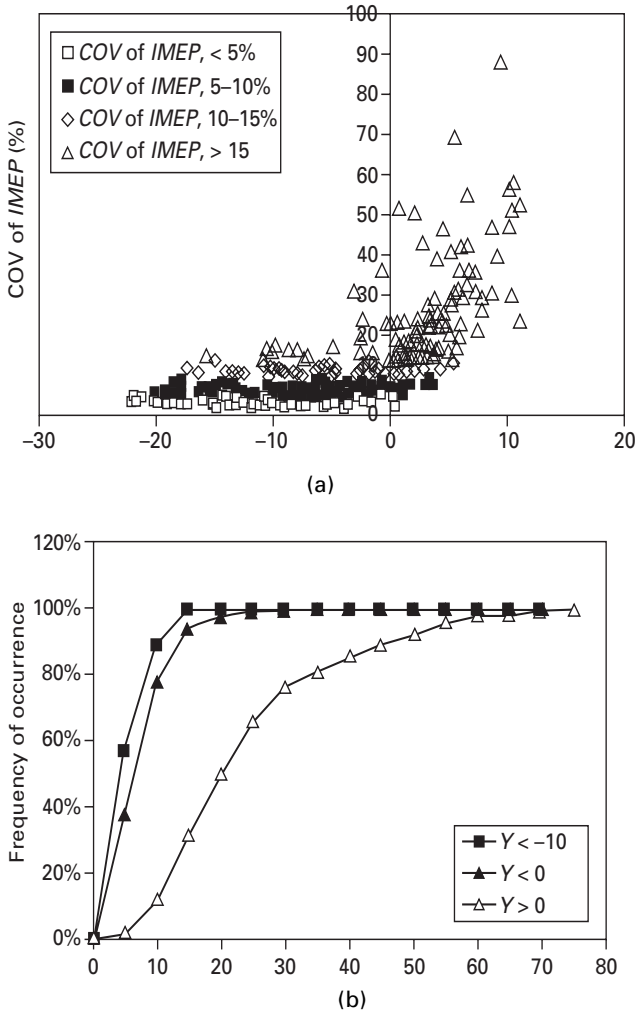

9.12 (a) *COV* of *IMEP* vs *Y* = 1.55CA50–52 Φ; (b) Cumulative occurrence of *COV* of *IMEP* plotted against level of *COV* of *IMEP* for different criteria for X = 1.55CA50–52 Φ.

9.7 *IMEP* and indicated efficiency

In Fig. 9.13 *IMEP*, the mean from 100 cycles, is plotted against the fuel energy content per cycle, *FEN* which is given by Equation 9.17 – the data are from Kalghatgi and Head (2006).

$$FEN = [m_{air}][\Delta H][\Phi]/\{[AFR][N]\} \qquad 9.17$$

Data are again classed by *COV* of *IMEP*. It is clear that mean *IMEP* is

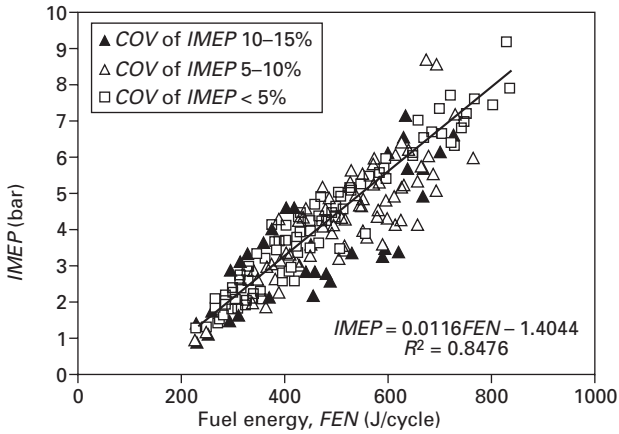

9.13 IMEP vs fuel energy per cycle, *FEN*. Data from Kalghatgi and Head (2006).

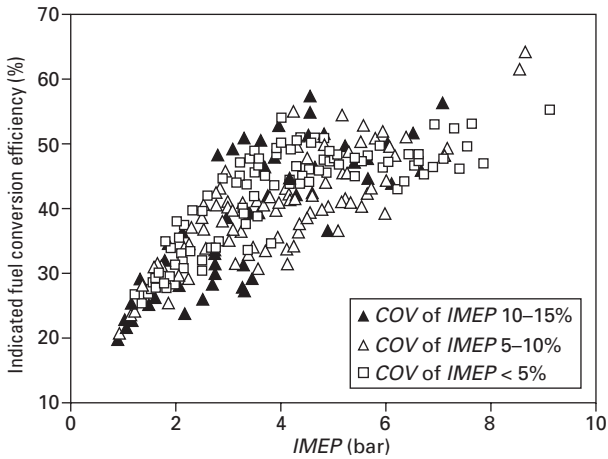

9.14 Indicated fuel conversion efficiency, η_i, plotted against *IMEP*.

strongly correlated to the mean fuel energy per cycle. We can calculate the indicated fuel conversion efficiency (η_i) as

$$\eta_i = [IMEP]\ V_d/FEN \qquad 9.18$$

where V_d is the displacement volume, 500 cc in this case.

The indicated specific fuel consumption (*isfc*) is given by

$$isfc = 1/(\eta_i\, \Delta H) \qquad 9.19$$

In Fig. 9.14, η_i, expressed as a percentage, has been plotted against *IMEP*. It increases with *IMEP* as also noted by Aroonsrisopon *et al*. (2002) where

IMEP is plotted against *isfc*. Regression analysis of the data showed that η_i decreases with increasing Φ, intake air density ρ, and intake temperature T_{in} but increases with increasing *CA50* and P_{max} if these parameters are varied individually while holding others constant (Kalghatgi and Head, 2006). Of course the different parameters on which η_i (or *MPRR* in Fig. 9.11) depends are related to one another. For instance if the intake pressure and temperature are held constant and Φ is increased for a given fuel, *CA50* decreases, *IMEP* increases and η_i will actually increase; however the increase in η_i in such a case occurs because the increase in P_{max} overcomes other effects.

Thus in order to get high *IMEP* on a given fuel and given engine speed, *FEN* has to be increased by increasing m_{air} by boosting the intake and/or by increasing Φ. This would lead to high *MPRR* and hence, depending on the acceptable limit on *MPRR*, there will be a limit on the *IMEP* that can be reached on a given fuel in a given engine with HCCI combustion; higher *IMEP*s can be reached with proper use of EGR. At low *IMEP*, m_{air} and/or Φ will be low, OI_0 will be low and with a given fuel, *CA50* will be large so that cyclic variation could be high unless temperatures are increased through internal EGR to levels where $(a + b)$ in Equation 9.13 is small (Fig. 9.10). These various interdependencies can be studied using the data presented above as discussed in the Appendix.

9.8 Other approaches to characterising fuel performance in HCCI engines

Montagne and Duret (2002) and Jeuland *et al*. (2003) have introduced the CAI index or the Controlled Auto-ignition Number (CAN) to enable the comparison of two fuels in an HCCI engine. In a given engine the operating boundaries, in terms of load and speed, are first established with a reference fuel. Thus in Fig. 9.15, the reference fuel could be run satisfactorily only within the area bound by the heavy lines – at a given speed, outside this boundary, for high loads the noise is too high and for low loads, the cyclic variation is too high. A similar operational region is then established for the test fuel – area bound by the dotted line in Fig. 9.15. CAN is then defined as the ratio of the operational area for the test fuel to the operational area for the reference fuel. If CAN is greater than unity, the test fuel can be run over a larger operational area compared to the reference fuel at the inlet pressure chosen and vice versa. In fact, Jeuland *et al*. (2003) suggest that there can be four different CANs associated with low/low, low/high , high/low, and high/high speed/load conditions respectively. This would be an informative way to compare fuels at a fixed condition but the CAN ranking of fuels will most likely change if the inlet is boosted in the quest for higher loads, since as discussed earlier, fuel auto-ignition behaviour changes significantly with pressure and temperature for fuels of different composition. Thus non-paraffinic

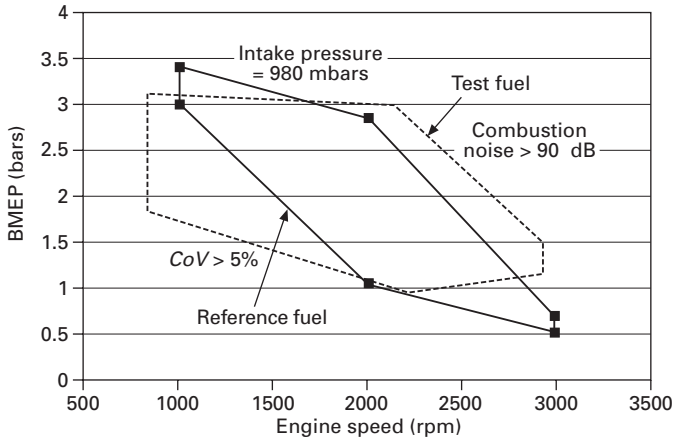

9.15 Operating range of a HCCI engine on two different fuels (after Jeuland *et al.,* 2003).

fuels get relatively more prone to auto-ignition as T_{comp15} is increased but less prone to auto-ignition as T_{comp15} is reduced. Needless to say, CAN will also depend on the composition of the reference fuel used.

Combustion in an HCCI engine has been shown to correlate well with combustion measurements in the IQT test for different fuels by Ryan and Matheus (2002). There has also been a lot of interest (e.g., Shibata and Urushihara, 2006) in attempting to understand fuel behaviour in HCCI engines in terms of the low temperature heat release (*LTHR*). This raises the possibility of using an IQT test to characterise the auto-ignition quality of fuels for HCCI operation perhaps with additional attention paid to the *LTHR*. Any procedure used to rank fuels must have a fully specified test method and a ranking scale such as the Octane scale based on PRF fuels. In view of the earlier discussion, any new auto-ignition scale, if it were to be set up, should be based on reference fuels that behave much more like practical fuels – perhaps toluene/n-heptane mixtures. HCCI engines operate over a wide range of pressure and temperature to cover a reasonable area of load and speed. As discussed in Section 9.3, auto-ignition behaviour varies significantly with pressure and temperature and, for gasoline-like fuels, also with fuel composition. At least three pieces of information are needed to characterise the auto-ignition behaviour of such fuels at different engine operating conditions – two measures such as *RON* and *MON* which describe auto-ignition at two very different pressure and temperature conditions and another parameter such as *K* in *OI*, which describes the actual engine operating condition in relation to these test conditions. Any new fuel-ranking test must take this into account in order to describe gasoline-like fuels. As discussed in Section 9.3, an IQT measurement at just one condition is probably sufficient to rank

fuels in the diesel auto-ignition range over a wide HCCI engine operating range.

9.9 Fuel requirements of HCCI engines

An IC engine can be run in HCCI mode on practically any fuel if the right design and operating conditions are chosen. However, practical engines must run over a wide range of speed and load with acceptable levels of noise, stability and emissions. A suitable fuel would enable this breadth of operation. Such a fuel must be volatile enough to allow sufficient pre-mixing of the fuel with air. The deficiency of a fuel in this respect can be overcome by better mixture-preparation strategies using direct injection, improved injector design, high injection pressures, multiple injection pulses, flow control and so on. Thus though it is extremely difficult to run an engine on HCCI mode on practical diesel fuels, which are relatively involatile, using port injection, it is much easier to do so using direct injection (Risberg *et al*., 2005).

The auto-ignition quality of the fuel must satisfy the changing requirements of the engine – *OI* must not be too far away from OI_0 – over as wide a range of operating conditions as possible. This is usually very difficult with a single fuel since OI_0 changes so widely but sensitive fuels, fuels which are not paraffinic, have an advantage in this respect (Risberg *et al*., 2003; Kalghatgi and Head, 2004; Kalghatgi, 2005). In such fuels their *OI* changes in the same direction as OI_0 as the engine is operated at different loads at the same speed. Again, engine control can be employed to overcome deficiencies of the fuel and enable the engine to continue running, though not necessarily at the best possible efficiency. For instance if *OI* is too large compared to OI_0, charge temperature could be increased sufficiently by retaining large amounts of internal EGR. If the temperature is high enough – in the region where $(a + b)$ tends to zero in Fig. 9.10 – auto-ignition could be ensured with most fuels. At high loads, with low λ and high P_{maxcomp} and T_{maxcomp}, OI_0 will be high and hence *OI* needs to be high while at low loads the failure to auto-ignite will be a problem and *OI* needs to be low.

9.9.1 Practical dual-mode engines

In practice HCCI engines will be dual-mode engines – running in HCCI mode where possible and reverting to conventional diesel or SI mode where they cannot, at start-up and high load. In such engines the fuel will have to support the conventional mode of combustion. Indeed the greatest incentive to bring in HCCI combustion is the potential reduction of NOx and particulates in diesel engines. Thus in practice HCCI combustion is far more likely to be implemented in engines that will be carrying conventional diesel fuel. These engines will run in HCCI mode at low loads by, say, early direct injection of

small quantities of fuel that will enable premixing of fuel and air. In fact modern practical diesel engines use many other strategies to promote premixed combustion such as the Nissan Modulated Kinetics (MK) system (e.g., Kimura *et al*., 2001) but the discussion of such strategies is beyond the scope of this article. However, at high loads, which require greater quantities of fuel, HCCI combustion will not be possible because of excessive heat release rates and the engine will switch to conventional diesel mode by direct injection of the fuel late in the cycle. In such engines, if the goal is to minimise the emissions by maximising the HCCI operation regime, the optimum diesel fuel will be as volatile as possible with the lowest cetane number that will still allow diesel operation. In other words a diesel fuel, as much like gasoline as the circumstances allow, will extend the HCCI operating range in such dual-mode engines. This is indeed found to be the case by Kitano *et al*. (2003) where the optimum fuel in a diesel/HCCI engine was found to be in the kerosene range with a cetane number of about 40. If, on the other hand, the goal is to reduce the noise levels at high loads, the optimum fuel might need to be of higher cetane.

SI/HCCI dual-mode engines will have higher compression ratios than current SI engines. Hence in the SI mode they will be more prone to knock. Such engines will require a fuel of high *RON* and high sensitivity (Kalghatgi, 2005).

9.9.2 'Full HCCI' engines

It is very unlikely that an engine that runs in HCCI mode over its entire operating regime will be developed in the foreseeable future, primarily because of the difficulty in achieving high loads in HCCI combustion. Figure 9.16 shows the range of auto-ignition and volatility characteristics of different fuels and some common refinery components. We will now consider the suitability of these components for 'Full HCCI' engines.

In such an engine, gasoline fuels would have an advantage over conventional diesel fuels because they are more volatile and also because conventional diesel fuels are too prone to auto-ignition with *OI* less than about 35. OI_0 with a compression ratio of 14 is around 50 at low loads and needs to be much higher at high loads (e.g., Fig. 9.9). Thus it will be much more difficult to attain satisfactory HCCI combustion with diesel fuels and get reasonable *IMEP* unless OI_0 is reduced by say, reducing the compression ratio. There are many strategies, such as charge stratification and use of EGR, that are being researched to moderate heat release rates so that higher loads can be reached in HCCI combustion even with diesel fuels. However with all things being equal, a fuel with a higher *OI* will enable a higher maximum load in HCCI operation. GTL fuels are, in general, even more prone to auto-ignition than conventional diesels though they have better volatility. Kerosenes would

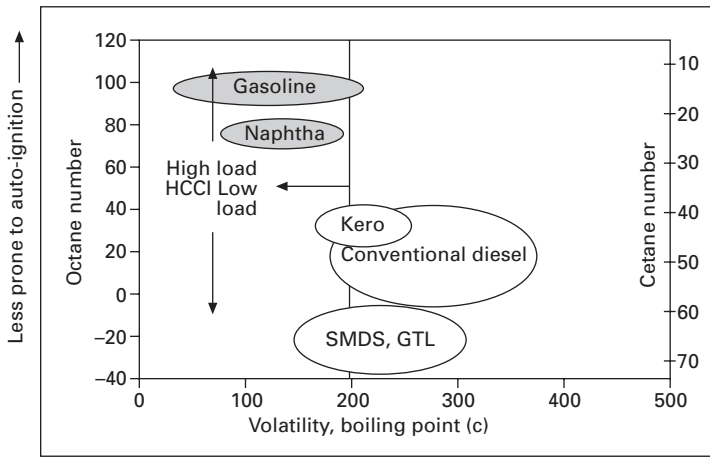

9.16 Auto-ignition quality vs volatility of different fuels and refinery streams.

be better than conventional diesels because of better volatility and lower cetane quality. On the other hand, there could be difficulties in ensuring that gasoline fuels can auto-ignite at low loads because of their high *OI*. However, as already discussed, this deficiency could be more easily overcome by control strategies such as retaining high levels of hot internal EGR or other thermal management.

Gasoline fuels can be blended to have high sensitivity and this gives them more flexibility in HCCI engines. In this respect they will be better than naphtha which will have the right volatility but will be less sensitive and it is possible that its *OI* will be lower than desired. In summary, conventional gasoline fuels are more suited for a 'full HCCI' engine than conventional diesel fuels. They need to be as sensitive as possible and but the optimum *RON* value will depend on the criterion used for optimisation. If reaching high loads is deemed to be important, *RON* levels of current gasolines would be required but Amann *et al*. (2005) report that in their experiments they found the optimum *RON* to be lower – around 80. If the engine has to run at higher speeds optimum RON could be even lower.

If reaching high loads in HCCI operation is considered to be the main challenge and on the basis of ease of mixture formation and flexible ignition quality which might make engine control a little easier, the fuels shown in Fig. 9.16 can be ranked, loosely, from the best to the worst for 'Full HCCI' engines as follows – gasoline, naphtha, kerosene, appropriate GTL cuts, conventional diesel. However, GTL components offer very high cetane numbers but with volatility in the gasoline range and hence offer some more flexibility in blending relatively volatile fuels with varying auto-ignition quality.

9.10 Summary

Gasoline-like fuels are defined as those fuels with $RON > \sim 60$ or cetane number, $CN < \sim 30$.

1. The combustion phasing is characterised by *CA50*, the crank angle position where 50% of the total heat release occurs. $CA50 = (a + b)[OI - OI_0]$ where *OI* is the octane index defining the fuel auto-ignition quality and is given by $OI = (1 - K)RON + KMON = RON - KS$ and *S* is the sensitivity of the fuel, $(RON - MON)$. For diesel-like fuels ($RON < \sim 60$), auto-ignition quality can be reasonably well defined by *CN* alone and *OI* for such fuels can be approximated by $(130–2.4CN)$
2. *K* and $(a + b)$ depend on T_{comp15}, the temperature when the pressure in the cylinder is 15 bar.
3. Compared to paraffinic fuels, non-paraffinic fuels become more resistant to auto-ignition as pressure is increased at a given temperature.
4. OI_0 increases as the maximum compression pressure and temperature increase and decreases as engine speed is increased or the mixture is made leaner or more dilute.
5. Maximum pressure rise rate, *MPRR*, increases with increasing equivalence ratio (Φ) and the inlet pressure (P_{in}) and decreases with increasing *CA50* and *S* if these parameters are varied individually with other parameters constant. Thus the fuel effect comes in through both *CA50* and *S*, with the sensitive fuels giving lower *MPRR* with all other things constant.
6. *CA50* should not be very much greater than 10 CAD for stable combustion. $Y = 1.55CA50–52\Phi$ can be used to discriminate between conditions of high and low cyclic variation and for reasonably stable operation, *Y* must certainly be less than zero.
7. *IMEP* increases with fuel energy content per cycle. Indicated efficiency η_i decreases with increasing Φ, intake air density ρ, and intake temperature T_{in} but increases with increasing *CA50* and P_{max} if these parameters are varied individually while holding others constant.
8. In order to characterise the auto-ignition quality of a gasoline fuel in a given HCCI test using a ranking method separate from the particular HCCI test, at least three pieces of information are needed – the auto-ignition measure of the fuel at two different pressure/temperature combinations in the ranking method (e.g., *RON* and *MON*) and a measure of how far the HCCI test condition is from one of the ranking test conditions (e.g. *K*). This information can be combined (e.g. *OI*) to provide a more accurate general description of auto-ignition quality.
9. In dual-mode engines the fuel requirement is determined by the requirements of the conventional mode. Thus in SI/HCCI engines, the fuel has to be high *RON* and high sensitivity. In 'Full HCCI' engines, if attaining high loads is considered to be the main challenge, gasoline-like

fuels have an advantage because of their high resistance to auto-ignition, high volatility and the possibility of blending them with high sensitivity.

9.11 References

Amann, M., Ryan, T.W. and Kono, N., 'HCCI fuels evaluations – gasoline boiling range fuels', SAE 2005-01-3727, 2005.

Andrae, J., Johansson, D., Björnbom, P., Risberg, P. and Kalghatgi, G., 'Co-oxidation reactions in the auto-ignition of primary reference fuels and n-heptane /toluene blends', *Combustion and Flame*, vol 140, pp 267–286, 2005.

Aroonsrisopon, T., Werner, P., Foster, D.E., Morikawa, T. and Iida, M., 'An investigation into the effect of fuel composition on HCCI combustion characteristics', SAE 2002-01-2830, 2002.

ASTM, 2005 Annual book of ASTM standards, Section 5, vol. 5.01, American Society of Testing Materials, 2005.

Bradley, D. and Morley, C., 'Auto-ignition in spark-ignition engines', Ch. 7 in 'Low-temperature combustion and auto-ignition', Editor, M.J. Pilling, vol. 35 of *Comprehensive chemical kinetics* edited by R.G. Compton and G. Hancock, Elsevier Science B.V., 1997.

Bradley, D., Morley, C. and Walmsley, H., 'Relevance of Research and Motor Octane numbers to the prediction of engine auto-ignition', SAE 2004-01-1970, 2004.

Ciezki, H.K. and Adomeit, G., 'Shock-tube investigation of self-ignition of *n*-heptane-air mixtures under engine relevant conditions', *Combustion and Flame* 93, 421–433 1993.

Cowell, L.H. and Lefebvre, A.H., 'Influence of pressure on auto-ignition characteristics of gaseous hydrocarbon-air mixtures', SAE 860068, 1986.

Davidson, D.F., Gauthier, B.M. and Hanson, R.K., 'Shock tube ignition measurements of iso-octane/air and toluene/air at high pressures', Proceedings of the 30th International Combustion Symposium, 2004.

Dec, J.E., 'A conceptual model of DI diesel combustion based on laser sheet imaging', SAE 970873, 1997.

Douaud, A.M. and Eyzat, P. 'Four-octane-number method for predicting the anti-knock behavior of fuels and engines', SAE 780080, SAE Trans., vol. 87, 1978.

Eng, J.A., 'Characterisation of pressure waves in HCCI combustion', SAE 2002-01-2859, 2002.

Fieweger, K., Blumenthal, R. and Adomeit, G., 'Self-ignition of SI engine model fuels: a shock tube investigation at high pressure,' *Combustion and Flame*, 109, 599–619 1997.

Gauthier, B.M., Davidson, D.F. and Hanson, R.K., 'Shock tube determination of ignition delay times in full-blend and surrogate fuel mixtures', *Combustion and Flame*, 139, pp 300–311, 2004.

Griffiths, J.F., 'Reduced kinetic models and their application to practical combustion systems', *Progress in Energy and Combustion Science*, vol. 21, p 25, 1995.

Griffiths, J.F., Halford-Maw, P.A. and Mohammed, C., 'Spontaneous ignition delays as a diagnostic of the propensity of alkanes to cause engine knock', *Combustion and Flame*, 111, pp 327–337, 1997.

Heywood, J.B., 'Internal combustion engine fundamentals', Ch. 9., McGraw Hill Book Co., 1988.

Hirst, S.L. and Kirsch, L.J., 'The Application of a Hydrocarbon Auto-ignition Model in

Simulating Knock and Other Engine Combustion Phenomena', in *Combustion Modeling in Reciprocating Engines*, edited by J. N. Mattavi and C. A. Amann, Plenum Publishing, New York, 1980.

Hultqvist, A., Christensen, M., Johansson, B., Richter, M., Nygren, J., Hult, J. and Alden, M., 'The HCCI combustion process in a single cycle – High-speed fuel tracer LIF and chemiluminescence imaging', SAE 2002-01-0424, 2002.

Jeuland, N., Montagne, X. and Duret, P., 'Engine and fuel related issues of gasoline CAI (Controlled Auto-Ignition) combustion', JSAE 20030349, SAE 2003-01-1856, 2003.

Kalghatgi, G., Risberg, P. and Ångström H-E, 'A method of defining ignition quality of fuels in HCCI engines', JSAE 20030120, SAE 2003-01-1816, 2003.

Kalghatgi, G.T. and Head, R.A., 'The available and required auto-ignition quality of gasoline-like fuels in HCCI engines at high temperatures', SAE 2004-01-1969, 2004.

Kalghatgi, G.T., 'Auto-ignition quality of practical fuels and implications for fuel requirements of future SI and HCCI engines', SAE 2005-01-0239, 2005.

Kalghatgi, G.T. and Head, R.A., 'Combustion limits and efficiency in a HCCI engine', *International Journal of Engine Research*, 2006.

Kimura, S., Aoki, O., Kitahara, Y. and Aiyoshizawa, E., 'Ultra-clean combustion technology combining a low-temperature and premixed combustion concept for meeting future emission standards', SAE 2001-01-0200.

Kitano, K., Nishiumi, R., Tsukasaki, Y., Tanaka, T. and Morinaga, M., 'Effects of fuel properties on pre-mixed charge compression ignition combustion in a direct injection diesel engine', JSAE 20030117 and SAE 2003-01-1815, 2003.

Koopmans, L., Stromberg, E. and Denbratt, I., 'The influence of PRF and commercial fuels with high octane number on the auto-ignition timing of an engine operated in HCCI combustion mode with negative valve overlap', SAE 2004-01-1967, 2004.

Leppard, W.R., 'The chemical origin of fuel octane sensitivity', SAE 902137, 1990.

Leppard, W.R., 'The autoignition chemistries of primary reference fuels, olefin/paraffin binary mixtures and non-linear octane blending', SAE 922325, 1992.

Livengood, J.C. and Wu, P.C., 'Correlation of auto-ignition phenomenon in internal combustion engines and rapid compression machines', Proceedings of Fifth International Symposium on Combustion, p 347, Reinhold, 1955.

Montagne, X. and Duret, P., 'What will be the future combustion and fuel-related technology challenges?', in *A new generation of engine combustion processes for the future*?, Editor P. Duret, Editions Technip, Paris, 2002, ISBN 2-7108-0812-9.

Naik, C.V., Pitz, W.J., Westbrook, C.K., Sjöberg, M., Dec, J.E., Orme, J., Curran, H.J. and Simmie, J.M., 'Detailed chemical kinetic model of surrogate fuels for gasoline and application to an HCCI engine', SAE 2005-01-3741, 2005.

Oakley, A., Zhao, H., Ladommatos, N. and Ma, T., 'Dilution effects on the controlled auto-ignition (CAI) combustion of hydrocarbon and alcohol fuels', SAE 2001-01-3606, 2001.

Owen, K. and Coley, T., 'Automotive fuels reference book', SAE, Warrendale PA, 1995.

Peters, N., Paszko, G., Seiser, R. and Seshadri, K., 'Temperature cross-over and non-thermal runaway at two-stage ignition of n-heptane', *Combust and Flame* 128, 38–59, 2002.

Risberg, P., Kalghatgi, G. and Ångström H-E, 'Auto-ignition quality of gasoline-like fuels in HCCI engines', SAE 2003-01-3215.

Risberg, P., Kalghatgi, G.T. and Ångström H-E., 'The influence of EGR on autoignition quality of gasoline-like fuels in HCCI engines', SAE Paper # 2004- 01 –2952, SAE Transactions, *Journal of Engines*, vol 113, 2004.

Risberg, P., Kalghatgi, G. and Ångström H-E., 'Auto-ignition quality of diesel-like fuels in HCCI engines', SAE 2005-01-2127, Also SAE Transactions, 2005.
Risberg, P., Johansson, D., Andrae, J., Kalghatgi, G., Björnbom, P. and Ångström, H-E., 'The influence of NO on combustion phasing in a HCCI engine', SAE 2006-01-0416.
Ryan, T.W. and Matheaus, A., 'Fuel requirements for HCCI engine operation', THIESEL 2002, *Thermo and Fluid Dynamic Processes in Diesel Engines*, 2002.
Shibata, G. and Urushihara, T., 'The interaction between fuel chemicals and HCCI combustion characteristics under heated intake air conditions', SAE 2006-01-0207, 2006.
Simmie, J.M., 'Detailed chemical kinetic models for the combustion of hydrocarbon fuels', *Progress in Energy and Combustion Science*, vol. 29, p 599, 2003.
Stone, R., 'Introduction to internal combustion engines', p 547, Macmillan Press Ltd., ISBN 0-333-74013- 0, 1999.
Tanaka, S., Ayala, F., Keck, J.C. and Heywood, J.B, 'Two-stage ignition in HCCI combustion and HCCI combustion control by fuels and additives', *Combustion and Flame*, vol. 132, pp 219–239, 2003.
Warnatz, J., 'Chemistry of high temperature combustion of alkanes up to octane', Twentieth Symposium (International) on Combustion, The Combustion Institute, Pittsburg, p 845, 1984.
Westbrook, C.K., 'Chemical kinetics of hydrocarbon ignition in practical combustion systems', *Proceedings of the Combustion Institute*, vol. 28, pp 1563–1577, 2000.
Westbrook, C.K. and Dryer, F.L., 'Chemical kinetic modelling of hydrocarbon combustion', *Progress in Energy and Combustion Science*, vol. 10, p 1, 1984.
Yates, A.D.B., Swarts, A., Viljoen, C.L., 'Correlating auto-ignition delays and knock-limited spark advance data for different types of fuel', SAE 2005-01-2083, 2005.
Zhao, H., Peng, Z., Williams, J. and Ladommatos, N., 'Understanding the effects of recycled burnt gases on the controlled auto-ignition (CAI) combustion in four-stroke gasoline engines, SAE 2001-01-3607, 2001.

9.12 List of notations

$(a + b)$	Slope of *CA50* vs *OI line*
a, b, c	Regression constants linking *CA50* to *RON* and *MON*
AFR	Air/fuel ratio
CA50	Crank angle when 50% of total heat is released
CAD	Crank angle degrees
CN	Cetane number
COV	Coefficient of variation = 100 (standard deviation/mean)
DCN	Derived cetane number from the IQT test
EGR_f	Exhaust gas recirculation mass fraction
FEN	Fuel energy content per cycle, J/cycle
GTL	Gas to liquids
ID	Ignition delay in an IQT test
IMEP	Indicated mean effective pressure, bar
IQT	Ignition quality test
isfc	Indicated specific fuel consumption

K	Parameter linking *OI* to *RON* and *MON*. Equation 10
LTHR	Low temperature heat release
m_{air}	Air consumption rate, g/s
MON	Motor octane number
MPRR	Mean maximum pressure rise rate, bar/crank angle degree
n	Polytropic index
N	Engine speed, rpm
NTC	Negative temperature coefficient
NVO	Negative valve overlap
OI	Octane index. Equation 9
OI_0	Requirement of the engine : *CA50* = 0 when $OI = OI_0$
P	Pressure
P_{in}	Inlet pressure, bar abs
P_{max}	Maximum pressure, bar abs
$P_{maxcomp}$	Maximum compression pressure, bar abs
Q	Heat released, J
RCM	Rapid compression machine
RON	Research octane number
S	Fuel sensitivity = *RON* – *MON*
T	Temperature
T_{comp15}	Compression temperature when pressure is 15 bar, K
T_{in}	Inlet temperature, C
$T_{maxcomp}$	Maximum compression temperature, C
V	Volume
V_d	Displacement volume
Φ	Equivalence ratio
λ	Normalised air/fuel ratio, $1/\Phi$
θ	Crank angle
η_i	Indicated fuel conversion efficiency
ΔH	Heat of combustion of fuel, MJ/kg
γ	Ratio of specific heats
τ	Ignition delay

Appendix HCCI predictor

The various quantitative relationships from experimental studies are brought together in this Appendix to enable operating parameters of interest to be estimated. Equations in A, have been based on two entirely different engines and can be used for any engine. Equations discussed in B, C and D below have been developed using data from only one engine – their applicability to other engines may not be quantitatively accurate.

Input data required –
RON, MON for the fuel. $S = RON - MON$

n – polytropic index during compression – will vary between 1.3 and 1.35
V_{min} – minimum volume at top dead centre
V_d – swept volume or displacement volume
P_{in}, T_{in} – intake pressure (bar abs) and temperature (K)
P_0, T_0, V_0, pressure (bar abs), temperature (K) and volume at the start of compression – P_0 and T_0 will depend on T_{in} and P_{in} and the amount of internal EGR and the heat losses during the intake process.
m_{air} g/s – fresh air flow rate into the engine
N – engine speed, in rpm
λ – normalised air/fuel ratio. Φ, equivalence ratio = $1/\lambda$
$\lambda^* = (1 + EGR_f)\ \lambda$ where, EGR_f is the EGR mass fraction.

A. Estimation of *CA50*
T_{comp15} , $K = T_0(15/P_0)^{(n-1)/n}$
for $T_{comp15} > 825$ K
$K = 0.0426\ (T_{comp15}) - 35.2$
For $T_{comp15} < 825$ K,
$K = 0.0056\ (T_{comp15}) - 4.68$ or
$K = 0.00497\ T_{comp15} - 0.135\lambda - 3.67$
$OI = (1 - K)RON + KMON = RON - KS$
$T_{maxcomp}$, $K = T_0\ (V_0/V_{min})^{(n-1)}$
$P_{maxcomp}$, $K = P_0\ (V_0/V_{min})^n$
$OI_0 = 59 + 0.015T_{maxcomp}\ (K) + 0.663P_{maxcomp}$ (bar abs) $- 2.6\lambda^* - 0.0123\ N$ (rpm)
From Figure 9.10,
If $1000 > T_{comp15} > 890$, $(a + b) = 1.06 - 0.001\ T_{comp15}$
If $890 > T_{comp15} > 780$, $(a + b) = 13.358 - 0.0148\ T_{comp15}$
If $780 > T_{comp15} > 600$, $(a + b) = 0.008\ T_{comp15} - 4.44$
If $600 > T_{comp15} > 500$, $(a + b) = 0.001\ T_{comp15} - 0.24$
$CA50 = (a + b)[OI - OI_0]$

B. Cyclic variation
$Y = 1.55CA50–52\ \Phi$, should be less than zero for low cyclic variation. In addition, *CA50* should probably be less than 10 CAD.

C. Maximum pressure rise rate (*MPRR*)
$x = 36.7[\Phi] + 2.86\ [P_{in}, \text{bar}] - 0.344[CA50, \text{CAD}] - 0.053[S] - 8.45$
MPRR, bar/CA deg $= 0.1196x^2 + 0.1404x + 1.2368$ (from Figure 9.11)
The acceptable limit for *MPRR* is subjective – Kalghatgi and Head (2006) report that in their set up the engine was considered too noisy for *MPRR* > 5 bar/CA deg.

D. *IMEP* and indicated efficiency, η_i
From Figure 9.13, *IMEP* (bar) = 0.0116 *FEN* (J/cycle) – 1.4044
FEN (J/cycle) = 120,000 $[m_{air}, \text{g/s}][\Delta H, \text{MJ/kg}][\Phi]/\{[AFR_{stoich}][N, \text{RPM}]\}$.
For a typical gasoline (Table 1), $\Delta H \sim 43.5$ MJ/kg and $AFR_{stoich} \sim 14.5$
indicated efficiency, $\eta_i = [IMEP]\ V_d/FEN$

Part III

Diesel HCCI combustion engines

10

Overview of HCCI diesel engines

J V PASTOR, J M LUJÁN, S MOLINA and
J M GARCÍA, CMT-Motores Térmicos, Spain

10.1 Introduction

In the previous part of this book, the basis of HCCI/CAI engines has been presented starting from current spark ignition engines. In this part, a similar development will follow, starting from the diesel side.

Whereas in gasoline HCCI engines the main advantage is the improved efficiency as well as ultra-low NOx emission, in the diesel HCCI, the objective when using these new combustion modes is to reduce both NOx and particulate matter (PM) emissions, keeping fuel consumption and engine performance, and trying to make the most of combustion control, in order to use as little after-treatment as possible. This chapter aims to provide a conceptual description of the fundamentals of HCCI engines, as an evolution of current diesel engines, and an overview of existing solutions.

As a starting point, an overview of the combustion process in current Diesel engines will be made in this chapter, highlighting those aspects which are critical for success in achieving a combustion mode close to the theoretical concept of HCCI combustion, on the basis of diesel-type engines. Then, a conceptual description of HCCI combustion will be depicted in terms of mixture formation, autoignition and combustion development, engine efficiency and pollutant formation.

Finally, an overview of the state of development of diesel HCCI engines will be made, highlighting the technology requirements and the potential of different technologies, keeping in mind that, at least in short-to-middle term, it is expected that the HCCI combustion mode will have to coexist with diffusion controlled diesel combustion modes.

A classification of diesel HCCI engine types will be made attending to the mixture formation process, leading to three clearly different types of engine operation which will be treated in more detail in Chapters 11 to 13. Although playing a major role, fuel effects will not be treated here, since Chapter 14 is dedicated to this topic.

10.2 Conventional diesel combustion

Conventional diesel combustion is a heterogeneous process from both temporal and spatial points of view.

Temporal description of the conventional diesel combustion can be made following the classical sequence, which is shown in Fig. 10.1.

When the liquid spray is injected into the high density environment of the combustion chamber it starts to disintegrate into small droplets, which increases the gas-liquid interphase. Besides, spray momentum plays a major role in mixture preparation, inducing movement to the hot air which is entrained by the spray. Consequently, liquid fuel temperature increases and evaporation starts. As the spray penetrates into the chamber, liquid phase changes into vapour, especially in the spray boundaries. In this period there is no radiation from the spray, indicating that there is no chemical reaction.

When vapour appears, the first phase of the autoignition process starts at low temperature (up to around 750 K). Slow fuel oxidation reactions lead to a slight increase of in-cylinder pressure associated with the production of free chemical radicals which is evidenced by chemiluminescence radiation of CH and formaldehyde. In parallel to this chemical activity, mixing of fuel with hot gases progresses, considerably increasing mixture temperature. The time interval from the start of injection up to this moment has been traditionally called ignition delay period, and lasts a few hundred microseconds in actual diesel engines.

Then, a high temperature autoignition stage starts, which has been traditionally labelled as premixed combustion phase, and is characterized by

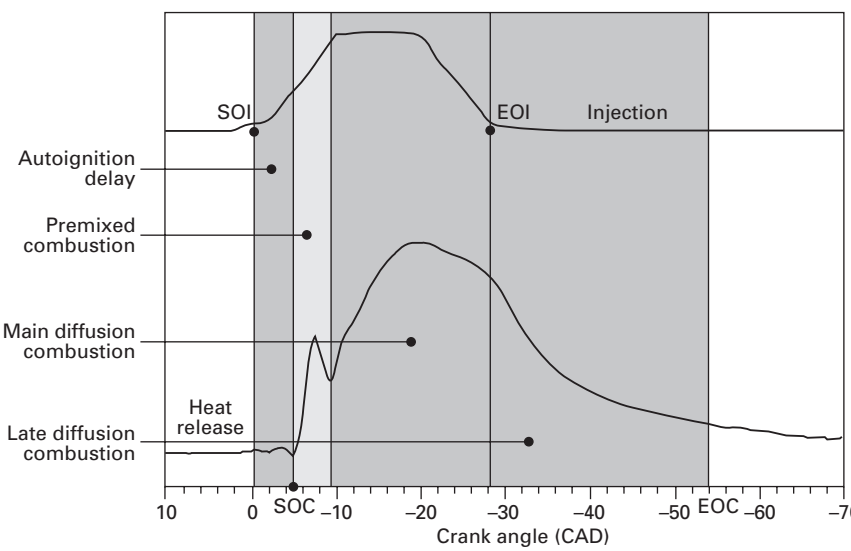

10.1 Temporal evolution of diesel combustion.

three basic phenomena. First, chemical kinetics enters into a phase of high temperature reactions so that fuel chemistry speeds up and heat release increases significantly. Final combustion products start to appear, as well as soot precursors. This leads to a second phenomenon characteristic of this phase, which is the appearance of incandescent soot in the spray front at the instants close to the maximum of the heat release rate curve. Thermal soot radiation will dominate during the rest of the combustion process, even after injection ends. Third, near the end of this phase, conditions for a self-sustained reaction are achieved and a flame front is established, which reveals the transient nature of this last stage of the autoignition process and constitutes the transition from the non-reactive spray to the diffusion flame. The basic quasi-steady structure of the flame will be maintained along the rest of the combustion process up to the end of injection as described later.

In the diffusion controlled combustion period, the visible flame is dominated by thermal soot radiation since soot particles occupy the main region of the spray. Its thermal radiation is very intense, but also chemiluminescence of OH radicals appears surrounding the sooting flame which, despite its far weaker intensity, can be used as a marker of the reaction front. This OH radicals radiation dominates in the region closer to the nozzle, defining the lift-off length, which determines the region where air is entrained to the spray core, upstream the reaction regions.

This structure is preserved up to the end of the injection process since fuel-air mixture is controlled by the fuel momentum flux and consequently, by the spray induced turbulence. Once the injection is over, momentum supplied by the spray ceases and consequently combustion rate decays. The oxidation process is then controlled only by the residual turbulence existing in the combustion chamber, either due to the charge motion or to the residual spray velocity.

On the other side, diesel combustion is also heterogeneous from the spatial point of view, and can be described by the conceptual model proposed by Dec (1997) for diffusion controlled combustion in diesel engines, schematically presented in the upper part of Fig. 10.2. Three different parts can be clearly observed:

- In the first region, close to the nozzle orifice, flame has the appearance of a non-reacting spray, since the reaction zone does not arrive at the nozzle due to the high injection velocity. In this region, phenomena of atomization, air entrainment and fuel evaporation occur in a similar way as in a non-reactive evaporative spray. Obviously, the presence of flame downstream modifies all these processes, but the physics is the same. The length of this first region is called flame lift-off length.
- After this lift-off length, the flame gets the structure of a typical diffusion flame, with an inner region occupied by soot and unburned fuel, surrounded by a thin reaction surface, where complete oxidation to CO_2 and H_2O

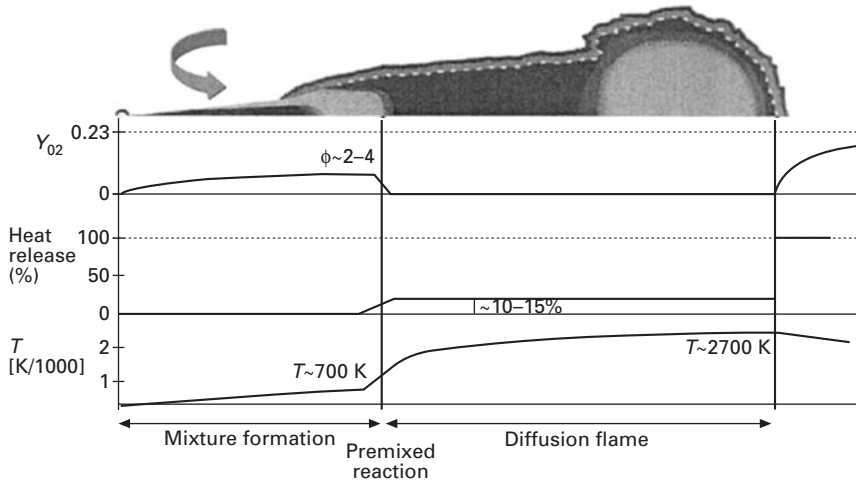

10.2 Direct injection (DI) diesel spray. Spatial distribution of main variables. Adapted from Dec (1997).

occurs when the fuel-air ratio becomes close to stoichiometric conditions. Nitrogen oxide is formed outside this flame front, where high temperature and oxygen concentrations are achieved simultaneously. Spray width in this region is higher than in the region close to the nozzle, owing to the gas expansion induced by the high temperatures appearing as a consequence of the heat released. Thus, the spray modifies the conical shape that occurs in non-reactive situations. Moreover, at the frontal part, a vortex with a higher concentration of soot particulates appears, which reveals the transient nature of the flame.

- Between both zones, a thin region appears where it is assumed that a premixed reaction occurs, and the oxygen entrained in the first region is consumed, so that in the inner region of the diffusion flame oxygen concentration is null. Products of this fuel-rich combustion (basically carbon monoxide and partially oxidized hydrocarbons) are precursors for soot formation in the inner part of the diffusion flame.

To improve understanding, it would be convenient to follow the path of a fuel element which is injected after the diffusion flame is established and travels along the flame axis. Just after injection such fuel element is atomized into droplets. Under conditions representative of normal diesel engine operation, complete atomization regime is achieved so that primary atomization occurs in a very effective way and fuel is completely atomized at a distance of approximately the equivalent nozzle orifice diameter (defined as the geometrical orifice diameter times the square root of the ratio of fuel density over air density). Secondary atomization, mainly due to aerodynamic stresses, is completed at a distance of the order of 10 times the equivalent nozzle orifice

diameter, leading to droplets with a Sauter mean diameter in this region of typically around 20 microns.

In this region where atomization dominates, the spray entrains hot air of the combustion chamber, whose temperature depends on the engine operating conditions and injection timing, but can be considered as around 950 K. Its composition will be a function of the time elapsed from the start of injection: for fuel elements close to the start of the injection, entrained gases will be basically intake air diluted with recirculated exhaust gases (if EGR is used) and residual gases inside the cylinder, whilst later in the combustion process, the spray also entrains an increasing fraction of burnt gases. In any case, entrainment of hot gases and thermal and mass diffusion in the droplet/gas interface are the two phenomena controlling fuel evaporation. Complete evaporation takes places at a distance of around 100 times the orifice diameter, although it depends of the in-cylinder temperature, fuel volatility and mixing rate. From this distance onwards, vapour fuel goes on mixing with air up to the end of the first zone of Fig. 10.2 where premixed combustion appears. At this point, the fuel element considered has diluted with air so that local equivalence ratio has decreased down to values of the order of 4, and temperature of the mixture has increased up to values around 800 K.

As our mixture element crosses the premixed combustion zone it burns and temperature increases up to around 1600 K. Since equivalence ratio is high, all the oxygen available is used for combustion and a large proportion of partially oxidized products appear, such as carbon monoxide, and light unsaturated hydrocarbons, which are supposed to be the true precursors of soot. In this part of the process, according to Flynn *et al*. (1999), between 10 and 15% of the energy is released. Next, our mixture element enters into the diffusion flame region where dilution with combustion products and nitrogen continues. Since there is no free oxygen in this region, no further heat release is expected. As the mixture element approaches the flame front, a sensitive increase in temperature takes place. It promotes formation of soot particles from partially oxidized products, which grow up reaching its maximum size near the flame front. When, finally, it crosses the flame front, diffusion of oxygen from the outer part of the spray allows complete burning of the partially oxidized products, leading to the release of the remaining energy (around 85% of the total energy in the fuel). Thus, maximum temperatures are achieved, which are of the order of the adiabatic flame temperature. Soot is also oxidized here due to the presence of high temperature and high concentration of OH radicals.

According to this description, it can be stated that in a diffusion flame fuel burns in two stages: first a rich premixed combustion and then a diffusion controlled high temperature combustion at the spray boundaries.

Calculations performed by Kitamura *et al*. (2002) for n-heptane at an ambient pressure of 60 MPa and a residence time of 2 ms, provide the

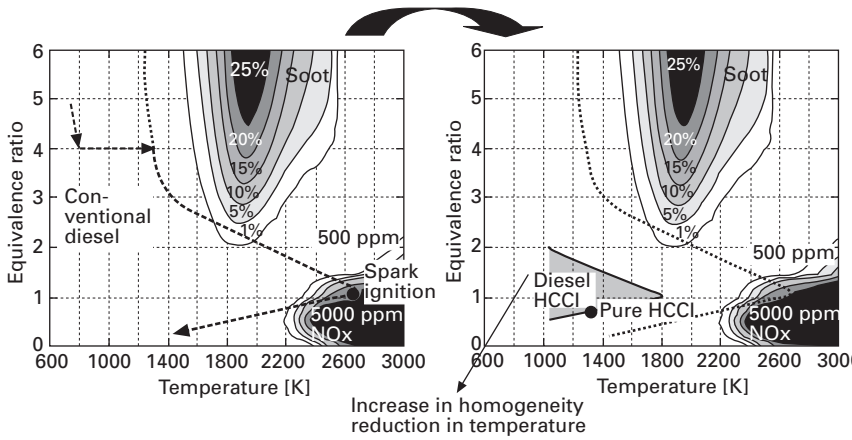

10.3 Equivalence ratio vs local temperature with the typical paths of different combustion concepts. Adapted from Kitamura *et al.* (2002).

regions of soot and NOx formation in the ϕ-T plane shown in Fig. 10.3. The solid line superimposed on the figure represents the adiabatic, equilibrium flame temperature computed for each equivalent ratio at an initial reactant temperature of 1000 K, assuming O_2 concentration of 21%. On the left side of this plot, for comparison purposes, the case of a stoichiometric port injection spark ignition engine combustion would be that represented by the symbol at $\phi = 1$, leading to substantial amount of NOx formation but no soot. However, for a diesel engine, according to the description for the diffusion controlled combustion depicted in the previous paragraphs, a representative fuel element would follow the dashed line leading to formation of both NOx and soot: NOx will be formed in the periphery of the diffusion flame, at high temperatures and low equivalence ratio, whilst soot formation, taking place in regions with rich mixtures and not so high temperatures, seems unavoidable in diesel flames.

This line is representative for a fuel parcel with a residence time of 2 ms; if a parcel travels faster or slower through the soot and NOx regions the quantity of these species will be different. Furthermore, in-cylinder turbulence can recycle formed and cooled soot particles into areas with higher temperatures and sufficient oxygen concentration leading to oxidation of these particles.

Since soot emission is a balance between formation and oxidation, conventional diesel engines usually reduce soot by means of increased oxidation, whilst in advanced diesel engines soot formation can be reduced by increased mixing. However, a potential way to reduce both NOx and soot simultaneously is to reduce heterogeneity and flame temperature, using new combustion concepts derived from the theoretical HCCI concept to practical situations, which is treated in the next section.

10.3 Fundamentals of HCCI combustion

From a conceptual point of view, HCCI would allow a drastic reduction of particulates and NOx emissions to near-zero levels on the basis of two basic processes: first a homogeneous mixture has to be formed, and second, this mixture autoignites due to compres-sion heat. However, these main characteristics are also the main challenges.

If a perfectly homogeneous mixture is created, the pressure and temperature rise during the compression stroke will lead to spontaneous ignition which differs from the classical diesel autoignition in the sense that it does not occur at a specific place in the spray, but simultaneously across the combustion chamber. Consequently, if autoignition occurs simultaneously in the whole cylinder, no high temperature flame front will appear as in the case of spark ignition engines. The absence of a high temperature flame front will lead to a practically negligible formation of nitrogen oxides, and due to the homogenized lean mixture, fuel rich zones are absent and therefore soot formation is also avoided.

The path followed by a typical fuel element in the case of an 'ideal' HCCI combustion has been represented by a dot in the right side of Fig. 10.3. It is assumed that all of the fuel is mixed with air to form a lean homogeneous mixture prior to the start of combustion, so the fuel path depicted is followed more or less simultaneously by all fuel elements. The path stays far away from the soot formation region and thus no soot will be formed. Depending on the fresh air composition, the local temperature can enter the NOx formation zone. However, these conditions represent high load, and in general the increase in load is stopped before these conditions occur because of knocking combustion. Due to the simultaneous combustion, there are very few or no pressure differences among the different regions in the chamber and there is no knocking. In practical situations this is true for lean mixtures, but knocking is one of the major limits in HCCI diesel engines at high loads (Sheppard *et al*., 2002).

Moreover, although from these calculations it seems that a wide range of equivalence ratio values is possible, in practice suitable values of mixture equivalence ratio are limited by two factors: for rich mixtures, knocking probability increases in a similar way as occurs in the CAI cases discussed in previous chapters; with too lean mixtures, the local burning temperatures can be so low that incomplete combustion occurs, leading to high CO and HC emissions.

To achieve the kind of combustion depicted in previous paragraphs, three major aspects should be addressed:

1. How to create a homogeneous mixture.
2. How to ignite such a mixture.
3. How to control combustion so that engine performance can be optimized.

10.3.1 Mixture formation

When diesel fuel is used, the level of homogenization achievable for the fuel air mixture is far from that in a spark ignition engine. In fact, it has been stated by some authors (Yanagihara, 2001) that rather than a homogeneous mixture, a homogeneous stratification should be more appropriate for lean HCCI diesel combustion. It means that mixture in the combustion chamber should consist of small clouds of rich mixture, homogenously distributed in the cool air of the combustion chamber. Chemical reaction should proceed simultaneously in every cloud, so that temperature will be limited and a lean combustion would be possible. In that case, the paths followed by fuel elements in diesel HCCI operation will spread over a wider area of the ϕ vs. T diagram. Moreover, Iida *et al*. (2004) have shown that some heterogeneity can be useful when trying to avoid a too intense heat release, so that noise, pressure gradients and tendency to knocking can be reduced.

Creating a homogeneous mixture using Diesel fuel presents some major problems: on the one side, time is needed for homogenization, which implies performing well-advanced injection either in the cylinder or at the intake ports. However, this means injecting fuel in environments at low density and temperature so that atomization and evaporation processes are strongly worsened, making unviable the use of conventional high pressure injection systems to minimize impingement against the engine walls. Instead, fuel injection systems capable of providing lean homogeneous mixtures, whilst keeping fuel away from the engine walls are strongly advisable. As a second problem, due to the low volatility of diesel fuel, vaporization becomes a major issue. With port or early injection, the low air temperature prevents significant evaporation, so that charge heating can be advisable in these cases.

Finally, assuming that a homogeneous, lean mixture is achieved, large autoignition delays are obtained that are not governed any more by physical phenomena, but mainly by chemistry. This means that the start of combustion is not triggered by the injection event, but by the high temperature achieved near the end of the compression stroke. In such cases, the high tendency to autoignition of diesel fuels, characterized by a high cetane index and a two-stage chemistry described below, will tend to provoke a too early autoignition which lead to a too advanced combustion.

10.3.2 Mixture autoignition

Autoignition phenomenon is one of the classical problems of combustion science and relies on the fact that any amount of air-fuel mixture at high temperature and/or pressure becomes unstable after a certain amount of time and, in the end, develops a combustion process. It is induced by the reaction

of radicals (non-equilibrium chemical species) generated due to the instability characteristics of the fuel-air mixture, and its development depends on many factors such as fuel properties, air composition, equivalence ratio, or temperature and pressure in the combustion chamber.

From a chemical point of view, autoignition is characterized by a set of several hundreds of species and complex reactions. However, from a conceptual point of view it is the result of particular thermal and fluid-dynamic conditions which lead to a spontaneous heat release, i.e. without any external source of energy.

Considering that diesel fuel consists of a complex and partially unknown blend of hundreds of hydrocarbon species, most of the studies available in the literature have been performed using fuel surrogates such as n-heptane, whose autoignition characteristics are similar to those of the commercial diesel fuels and for which kinetic mechanisms have been established and validated, (e.g., Curran *et al*. 1998). In all the studies performed with either diesel fuel or surrogates, it has been verified that autoignition process consists of two stages. In the first stage, low temperature reactions occur, so that fuel is consumed through an initial breakdown of fuel molecules, leading to formation of free radicals, aldehydes and hydrogen peroxide. Such reactions are initiated at temperatures of the order of 700 K and occur at modest reaction rates. Due to the heat released in this stage, the mixture temperature rises and, when temperatures of the order of 900 K are achieved, a high temperature stage starts. The process becomes highly exothermic, mixture temperature rises rapidly and reactions shift towards final combustion products. Oxygen and fuel molecules are fully consumed, and radical reactions lead to carbon dioxide and water, as well as carbon monoxide, hydrogen and several species considered as soot precursors.

If the mixture is induced by a spray-type flow, i.e. if the mixture is not homogeneous but a spray structure remains, the problem becomes more complicated: physical phenomena may play an important role, and combustion development follows a pattern closer to that described for the conventional diesel combustion. However, the two-stage autoignition pattern is maintained.

10.3.3 Heat release and combustion control

The two-stage autoignition chemistry is also reflected in the heat release patterns observed for combustion of homogeneous mixtures in engine situations. As shown by, e.g. Shibata and Urushihara (2004), cool flames arising from the first stage of the autoignition process provide a significant heat release, followed by a period with no apparent heat release corresponding to the so-called negative temperature coefficient chemistry which lasts up to the high temperature stage leading to the main heat release which will control engine performance.

This two-stage autoignition chemistry is also observable in HCCI diesel engine situations, as shown in Fig. 10.4 which corresponds to a heavy duty diesel engine. If fuel injection is performed early in the compression stroke, the first stage of the autoignition chemistry results in the first peak in heat release. The temporal location of this combustion phase is controlled by charge temperature. If no other engine setting is modified, autoignition takes place at a given crank angle position independently of the start of injection, provided that enough time is made available to create a more or less homogeneous mixture. However, the high temperature stage of the autoignition process is indeed affected by the injection timing due to the difference in the mixing process. If either the start of injection is further delayed, or the quantity of fuel injected is too high, knocking combustion can occur as shown in Fig. 10.5.

If the high temperature threshold controlling the second stage of the autoignition chemistry is reached too early in the compression stroke, the combustion phasing becomes too advanced, leading to penalties in the efficiency, high noise, increase knocking probability and, consequently, risk of engine damage. However, if this temperature threshold is reached too late, there is a high probability of misfiring which leads to very high HC emissions and reduced performance.

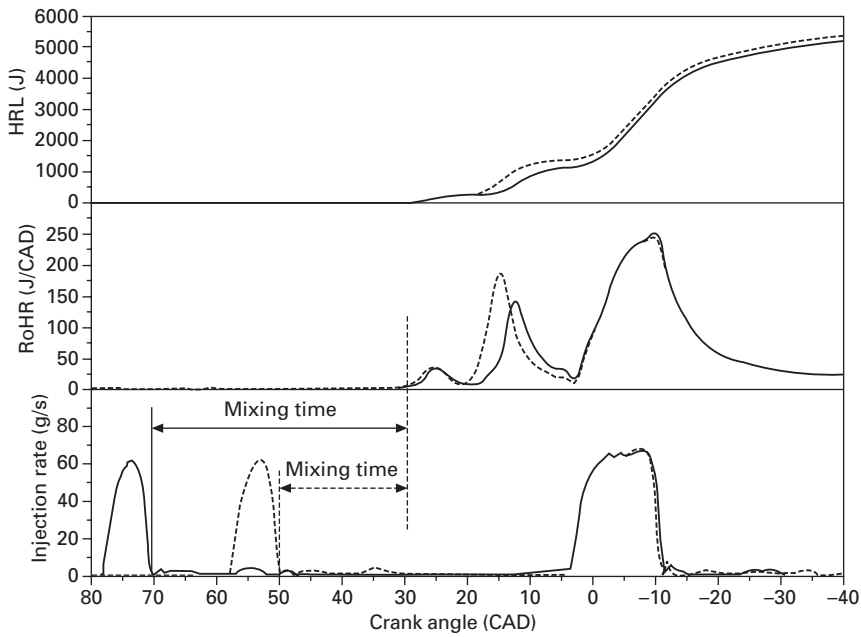

10.4 Effect of mixing time on early plot injection combustion process.

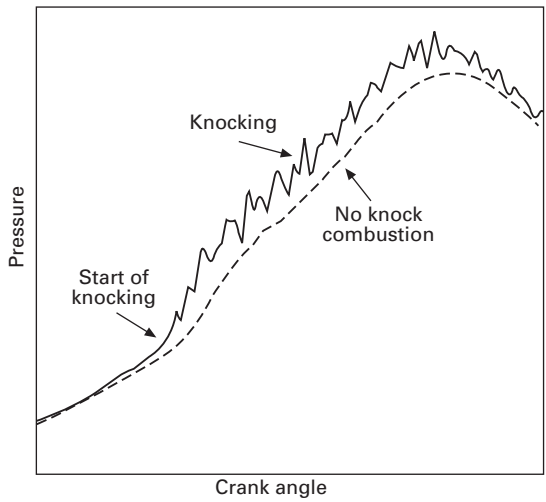

10.5 Knocking combustion in a heavy duty diesel engine.

From a theoretical point of view, control of combustion phasing can be made either controlling the mixture reactivity (either acting on fuel composition by means of blends, additives or fuel pre-conditioning, or on intake charge composition by means of EGR or residuals fraction regulation) or the temperature evolution along the engine cycle. From a practical point of view, several alternative strategies exist that can control the start of combustion to some extent:

- Controlling the temperature of the intake charge (Nishijima *et al*., 2002).
- Altering the composition of the intake charge by changing the EGR rate (Ladommatos *et al*., 2000), the equivalence ratio (Husberg *et al*., 2005), adding ozone (Yamada *et al*., 2005, Nishida and Tachibana, 2006), controlling homogeneity of air fuel mixture (Richter *et al*., 2000), or using dual fuel systems (Olsson *et al*., 2001).
- Modifying the gas temperature during the compression by means of a variable compression ratio (Ryan *et al*., 2004), variable valve timing (Milovanovic *et al*., 2004) or water injection (Kaneko *et al*., 2002, Nishijima *et al*., 2002).

Nevertheless, most of these methods are too slow for a cycle-to-cycle control. This disadvantage has led to strategies where the mixture homogeneity is reduced but where the control on the start of combustion is easier.

These strategies can be divided into early injection strategies (injection early in compression stroke), and late injection strategies (after TDC). These strategies, which will be treated in detail in the next three chapters, provide different levels of air fuel mixture homogenization, as well as different

ignition timings. Especially with late injection strategies, the control over the start of combustion is easily achievable but the lowest level of homogenization is reached. Some authors defend that these are not HCCI systems but rather some types of Low Temperature Combustion (LTC) systems. Although acceptable, such distinction will not be followed in this chapter.

Finally, it must be mentioned that fuel characteristics are of major importance in HCCI combustion. Especially the evaporation properties and the autoignition quality, play a major role in the level of homogenization and in the thermodynamic conditions where the combustion starts. However, owing to the fact that HCCI combustion can only cover part of the operating range of an engine, it is expected that in the medium to long-term, and especially in passenger car engines, HCCI modes will have to coexist with conventional diffusion controlled combustion modes in the same engine. Because of this, this chapter will only consider HCCI combustion using conventional diesel fuel, leaving the analysis of effect of alternative fuels for Chapter 14.

10.4 Overview of diesel HCCI engines

Several practical solutions more or less close to the theoretical concept described in the previous section have been proposed during the last decade, operating in more or less modified diesel engines. From the point of view of the injection process, such new combustion concepts can be classified into three main groups which are treated in the following subsections and sketched in Fig. 10.6.

10.4.1 Port fuel injection (PFI) diesel HCCI engines

Considering that time is needed for mixture preparation, fuel injection in the intake port is the most straightforward method to prepare a homogeneous mixture, and the highest rate of homogenization is achieved by port fuel injection compared with other alternatives.

The principle is exactly the same as in conventional spark-ignition engines, i.e. fuel is injected upstream of the intake valve, and consequently requirements on the injection system operation are not very different to those in conventional spark-ignition engines. Mixture is thus homogenized during the intake and compression strokes, and autoignition occurs due to compression.

For PFI HCCI engines, NOx emissions levels of around 100 times lower than conventional combustion have been reported, with soot levels also very low, depending on the degree of evaporation and homogenization (Christensen *et al.*, 1997, 1998, Christensen and Johansson, 1998, 1999). However, emissions of HC and CO tend to be much higher than for conventional diesel combustion, and are also dependent on the level of homogenization.

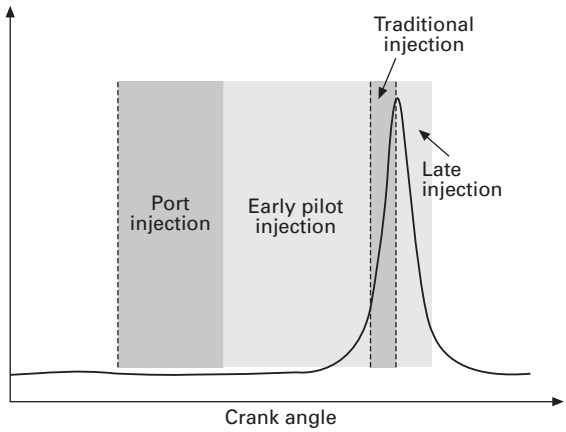

10.6 HCCI combustion concepts classification according to injection timing.

In these systems, the main issue concerns fuel evaporation. In general, full evaporation of diesel fuel only occurs at a temperature that is much higher than that normally found in the intake manifold. If no precautions are taken to enhance the fuel evaporation, a significant part of the fuel evaporates late in the compression stroke even after the start of combustion. This leads to a heterogeneous mixture losing the benefits found in HCCI combustion. Moreover, impingement or condensation of fuel on the engine walls can lead to high levels of unburned hydrocarbons and oil dilution (Ryan and Gray, 1997). These levels can be so high that they have a significant influence on the combustion efficiency (part of the fuel does not burn). So, a common strategy to enhance evaporation is to heat up the intake charge to enhance evaporation (Ryan and Callahan, 1996).

If the diesel fuel is evaporated properly and homogenized adequately at the intake port, this mixture is heated up during the compression stroke up to the ignition temperature. However, with conventional diesel compression ratios, this ignition temperature is reached too early in the compression stroke, far before TDC, leading to problems with efficiency and noise, and this is especially critical if intake charge is heated to enhance fuel evaporation, since this leads to higher temperature at the start of the compression stroke and consequently combustion will start earlier in the engine cycle.

Christensen *et al*. (1997, 1998) and Christensen and Johansson (1998, 1999) reported that start of ignition should be timed in advance to TDC with a certain margin to anticipate possible variation and ensure good combustion stability.

A reduction in oxygen concentration of the intake charge – EGR – is an effective way for retarding the start of ignition (Christensen and Johansson, 1998); furthermore, the heat of the recycled exhaust gases can promote the

evaporation of the fuel. However, EGR also increases the CO and HC emissions (Ryan and Gray, 1997).

The typical high burning rate in a HCCI engine can be also reduced by utilizing high air fuel ratios (Christensen *et al*., 1997, 1998), or water injection (Christensen and Johansson, 1999). As the upper limit of the load range is mainly limited by too high burning rate (leading to knocking combustion), the same strategies are used for increasing the load range.

Recent works (Guezennec *et al*., 2002, 2004, Midlam-Mohler *et al*., 2003, Canova *et al*., 2005) avoided the problems associated with the evaporation of diesel fuel by using a highly effective atomization device, which has some similar characteristics to the fumigation device used in the first work with diesel HCCI of Alperstein *et al*. (1958). Due to the high surface to volume ratio of the fuel droplets, these droplets have good evaporation dynamics, and the heat during the compression stroke is sufficient to evaporate all the fuel. They demonstrated diesel HCCI operation with external mixture formation at a compression ratio of 18:1, intake temperatures in the range of 15–60°C, and up to a maximum load of 4.7 bar IMEP. The traditional problems of PFI diesel mixture formation, such as high intake heating, low compression ratio, wall wetting and soot formation are largely avoided.

In theory, PFI HCCI combustion should have a better efficiency than a conventional combustion since, due to the good homogenization, almost all fuel burns simultaneously, leading to a very fast combustion. However, this is not the case in practice. This combustion can be so fast that before medium load is achieved, the pressure gradient is too high and knocking combustion occurs with high risk of engine damage. Commonly, these phenomena are anticipated by reducing the compression ratio (Ryan and Gray, 1997), but it can lead to a serious reduction in the maximum achievable efficiency of the engine.

Thus, due to the limited efficiency, high unburned hydrocarbon emission and high noise, PFI HCCI combustion is not nowadays considered a real alternative for conventional diesel combustion, despite its advantages on NOx and soot emission. Besides problems of fuel evaporation, control of combustion phasing is a main issue in PFI HCCI engines, which limits the maximum achievable load. Nevertheless, the research on this type of combustion has increased the understanding of the fundamentals of HCCI combustion.

An alternative to extend the load range is to combine the port fuel injection with a direct injection around TDC, which will lead to a conventional diesel combustion mode at higher loads (Christensen *et al*., 1997, 1998, Christensen and Johansson, 1998, 1999, Guezennec *et al*., 2002, 2004, Midlam-Mohler *et al*., 2003, Canova *et al*., 2005).

10.4.2 Early direct injection HCCI engines

A homogeneous mixture can also be obtained when fuel is injected directly in the combustion chamber during the compression stroke well before TDC. If properly chosen, sufficient time is available between the end of injection and the start of ignition to assure a relatively good homogeneous mixture, which will result in fully premixed combustion. This generic combustion concept with early injection has been classified by some authors as PCCI (Premixed Charge Compression Ignition) combustion (Hardy and Reitz, 2006).

Compared to port fuel injection, there is a major advantage for early injection strategies: since fuel is injected during the compression stroke, the gas temperature and density are higher than at intake conditions, which enhances the evaporation process and thus reduces the time for preparing the mixture, avoiding the need to heat up the intake air. This leads to lower temperature during the compression stroke and fewer problems with a too early start of ignition. But the control of the start of combustion is still critical because there is no direct relation between the start of injection and the start of ignition.

A second advantage is that the same fuel injection system can be used for both early injection HCCI combustion and direct injection conventional diesel combustion. This opens possibilities for controlling combustion and should allow an easier transition from the low load HCCI combustion type to the high load conditions requiring conventional diesel combustion. However, since early injection is performed against a low density environment, avoiding fuel impingement and cylinder wall wetting is a major challenge which requires re-designing of either the injection system itself (which presents stability problems at low injection pressures) or the geometrical arrangement. If wall wetting is avoided an effective reduction of unburned hydrocarbons emissions is obtained and fuel efficiency increases (Akagawa *et al*., 1999, Kaneko *et al*., 2002, Walter and Gatellier, 2002).

As a drawback, with early direct injection less time is available for mixing the fuel with the air, compared to a port fuel mixing system. This results in a less homogeneous mixture, leading to emissions of NOx and soot that are higher than those achieved with port mixing HCCI (but still much lower than for conventional diesel combustion).

Several approaches exist to early direct injection HCCI combustion, utilizing one or more injectors and single or multiple injection events. The most important systems are: PREDIC and MULDIC, HiMICS, PCI, UNIBUS and NADI; these systems are summarized in the following paragraphs.

- The PREDIC (PREmixed lean DIesel Combustion) and MULDIC (MULtiple stage DIesel Combustion) combustion concepts were developed by the New ACE Institute in Japan.
  In a first study presented by Takeda and Keiichi (1996), different injector

configurations and locations were studied in combination with variation of injection timing. Due to the good mixing, low NOx and soot emission were achieved, but results were largely affected by the injection timing and geometrical arrangement and charge dilution. The large emissions of HC and CO found with a conventional diesel DI injector, were significantly reduced by using two side injectors or reducing the nozzle orifice diameter in combination with an increase in the number of orifices. A maximum load of 5 bar IMEP was achieved at very advanced start of injection (Ishii *et al*., 1997). Later on, Harada *et al*. (1998) used a swirling-flow pintle-nozzle injector, which resulted in a more uniform mixture with lower HC emission and higher combustion efficiency. Several improvements are presented by Akagawa *et al*. (1999), showing that a maximum load of around 50% of the IMEP that could be achieved with a natural aspirated diesel engine was the upper limit of PREDIC, whilst with lowered compression ratio and supercharging, power output could be nearly doubled.

As in most early-injection HCCI systems, the start of injection is limited by misfiring due to over mixing in case of too early injection, and for the case of too late injection, knocking occurs (Akagawa *et al*., 1999).

In order to increase the operation range of the PREDIC system, a second injection around TDC was introduced by Hashizume *et al*. (1998), leading to the so-called MULDIC system, which combines a lean premixed combustion (PREDIC) with a more conventional diffusion combustion separated in time. Since the second stage of combustion closely resembles conventional diesel combustion, the emission of NOx and soot are much higher than those for PREDIC combustion, but NOx emissions were found to be one-sixth those of conventional diesel combustion. Engine efficiency was improved in the Japanese 13-mode test cycle and particulate emissions were found higher than in conventional diesel operation. However, the high soluble organic fraction of the particles found makes it possible to use a simple oxidation catalyst.

- The HiMICS combustion concept (Homogeneous charge Intelligent Multiple Injection Combustion System) was developed at Hino Motors Ltd. (Suzuki *et al*., 1997a, 1997b). A conventional common rail system is used and multiple injection strategies are applied. It uses a hybrid injection pattern, combining a very advanced injection with a main injection around TDC and eventually a post injection after TDC to reduce soot.

  A conventional 6-orifice nozzle was used and, in order to improve the mixture formation, a 30-orifice 3-row nozzle was also evaluated. The 30-orifice nozzle was found to be good for forming a well-homogenized mixture while the 6-orifice nozzle was found to be better for the injection

around TDC, leading to the conclusion that a double nozzle injection system was necessary.

- The PCI (Premixed Compression Ignition) combustion concept, developed by Mitsubishi (Iwabuchi *et al.*, 1999), uses a conventional DI diesel injector nozzle, early start of injection and a reduced compression ratio. In an initial study, the enclosed angle between the orifices was varied, and an angle of 80° was found to give the best compromise, using a single injection at around 60–40 CAD BTDC. Very low NOx and acceptable HC emission were observed; however, these were accompanied by very high soot emission.

  Using a novel nozzle tip with two rows of orifices drilled in such a way that the sprays impinge with each other, fuel dispersion is enhanced and spray penetration is reduced, so that soot emissions are reduced to nearly zero.

  The hydrocarbon emissions of the PCI system are relatively high, but with the use of an oxidation catalyst, similar levels as a conventional diesel engine without catalyst are achieved.

  Cooled EGR was found to retard the start of combustion and thus increase the maximum load. If combined with a boost pressure of 1.80 bar, similar performance was obtained as with a natural aspirated diesel engine, with 90% less NOx, almost no soot emission and similar fuel consumption.

  The load range of the PCI combustion concept can be extended using a split injection. While the first injection leads to PCI combustion, the second injection event leads to a more conventional combustion (Okude *et al.*, 2004). This results in reductions in NOx and soot, and avoids high combustion noise at high load.

- The UNIBUS (UNIform BUlky combustion System) system, developed by the Toyota Motor Corporation, (Akihama *et al.*, 2001, Yanagihara, 2001, 2002, Hotta *et al.*, 2002, Hasegawa *et al.*, 2004, Hildingsson *et al.*, 2005), was introduced on the market in 2000 and is currently used as a rich combustion strategy for the Toyota DPNR system (DeNOx and Particulate Number Reduction) (Matsuda, 2005). Despite the fact that the system is commercialized, there is not too much information available in the literature, and only by comparison of different articles and assumption of the missing links, can one guess how this combustion concept works. UNIBUS mode is restricted to the low load, low speed region, whilst conventional diesel combustion is used in the high load and high speed region as sketched in Fig. 10.7.

  The combustion concept relies on a combination of an early injection (around 50 CAD BTDC) and a late injection after TDC. The first injection creates a homogeneous mixture that shows spontaneous low temperature heat release close to TDC but prior to the second injection. The second

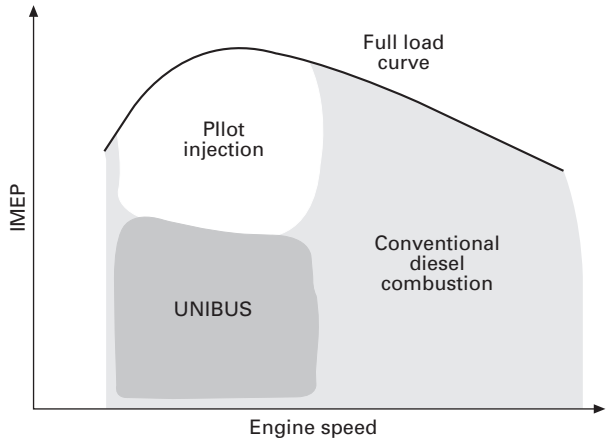

10.7 Operation map of UNIBUS engine.

injection triggers burning of the premixed fuel of the second injection and of the partly burned fuel of the first injection. This strategy is reported to improve combustion efficiency without causing excessive HC and CO emissions.

- In the NADI (Narrow Angle Direct Injection) combustion concept, developed at the IFP (Institut Français de Pétrole) (Walter and Gatellier, 2002), the combustion chamber design and spray formation are optimized for early injection HCCI combustion, without losing the ability to function as a conventional DI diesel combustion. It makes use of a nozzle with a narrow included angle of around 80 degrees, so that fuel can be injected early in the compression stroke when density and temperature are relatively low, without causing cylinder liner wetting (see Plate 10) (between pages 268 and 269). With a careful design of the piston-bowl geometry, it can operate at full load in conventional diffusion combustion with the same injector. At low to medium load the engine works in a HCCI regime and is switched to a conventional combustion for higher load.

  The latest version of the NADI combustion concept features a 3rd generation common rail system. This allows for split injection strategies at low load conditions, which reduce HC and CO emissions (Walter *et al.*, 2004). Under conventional combustion, split injections were found to create vortices with the narrow bowl which improve the soot oxidation (Revaille *et al.*, 2004). The transient control of the combustion and switching between different combustion modes has been demonstrated despite the high requirements for the EGR rate control. Very low NOx and soot emissions were achieved at a maximum power of 63kW/l with a high efficiency and acceptable CO and HC emissions (Duret *et al.*, 2004).

10.4.3 Late direct injection

In the previous paragraphs, it has been discussed that in early injection HCCI combustion, fuel is injected well before the expected start of ignition, early in the compression stroke, which allows sufficient time to form a homogenized mixture. The more the injection approaches TDC, the higher the gas temperature and density and the shorter the autoignition delay, up to the moment that the combustion resembles a more classic DI combustion than HCCI combustion.

However, if the injection is further retarded, starting from a conventional combustion with injection just before TDC, towards later crank angles, then gas temperature and density decrease – due to the expansion movement of piston – leading to a longer autoignition delay, and an improved mixture formation. In fact, the conditions are again favourable for HCCI combustion. If, in addition, high EGR rates are used, then the ignition delay can be sufficiently long as to allow the development of an intense premixed combustion mode that should inhibit soot formation, together with low combustion temperatures that can prevent NOx formation.

This effect is illustrated in Fig. 10.8, extracted from Benajes *et al.* (2004), showing the effect of retarding the injection on the rate of heat release. When changed in a range that is common for conventional diesel engines, the RoHR does not change too much. However, when the SOI is retarded further, the shape of the RoHR curves start to change; the premixed burning fraction increases while the diffusion combustion becomes less important, this is accompanied by a large reduction in NOx and soot emissions.

Although the challenge is again the maximum load achievable with an acceptable efficiency, two major advantages of the late injection strategies are, first, that they are applicable in conventional diesel engines or in natural

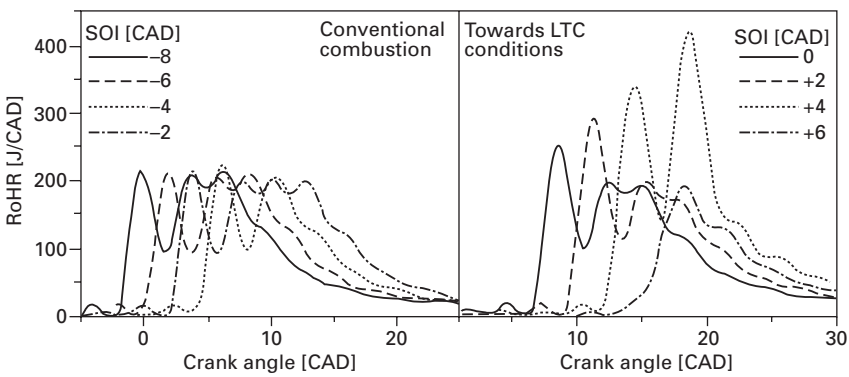

10.8 Injection retarding, from conventional combustion towards LTC conditions.

technological evolution of current engines, and second, that injection and combustion processes are not completely decoupled, so that combustion phasing is controlled by injection timing.

This concept is the basis of the MK (Modulated Kinetics) and HPLI (Highly Premixed Late Injection) developments.

The MK (Modulated Kinetics) combustion system was developed by the Nissan Motor Corporation (Mase *et al*., 1998, Kimura *et al*., 2002), and is well covered in a later chapter. It was introduced in the Japanese literature in 1995 and brought into the Japanese market in 1998 for high-speed diesel engines.

In the first generation of the MK system, success of combustion with HCCI characteristics relies on three factors: first, the oxygen concentration of the intake air was reduced with EGR, which leads to a drastic reduction in NOx emission with a penalty on soot and HC; second, the start of ignition was retarded leading to a more premixed combustion with lower NOx, lower soot, but higher HC emission; and third, a high swirl ratio was used in order to improve the mixture formation, further reduce soot emission, and get a serious reduction in HC emission. These three factors contribute to increased ignition delay, so that all the fuel is injected before the start of combustion (Kimura *et al*., 2002, Ryan and Gray, 1997).

In the second generation of the MK combustion system the load and speed range of the MK combustion was extended following the main principles of this combustion. The autoignition delay was increased by means of a reduction in the compression ratio and EGR cooling. The injection duration was reduced by means of higher injection pressure in combination with an increase in nozzle orifice diameter. The combination of a reduced oxygen concentration and a retarded start of injection led to a simultaneous reduction of NOx and soot. In the case that all fuel is injected before the start of combustion, the soot emission can be very low, independent of the equivalence ratio (Kimura *et al*., 2001).

The HCLI (Homogeneous Charge Late Injection) and HPLI (Highly Premixed Late Injection) combustion concepts are currently being developed by AVL (Pfahl, 2005, Wimmer *et al*., 2006) and appeared only recently in the international literature.

As shown in Fig. 10.9, the HCLI combustion is used at low load, HPLI combustion is used at medium load, and high load is achieved with a conventional DI diesel combustion.

In the HCLI combustion concept, injection is performed at around 40 degrees before TDC, so that a rapid homogenization takes place. As in other early injection HCCI combustion modes, the start of combustion and the burn rate cannot be controlled by the rate of injection but only depend on the reaction kinetics of cylinder charge and are thus determined by the variables and composition of the charge at the end of intake. In order to reduce the

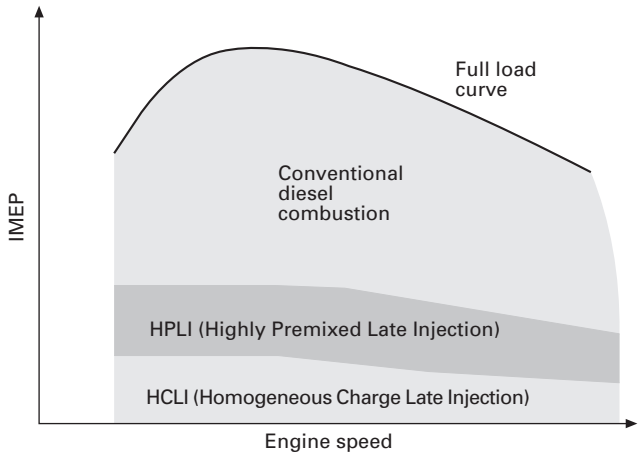

10.9 Operation map of engine using HCLI and HPLI combustion concepts.

tendency for premature autoignition, it is necessary to slightly reduce the compression ratio as compared to conventional DI diesel engines and to dilute the mixture by using rates of EGR typically higher than 65%. As in other cases, the problems of a high combustion speed, which leads to very high rates of pressure rise and combustion noise persists, and the high efficiency of the conventional diesel combustion is not achieved either.

In the HPLI combustion mode, injection is performed after TDC. In order to prevent conventional combustion, the start of injection is chosen sufficiently late as to ensure an ignition delay high enough to allow for mixture homogenization before combustion. In this case, the interval between the end of injection and the start of combustion is decisive for proper mixture formation. If the injection and combustion phases overlap, a considerable amount of soot is produced, so that it is necessary to ensure complete soot oxidation keeping slightly higher temperatures at the end of the combustion process. Simultaneous reduction of the NOx emissions is achieved by EGR rates of the order of 40%.

10.5 Summary

Homogeneous Charge Compression Ignition (HCCI) is one of the most widely accepted acronyms to identify new combustion strategies based on the enhancement of premixed combustion modes. The basic process consists of the preparation of a homogeneous (or highly premixed) mixture under autoignition conditions. This mixture will undergo simultaneous and distributed oxidation so that no flame front is present, local temperatures are kept low, and NOx formation can be avoided. Besides, by keeping local fuel-air ratio

values low, soot formation, typical of conventional non-premixed flames, can also be also prevented.

Attempts to achieve practical solutions towards the theoretical concept of Homogeneous Charge Compression Ignition combustion have shown a large potential to reduce NOx and soot emissions in current diesel engines, keeping its low fuel consumption. However, due to the peculiarities of both diesel fuel and diesel combustion concept, current developments operate properly at low load, and increasing the operation range remains the main challenge which needs further development.

Conventional diesel combustion is highly heterogeneous from both spatial and temporal points of view and many different possibilities appear to reach combustion modes somehow close to the HCCI concept, each of them dealing with particular difficulties and requiring engine adaptations or technological developments. Thus plenty of denominations have been used for the resulting processes but, in any case, the idea is to promote premixed combustion modes.

Since creating a homogeneous mixture requires time, port fuel injection appeared as one the simplest solutions. But due to the low volatility of the diesel fuel and its high cetane number both evaporation process and autoignition control appear as the main problems. Thus, due to the limited efficiency of the technical solutions found, the high emissions of unburned hydrocarbon and noise, and the limited operation range, PFI HCCI combustion alone is nowadays not considered a real alternative for conventional diesel combustion, despite its advantages on NOx and soot emission. Nevertheless, the research on this type of combustion has increased the understanding of the fundamentals of HCCI combustion and some potential is offered if combined with direct injection strategies.

With early injection HCCI combustion strategies, a homogeneous or highly premixed fuel-air mixture is obtained by means of an injection event located early in the compression stroke. But due to the low in-cylinder density in which injection takes place, cylinder wall impingement is a major inconvenience, both in terms of cylinder liner erosion and fuel interaction with oil. This has led to the development of different versions of injection systems and strategies trying to overcome such disadvantages.

Developments in this group have been based either on optimization of multiple injection strategies, to achieve highly premixed combustion rates, or on a modification of the traditional single centred injector configuration. The former option does not bring any new requirement on the injection system, whereas the latter involves different possibilities, either using hollow cone nozzles or impinged spray nozzles to limit spray penetration and wall impingement, or using more than one injector per cylinder, and a special nozzle with a large number of micro-orifices.

If such problems are solved, serious reduction in soot and NOx emissions

are achieved; not as large as can be achieved by PFI HCCI, but still far below the emission levels of conventional diesel combustion.

Late injection low temperature combustion is the easiest way to obtain realistic real-world HCCI combustion if combined with high EGR rates. In order to obtain optimal results, injection has to be finished within the autoignition delay time, which brings in the necessity of high mixing rates, i.e. high injection rates. These late injection systems do not have the same characteristics of 'ideal' (PFI) HCCI engines, but are more a mix between the characteristics of conventional combustion and HCCI combustion. In general, the control of the start of combustion is easier than with any other HCCI concept. Late injection HCCI is the most successful application of HCCI combustion due to the minor modifications of the hardware components, and the easy control of the start of combustion.

Current views on all these new combustion modes show that, in general, they can only represent alternatives to conventional engines in part-load operating conditions. Although full load HCCI operation has been recently achieved in a single cylinder heavy duty engine by Caterpillar (Duffy *et al*., 2004), achieving 21 bar BMEP while meeting future emissions standards, details on how it can be achieved is not published, application to real production engines is still a challenge and the limits of application to lower size engines is not clear with current technology. A reasonable practical solution in the short-to-medium term would be a dual system in which both conventional and new combustion processes are used, the former for full load conditions, the latter for partial and low load.

Extending the operating limits require important developments in terms of combustion control, and the use of advanced technologies such as advanced boosting, variable valve actuation or variable compression ratio, or new developments in injection systems. On this last concern adaptations of current injection systems for new combustion modes should deal with hardware requirements rather than with injection operation.

10.6 References

Akagawa H, Miyamoto T, Harada A, Sasaki S, Shimazaki N, Hashizume T (1999), 'Approaches to solve problems of the premixed lean Diesel combustion', SAE International, SAE no. 1999-01-0183.

Akihama K, Takatori Y, Inagaki K, Sasaki S, Dean A (2001), 'Mechanism of the smokeless rich Diesel combustion by reducing temperature', SAE International, SAE no. 2001-01-0655.

Alperstein M, Swim W B, Schweitzer P H (1958), 'Fumigation kills smoke – improves Diesel performance', SAE International, SAE no. 580058.

Benajes J, Molina S, Riesco J M, Novella R (2004), 'Enhancement of the premixed combustion in a heavy duty Diesel engine by adjusting injection conditions', Proceedings of conference on thermo-and fluid dynamic processes in Diesel engines, Thiesel 2004, Valencia, Spain.

Canova M, Garzarella L, Ghisolfi M, Midlam-Mohler S, Guezennec Y, Rizzoni G (2005), 'A mean-value model of a turbocharged HCCI Diesel engine with external mixture formation', SAE International, SAE no. 2005-24-034.

Christensen M, Johansson B (1998), 'Influence of mixture quality on homogeneous charge compression ignition', SAE International, SAE no. 982454.

Christensen M, Johansson B (1999), 'Homogeneous charge compression ignition with water injection', SAE International, SAE no. 1999-01-0182.

Christensen M, Einewall P, Johansson B (1997), 'Homogeneous charge compression ignition (HCCI) using isooctane, ethanol and natural gas – A comparison with spark-ignition operation', SAE International, SAE no. 972874.

Christensen M, Johansson B, Amneus J, Mauss F (1998), 'Supercharged homogeneous charge compression ignition', SAE International, SAE no. 980787.

Curran H, Gaffuri P, Pitz W, Westbrook C (1998), 'A comprehensive modeling study of n-heptane oxidation', *Combustion and Flame*, Vol. 114, pp 149–177.

Dec J E (1997), 'A conceptual model of DI Diesel combustion based on laser-sheet imaging', SAE International, SAE no. 970873.

Duffy K, Coleman G, Donaldson G (2004), 'Diesel HCCI development', FY 2004 Progress Report for Advanced Combustion Engine Research and Development, Part II.A.14.

Duret P, Gatellier B, Monteiro L, Miche M, Zima P, Maroteaux D, Guezet J, Blundell D, Spinnler F, Zhao H, Perotti M, Araneo L (2004), 'Progress in Diesel HCCI combustion within the European space light project', SAE International, SAE no. 2004-01-1904.

Flynn P, Durret R, Hunter G, zur Loye A, Akinyemi O, Dec J E, Westbrook Ch K (1999), 'Diesel combustion: An integrated view combining laser diagnostics, chemical kinetics and empirical validation', SAE International, SAE no. 1999-01-0509.

Guezennec Y, Midlam-Mohler S, Rizzoni G (2002), 'A mixed mode HCCI/DI engine based on a novel heavy fuel atomizer', Proceedings of 8th Diesel engine emission reduction conference 2002, San Diego, USA.

Guezennec Y, Midlam-Mohler S, Rizzoni G, Haas S, Berner H, Bargende M (2004), 'Mixed-mode Diesel HCCI/DI with external mixture preparation', Proceedings of FISITA 2004 world automotive congress, F2004V258.

Harada A, Shimazaki N, Sasaki S, Miyamoto T, Akagawa H, Tsujimura K (1998), ´The effects of mixture formation on premixed lean Diesel combustion', SAE International, SAE no. 980533.

Hardy W, Reitz R D (2006), 'A study of the effects of high EGR, high equivalence ratio, and mixing time on emissions levels in a heavy-duty Diesel engine for PCCI combustion', SAE International, SAE no. 2006-01-0026.

Hasegawa R, Sakata I, Yanagihara H, Hildingsson L, Johansson B, Collin R, Nygre J, Richter M (2004), 'Analysis on homogeneity effects in HCCI combustion using simultaneous OH and formaldehyde LIF measurements', *Aachener Kolloquium Fahrzeug- und Motorentechnik*, Vol. 13.

Hashizume T, Miyamoto T, Akagawa H, Tsujimura K (1998), 'Combustion and emission characteristics of multiple-stage Diesel combustion', SAE International, SAE no. 980505.

Hildingsson L, Persson H, Johansson B, Collin R, Nygren J, Richter M, Alden M, Hasegawa R, Ranagihara H (2005), 'Optical diagnostics of HCCI and UNIBUS using 2-D PLIF of OH and formaldehyde', SAE International, SAE no. 2005-01-0175.

Hotta H, Inayoshi M, Nakakita K (2002), 'Achieving lower exhaust emissions and better performance in a HSDI Diesel engine with multiple injection', R&D review of Toyota Central R&D Labs, Vol: 37 no. 3, 9–16.

Husberg T, Gjirja S, Dentratt I, Engström J (2005), 'Fuel equivalence ratio and EGR

impact on premixed combustion rate and emission output on a heavy-duty Diesel engine', SAE International, SAE no. 2005-24-046.

Iida N, Yamasaki Y, Sato S (2004), 'The key points of HCCI combustion controls', IFP International Conference Which fuels for low CO_2 Engines? Rueil-Malmaison, France.

Ishii H, Koike N, Suzuki H, Odaka M (1997), 'Exhaust purification of Diesel engines by homogeneous charge with compression ignition – part 2: analysis of combustion phenomena and NOx formation by numerical simulation with experiment', SAE International, SAE no. 970315.

Iwabuchi Y, Kawai L, Shoji T, Takeda Y (1999), 'Trial of new concept Diesel combustion system – Premixed Compression Ignition Combustion', SAE International, SAE no. 1999-01-0185.

Kaneko N, Ando H, Ogawa H, Miyamoto N (2002), 'Expansion of the operating range with in-cylinder water injection in a premixed charge compression ignition engine', SAE International, SAE no. 2002-01-1743.

Kimura S, Aoki S, Kitahara Y, Aiyoshizawa E (2001), 'Ultra-clean combustion technology combining a low-temperature and premixed combustion concept for meeting future emission standards', SAE International, SAE no. 2001-01-0200.

Kimura S, Ogawa H, Matsui I, Enomoto Y (2002), 'An experimental analysis of low temperature and premixed combustion for simultaneous reduction of NOx and particulate emission in direct injection Diesel engines', *International Journal of Engine Research*, Vol. 3 no. 4, 249–259.

Kitamura T, Ito T, Senda J, Fujimoto H (2002), 'Mechanism of smokeless Diesel combustion with oxygenated fuels based on the dependence of the equivalence ratio and temperature on soot particle formation', *International Journal of Engine Research*, Vol. 3 no. 4, Page 223–248.

Ladommatos N, Abdelhalim S, Zhao H (2000), 'The effects of exhaust gas recirculation on Diesel combustion and emissions', *International Journal of Engineering Research*, Vol. 1 no. 1, Page 107–125.

Mase Y, Kawashima J, Eguchi M, Sato T (1998), 'Nissan's new multivalve DI Diesel engine series', SAE International, SAE no. 981039.

Matsuda Y (2005), 'Toyota's environmental challenge: Prius lobbying kit', Presentation at SAE Fuel & lubricant meeting 2005, Rio de Janeiro, Brazil.

Midlam-Mohler S, Guezennec Y, Rizzoni G (2003), 'Mixed-mode Diesel HCCI with external mixture formation: preliminary results', Proceedings of 9th Diesel engine emission reduction conference 2003, Newport, USA.

Milovanovic N, Chen R, Turner J (2004), 'Influence of variable valve timing strategy on the control of a homogeneous charge compression (HCCI) engine', SAE International, SAE no. 2004-01-1899.

Nishida H, Tachibana T (2006), 'Homogeneous charge compression ignition of natural gas/air mixture with ozone addition'. *Journal of Propulsion and Power*, Vol. 22, no. 1.

Nishijima Y, Asaumi Y, Aoyagi Y (2002), 'Impingement spray system with direct water injection for premixed lean Diesel combustion control' SAE International, SAE no. 2002-01-0109.

Okude K, Mori K, Shiino S, Moriya T (2004), 'Premixed Compression Ignition (PCI) combustion for simultaneous reduction of NOx and soot in Diesel engine', SAE International, SAE no. 2004-01-1907.

Olsson J, Tunestal P, Johansson B (2001), 'Closed-loop control of an HCCI engine', SAE International, SAE no. 2001-01-1031.

Pfahl U (2005), 'Combustion, aftertreatment and control key elements for emission reduction of US HSDI Diesel engines', Proceedings of ERC – 2005 symposium, Madison, USA.

Revaille B, Miche M, Jay S, Heinriot S (2004), 'Contribution of 3D CFD tools to the development and understanding of Diesel engines: improving today's engines and designing tomorrow's power units', Congrès Le Diesel: aujourd'hui et demain, Société des ingénieurs d'automobile, Lyon, France.

Richter M, Engström J, Franke A, Aldén M, Hultqvist A, Johansson B (2000), 'The influence of charge inhomogeneity on the HCCI combustion process', SAE International, SAE no. 2000-01-2868.

Ryan T W, Callahan T J (1996), 'Homogeneous charge compression ignition of Diesel fuel', SAE International, SAE no. 961160.

Ryan T W, Gray A W (1997), 'Homogeneous charge compression ignition (HCCI) of Diesel fuel', SAE International, SAE no. 971676.

Ryan T W, Callahan T J, Mehta D (2004), 'HCCI in a variable compression ratio engine – effects of engine variables', SAE International, SAE no. 2004-01-1971.

Sheppard C, Tolegano S, Woolley R (2002), 'On the nature of auto-ignition leading to knock in HCCI engines', SAE International, SAE no. 2002-01-2831.

Shibata G, Urushihara T (2004), 'The effect of fuel properties on HCCI Engine Combustion characteristics and Performances', IFP International Conference Which fuels for low CO_2 Engines? Rueil-Malmaison, France.

Suzuki T, Kakegawa T, Hikino K, Obata A (1997a), 'Development of Diesel combustion for commercial vehicles', SAE International, SAE no. 972685.

Suzuki T, Yokata H, Kudo Y, Nakajima H, Kakegawa T (1997b), 'A new concept for low emission Diesel combustion', SAE International, SAE no. 970891.

Takeda Y, Keiichi N (1996), 'Emission characteristics of premixed lean Diesel combustion with extremely early staged fuel injection', SAE International, SAE no. 961163.

Walter B, Gatellier B (2002), 'Development of the high-power NADI concept using dual-mode Diesel combustion to achieve zero NOx and particulate emissions', SAE International, SAE no. 2002-01-1744.

Walter B, Monteiro L, Miche M, Gatellier B (2004), 'Improvement of exhaust and noise emissions of the NADI concept using pre-mixed type combustion with multiple stages injection', Congrès Le Diesel: aujourd'hui et demain, Société des ingénieurs d'automobile, Lyon, France.

Wimmer A, Eichlseder H, Klell M, Figer G (2006), 'Potential of HCCI concepts for DI Diesel engines', *International Journal of Vehicle Design* Vol 41, no. 1–4 pp. 32–48.

Yamada H, Ohtomo M, Yoshii M, Tezaki A (2005), 'Controlling mechanism of ignition enhancing and suppressing additives in premixed compression ignition', *International Journal of Engine Research*, Vol. 6, no. 4, pp. 331–340.

Yanagihara H (2001), 'Ignition timing control at Toyota UNIBUS combustion system', IFP international Congress, Rueil-Malmaison, France.

Yanagihara H (2002), 'A study on combustion structure of premixed compression ignition Diesel engines', Proceedings of conference on thermo-and fluid dynamic processes in Diesel engines, Thiesel 2002, Valencia, Spain.

11

HCCI combustion with early and multiple injections in the heavy-duty diesel engine

Y A O Y A G I, New ACE, Japan

11.1 Introduction

Electrically controlled common rail injection systems have allowed diesel engines to vary injection timing widely and have the capability of multi-injections [1, 2]. As a result, homogeneous compression ignition combustion (HCCI) can be realized not only through the adoption of a fuel supply in the intake port [3, 4], but also direct injection into the cylinder [5]. Using those technologies, New ACE has proposed an advanced combustion system [6, 7]. Many automobile companies, institutions, and universities have undertaken numerous research efforts concerning HCCI [8–10]. Recently, it is interesting to note that Shimazaki *et al.* [11], Walter *et al.* [12] and authors [37] have studied combined systems of premixed compression ignition and diesel combustion with a narrow spray angle of the injection nozzle. Christensen, Johansson *et al.* [3, 4], Harada *et al.* [13], and Ogawa *et al.* [14] have examined combustion at high loads using alcohol-based high-octane fuel.

Authors adopted a new combustion system with early fuel injection into the cylinder, along with mixture formation during the compression stroke, and compression ignition at near the TDC. We call this system 'premixed diesel combustion (PREDIC)' and have continued studying this system [6, 7]. Initially, based on a conventional natural aspiration (NA) diesel engine, this PREDIC system had used the fuel with a lower cetane number, which is from 20 to 40, than conventional diesel fuel in order to avoid the knock tendency. Although PREDIC was able to reduce NOx and soot dramatically, this system was unable to maintain the normal air excess ratio $\lambda = 1.3\sim1.5$ required for conventional diesel engines, thereby presenting the problem that the engine was capable of achieving only half the torque of a normal diesel engine.

An engine was supercharged with much more air with the intention of improving poor engine torque to solve this problem. Supercharging prompted ignition earlier. It was necessary to greatly increase the air excess ratio λ to improve this situation of premature ignition. Consequently, although the

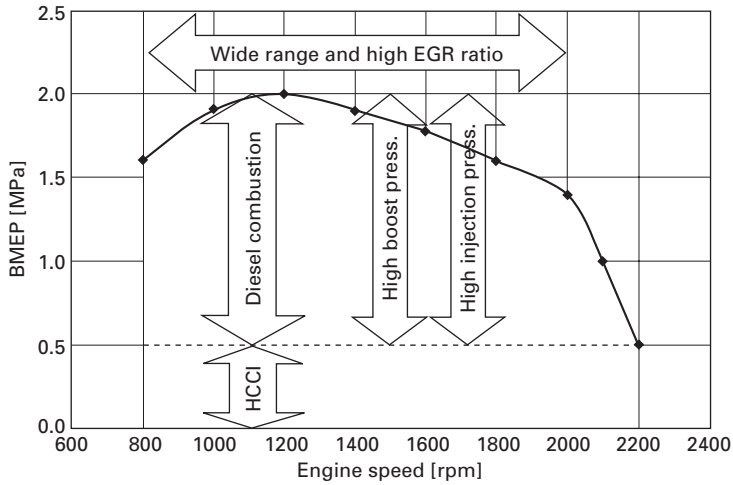

11.1 Combustion concept for Super Clean Diesel Engine.

engine achieved low NOx and smoke, the engine required high boost-pressure to achieve sufficient engine power and torque to provide comparable performance to that of conventional NA diesel engines [7, 15–18]. By merits of the high pressure fuel injection and turbo intercooler [19–22], the current engines have been improved. And recent diesel engines have become cleaner by combining EGR [23, 24] and after-treatment devices as clean emission technology [25, 26, 27].

To achieve HCCI combustion using production-ready technologies, it can be considered that an engine should adopt HCCI at partial load range. On the other hand, engines should adopt high performance diesel combustion at a medium and high load range where high brake mean effective pressure (BMEP) and low fuel consumption are required [28–35]. Authors have conducted research based on the concept that engines should use highly boosted diesel combustion from medium to high loads and use premixed compression ignition combustion at light loads, which is shown in Fig. 11.1 [29]. This chapter presents research achievements in the author's laboratory related to premixed compression ignition combustion.

11.2 Experimental apparatus

The current specifications of a single cylinder test engine are shown in Table 11.1 and this engine is a four-stroke and direct injection diesel engine. On the premise of high boost pressure, the engine was able to withstand maximum cylinder pressure of P_{max} = 30 MPa. A new monotherm piston was designed for this engine[36]. Figure 11.2 shows the piston shape and ring set. The piston cavity is a shallow-dish type with a compression ratio of ε = 16.5. The

Table 11.1 The current specifications of single cylinder test engine

Item	Specifications
Engine type	DI single cylinder
Bore and stroke	135 × 140 mm
Displacement	2004 cm^3
Cylinder head	4 valve
Piston	Monotherm steel piston
Comb. chamber	D = 98 mm, shallow dish
Compression ratio	16.5
Swirl ratio	1.4, 0.5 ~ 5.6
Air charging	External super charger
Injector, center	Hole nozzle, 0.17 × 8
Injection pressure	100 ~ 200 MPa
Engine speed	800 ~ 2000 rpm

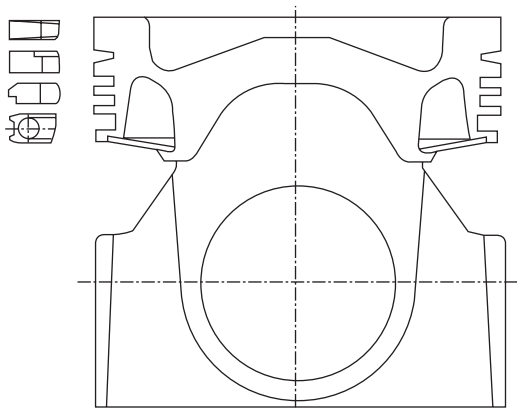

11.2 Combustion chamber shape and monotherm steel piston for P_{max} 30 MPa.

injection system is a common rail type. The injection pressure was capable of increased pressures up to 230 MPa, and this HCCI experiment was performed at 100~120 MPa. In this experiment, the fuel injectors were a hole nozzle type installed in the cylinder center and side.

An independent supercharger and charged air cooler on the single cylinder engine allowed the boost pressure and temperature to be changed independently. Furthermore, the EGR ratios were also controlled independently of the boost pressure.

Figure 11.3 shows an outline of the experimental apparatus and Fig. 11.4 shows the relationship between injection quantity and boost pressure at 1200 rpm. The boost pressure was controlled based on of the operation of a 6-cylinder engine. A series of HCCI tests were conducted at naturally aspirated

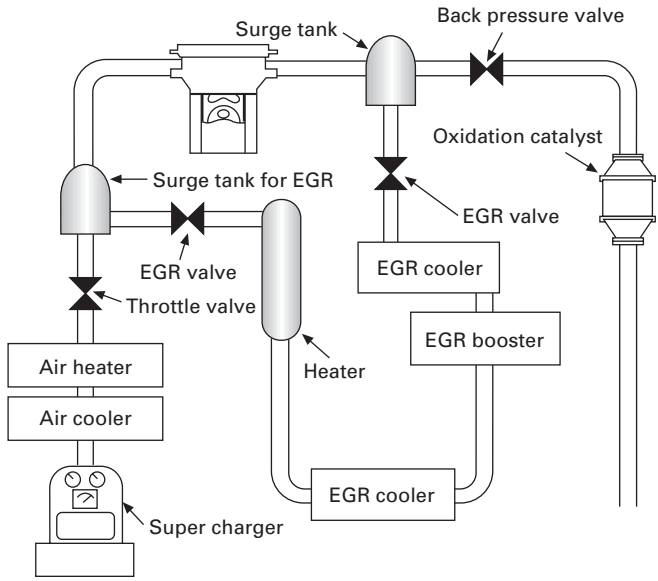

11.3 External supercharger and EGR system for single cylinder engine.

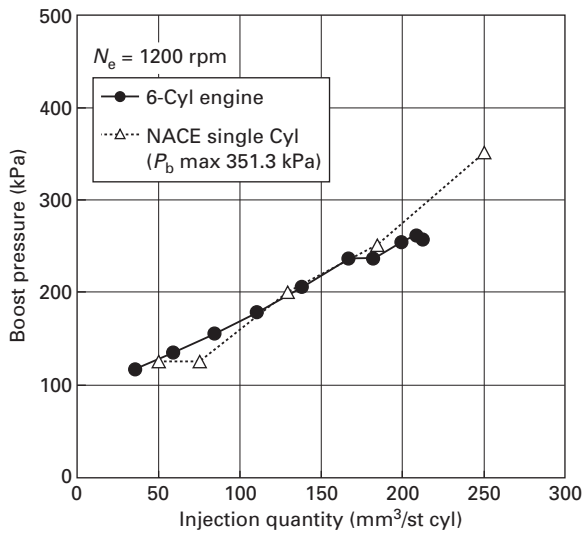

11.4 The relationship between boost pressure and injection quantity at 1200 rpm.

condition and at the light load condition with constant boost pressure of P_b = 151.3 kPa.

The engine torque was measured by Meidensha 110 kW dynamometer. The rate of heat release was analyzed by Ono Sokki DS2000 based on the in-cylinder pressure measurements using a Kistler pressure transducer. Horiba MEXA-9100 measured the gaseous exhaust emissions. PM was sampled by Horiba Micro-tunnel MDLT-1302TM and was analyzed by Horiba MEXA-1370PM. Filter smoke numbers were measured by AVL415S.

11.3 Early injection HCCI (PREDIC) by low cetane fuel

A system with pre-mixed compression-ignition combustion, which author calls PREDIC, is shown schematically in Fig. 11.5. In this figure the difference in mixture processes between PREDIC and conventional diesel is described. Horizontal and vertical coordinates respectively denote excess air ratio λ and the quantity of fuel/air mixture immediately before ignition, whose distributions are derived from numerical analyses with KIVA code. Because fuel injection takes place near the TDC in conventional combustion, over-rich fuel/air mixture is obtained immediately after injection. On the other hand, in PREDIC, fuel injection is performed at an early timing, 90°BTDC, so that the period of 90° is used for generation of the fuel/air mixture. The over-rich fuel/air mixture is then made lean as it mixes with air. Therefore, in spite of the same overall excess air ratio, PREDIC is a leaner combustion than conventional one.

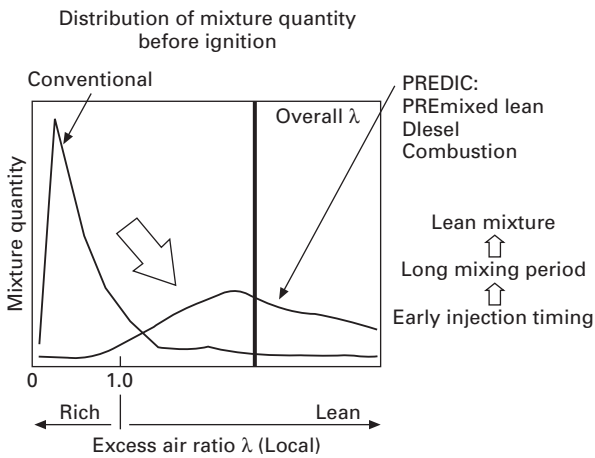

11.5 The difference in mixture processes between PREDIC and conventional diesel.

Figure 11.6 compares the injector layout in combustion chamber between PREDIC and conventional diesel. Side injectors are employed for PREDIC and MULDIC as a pre-mixed compression ignition combustion. These side injectors increase the distance between the injector and the cylinder wall in comparison with center injector, and can thereby reduce fuel adherence to the cylinder wall. Hence, the injectors are advantageous for fuel/air mixture generation. The specifications of PREDIC and MULDIC engine are shown in Table 11.2 and some of items are different to Table 11.1.

Figure 11.7 compares combustion processes in PREDIC with conventional combustion, at two different injection timings at air excess ratio $\lambda = 2.7$. The

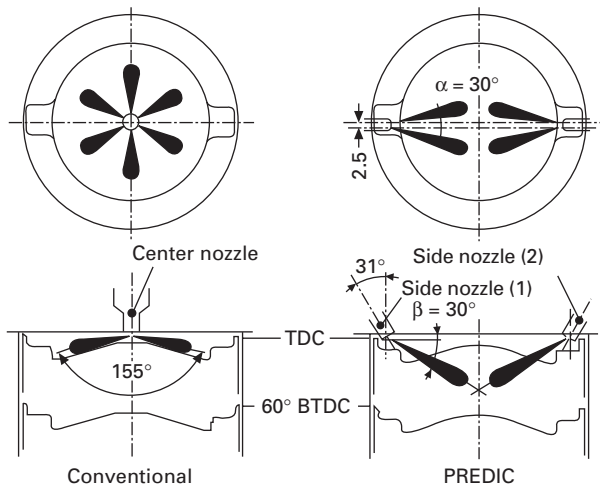

11.6 The comparison of injector layout between PREDIC and conventional diesel.

Table 11.2 PREDIC and MULDIC engine specifications

Item	Specifications
Engine type	DI single cylinder
Bore and stroke	135 × 140 mm
Displacement	2004 cm^3
Cylinder head	4 valve
Piston	Alminum piston
Comb. chamber	D = 98 mm, shallow dish
Compression ratio	16.5
Swirl ratio	0.5
Air charging	External super charger
Injector, center	Hole nozzle, 0.17 × 6
Injector, sides	Hole nozzle, 0.17 × 2
Injection pressure	100 MPa
Engine speed	1000 rpm

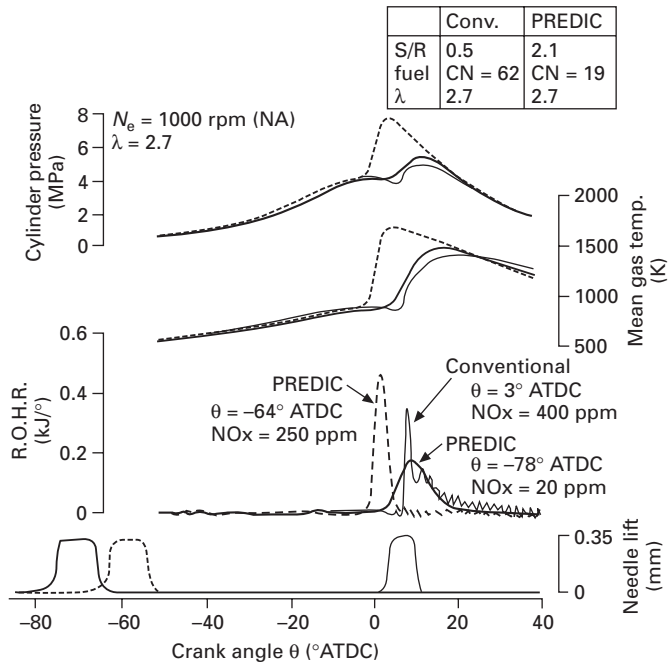

11.7 The comparison of combustion between PREDIC and conventional diesel.

dashed line represents a PREDIC case with injection timing at 64°BTDC, where NOx is reduced by half compared with conventional combustion. With earlier injection timing at 78°BTDC, lean combustion prevails and NOx is reduced to 1/20 of the level of conventional diesel. Further advancement of injection of lean fuel/air mixtures can cause misfires that prevent proper driving operation.

Figure 11.8 presents the exhaust emissions at various air excess ratio λ and changing injection timing. Watching the case of λ fixed at 2.7, when the injection timing is later than 64°BTDC, the fuel/air mixture gets richer and its combustion becomes fast. Further injection timing retards induces uncontrolled fast combustion and knocking. Although PREDIC uses low cetane fuel such as CN = 19, fuel consumption is affected a little even though NOx is reduced to 1/10, as indicated also by the cylinder pressure in Fig. 11.7. Because PREDIC allows low NOx even though it uses iso-volumetric combustion, proper control of ignition timing will further improve fuel consumption. Current issues on PREDIC include torque of only half that of conventional combustion because of the minimal limit of λ at 2.5, along with high unburned hydrocarbons (THC) and exhaust CO concentration.

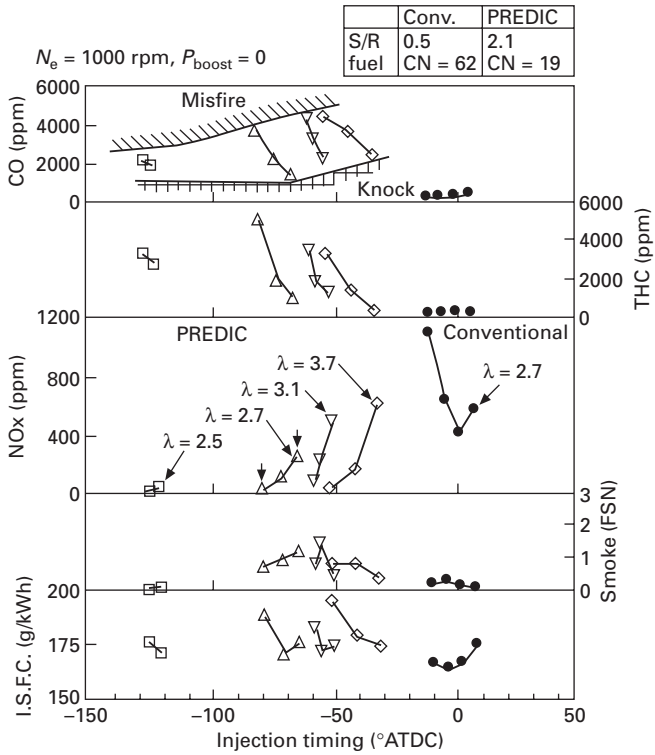

11.8 The exhaust emissions of PREDIC and conventional diesel.

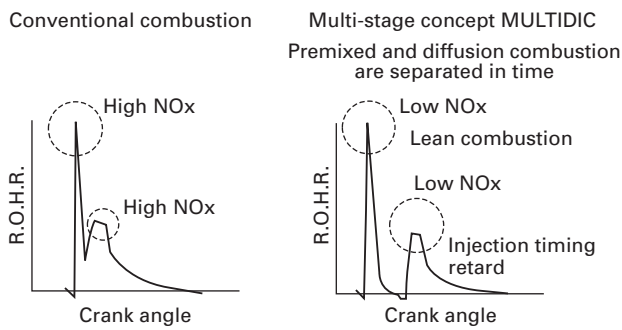

11.9 Multi-stage diesel combustion (MULDIC).

11.4 Multiple injections HCCI by low cetane fuel (two-stage combustion, MULDIC)

MULDIC is a kind of two-stage combustion and was introduced in order to improve torque upper limit in PREDIC [12]. Figure 11.9 explains the multi-stage diesel combustion (MULDIC). It employs PREDIC at first to reduce

NOx and smoke. Combustion with injection timing retarded at high λ might suppress NOx and smoke and allow combustion of sufficient torque with the aid of an internal EGR-like effect. Figure 11.10 illustrates injection timing in MULDIC. Particularly great injection timing retarding at stage 2 compared to that of conventional diesel reduces NOx without misfires.

Effects of injection timing retarding in MULDIC on fuel consumption and exhaust emissions are shown in Fig. 11.11 and NOx becomes minimal at

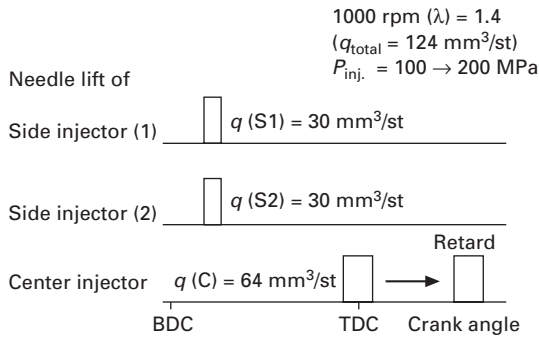

11.10 Fuel delivery in MULDIC.

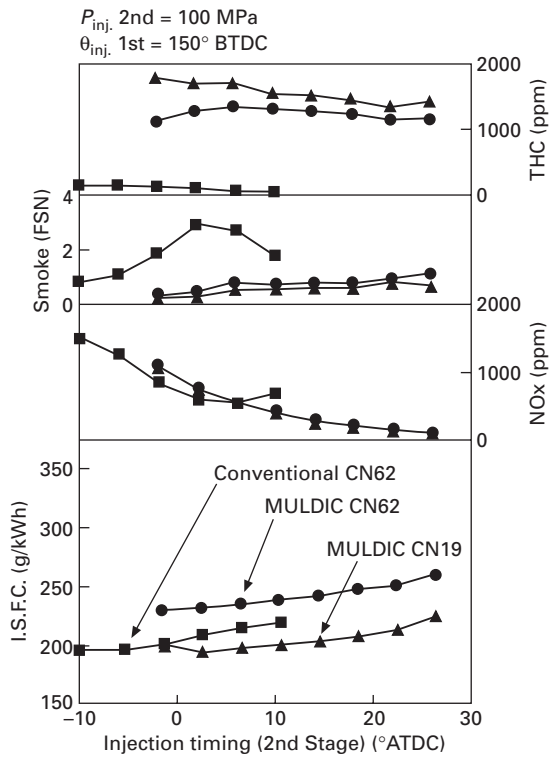

11.11 The exhaust emissions of MULDIC and conventional diesel.

around TDC injection in conventional combustion, whereas MULDIC can achieve further NOx reduction by retarding the second injection of the center injector. In Fig. 11.12, fuel consumption, smoke and THC in MULDIC are presented in comparison with conventional diesel. In this figure NOx of MULDIC became 40% of conventional diesel. Furthermore, MULDIC reduces smoke as well as NOx and fuel consumption is improved to the level of the conventional diesel with low cetane number of fuel, CN = 19. Because MULDIC, as well as PREDIC, can reduce NOx in spite of high degree of constant volume like otto cycle, it might achieve further improvement of fuel consumption with ignition timing control and selection of fuel property.

Current issues on MULDIC include high unburnt hydrocarbon (THC) and high exhaust CO concentration. An injector that suppresses spray penetration is under examination as a countermeasure to eliminate this issue [13]. However, the after-treatment of exhaust gas is required using a high-performance of oxidation catalyst.

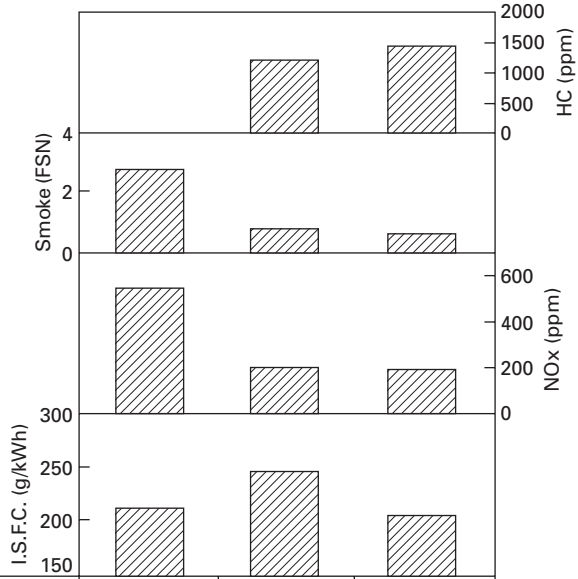

Cetane no.		CN62	CN62	CN19
Injection timing	1st	6° ATDC	150° BTDC	150° BTDC
	2nd	————	18° ATDC	18° ATDC
Injection pressure	1st	100 MPa	100 MPa	100 MPa
	2nd	————	100 MPa	100 MPa
Type		Conventional	MULDIC	MULDIC

11.12 The comparison of exhaust emissions and ISFC between MULDIC and conventional diesel.

11.5 HCCI for normal cetane fuel

11.5.1 Combustion experiment with the research engine

The engine used sulfur-free diesel fuel with sulfur concentration of 3 ppm and the fuel properties are shown in Table 11.3. This experiment used a multi-hole nozzle shared between diesel combustion and premixed compression ignition combustion with the narrower spray angle of 120°, which enabled earlier injection than the normal angle of 150° [37]. Figure 11.13 shows the position in the piston where the fuel spray impinges with different injection timings of 20, 30, 40, and 50° BTDC for cases in which the spray angles are 150 and 120°. For a spray angle of 120°, when the fuel injection timing is retarded from 45° BTDC, much injected fuel remains in the piston cavity. Furthermore, because the injected fuel spray impinges on the piston cavity wall, the injection timing greatly affects the combustion behavior and combustion changes continuous from 45° BTDC to TDC. However, when injection timing is advanced from 50° BTDC, the position of fuel spray impingement changes from the cavity wall to the top surface of the piston. Consequently, dramatic variations are predicted in exhaust emissions and torque.

In this experiment, the operating range of injection timing was from T_{inj} = 50° BTDC to TDC, EGR ratio, R_{egr}, from 0.0 to 75%, and swirl ratio R_s from 1.4 to 5.6 (the standard swirl ratio was R_s = 1.4). Other parameters were constant, such as engine speed N_e = 1200 rpm, boost pressure P_b = 151.3

Table 11.3 Fuel properties for test

Category	Unit	Properties	Category	Unit	Properties
Density 15°C	g/cm^3	0.8217	Elements	C	86.1
Kinematic	mm^2/s	3.355	mass %	H	13.8
viscosity 30°C				O	<0.1
Flash point	°C	64.0		N	<0.1
Cetane index		61.1	Components	Saturates	80.3
(JIS K2280)			Vol. %	Olefins	0.0
Cetane number		58.3		Aromatics	19.7
Distillation	IBM	165.0		Mono-	17.5
°C	5%	191.5		Di-	1.9
	10%	204.5		Tri-	0.3
	50%	282.5	Gross calorific	kJ/kg	45,980
	90%	332.5	value		
	EP	353.0	Lower calorific	kJ/kg	43,092
			value		
Sulfur	mass ppm	3	(calculated)		

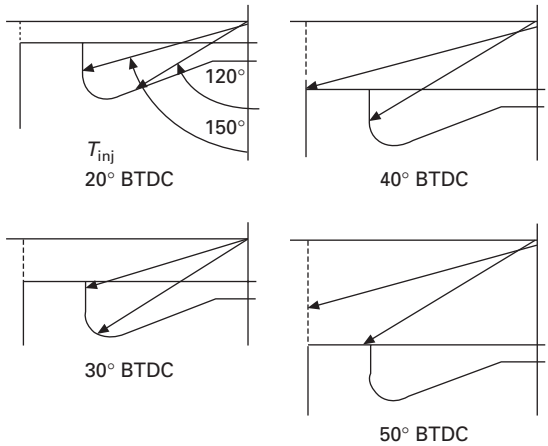

11.13 Fuel spray impingment between injection timing and piston position.

kPa, intake-air temperature T_a = 35°C, compression ratio ε = 16.5, fuel injection quantity q = 50 mm^3/st, and fuel injection pressure P_{inj} = 120 MPa. Both diesel and premixed compression ignition combustion were studied simultaneously varying the injection timing from 50° BTDC to TDC.

11.5.2 Pressure diagram and heat release process for different EGR ratios

Figure 11.14 shows combustion characteristics in changing EGR ratios from 0 to 75% at light loads and the injection timings of T_{inj} = 40° BTDC. This figure shows that there is low temperature heat release soon after fuel injection finishes and it is followed by the main combustion that takes place throughout the combustion chamber. In this case ignition delay becomes long because compressed air temperature is low due to early injection. This is typical premixed compression ignition combustion. Even though the combustion speed is slow, the rate of pressure increase is 2–4 times higher than that of diesel combustion under high boost-pressure. Future efforts should be undertaken to further decrease the rate of pressure increase. The pressure diagrams show almost identical profiles. The profiles of mean gas temperature in the cylinder showed little difference when the EGR ratio varied. The combustion of high EGR ratio was accompanied with high mean gas temperature.

In Fig. 11.15, in the case of T_{inj} = 30° BTDC, the ignition delay period becomes shorter than that of T_{inj} = 40° BTDC. Moreover, with a higher EGR ratio, the mean gas temperature in the cylinder, pressure diagram, the rate of

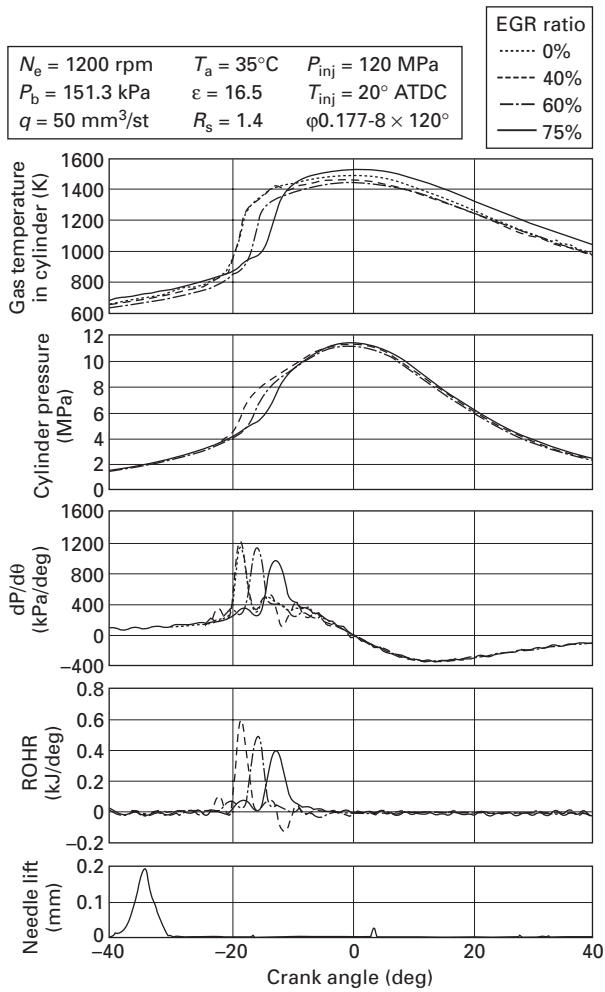

11.14 Combustion characteristics by changing EGR ratios at light load (T_{inj} = –40° ATDC).

pressure increase, and heat release show almost identical results to T_{inj} = 40° BTDC.

Figure 11.16 shows the result with T_{inj} = 20° BTDC and the ignition delay period is extremely short. Ignition began while the needle is lifting. It has less cool flame combustion. This pattern is that of conventional diesel combustion rather than premixed compression ignition combustion. Nevertheless, when the EGR ratio is 75%, the ignition delay period becomes longer, both cool flame and main heat release rate exist. The main heat release rate occurs after injection is finished. Therefore, it is possible to call

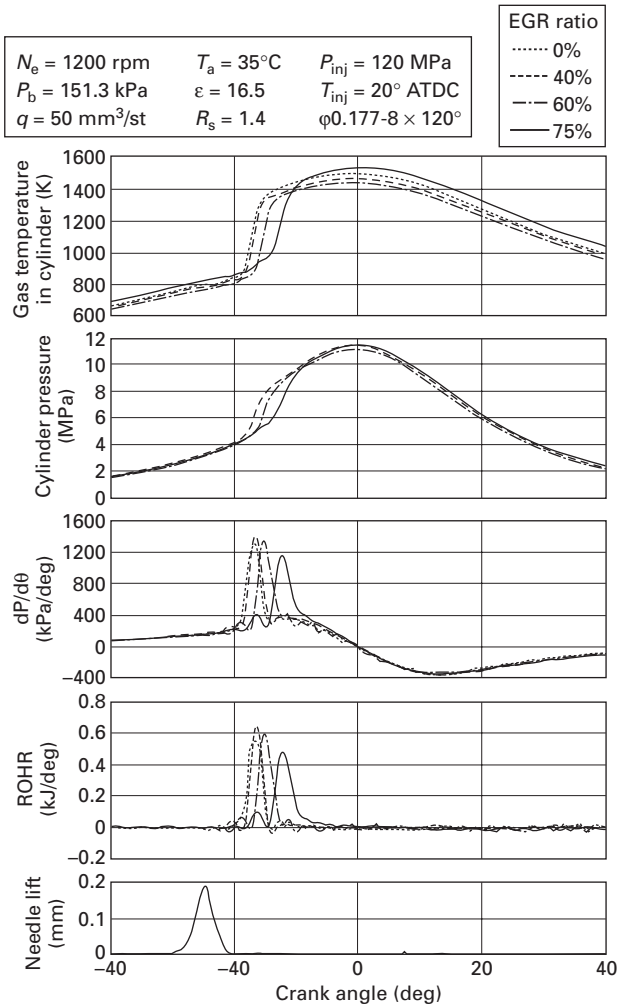

11.15 Combustion characteristics by changing EGR ratios at light load (T_{inj} = –30° ATDC).

this phenomenon premixed compression ignition combustion in 75% EGR ratio.

11.5.3 Thermal efficiency and brake mean effective pressure (BMEP) by varying injection timing

Figure 11.17 shows brake thermal efficiency η e, brake specific fuel consumption (BSFC), brake mean effective pressure (BMEP), and the excess air ratio λ by varying injection timing and EGR ratio at a light load. λ is

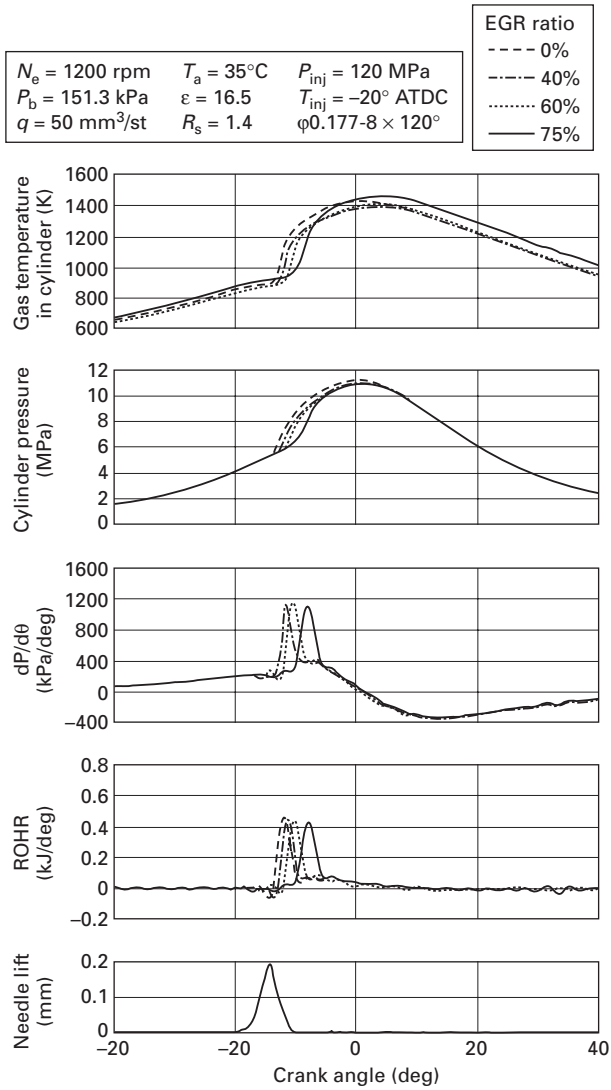

11.16 Combustion characteristics by changing EGR ratios at light load (T_{inj} = – 20° ATDC).

constant with the same EGR ratio. Replacement of fresh air with increased burned gas naturally decreases the value of λ when the EGR ratio increases. It is possible to regard this situation as premixed compression ignition combustion, as described in heat release rate, when the injection timing is retarded to 25° BTDC or more.

BSFC worsens and unburned properties increase with advanced injection timing. The discontinuity area in BMEP and BSFC appears with T_{inj} = 45°

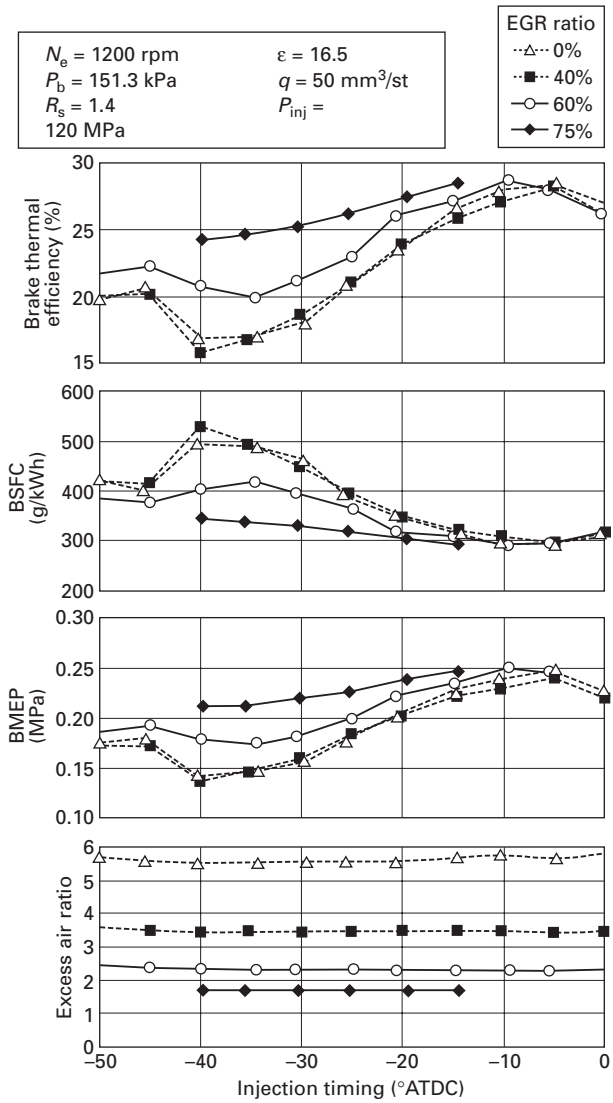

11.17 Engine performance by changing injection timing and EGR ratio at light load.

BTDC. It appears to be overflow fuel spray from the piston cavity. With injection timing advanced to 20° BTDC or more, it can be described as diesel combustion. From the point of view of BMEP and BSFC, It can be said that diesel combustion presents advantages even in light load. The premixed compression ignition combustion with high EGR ratio at light load condition improves BMEP and BSFC.

11.5.4 Exhaust emissions by varying injection timing

Figures 11.18a and 11.18b respectively show exhaust emissions such as BSSoot, BSNOx, BSHC, and BSCO in mass per kWh and ppm concentration by varying the injection timing and EGR ratio. First, Fig. 11.18a shows the peak value of BSNOx with injection timing of 25° BTDC when the EGR ratio is 0%; then BSNOx decreases with retarded injection timing. Finally, their values indicate the pattern of diesel combustion. BSNOx decreases with injection timing advanced; their values indicate the pattern of premixed compression ignition combustion.

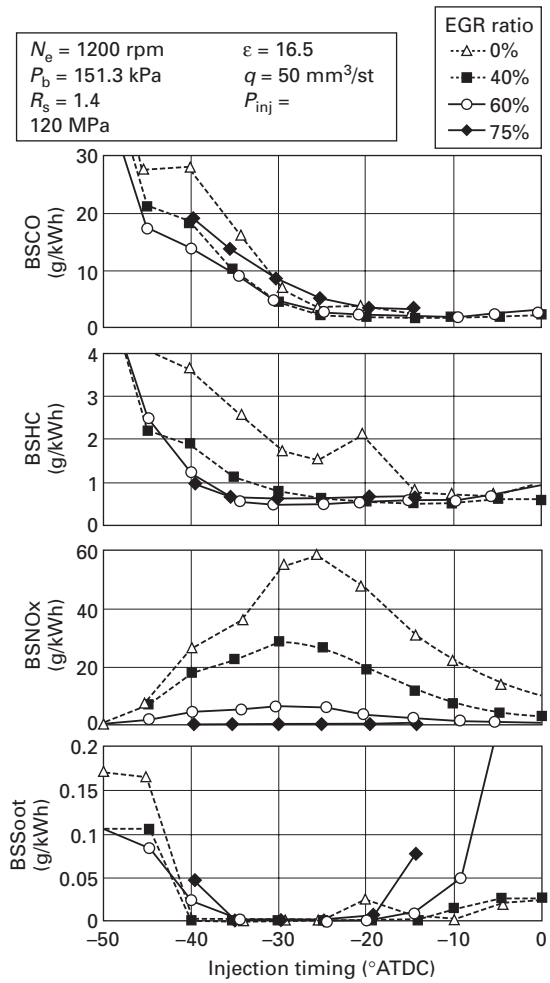

11.18 (a) Exhaust emissions (g/kWh) by changing injection timing and EGR ratio at light load; (b) Exhaust emissions (ppm and FSN) by changing injection timing and EGR ratio at light load.

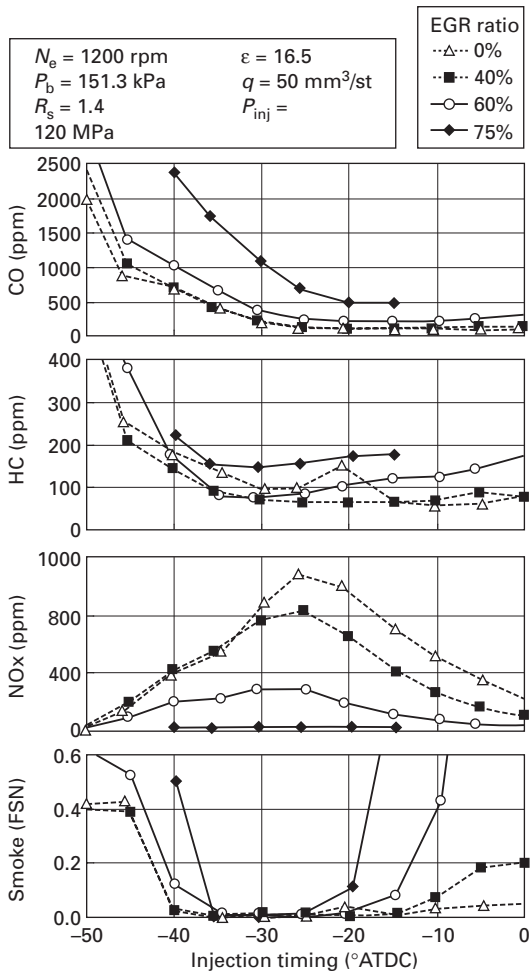

11.18 (b) *Continued*

The fuel spray was unable to fit into the piston cavity sufficiently and BSSoot, BSHC and BSCO were extremely high when injection timing was advanced to 45° BTDC or more. Moreover, because BSSoot with EGR ratio of 75% were very high, the exhaust passage became dirty; therefore, we did not attempt measurement at 45° BTDC. The value of BSSoot tended to worsen when injection timing was retarded to 20° BTDC or more. In the case of EGR ratio of 75%, when injection timing was advanced to 10° BTDC or more, we also did not attempt any measurement.

Judging from the tendency of exhaust emissions in Fig. 11.18a, the premixed compression ignition combustion with a high EGR ratio of 75% and injection timing of 20~30° BTDC minimizes BSNOx and BSSoot and achieves better

fuel consumption. The expression in ppm concentrations in Fig. 11.8b indicates that the highest CO concentration was obtained with the EGR ratio of 75% at 40° BTDC. In addition, the weight expression in Fig. 11.18a indicates the highest BSCO with an EGR ratio of 40% at 40° BTDC. In the weight expression a high EGR ratio has a big advantage.

Results for HC concentration indicate a very similar trend. It goes without saying that the quantity of the exhaust gas decreases with EGR even though the exhaust emission concentration is high. Consequently, the quantity of the exhaust gas decreases, namely special attention should be given to the extremely different trends of expressions for concentration and weight. For selection of diesel combustion, the condition of T_{inj} = 15° BTDC with an EGR ratio of 60% is best. As described above, at light load conditions, premixed compression ignition combustion has the potential to reduce BSSoot and BSNOx simultaneously, in contrast to diesel combustion.

11.6 Summary

The need for clean exhaust emissions in diesel engines will be greater in the future. Diesel combustion with high boost is a basic concept to meet that requirement in medium and high load and HCCI is the one for light load. This chapter has mainly described the use of premixed compression ignition combustion for light load operations.

1. Research of a low-emission and clean diesel engine is a difficult challenge. Based on the premise of using after-treatment devices, engine emissions should be improved. Based on the premise of using sulfur-free diesel fuel, it can be considered that the combination of diesel combustion at high load ranges and premixed compression ignition combustion to reduce exhaust emissions at light load ranges is effective to improve combustion.
2. Based on the premise of using low cetane diesel fuel, it can be considered that the combination of PREDIC and two-stage combustion MULDIC from light to high load is effective to improve combustion.
3. Use of a high EGR ratio at a light load range could decrease both NOx concentration and exhaust gas weight. By both of these, the weight of exhaust NOx is reduced greatly. The combination of a high EGR ratio and proper injection timing in premixed compression ignition combustion is capable of reducing exhaust emissions and achieving good BSFC. Premixed compression ignition combustion strategy is a forward-looking technology that offers compatibility between achieving low emissions and increasing thermal efficiency. Further efforts will be needed by the adoption of this combination. Future engine research with sulfur-free diesel fuel for clean exhaust emissions should be promoted vigorously.

11.7 Acknowledgements

The authors wish to acknowledge the New ACE's investors and the project to promote development of Next Generation Low Emission Vehicles of Ministry of Land, Infrastructure and Transport, who financially supported this study.

11.8 References

1. H. Sugihara, H. Nakagawa, K. Shouyama and A. Yamamoto, Hino New K13C Diesel Engine Equipped With Common-rail Type Fuel Injection Equipment (in Japanese), *Engine Technology*, Vol. 01 No. 04, pp. 40–45 (1999).
2. S. Itoh and K. Nakamura, Reduction of Diesel Exhaust Gas Emission with Common Rail System (in Japanese with English summary), *Journal of JSAE*, Vol. 55, No. 9, pp. 46–52 (2001).
3. M. Christensen *et al*., Supercharged Homogeneous Charge Compression Ignition, SAE paper No. 980787, (1998).
4. H. Persson *et al*., The Effect of Intake Temperature on HCCI Operation Using Negative Value Overlap, SAE paper, 2004-01-0944 (2004).
5. H. Yanagihara, *et al*., A Simultaneous Reduction of NOx and Soot in Diesel Engines under a New Combustion System (Uniform Bulky Combustion System – UNIBUS), 17th International Vienna Motor Symposium (1996).
6. Y. Takeda, K. Nakagome and K. Niimura, Emission Characteristics of Premixed Lean Combustion with Extremely Early Staged Fuel Injection, SAE paper 961163.
7. T. Hashizume, T. Miyamoto, H. Akagawa and K. Tsujimura, Combustion and Emission Characteristics of Multiple Stage Diesel Combustion, SAE paper No. 980505 (1998).
8. H. Yokota, Y. Kudo, H. Nakajima and T. Kakegawa, New Concept for Low Emission Diesel Combustion, *Journal of JASE*, Vol. 51, No. 9, p. 47–52 (1997).
9. A. Helmantel *et al*., HCCI Operation of a Passenger Car Common Rail DI Diesel Engine With Early Injection of Conventional Diesel Fuel, SAE Paper, 2004-01-0935 (2004).
10. G. Shibata, K. Oyama, T. Urushihara and T. Nakano, The Effect of Fuel Properties on Low and High Temperature Heat Release and Resulting Performance of HCCI Engine, SAE paper, 2004-01-0553 (2004).
11. N. Shimazaki, H. Akagawa and K. Tsujimura, Attempt of Premixed Lean Diesel Combustion with High Pressure Fuel Injection nearly TDC, No. 75 JSME Congress, Proceedings No. 3 (in Japanese with English summary), p. 448–449, (1998).
12. B. Walter *et al*., Improvement of Exhaust and Noise Emissions of the NADI Concept using Pre-Mixed Type Combustion with Multiple Stages Injection, Congres Le diesel, p. 1–18, (2004).
13. A. Harada, Y. Asaumi and Y. Aoyagi, A Study of Ignition Timing Control on Premixed Lean DI Compression Ignition Engine, *Transactions of JSME* (in Japanese with English summary), Series B, Vol. 68, No. 670, p. 227–232 (2002).
14. H. Ogawa, K. Azuma and N. Miyamoto, Combustion Control in a PCCI engine with Suppression of Low Temperature Oxidation by Methanol, JSME Autumn Congress, JSAE Paper (in Japanese with English summary), 20045727 (2004).
15. A. Harada, T. Miyamoto, Y. Asaumi and Y. Aoyagi, Premixed Lean Diesel Combustion Characteristics on Supercharged Diesel Engine, *Transactions of JSME* (in Japanese with English summary), Series B, Vol. 66, No. 649, p. 237–263 (2000).

16. A. Harada, Y. Asaumi and Y. Aoyagi, Study of Operation Region and Combustion Characteristics of Premixed Compression Ignition Engine, *Transactions of JSME* (in Japanese with English summary), Series B, Vol. 67, No. 653, p. 257–263 (2001).
17. A. Harada, Y. Asaumi and Y. Aoyagi, Combustion and Emission Characteristics of Supercharged Premixed DI Diesel Engine, *Transactions of JSME* (in Japanese with English summary), Series B, Vol. 67, No. 657, p. 180–186 (2001).
18. A. Harada, Y. Asaumi and Y. Aoyagi, A Study of Ignition Characteristics on Premixed Lean DI Diesel Engine, *Transactions of JSME* (in Japanese with English summary), Series B, Vol. 67, No. 660, p. 227–232 (2002).
19. T. Suzuki, A. Sato and K. Suenaga, Development of a Higher Boost Turbocharged Diesel Engine for Better Fuel Economy in Heavy Vehicles, SAE Paper 830379 (1983).
20. A. Sato, K. Suenaga, M. Noda and Y. Maeda, Advanced Boost-up in Hino EP100-II Turbocharged and Chargecooled Diesel Engine, SAE Paper 870298 (1987).
21. M. Tsujita, S. Niino, T. Ishizuka, A. Kakinai and A. Sato, Advanced Fuel Economy in Hino New P11C Turbocharged and Charge-Cooled Heavy Duty Diesel Engine, SAE Paper 930272 (1993).
22. T. R. Stover, D. Reichenbach and E. Lifferth, The Cummins Signature 600 Heavy Duty Diesel Engine, SAE Paper 981035 (1998).
23. H. Sugihara, K. Miyoshi, T. Takakura, Technologies to Reduce Exhaust Gas Emissions of Heavy Duty Diesel Engines, JSME Autumn Congress, JSAE Paper (in Japanese with English summary), 20045619 (2004).
24. W. Knecht, European Emission Legislation of Heavy Duty Diesel Engines and Strategies for Compliance, Proceedings of the Thermofluidynamic Processes in Diesel Engines (THIESEL 2000), pp. 289–302 (2000).
25. K. Hirata, N. Masaki, H. Ueno and H. Akagawa, The development of Urea-SCR System for a heavy duty commercial vehicle (First Report), JSME Autumn Congress, JSAE Paper (in Japanese with English summary), 20045683 (2004).
26. N. Masaki, K. Hirata, M. Kikuchi, M. Iijima and H. Akagawa, The development of Urea-SCR System for a heavy duty commercial vehicle (Second Report), JSME Autumn Congress, JSAE Paper (in Japanese with English summary), 20045687 (2004).
27. T. Tanaka, After-Treatment Systems and Fuel Properties for Controlling Engine Emissions, Proceedings of the International Workshop on Next Generation Power Systems for Automobiles (IWPS2000), p. 58–67, (2000).
28. M. Woods, R. Kamo and W. Bryzik, High Pressure Fuel Injection for High Power Density Diesel Engines, SAE Paper 2000-01-1186 (2000).
29. Y. Aoyagi, Super Clean Diesel Engine, Proceedings of IWEFV2004, pp. 199–208 (2004).
30. Y. Aoyagi, E. Kunishima, Y. Asaumi and Y. Aihara, Diesel Combustion and Emission using High Boost and High Injection Pressure in a Single Cylinder Engine, *JSAE International Journal* Series B, Vol. 48, No. 4, pp. 648–655 (2005).
31. Y. Aoyagi, H. Osada, M. Misawa, T. Hirosawa, M. Odaka and Y. Goto, Diesel Emission Reduction using High Boost and High EGR Rate in a Single Cylinder Engine, *JSAE Review of Automotive Engineering*, Vol. 26, No. 4, (2005).
32. M. Misawa, Y. Aoyagi, M. Kobayashi, M. Odaka and Y. Goto, High EGR Diesel Combustion and Emission Reduction Study by Single Cylinder Engine (First Report) (in Japanese with English summary), JSAE Paper No. 20045308 (2004).

33. M. Misawa, Y. Aoyagi, Y. Hyodo, M. Kobayashi, M. Odaka and Y. Goto, High EGR Diesel Combustion and Emission Reduction Study by Single Cylinder Engine (Second Report) – Install to Multi-cylinder Engine, (in Japanese with English summary), JSAE Paper 20045610, (2004).
34. Yuzo Aoyagi, Development of Super Clean Diesel Engine, (in Japanese), Tokyo Motor Show Symposium 2004, Proceedings pp. 93–102 (2004).
35. Y. Aoyagi, H. Osada, M. Misawa, T. Hirosawa, M. Odaka and Y. Goto, Advanced Diesel Combustion using Wide Range, High Boosted and Cooled EGR System by Single Cylinder Engine, SAE Paper 2006-01-0077, (2006).
36. P. Kemnitz, O. Maier and R. Klein, Monotherm, a New Forged Steel Piston Design for Highly Loaded Diesel Engines, SAE Paper 2000-01-0924 (2000).
37. Y. Aoyagi and Y. Hyodo, Challenging Technology for Premixed Compression Ignition Combustion (HCCI) In Heavy Duty Diesel Engine, *Engine Technology*, Vol. 7, No. 2, p. 33–38 (2005).

11.9 Nomenclature

BMEP	: Brake mean effective pressure	kPa, MPa
IMEP	: Indicated mean effective pressure	kPa, MPa
N_e	: Engine speed	rpm
P_b	: Boost pressure	kPa
P_{inj}	: Injection pressure	MPa
T_{inj}	: Injection timing	°CA
T_a	: Intake air temperature	°C
q	: Injection fuel quantity	mm^3/st
R_{egr}	: EGR ratio	%
R_s	: Swirl ratio	
ROHR	: Rate of heat release	kJ/°CA
BSNOx	: Brake specific NOx	g/kWh
BSCO	: Brake specific CO	g/kWh
BSHC	: Brake specific HC	g/kWh
SMOKE	: Smoke	FSN
ε	: Compression ratio	
λ	: Air excess ratio	
η v-a	: Volumetric efficiency of new intake air %	
η e	: Brake thermal efficiency	%
η i	: Indicated thermal efficiency	%
η e-6	: 6 cylinder brake thermal efficiency	%
$dp/d\theta$	: Rate of pressure change	MPa/deg

12

Narrow angle direct injection (NADI^{TM}) concept for HCCI diesel combustion

B GATELLIER, IFP, France

12.1 Introduction

The agreement between the ACEA and the European Parliament to reduce the fleet consumption of new passenger cars to 140 g of CO_2 per kilometre in 2008 and the more and more stringent regulation of emissions represent a great challenge. The diesel engine is one of the best candidates facing CO_2 reduction and its market share will probably increase further over the next few years. However, fuel efficient combustion produces high NOx emissions. Despite the impressive progress made in the last decade, the diesel engine is still facing the well known NOx and particulate trade-off. It is obvious that such limits will require new advanced technologies and/or new combustion processes.

As an answer to this challenge, a combined NOx/particulate after-treatment solution could be found but with some drawbacks in terms of complexity, robustness, fuel dependency, infrastructure and then cost.

An alternative would be to apply new combustion processes efficient enough to solve the NOx/CO_2 dilemma. Different approaches have been the subject of R&D work for a number of years in order to achieve low temperature combustion avoiding the formation of NOx and in some cases the formation of particulate [1–8]. However, applying such new combustion process to engines involves some difficulties:

- Mixture preparation: the main problems are to avoid wall impingement and to promote fuel vaporisation and air mixing, so as to limit particulate and HC emissions, and to prevent oil dilution.
- Operating range: at high load, operation at high fuel/air equivalence ratio is limited by combustion stability, excessive heat release rate, knock and noise.
- Control of combustion: it is the key point in highly premixed combustion, especially to extend the operating range and power output.

Since 2000, IFP has been working to solve these problems and has developed

the NADI™ (Narrow Angle Direct Injection) concept which is a dual mode engine, using Highly Premixed Combustion (HPC) at low and medium loads and conventional diesel combustion at high and full loads [9–17].

First, the approach of IFP, based on modelling and single cylinder engine testing, to define the NADI™ concept is described. Then, the first results obtained are summarised and the main limitations and ways of progress are discussed.

Secondly, the development of the concept to overcome the noticed barriers is addressed. Some of the work performed using the methodology of improvement used at IFP and the results achieved regarding the engine injection strategies, injection system and compression ratio aspects are presented in more detail.

Finally, preliminary results obtained at full load and at part load on a multi-cylinder engine, in steady state operation, are presented. The causes of poorer performances compared to single cylinder engine results are commented. Solutions are proposed and works currently in progress are listed in the last part of this chapter.

12.2 The NADI™ concept overview

12.2.1 IFP approach

To overcome the limitations in power output, IFP has developed a 'dual mode' engine, using HPC combustion at low and medium loads and conventional diesel combustion at high loads, which is called NADI™ (Narrow Angle Direct Injection). That means that the combustion system should be able to switch between the two combustion modes.

At an early development stage, it was decided to keep the general architecture of a conventional diesel combustion system:

- direct injection
- flat cylinder head
- combustion piston bowl.

A common rail fuel injection system has been selected due to its continuously increasing flexibility, especially in terms of injection events. A narrow spray cone angle was selected (around 70°) to limit fuel wall impingement and to promote fuel/air mixture, while having a great flexibility in terms of injection timing (very early or late injection). Concerning the compression ratio, a lot of work pointed out the advantage to have a moderate compression ratio in order to better control the start of combustion, especially to extend the engine HPC operating range. In the present study, the engine geometric compression ratio has been set lower or equal to 16:1.

Figure 12.1 gives an overview of the NADI™ combustion system concept whose main features can be listed as:

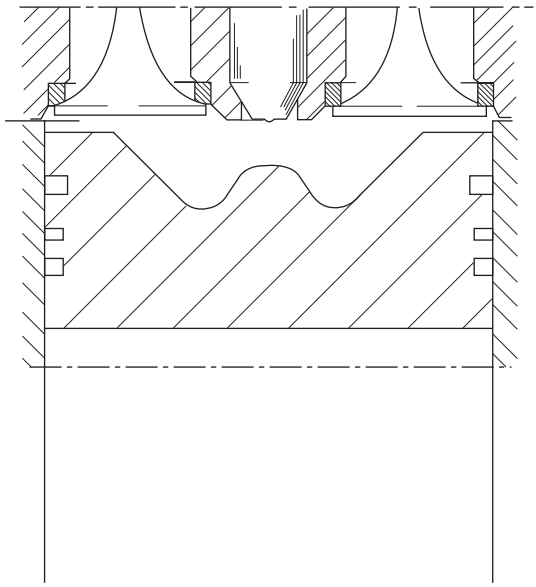

12.1 Overview of the NADI™ combustion system.

- conventional flat cylinder head
- narrow spray cone angle (around 70°)
- reduced geometric compression ratio (≤16:1)
- multi-stage injection (common rail FIS).

12.2.2 Combustion system definition

The first objective was to find a combustion chamber design well adapted to the specific narrow spray cone angle in order to reach a good conventional diesel combustion behaviour, especially at full load. The first challenge was to make a proper transport and mixing with air of the fuel injected inside the piston bowl. The idea was to use a fuel wall guided effect thanks to the kinetic energy of the injected fuel. Several combustion chamber shapes associated with nozzle geometry and swirl motion variations have been computed. The computed output power against burned mass fraction (BMF) just before the exhaust valve opening is shown in Fig. 12.2. This figure shows an iteration process which allows a shift from about 73% BMF and 72% power to about 98% BMF and 120% power. This improvement is the result of a work on different parameters of the bowl. The bowl dome was modified so as to have more space under the spray in order to promote fuel/air mixing and then to reduce the auto-ignition delay. Moreover, a main

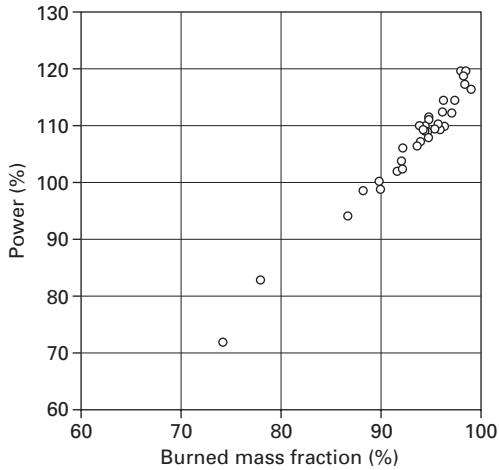

12.2 CFD results at 4000 rpm, full load.

characteristic of this design is to promote fuel vapour progression along the bowl shape. The fuel has to go out of the bowl so as to reach the air in the squish area. So, a work on the total length of the bowl and its out-section allows an increase of the 'extraction' speed of the vapour from the bowl, and finally improves the power and efficiency of this concept. After a few iterations, some combustion chambers, associated with nozzle and swirl definition, adapted to narrow spray cone angle, have been found.

Plates 11 and 12 (between pages 268 and 269) shows the combustion process at 4000 rpm, full load, with a conventional combustion chamber geometry (cone angle higher than 145°) and with the NADI^{TM} concept. The fuel air mixture is represented in a colour that depends on the lambda value: the fuels droplets in black, the fuel vapour in red, the air in blue. With conventional combustion system, the fuel is injected towards the bowl periphery. Due to fuel/wall interaction, the majority of the fuel is sent to the center of the bowl, mixes with air and burns. Some fuel mixes with air and burns in the squish area. With the NADI^{TM} concept, the fuel is injected at the center of the combustion piston bowl. Due to fuel/wall interaction, fuel is transported to the piston bowl periphery, mixes with air and burns.

12.3 First results and limitations

The first target was to validate the concept on a single cylinder engine. The main characteristics are a bore × stroke of 78.3 × 86.4 mm, leading to a displacement of 416 cm^3, and a compression ratio of 16:1 or 14:1 (tested only in HPC combustion mode).

The intake ducts have been modified in order to adapt the swirl motion to a low value (about 1.3). A production Bosch first generation common rail

fuel injection system (FIS) was used. The engine was externally boosted and the exhaust pressure was controlled by a throttle valve in accordance with intake pressure and EGR values. This part quickly summarises these first results obtained in 2001 [9] and points out the main limitations.

12.3.1 Initial results at part load using HPC combustion mode

The engine was evaluated at 1500 and 2500 rpm, using early injection timings (at least 20 crank angle before top dead centre). Two compression ratios were tested (16:1 and 14:1). The results obtained in HPC mode with the NADI^{TM} concept geometry were compared to results with a standard geometry using a conventional combustion mode with a compression ratio of 18:1, and parameter settings consistent with Euro III emissions standard. These initial results have shown a great potential to strongly reduce NOx and particulate emissions while maintaining fuel efficiency. Nevertheless some points have to be addressed such as CO and HC emissions at low engine loads and combustion noise at high engine loads. Figures 12.3 to 12.5 present the results obtained at 1500 rpm, same trends have been observed at 2500 rpm.

Fuel consumption

For low load points, the ISFC was close to the reference one with both compression ratios. For higher load points we observed a fuel consumption

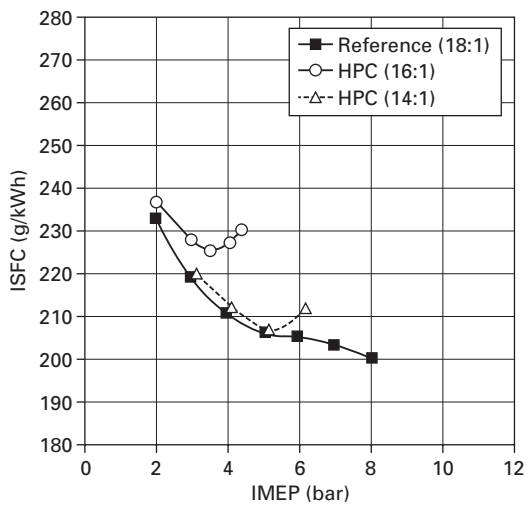

12.3 Specific indicated fuel consumption against engine load at 1500 rpm.

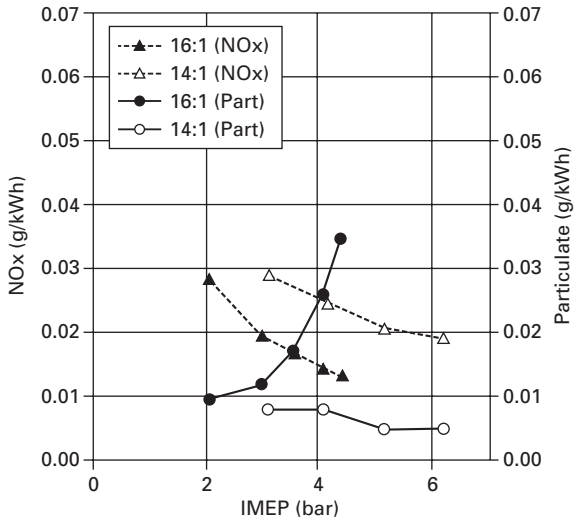

12.4 NOx and particulate emissions against engine load at 1500 rpm.

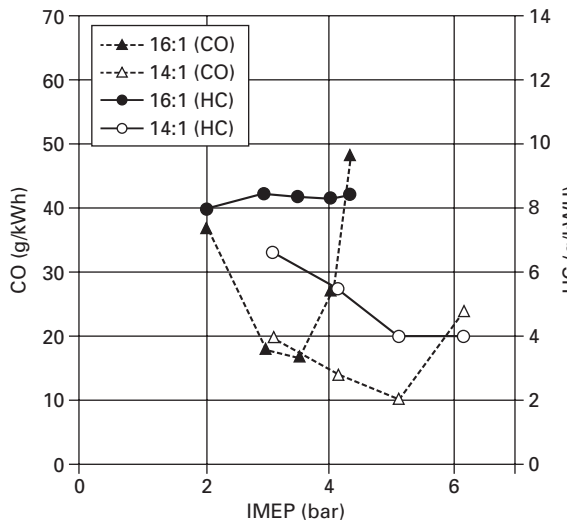

12.5 CO and HC emissions against engine load at 1500 rpm.

penalty mainly due to high unburned emissions (HC and CO). This phenomenon was more sensitive for high CR values (16:1).

NOx and particulate emissions

Concerning NOx and particulate emissions, the levels were near zero (always below 0.05 g/kWh). NOx emissions were more than 100 times lower than

with conventional diesel engines and particulate emissions were more than 10 times lower.

HC and CO emissions and exhaust gas temperature

Here are the main drawbacks of such type of combustion. Nevertheless, the HC and CO emissions were at the same levels as direct gasoline engines. However, due to the combustion process used, exhaust temperatures were quite low compared with gasoline engines, especially at low load, and could be problematic regarding exhaust gas after-treatment.

Combustion noise

Due to early injections, noise levels increase significantly with engine speed and load. If the final level at 1500 rpm (about 86 dB) could be acceptable, engine speed and load increase leads to high levels of noise which remained over 90 dB for almost all loads at 2500 rpm, leading to too high pressure gradient values.

Load range

For this first NADI engine, we tried to limit the particulates to near zero and the operating range was consequently limited to 0.4 MPa and 0.6 MPa at 1500 rpm and to 0.6 MPa and 0.9 MPa at 2500 rpm (respectively with CR 16:1 and 14:1 for the two engine speeds). This operating range seems too short to run all the MVEG cycle in HPC mode especially regarding downsizing applications. In addition, some slightly more optimistic considerations were made to fix single cylinder intake pressure levels, especially for the higher loads in the HPC area.

12.3.2 Initial results at full load using conventional combustion

With a CR of 16:1, the maximum power reached was 54 kW/l with a high intake pressure of 280 kPa, due to a limitation in the maximum fuel/air equivalence ratio (0.62).

At 2000 rpm, full load, the maximum specific torque was lower than the future diesel engine requirement. This first version of the concept reached 145 Nm/l at a smoke level of 3 FSN and with some problems to limit combustion noise (about 90 dBa, estimated with an AVL noise meter). Here again, the air in the cylinder was not well used, and the maximum fuel/air equivalence ratio was just about 0.73.

12.4 Development of the concept

12.4.1 Ways of improvement

In order to improve NADI performances at full load and part load, important works were performed in single cylinder engines assisted with CFD and optical diagnosis tools. These works allowed some major improvements:

- in HC and CO emissions, particularly at low loads
- in combustion noise emissions
- in the intake pressure, with a reduction at the higher loads
- in HPC load range
- in torque and power.

Below is presented some of the work performed using the methodology of improvement used at IFP and the results achieved regarding the engine injection strategies, injection system and compression ratio aspects.

Injection strategies

In order to evaluate and understand the fuel spray behaviour and fuel/air mixing formation for different injection strategies, several scientific tools were used to investigate these phenomena.

The CFD tool was used with an accurate HPC combustion model. Three different experimental devices completed this toolbox, using optical visualisation to analyse combustion and fuel/air mixture formation:

- The first one consisted of a single-cylinder engine equipped with a special cylinder head that allows combustion chamber optical endoscopies access to directly visualise the physiochemical phenomena in the combustion chamber.
- The second one consisted of an optical engine equipped with a special optically accessible transparent piston bowl chamber with a small transparent crown liner using the conventional optical diagnosis (CCD camera and laser beam) with fluorescence techniques.
- The third one consisted of a high pressure electrical heated cell equipped with a common rail injector and a 1/6 piston bowl sector in order to evaluate the fuel spray and piston bowl shape interaction (fuel spray guiding effect).

These tools allowed identification and understanding of some fuel/air mixture formation phenomena and particularly underlining of the piston bowl shape and fuel spray interaction within these fuel/air mixture mechanisms. Depending on the injection timing, the piston bowl – fuel spray interaction can play an important role in the fuel/air mixture formation.

All these results lead to injection strategies using the fuel/wall interaction ability of the concept. The latest fuel injection strategies used with the NADI™ concept are based on different injection events per engine cycle according to engine load.

Strategies at part load

Early injections: This strategy gives the most homogeneous mixture and leads to the lowest NOx and smoke levels for a given intake mass composition and temperature. As, it will be seen, this injection strategy is well adapted to low engine load. At low load, as injected quantity is limited, noise level is acceptable. For higher loads, this pre-mixed combustion becomes too fast and too early with a negative impact in noise level. Moreover, as the injected quantity grows, fuel liner wetting could appear, even with a reduced spray cone angle.

The CFD tools were used to optimise the injection timing in HPC mode at low load. Indeed, it was possible to reduce fuel wall wetting, which represents, as said before, one of the main HPC drawbacks. These 3D calculations showed that injections before 90° BTDC were not useful, because of too large a liquid penetration. Plate 4 (between pages 268 and 269) illustrates this point. Moreover optical engine tools confirmed the drawbacks of very early injections at such thermodynamic conditions due to the fuel spray penetration, on one hand, and a low fuel vaporisation, on the other hand. In such conditions the injected fuel spray will persist during some crank angle degrees with a poor fuel vaporisation. Due to the combustion chamber aerodynamics, namely the swirl motion, as fuel spray droplets persist they will be centrifuged to the combustion chamber walls (liner).

Early multiple injection strategies are an important way to improve unburned emissions at very low loads. As it can be seen in Fig. 12.6, a well fitted multiple injection strategy set and timing allowed significant reductions in HC and CO emissions at very low loads. The main issue is to be able to avoid fuel piston bowl and liner impingement and confine the fuel injected spray in the piston bowl chamber, therefore precise injection quantities and timing control are important.

Late injections: This kind of injection, usually with main injection after TDC, allows control of the start of combustion and, as combustion temperatures are lower, leads to lower NOx levels. Therefore, using this strategy, it is possible to decrease the EGR rate from 55% to 45% and so to increase air flow and have a better localisation in the compressor map.

Moreover, late injection allows lower combustion noise and smoke levels. The major drawback is a fuel consumption increase especially at high HPC loads. This is a reason why a double late injection called ‘TDC split injection’ has been developed.

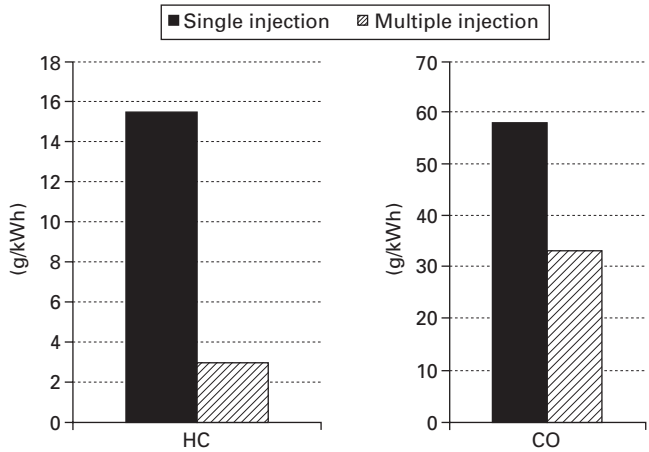

12.6 Multiple injection strategy effect on HC and CO emissions – 1500 rpm, BMEP = 0.1 MPa, NOx = 0.15 g/kWh.

Split injections: When engine load increases, there is a clear advantage to use a fuel injection strategy named 'TDC split injection'. This is a two-injection event strategy whose first injection is timed before TDC and the other one after TDC.

3D calculations showed the interest of split injections. As can be seen in Plate 13 (between pages 268 and 269) the first injection is wall guided by the piston bowl shape. If the fuel spray momentum is high enough, fuel air entrainment generates an additional air vortex in the fuel spray direction and therefore some fresh air is driven to the piston bowl dome, replacing the fuel/air mixture, allowing for the second injection to take place in a 'fresh' air area and hence leading to an improved bulk air utilisation.

In addition, the combustion process in two steps allows better control of maximum heat release leading to less combustion noise and NOx emissions at a given air dilution by EGR.

Compared to late injection, the trade off between pollutant emissions, noise and fuel consumption is improved. As an example, at 1500 rpm, IMEP = 0.8 MPa, for a given very low NOx emissions (0.02 g/kWh) and combustion noise (81 dBa), the use of 'TDC split injection' leads to less smoke (by 1.5 FSN), less CO (by 20 g/kWh), less HC (by 2 g/kWh) and less fuel consumption (by 15 g/kWh).

These new injection strategies, coupled with a decreased EGR rate, allowed enlargement of the HPC operating range of the engine: with CR 14:1, up to 1500 rpm, 0.8 MPa of BMEP was reached with no fuel penalty (except at the highest load) and with significant reduction of noise levels, especially at 2500 rpm.

Strategies at full load

At 2000 rpm full load, the main limitations for this first NADI engine were essentially due to a non-optimal use of the air inside the cylinder, with poor fuel/air equivalence ratios. CFD, used to better understand fuel air mixing, indicated that some air volume over the piston is not reached by the injected fuel and therefore is not used for combustion.

The idea was to use dedicated injection strategies so as to provide fuel in this area. At 2000 rpm, the performances have been improved using a post injection. At similar smoke levels (2 FSN), it is possible to increase the fuel/air equivalence ratio by 0.05 and hence an increase in IMEP by 5%.

Fuel injection system

'TDC split injection' strategy, because of its sensitivity to injection timing, requires very close behaviour for all the injectors. A comparison between two fuel injection systems (second and third generation from Bosch) fitted with the same combustion system highlights the impact of the injector's capability of multiple injections on the results at 1500 rpm. As it can be seen in Fig. 12.7, the main advantages of a piezoelectric injector system is a larger highly premixed combustion operating range which reaches 0.8 MPa of BMEP with CR 16:1 without any significant penalty in terms of fuel consumption, noise, NOx and particulate emissions. It has to be noticed that HC and CO emissions are drastically reduced due to lower fuel/air equivalence ratios allowed by injection strategies used with the third generation injection system.

At full load, there is a clear advantage in improving the linear momentum of the spray in order to reach the bowl periphery and the squish area earlier. At the same time, it is obvious that the reduction of injection duration for a given injected quantity allows higher combustion speed and then less smoke and exhaust temperatures. That is the reason why we have used a third generation Bosch FIS with higher injection pressure and needle lift speed. Table 12.1 summarises the differences between the two injection systems used, it can be seen that the nozzle flow has been reduced in order to improve the fuel/air mixing.

Figure 12.8 presents the results obtained with a single cylinder engine equipped with a NADI^{TM} combustion system (unit displacement of 550 cm^3, compression ratio of 16:1) at 4000 rpm, full load. These curves confirm that the improved injection system leads to better performance levels, and that the differences are more important for higher air mass flows. In addition, the third generation Bosch injection system improves output power by about 2% for the same injection pressure (160 MPa) and air flow.

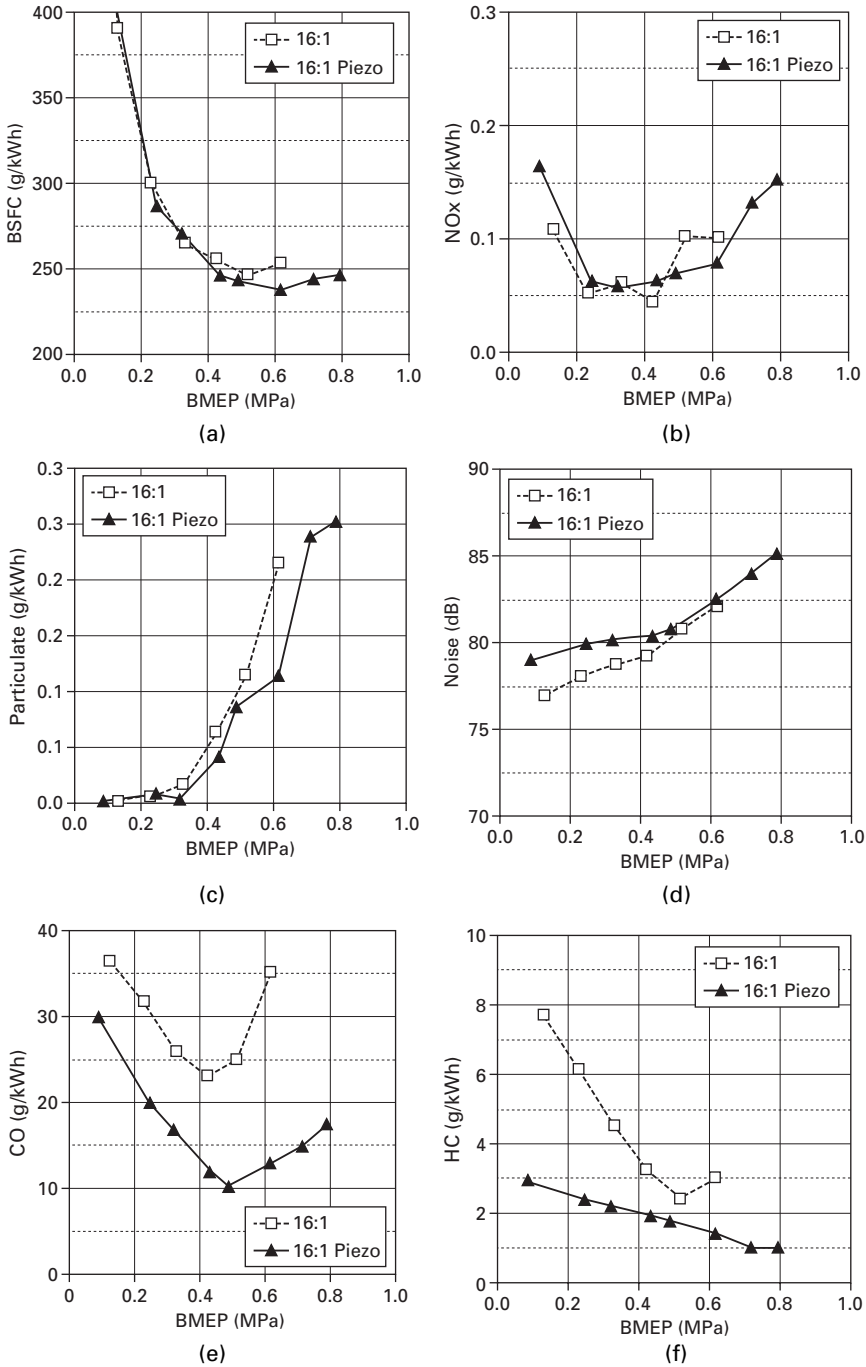

12.7 Injection system effects on engine results, 1500 rpm, compression ratio of 16:1.

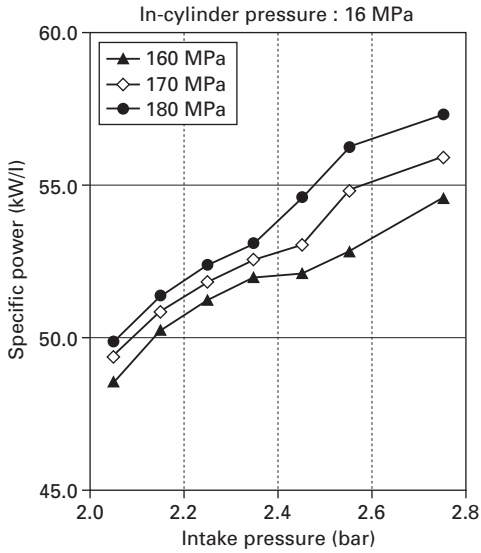

12.8 Injection pressure effect on output power at 4000 rpm, full load, CR 16:1, I in-cylinder maximal pressure 16 MPa.

Table 12.1 Difference between second and third generation Bosch system features

	Second generation Bosch FIS	Third generation Bosch FIS
Maximum injection pressure	1600 bar	1800 bar
Nozzle flow	450 ml/30 s @ 100 bar	425 ml/30 s @ 100 bar
Nozzle type	VCO	Mini-sac
Nozzle hole geometry	6 holes, 60°, K = 0	6 holes, 60°, K = 1.5
Needle speed	About 1 m/s	Up to 2 m/s

Compression ratio

Because of its effects on in-cylinder temperature and pressure during the compression phase, the engine compression ratio has an influence on the auto-ignition phase of the combustion: a reduction prolongs the air/fuel mixing process before combustion. Different works performed on experimental single cylinder engines showed this significant advantage. The results, presented in Fig. 12.9, highlight improvements obtained by the 14:1 value compared to 16:1 in terms of operating range, fuel consumption, NOx and particulate emissions and combustion noise, at 1500 rpm.

At full load, the compression ratio of 14:1 allows a significant increase in torque and power output with values reaching respectively 180Nm/l and 63 kW/l compared to 150 Nm/l and 50 kW/l obtained with the compression

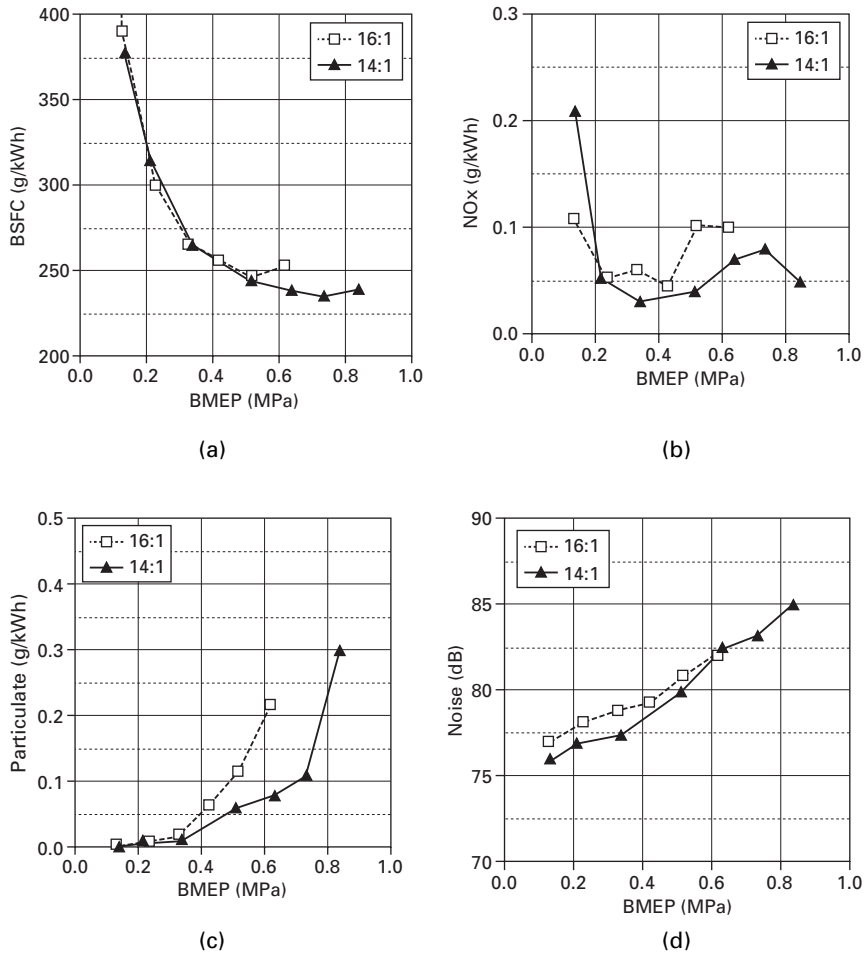

12.9 Compression ratio effect on engine results at part load, 1500 rpm.

ratio of 16:1. These results have been obtained with the same limiting factors such as smoke, maximum cylinder pressure (16 MPa) and exhaust temperature.

One of the main drawbacks of the compression ratio reduction is cold start and engine running stability. However, new technologies will be available in the near future as new glow plugs (made of ceramic, spark glow plug, flame glow plug), or electric air heater. Higher engine crank speed thanks to high speed starter or integrated starters generators (ISG) could be also methods of great improvement.

12.4.2 Results of the improved concept

Results at full load using conventional combustion

The results achieved at 4000 rpm full load with CR of 14:1 and 16:1 are presented in Fig. 12.10 and compared to the initial results. Levels of 63 kW/l and 56 kW/l have been achieved at nominal conditions (0.25 MPa of intake air pressure), respectively at CR of 14:1 and 16:1. At CR 14:1 there is a potential to increase specific power output up to 72 kW/l with an increased air pressure and revised in-cylinder maximal pressure. The boundary conditions are described in Table 12.2.

At 2000 rpm, 180 Nm/l have been reached with 85 dBA of combustion noise level at the nominal conditions (0.25 MPa of intake air pressure, 0.3 MPa of exhaust pressure, 50°C of intake air temperature, 3 FSN of smoke and 15 MPa of in-cylinder maximal pressure). Up to 205 Nm/l have been achieved for an increased air flow, with constant combustion noise emissions and fuel/air equivalence ratio (respectively 85 dBa and 0.87).

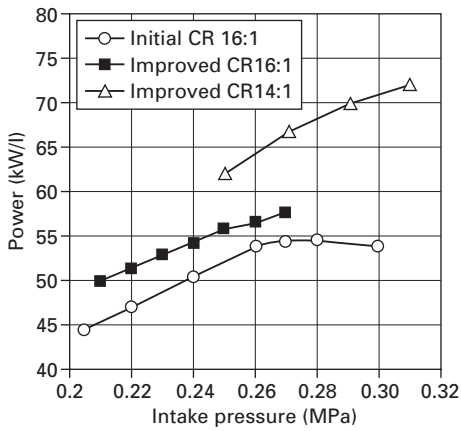

12.10 4000 rpm, full load.

Table 12.2 Synthesis of the engine nominal and revised boundary conditions

Boundary conditions	Nominal	Revised
Δ Exhaust-intake pressure (MPa)	0.06	0.06
Intake air temperature (°C)	50	50
In-cylinder maximal pressure (MPa)	16	18
Smoke (FSN)	3	3
Maximal exhaust temperature (°C)	750	750

Results at part load using HPC combustion mode

Within the HPC mode load range, some improvements have been made to reduce HC and CO emissions at very low loads (at 1500 rpm), to extend the HPC load range at 1500 rpm and to reduce combustion noise and required intake pressure at the higher loads. The results at 1500 rpm and 2500 rpm are presented in Figs. 12.11 and Fig. 12.12.

HC and CO emissions have been significantly reduced at very low loads and low engine speed thanks to early multiple injection strategy. Noise emissions are very low for the lower loads and increase for higher loads but still below 84 dBa at 1500 rpm and 87 dBa at 2500 rpm. Compared with the initial combustion noise levels, these values have been significantly reduced

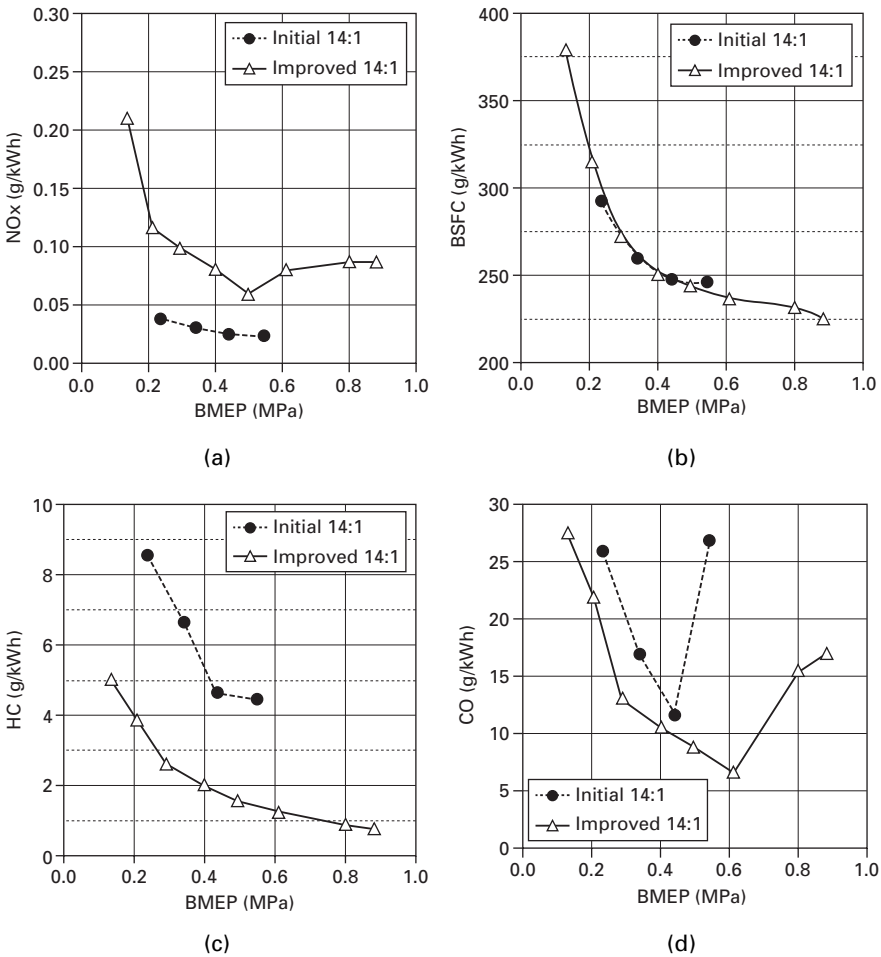

12.11 Results obtained at 1500 rpm, part load using HPC combustion.

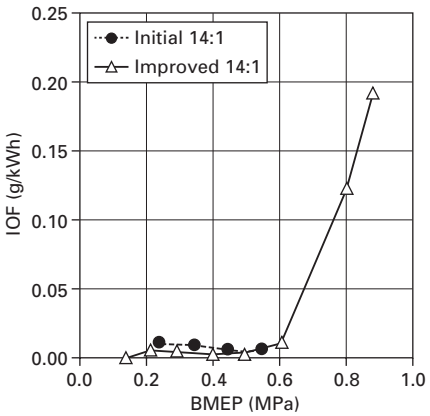

(e)

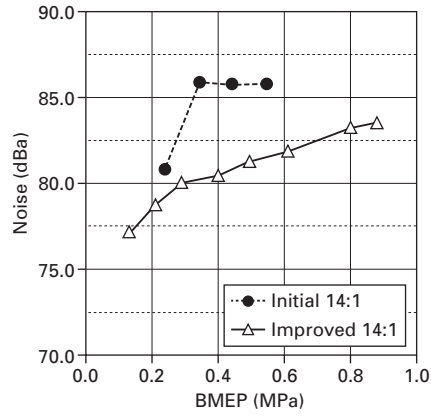

(f)

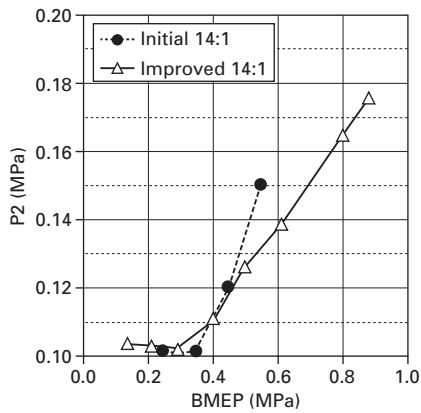

(g)

12.11 Contined

particularly at 2500 rpm. Thanks to the split injection strategy and better combustion control, the intake pressure has been also reduced for the higher loads, particularly at 2500 rpm. Nevertheless, due to this intake pressure reduction and therefore EGR rate reduction, particulate emissions were consequently slightly increased, but NOx emissions still remain less than 0.1 g/kWh. Some major improvements have been made to reduce fuel consumption (BSFC) and extend the HPC load range. Good results have been reached, particularly at 1500 rpm, with upper load range extended from 0.5 MPa to 0.9 MPa of BMEP without fuel consumption penalty, compared to a conventional engine. At 2500 rpm, there is still a fuel consumption penalty at the higher loads. Particulate emissions are always zero up to 0.6 MPa of BMEP; they increase for the higher loads but remain under 0.2 g/kWh.

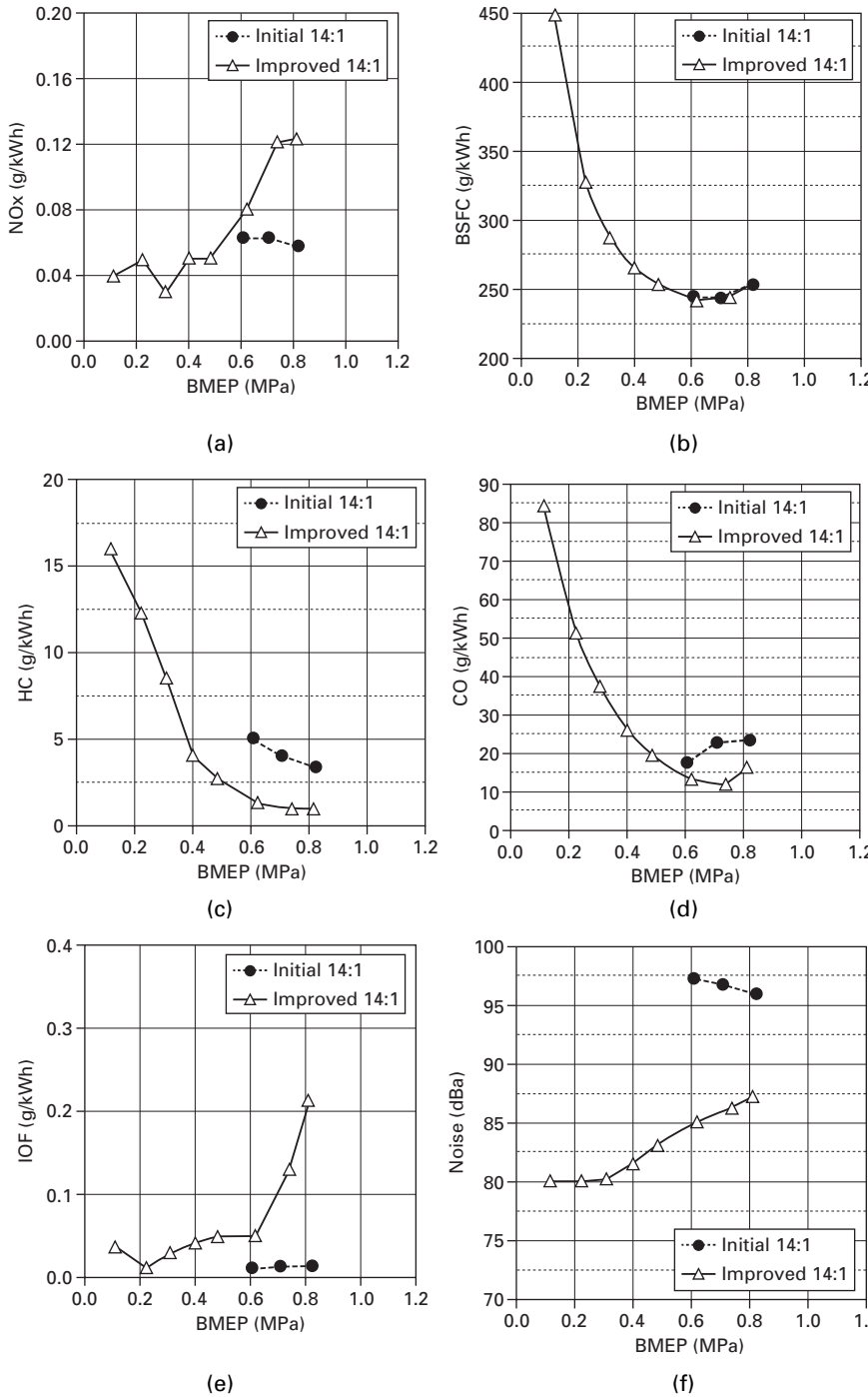

12.12 Results obtained at 2500 rpm, part load using HPC combustion.

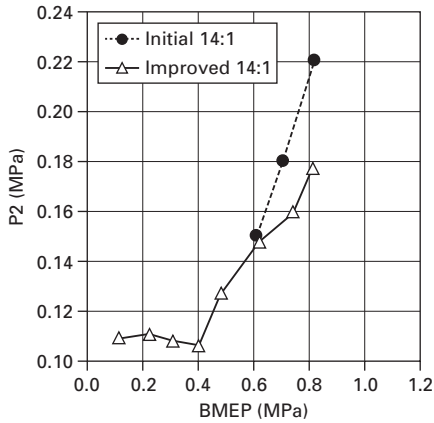

(g)

12.12 Continued

12.5 Evaluation of the concept in a multi-cylinder engine

This part of the chapter presents the preliminary results obtained at full load and at part load in a multi-cylinder engine, in steady state operations.

12.5.1 Engine configuration

This section aims to describe the engine hardware used in terms of combustion chamber parts, compression ratio, turbocharger and type of EGR circuit.

The multi-cylinder application is based on a production in line four-cylinder engine with a bore of 87 mm and a stroke of 92 mm leading to a displacement of 2.188 litres. The piston bowl was designed with the NADI^{TM} bowl drawing specifications with a compression ratio of 14:1. The intake ducts of the cylinder head were modified in order to adapt the swirl motion to the required swirl number of 1.3 at BDC. All the results shown in this paper, including full load conditions, were obtained with the same swirl number, without any inlet duct closure.

A conventional air loop architecture has been considered for this first multi-cylinder application. The turbocharger has been slightly improved compared to the production one in order to reach the power target fixed at about 60 kW/l. The production high pressure EGR circuit was upgraded in order to reach higher intake air dilution by burned gases. The revised EGR circuit, in order to increase its permeability and the cooler power, includes a specific cooler which is supplied by a special low temperature water circuit. The EGR cooler can be by-passed, which allows an increase of the intake temperature favourable to HC and CO emissions at very low engine loads.

12.5.2 Full load tests

Two engine speeds, representative of full load curve, were selected to make the comparison with the production engine using a compression ratio of 18:1, and parameter settings consistent with Euro IV emissions standards:

- 4000 rpm, where the maximum engine power is reached
- 2000 rpm, where the maximum engine torque is reached.

The same limiting factors have been considered:

- Maximum in-cylinder pressure: 16 MPa
- Maximum exhaust temperature: 750°C
- Maximum smoke at the exhaust: 3 FSN.

For the full load tests on the NADI™ engine, the fuel injection system has been up-graded in order to increase the injection pressure from 160 MPa to 180 MPa. Table 12.3 gives the main results obtained by the two engines.

The NADI™ engine allows better torque and power. This is mainly due to the lower compression ratio and the improved turbocharger, which allow an increase in the intake pressure for a given maximum in-cylinder pressure level. At 2000 rpm, the maximum output torque level reached by the NADI™ engine is 380 Nm, which corresponds to 172 Nm per litre. At 4000 rpm, the maximum output power of 129 kW, which corresponds to almost 59 kW per litre. Such performances are quite compatible with future standards even if some improvements have to be made to reach 180 Nm per litre and 60 kW per litre respectively.

12.5.3 Part load tests

Two engine speeds of 1500 rpm and 2500 rpm were selected to evaluate the dual mode combustion NADI™ concept at part load and make a comparison with the production engine using a compression ratio of 18:1, and conventional parameter settings consistent with Euro IV emissions standards. For the NADI™ engine, two combustion modes were used for each engine speed:

Table 12.3 Multi-cylinder engine results at full load

	2000 rpm		4000 rpm	
	Conventional	NADI™	Conventional	NADI™
Torque output (Nm)	330	380	–	–
Power output (kW)	–	–	99	129
Smoke (FSN)	1.9	2.0	3.0	3.0
Combustion noise (dBa)	87	83.5	–	–
Intake pressure (kPa)	230	260	220	270

the HPC mode to reach very low NOx emissions with a high EGR rate and the more conventional combustion mode for higher engine loads beyond the normalised cycle with a lower EGR rate. Figure 12.13 and Fig. 12.14 make a comparison between the two engines and show fuel consumption, pollutant emissions, combustion noise and air fuel equivalence ratio (1/λ) versus engine load.

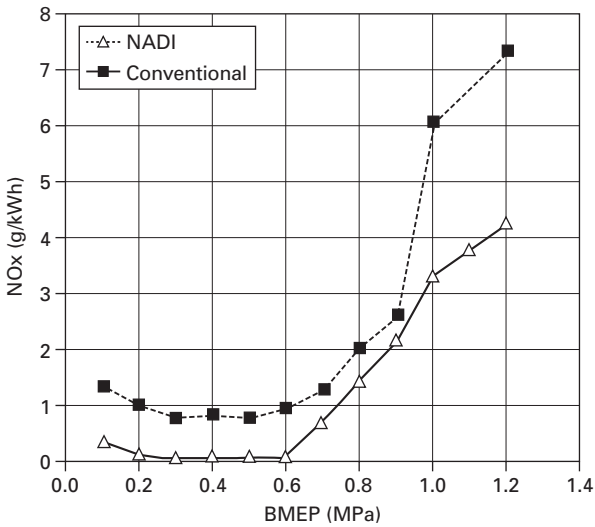

(a)

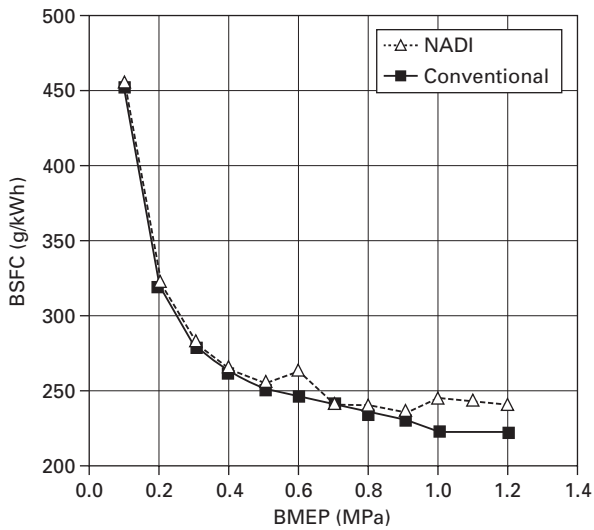

(b)

12.13 Multi-cylinder engine results at 1500 rpm, part load.

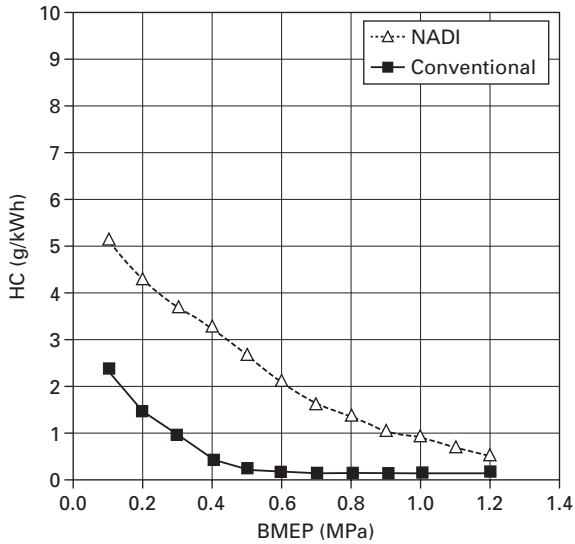

(c)

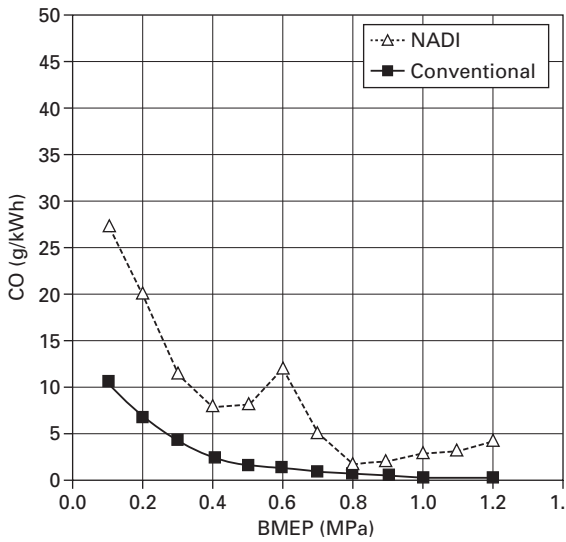

(d)

12.13 Continued

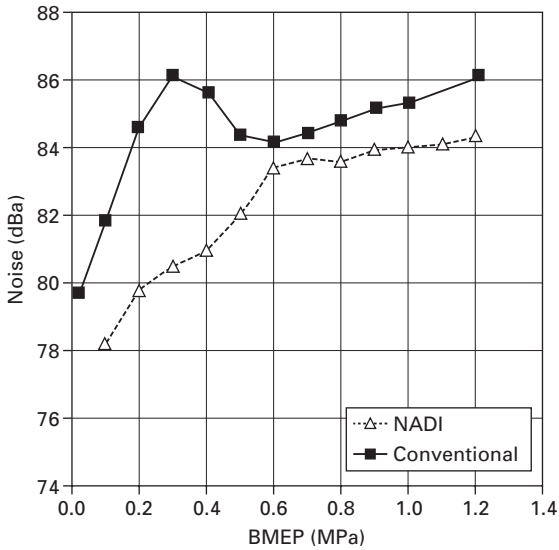

(e)

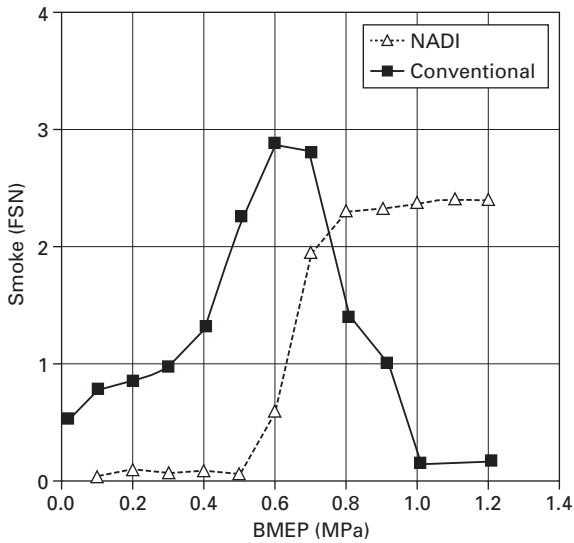

(f)

12.13 Continued

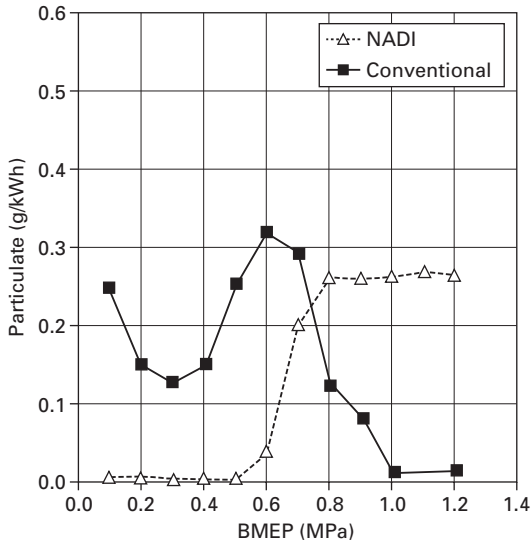

(g)

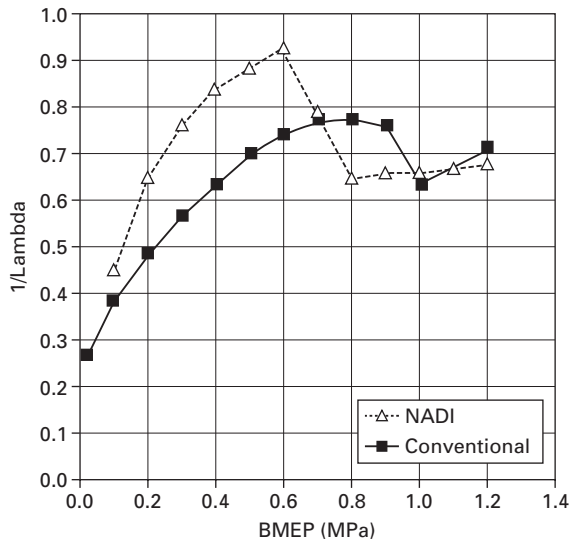

(h)

12.13 Continued

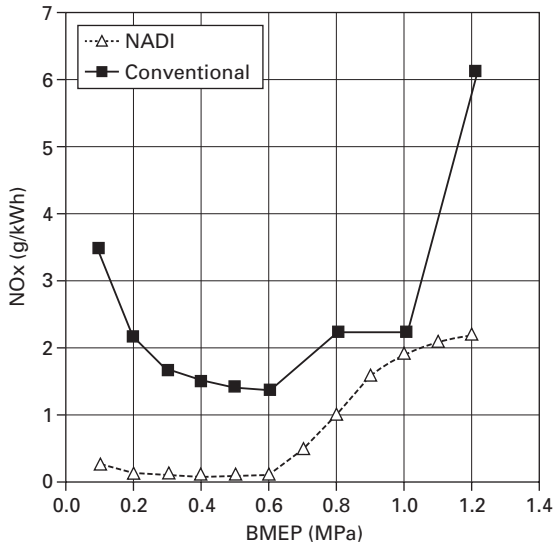

(a)

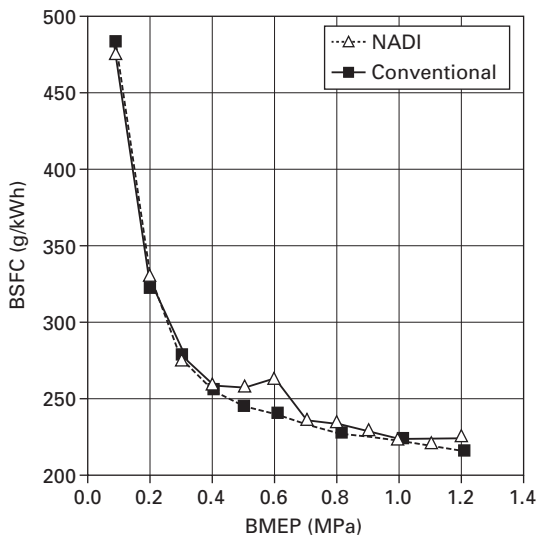

(b)

12.14 Multi-cylinder engine results at 2500 rpm, part load.

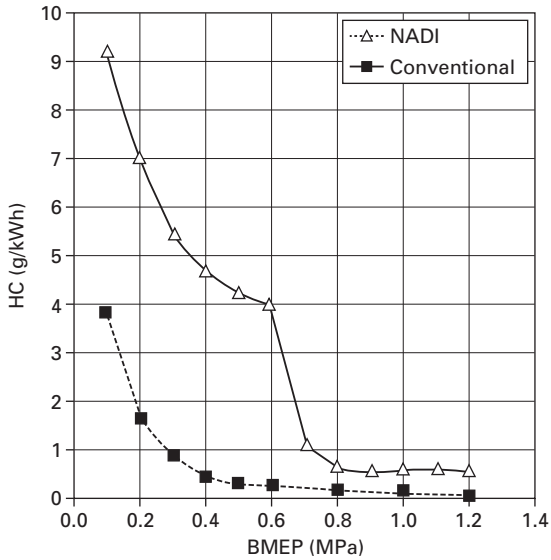

(c)

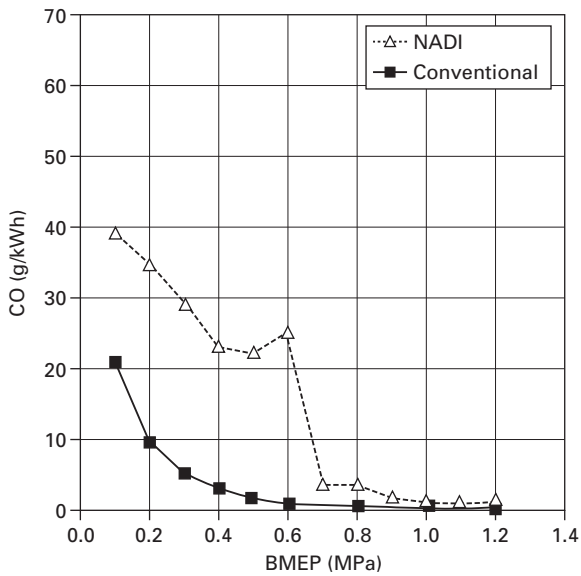

(d)

12.14 Continued

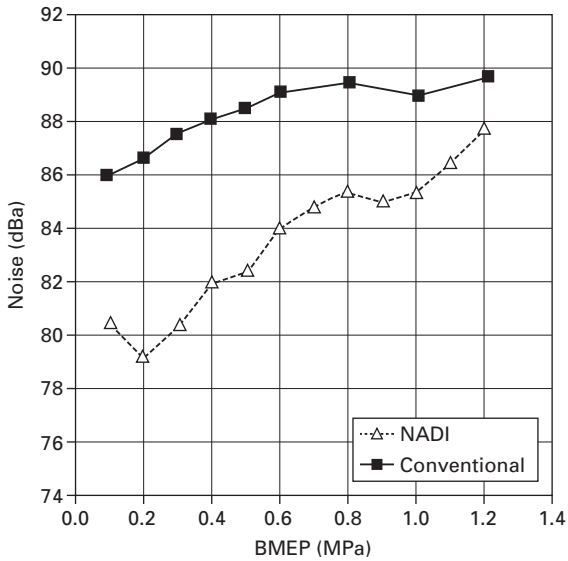

(e)

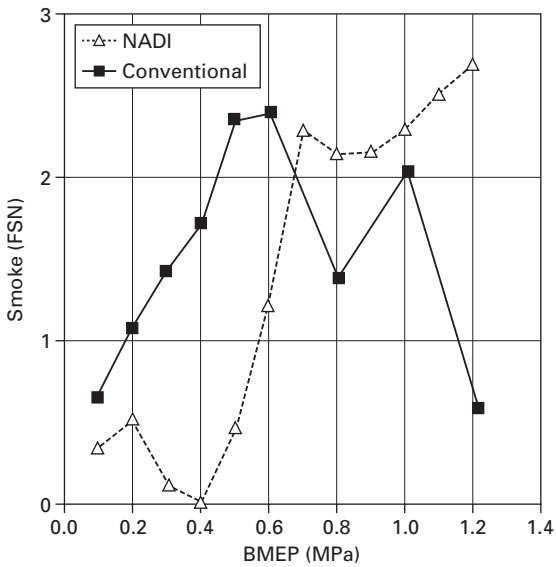

(f)

12.14 Continued

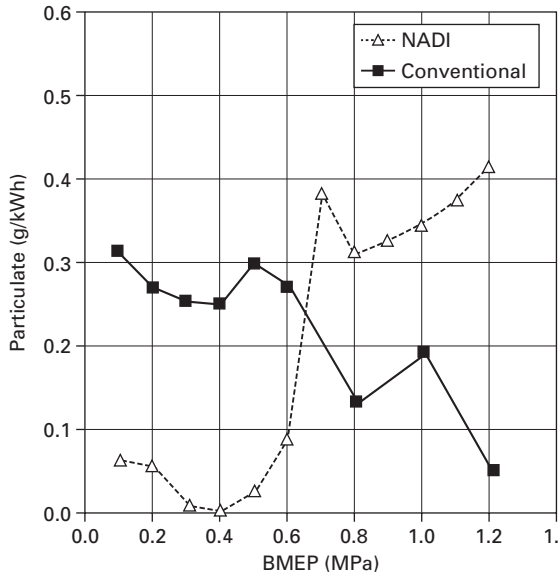

(g)

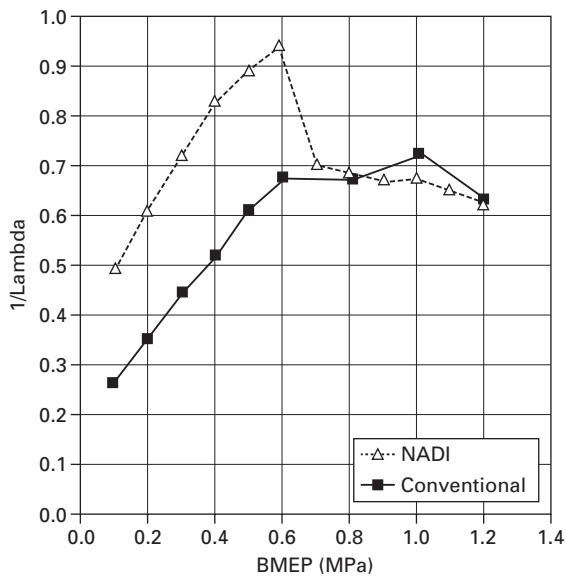

(h)

12.14 Continued

First of all, the HPC operating range with NOx emissions near zero is only up to 0.6 MPa of BMEP for both engine speeds. Compared with single cylinder engine results, the limitation of the operating range in the HPC mode observed during the multi-cylinder test is mainly due to the lack of intake boosting. As a matter of fact, more and more air dilution is needed to control the heat release, in order to keep an acceptable combustion noise, as the engine load increase. As a consequence, the required intake pressure level increases with engine load, with a snowball effect, to maintain enough oxygen excess, in order to limit CO emissions. A lot of tests conducted on single cylinder engines have pointed out that λ does not exceeded 1.1. At a certain step, the lack of balance between energy on the turbine and the energy required by the compressor does not allow HPC mode to be applied. Indeed, the energy on the turbine decreases due to the reduced exhaust gases flow, and the energy required by the compressor increases due to the lower efficiency induced by the reduction of air flow. Turbocharger efficiency improvement is thus a major way of extending the operating range of the highly premixed combustion. Alternative solutions, such as low pressure EGR or two stages turbocharger, could offer larger improvement. This point will be discussed later on, in Section 12.6.

Nevertheless, the results obtained within the HPC operating mode are very promising:

- The trade off between NOx and particulate emissions has been deeply improved. NOx emissions are near zero and particulates are at a very low level.
- The fuel consumption is maintained at a good level compared to the conventional combustion, except at the highest load of the HPC combustion mode. TDC split injection strategy allows near zero NOx emissions without too high a fuel consumption penalty compared to the late injection strategy.
- The noise levels are significantly lower than conventional combustion levels. That is partly due to the EGR effect but, above all, to the injection strategy effect which slows down the combustion heat release rate.
- However, HC and CO emissions overtake conventional combustion levels, but they are well reduced at low engine loads thanks to hot EGR and injection strategies. Indeed, at low engine load, the intake temperature increase helped fuel vaporisation which leads to better local air/fuel mixing. So unburned HC are reduced and combustion produces less CO. Multi-stage injections still improve HC and CO emission levels at low load by injecting very small amounts of fuel without any large wall wetting. Nevertheless, tests with advanced oxidation catalyst have to be done to verify the compatibility with future emissions standards.

Beyond 0.6 MPa of BMEP, highly premixed combustion cannot be operated

and the engine runs in conventional combustion. However, it should be noted that comparison between results obtained at medium and high load with the NADI^{TM} concept geometry and conventional geometry is quite difficult because of the very different NOx emission levels targeted with each concept. As a consequence, EGR rate or equivalence ratio ($1/\lambda$) is not the same. Moreover, noise levels targeted with the NADI^{TM} concept geometry are lower than noise levels relative to conventional geometry. So, higher fuel consumption and smoke emission levels related to the NADI^{TM} concept geometry are mainly due to the difference of compromise between NOx emissions and fuel consumption achieved with each concept. For instance, with conventional geometry, EGR is cut off from 1.0 MPa of BMEP at 1500 rpm and always apply with NADI^{TM} geometry to reduce NOx emissions whatever the engine load. However, without EGR, the NADI^{TM} concept is able to achieve the same fuel consumption with NOx emission levels at 6 g/kWh.

12.6 Future trends

Regarding the engine results obtained on the test bench, the NADI^{TM} concept proposed by IFP seems to be a promising solution to meet future pollutant emission standards by 2010, while maintaining the diesel engine advantages and foremost its low fuel consumption. Nevertheless, a lot of work has to be done in order to put this concept into production. First, HPC operating range has to be improved. As we have highlighted, the air loop circuit definition will have a great importance. Secondly, as the HPC combustion is partly controlled by intake gases composition and temperature, the engine management will have to integrate advanced devices.

12.6.1 Air loop circuit

The air loop circuit has to be suitable for running conditions at both full load and part load. At full load, the output torque and power specifications impose the air mass flow required by the engine according to the geometric compression ratio, maximum in-cylinder pressure and fuel consumption target. At part load, the HPC mode needs high EGR mass flow. At very low engine load, there is no problem because the corresponding air mass flow required by the engine is low. But when engine load increases, the compressor must supply sufficient air flow to ensure engine load with lambda value above 1.1, while high burnt gases mass flow is needed for combustion control.

Using conventional air loop circuit with high pressure EGR (burnt gases are picked up upstream of the turbine and mixed to fresh air downstream of the compressor), the main method of improvement concerns the compressor itself, in order to increase its efficiency for low flow-rate and high compression

ratio. In this context, a variable geometry compressor is an interesting way to develop by continuously tuning the compressor map to the engine running point.

An alternative way, using one conventional turbocharger, is to modify the EGR circuit by adopting low pressure EGR. In this EGR circuit layout, burnt gases are picked up downstream of the turbine, after the particulate filter and mixed with fresh air upstream of the compressor. Fresh air and burnt gases thus pass through the compressor and the turbine. That leads to a better use of the turbocharger. Indeed, compressor working points go away from the compressor surge line by increasing gas mass flow and they are situated in an improved compressor efficiency zone. It is the same for the turbine which is crossed by the whole gas mass flow and then operates in a better efficiency zone. This solution leads to some drawbacks, such as the increase of pumping losses at low load and particulate filter fouling, as the whole gas flow passes through the filter. But, it offers some advantages, such as increased EGR circuit durability in terms of EGR cooler and valve fouling due to cleaned burnt gases picked up downstream of the particulate filter, or better cylinder to cylinder EGR repartition.

Other solutions consist of using more than one turbocharger. A two-stage turbocharger in series can be used to obtain a higher compression ratio, which allows more air to be introduced in the engine for a given burnt gases mass flow. The use of two turbochargers in parallel allows optimisation, for high EGR demands, of one of the two turbochargers.

Finally, mild turbocharger hybridising such as E-boosts and turbocharger electrical assistance are other solutions to compensate for the lack of exhaust energy when gas temperature is low.

12.6.2 Engine control development

Engine management is nowadays a key point in new production engines. Because highly premixed combustion is more sensitive to tuning than conventional diesel combustion and due to the fact that transition between several combustion modes must be managed during transient operations, the control of NADI^{TM} concept engine requires specific development, currently in progress [18] and [19].

Air loop control

Indeed, Highly Premixed Combustion (HPC) depends closely on thermodynamic behaviour inside the combustion chamber. Then fast and precise EGR control is also required. In addition, EGR circuit response time is long, particularly in the case of the low pressure EGR layout that complicates the follow-up of the targeted EGR rate. Several actuators are used (intake

throttle, waste gate or VGT, EGR valves) to control the air loop. A multivariable control has to be set up to manage these actuators.

Fuel control

Precise injection models with multi-injection capacities are required. Special attention must be paid to insure the injections phasing and quantity during HPC combustion and modes changes.

Combustion control

Disparities between cylinders can dramatically reduce NADI^{TM} combustion potential. Therefore, IFP has developed advanced cylinder to cylinder control based on air/fuel ratio and torque observers. The air/fuel ratio observer gives air/fuel ratio disparities between cylinders with the help of the measurement of a unique lambda exhaust sensor which could be placed after the turbine. The torque observer translates the measurement of crankshaft speed into individual energy release of each combustion event. Controllers are used to minimise the observed disparities between cylinders.

12.7 References

1. G. R. Pucher, D. P. Gardiner, M. F. Bardon and V. Battista. 'Alternative Combustion Systems for Piston Engines Involving Homogeneous Charge Compression Ignition Concepts – A review of Studies Using Methanol, Gasoline and Diesel Fuel'. SAE Paper 962063 (1996).
2. R. H. Stanglmaier and C. E. Roberts. 'Homogeneous Charge Compression Ignition (HCCI): Benefits, Compromises, and Future Engine Applications' SAE Paper 1999-01-3682, (1999).
3. P. M. Najt and D. E. Foster. 'Compression – Ignited Homogeneous Charge Combustion' SAE Paper 830264, (1983).
4. M. Christensen and B. Johansson. 'Supercharged Homogeneous Charge Compression Ignition (HCCI) with Exhaust Gas Recirculation and Pilot Fuel' SAE Paper 2000-01-1835, (2000).
5. H. Yokota, H. Nakajima and T. Kakegawa. 'A new Concept for Low Emission Diesel Combustion (2nd Rep.: Reduction of HC and CO Emission, and Improvement of Fuel Consumption by EGR and MTBE Blended Fuel' SAE Paper 981933, (1998).
6. H. Yanagihara, Y. Sato and J. Mizuta. 'A simultaneous reduction of NOx and soot in diesel engines under a new combustion system (Uniform Bulky Combustion System – UNIBUS' VDI 1996 no. 267, (1996).
7. Y. Iwabuchi, K. Kawai, T. Shoji and Y. Takeda. 'Trial of New Concept Diesel Combustion System – Premixed Compression – Ignited Combustion' SAE Paper 1999-01-0185, (1999). Mitsubishi Motors Corporation.
8. S. Kimura, O. Aoki, Y. Kitahara and E. Aiyoshizawa. 'Ultra-Clean Combustion Technology Combining a Low-Temperature and Premixed Combustion Concept for Meeting Future Emission Standards' SAE Paper 2001-01-0200, (2001).

9. B. Gatellier, B. Walter. and M. Miche. 'New Diesel combustion process to achieve near zero NOx and particulates emissions'. IFP International Congress – A new generation of engine combustion processes for the future? (2001).
10. B. Walter and B. Gatellier. 'Development of the High Power NADI^{TM} Concept Using Dual Mode Diesel Combustion to Achieve Zero NOx and Particulate Emissions'. SAE paper 2002-01-1744.
11. B. Gatellier and B. Walter. 'Development of the High Power NADI^{TM} Concept Using Dual Mode Diesel Combustion to Achieve Zero NOx and Particulate Emissions'. Thiesel Conference on Thermo and Fluid Dynamic Processes in Diesel Engines (2002).
12. B. Walter and B. Gatellier. 'Near Zero NOx Emissions and High Fuel Efficiency Diesel Engine: the NADI^{TM} Concept Using Dual Mode Diesel Combustion'. *Oil and Gas Science and Technology*, Vol 58 (2003), No 1, pp. 101–114.
13. A. Ranini, S. Potteau and B. Gatellier. 'New developments of the NADI^{TM} concept to improve operating range, exhaust emissions and noise'. Thiesel Conference on Thermo and Fluid Dynamic Processes in Diesel Engines (2004).
14. B. Walter, L. Monteiro, M. Miche and B. Gatellier. 'Improvement of Exhaust and Noise Emissions of the NADI^{TM} Concept Using Pre-Mixed Type Combustion with Multiple Stages Injection'. SIA Congress : The Diesel Engine : today and tomorrow, 2004.
15. B. Gatellier, A. Ranini and M. Castagné. 'Neue Entwicklungen des NADI^{TM} Konzepts zur Verbesserung des Kennfeldbereiches, der Abgas-Emissionen und der Lärmentwicklung'. 13. Aachener Kolloquium Fahrzeug und Motorentechnik 2004.
16. B. Gatellier, B. Gessier, J. Genoist and A. Ranini. 'Neue Technologien zur Erfüllung der Abgasnorm Euro 5', *MTZ* 6/2005 Jahrgang 66, pp. 434–443.
17. B. Gatellier, A. Ranini and M. Castagné. 'New development of the NADI^{TM} Concept to improve operating range, exhaust emissions and noise. Combustion'. *Oil and Gas Science and Technology*, Vol. 61 (2006), No 1, pp. 7–23.
18. A. Albrecht, O. Grondin, F. Le Berr and G. Le Solliec. 'Towards a stronger simulation support for engine control design: a methodological point of view', Les Rencontres Scientifiques de l'IFP – New Trends in Engine Control, Simulation and Modelling; 2006.
19. J. Chauvin, G. Corde, N. Petit and P. Rouchon. 'Experimental air path control of a Diesel engine', Les Rencontres Scientifiques de l'IFP – New Trends in Engine Control, Simulation and Modelling, 2006.

13

Low-temperature and premixed combustion concept with late injection

S KIMURA, Nissan Motor Company, Japan

13.1 Introduction

Nitrogen oxide (NOx) and particulate matter (PM) emissions of diesel vehicles are regarded as a source of air pollution, and there is a global trend to enforce more stringent regulations on these exhaust gas constituents in the early years of the 21st century. On the other hand, the excellent thermal efficiency of diesel engines is certainly a welcome attribute from the standpoints of conserving energy and curbing global warming.

Figure 13.1 shows how much NOx emissions would have to be reduced for a conventional DI diesel that does not incorporate any emission reduction technologies in order to comply with current and future regulations. NOx emissions would have to be reduced by 87.5% to meet the current standard for EURO4 and by 98% to clear the more stringent standard for ultra low emission vehicle (ULEV) regulations of the US set to be enforced in 2007. Moreover, a reduction of 99.4% would be required to reach super ultra low emission vehicle (SULEV) level, which is the toughest exhaust emission

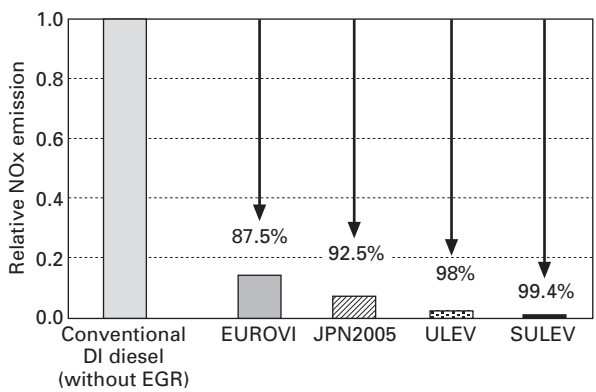

13.1 Regulation level in the world.

target now being considered, albeit it is not a regulation value. Recently, many research institutes and engine researchers around the world have been researching emission control technologies in high-efficiency direct injection diesel engines so as to obtain clean internal combustion engines.

The lean premixed combustion technologies [1–7] like homogeneous charged compression ignition (HCCI) are considered one of the most promising techniques that has the excellent potential of significant reduction in NOx and soot emissions. This kind of lean premixed combustion requires a long time for mixture preparation. One of approaches to accomplish a long mixing time is early fuel injection into the cylinder during the compression stroke [4, 5]. With early fuel injection, the lean and homogeneous condition was performed and NOx level is significantly reduced without increase in soot. The previous study [1] indicated HCCI with early injection could reduce NOx emissions by 98% in comparison to conventional diesel combustion at half load region. However, HC and CO emission levels of HCCI are extremely high and there are deteriorations in fuel consumption [6]. Furthermore, the onset of combustion that significantly influences exhaust emissions and fuel consumption is strongly dependent on injection timing and the equivalent ratio. The main technical challenge of this combustion to be of practical use is controlling the onset of combustion [7].

In this chapter, the combination of low-temperature and premixed combustion with late injection is investigated with the aim to reduce both NOx and PM without the increase of HC emission and fuel consumption. Based on experimental results, it also describes the characteristics of this low-temperature and premixed combustion through the instantaneous heat flux measurement and high-speed photographs.

13.2 Basic concept of low-temperature and premixed combustion

A new combustion concept, which the authors named as modulated kinetics or MK combustion, can be essentially characterized as a low-temperature, premixed combustion system that is aimed at simultaneously reducing NOx and PM emissions, which is a major issue for DI diesel engines. This combustion does not require homogeneous condition like HCCI. The basic concept of MK combustion is explained schematically in Fig. 13.2.

Because NOx formation is strongly dependent on the combustion temperature, one effective way to reduce NOx emissions is to lower the combustion temperature. Low-temperature combustion is accomplished in MK combustion concept by applying heavy exhaust gas recirculation (EGR), to reduce the oxygen concentration, and by employing a lower compression ratio. Usually, reducing the oxygen concentration, however, results in a higher smoke level. Since it was expected that a higher smoke level would be

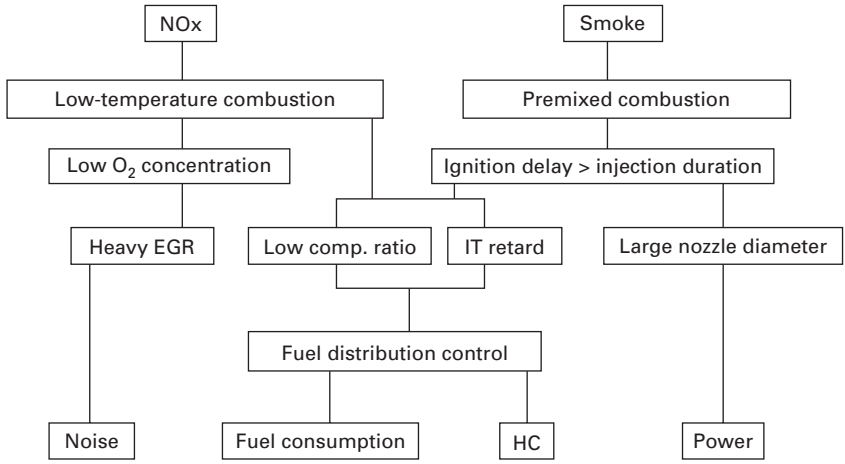

13.2 Schema of MK combustion concept.

unavoidable with diffusion combustion, an investigation was made of a premixed combustion process, marking a departure from the methodology pursued previously. An attempt was made to reduce NOx and smoke emissions simultaneously through the use of low-temperature combustion and premixed combustion, respectively.

To achieve premixed combustion, the fuel and oxygen must be thoroughly mixed prior to ignition. In MK combustion, sufficient mixing time is secured by prolonging the ignition delay. To obtain a prolonged ignition delay, the fuel injection timing is retarded significantly and the low compression ratio is applied. On the other hand, the injection timing retard and low compression ratio lead the deteriorations of isochoric efficiency and unburned HC emissions. The control of injected fuel distribution in the cylinder has been adopted to suppress the formation of HC and soluble organic fraction (SOF) and to reduce the cooling loss. One of the approaches to promote the optimal fuel distribution is the combination of a toroidal combustion chamber shape and a higher swirl ratio. Experimental results have further confirmed that this combustion system is effective in reducing cooling losses [8, 9].

13.3 Characteristics of combustion and exhaust emissions with modulated kinetics (MK) combustion

13.3.1 Combustion photographs

The main specifications of the single-cylinder test engine used in the experiments are given in Table 13.1. Combustion conditions were observed on the basis of high-speed photographs to confirm that the MK concept

Table 13.1 Engine specifications

Engine type		Single cylinder
Combustion system		Direct injection
Bore × Stroke		ϕ 89 mm × 100 mm
Displacement		622 cm^3/cyl
Compression ratio		16.0:1
Combustion chamber		Toroidal type
Swirl ratio		3.6 ~ 10.0
Injection system	Pump	Common rail system
	Nozzle	ϕ 0.23 mm × 5

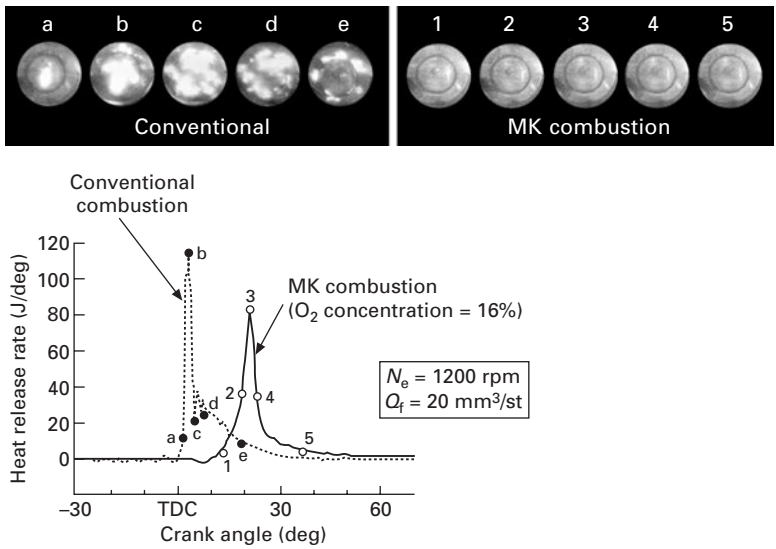

13.3 Comparison of combustion photographs between conventional and MK combustion.

works to promote low-temperature, premixed combustion in a DI diesel engine. Photographs of MK combustion are compared in Fig. 13.3 with those of the conventional DI combustion process, typified by no EGR and a standard injection timing and swirl ratio. The heat release rate curves measured for each combustion process are also given in the figure.

Looking at the heat release rates, it is seen that the onset of heat release with the MK concept was plainly later than for the conventional combustion process, owing to the large retardation of injection timing. Another characteristic of MK combustion is the low heat release rate following the onset of heat release. This is attributed to the low rate of increase in cylinder pressure, which is thought to lead to a reduction of combustion noise. Although the initial heat release rate was low with the MK concept, combustion subsequently

proceeded vigorously and the overall combustion period was virtually comparable to that of the conventional combustion process. Moreover, the general shape of the heat release rate curve for the MK concept shows a single stage of entirely premixed combustion. This is in clear contrast to the two-stage profile observed for the standard DI process, which is divided between an initial stage of premixed combustion and the main stage of diffusion combustion.

In the combustion photographs for the MK concept, virtually no clear sign of a brilliant flame is observed throughout the entire combustion period. By analogy with the high transparency of the flame, this is taken as proof not only of the weak luminous intensity of the flame but also of its low soot concentration on account of the low combustion temperature. Although the reduced combustion temperature cannot be substantiated directly from the photographs, they are thought to confirm a more advanced state of premixing, which was the original aim.

13.3.2 Performance characteristics

The effect of each combustion factor in the MK concept on exhaust emissions and thermal efficiency is shown individually in Fig. 13.4. With a lower oxygen concentration, NOx emissions were dramatically reduced by approximately 90%, and retarded injection timing reduced the smoke level markedly. Moreover, it is seen that the higher swirl ratio played a part in reducing smoke and unburned HC emissions. Figure 13.4 shows the effect of each combustion factor on thermal efficiency. With a lower oxygen concentration, which has a pronounced effect on reducing NOx emissions, the thermal efficiency improved; however, the thermal efficiency deteriorated with retarded injection timing. A higher swirl ratio improved the thermal efficiency over the level of ordinary combustion.

According to these results, it is clear that a higher swirl ratio is the key factor to reduce soot, HC emissions and cooling losses. Then, to investigate this mechanism of a higher swirl ratio, the combustion phenomena of this MK combustion with low and high swirl ratios was examined using the transient heat flux measurement.

13.3.3 Experimental measurement of transient heat flux

The heat flux of the piston was measured with the thin-film thermocouple [10]. The body of this thermocouple is made of the same material as that of the piston. The hot junction is formed by a copper thin film with a thickness of 10 μm and a constant wire of 0.15 mm diameter separated from each other by a dielectric film. Another thermocouple is placed at 3.2 mm from the surface to form the cold junction that records the body temperature. The

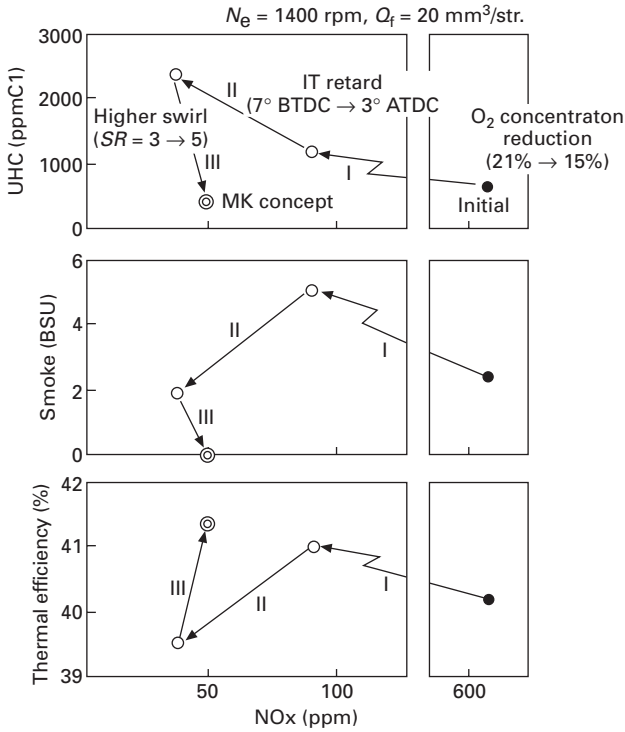

13.4 Effects of each combustion factor on exhaust emissions and thermal efficiency.

locations of thin-film thermocouples on the piston surfaces are shown at the bottom of Fig. 13.5.

To investigate the influence of these locations on heat flux, the heat flux measurement was conducted using three different injectors whose orifices are aimed in different directions relative to the measurement locations.

The plots are the mean heat flux averaged over a period of a 60° CA from the start of combustion for three nozzles. The results reveal that the mean heat fluxes at piston side wall (S1) and piston head (H1) are always lower for the high swirl ratio irrespective of the different relative locations between heat flux sensors and nozzle holes. This implies that relatively homogeneous mixtures are formed during the long ignition delay observed in the heat release curves.

The heat release rate and heat flux pattern measured at cavity side wall, S1, and piston head, H1, for low and high swirl ratios under a condition of a reduced oxygen concentration are compared in Figs 13.6 and 13.7. The heat release rate in the initial period is almost the same for both swirl ratios, but the low swirl ratio has a lower peak value and the end of combustion was

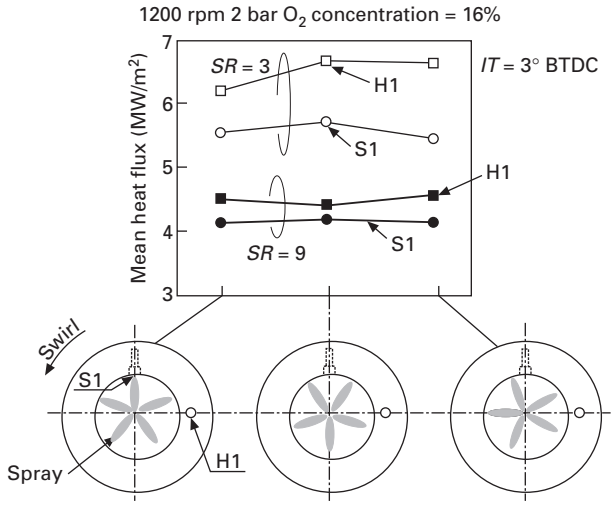

13.5 Comparison of mean heat flux between low and high swirl conditions.

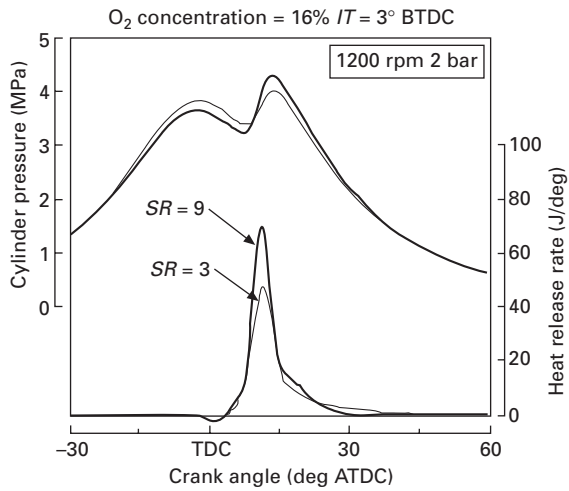

13.6 Heat release pattern of low and high swirl conditions.

prolonged. On the other hand, the heat flux pattern under a low swirl ratio condition indicates that heat flux rose at an earlier crank angle at the cavity side wall and at a later crank angle at the piston head. These results also indicate the heat flux with the low swirl ratio was greater than that with the high swirl ratio. The reason for this greater heat flux initially at the cavity side wall is presumed to be due to the approach of hot combustion gas rather than to a change in the rate of combustion. This assumption is based on the

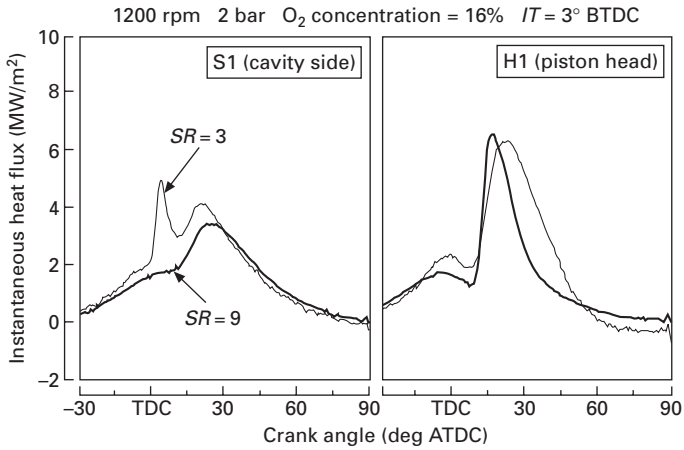

13.7 Comparison of heat flux between low and high swirl conditions.

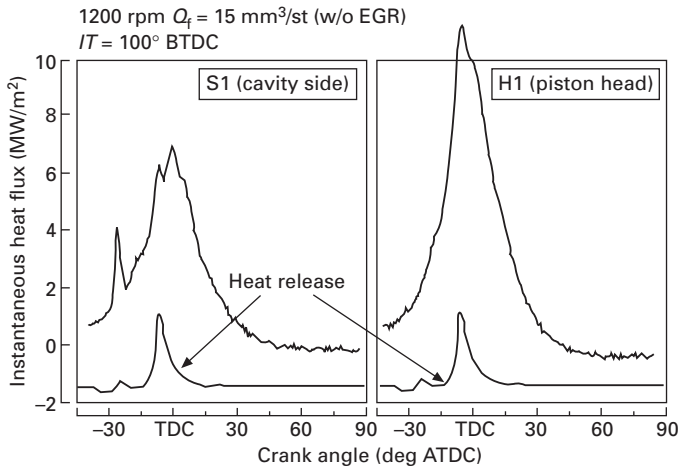

13.8 Heat flux pattern of early injection timing.

fact that no significant change is seen in heat release in the initial period with a low swirl ratio.

To confirm this assumption, the distribution of equivalent ratio in cylinder with a three-dimensional simulation code; Turbo-KIVA [11], was used. Figure 13.8 shows the calculated results as a function of the swirl ratio. With a high swirl ratio, the injected fuel was concentrated in the center of the combustion chamber. On the other hand, with a low swirl ratio the injected fuel reached the cavity side wall. It is thought that the straight-line directionality of the fuel spray increases under a low swirl ratio, resulting in mixture formation near the cavity side wall, which would account for the larger heat

flow rate seen there. Then, this fuel near the cavity side wall reached near the cylinder liner wall with the falling of piston. It is thought that this is the reason why HC emissions were reduced with a high swirl ratio. The results of these heat flux measurements make it clear that cooling losses and HC emissions were reduced by the fuel distribution control in the cavity.

Plate 14 (between pages 268 and 269) compares the heat release rate and the heat flux pattern between homogeneous condition using early injection timing, 100 deg BTDC, and MK combustion condition. With early injection timing, the pre-heat release by low temperature oxygen reactions was occurred before main combustion. At this timing, the heat flux rose at the cavity side wall and did not rise at the piston head. These heat flux phenomena of HCCI correspond with those of MK combustion with low swirl condition. In view of these results, it is conjectured that the initial heat release rate of MK combustion is formed by low temperature oxygen reactions. The total heat flux of homogeneous condition is larger than that of MK combustion due to early combustion start. These results indicate that it is very important to control the combustion start of HCCI for obtaining high thermal efficiency.

13.4 Second generation of MK combustion

13.4.1 Challenges for MK combustion

In trying to apply MK combustion to the high-load region, it is predicted that two problems will have to be resolved. The first problem is that the ignition delay is shortened by the higher temperature of the EGR gas. The second problem is that the injection duration is prolonged by the greater quantity of fuel injected. The multiplied effects of these two problems make it impossible to complete the injection of all fuel prior to ignition, which is one of the necessary conditions for accomplishing premixed combustion.

Consequently there are two approaches that can be considered for expanding the MK combustion region to the high-load range. One approach is to prolong the ignition delay and the other approach is to shorten the injection duration. The fundamental objective of prolonging the ignition delay is to lower the gas temperature of the combustion field at top dead center (TDC) of the compression stroke. Specific ways of accomplishing that objective include cooling the EGR gas and lowering the compression ratio. On the other hand, the injection duration can be shortened with high-pressure injection or a larger nozzle hole, among other approaches.

13.4.2 Effects of prolonging ignition delay

Figure 13.9 shows the effects of the intake gas temperature on prolonging the ignition delay, as a result of cooling the recirculated exhaust gas. In this

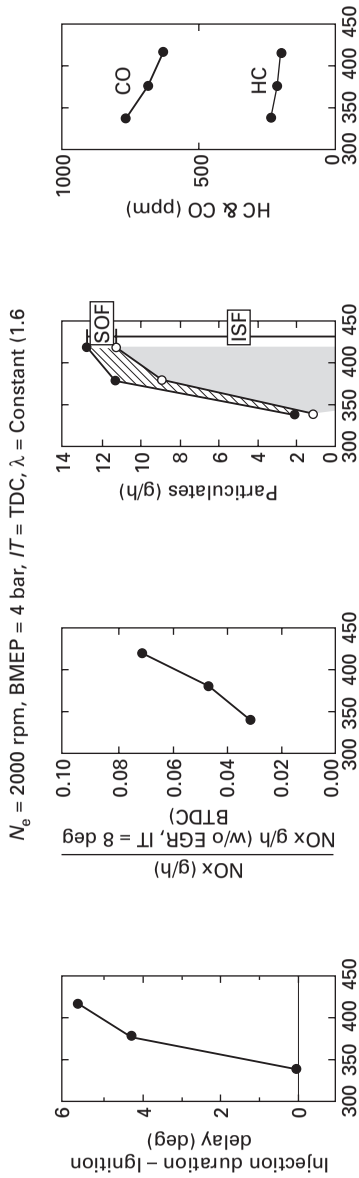

13.9 Correlation between ignition delay and exhaust emission.

operating region, the injection duration was over 9 crank angle degrees. Without cooling the EGR gas, the intake gas temperature was about 420 K and the ignition delay was shorter than 6 CA degrees. When the intake temperature was under 350 K, the ignition delay was prolonged to the length of the injection duration.

Figure 13.9 also shows the effect of cooling the EGR gas on NOx reduction rate, particulate matter, HC and CO emissions. To avoid any effect on volumetric efficiency due to the lower intake gas temperature, the excess air ratio was maintained at the same level, 1.6. As seen in the figure, NOx emissions were steadily reduced with a lower intake gas temperature. The PM level was significantly reduced by lowering the intake air temperature from 390 K to 340 K, which prolonged the ignition delay to the length of the injection duration. In this case, the dry soot, insoluble fraction (ISF), and soluble organic fraction (SOF) simultaneously reduced with the prolonging ignition delay. Furthermore, HC and CO emissions did not increase significantly with the lower intake gas temperature. These results indicated that the prolonging ignition delay to the length of the injection duration significantly reduced the dry soot without the increase of unburned fuel. In short, this data also indicates that the dry soot oxidized due to the improvement of mixing performance. If the combustion temperature decreased without the improvement of mixing, the unburned fuel increased with the reduction of soot. Then, these results led to the conclusion that the prolonging ignition delay of MK combustion progresses the premixing condition.

13.4.3 Effects of combination between prolonging ignition delay and shortening injection duration

The foregoing results showed the effects of prolonging ignition delay due to the decrease of intake gas temperature using EGR cooling on ignition delay. The second approach to accomplish the premixed combustion is to shorten the injection duration, which is possible with a high-pressure injection system, such as a common rail system, or with a larger nozzle hole diameter. Next, the effects of shortening the injection duration were investigated. The injection duration was changed by the common rail system, which allows easy control of the injection pressure.

Figure 13.10 shows the trade-offs among NOx, PM and the relationship between ignition delay and injection duration under operating conditions where MK combustion was accomplished at a reduced load level with λ of 1.3, this is the minimum λ to avoid the deterioration of thermal efficiency [12]. A constant compression ratio of 16:1 was used in these tests. At a low injection pressure with 30% EGR, the NOx level was reduced, but PM emissions increased noticeably owing to greater smoke formation. In this condition, the ignition delay shortened than injection duration. Retarding the

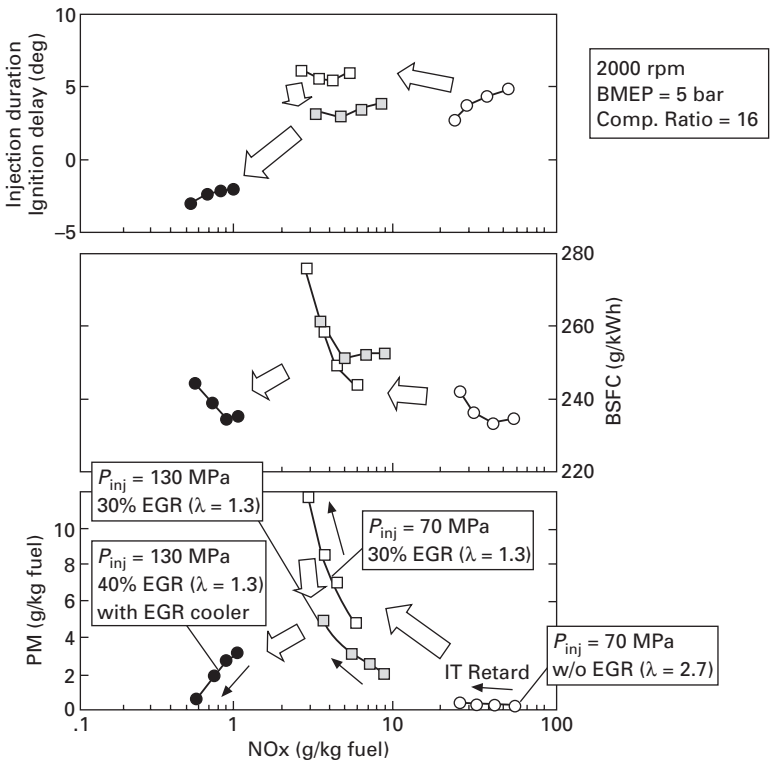

13.10 Effects of low compression ratio, high injection pressure and EGR cooling.

injection timing resulted in a NOx reduction, but the PM level rose, indicating that this trade-off was not improved. In contrast, with high-pressure injection with 30% EGR, PM emissions were reduced, but the NOx level increased. In this case, injection duration was shortened by the increase of injection pressure, however ignition delay was no longer than the injection duration. Then, the performance trade-off accompanying the retardation of injection timing was not improved. The combination of a low compression ratio, high injection pressure and EGR cooling resulted in a longer ignition delay than the injection duration. Then the NOx level was reduced markedly by approximately 95% compared with the result obtained when EGR was not applied. Retarding the injection timing worked to reduce NOx and PM emissions simultaneously. With retarded injection timing, PM emissions were reduced to nearly the same level as under the initial condition without EGR. Additionally, fuel economy was improved to almost the same level as that of the initial condition.

According to these results, the shortened injection duration is also an effective way to accomplish the premixed combustion.

13.4.4 HC emission with low compression ratio in cold condition

The foregoing discussion has shown that a combination of a lower compression ratio, high-injection pressure and EGR gas cooling can prolong ignition delay longer than injection duration in the high-load region. However, it was feared that a lower compression ratio might cause HC emission performance to deteriorate in cold-condition. Ordinarily, the effective approach to reduce HC emission in cold-condition is the avoiding fuel-cavity wall interaction. A small nozzle hole is one way to avoid the fuel-wall interaction; however this leads to prolonging injection duration, which is an opposite tack of MK combustion. So, the large cavity diameter is used to avoid HC emissions in cold-condition.

Figure 13.11 compares HC emissions as a function of coolant temperature. HC emissions under hot-condition did not change on account of the large cavity diameter. Under the cold-condition, coolant temperature was 313 K, HC emission with the large cavity diameter was significantly reduced. According to these results, the following experiments were conducted using the large cavity diameter.

13.5 Emission performance improvement of second generation of MK combustion

13.5.1 Smoke characteristics

The foregoing results indicated that the combination of low compression ratio, EGR cooling and high injection pressure could make the ignition delay longer than the injection duration. An attempt was then made to achieve MK combustion over nearly the entire load range by substantially changing the ignition delay as a result of cooling the EGR gas. The results obtained are

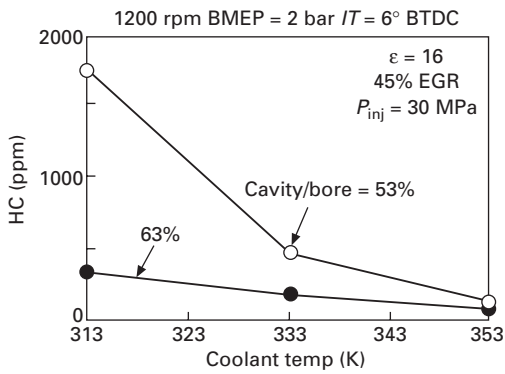

13.11 Effect of enlarging cavity diameter on cold-start HC emission.

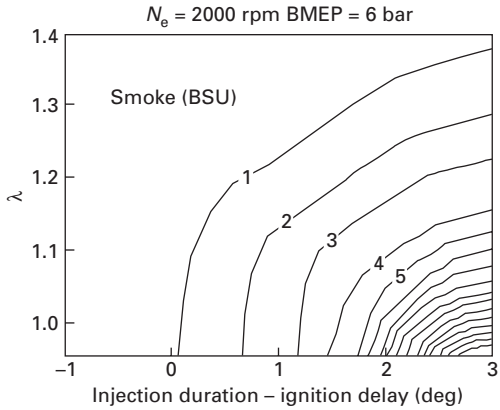

13.12 Effects of prolonging ignition delay on smoke level.

shown in Fig. 13.12, which presents a map indicating the effect on the smoke concentration of the difference between the injection duration and the ignition delay and the excess air ratio λ. The data were obtained under conditions of an engine speed of 2000 rpm and 6 bar break mean effective pressure (BMEP). It is seen that smoke increased with a smaller λ value in the region of a short ignition delay, i.e., the area where the horizontal axis values are greater than zero. The smoke level shows an especially sharp increase at λ values below 1.2. By contrast, the smoke level decreased in the region where the ignition delay exceeded the injection duration, and even at λ values below 1, the smoke level was less than 1 BSU. These results indicated that smoke generation can be suppressed even in the region near a stoichiometric mixture ratio by making the ignition delay longer than the injection duration.

13.5.2 Comparison of performance between conventional and MK combustion

The NOx reduction rate and particulate emissions on conventional and MK combustion are compared in Fig. 13.13. The conventional combustion was run with several injection pressure levels, from 700 to 1600 bar. Looking at the NOx reduction rate (NOx/NOx baseline), NOx reduction rate of MK combustion is over 98% and the limit of NOx reduction rate with conventional combustion is from 90 to 92%.

13.5.3 Possibility of obtaining a clean diesel with MK combustion

The extension of MK combustion to the high-load range showed that NOx emissions could be reduced by more than 98% over the entire range of

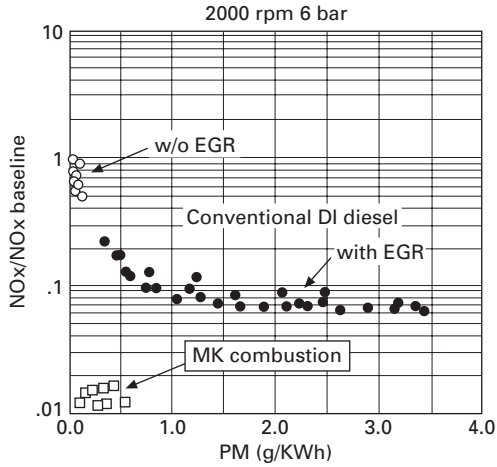

13.13 Emission comparison: MK combustion vs. conventional DI diesel.

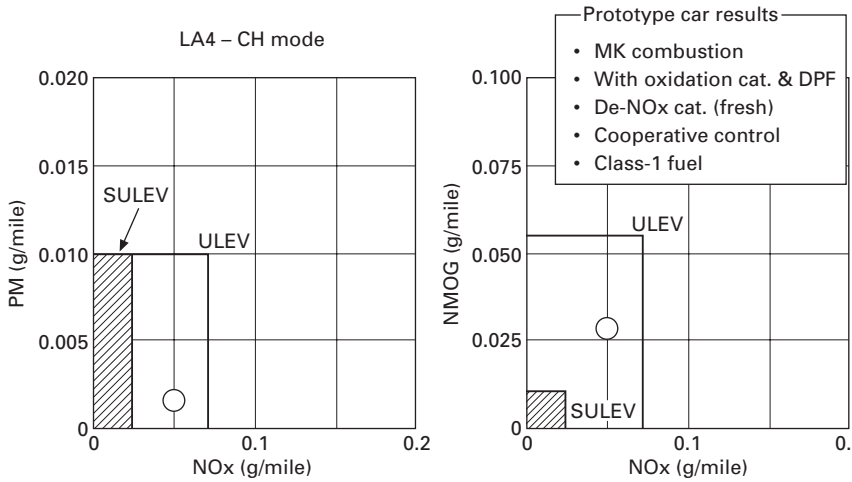

13.14 Test car results with MK combustion and 5-way catalyst.

everyday driving without having a large adverse effect on smoke formation and fuel consumption. Furthermore, the second-generation MK combustion system with the excess air ratio limit expanded to near the stoichiometric air-fuel ratio level without increase of smoke offers the potential of more effective reduction in NOx emissions using more robust NOx catalyst.

The test car results with second-generation MK combustion and 5-way catalyst are shown in Fig. 13.14. The 5-way catalyst consists of the oxidation catalyst, particulate filter and de-NOx catalyst. In this experiment, NOx

adsorber is used for de-NOx catalyst. The sulfur content of the fuel is maintained below 10 ppm. According to the test car results, the combination of second-generation MK combustion and 5-way catalyst has the possibility of meeting the ULEV emission (NOx < 0.07g/mile, PM < 0.01g/mile) with 5000 lb gross vehicle weight rating (GVWR).

13.6 Future trends

13.6.1 Concept for SULEV compliance

The previous results indicate that low temperature and premixed combustion concept with late injection has the potential to achieve emission levels comparable to those of a gasoline engine, ULEV. Furthermore, the result of Fig. 13.14 indicates that the PM level satisfies the Super ULEV regulation. However, a further reduction of NOx and NMOG emissions is necessary for compliance with the SULEV regulations that impose the most stringent requirements.

Subsequent in-vehicle evaluations have made it clear that reducing cold-start emissions is an issue that must be addressed to attain a further improvement in the emission performance of a diesel engine that combines the MK combustion concept with an after-treatment system. The catalytic converter does not exhibit sufficient conversion performance until the after-treatment system lights off under a cold-start engine condition. Consequently, exhaust gas emitted from the engine is discharged into the atmosphere without reacting with the catalyst. Moreover, the stability of the MK combustion process, which uses a low compression ratio, tends to decline under a cold-start condition on account of the increased ignition delay due to the cool combustion chamber and cylinder walls. As a result, there is an especially noticeable increase in the THC level. The EGR rate was set lower in an attempt to inhibit this rise in the THC level caused by the decline in combustion stability in a low-temperature condition. However, this approach is not a rational way of reducing exhaust emissions because of the trade-off with a higher NOx level.

To reduce exhaust emissions for SULEV compliance, this study focused on gas-to-liquid (GTL) fuel that has a high cetane number and a high level of paraffin compounds. However, because MK combustion requires a long ignition delay, an investigation was made of the combination of a lower compression ratio (14:1) and GTL fuel to examine the potential effect on reducing cold-start exhaust emissions.

13.6.2 Effects of future fuel

The influence of both the compression ratio and the cetane number on HC emissions under the cold condition with GTL fuel is shown in Fig. 13.15.

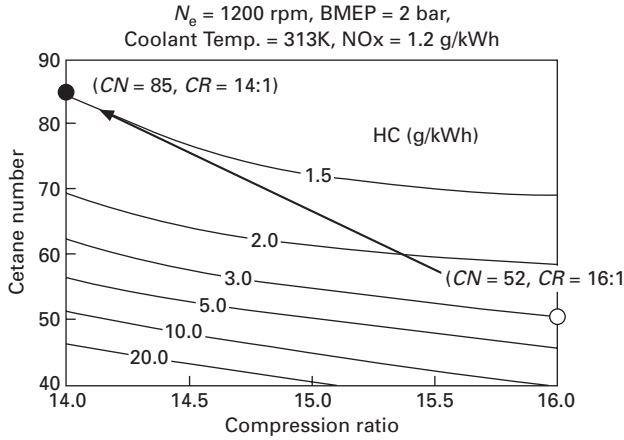

13.15 Influence of CN and CR on HC emissions.

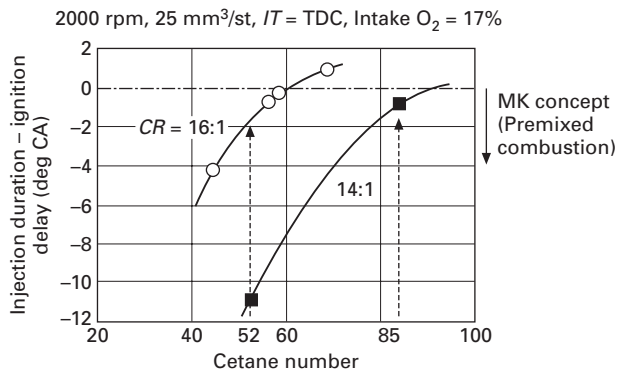

13.16 Influence of CN and CR on ignition delay.

This map shows that HC emissions increased significantly when the cetane number was 50 or lower. The map also indicates that the HC emission level obtained with the combination of a compression ratio of 16:1 and a CN 52 fuel (Class 1), which was used in the prototype ULEV vehicle mentioned above, can be reduced by half by using the combination of a compression ratio of 14:1 and a cetane number fuel of 85.

Using higher cetane number fuel is effective in reducing HC emissions under a cold condition. However, using a higher cetane number fuel might impede MK combustion due to a shorter ignition delay, especially in a higher load condition. Therefore, the influence of both the cetane number and the compression ratio on the relationship between the ignition delay and injection duration was investigated. The results shown in Fig. 13.16 indicate that it is possible to keep a sufficiently long ignition delay to obtain the desired

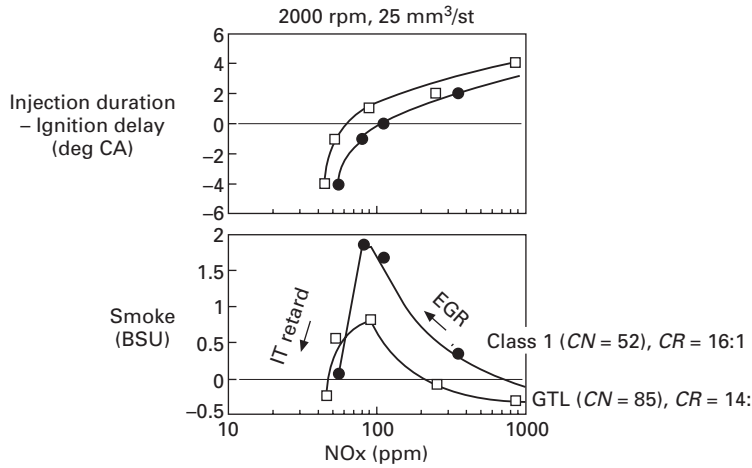

13.17 Combining MK concept with high cetane number fuel.

premixed condition even with a CN 80 or higher fuel by lowering the compression ratio to 14:1.

Figure 13.17 compares the emission characteristics obtained with a combination of a compression ratio of 16:1 and a CN 52 fuel (Class 1) and a combination of a compression ratio of 14:1 and a CN 85 fuel. The ignition delay of the latter combination was shorter than that of the former, but both combinations provided a sufficiently long ignition delay to achieve premixed combustion.

13.6.3 Possibility of meeting SULEV standard

The test car results obtained with MK combustion using a compression ratio of 14:1, GTL fuel with a cetane number of 85 and the 5-way catalyst system are shown in Fig. 13.18. The combination of a lower compression ratio and the high cetane GTL fuel reduced cold-start emissions without any deterioration of emission performance under high load conditions. The test car results indicate that the combination of MK combustion and GTL fuel has the possibility of meeting the SULEV standards.

Combustion concepts such as HCCI have been investigated by many researchers and institutes for more than 10 years. On the other hand, the recent circumstances around diesel engines is changing rapidly.

For example, Diesel Particulate Filter (DPF) first appeared a few years ago, but recently DPF are becoming a standard technology for diesel vehicles. Concerning market situation, diesel car share in Europe has been increasing and reached near 50%. On the other hand, diesel share of passenger cars in Japan has significantly reduced. And there is a global trend to enforce more stringent regulations to the same level as that of gasoline engines. The current

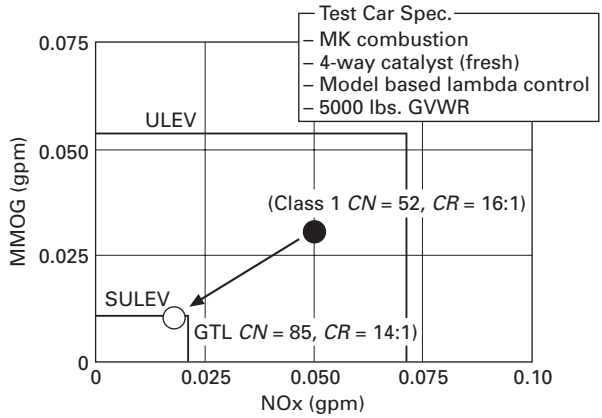

13.18 Possibility of attaining SULEV emission levels.

situation provides key direction for the future; customer value, DPF as standard equipment and low NOx technology. To consider new combustion concepts based on these future key direction, Low NOx combustion with DPF is proposed as one of candidates for future research direction. And as this chapter points out, the main subject of low NOx combustion is HC emission control. Furthermore, robust controls, fuel distribution management and high cetane number are suggested as the key solutions of HC reduction for future diesel combustion improvement.

13.7 References

1. Allen W. Gray and Thomas W Ryan, 'Homogenious Charge Compression Ignition (HCCI) of Diesel Fuel', SAE Paper No. 971676, 1997.
2. Iida N., 'Alternative Fuels and Homogeneous Charge Compression Ignition Combustion Technology', SAE Paper No. 972071, 1997.
3. Furutani M., Ohta Y., Konno M. and Hasegawa, M., 'An Ultra-Lean Premixed Compression-Ignition Engine Concept and Its Characteristics', Proceedings of the Fourth International Symposium COMODIA 98, pp. 173–177, 1998.
4. Takeda Y., Nakagome K. and Niimura K., 'Emission Characteristics of Premixed Lean Diesel Combustion with Extremely Early Staged Fuel Injection', SAE Paper 961163, 1996.
5. Yanagihara H., Sato Y. and Mizuta J., 'A Study of DI Diesel Combustion under Uniform-Higher Disparaged Mixture Formation', The 13th International Combustion Engine Symposium Lecture, 1996, pp. 365–369 [in Japanese].
6. Akagawa H., Miyamoto T., Harada A., Sasaki S., Shimazaki N., Hashizume T. and Tsujimura K., 'Approaches to Solve Problems of the Premixed Lean Diesel Combustion', SAE Paper No. 1999-01-0183, 1999.
7. Rudolf H., Stanglmaiar and Charles E. Roberts, 'Homogeneous Charge Compression Ignition (HCCI): Benefits, Compromises, and Future Engine Applications', SAE Paper No. 1990-01-3682, 1999.

8. Kimura S., Matsui Y. and Itoh T., 'Effects of Combustion Chamber Insulation on the Heat Rejection and Thermal Efficiency of Diesel Engines', SAE Paper 920543, SAE Trans., 1992.
9. Kimura S., Matsui Y., Ogawa H. and Enomoto Y., 'Effects of Combustion Chamber Specifications and Swirl Ratio on Performance of Light-Duty DI Diesel Engines', Proceedings of FISITA Congress 96, 1996, pp. 02, 13.
10. Enomoto Y., Ishii A., Kimura S. and Iida N., 'Thin Film Thermocouple for Instantaneous Surface Temperature Measurement of a Metallic and Ceramic Combustion Chamber Wall', IMechE Paper C496/011/95, 1998.
11. Ogawa H., Matsui Y., Kimura S. and Kawashima J., 'Three-Dimensional Computation of the Effects of the Swirl Ratio in Direct-Injection Diesel Engines on NOx and Soot', SAE Paper 961125, 1996.
12. Kimura S., Aoki O., Ogawa H., Muranaka S. and Enomoto Y., 'New Combustion Concept for Ultra-Clean and High-Efficiency Small DI Diesel Engines', SAE Paper 1999-01-3681, SAE Trans., 1999.

14

HCCI fuel requirements

T W RYAN III, SWRI, USA

14.1 Introduction

HCCI involves complex physical processes including atomization, mixing and evaporation, as well as complex chemical reactions that occur over a range of temperatures from 700–1000K. Fuel properties and composition are important in all of the physical and chemical processes. This chapter focuses on a summary of the more important findings regarding the fuel effects on HCCI operation. The historical background is presented first, followed by separate descriptions of the diesel-like fuel and the gasoline-like fuels for HCCI operation. An effort is made to lead the reader to the conclusion that optimum HCCI operation requires a fuel specially formulated for HCCI. The chapter concludes with a discussion of the fundamental aspects of fuel composition interactions in HCCI and a brief outline of work required for development of an HCCI fuel specification.

14.2 Background

The development of fuels for use in internal combustion engines has historically been an evolutionary process in which fuel-related problems are encountered and critical fuel properties are identified and specific limits (or specifications) defined to mitigate the problem. Typically, these critical properties are identified through engine experiments and, for the most part, simplified laboratory tests or measurements are developed to measure the critical property. This process of fuel 'specification' is exemplified in the ASTM D975 specification for diesel fuel and ASTM 4814 for motor gasoline.

The properties or characteristics listed and limited in the specifications are generally called performance properties because they identify some critical performance characteristic when used in normal engine service. There have historically been very few composition based specification properties. The specifications may include properties that affect engine operation or durability. Examples of specified operational properties of diesel fuel include pour and

cloud point, viscosity, and specific gravity. Durability properties include particle contamination, high temperature stability, and lubricity. The gasoline specification includes similar operation and durability properties.

The only specification properties directly related to combustion include the cetane number (ASTM D613) for diesel fuel and octane number (ASTM D2669 or ASTM D2700) for gasoline, and these are really performance properties related to ignition characteristics as measured in specified test engines. Cetane number, as measured in a variable compression ratio CFR engine, is basically a measure of the ease of auto igniting the given diesel fuel sample. It is really a measure of the compression ignition temperature at constant ignition delay time, measured at a specific test condition. Cetane number is important in diesel engines because it defines the required compression ratio for starting and for cold smoke elimination. The octane number of gasoline is also measured in a variable compression ratio CFR test engine, but of different design than the cetane rating engine. In the case of octane number, the measurement is an indication of the propensity of the given fuel to resist auto ignition. It is really a measure of the propensity of the gasoline sample to auto ignite at specific engine test conditions, and as compared to reference fuels run at the same engine conditions. Octane number is important because it provides an indication of the gasoline sample's ability to resist knock, a potentially damaging reaction mode in spark ignition engines.

A relatively new internal combustion engine concept receiving a great deal of attention involves what most generally can be called low temperature combustion. There are several different approaches being examined to achieve these low temperatures, and thus low NOx emissions, concepts each with its own acronym. In what is considered by the author to be the purest form of low temperature combustion, HCCI involves compression ignition of a homogeneous fuel-air mixture, providing the lowest emissions and highest efficiency potential. The recent dramatic increase in the technical literature on HCCI provides an indication of the international interest in low emissions combustion technology. Initially, the efforts reported in the literature focused on developing engine concepts that could use either existing gasoline or diesel fuel. Much of this work continues with compromises in terms of the operating range and/or in the achievement of 'pure HCCI', introducing corresponding degradation of the fuel consumption and engine out emissions levels.

It is worthwhile spending some time here on defining in detail 'pure HCCI'. In the most literal case, a homogeneous mixture is one in which there are no gradients in composition or temperature. If this mixture condition is maintained in the engine throughout the intake and compression processes then reactions will begin when the compression temperature reaches the auto ignition temperature of the mixture, and reaction would occur throughout the mixture at the rate primarily defined by the thermodynamic conditions at the

start of reactions. As indicated by Dec *et al.* [1] and demonstrated in Fig. 14.1, the reaction duration under these conditions would be in the order of 1°CA, resulting in extremely high rates of pressure rise. As indicated in the figure, the actual reaction duration is typically on the order of 3 to 7°CA, due to thermal and composition stratifications.

Fuel composition (assuming normal hydrocarbon-based fuels) has little impact on the reaction rate and reaction duration once reaction is initiated. Composition, however, does define the initiation temperature, or the auto ignition temperature.

Reactions in HCCI engines generally involve a two-stage process, including both the so-called low temperature and high temperature reactions. In general, the initial reactions do start at relatively low temperatures, on the order of 750 K. The high temperature reactions typically start in the range of 950 K. Plate 15 (between pages 268 and 269) is a set of typical heat release rate diagrams from an HCCI engine operating on a fuel that does demonstrate significant amounts of low temperature reaction. Also shown in Plate 15 (between pages 268 and 269) is a significant problem inherent in going to higher loads in HCCI engines, and that is the very strong tendency for the main reaction to advance resulting in unacceptable heat release rates and rates of pressure rise.

A more detailed analysis of Plate 15 (between pages 268 and 269) indicates that two things happen as load increases. First the start of the low temperature reactions occurs earlier, presumably due to increased engine temperatures as the load is increased. The second observation is that the amount of energy liberated in the low temperature phase increases, due to introduction of increased quantities of the components contributing to the low temperature

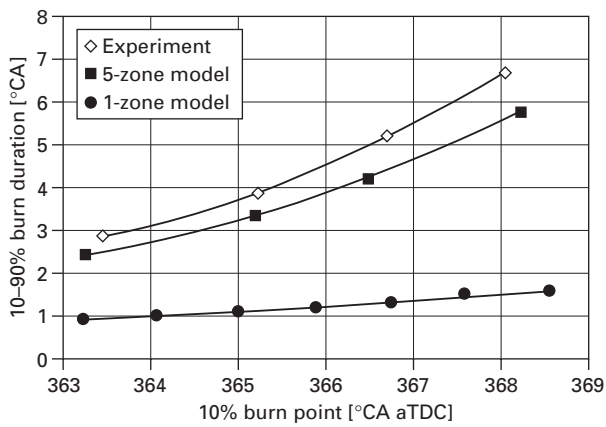

14.1 Reaction durations as function of equivalence ratio (Dec *et al.* [1]).

reactions as associated with the increased total fuel quantities. A third observation is the fact that the combination of advanced low temperature reactions and increased energy liberation in the low temperature reactions results in significant advances and higher heat release rates in the main reaction.

It should be noted that fuel composition mainly affects the amount of low temperature reaction that occurs in HCCI engines, and this in turn affects when reaction is initiated and where in the cycle the main reactions occur. Fuels like gasoline exhibit little or no low temperature reaction and initiation temperatures on the order of 950K in HCCI engines. Fuels like diesel fuel exhibit significant low temperature reaction and corresponding initiation temperatures in the range of 750K in HCCI engines. The specific effects of composition will be discussed in the following sections.

14.3 Diesel fuel HCCI

Early HCCI engine developments were based primarily on diesel engines using diesel fuel. This was, in fact, a logical approach at the time, due to the significant difficulty of catalytically reducing NOx in lean combustion systems and also due to the existing mode of compression ignition used in both diesel and HCCI mode. This work continues, but more recently has focused on limiting the required compromises in both the engine operating range and the potential HCCI emissions and fuel consumption opportunities.

Some of the earliest diesel fuel based HCCI demonstrated the limits of using diesel fuel in the 'pure HCCI' mode [2–4]. Diesel fuels typically have 90% distillation points in the range of 340°C. The volatility, or the distillation characteristics of the fuel, dominates the evaporation of the fuel in the combustion chamber. For true HCCI engine operation, all of the fuel must be evaporated, and at least partially mixed, prior to the start of reaction. It has been shown [2–4] that if liquid fuel survives through the start of reaction, these fuel droplets, or packets, will burn as diffusion flames with dramatically elevated production of soot and NOx. It can be observed that an increase in soot formation, as indicated by an increase in BSN (Bosch Smoke Number) from zero, signals the onset of non-HCCI operation. It appears that this onset occurs in the range of intake air temperatures from 130 to 150°C, for diesel fuel and blends of gasoline and diesel fuel. These trends are demonstrated in Fig. 14.2, where the BSN is plotted versus intake air temperature. In general, the presence of gasoline tends to reduce the temperature, but the limit is still above 130°C. Droplet evaporation calculations were performed to determine the fate of the fuel during compression. These calculations indicated that the intake temperature had to be greater than 120°C for all of the diesel fuel blends. This temperature is of concern because of the potential impact on the volumetric efficiency. In addition, it was observed that this intake temperature

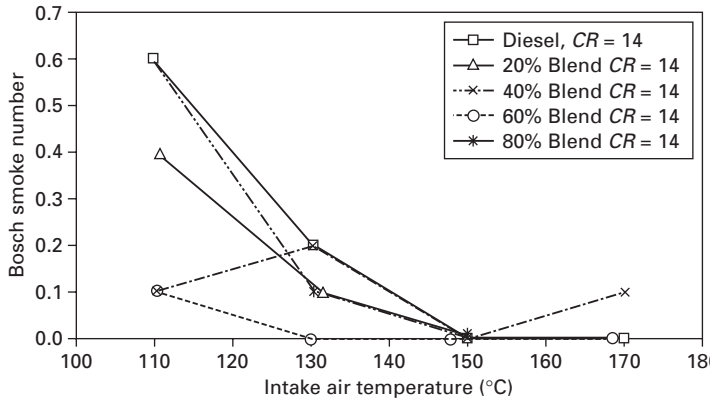

14.2 BSN versus intake air temperature for various gasoline and diesel fuel blends. *CR* = 14:1, *A/F* = 40:1, no EGR.

leads to early start of reaction (SOR) for diesel fuel and all of the blends that contain diesel fuel. Acceptable HCCI operation (close to 'pure HCCI') on diesel fuel was only possible at intake manifold temperatures of 130°C or higher, and compression ratios of 8:1 or less.

The SOR appears to be dominated by the auto ignition temperature of the fuel and the temperature history of the fuel air mixture. In an effort to control the SOR, a variety of different fuels have been considered. One interesting fuel tested at Southwest Research Institute was naphtha from Fischer Tropsch processing of natural gas. The results of these experiments indicated that this particular fuel addressed the volatility, or mixture preparation problem, but it did not totally address the SOR issues.

The results of engine SOR analysis for gasoline-diesel fuel blends and for Fischer Tropsch naphtha are shown in Fig. 14.3. It should be noted that the results in Fig. 14.3 were based on tests designed to achieve the maximum load at each condition, so that air-fuel ratio did vary from test to test. The EGR level was zero in all cases. The lowest intake manifold temperatures that could be used with the gasoline and diesel fuel blends were in the range of 110 to 130°C. Attempts to use lower temperatures resulted in the onset of sooty diffusion burning. The exception was gasoline. Gasoline would not react at the lower temperatures, even when the compression ratio was increased to 16:1. There were no temperature limits on the Fischer Tropsch naphtha. In fact, it can be seen that the use of the naphtha actually improved the performance in two ways. First, it did not revert to sooty diffusion burning, even as the intake temperature was reduced to ambient levels (the BSN was zero for all of the Fischer Tropsch naphtha runs). Second, the SOR was retarded due to the reduced intake temperature.

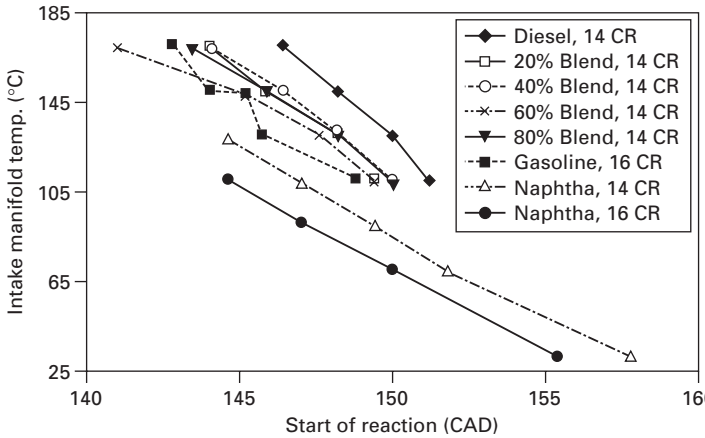

14.3 Intake manifold temperature versus start of reaction.

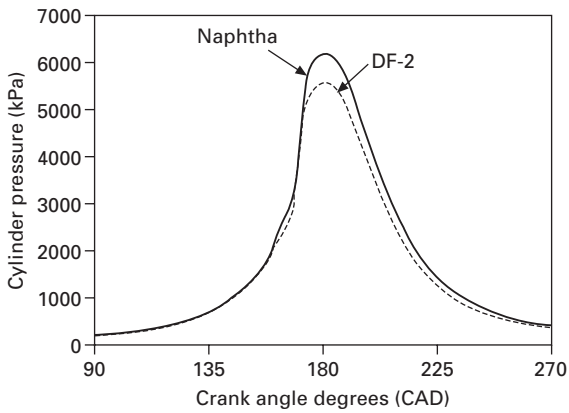

14.4 Cylinder pressure comparison (same conditions as Fig. 14.2).

The results for the naphtha fuel used in testing were encouraging with respect to intake temperature and combustion characteristics. Naphtha has reaction timing similar to that of DF-2 fuels at similar temperatures; however, it also provides the HCCI reaction at ambient intake air temperatures. There is no comparison of the smoke levels of the two fuels because, as indicated above, naphtha fueled HCCI produced zero smoke at all tested conditions, indicating that total fuel evaporation was possible at low intake manifold temperature when using the naphtha.

Review of the combustion data reveals that the peak cylinder pressure is greater for naphtha fueled HCCI (Fig. 14.4), the peak value of the main heat release rate is less (Fig. 14.5), and the cumulative heat release is greater (Fig. 14.6). These results were obtained at approximately the same IMEP, but at

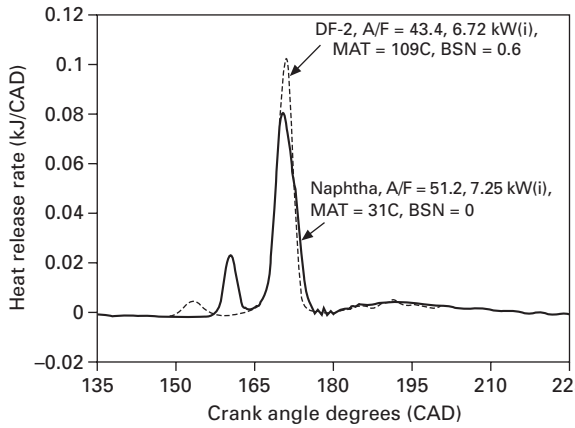

14.5 Heat release rate comparison (same conditions as Fig. 14.2).

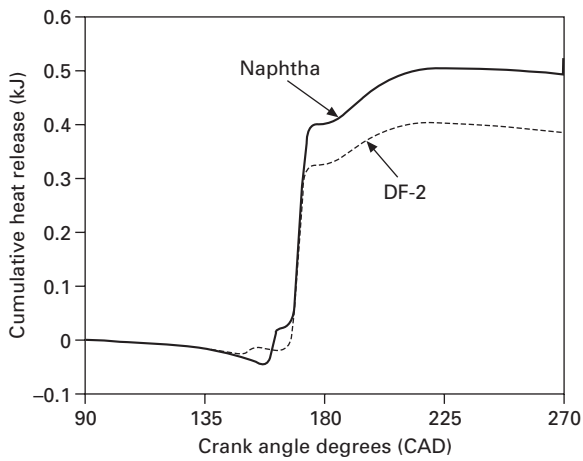

14.6 Cumulative heat release comparison (same conditions as Fig. 14.2).

different MATs, with the diesel tested at approximately 130°C and the Fischer Tropsch naphtha tested at approximate 28°C MAT. The reaction characteristics of HCCI are very interesting. As indicated above, the reaction of hydrocarbon fuels in an HCCI engine typically demonstrate a two-phase type of reaction. This is demonstrated in Fig. 14.5, where the heat release rate diagrams for diesel fuel and Fischer Tropsch naphtha are compared. It can be seen that the naphtha, in addition to having a larger pre-reaction heat release, also had a significantly delayed SOR (start of reaction), based on the pre-reaction heat release. It should also be noted, however, that the main heat release occurred at the same timing as that of the diesel fuel.

The most noticeable difference in the shape of the heat releases shown in the Fig. 14.6 is that the initial heat release of the naphtha run is greater than that of the diesel fuel run. The SOR occurs later in the engine cycle and a greater fraction of the fuel is consumed during the initial heat release. This has the effect of moving the peak cylinder pressure closer to TDC. The cumulative heat release rate is different than typical diesel combustion, most likely due to completion of combustion prior to TDC.

Prior to testing, it was expected that the cetane number (CN) of the naphtha would be significantly lower than that of the diesel fuel. In fact, it was found to be the same as the diesel fuel, 46CN. This observation raised the question as to the application of CN as a fuel rating parameter for SOR in HCCI engines. The results presented in Fig. 14.5 indicate very clearly that the CN is not a universal indicator of the fuels SOR characteristics in an HCCI engine. In this case the CN variation is negligible but the engine results indicate that the SOR does have a large variation. These results suggested that some measure of the auto ignition temperature might provide a better indication of the fuels propensity for reaction in an HCCI engine.

The results presented in Fig. 14.7 clearly demonstrate the validity of this assumption, where the temperature histories for a number of HCCI runs on the same diesel fuel are compared. These temperature histories were computed from the measured cylinder pressures, using the ideal gas assumptions. The differences in the runs are intake temperatures, compression ratio, and load. In all cases the temperature at SOR (based on the timing of the pre-reaction heat release) was approximately the same, as indicated by the end points (approximately 400°C) in the plots. The absolute value of 400°C may not be

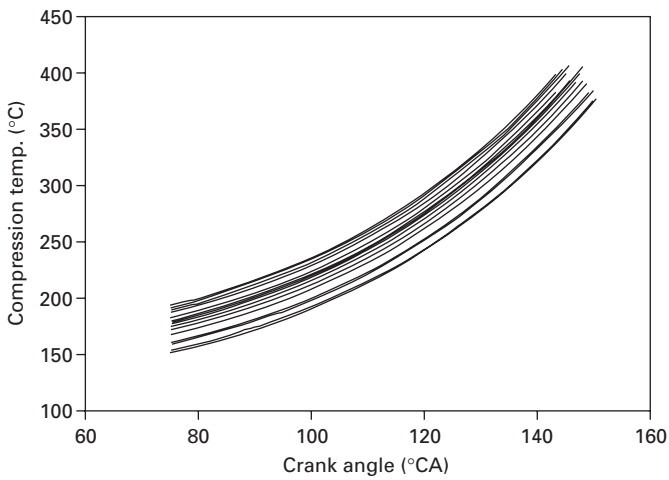

14.7 Bulk gas temperature during compression and SOR temperature.

accurate due to the assumptions used in the calculation of the compression temperature histories. The largest errors are probably introduced through the assumed initial temperature, where heat transfer during the intake process was not accounted for in the calculation.

Fundamentally, the start of reaction is related to the time-temperature history of the fuel-air mixture, the ratio of fuel to air, and the activation energy of the fuel. The thermodynamic history is relatively easy to address through calculation, however, the activation energy is very difficult to determine as a fuel specification property and even more difficult to apply in the changing thermodynamic environment of the engine. The SwRI engine experiments provided some indication that the start of reaction can be related to the auto ignition temperature of the fuel. Current standard test methods for determining the auto ignition are generally related to atmospheric condition safety issues and do not provide data representative of the conditions encountered in engines. Researchers at Southwest Research Institute have developed a new test method that is claimed to be effective in defining the required ignition characteristics for HCCI engine operation. This will be discussed further in the next section.

14.4 HCCI fuel ignition quality

The ignition and reaction characteristics presented in the heat release rate diagrams presented in Fig. 14.6, are typical of fuels with relatively large levels of low temperature reaction. As indicated above, this is typical of diesel-like fuels, or fuels which auto ignite easily at relatively low temperatures. The effects of fuel composition on the low temperature reactions are discussed in another section.

The approach taken in the Southwest Research Institute work [5] was to determine the ignition delay time as a function of the initial air temperature in a commercially available constant volume combustion bomb apparatus currently used in diesel fuel cetane rating (ASTM D6890), called the Ignition Quality Tester, or IQT. The goal was to develop relationships between the ignition delay time and the test temperature, or conversely, ignition temperature (test temperature) as a function of the delay time.

Four different sets of fuels were examined in this effort. The sets consisted of the following:

1. Hexadecane and heptamethylnonane blends (primary reference fuels for cetane number rating).
2. Isooctane and n-Heptane blends (primary reference fuel for octane number rating).
3. Diesel fuel and gasoline blends
4. Fischer Tropsch naphtha (FTN) and ethyl hexyl nitrate (EHN) (additized fuels to test alternative method for cetane number variation).

All of the fuels were tested in the IQT at approximately the same initial temperatures, 460, 480, 500, and 530°C. A fuel residence time, or ignition delay time, typically encountered in an HCCI engine was selected, and using this ignition delay time and the IQT data it was possible to determine the temperature required to give this ignition delay time. This temperature represents the point at which each fuel starts to react in the same time period in the HCCI engine, and it is called the elevated pressure auto ignition temperature, or EPAIT.

In addition to the ignition temperature versus the ignition delay time relationships, the cetane numbers of each test fuel were also either defined by the blend ratio (primary reference fuels) or determined in the IQT. It was possible to plot the EPAIT versus the cetane number. These data are presented in Fig. 14.8, where the EPAIT is plotted for all test fuels versus the cetane number. The results demonstrate what appears to be some relationship between the EPAIT and the cetane number, however, the relationship is not universal and there is some scatter about the line. The un-additized FT fell on the curve, but the data for the additized FT fuels deviated from the curve. It is not suggested that CN be used as a measure of ignition quality for HCCI engine fuels. The correlation is presented only to demonstrate the problem associated with the use of CN for this purpose. As will be demonstrated, octane number (ON) is even a worse indicator of ignition quality in these engines.

One of the test fuel sets consisted of blends of the primary reference fuels for octane rating of gasolines. Since the cetane numbers of these reference fuel blends were also determined in the IQT experiments, it was possible with the IQT data to relate the cetane and the octane numbers. These data are

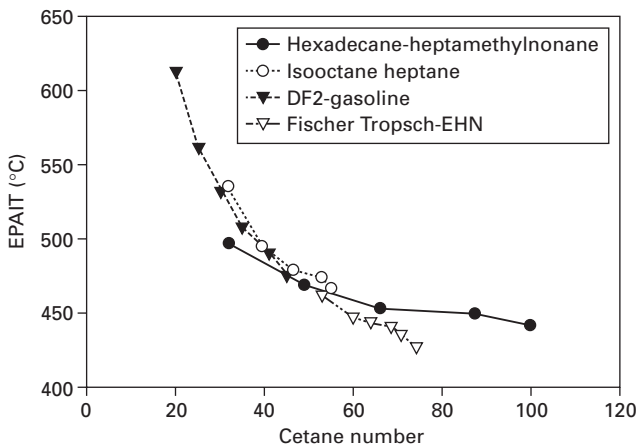

14.8 Elevated pressure auto ignition temperature versus cetane number.

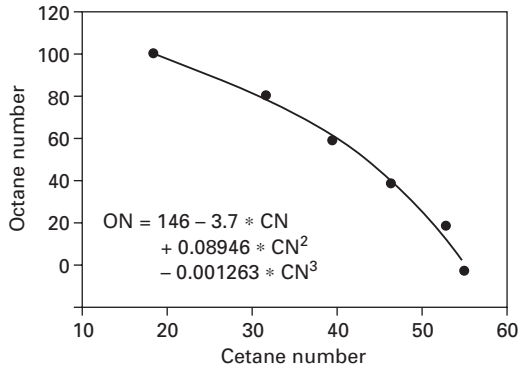

14.9 Relationship between octane and cetane numbers using isooctane and heptane fuels.

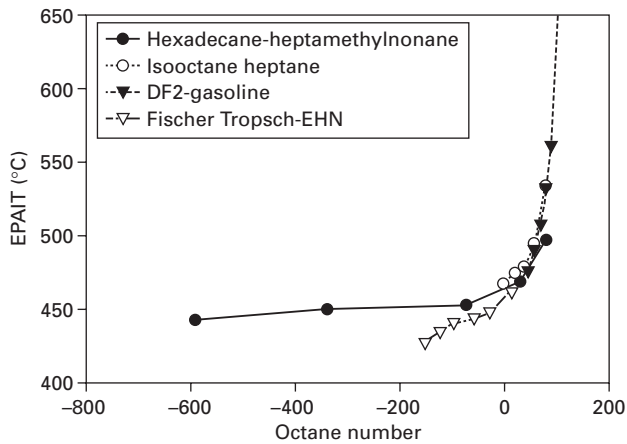

14.10 Elevated pressure auto ignition temperature versus octane number.

plotted in Fig. 14.9. The regression equation, relating the ON to the CN is also presented in Fig. 14.9.

While the expression presented in Fig. 14.9 may not be universally applicable it was used to estimate the ON of all of the other test fuels. (In fact, extrapolation over the entire cetane number range (15 to 100) results in extremely negative octane numbers.) It was then possible to plot the EPAIT versus the ON, as presented in Fig. 14.10. As can be seen, there is a relationship between the EPAIT and ON, but it requires significant extrapolation of the ON scale into the negative ON range, a meaningless extrapolation. In addition, in the range of application of the ON scale the slope is very steep. It should be noted that all of the test fuels have been successfully tested in the HCCI engine, meaning

that the fuel actually reacted and produced work in the engine. Under these circumstances reactions were initiated, thus indicating that there is some fuel property that represents their ignition characteristic in the engine. It is clear that ON is not a good parameter for this purpose.

The results of these experiments indicate that the IQT can be used to determine the EPAIT of candidate HCCI fuels. It is also apparent that this parameter is somewhat related to both the ON and CN. The results also do indicate, however, that ON and CN are not necessarily good rating parameters for all of the potential HCCI fuel candidates because of the limitations on the ranges of these two methods that are imposed by the use of the specific reference fuels. In other words, neither ON nor CN have adequate range to provide the needed scale for all possible HCCI fuel candidates. The EPAIT, on the other hand, is a fundamentally based measurement, not dependent on specific reference fuel behavior, and not limited in range.

It has also been observed that fuels can have the same EPAIT and significantly different locations of the main, or high temperature reactions. This phenomenon is presented in Fig. 14.11, where the cumulative heat release rate diagrams are presented for three fuels that have similar EPAIT and ON. Note that the EPAIT does accurately predict the start of the low temperature reactions (all fuels have the same start of reaction). Note, also that the magnitudes of the cool flame reactions are significantly different and that the start of the main reactions appear to be related to the magnitude of the low temperature reactions. Figure 14.12 is a plot showing the relationship between the magnitude of the low temperature reactions and the timing, or phasing between the start of the low temperature reactions and the start of the high temperature reactions.

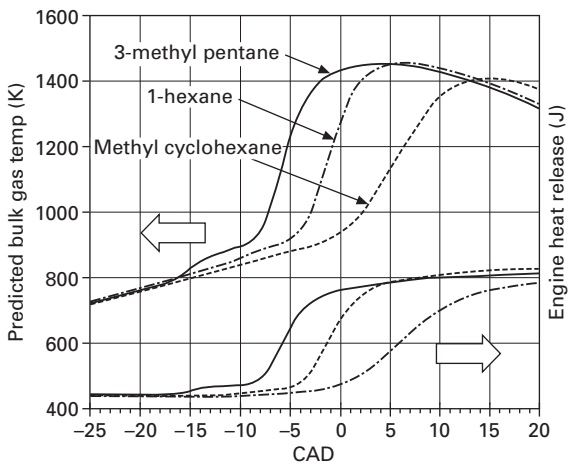

14.11 Cumulative heat release rate diagrams for three fuels with the same EPAIT.

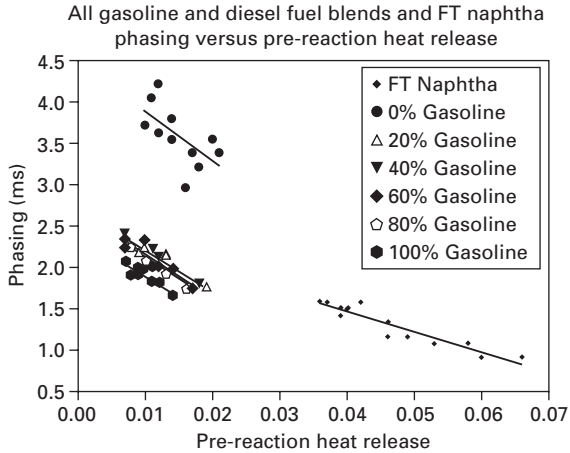

14.12 Phasing between the low temperature reactions and the high temperature reactions for fuels that support low temperature reactions.

It is clear in Fig. 14.12 that the onset of the main reaction is dependent on the magnitude of the low temperature reactions, for fuels that demonstrate low temperature reaction. Basically, the low temperature reaction increases the temperatures in cylinder, leading to earlier onset of the high temperature, or main reactions. This is clearly demonstrated in experiments with increasing load (richer air-fuel ratios) as shown in Fig. 14.13, where it can be seen that the magnitude of the low temperature reactions increase with richer mixtures (higher loads), due simply to the fact that there are larger quantities of the fuel components that produce low temperature reactions in these richer mixtures. This is not the case for fuels that exhibit little or no low temperature reactions. Dec *et al.* [6–7] have shown this in Plate 17 (between pages 268 and 269) using a modeling approach. It can be seen in the figure that the reaction timing is not affected by load as it was in the case of the fuel with low temperature reactions.

14.5 Gasoline HCCI

As pointed out above, mixture preparation in HCCI engines is dramatically easier with gasoline-like fuels than with diesel-like fuels. It was also pointed above, however, that it is very difficult to initiate reaction in gasoline HCCI engines due to the high auto ignition temperature of gasoline. The EPAIT for a representative gasoline and a representative diesel fuel, and other fuel blends are presented in Fig. 14.14. The plot is similar to Fig. 14.8, but with the addition of the data for the representative gasoline, diesel fuel, and the Fischer Tropsch naphtha. As can be seen, the diesel fuel falls in the lowest

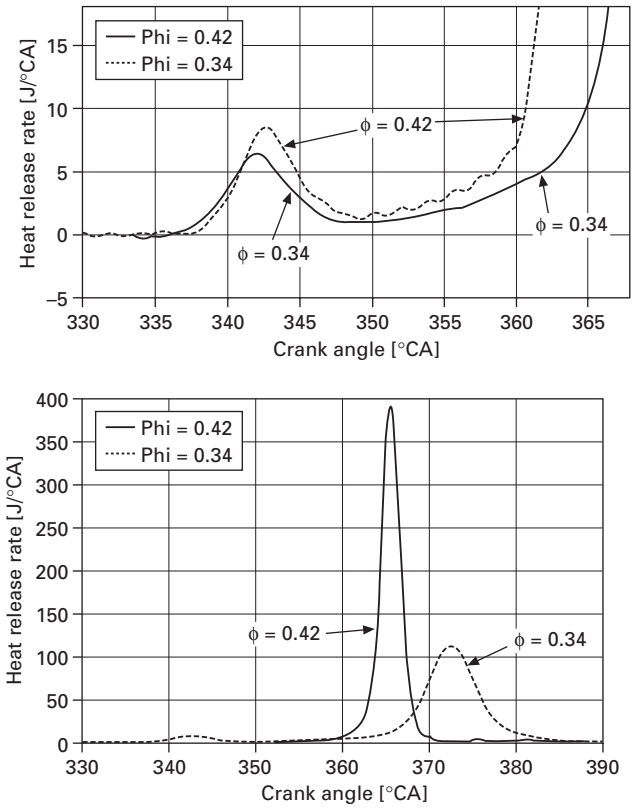

14.13 Heat release rate diagrams for two different equivalence ratio tests using a fuel that demonstrates low temperature reactions (Dec *et al.* [7]).

range, with EPAIT values in the order of 450°C, while gasoline falls in the highest regions, with EPAIT values in the range of 650°C.

Cycle simulation analysis has been used to compute the compression temperature histories as a function of compression ratio (11.5–17.5:1), intake manifold temperature (20–100°C), and engine speed (1200–2400 rpm). These predictions are presented in Figs 14.15–14.17, where the gasoline and diesel fuel EPAITs are also plotted and annotated. As can be seen, the start of reaction is very early for fuels with ignition characteristics like diesel fuel, or fuels with EPAIT values in the range of 400–450°C (723–773 K). On the other hand, fuels with EPAIT values in the range of gasoline, 600–650°C (923–973 K), may not react under any of the engine operating conditions examined in the figures. These results indicate that neither gasoline nor diesel fuel have the correct EPAIT for operation in practical conventional engines.

Researchers have worked diligently to increase the compression temperatures in gasoline-fueled HCCI engines to overcome the high EPAIT with gasoline.

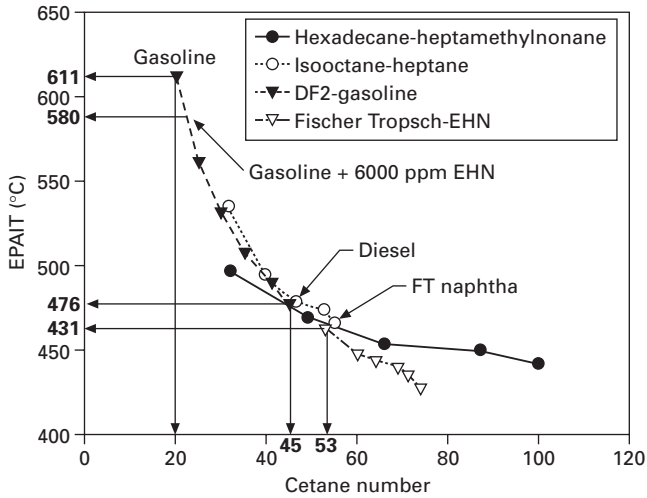

14.14 EPAIT versus cetane number for a variety of fuels.

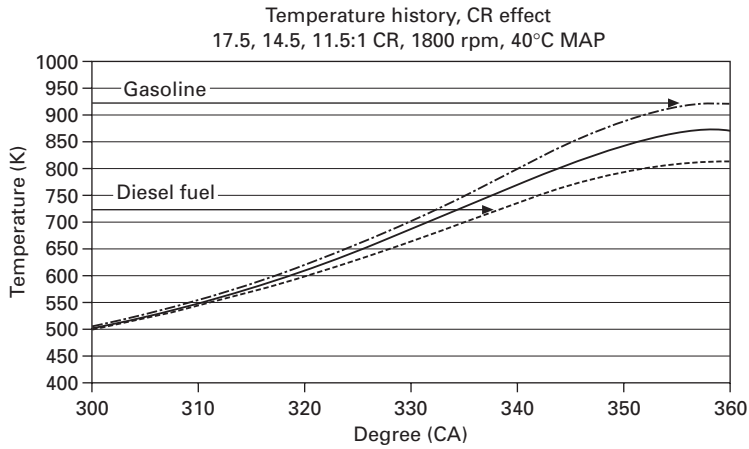

14.15 Predicted compression temperature histories at three compression ratios.

The most popular approach is to use internal EGR, this is exhaust gas that is retained in-cylinder usually through early exhaust valve closing. Promising work in this area, generally referred to as negative valve overlap, incorporates direct injection, with some fuel being injected during re-compression resulting from the lack of overlap between the exhaust and intake processes. This is demonstrated in Fig. 14.18 and 14.19, where various injection timings are annotated on a valve actuation schedule in Fig. 14.18 and the resulting heat release rate diagrams are presented in Fig. 14.19. Note that DI HCCI is

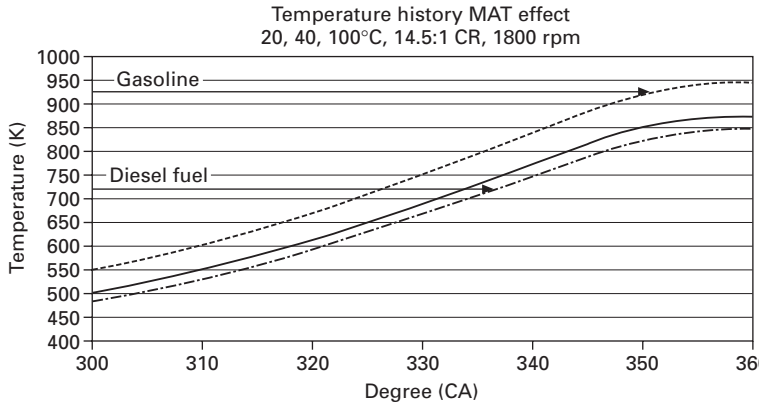

14.16 Predicted compression temperature histories with three different intake air temperatures.

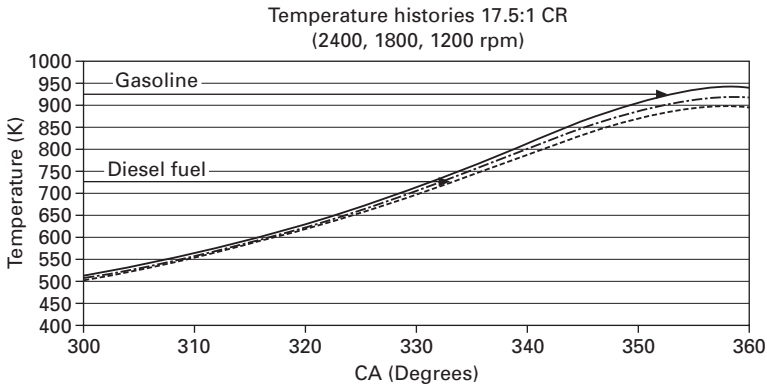

14.17 Predicted compression temperature histories at three different engine speeds.

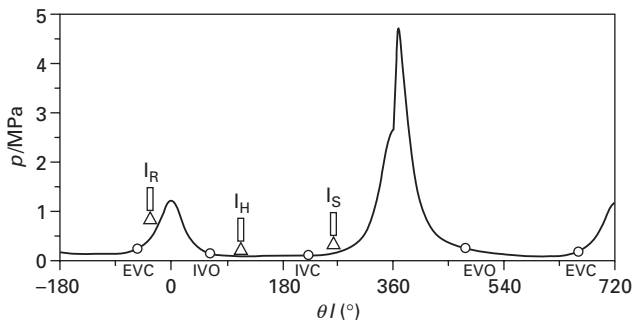

14.18 Cylinder pressure diagram showing valve timing and DI fuel injection strategies to achieve acceptable ignition in gasoline HCCI [8].

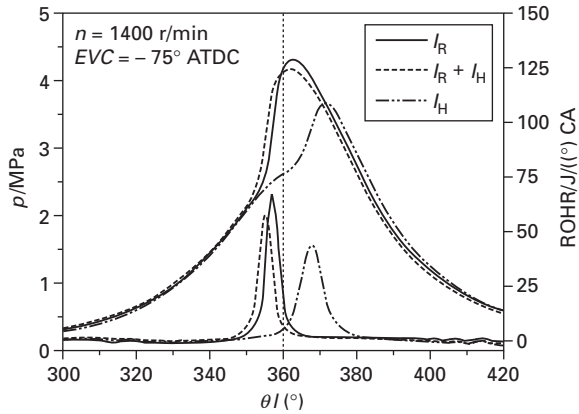

14.19 Heat release rate diagram for different fuel injection strategies [8].

possible with gasoline because gasoline will atomize and evaporate with a characteristic time equivalent to or less than the ignition delay time of the fuel. This relates to the fact that gasoline typically exhibits little or no low temperature reaction.

14.6 HCCI fuel specification

It should be clear from the discussion above that mixture preparation in HCCI engines is greatly enhanced if the boiling point distribution of the fuel is more like gasoline than diesel fuel. It is possible that end points higher than gasoline may be acceptable, but the end point of diesel fuel is definitely too high for acceptable HCCI engine operation. It is also clear that the ignition temperatures (EPAIT) of diesel fuels are too low, while those for typical gasolines are too high for practical conventional engine design.

Volatility and ignition characteristics are the two properties that will ultimately differentiate HCCI fuels from gasoline and diesel fuel. As mentioned above, the ideal HCCI fuel will have 90% and end points below current diesel fuel. The optimum maximum end point has not yet been defined. The ignition characteristics that are important are the temperature at which reaction begins and the magnitude of the low temperature reactions.

As indicated previously, Southwest Research Institute researchers have developed a fuel specification type test method for rapidly evaluating and rating the ignition characteristics of HCCI fuels. The start of reaction temperature is measured using the ASTM D6890 specified apparatus. This temperature is called the Elevated Pressure Auto ignition Temperature, or EPAIT. This parameter accurately identifies the temperature at which reactions begin for fuels that have all levels of low temperature reactions. In the case

of fuels with low temperature reaction the EPAIT identifies the temperature at which these reactions are initiated. The EPAIT identifies the start of the high temperature reactions for those fuels that have no low temperature reactions. This observation is demonstrated in Fig. 14.14, where the diesel fuel did display significant low temperature reactions and this is reflected in the low EPAIT values. The gasoline, on the other hand did not have low temperature reactions and this is reflected in the high value of the EPAIT. As a gross simplification, low temperature reactions typically occur in the range of 750 K (470°C), close to the measured EPAIT for diesel fuel. The high temperature reactions are usually assumed to occur in the range of 950 K (670°C), very close to the measured EPAIT for the gasoline sample shown in Fig. 14.14.

The second important fuel ignition characteristic for HCCI engine operation is the magnitude of the low temperature reactions. For fuels that exhibit low temperature reaction, the magnitude of the low temperature reaction is proportional to the fueling rate, or load – more fuel gives more low temperature reaction. It was shown above that the timing of the main or high temperature reactions is directly related to the magnitude of the low temperature reactions. So in addition to the EPAIT, the ASTM D6890 apparatus is being used to directly measure the magnitude of the low temperature reactions. Figure 14.20 shows a heat release rate diagram measured in the IQT (ASTM D6890). As can be seen, the heat release rate diagram is very similar to the typical HCCI engine heat release rate diagram. This offers the opportunity to use the same apparatus and test method to measure both ignition characteristics, the EPAIT and the low temperature reactions.

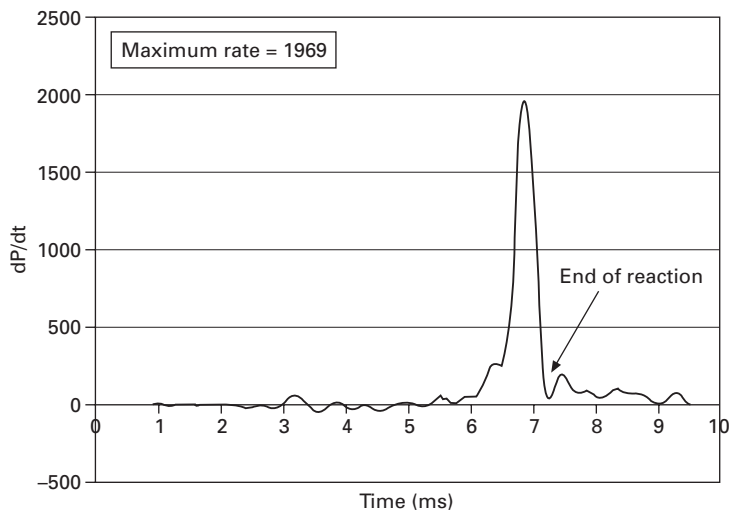

14.20 Heat release rate diagram measured in the IQT.

While a great deal of information is available in the literature regarding the optimum HCCI fuel, as of now there are no clearly defined specifications. As indicated above, the volatility of the optimum fuel will include the gasoline boiling range, extending perhaps into the kerosene range. One very clear limit is that the 90% and end point should not exceed the jet fuel limits.

Roughly, the optimum ignition quality should fall in between gasoline and diesel fuel. Gasoline auto ignition temperature is too high and diesel fuel ignition quality is too low. While not universally accurate in rating the ignition quality of HCCI fuels, cetane and octane do provide a somewhat empirical impression of the requirements. Using these more traditional parameters, it appears that the ideal fuel should have a cetane number in the range of 30 and an octane number in the range of 75. Based on the preliminary work at Southwest Research Institute, the EPAIT specification will likely fall in the range of 550°C with cool flame magnitudes in the range of 5–10% of total heat release.

14.7 Fundamental fuel factors

Control of a fuel's EPAIT and cool flame magnitude are fundamentally related to composition. The effects of fuel composition have been studied extensively and a clear understanding has been developed between composition and the EPAIT and the magnitude of the cool flame. In general terms, normal paraffins tend to lower EPAIT and increase the magnitude of the cool flame reactions. The cyclic hydrocarbons tend to suppress the low temperature reactions so that the EPAIT is increased and the low temperature reactions reduced with the addition of these materials. Everything else has very low propensity for low temperature reactions and there seems to be little specific correlation with the start of the high temperature reactions, with some exceptions such as methane.

Shibata *et al.* [9–10] have presented probably the most extensive data base and analysis of the specific fuel component effects. The effects of the normal paraffins and the aromatic compounds are demonstrated in Fig. 14.21 where it can be seen that as little as 6.5% of n-heptane added to a base fuel can dramatically advance and increase the low temperature reactions, which in turn advances the high temperature reactions. In addition, it can be seen that the addition of as little as 6.5% toluene delays and reduces low temperature reactions, resulting in a delayed main reaction, with lower peak heat release rate.

Shibata [9] has also quantified that the relative effects of various hydrocarbon types on the HCCI reactions. Their rankings are presented in Fig. 14.22, where the coefficients of a regression equation predicting the CA50 point (crank angle location of the 50% burn point). The coefficients indicate that the normal paraffins have large effect on advancing the 50% burn point, while the aromatics have a large effect on retarding the 50% burn point.

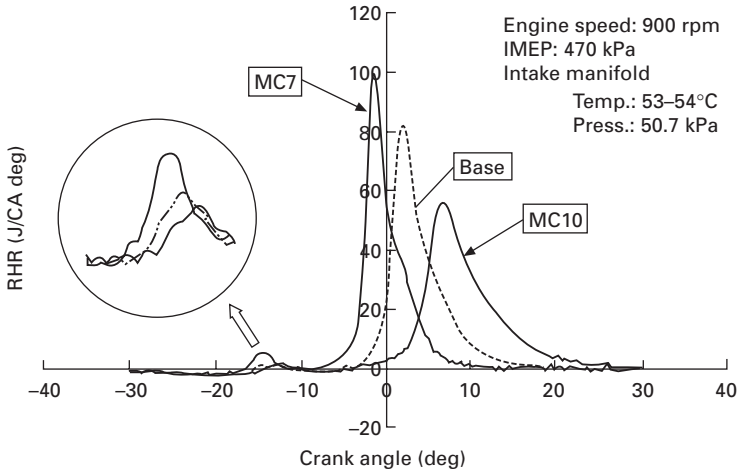

14.21 Effects of fuel composition in low and high temperature reactions [9].

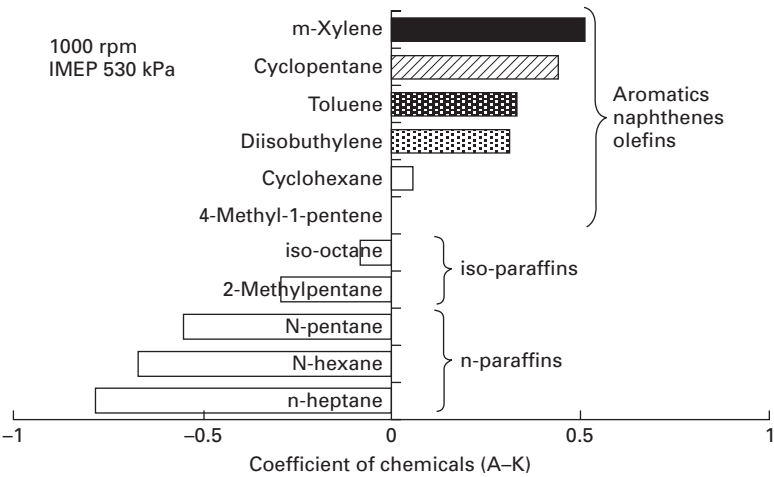

14.22 Coefficients of CA50 prediction equations [9].

14.8 Future trends

The ultimate goal of future HCCI fuel research should be the development of a specification for HCCI fuels. In order to further this goal, additional data are needed on the effects of fuel composition on low temperature reactions. These data must include consideration of the interactions of the various constituents, perhaps in the most global sense of hydrocarbon types, as least as a first step. The data must include the interaction of other important factors associated with the use of EGR and factors associated with engine

design, such as intake manifold conditions, compression ratio, and in-cylinder temperatures and compositions.

The future specification must include some measure of the ignition characteristics and it is clear from the literature that neither octane number nor cetane number is adequate for this purpose. Ryan *et al*. [3] propose the use of two parameters, EPAIT and cool flame magnitude, both measured using a modified ASTM D6890 approach. This is a fundamental approach that is based on simple measurements in a constant volume combustion bomb. The approach suggested by Kalghatgi [11] involves the use of octane sensitivity in a technique that must be calibrated for each engine.

Fuel volatility is important in HCCI mixture preparation and additional data is needed in order to define the appropriate boiling range. Materials in the gasoline boiling range are clearly appropriate, but some limited data with jet fuels indicate that the range could possibly be extended into the distillate fraction.

14.9 References

1. M. Sjoberg, J.E. Dec and N.P. Cernansky, 'Potential of Thermal Stratification and Combustion Retard for Reducing Pressure-Rise Rates in HCCI Engines Based on Multi-Zone Modeling and Experiments' SAE Paper 2005-01-0113, April 2005.
2. T.W. Ryan and T.J. Callahan, 'Homogeneous Charge Compression Ignition (HCCI) of Diesel Fuel' SAE Paper 961160, May, 1996, SAE Trans.
3. A.W. Gray and T.W. Ryan, 'Homogeneous Charge Compression Ignition (HCCI) of Diesel Fuel' SAE Paper 971676, May, 1997, SAE Trans.
4. T.W. Ryan and A. Matheaus, 'Fuel Requirements for HCCI Engine Operation' SAE Paper 2003-01-1813, June 2003, SAE Trans.
5. L.N. Allard, *et al*., 'Analysis of the Behavior of the ASTM D613 Primary Reference Fuels and Full Boiling Range Diesel Fuels in the Ignition Quality Tester (IQT) – Part III', SAE Paper 1999-01-3591, 1999.
6. M. Sjoberg and J. Dec, 'Smoothing HCCI Heat-Release Rates using Partial Fuel Stratification with Two-Stage Ignition Fuels' SAE Paper 2006-01-0629, April 2006.
7. J. Dec, W. Hwang and M. Sjoberg, 'An Investigation of Thermal Stratification in HCCI Engines using Chemiluminescence Imaging' SAE Paper 2006-01-1518, April 2006.
8. T. Guohong, W. Zhi, W. Jianxin, S. Shijin, A. Xinliang, 'HCCI Combustion Control by Injection Strategy with Negative Valve Overlap in a GDI Engine' SAE Paper 2006-01-0415, April 2006.
9. G. Shibata *et al*., 'Correlation of Low Temperature Heat Release with Fuel Composition and HCCI Engine Combustion' SAE Paper 2005-01-0138, April 2005.
10. G. Shibata *et al*., 'The Interaction Between Fuel Chemicals and HCCI Combustion Characteristics Under Heated Intake Air Conditions' SAE Paper 2006-01-0207, April, 2006.
11. Kalghatgi, G., *et al*. 'A Method of Defining Ignition Quality of Fuels in HCCI Engines' SAE Paper 2003-01-1816, May 2003.

Part IV

HCCI/CAI combustion engines with alternative fuels

15

Natural gas HCCI engines

N IIDA, Keto University, Japan

Homogeneous charge compression ignition (HCCI) is regarded as the next generation combustion regime in terms of high thermal efficiency and low emissions. It is difficult to control auto-ignition timing and combustion duration because they are controlled primarily by the chemical kinetics of fuel-air mixture. In this chapter, the characteristics of HCCI combustion of natural gas in HCCI engines are discussed. As natural gas consists of methane, ethane, propane and butane, so the influence of n-butane in natural gas on auto-ignition and combustion processes are discussed.

15.1 CNG HCCI engine experiment and calculation conditions [1]

The research engine used for this study is a YANMAR TS230R series. This engine is a four-stroke single cylinder diesel engine with a bore of 112 mm and a stroke of 115 mm. Figure 15.1 shows the experimental setup and Table 15.1 the engine specifications. In order to form homogeneous charge, the fuel was injected into the intake manifold about 1500 mm from the intake valve. The flow rate of air was measured by a laminar flow meter. The flow rate of fuel was controlled by a mass flow controller. The intake air was preheated by an electric heater installed in the intake manifold. The intake temperature (T_{in}) was measured at about 50 mm from the intake valve using a K-type sheathed thermocouple. The exhaust gas temperature (T_{ex}) was measured at about 110 mm from the exhaust valve. It was possible to adjust the intake air pressure to a selected value by controlling the compressor. The in-cylinder gas pressure was measured with a piezoelectric pressure transducer for all operating conditions. For each test point, the cylinder pressure was sampled over 64 cycles at intervals of 1 degree crank angle. The concentrations of THC, NOx, CO and CO_2 were measured by FID, CLD and NDIR.

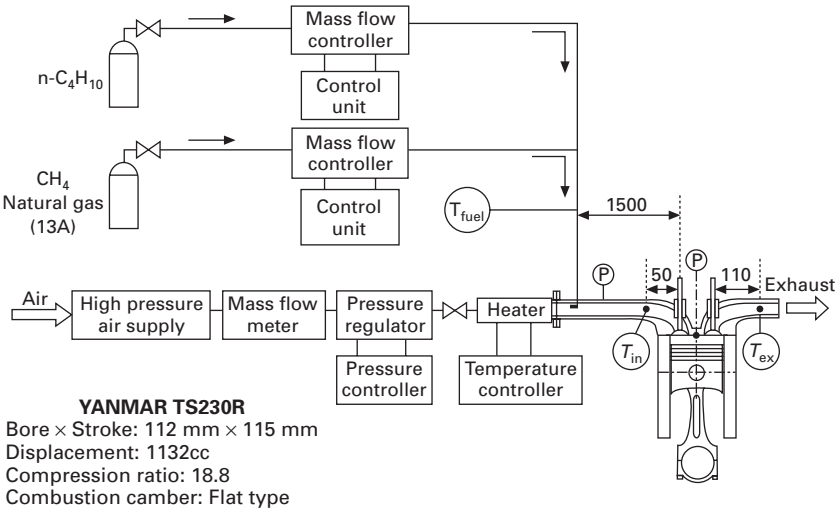

15.1 Experimental setup [1].

Table 15.1 Engine specification of experiment and calculation [1]

	Experiment	Calculation
Process	4 stroke	Only one compression/ expansion process
Number of cylinders	1	–
Displacement	1132cc	←
Bore	112 mm	←
Stroke	115 mm	←
Length of conrod	250 mm	←
Crank radius	57.5 mm	←
Intake valve close	ABDC 48°	←
Compression ratio	18.8	←
Combustion chamber	Disk type	–
Engine speed	800 rpm	←

15.2 CNG composition

Natural gas was selected as the fuel, which is 13A gas used in major cities of Japan. It consists of methane, ethane, propane and butane. The composition of the natural gas (13A) is shown in Fig. 15.2. Table 15.2 shows the properties of methane, n-butane and natural gas (13A) [1].

Figure 15.3 and Figure 15.4 show the operation region of experiment for various intake temperatures at a constant intake pressure and intake pressures at a constant intake temperature. It can be seen that there are three regions in figures: misfiring region, firing region and knocking region. Knocking limit was judged by the cylinder pressure, which starts to show high frequency

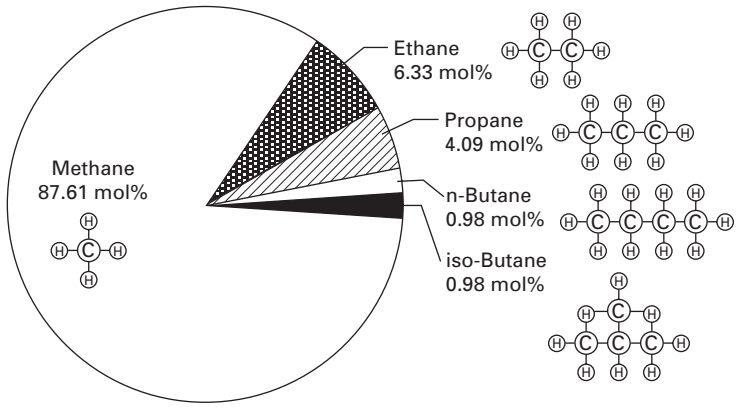

15.2 Composition of natural gas (13A) [1].

Table 15.2 Properties of methane, n-butane and 13A [1]

	Methane	Natural gas (13A)	n-Butane
Chemical structure	CH_4	–	C_4H_{10}
Mole weight (g/mol)	16.04	20.75	58.12
H/C	4	–	2.5
C (% wt.)	75	–	83
H (% wt.)	25	–	17
Octane number	105	–	91.8
Cetane number	< 10	–	< 10
Stoich. A/F ratio (kg/kg)	17.19	16.89	15.46
Low calorific value (MJ/kg)	32.87	41.7	112.32
Ignition limits (Φ)	0.5/1.67	–	0.5/2.8
Auto-ignition temperature (K)	905	–	703
Combustion type	Only HTR	Only HTR	LTR & HTR

pressure fluctuation. Misfiring was defined as rates of heat release calculated from the total averaged cylinder pressure of 64 cycles, when the integrated value of heat release rate is below 1% of the total heat values of introduced fuel. As the intake temperature increases at a constant intake pressure, the firing region slides to the lean side. The firing region is not expanded because the knocking region also slides to the lean side with increasing intake temperature. The misfiring limit and knocking limit slide to the lean side with increasing intake pressure at a constant intake temperature.

Figure 15.5 shows the relationship between the operating equivalence ratio and the total heating value of supplied fuel for various intake pressures. The misfiring limit slides to the lean side with increasing intake pressure as intake pressure increases and the total heating value of supplied fuel at misfiring limits have almost constant values. The misfiring limit depends on

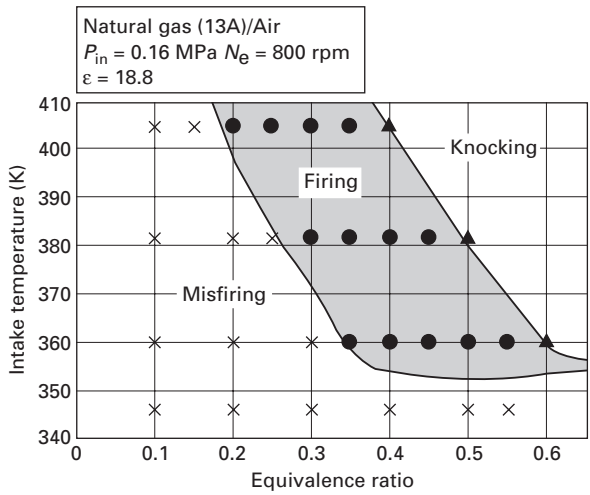

15.3 Operation area for various intake temperatures at a constant intake pressure [1].

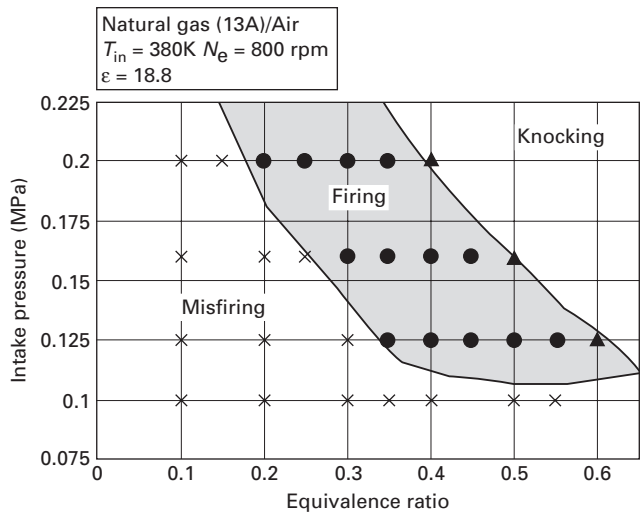

15.4 Operation area for various intake pressures at a constant intake temperature [1].

the total heating value of introduced fuel in a range of intake pressure from 0.125 MPa to 0.2 MPa. Though the knocking limit slides to the lean side with increasing intake pressure, the total heating value of introduced fuel becomes higher. This is because the specific heat becomes higher by increasing the mass of air.

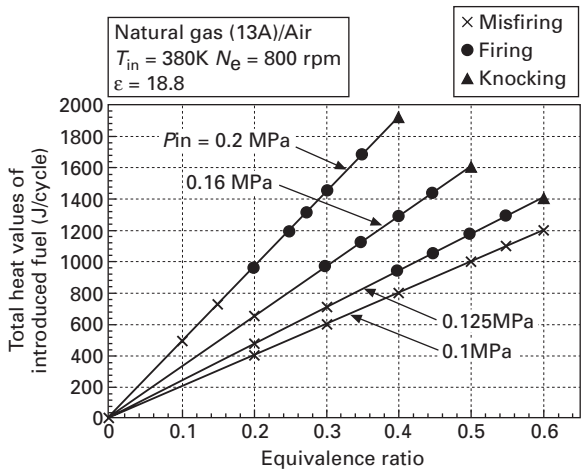

15.5 Relationship between the operation area and the total heat values of introduced fuel for various intake pressures [1].

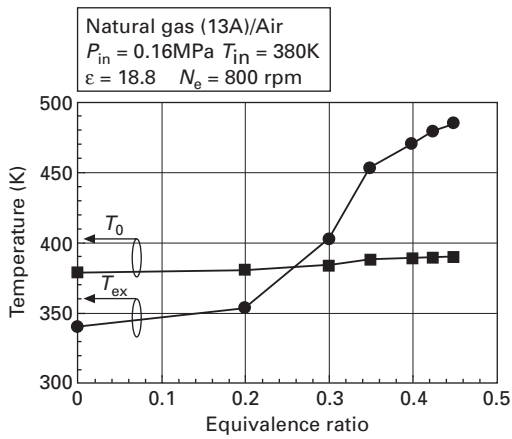

15.6 Initial gas temperature and exhaust gas temperature for various equivalence ratios [1].

15.3 Influence of equivalence ratio

In experiment, the fresh gas introduced into the combustion chamber is diluted by high temperature residual gas left over from the previous cycle. Figure 15.6 shows the initial gas temperature (T_0) and exhaust gas temperature (T_{ex}) for various equivalence ratios at intake temperature of 380K, intake pressure of 0.16MPa, engine speed of 800 rpm and compression ratio of 18.8. The initial gas temperature T_0 is calculated from equation 15.1.

$$T_0 = \frac{m_s \cdot Cp_s \cdot T_{in} + m_r \cdot Cp_r \cdot T_r}{m_s \cdot Cp_s + m_r \cdot Cp_r} \quad 15.1$$

Where T_0 is the initial gas temperature when the intake valve is closed (BTDC132°), T_{in} and T_r are the temperatures of fresh gas and residual gas, m_s and m_r are the mass of fresh gas and residual gas, and Cp_s and Cp_r are specific heat of fresh gas and residual gas, (T_r) is assumed to the exhaust gas temperature (T_{ex}) measured at 110 mm from the exhaust valve. As equivalence ratio increases from 0 to 0.45, the initial gas temperature becomes higher about 10K higher.

Figure 15.7 shows the profiles of in-cylinder gas pressure, rate of heat release and in-cylinder gas temperature for various equivalence ratios. The equivalence ratio was changed from 0 to 0.45. In-cylinder gas pressures are the total averaged pressures of 64 cycles. The rate of heat release was calculated from in-cylinder gas pressure using a single zone model. In-cylinder gas temperature was calculated from adiabatic equation before auto-ignition,

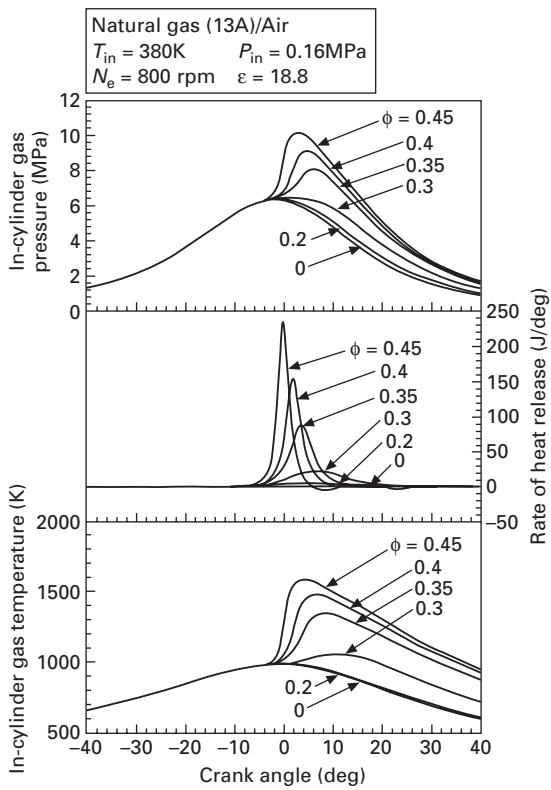

15.7 Profiles of in-cylinder gas pressure, rate of heat release and in-cylinder gas temperature for various equivalence ratios [1].

and after it was calculated from perfect gas equation of state.

As the equivalence ratio increases, the occurrence of heat release advances, and the maximum cycle pressure and temperature become higher.

15.4 Auto-ignition timing and combustion duration

Figure 15.8 shows the definition of auto-ignition timing and combustion duration. Auto-ignition timing is defined as the crank angle when the integrated value of heat release rate reaches 1/100 of total heat values of introduced fuel. The end timing of combustion is defined as the crank angle of intersection of heat release rate of 0J/deg and tangential to hold maximum slope (negative gradient) in heat release rate profiles.

Figure 15.9 shows auto-ignition timings and combustion durations for various equivalence ratios, intake temperatures and intake pressures. As equivalence ratios increase, intake temperature and intake pressure, auto-ignition timing becomes earlier. As the equivalence ratio increases from 0.2 to 0.3, combustion duration becomes longer. The combustion duration depends on combustion temperature. Since the auto-ignition take place after TDC at equivalence ratio of 0.2, the combustion temperature decreases with increasing volume of the combustion chamber. Therefore, the reaction of fuel-air mixture is terminated by the low combustion temperature. At the equivalence ratios

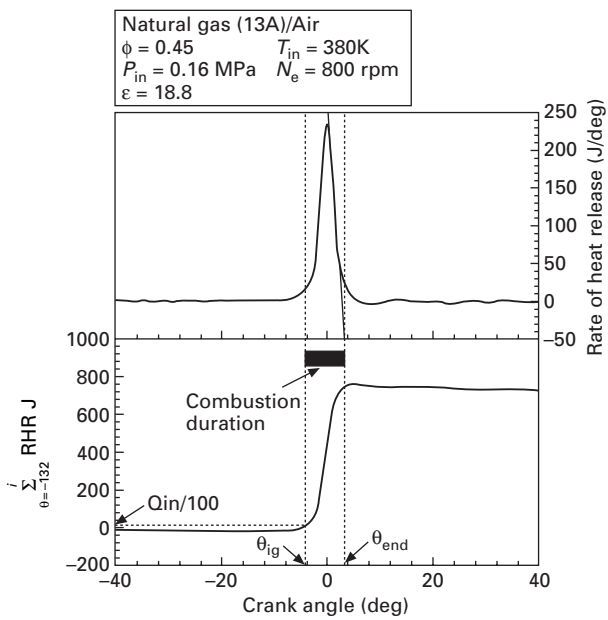

15.8 Definition of auto-ignition timing and combustion duration [1].

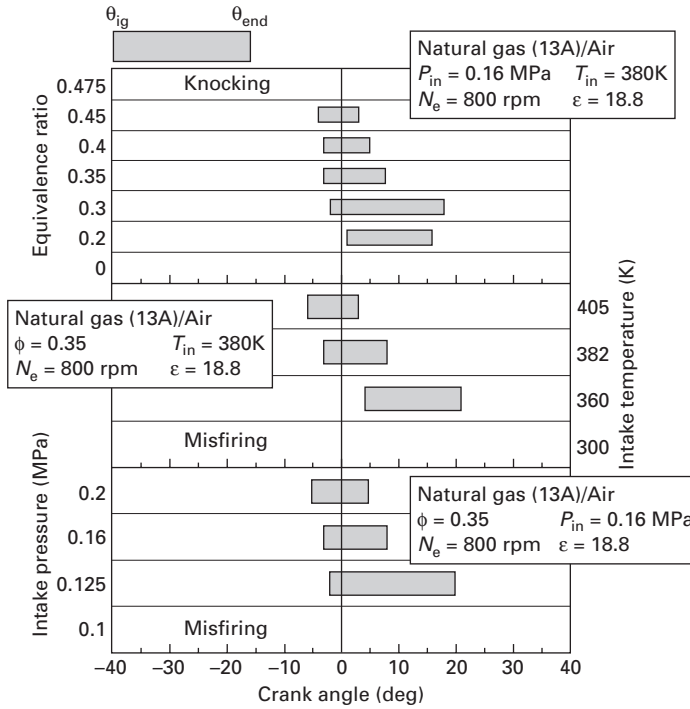

15.9 Auto-ignition timings and combustion durations for various equivalence ratios [1].

of more than 0.3, combustion duration becomes shorter with increasing equivalence ratio. The combustion duration decreases with increasing intake temperature and intake pressure.

15.5 Auto-ignition temperature and auto-ignition pressure

Figure 15.10 shows P-T diagrams for various equivalence ratios, intake temperatures and intake pressures. Auto-ignition temperature and auto-ignition pressure are constant regardless of equivalence ratio. As intake temperature decreases and intake pressure increases, auto-ignition pressure becomes higher, and auto-ignition temperature becomes lower. The relationship between auto-ignition temperature and auto-ignition pressure is shown in Fig. 15.11. The auto-ignition temperature becomes lower with increasing auto-ignition pressure.

Figure 15.12 shows profiles of in-cylinder gas temperature for various engine speeds. The x-axis is the period from compression start. With increasing engine speeds, the time from start of compression to auto-ignition becomes shorter. The auto-ignition temperature slightly decreases with increasing

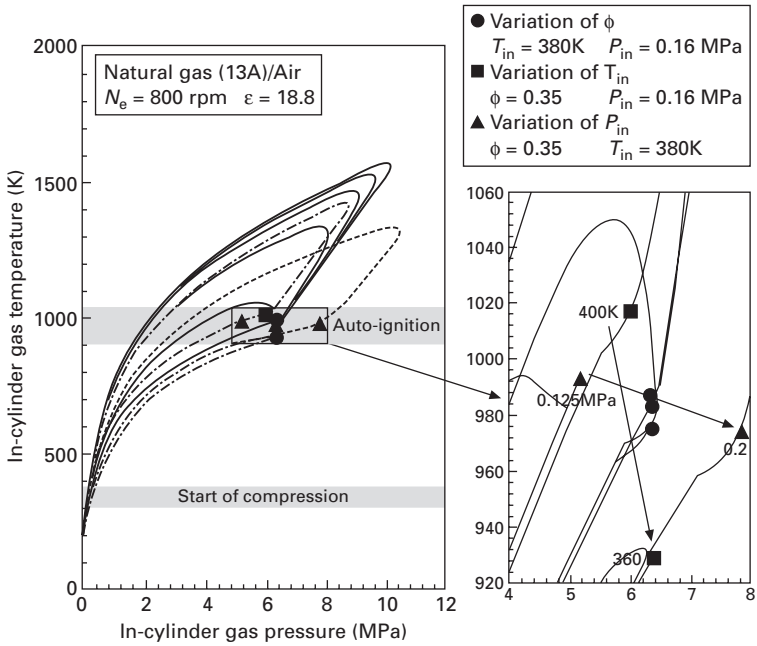

15.10 P-T diagrams for various equivalence ratios, intake temperatures and intake pressures [1].

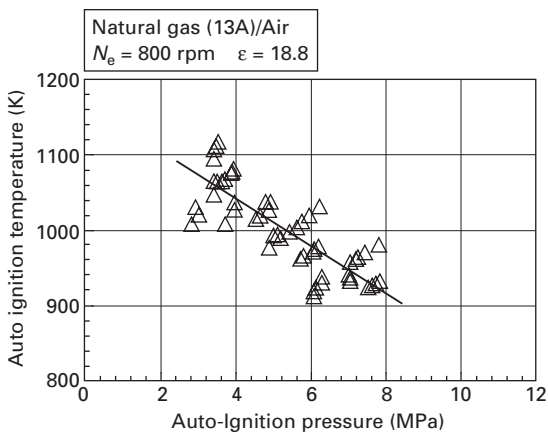

15.11 Auto-ignition temperatures and auto-ignition pressures for various equivalence ratios, intake temperatures and intake pressures [1].

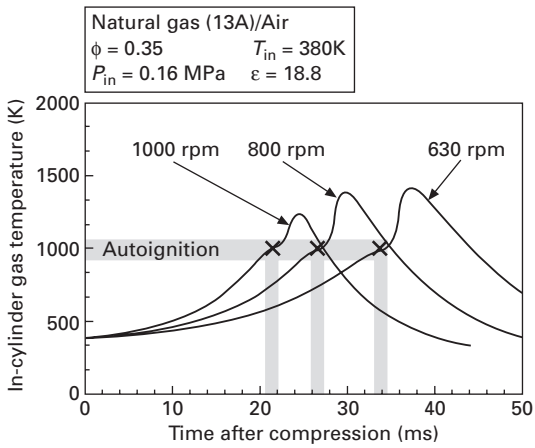

15.12 Profiles of in-cylinder gas temperature for various engine speeds [1].

engine speed from 630 rpm to 1000 rpm. In a hydrocarbon-air mixture, the low temperature oxidation reaction process becomes dominant at a temperature range of 700K–900K. It is said that a mixture leads to high temperature oxidation via the low temperature oxidation ignition process [3]. As engine speed decreases, the period that mixture passes this temperature region lengthens, and auto-ignition temperature becomes lower. However, the range of engine speed investigated in this study is so small that it is necessary to investigate over a wider range.

15.6 Exhaust emission, maximum cycle temperature and combustion efficiency

In HCCI engines, the low combustion temperature results in low NOx emissions, but the combustion temperature becomes too low to oxidize the fuel completely. This low combustion temperature leads to incomplete combustion, which results in high emissions of THC and CO emissions.

Figure 15.13 shows the emissions of THC, CO, CO_2, maximum cycle temperatures and combustion efficiencies for various equivalence ratios. Combustion efficiency was calculated from the following equation:

$$\eta_{com} = \sum RHR/Q_{in} \times 100 \qquad 15.2$$

where $\sum RHR$ is integrated value of heat release rate; Q_{in} is total heat values of introduced fuel.

The cooling losses by the convective, radiative and conductive heat transfer through the wall of combustion chamber were not considered.

THC emission is initially proportional to supplied fuel quantity before

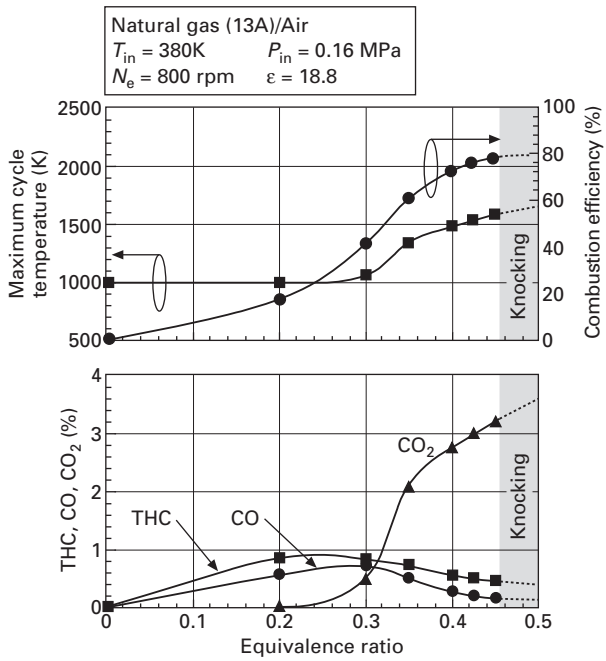

15.13 Emissions of THC, CO, CO_2, maximum cycle temperatures and combustion efficiencies for various equivalence ratios [1].

auto-ignition. But at equivalence ratios more than 0.25, it is reduced with increasing equivalence ratio. Similarly, CO emission increases initially and then decreases as equivalence ratio is more than 0.3. NOx emission is lower than 20 ppm under these conditions.

Maximum cycle temperature and combustion efficiency increase with increasing equivalence ratio. When equivalence ratio reaches about 0.45, maximum cycle temperature is 1500K, combustion efficiency is over 80%, and CO emission is reduced to about 0.2%.

Figure 15.14 shows the relationship between maximum cycle temperatures and CO, CO_2 emissions, combustion efficiencies. CO emission increases at the maximum cycle temperature of 1100K. While at maximum cycle temperature more than 1100K, CO_2 emission becomes higher with the increasing maximum cycle temperature. When maximum cycle temperature is over 1500K, CO emission reduces to 0.2%. Therefore, to oxidize CO to CO_2 completely, it is necessary for the mass averaged in-cylinder gas temperature to exceed the temperature of 1500K. Moreover, in the case of the maximum cycle temperature over 1500K, combustion efficiency reaches 80%. Consequently the maximum cycle temperature must be over 1500K in order to maintain high thermal efficiency as well as low CO emission in HCCI engine.

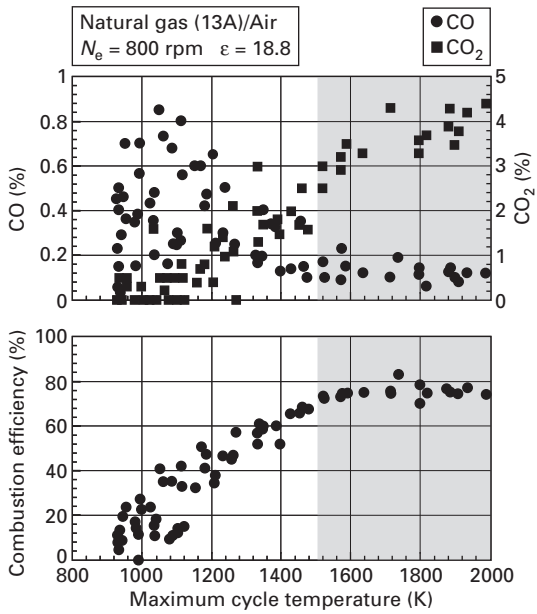

15.14 Relationship between maximum cycle temperatures and CO, CO_2 emissions and combustion efficiencies [1].

15.7 Influence of n-butane on auto-ignition and combustion in methane/n-butane/air mixtures

Natural gas consists of methane and ethane, propane and butane. The decomposition of hydrocarbons starts with the abstraction of H-atom by O_2, O, H, OH, HO_2 and CH_3. A C–H bond in a methane molecule is stronger than a C–H bond in the primary carbon atom. A H-atom is more easily abstracted from n-butane molecule with two secondary carbon atoms than ethane and propane [4]. To investigate the influence of n-butane on auto-ignition and combustion in natural gas, the blend ratio of n-butane in methane/n-butane/air mixtures is varied.

Figure 15.15 shows the blend ratios of n-butane and methane and the variation of equivalence ratio at each blend ratio in methane/n-butane/air mixtures. The blend ratio of n-butane is changed from 0 mol% to 10 mol% at intake temperature of 380K, intake pressure of 0.16 MPa, engine speed of 800 rpm and compression ratio of 18.8. The total heat values of introduced fuel (Q_{in}) are a constant of 1300 ±10J in all conditions. The equivalence ratio is in a range of 0.3 ± 0.02.

Figure 15.16 and Figure 15.17 show profiles of in-cylinder gas pressure of n-butane/air mixtures and methane/air mixtures for various equivalence ratios. In n-butane/air mixtures, the pressure is raised slightly by combustion

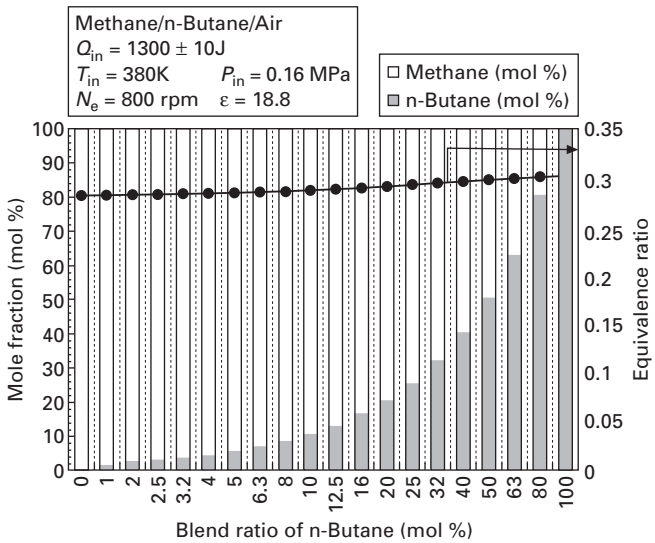

15.15 Blend ratios of n-butane and methane and the variation of equivalence ratio at each blend ratio in methane/n-butane/air mixtures [1].

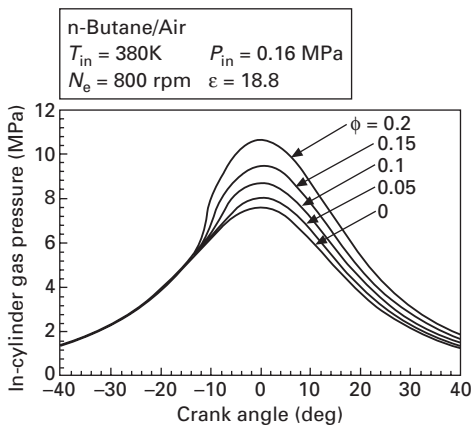

15.16 Profiles of in-cylinder gas pressure of n-butane/air mixtures for various equivalence ratios [1].

from equivalence ratio of 0.05. The maximum cycle pressure increases with rising equivalence ratio. The equivalence ratios were changed from 0 to 0.45 in methane/air mixtures. The methane/air mixtures do not reach stable combustion under these conditions.

Figure 15.18 shows the rate of heat release in methane, natural gas (13A) and n-butane/air mixture. Two-stage ignition can be seen with low temperature reaction (LTR) and high temperature reaction (HTR) in n-butane/air mixture.

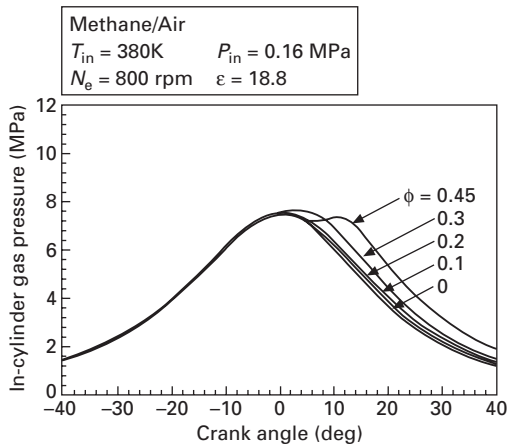

15.17 Profiles of in-cylinder gas pressure of methane/air mixtures for various equivalence ratios and various blend ratios of n-butane [1].

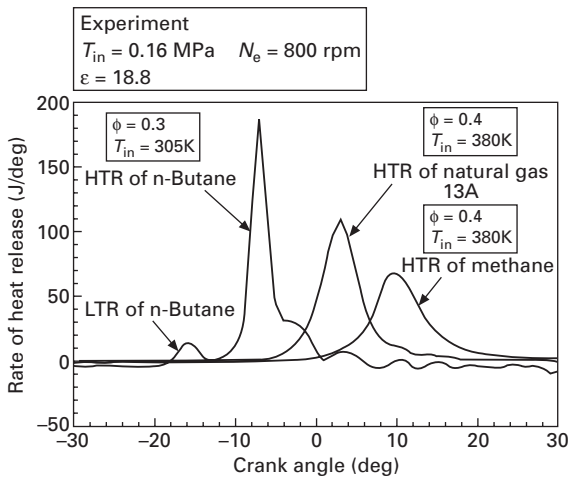

15.18 Profiles of heat release rate of methane, natural gas (13A) [1].

In higher hydrocarbon/air mixtures, the low temperature reaction process becomes dominant at the temperature from 700K to 900K. It is said that a mixture leads to high temperature reaction via the low temperature reaction process [4]. In the case of methane/air and natural gas (13A)/air mixture, only the high temperature reaction is shown.

Figure 15.19 shows the main chemical reaction path of n-butane [4, 5]. The low temperature reaction starts with the abstraction of H-atom in secondary carbon atom since the C-H bond energy of secondary carbon atom is a few kilocalories less than that of primary carbon atom. Next, alkyl radicals react

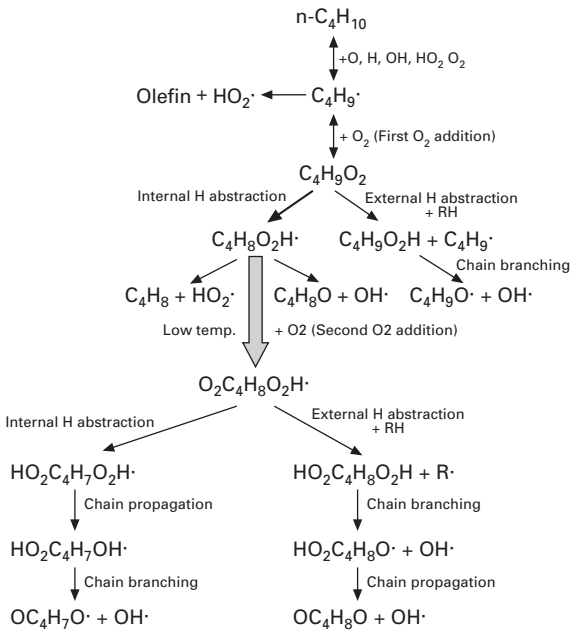

15.19 Main chemical reaction path of n-butane [1].

with O_2 and form $C_4H_9O_2$ (1st O_2 addition). $C_4H_9O_2$ can undergo external or internal H-atom abstraction. The external H-atom abstraction leads to chain branching, whereas internal H-atom abstraction only leads to chain propagation. However, the external H-atom abstraction is much slower than the internal H-atom abstraction. The internal H-atom abstraction gives rise to the second O_2 addition. $C_4H_9O_4$ generated by the 2nd O_2 addition undergoes a chain branching reaction and continues to oxidize. The second O_2 addition is dominated in a temperature range from 700K to 900K. $C_4H_9O_4$ decomposes back to $C_4H_9O_2$ and O_2 at high temperatures. This mechanism gives rise to the NTC region. At temperatures more than 1000K, HTR is dominant.

Figure 15.20 shows profiles of in-cylinder gas pressure, rate of heat release and in-cylinder gas temperature for various blend ratios of n-butane in methane/n-butane/air mixtures. As the blend ratio of n-butane increases, heat release occurs earlier. This is because the in-cylinder gas temperature becomes higher, and more radicals, which initiate methane oxidation, are created with the increasing blend ratios of n-butane.

Figure 15.21 shows P-T diagrams for various blend ratios of n-butane. Auto-ignition temperature and auto-ignition pressure are constant at n-butane blend ratios of 0%–2%. At the n-butane blend ratio of more than 2%, auto-ignition temperature and auto-ignition pressure decrease with increasing blend ratio of n-butane. Auto-ignition temperature is 25K lower, and auto-ignition

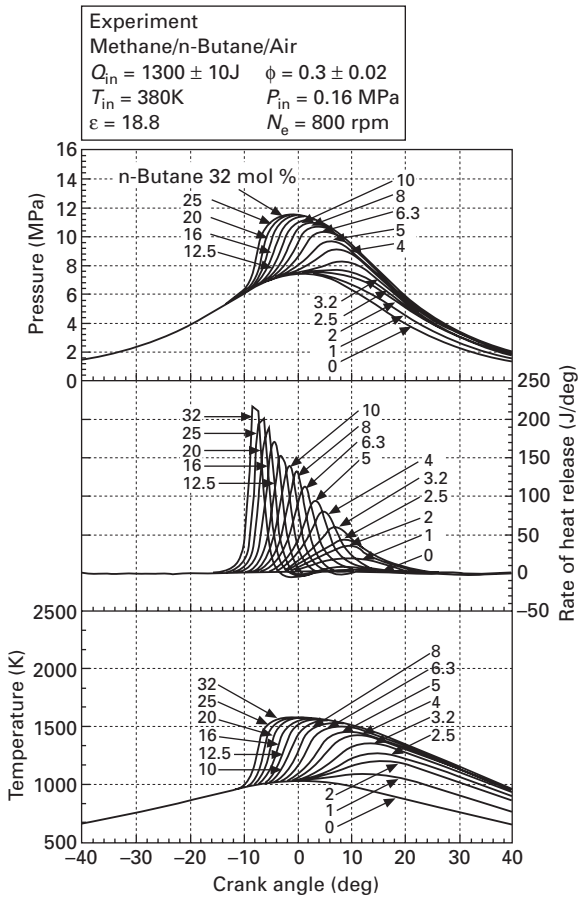

15.20 Profiles of in-cylinder gas pressure, rate of heat release and in-cylinder gas temperature for various blend ratios of n-butane in methane/n-butane/air mixtures [1].

pressure is 0.8MPa lower by increasing n-butane blend ratio of 10%. When the blend ratio of n-butane is over 8%, the combustion efficiency is over 80%.

Figure 15.22 and Figure 15.23 show the auto-ignition timing and auto-ignition temperature of experiment and calculation for various blend ratios of n-butane. In calculation and experiment, the auto-ignition advances and the auto-ignition temperature becomes lower with increasing the blend ratio of n-butane. However, these effects are most sensitive to the small blend ratio of n-butane, further amounts of n-butane have a comparatively smaller effect.

Figure 15.24 shows the maximum cycle temperature, combustion efficiency and the emissions of THC, CO, CO_2. In calculation, the maximum cycle

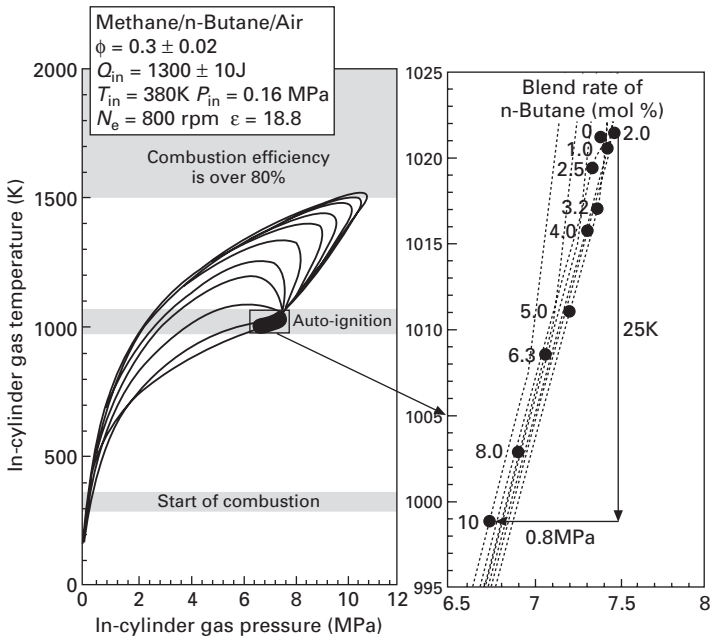

15.21 P-T diagrams for various blend ratios of n-butane in methane/n-butane/air mixtures [1].

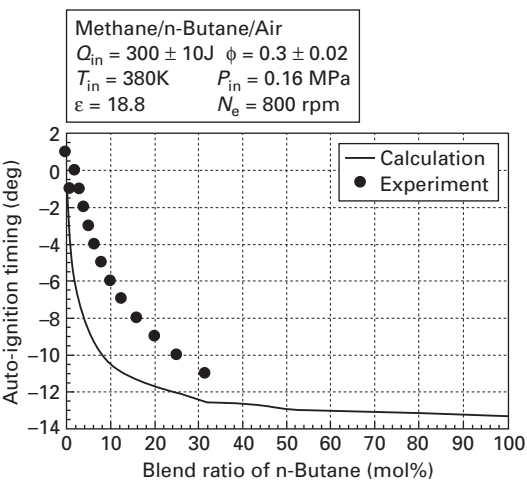

15.22 Auto-ignition timing of calculation and experiment for various blend ratios of n-butane in methane/n-butane/air mixtures [1].

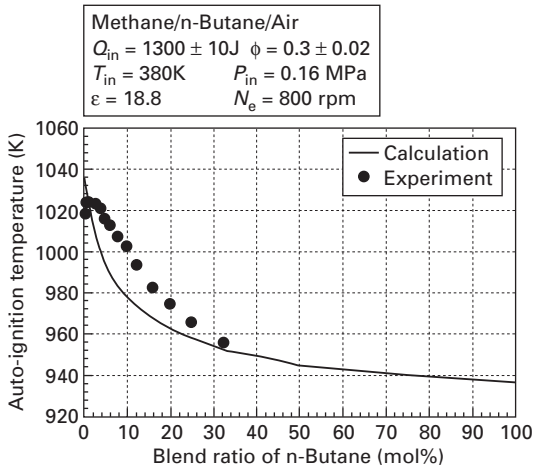

15.23 Auto-ignition temperature of experiment for various blend ratios of n-butane in methane/n-butane/air mixtures [1].

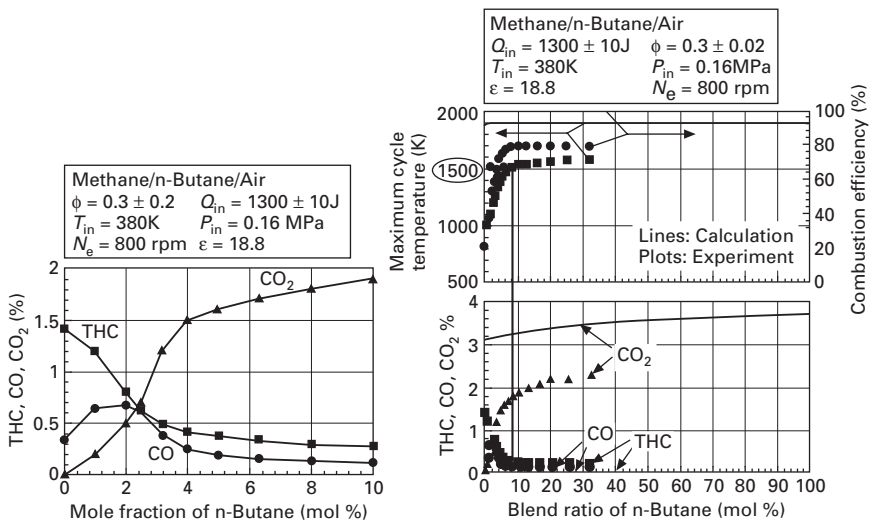

15.24 THC, CO and CO_2 emissions for various blend ratios of n-butane [1]

temperatures are about 1800K, the combustion efficiencies are 100%, and the emissions of THC and CO are about 0% regardless of the blend ratio of n-butane. In the case of experiment, the emissions of THC and CO reduce proportional to the blend ratio of n-butane. The maximum cycle temperature and combustion efficiency become higher with increasing blend ratio of n-butane. When the blend ratio of n-butane is over 6.3 mol%, the maximum

cycle temperature is over 1500K, and the combustion efficiency is over 80%.

15.8 Summary of naturally aspirated natural gas HCCI engine

In this study, the characteristics of auto-ignition and combustion of natural gas (13A) were investigated at engine speed of 800 rpm and compression ratio of 18.8 in a 4-stroke cycle HCCI engine. The influence was clarified of n-butane blend ratio on auto-ignition and combustion of methane/n-butane/air mixtures at total heat values of introduced fuel of 1300 ± 10J, intake temperature of 380K, intake pressure of 0.16 MPa, engine speed of 800 rpm and compression ratio of 18.8.

1. The HCCI region and knocking region slides to the lean side with increasing intake temperature and intake pressure.
2. The auto-ignition temperature of natural gas (13A) becomes lower with increasing auto-ignition pressure.
3. The auto-ignition timing advances, and combustion duration becomes shorter with increasing equivalence ratio, intake temperature and intake pressure.
4. To realize high thermal efficiency and low THC, CO emission, it is necessary to prepare operation conditions at which maximum cycle temperature is over 1500K.
5. As blend ratio of n-butane increases, the auto-ignition temperature and auto-ignition pressure become lower in methane/n-butane/air mixtures.
6. Maximum cycle temperature increases, and THC, CO emissions reduce by rising blend ratio of n-butane.

15.9 Supercharged natural gas HCCI engine set-up and experiments

The possibility of turbocharging into a natural gas homogeneous charge compression ignition (HCCI) engine is investigated experimentally and by simulation. Experiments are performed using a four-cylinder naturally aspirated engine fitted with an external supercharger and a butterfly valve for back pressure control to simulate a turbocharger with efficiency of 0.64. Based on the test results, the performance and emission characteristics are studied in detail through numerical one-dimensional cycle simulations. The results indicate that the thermal efficiency can be improved by raising the engine compression ratio and lowering the turbocharging pressure. At an engine compression ratio of 21 and turbocharging pressure of 1.9 bar, the brake thermal efficiency reaches 0.43, with NOx emissions of only 10 ppm or less.

The cycle simulations demonstrate that performance comparable to that achieved in the external supercharging test can be obtained by optimizing engine and turbocharger specifications.

The base engine used for this test was a naturally aspirated, water-cooled, 4-cylinder, 4-cycle natural gas engine. For the supercharging trial, the engine was remodeled to allow a maximum operating in-cylinder pressure of 150 bar. The main elements of the test system are shown in Table 15.3. The combustion chamber was dog-dish in shape with an aperture ratio of 0.9. Figure 15.25 provides an outline of the test equipment. An electric heater was fitted to the intake system to maintain the intake temperature at a specified constant value, which was measured by a J-type thermocouple positioned 100 mm upstream of the intake port of the no. 2 cylinder. The intake air was

Table 15.3 Engine specifications [6]

Engine type	Four cylinder, water cooled
Bore × stroke	98 mm × 110 mm
Displacement	3,318 cm^3
Compression ratio	17:1, 19:1, 21:1
Boost pressure	1.9–2.5 bar
Combustion chamber	Dog-dish
Intake air temperature	~573K (electric heaer)

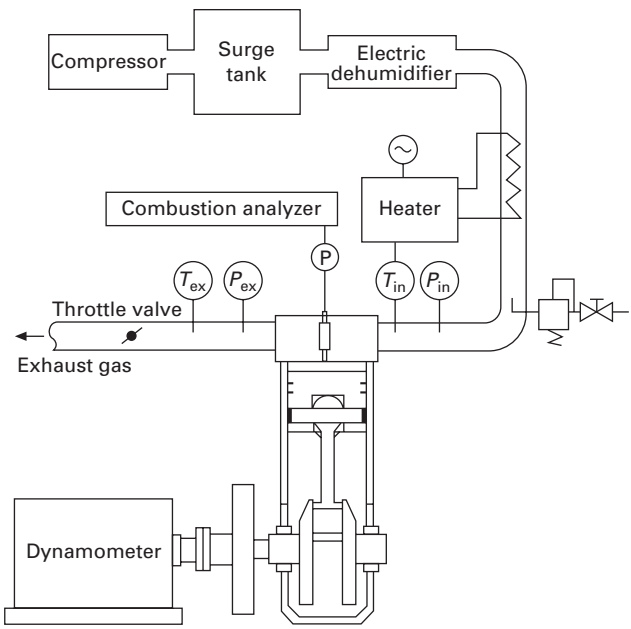

15.25 Experimental setup [6].

pressurized to 8.0 bar by a screw compressor, dehumidified by a refrigeration-type air dehumidifier, and then adjusted to the specified pressure by a regulator. A butterfly valve was installed in order to apply back pressure in the exhaust system. The fuel used in the experiment was 13A natural gas (typical composition: CH_4 88%, C_2H_6 6%, C_3H_8 4%, C_4H_{10} 2%). After the pressure was reduced by the regulator from 8.0 bar to 5.0 bar, the main fuel was supplied continuously through a nozzle positioned in the intake line 1000 mm upstream of the cylinder head. To eliminate dispersion of fuel among the cylinders, a very small quantity of fuel was supplied to each of the cylinders. The nitrogen oxides (NOx) in the exhaust gas were measured by chemiluminescence analysis, carbon monoxide (CO) and carbon dioxide (CO_2) were measured by infrared analysis, total hydrocarbons (THC) were measured by flame ionization detection (FID) analysis as the quantity of CH_4 equivalent, and oxygen (O_2) was measured using a magnetopneumatic. The upper limit of the equivalence ratio in operation was determined by the maximum in-cylinder pressure and engine knock. The upper limit of in-cylinder pressure was determined to be 150 bar. The knock intensity was defined as the amplitude of the signal wave obtained by processing the in-cylinder pressure through a band-pass filter, and the knock limit was defined as the equivalence ratio at which the average maximum knock intensity exceeds 2.0 bar.

In the experiment, the opening of the butterfly valve in the exhaust system was adjusted to simulate back pressure induced by a turbocharger with efficiency of 0.64. The turbocharger efficiency is defined as the ratio of compressor work to turbine work, as calculated using the specific heat of the working fluid for the measured values of intake and exhaust gas pressures, exhaust temperature, ambient temperature and air composition. In the calculation, atmospheric pressure at the compressor inlet and turbine outlet was assumed.

15.10 Performance and exhaust gas characteristics at a compression ratio of 17

With the compression ratio fixed at $\varepsilon = 17$, engine speed at $\eta_e = 1800$ rpm, boost pressure at $p_b = 2.5$ bar, and assumed a turbocharging efficiency at $\eta_{T/C} = 0.64$, the intake air temperature T_{in} and equivalence ratio Φ were varied. Figure 15.26 shows the combustion efficiency η_c, brake thermal efficiency η_e and brake mean effective pressure BMEP, calculated from the measured values of THC and CO in the exhaust gas and the fuel flow rate. The results are shown for different values of T_{in} and Φ.

As T_{in} is reduced, the operating range shifts towards higher values of Φ. Comparing the η_c at a fixed value of Φ, the combustion efficiency tends to improve as T_{in} increases.

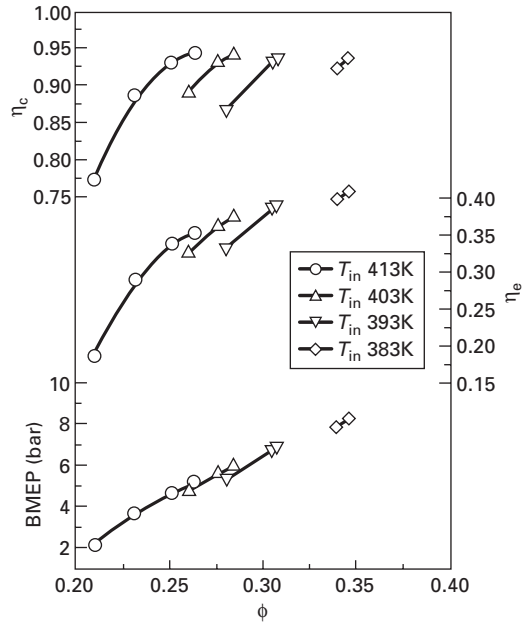

15.26 Influence of intake air temperature on engine performance under supercharging conditions (engine speed 1800 rpm, compression ratio 17, and boost pressure 2.5 bar) [6].

However, the maximum value of η_c does not depend on T_{in} and Φ, as it is more or less constant at around 0.94. It can also be seen that η_e improves as T_{in} becomes lower, reaching a maximum value of 0.4. BMEP varies in the same way as η_c, reaching a maximum value of 8.5 bar.

Figure 15.27 shows the variation of CO, THC and NOx in the exhaust gas with respect to T_{in} and Φ. CO and THC become lower as either T_{in} or Φ is increased. NOx is extremely low regardless of the value of Φ.

Figure 15.28(a) shows the variation of in-cylinder pressure p, and heat release rate $dq/d\theta$ as the temperature T_{in} of cylinder #2 changes. The lower the value of T_{in}, the later the heat release starting point and the higher the heat release peak. The later the heat release starting point, the lower the in-cylinder pressure. The increasing lateness of the heat release starting point as T_{in} decreases can be explained as follows. The lower the temperature at the start of compression, the longer it takes to reach auto ignition temperature, which in the case of natural gas is 1000–1100K [7, 8] (the crank angle at auto ignition is retarded). Figure 15.28(b) shows the variation of $dq/d\theta$ for each cylinder at the knock limit of T_{in} = 383K. As a result of fuel charge control for limiting dispersion among cylinders, there is little deviation in the heat release starting point and peak. As shown above, η_e increases as T_{in} decreases. This is thought to be due to the reduction in cooling loss resulting from the

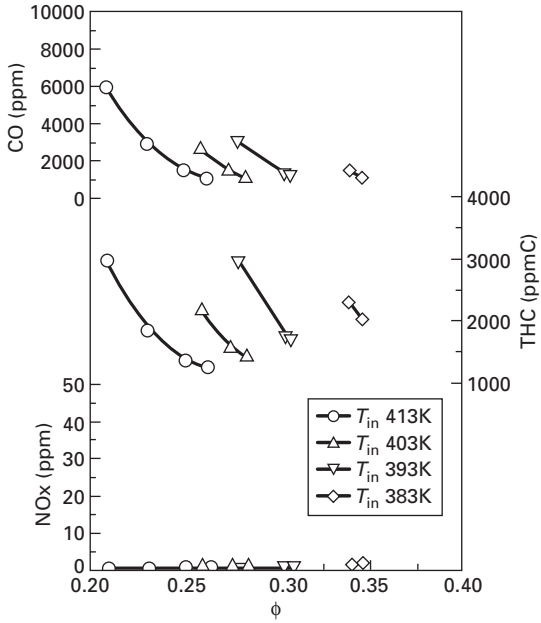

15.27 Influence of intake air temperature on emission characteristics under supercharging (engine speed 1800 rpm, compression ratio 17, boost pressure 2.5 bar) [6]

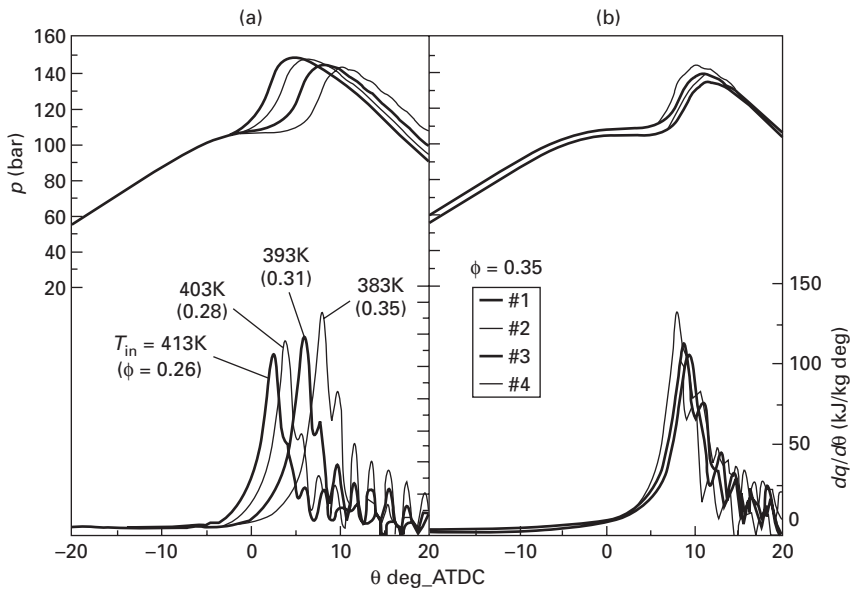

15.28 In-cylinder pressure and heat release rate over time (engine speed 1800 rpm, compression ratio 17, boost pressure 2.5 bar). (a) change in p and $dq/d\theta$ with intake air temperature, and (b) change in p and $dq/d\theta$ for each cylinder at knock limits [6].

lag in heat release starting point, an increase in the fuel charge quantity, and a change in the temperature profile due to the decrease of T_{in} [9].

15.11 Performance and emission characteristics at a compression ratio of 21

A characteristic of the HCCI engine is that the brake thermal efficiency η_e improves as the intake air temperature T_{in} is reduced. At a compression ratio ε of 17, the lower operating limit for T_{in} was relatively high (383K). In view of this, the authors attempted to improve η_e by extending the lower operating limit of T_{in} while increasing the compression ratio.

With the system parameters fixed at $\varepsilon = 21$, $\eta_e = 1800$ rpm, $T_{in} = 383$K and $\eta_{T/C} = 0.64$, the boost pressure p_b and Φ were varied. Figure 15.29 shows the variation in η_c, η_e and BMEP under these conditions. It can be seen that η_c rises as p_b is reduced, and that η_e and BMEP both improve with decreasing p_b, with the former reaching a maximum value of 0.42.

Figure 15.30 shows the emissions from this engine. It can be seen that as the intake air temperature decreases, the operating equivalence ratio increases, which in turn results in reduced levels of CO and THC. The NOx emission concentration is also extremely low under all conditions. The maximum value of η_c improves with decreasing p_b, due to the fuel charge reduction

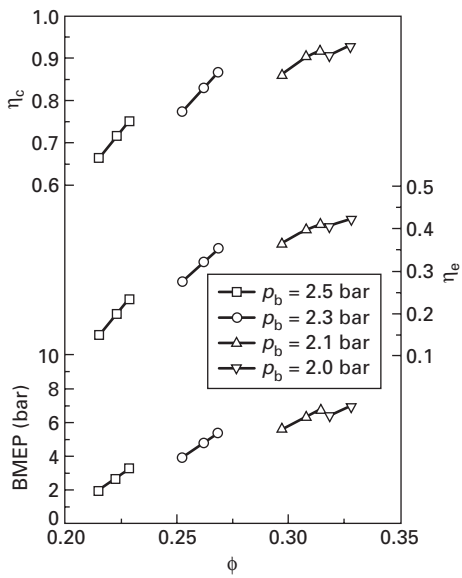

15.29 Effect of boost pressure on engine performance (engine speed 1800 rpm, compression ratio 21, intake air temperature 353K) [6].

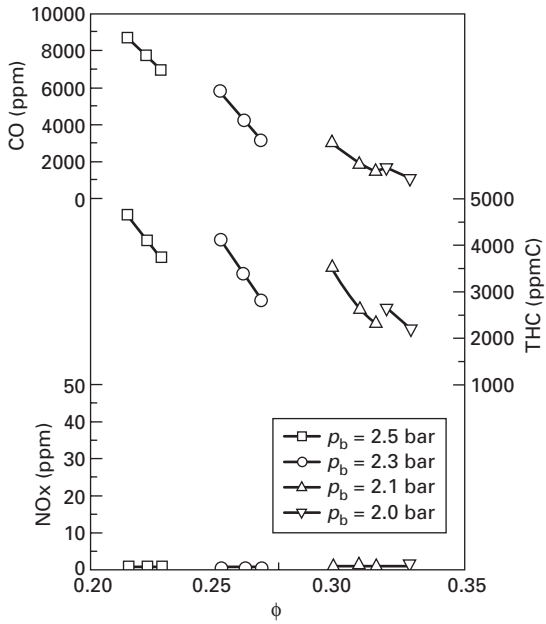

15.30 Effect of boost pressure on emission characteristics (engine speed 1800 rpm, compression ratio 21, intake air temperature 353K) [6].

required at high boost pressure to limit in-cylinder pressure. This condition also reduces the maximum attainable temperature [7].

In the previous tests of performance and emission characteristics, T_{in} was fixed at 353K. Figure 15.31 shows the upper limit of BMEP for all the test values of T_{in} and p_b. The fine lines in the figure represent η_e, the light gray region shows dependence of the upper operating limit on p_{max}, and the dark grey region shows the dependence of the upper operating limit on knock. From this figure, it appears to be possible to operate the engine over a relatively wide range of BMEP by suitably adjusting T_{in} and p_b. When p_b is over 2.1 bar, the upper operating limit is determined by p_{max}, regardless of T_{in}. Below $p_b = 1.9$ bar and $T_{in} = 373$K, the upper operating limit is determined by engine knock. The figure also shows that in the range of BMEP from 7.5 bar to 9.0 bar, it is possible to attain a brake thermal efficiency higher than 0.42.

15.12 Potential of natural gas turbocharged HCCI engines

Figure 15.32 shows the upper operating limit values of BMEP and η_e with variation in T_{in} and Φ at fixed values of ε and p_b. At $\varepsilon = 17$ and $p_b = 1.6$ bar,

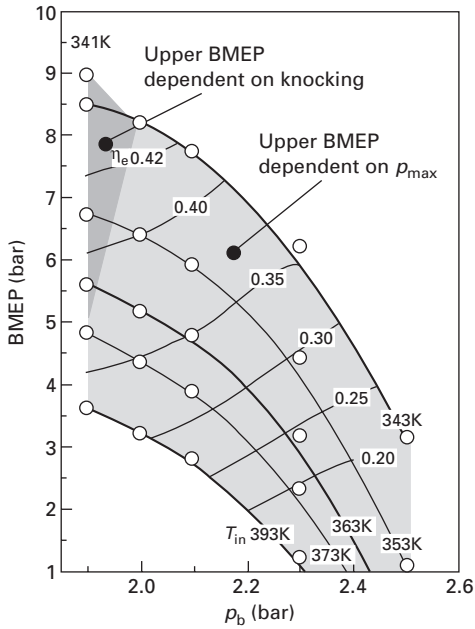

15.31 Brake thermal efficiency and brake mean effective pressure with variation of boost pressure and intake air temperature at a compression ratio of 21 [6].

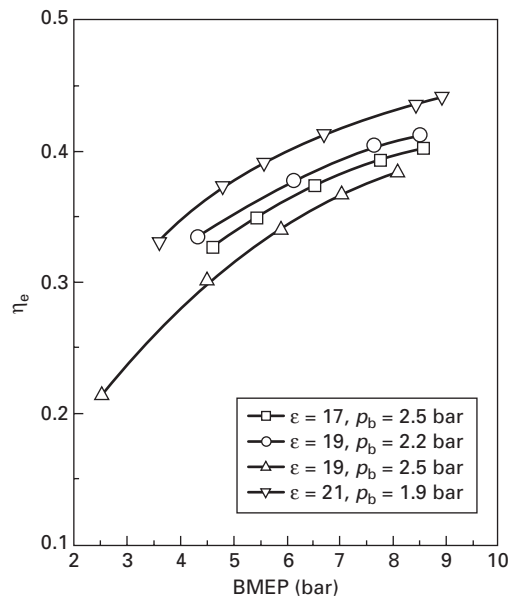

15.32 Performance of natural gas supercharged HCCI engine characteristics (engine speed 1800 rpm, assumed turbocharging efficiency 0.64) [6].

the maximum value of η_e is approximately 0.4. However, when ε is increased to 19 and p_b = 2.5 bar, η_e decreases from the value at ε = 17. This is because the upper operating limit is limited by p_{max}. By setting p_b to 2.3 bar and changing the in-cylinder pressure profile to reduce p_{max}, η_e can be improved to 0.41. At ε = 21 and p_b = 1.9 bar, the thermal efficiency can be improved even further (approximately 0.43). Regardless of the values of ε and p_b, the value of BMEP at the upper operating limit is around 8.0–9.0 bar.

Under high thermal efficiency operating conditions, the heat release process is extremely sensitive to the fuel charge. Even a tiny change in the fuel charge can lead to knock or accidental fire, requiring a sophisticated control method to ensure continuous stable engine operation. The concentration of NOx in exhaust gas is below 10 ppm under all operating conditions. From these results it can be concluded that when the maximum in-cylinder pressure is limited, increasing the engine compression ratio to minimize the lower operating limit temperature and reducing the boost pressure makes it possible to achieve high thermal efficiency and extremely low NOx emission concentration.

This analysis reveals that turbocharging into a natural gas-fueled homogeneous charge compressed ignition engine has considerable potential. Due to the characteristics of natural gas as a fuel, a high intake air temperature is necessary to achieve auto-ignition, but with the application of turbocharging, intake air heating becomes unnecessary, which is another advantage.

15.13 Summary

The engine performance and exhaust gas characteristics of a natural gas-fueled HCCI engine with external supercharger were examined in order to explore the potential of HCCI engines. The performance of a turbocharged HCCI engine was also predicted through one-dimensional cycle simulations. The main conclusions of the present study are as follows.

From the experimental results:

1. Under conditions restricting the upper operating limit (i.e. maximum BMEP) by in-cylinder pressure, the combustion efficiency was low, attributable to the low maximum combustion temperature. The brake thermal efficiency was also low for this reason.
2. When the in-cylinder pressure during operation is limited by the allowable cylinder strength, increasing the engine compression ratio and reducing the boost pressure improve the thermal efficiency.
3. Under a compression ratio of 21, boost pressure of 1.9 bar, and air intake temperature of 333K, it is possible to operate at a brake thermal efficiency of 0.43 and break mean effective pressure of 9.0 bar, with NOx emission below 10 ppm.

15.14 References

1. Daesu Jun, Kazuaki Ishii and Norimasa Iida, 'Combustion Analysis of Natural Gas in a Four Stroke HCCI Engine Using Experiment and Elementary Reactions Calculation', SAE Paper 2003-01-1089 (2003).
2. TNO report, 12 of 76, Table 2.1, 14, June (1996).
3. C. Chevalier, P. louessard, U.C. Muller and J. Warnatz A, 'Detailed Low-Temperature Reaction Mechanism of n-Heptane Auto-Ignition', COMODIA 90, pp 93–97 (1990).
4. C.K. Westbrook, W. J. Pitz, W.R. Leppard, 'The Autoignition Chemistry of Paraffinic Fuels and Pro-Knock and Anti-Knock Additives: A Detailed Chemical Kinetic Study', SAE Paper 912314 (1991).
5. S. Kojima, 'Detailed Modeling of n-Butane Autoignition Chemistry' *Combustion and Flame* 99, pp 87–136 (1994).
6. Takahiro Sako, Satoshi S. Morimoto, Hiroumi Fujimoto, Ryoji Okada and Norimasa Iida, 'A Study on Supercharged HCCI Natural Gas Engines', JSAE 20056503/ SAE Paper 2005-32-0021 (2005).
7. Deasu Jun and Norimasa Iida, 'A Study of High Combustion Efficiency and Low CO Emission in a Natural Gas HCCI Engine', SAE Paper 2004-01-1974 (2004).
8. Takahiro Sako, Shunsaku Nakai, Koji Moriya and Norimasa Iida, 'Performance and Exhaust Emission in a Natural-Gas Fueled Homogeneous Charge Compression Ignition Engine', Transactions of Japan Society of Mechanical Engineers, 70-694, B, pp. 197–203 (2004) (in Japanese).
9. Takuji Ishiyama, Masahiro Shioji, Hiroki Tanaka, Hideki Nakagawa, Shunsaku Nakai, 'Performance and Exhaust Emissions of a Premixed Charge Compression Ignition Engine Fueled with Natural Gas Employing Direct Injection', JSAE Lecture Proceedings, 236, pp. 15–20 (2002) (in Japanese).

16

HCCI engines with other fuels

N IIDA, Keio University, Japan

16.1 Characterization of DME

The properties of dimethyl ether (DME) compared with n-Butane, methane and diesel oil are summarized in Table 16.1 [1].

DME is generated from various abundant hydrocarbons, such as natural gas, coal, and biomass. DME is easily vaporized because of its low boiling point and vapor pressure. Furthermore smokeless combustion is possible because it has no C-C combinations and no sulfur.

Figure 16.1 shows the ignition delay of DME in comparison to n-Butane and methane in numerical calculation. DME has a two-step heat release called low temperature reaction (hereafter, LTR) and high temperature reaction (hereafter, HTR). It may be said that DME is a superior fuel in ignition characteristics because its ignition delay is much shorter than the other gaseous fuels and it has a high cetane number. Besides, it is also superior in combustion characteristics as it has high combustion velocity and low ignition temperature.

As mentioned above, DME has a lot of advantages as an alternative fuel, and it is a suitable fuel for compression ignition engines on account of its superior ignition and combustion characteristics.

Table 16.1 Properties of DME compared to n-butane, methane and diesel Oil [1]

	n-Butane C_4H_{10}	Methane CH_4	Diesel oil	DME CH_3OCH_3
Boiling point °C	–0.5	–162	200–350	–25
Low calorific value kcal/m^3	26,504	8,600	–	14,143
Ignition temp. °C	430	632	230–250	350
Adiabatic flame temp. °C		1,963	2,125	1,954
Combustion velocity cm/s	41	37	–	50
Viscosity coefficient 10^{-3} kg/ms		–	2–4	0.15
Cetane number	<10	0	10–55	55–60
Others				Catalysis

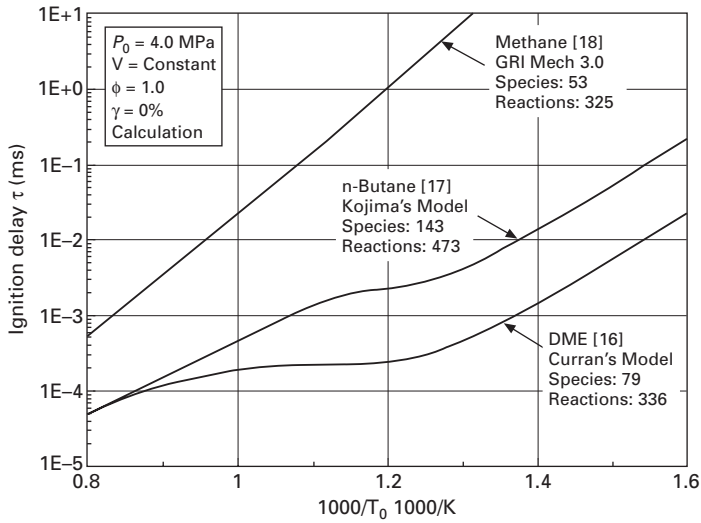

16.1 Logarithmic plot of DME, n-Butane and methane ignition delays [10].

16.2 DME HCCI engine

The HCCI engine has potential for diesel-like thermal efficiency with very low NOx emission and particulate matter (PM). In spite of those advantages, the HCCI engine has some problems, which are high-unburned hydrocarbon and CO emissions, difficulty in controlling the combustion phasing, and high-load operating limit by knocking.

A DME HCCI engine has a lot of excellent characteristics. DME/air mixture naturally aspirated to a HCCI engine is subject to increasing pressure and temperature as it is compressed by the piston, causing two stages of heat release by LTR at first and HTR later. DME has the feature that the temperature at the beginning of LTR is about 650K, which is lower than 850K of petroleum-derived fuels. The heat release value in the LTR is larger than that of petroleum fuels. These features are excellent characteristics that are able to solve the problem of HCCI engines. In this chapter, the focus is on the combustion research of DME HCCI engines for reducing unburned hydrocarbon and CO emissions with the aid of chemical reaction calculation [2, 3].

16.3 DME chemical reaction model

DME has two-stage-ignition during the auto-ignition process as the alkane family fuels whose number of C is more than four. In order to compare with experimental results, it is necessary to choose a DME reaction scheme that

can re-create this characteristic of two-stage ignition. The following DME reaction schemes are proposed: Curran *et al*.'s scheme [4]; and Dagaut *et al*.'s scheme [5]; Koyama *et al*. [6] reported that Curran *et al*.'s scheme can re-create both LTR and HTR and has good agreement with experimental data in respect of the appearance timing of both LTR and HTR, and can be qualitatively used for the prediction of the influence of equivalence ratio and temperature on the appearance timing.

The main reaction mechanism of DME is shown in Fig. 16.2. In this figure, the vertical axis shows energy, and the activation energies are quoted from Curran's scheme.

LTR begins with the breakage of C–H bond of DME. Next, O_2 attaches to a C atom in place of the abstracted H atom, forming $C_2H_5O_3$ (1st O_2 addition). A subsequent isomerization reaction gives rise to the second O_2 addition. Governed by equilibrium conditions, $C_2H_5O_3$ without the 2nd O_2 addition can undergo a chain propagation reaction, after which oxidization apparently stops. $C_2H_5O_5$, on the other hand, generated by 2nd O_2 addition is dominated by temperature. Under 800K, the equilibrium of the system $C_2H_5O_3 + O_2 = C_2H_5O_5$ is directed toward the right. However, the reaction tends toward the left at higher temperatures, and oxidation is inhibited. This equilibrium system gives rise to the NTC region.

At temperatures exceeding 1000K, HTR is dominant. HTR begins with the abstraction of H from DME in a similar way to LTR. After H abstraction, C–O bonds are broken and the DME is broken and subsequently oxidized.

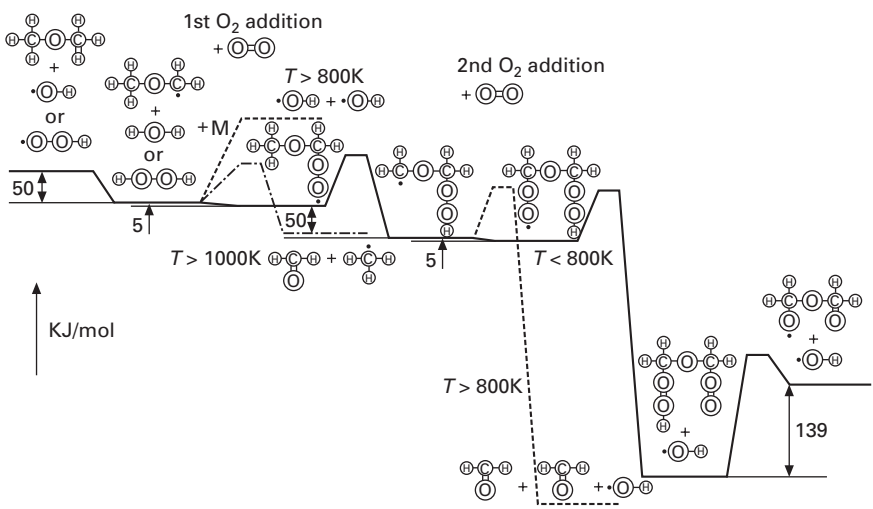

16.2 Main chemical reaction path of DME/Air [4].

16.4 Combustion completeness in the DME HCCI engine

16.4.1 Influence of equivalence ratio

(a) Pressure, temperature and rate of heat release

Figure 16.3 shows pressure and temperature histories at various equivalence ratios obtained from calculation (initial temperature $T_0 = 300$K, initial pressure $P_0 = 0.1$ MPa, compression ratio $\varepsilon = 12.5$ and engine speed $N_e = 800$ rpm). The 0-dimensional calculation with CHEMKIN II [7] and SENKIN [8] makes use of Curran's scheme for the simulated 4-stroke HCCI engine. In the temperature history figure, η_{comb} shows combustion efficiency. At an equivalence ratio of $\Phi = 0.2$, there is only one stage pressure and temperature rise. And at an equivalence ratio of $\Phi = 0.236$, there are two stages in pressure and temperature rise. With a higher equivalence ratio, the cylinder pressure and temperature have lower values in the compression stroke, because of lower specific heat ratio. However, as equivalence ratio is increased, the maximum values of pressure, temperature and combustion efficiency become higher.

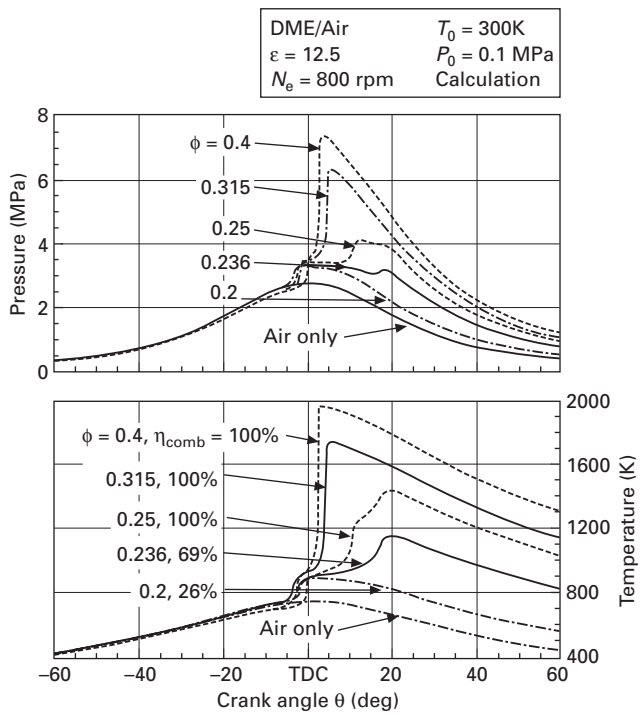

16.3 Pressure and temperature histories for various equivalence ratios and combustion efficiencies (calculation) [3].

Figure 16.4 shows pressure and temperature histories at various equivalence ratios obtained from experiment (intake temperature T_{in} = 300K, intake pressure P_{in} = 0.1 MPa, compression ratio ε = 12.9 and engine speed N_e = 800 rpm). At equivalence ratio Φ = 0.2, one stage pressure and temperature rise is observed, and at more than Φ = 0.25, a two-stage rise is observed. And, similar to calculation results, as equivalence ratio is increased, combustion efficiency increases. But in the experiment result, when equivalence ratio increases, pressure and temperature rising timing produced results contrary to calculations.

Figure 16.5 shows rate of heat release profiles at various equivalence ratios obtained from calculation. In this figure, the solid lines show the rate of heat release profiles of no EGR condition. At the equivalence ratio of Φ = 0.2, one peak heat release, LTR is observed. In case of the equivalence ratio Φ = 0.24, heat release of the LTR becomes larger and HTR appears, as a result, the heat release rate curve have two peaks. In the case of Φ = 0.28, the heat release of the HTR becomes larger and heat release curve at the HTR has two peaks. But two peaks at the HTR are united in one peak in the case of Φ = 0.4.

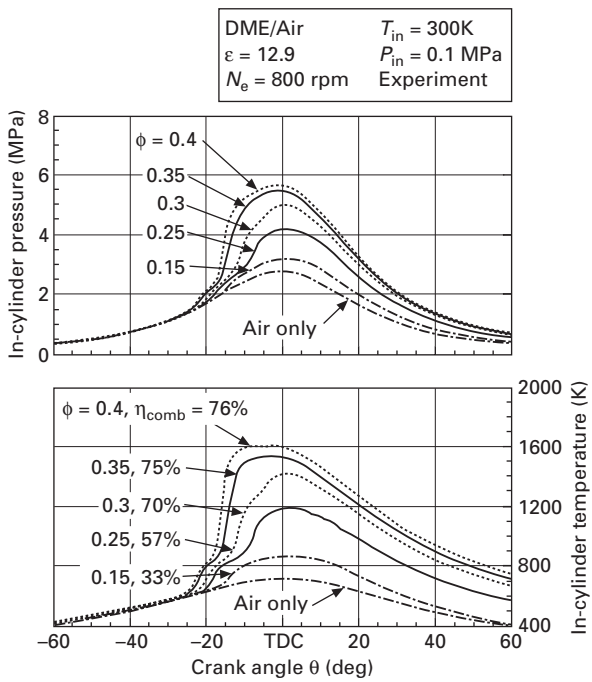

16.4 Pressure and temperature histories for various equivalence ratios and combustion efficiencies (experiment) [3].

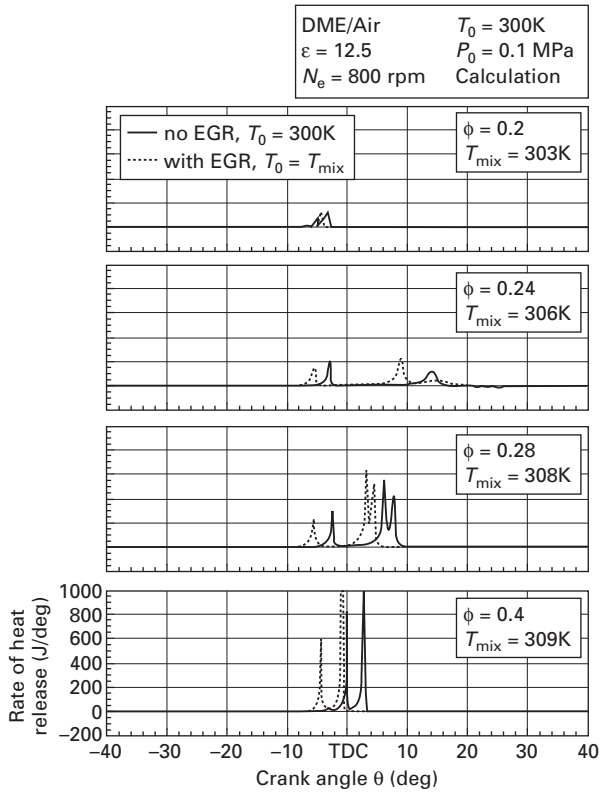

16.5 Rate of heat release profiles for various equivalence ratios (calculation) [3].

This tendency of the HTR curve was also seen in the experiment in Fig. 16.6. At higher equivalence ratio, the maximum value of the rate of heat release increases in the simulation. However, in the experimental results, the maximum value of LTR remained almost constant. In addition, the appearance timing of LTR is retarded in the calculation. In the experimental results, the appearance timings of both LTR and HTR were advanced. The differences between calculation and experiment are thought to be due to residual gas. In the experiment, residual gas supplied enthalpy to the next cycle and the temperature at the start of compression is not constant because of the residual gas, i.e. internal EGR gas. On the other hand, in the calculation only one cycle is calculated and this does not take account of residual gas.

So the effects of the residual gas were taken into account, and the calculation was carried out. In Fig. 16.5, the broken lines show the heat release profiles at the condition with internal EGR for various equivalence ratios. With higher equivalence ratio, the temperature at the start of compression T_{mix}

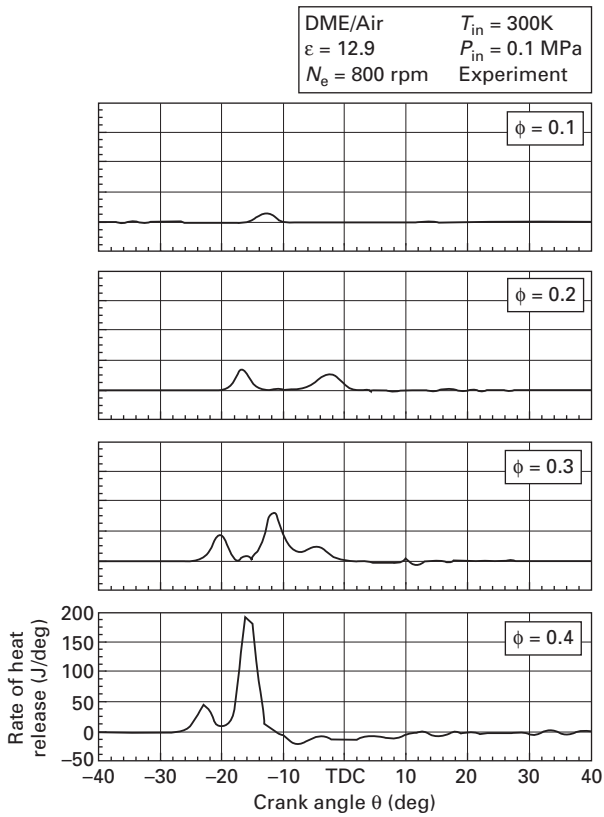

16.6 Rate of heat release profiles for various equivalence ratios (experiment) [3].

becomes higher. As a result, the appearance timings of LTR are almost constant against various equivalence ratios.

(b) Combustion efficiency and exhaust emissions

Figure 16.7 shows combustion efficiency and exhaust emissions as CO, CO_2 and THC (total hydro carbon) concentration for equivalence ratio variation in the calculation. Exhaust emissions' values were calculated with the exhaust valve open and combustion gas expanded to atmospheric pressure. Though combustion efficiency decreases till about $\Phi = 0.15$, if more than $\Phi = 0.15$ it increases. In addition, from $\Phi = 0.25$ to $\Phi = 0.75$ combustion efficiency reaches 100%. CO_2 emission increases as equivalence ratio become high. From $\Phi = 0$ to 0.22 THC and CO emissions increase. But if it is more than $\Phi = 0.25$, at which combustion efficiency reaches 100%, THC and CO emissions become almost zero.

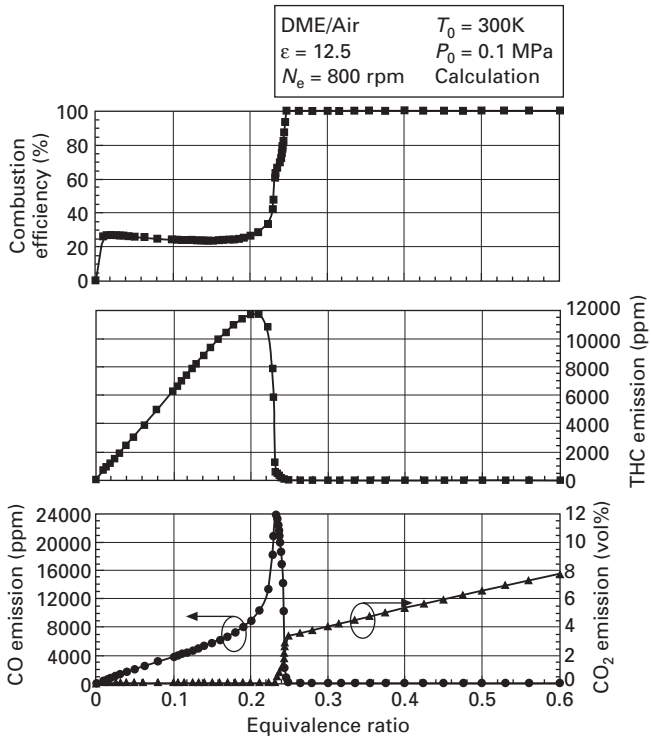

16.7 Relationship between equivalence ratio and combustion efficiency, THC, CO, CO_2 emissions (calculation) [3].

Figure 16.8 shows combustion efficiency and exhaust emissions as CO, CO_2 and THC (total hydro carbon) concentration for equivalence ratio variation in the experiment. In the experiment, THC emission was measured by FID, CO and CO_2 by NDIR. In the experiment, if equivalence ratio is more than $\Phi = 0.4$, the operating of the engine was impossible. With higher equivalence ratio, combustion efficiency and CO_2 emission become higher. This tendency is the same as the calculation result. THC emission increases until $\Phi = 0.15$, and CO emission until $\Phi = 0.25$, but both emissions decrease if the equivalence ratio is higher than $\Phi = 0.25$, at which combustion efficiency reaches 60%. However, THC and CO emissions' maximum values are lower than those of the calculation result. Finally it should be mentioned that unburned fuels near the cylinder wall and in the piston quench area are not taken into consideration in the calculations.

16.4.2 Influence of initial temperature

Figure 16.9 shows the temperature-pressure diagram for various initial temperatures in calculation (equivalence ratio $\Phi = 0.2$, initial pressure $P_0 =$

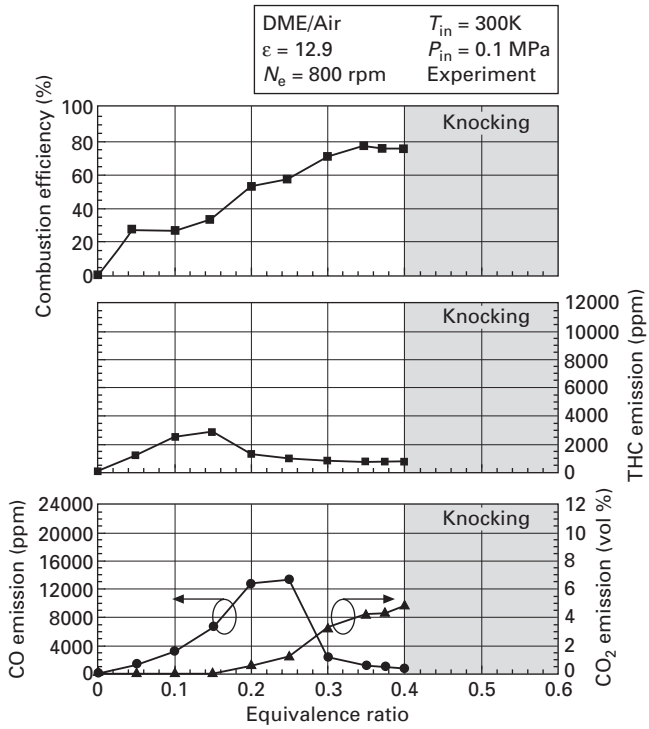

16.8 Relationship between equivalence ratio and combustion efficiency, THC, CO, CO_2 emissions (experiment) [3].

0.1 MPa, compression ratio ε =12.5 and engine speed N_e = 800 rpm). The combustion efficiency and maximum temperature and pressure of the cycle increased as initial temperature increased. In this condition, it is clarified that combustion efficiency is ensured to be over 90% as the temperature in a cycle exceeded 1250K, regardless of maximum pressure, and then reached 100% as the temperature exceeded 1400K.

Figure 16.10 shows the rate of heat release profiles at various initial temperatures obtained from calculation. As the initial temperature is increased, the timing of the occurrence of heat release by LTR and HTR advances, and the maximum value of the rate of heat release from LTR decreases. The maximum value of the rate of heat release from HTR increases. The advance of LTR occurrence timing was also observed in the result of equivalence ratio variation, especially in the experiment.

16.4.3 LTR and HTR appearance conditions

Figure 16.11 shows pressure and temperature at LTR and HTR at various equivalence ratios and initial temperatures obtained from calculation. Solid

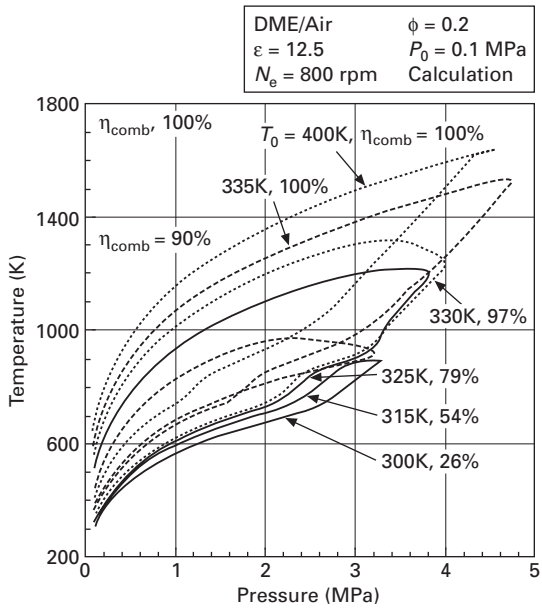

16.9 Temperature-pressure diagram for various initial temperatures (calculation) [3].

symbols show LTR appearance points and open symbols HTR appearance points. LTR appears in the range from 700K to 750K and HTR about 1000K. In these results, appearance of both reactions largely depends not on pressure but temperature of pre-mixture.

16.4.4 Chemical species concentration profile

Mole fraction histories of each chemical species at $\Phi = 0.24, 0.28$ are shown in Fig. 16.12 and Fig. 16.13. These figures include temperature profiles and heat release profiles in each condition. At equivalence ratio $\Phi = 0.24$, two temperature increases and two peaks of heat release rate are observed. At the same timing of heat release, DME (CH_3OCH_3) begins to be reduced and the concentrations of CO, CO_2, HCHO and H_2O_2 rapidly increase. Behavior of OH mole fraction has the same tendency as rate of heat release value. And about 1/2 of DME (CH_3OCH_3) decreases during LTR. In this condition, HCHO and H_2O_2 and DME (CH_3OCH_3) concentrations begin to decrease quickly at the beginning of HTR heat release. However, CO mole fraction increases at the same time. Combustion efficiency is 74% and CO still remains. In other words, appearance of both LTR and HTR does not mean complete combustion. At equivalence ratio $\Phi = 0.28$, two spikes are observed in HTR, three spikes are in HRR. After the third spike, CO emission is almost oxidized

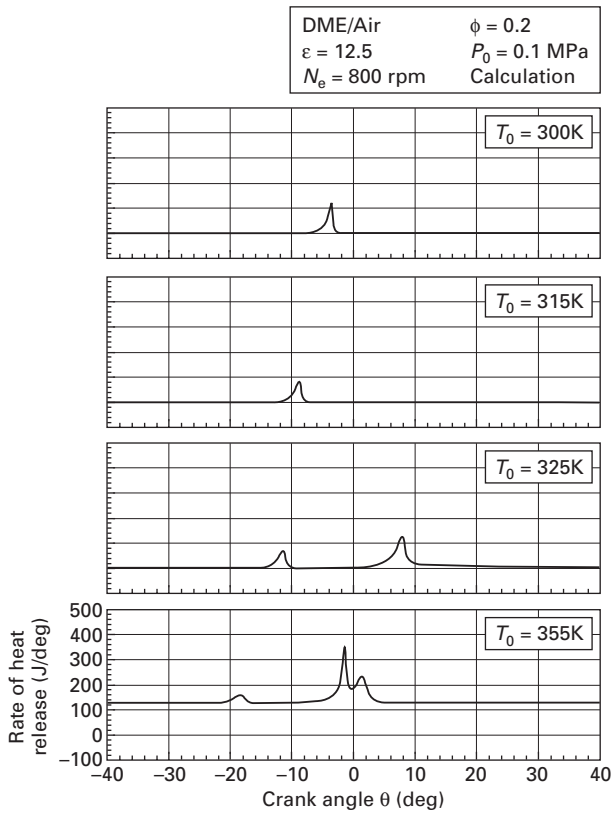

16.10 Rate of heat release profiles for various initial temperatures (calculation) [3].

and the combustion efficiency is 100%. In this case, HCHO, H_2O_2 and DME (CH_3OCH_3) but also CO decreases gradually at the late term of HTR with increasing CO_2. The maximum temperature becomes about 1600K.

From exhaust emissions, in case of $\Phi = 0.24$, THC emission was about 200 ppm and CO emission about 19,000 ppm and these emissions came at incomplete combustion. In order to complete combustion, it is thought that the temperature in a cycle was a very important factor.

16.4.5 Necessary factor for high combustion efficiency and low emissions

In this way, maximum temperature is thought to be an index of combustion efficiency. Figure 16.14 shows the relationship between maximum temperatures of the cycle and combustion efficiencies and THC, CO and CO_2 emissions in calculation. The plots in the figure show all of the calculation results. As

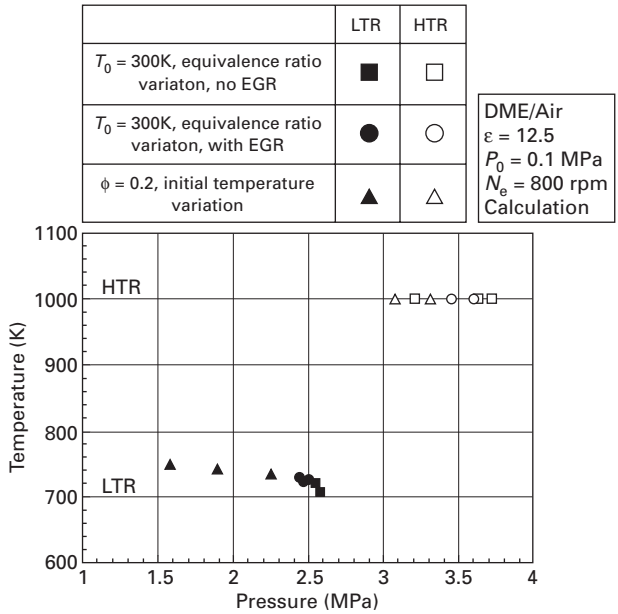

16.11 Temperatures at appearance timings of LTR and appearance timings of HTR for various initial temperatures and equivalence ratios [3].

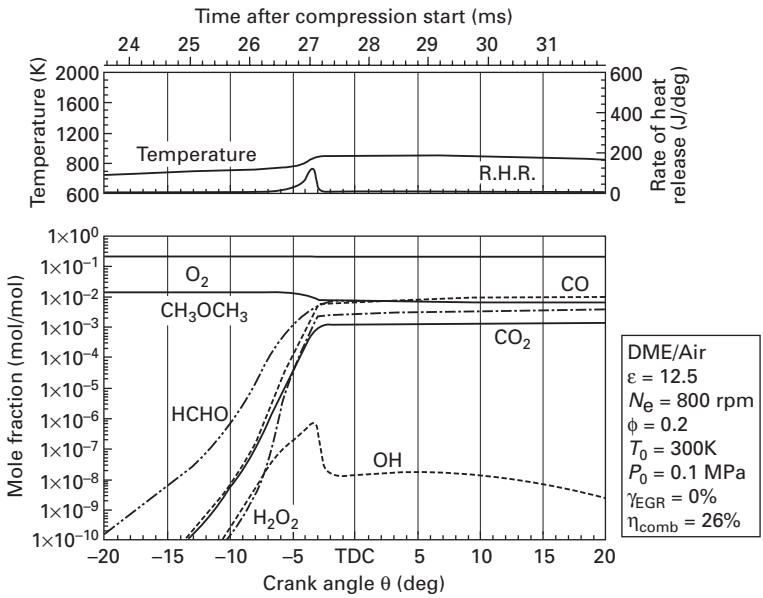

16.12 Mole fraction histories of major chemical species (Φ = 0.24, calculation) [3]

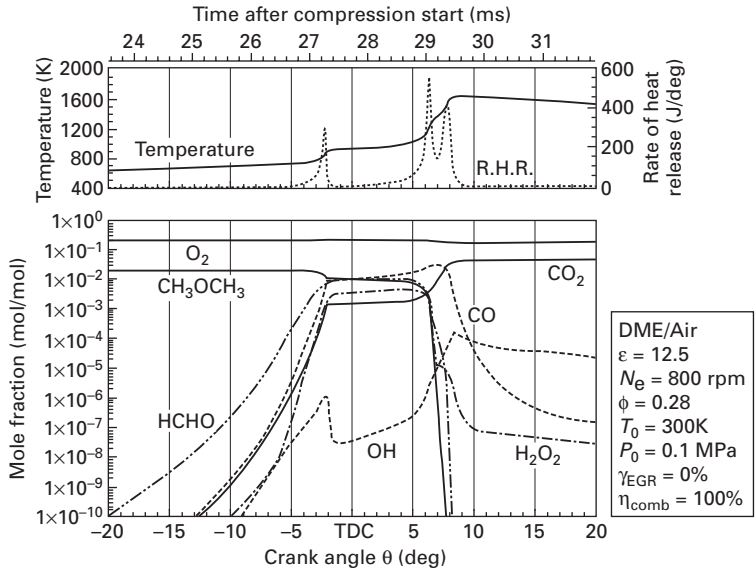

16.13 Mole fraction histories of major chemical species (Φ = 0.28, calculation) [3].

combustion efficiency and maximum temperature increased, THC and CO first increased and after that decreased, and CO_2 increased. When maximum temperature reached 1250K, combustion efficiency became 90%. Under the condition that the maximum temperature was over 1400K, CO and THC was almost zero and the combustion efficiency was 100%.

In order to compare this result with experiment, exhaust emissions obtained from experimental results were investigated. Figure 16.15 shows the relationship between maximum temperatures of the cycle and combustion efficiencies and THC, CO and CO_2 emissions in experiment. Similar CO and CO_2 emission characteristics are observed experimentally as in the calculations. However, lower THC emissions are observed experimentally. When maximum temperature reached 1600K, combustion efficiency became about 80%.

From those results, the necessary condition to keep high combustion efficiency and to reduce both THC and CO emissions is that in which the maximum temperature is more than 1600K in a combustion cycle by any method.

In conclusion, the maximum temperature in cycle has a great influence on combustion completeness. Although the increment of the maximum temperature follows an increase of combustion efficiency, if the maximum temperature reaches 1200K, HC emission will be almost 0% in the process. However, it is understood that the maximum temperature needs to be over 1500K for CO

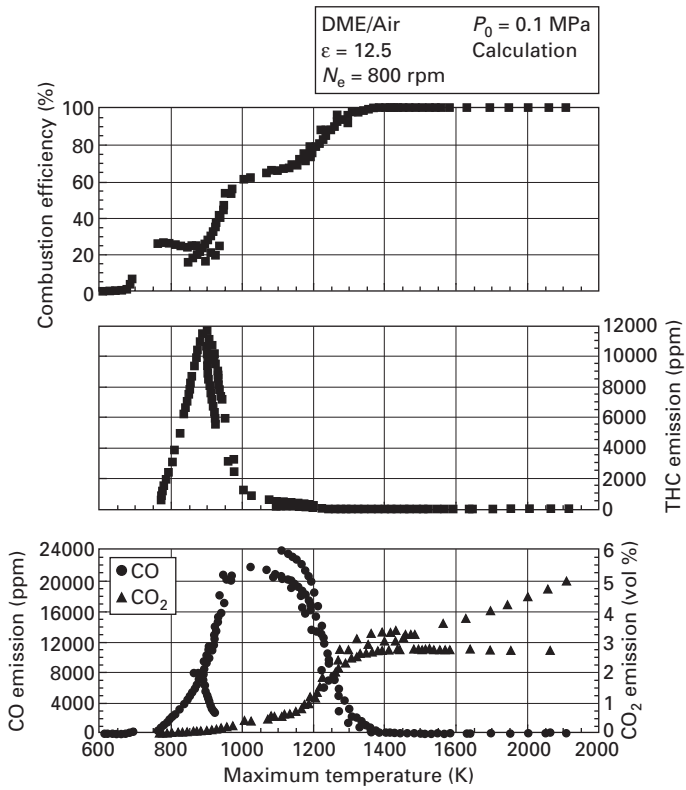

16.14 Relationship between maximum temperature and combustion efficiency, THC CO, CO_2 emissions (calculation) [3].

emissions to become 0%. Therefore, a combustion temperature over 1500K is needed for the complete DME HCCI combustion.

16.4.6 Summary of characteristic of auto-ignition of DME

In the above analysis, the characteristics of auto-ignition of DME/Air mixture in a HCCI engine are analyzed with the aid of chemical kinetics of elementary reactions. It was assumed that the temperature, pressure and composition of the mixture are always spatially uniform and the mixture is adiabatic. The calculation was carried out with changing equivalence ratio and initial temperature compared with the experimental results. The summary is as follows:

1. In the calculation, the start of LTR is retarded as the equivalence ratio is increased, while in the experiment that timing advanced. This phenomenon results from the existence of residual gas.

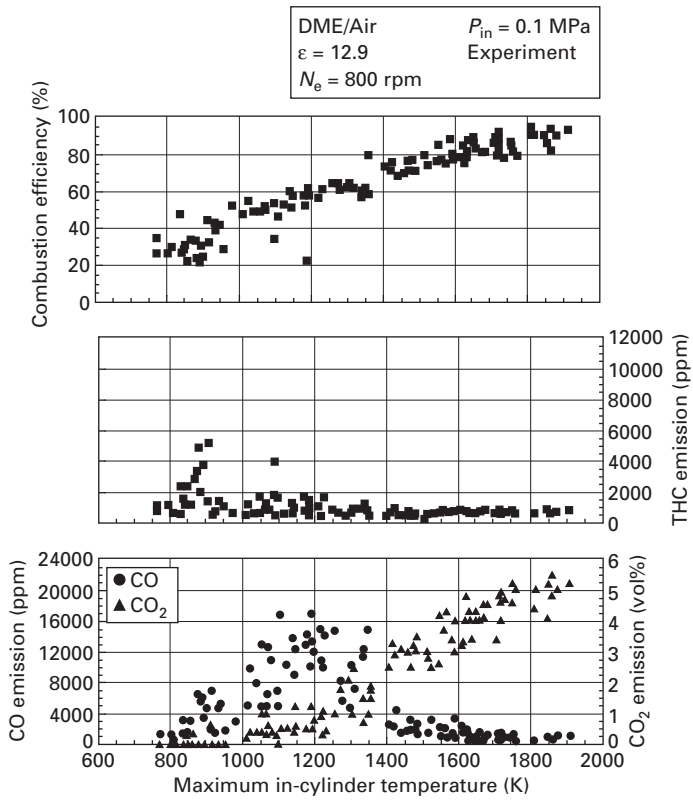

16.15 Relationship between maximum temperature and combustion efficiency, THC CO, CO_2 emissions (experiment) [3].

2. The start of both LTR and HTR are advanced with higher initial temperature.
3. LTR appears in the range from 700K to 750K and HTR at about 1000K. In addition, appearance of both LTR and HTR reactions largely depends not on pressure but temperature of pre-mixture.
4. Heat release by HTR can be separated into two stages. In the first stage is oxidation of HCHO and H_2O_2 in the same way as for LTR, the later stage is mainly CO oxidation and H_2O generation reactions.
5. In HCCI engines, ignition doesn't lead to complete combustion. The necessary condition to keep high combustion efficiency is to have a maximum temperature more than 1500K.
6. If maximum temperature of the cycle can reach 1500K, THC and CO emissions rapidly decrease.

16.5 Combustion control system for a small DME HCCI engine [9–10]

Since compressed auto-ignition temperature of DME is low, HCCI combustion can be realized in an engine with a low compression ratio. A research consortium led by Keio University has taken advantage of it and developed a HCCI engine for a small electric generator [9]. The weight of the DME HCCI engine is minimized by limiting its maximum power output. The main features are described here. To assume a simple structure, the engine doesn't have any variable mechanism of the compression ratio and the valve timing, etc. needed as in some other HCCI engines. The engine is operated with the stoichiometric mixture in order to use a conventional 3-way catalyst to reduce the emissions. Wide-ranging HCCI combustion has been optimized by adjusting the amount of the supply of external EGR gas with internal residual gas by operating four throttle valves, and managing the temperature of the charging air-fuel mixture. Figure 16.16 shows the schematics of the engine system and Fig. 16.17 shows the block diagram of the engine. A two-stage exhaust cam mechanism that opens the exhaust valve in the intake stroke as an internal EGR method is used. As a result, the engine was developed with IMEP upto 0.45MPa and the indicated thermal efficiency as high as 41%.

16.5.1 Specifications of DME HCCI engine

The DME HCCI engine was a modified engine of HONDA GX340 K1, 337 cc, single cylinder, air-cooled, gasoline engine, used in an electric generator EM4500 [10]. Figure 16.18 shows the sectioned drawing around the combustion chamber and the specifications of the engine. Compression ratio is variable

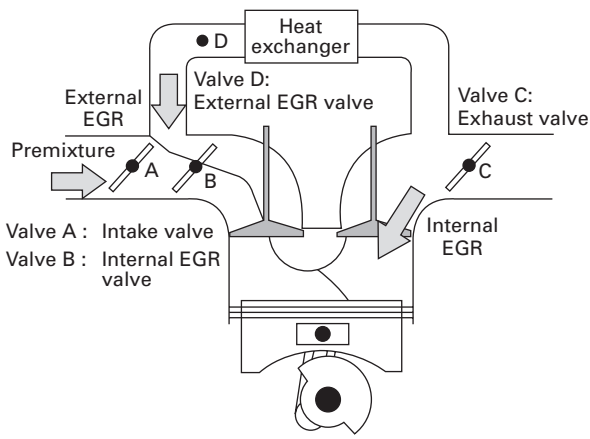

16.16 DME HCCI engine [9].

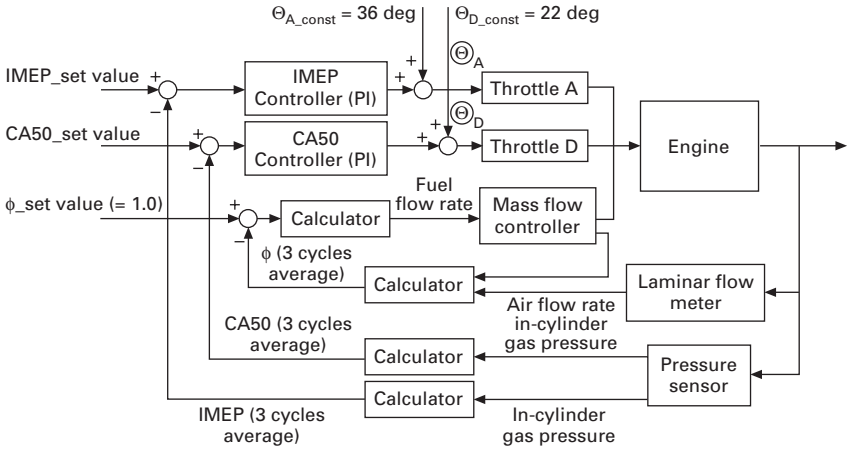

16.17 The engine control block diagram [9].

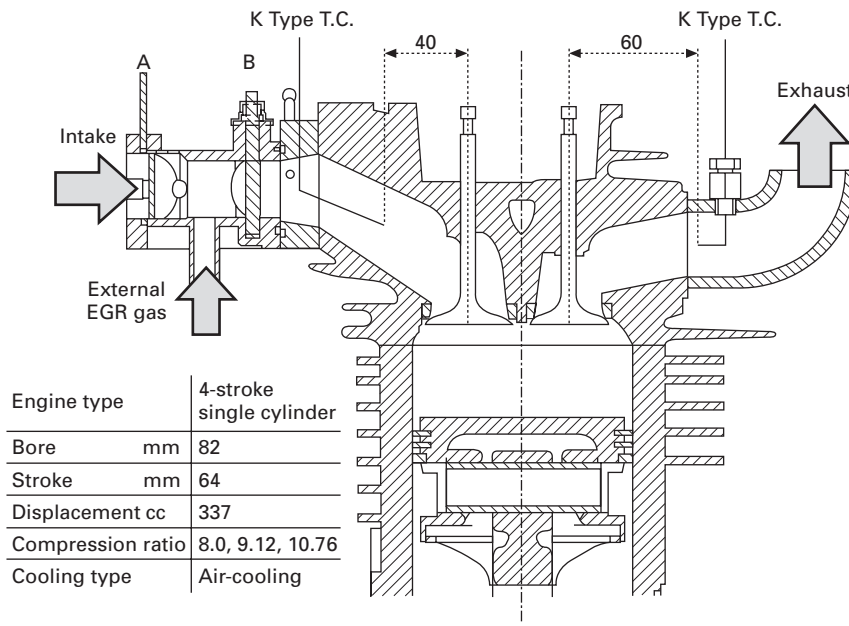

Engine type		4-stroke single cylinder
Bore	mm	82
Stroke	mm	64
Displacement	cc	337
Compression ratio		8.0, 9.12, 10.76
Cooling type		Air-cooling

16.18 Sectioned drawing around the combustion chamber and specifications of the reference engine [10].

to 8.0, 9.12, 10.76 with changing cylinder head and gasket. An in-cylinder pressure sensor is fitted at the top of cylinder head in order to detect the auto-ignition timing of HCCI combustion process of the engine. Thermocouples are mounted on both intake port and exhaust port to measure intake and

exhaust gas temperatures in order to estimate the mass averaged gas temperature of the charged gas trapped in the combustion chamber.

16.5.2 Combustion control method of DME HCCI engine

This section describes the combustion control method for combustion phasing, avoidance of knocking and securing of combustion completeness of the DME HCCI engine.

(a) Ignition timing control

In a HCCI engine, auto-ignition timing is strongly dependent on the in-cylinder gas temperature. Each fuel has a particular auto-ignition temperature, and oxidation reaction takes place at the timing when the in-cylinder gas temperature reaches its auto-ignition temperature during compression processes by the piston.

The temperature rise is evaluated assuming adiabatic compression. At a constant compression ratio, temperature history is decided as a function of crank angle from the temperature at the start of compression, thus adjusting temperature at compression start can control ignition timing. In-cylinder gas temperature at compression start, that is necessary to reach the required ignition temperature at an arbitrary timing, is calculated with Eq. 16.1.

$$T_{\mathrm{IVC}} = T_{\mathrm{HTR}}\left(\frac{V(\theta)}{V_{\mathrm{IVC}}}\right)^{\kappa-1} \tag{16.1}$$

T_{IVC}	Temperature at compression start	K
T_{HTR}	Temperature at appearance timing of HTR	K
$V_{(\theta)}$	In-cylinder gas volume	m^3
V_{IVC}	Gas volume at compression start	m^3
κ	Specific heat ratio (c_p/c_v)	–

In the meantime, fresh gas at low temperature and internal EGR gas at high temperature coexist in the combustion chamber at the time when the intake valve is closed. Therefore the temperature at the start of compression is calculated with equation of enthalpy balance, using mass, specific heat at constant volume and temperature of both fresh gas and internal EGR gas, expressed in Eq. 16.2. As the amount of internal EGR gas increases, initial charge temperature increases and ignition timing advances. The mass ratio of internal EGR gas is one of the measured control factors for combustion phasing control.

$$T_{\mathrm{IVC}} = \frac{c_{\mathrm{p_in}} m_{\mathrm{in}} T_{\mathrm{in}} + c_{\mathrm{p_IEGR}} m_{\mathrm{IEGR}} T_{\mathrm{IEGR}}}{c_{\mathrm{p_in}} m_{\mathrm{in}} + c_{\mathrm{p_IEGR}} m_{\mathrm{IEGR}}} \tag{16.2}$$

T_{in}	Temperature of fresh gas	K
T_{IEGR}	Temperature of internal EGR gas	K
c_{p_in}	Specific heat of fresh gas	J/mol/K
c_{p_IEGR}	Specific heat of internal EGR gas	J/mol/K
m_{in}	Mass of fresh gas	kg
m_{IEGR}	Mass of internal EGR gas	kg

(b) Avoidance of knocking combustion

Since the engine operates with HCCI combustion mode, HTRs occur almost simultaneously throughout the chamber, a very high heat release rate causes knocking at high load. Generally reaction speed of chemical kinetics including elementary reactions grows very large so that rate constant increases with temperature rise expressed in Arrhenius equation in Eq. 16.3.

$$k = AT^{\beta} \exp\left(-\frac{E}{RT}\right) \tag{16.3}$$

A	Pre-exponential factor	
E	Activation energy	J/mol
k	Rate constant	
R	Universal gas constant	J/mol/K
β	Temperature exponent	

The use of external EGR at low temperature, which includes a lot of inert gas like CO_2, is effective to prevent a sudden temperature rise. The mass ratio of external EGR gas, which is cooled off with a heat exchanger, is one of the control parameters to avoid knocking.

(c) Securing of combustion efficiency

The combustion speed is governed by chemical kinetics and so is strongly influenced by the concentration of the reactive species. As a result, only lean mixture can burn without knocking. Therefore gas temperature does not rise high enough to achieve high combustion efficiency.

Kojima *et al.* [11] investigated the mechanism of the combustion completion and reported that it is necessary to keep a maximum gas temperature at least above 1600K in order to complete the CO oxidation in HCCI combustion processes and to get high combustion efficiency.

The equation used to calculate the maximum gas temperature is shown as Eq. 16.4 based on the first law of thermodynamics.

$$T_{max} = \frac{c_{p_IVC} m_{IVC} T_{IVC} + Hum_{fuel} + c_{p_i} m_i T_{IVC} (\varepsilon^{\kappa-1} - 1)}{c_{p_c} m_c} \tag{16.4}$$

H_u	Low calorific value	kJ/kg
m_{fuel}	Mass of input fuel	kg
ε	Compression ratio	

In Eq. 16.4, mass of input fuel becomes a dominant variable. As the amount of fuel is increased, maximum gas temperature increases and high combustion efficiency can be achieved. In this study, premixed mixture of air and fuel at stoichiometric ratio is used as a control factor to secure combustion efficiency.

16.5.3 Control system of DME HCCI engine

As previously stated, stoichiometric mixture, internal EGR gas at high temperature and external EGR at low temperature are used as control factors to overcome the problems of the HCCI engine for avoidance of knocking, securing of combustion efficiency and ignition timing control.

Figure 16.19 shows the effects of the gas fraction of air/fuel mixture, internal EGR gas and external EGR gas. Figure 16.20 shows the relationship between the aforesaid control factors and control outputs. The proposed control method is based on the following observations:

1. IMEP (I axis) becomes high as the fraction of air/fuel mixture increases.
2. Temperature at the start of compression (II axis) rises and (A) ignition timing advances as the fraction of internal EGR gas increases.
3. Maximum gas temperature (III axis) is contained and combustion reaction

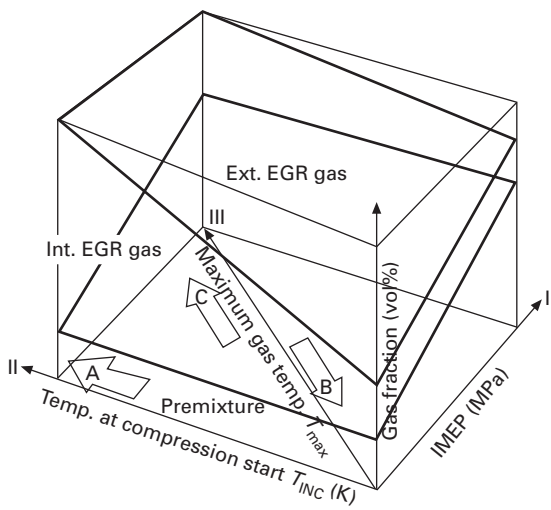

16.19 The effects of the gas fraction of air/fuel mixture, internal EGR gas and external EGR gas [10].

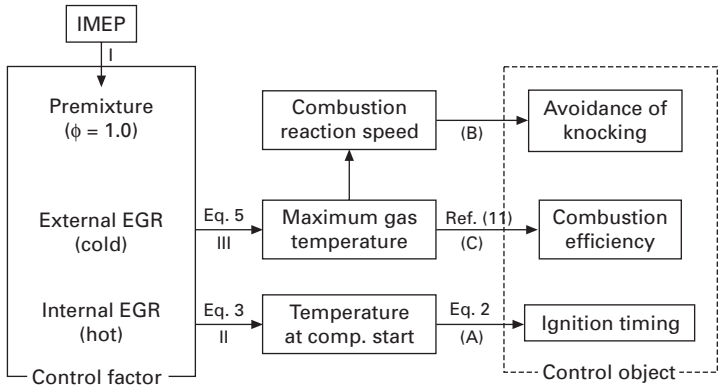

16.20 Relation between control factors and outputs [10].

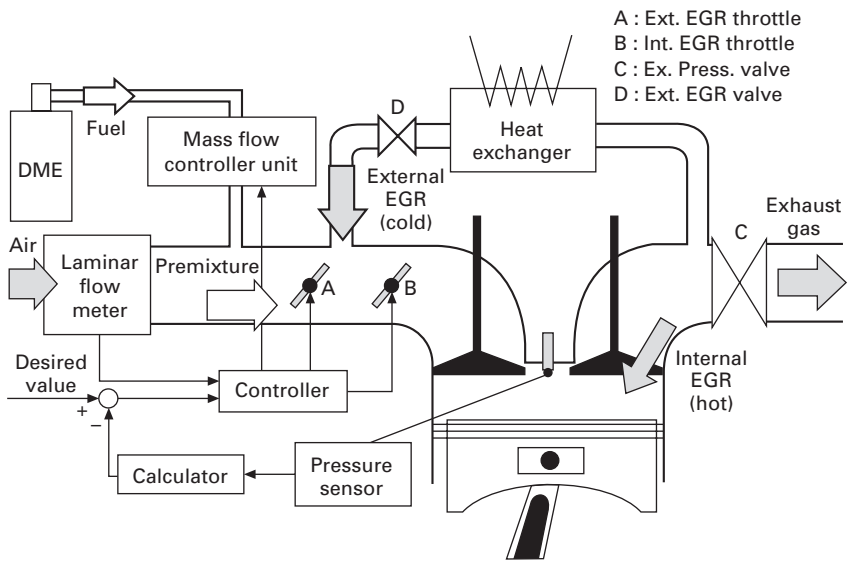

16.21 Combustion control system of stoichiometric DME HCCI engine [10].

speed becomes low as the fraction of external EGR gas increases and gas air/fuel mixture decreases. Then (B) knocking is prevented.

4. Maximum gas temperature (III axis) reaches high and (C) combustion efficiency becomes high as the fraction of air/fuel mixture increases and external EGR gas decreases.

The constructed system is shown in Fig. 16.21. Air and fuel are premixed quite upstream in the intake system. Some of the combustion gas remains in the combustion chamber as internal EGR gas and some is returned to the intake port as external EGR after cooling off with a heat exchanger.

In order to adjust the fraction of air/fuel mixture, internal EGR gas and external EGR gas, two throttles and two valves are fitted in this system. Throttle A for air/fuel mixture control, throttle B for internal EGR gas control, valve C for exhaust pressure control and valve D for external EGR gas control. For example, the fraction of air/fuel mixture decreases and external EGR gas increases with throttle A closed or valve D open. Internal EGR gas increases with throttle B closed or valve D closed.

16.5.4 Two-stage exhaust cam system

A two-stage exhaust cam system is adopted to introduce the internal EGR gas. As shown in Fig. 16.22, the exhaust valve reopens in the intake process in order to return the combustion gas into the combustion chamber as internal EGR gas.

In this study, three kinds of camshaft, which have different valve lifts at secondary exhaust process, are designed. And each camshaft is named according to the height of the secondary exhaust cam. Basically, the fraction of internal EGR gas is adjusted with two-stage exhaust cam and throttle B as explained before.

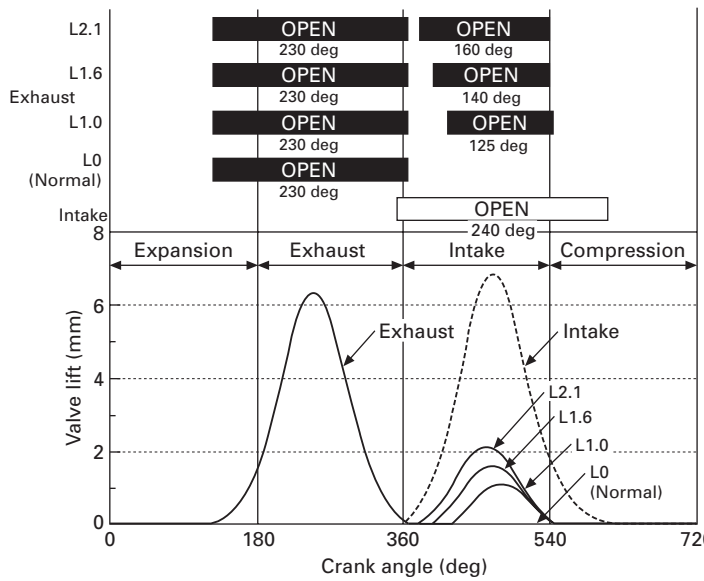

16.22 Valve timing of the designed two-stage exhaust cam system [10].

16.5.5 Calculation and experimental conditions

(a) Calculation conditions

Calculation conditions are shown in Table 16.2. In a single zone model it is assumed that the combustion chamber is a well-stirred reactor with a uniform temperature, pressure and composition. CHEMKIN II [7] and SENKIN [8] are used as calculation programs. In the numerical calculation, compression ratio is set to 12.0 and engine speed is set to 500 rpm to assure the ignition.

(b) Experimental conditions

Experimental conditions are also presented in Table 16.2. The set parameter is the gas fraction of air/fuel mixture, internal EGR gas and external EGR gas. Gas fraction is adjusted by using throttles and valves in Figure 16.21 before and throttle B for internal EGR gas control and valve D for external EGR gas control are used in this paper. Compression ratio is set to 8.0, 9.12 and four kinds of designed two-stage exhaust cam are used in the experiment.

(c) Calculation method of gas temperature

In-cylinder gas temperature and rate of heat release are calculated as follows using pressure data provided at every crank angle by the pressure sensor, which is fitted at the top of the cylinder head.

Since fresh gas and internal EGR gas coexist in the combustion chamber when the intake valve closes, temperature at compression start is calculated using equation of enthalpy balance shown in Eq. 16.2 before. At this point, fresh gas temperature is measured at 40 mm above intake valve and internal EGR gas temperature is measured at 60 mm after the exhaust valve with K type thermocouple.

Table 16.2 Calculation and experimental conditions [10]

	Calculation	Experiment
Fuel	DME	DME
Displacement	337 cc	337 cc
Cam type	–	L2.1, L1.6, L1.0, L0
Engine speed	500 rpm	1500 rpm
Compression ratio	12.0	8.0
Premixture rate	10–85 vol%	2.0–747 vol%
Equivalence ratio	10	0.7–1.0
Internal EGR rate	10–90 vol%	25.3–98.0 vol%
Throttle B open angle	–	10–80 degree
External EGR rate	0–80 vol%	0–5.0 vol%
Valve D open angle	–	0–100%
Calculation program	SENKIN CHEMKIN II	–

From the compression start to ignition occurring, in-cylinder gas temperature is calculated with equation of adiabatic change expressed in Eq. 16.5, because it is thought that oxidation reactions take place at the center of the cylinder without heat transfer.

$$T(\theta_{\mathrm{i}}) = T(\theta_{\mathrm{i-1}}) \cdot \left(\frac{P(\theta_{\mathrm{i}})}{T(\theta_{\mathrm{i-1}})} \right)^{\frac{\kappa_{\mathrm{i-1}}-1}{\kappa_{\mathrm{i-1}}}} \tag{16.5}$$

$P(\theta)$	In-cylinder gas pressure	MPa
$T(\theta)$	In-cylinder gas temperature	K

After the ignition, equation of state of ideal gas shown as Eq. 16.6 is used to calculate in-cylinder gas temperature.

$$T(\theta_{\mathrm{i}}) = \left(\frac{P(\theta_{\mathrm{i}}) \cdot V(\theta_{\mathrm{i}}) \cdot n(\theta_{i-1}) \cdot T(\theta_{i-1})}{P(\theta_{\mathrm{i-1}}) \cdot V(\theta_{\mathrm{i-1}}) \cdot n(\theta_{\mathrm{i}})} \right) \tag{16.6}$$

n	Number of moles	mol

Where rate of heat release is calculated with Eq. 16.7

$$\frac{dQ}{d\theta_{\mathrm{i}}} = \frac{1}{\kappa_{\mathrm{i-1}} - 1} V(\theta_{\mathrm{i}}) \frac{dP}{d\theta_{\mathrm{i}}} + \frac{\kappa_{\mathrm{i-1}}}{\kappa_{\mathrm{i-1}} - 1} P(\theta_{\mathrm{i}}) \frac{dV}{d\theta_{\mathrm{i}}} \tag{16.7}$$

$dQ/d\theta$	Rate of heat release	J/degree

Ignition is defined as at the point where rate of heat release gets over 0.3 J/degree.

(d) Definition of combustion reaction speed

In this study, combustion reaction speed is defined to estimate the rapidity of the oxidation reactions in HCCI combustion. It is defined as the ratio of the maximum rate of heat release and mass of fuel supplied,

$$v_{\mathrm{c}} = \left(\frac{dQ}{dt} \right)_{\max} \Big/ m_{\mathrm{fuel}} \tag{16.8}$$

v_{c}	Combustion reaction speed	J/ms/g
dQ/dt	Rate of heat release	J/ms

16.5.6 Calculation and experimental results

This section shows the calculation and experimental results. Combustion characteristics of DME and the effects of EGR are described. Additionally the performance of the developed HCCI engine is discussed in comparison to conventional engines.

(a) Combustion characteristics

Figure 16.23 shows the temperature and rate of heat release history for different internal EGR rates through experiments. Two-step heat release called LTR and HTR is observed. Heat release in LTR accounts for about 7% of total heat release at high internal EGR rate. And HTR starts at a temperature around 879 K. It is lower than the other gaseous fuels, such as methane at about 1000 K [12] and that of n-Butane at about 950 K [11]. Consequently, it can be said that DME is superior in ignition characteristics. Igarashi *et al.* [13] investigated ignition and combustion characteristics of n-Butane and DME in HCCI engines. According to their study, Igarashi reported that heat release in LTR of DME is much larger than that of n-Butane and concluded that DME is suitable fuel for the HCCI combustion.

Figure 16.24 shows the exhaust characteristics of DME in the experiment. CO, CO_2 and NOx emissions have strong relations to maximum gas temperature. CO_2 emission increases and CO emission decreases as maximum gas temperature increases. Besides, NOx is emitted when maximum gas temperature is high. Especially NOx emission increases rapidly as maximum

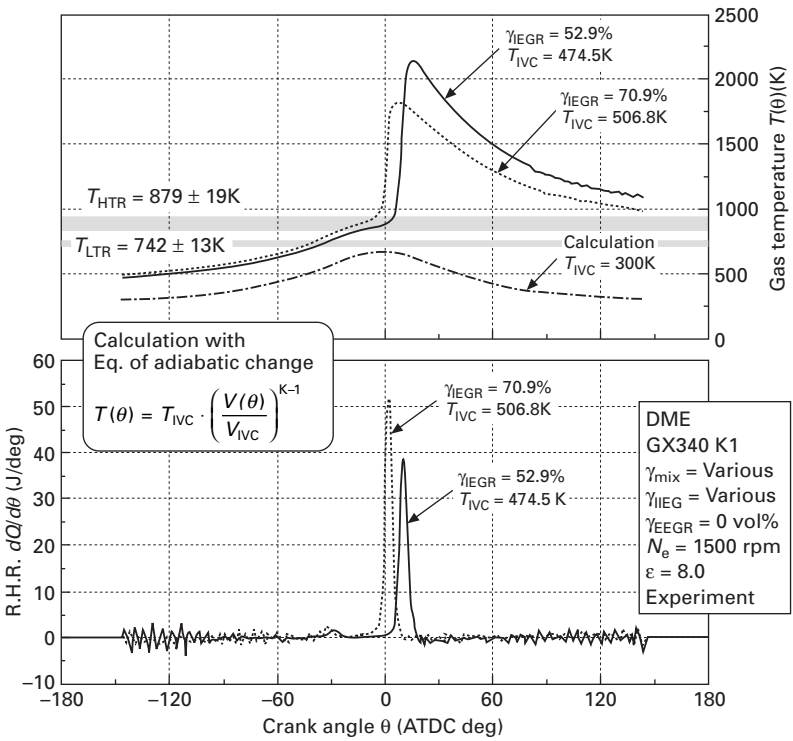

16.23 Temperature and rate of heat release history on internal EGR rate in experiment [10].

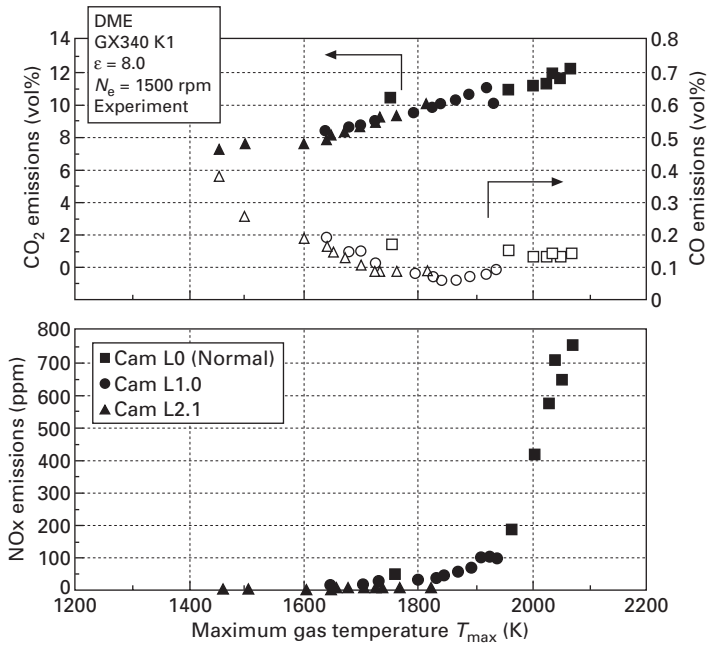

16.24 Exhaust performances of DME [10].

gas temperature reaches over 1900 K. Hence maximum gas temperature needs to be controlled in narrow range in order to prevent NOx emission and to get high combustion efficiency.

(b) The effect of EGR

Figure 16.25 shows the combustion reaction speed and Fig. 16.26 shows the maximum gas temperature from calculations. A means the fraction of air/fuel mixture from 10 to 85 vol% and B axis is the fraction of internal EGR gas and external EGR gas.

Either increasing the fraction of gas air/fuel mixture or decreasing external EGR gas causes the combustion reaction speed to increase. Maximum gas temperature also becomes high at the same time. That is, combustion reaction speed is dependent on the maximum gas temperature, and external EGR is effective in avoiding knocking combustion as it includes a lot of inert gas.

Figure 16.27 shows the temperature history and rate of heat release with external EGR gas. As shown in this figure, maximum gas temperature and heat release are reduced when a little external EGR gas is included. In this study, ignition cannot be assured when external EGR rate becomes more than 1.2 vol%.

Figure 16.28 shows the relation between maximum gas temperature and

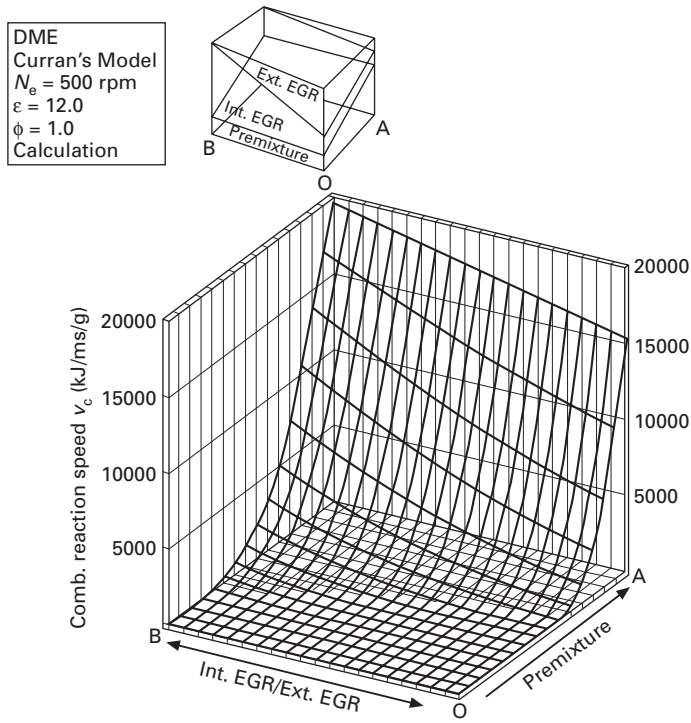

16.25 Combustion reaction speed in calculation [10].

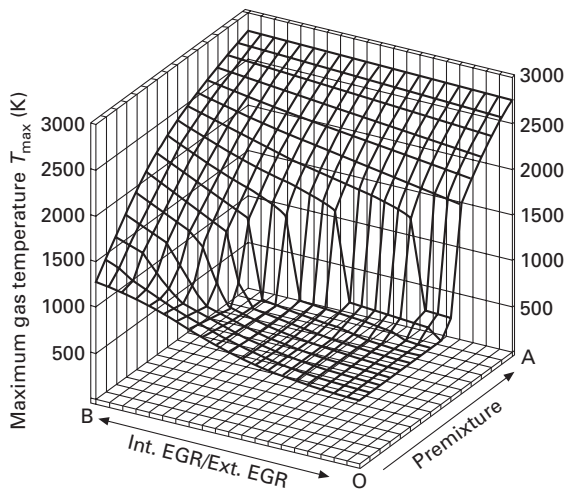

16.26 Maximum gas temperature in calculation [10].

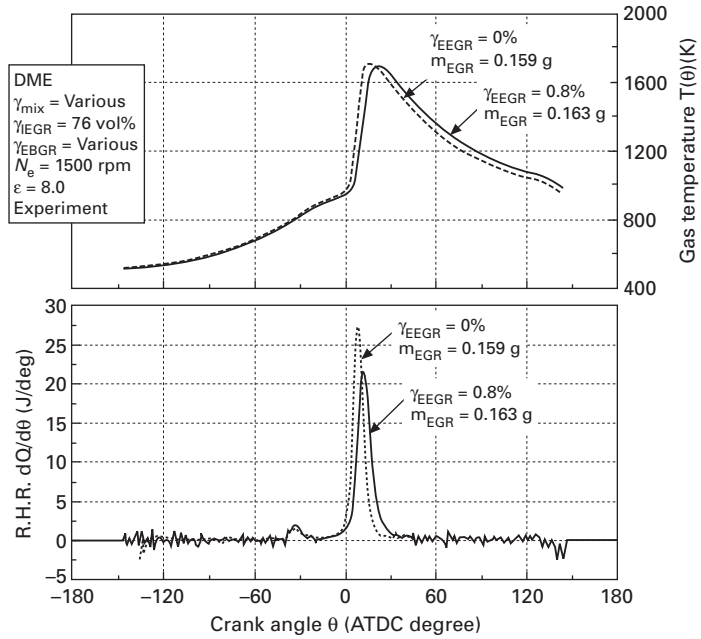

16.27 The temperature history and rate of heat release on external EGR gas [10].

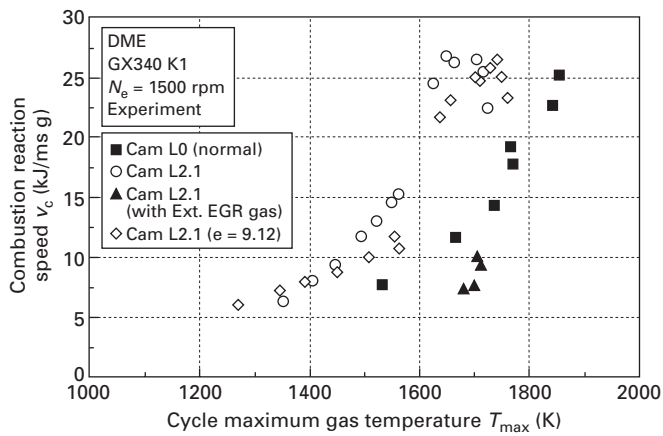

16.28 Combustion reaction speed in experiment [10].

combustion reaction speed. Calculation results also show that, as maximum gas temperature increases, combustion reaction speed increases without being affected by parameters such as equivalence ratio, internal EGR rate, external EGR rate or compression ratio.

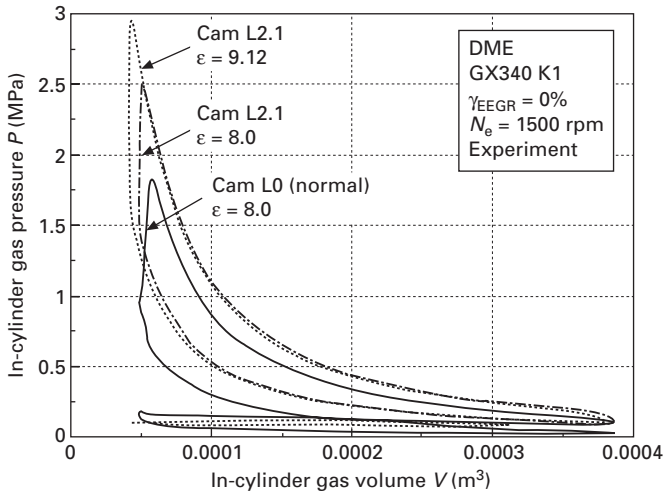

16.29 Pressure and volume diagram on the change of camshaft and compression ratio [10].

As mentioned before, external EGR is an effective method of preventing rapid combustion reactions. Accordingly, it is possible to increase the fraction of air/fuel mixture with more external EGR gas.

(c) Engine performance

Figure 16.29 shows the pressure and volume diagram with the change of camshaft and compression ratio. A large pumping loss occurs with the two-stage exhaust cam system because negative pressure in the intake port needs to be created in order to return the combustion gas as internal EGR gas. However, pumping loss can be reduced by making the secondary exhaust cam lift bigger and opening length longer. In addition, higher indicated work and thermal efficiency can be achieved by increasing the compression ratio to 9.12.

Figure 16.30 shows the engine performance comparison between the developed HCCI engine and conventional engines. Though high indicated thermal efficiency is achieved compared to the original SI engine, much lower indicated mean effective pressure (hereafter, IMEP) is achieved than in conventional engines, due to knocking at high load.

As stated before, external EGR is an effective method of preventing the rapid temperature rise. It is expected to achieve higher thermal efficiency and IMEP by increasing the compression ratio and the fraction of both air/fuel mixture and external EGR gas.

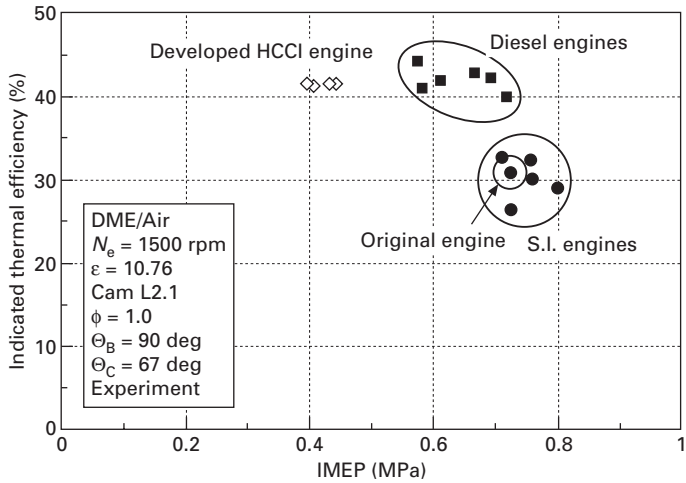

16.30 Engine performance comparison between developed HCCI engine and conventional engines [10].

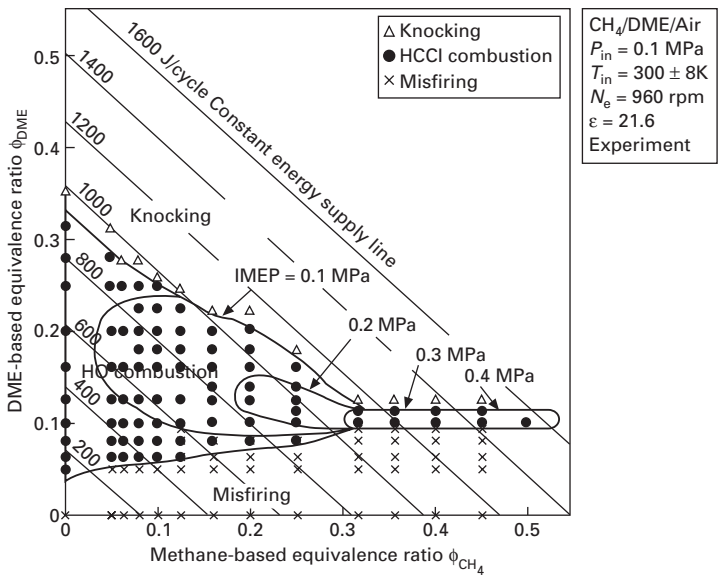

16.31 Relation of mixing ratio between methane with DME in HCCI operating range [14].

16.6 Method of combining DME and other fuels

The auto-ignition temperature is one of the innate characteristics of a fuel. If we alter the mixing ratio in mixed fuel HCCI combustion, it offers a way to control the combustion phasing by changing the auto-ignition temperature.

The auto-ignition temperature can be altered over a wide range of values by fuel mixing ratio of poor-igniting methane and good-igniting DME. Iida *et al*. [14], Konno *et al*. [15] and Yoshida *et al*. [16] have shown that a HCCI engine can be operated in a wide range of operating conditions using different mixing ratios with methane with DME. Figure 16.31 shows the example of a HCCI combustion operation domain [14]. The HCCI engine can be operated by the combination of partial equivalence ratios of DME and methane from idling to the load condition up to 0.46MPa IMEP without using a variable mechanism of the engine at all.

Ogawa *et al*. [17] used DME and methanol mixing fuel. DME is supplied from the intake manifold of the HCCI engine and methanol is directly injected in the combustion chamber. By optimizing the injection quantity of methanol, this engine can operate up to 0.9MPa by IMEP.

Moreover, Shudo *et al*. [18] developed the DME reforming system as shown in Fig. 16.32. The hydrogen and the carbon monoxide are reformed from DME, and they are supplied to the DME HCCI engine. The heat energy by exhaust gas of the engine can be recovered because the reforming reaction is an endoergic reaction, and it contributes to the thermal efficiency improvement. Because the mixing ratio of DME with the reforming gas is optimized, the maximum thermal efficiency 40% is achieved as shown in Fig. 16.33.

16.7 Reducing pressure rise rate by introducing 'unmixed-ness' of DME/air mixture

Controlling the combustion duration, and hence the rate of heat release and pressure rise, is a major issue. The rapid pressure rise can result in heavy knocking operation in high loads.

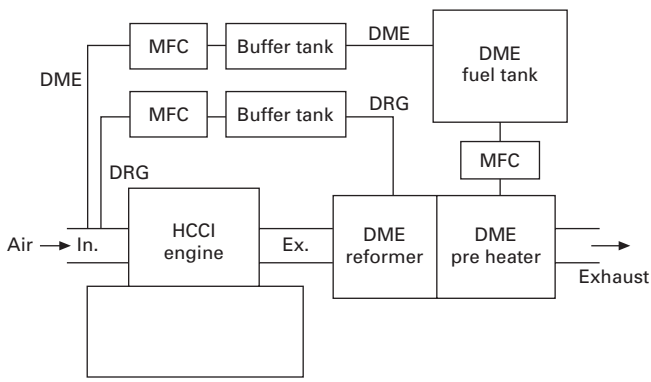

16.32 HCCI engine that operated with DME reforming gases as fuel [18].

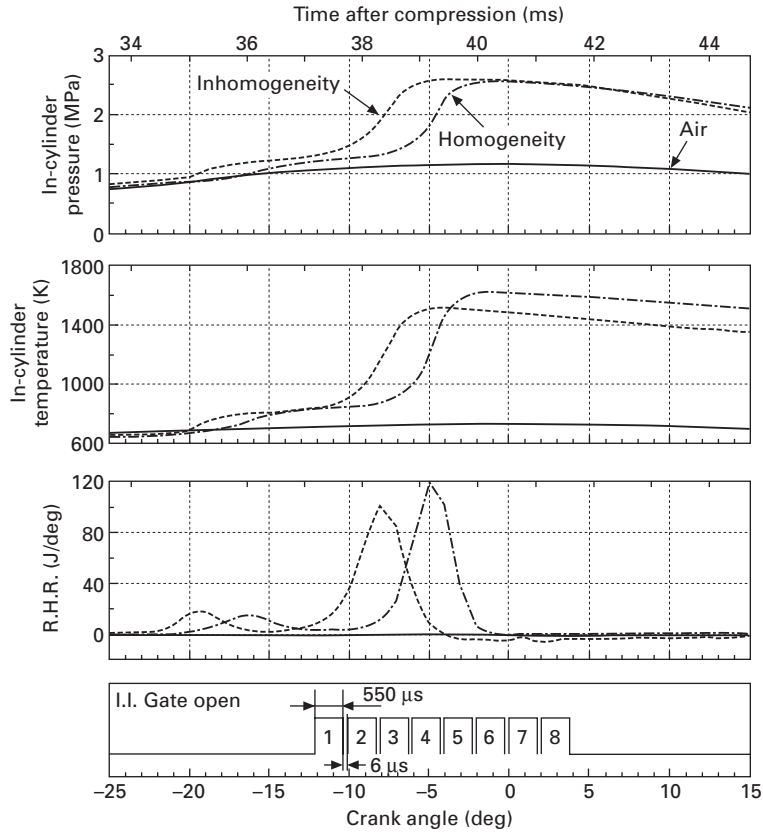

16.33 Efficiency and emissions of DME and reforming gas HCCI engine [18].

In order to reduce the excessive pressure rise rate (PRR) in HCCI combustion processes at high power output, Sjoberg, *et al*. [19] reported the potential of thermal stratification and combustion retard for reducing pressure rise rate in HCCI engines.

Kumano and Iida [20] demonstrated the effect of inhomogeneity of in-cylinder charge on HCCI combustion processes in a DME HCCI engine. The luminescence images during auto-ignition and combustion processes in the combustion chamber of a single cylinder HCCI engine were observed. The combustion characteristic is shown in Fig. 16.34 and the luminescence image is shown in Plate 16 (between pages 268 and 269). When the degree of unmixed-ness of charging DME/air mixture is high (an inhomogeneous condition), the maximum heat release rate and pressure rising rate is low compared with a homogeneous case, and the combustion duration becomes long. The whole area in the combustion chamber causes luminescence at the

same time, and luminescence for a short term is observed in a homogeneous condition. On the other hand, local regions in the combustion chamber begin to produce strong chemiluminescence at different timings. The first-ignited regions begin to burn out while the later ignited regions are still burning. The local region where chemiluminescence is observed once for a short time, never cause chemiluminescence again.

Since the heat release of DME of low temperature oxidation reaction is large, a temperature rise occurs in proportion to the fuel concentration in fuel-air mixture in each local area. There is a strong thermal stratification in the timing of regenerated reaction timing (at end of LTR and/or at the beginning of the HTR), with the result that each local area has different auto-ignition timing and HTR timing in the combustion chamber. The overall heat loss rate in the combustion chamber becomes lower as a result. In the DME

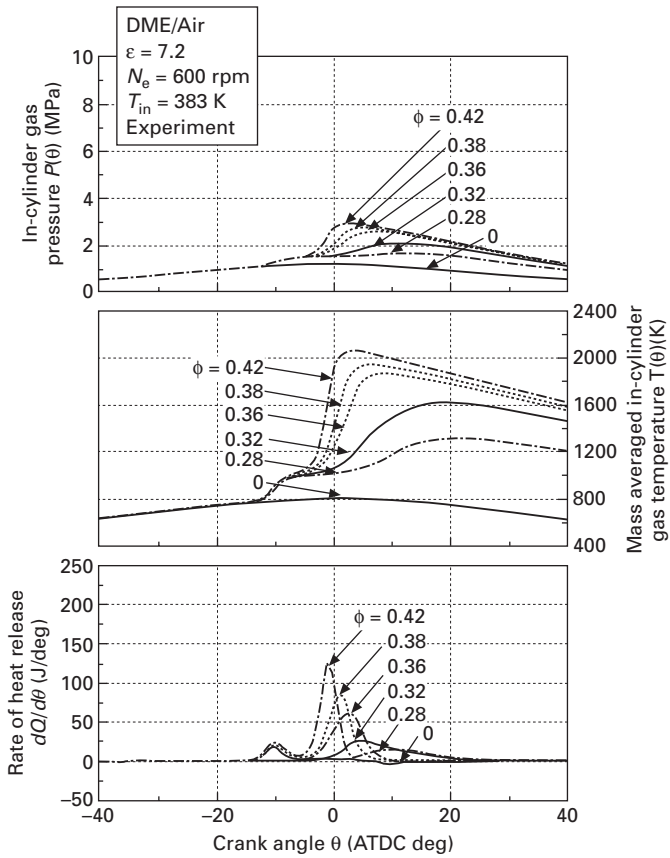

16.34 Histories of in-cylinder gas pressure, mass averaged temperature and heat release rate (comparison for cases of homogeneous mixture and inhomogeneous mixture) [20].

HCCI engine, an introduction of an unmixed-ness of the fuel can be said to be one of the most effective methods to avoid knock at high load conditions.

16.8 Summary

The in-cylinder gas pressure history of the combustion cycle in HCCI engines optimized for DME, n-Butane and natural gas are shown in Figs 16.34, 16.35, 16.36 and 16.37. Moreover, the combustion characteristic value related to HCCI combustion is shown in Table 16.3.

Auto-ignition temperature of DME is low and a naturally aspirated engine is also possible for the operation of an HCCI engine at a low compression ratio. Since the maximum pressure value of in-cylinder gas pressure in a cycle is low, the conformity of DME as fuel is high in lightweight and small engines. Moreover, also in low load, engine operation with little pumping loss is possible by using the system of negative overlap or re-breathing VVT

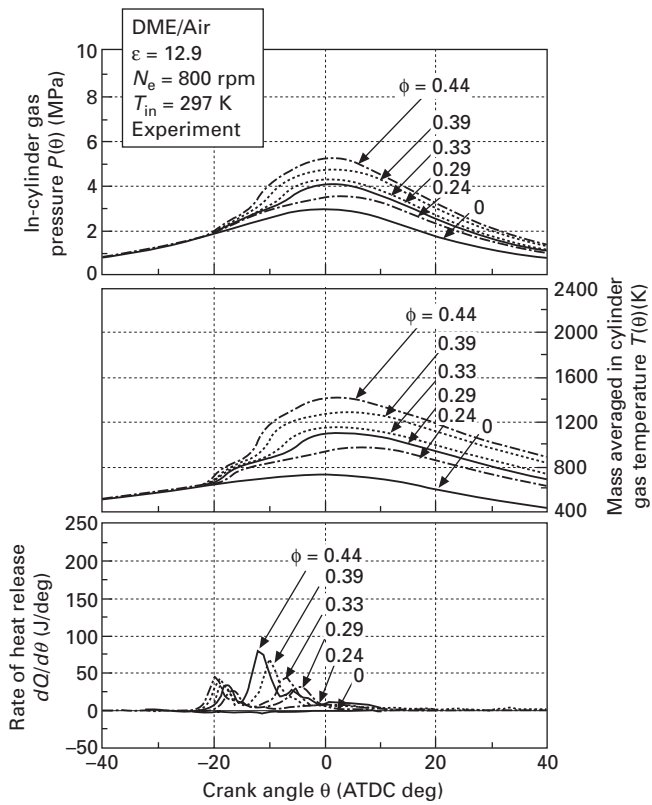

16.35 Pressure, temperature histories and rate of heat release for various equivalence ratios of fuel with DME HCCI combustion (ε= 7.2).

control and introducing a lot of internal EGR. There is a point at which care must be taken, when using DME as fuels for HCCI engine. It is the problem of freezing of CO in the HCCI combustion processes. Although ignition will occur DME/air mixture if it reaches the auto-ignition temperature, in the HCCI combustion process, ignition does not secure the conclusion and/or completeness of combustion. When an equivalence ratio is small, even if it carries out auto-ignition by 950K, CO will freeze without the ability to reach 1500K, which is the temperature at which CO can oxidize. This is the reason why operating efficiency is low in idling or low load condition. The amount of heat release during a low temperature reaction period of DME is relatively higher than that of other fuels. By applying the fuel stratification charge to a DME HCCI engine, large temperature differences between local regions in

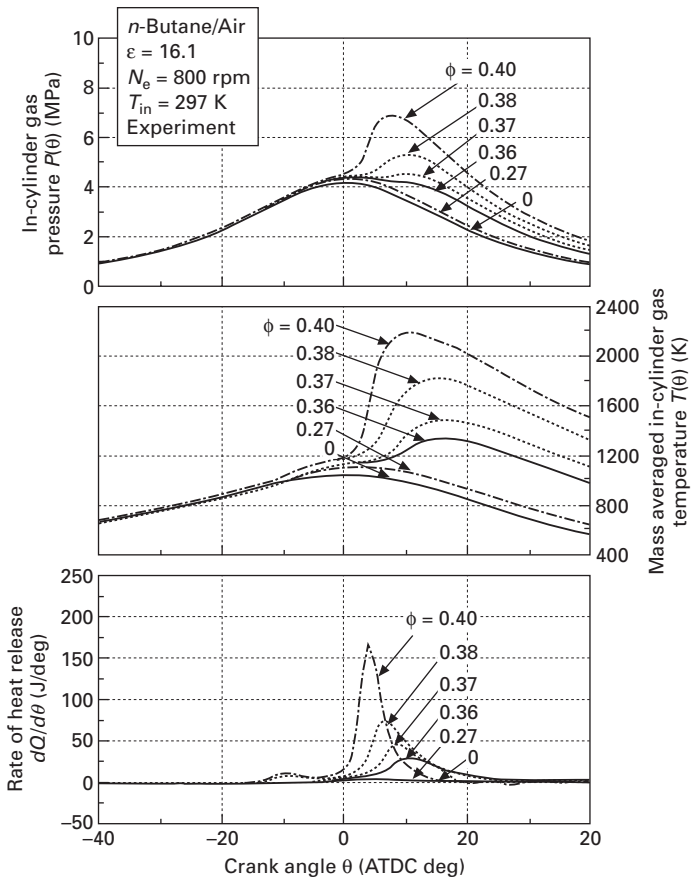

16.36 Pressure, temperature histories and rate of heat release for various equivalence ratios of fuel with n-Butane HCCI combustion (ε= 16.1).

the combustion chamber are obtained at a timing of auto ignition and result in a considerable reduction of the maximum pressure rise rate. As a result, fuel stratification enables smooth operation even for high load without knocking. It is the main feature of DME. On the other hand, natural gas requires a high auto-ignition temperature. Therefore, since the high degree of charging temperature is needed with the engine of a low compression ratio in order to realize HCCI combustion operation, generally heat loss increases and engine thermal efficiency is not as expected in many cases. In the gasoline SI engine, in which the compression ratio is around 10, when the combustion mode is changed to a HCCI combustion mode at lower load and the lower speed domains, there is a tendency for heat loss to increase for

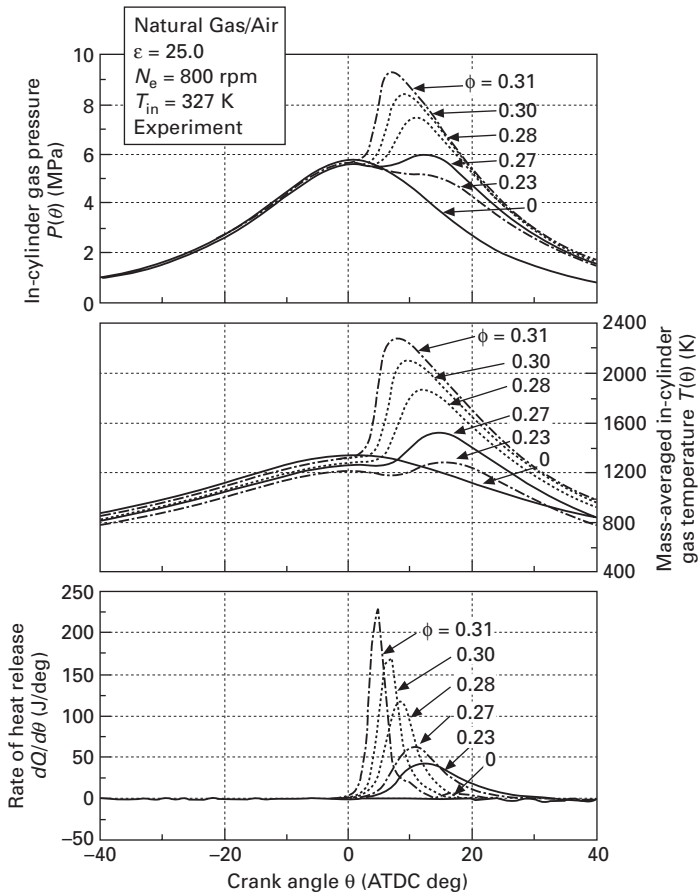

16.37 Pressure, temperature histories and rate of heat release for various equivalence ratios of fuel with natural gas HCCI combustion (ε = 25.0).

Table 16.3 Combustion characteristic value related to HCCI combustion fuel with DME, n-Butane and propane

		DME (CH_3OCH_3)	*n*-Butane (C_4H_{10})	Propane (C_3H_8)
Low temperature reaction	Start temperature	705 ± 7K	724 ± 9K	–
	Heat release	17–30%	4–12%	–
High temperature reaction	Start temperature	904 ± 17K	855 ± 11K	798 ± 6K
	Heat release	70–87%	88–96%	100%

the same reason. Therefore, as for the compression ratio of natural gas HCCI engine, the high compression ratio of 20 to 25 should be set up, and a strong structure where natural gas HCCI engine can be borne at very high maximum in-cylinder gas pressure is required as a result. Natural gas HCCI engines are the best for stationary engine applications of a medium and a large-sized heavy weight class. The auto-ignition temperature demand of natural gas is in the region of 1200K, and since this value is close to 1500K, which is the oxidization demand temperature of CO, it has the advantage that the freezing of CO does not produce operation of comparatively low load, either. Thus, when designing an HCCI combustion engine unlike an SI combustion engine, the auto-ignition temperature of fuel is an important factor, and a natural gas HCCI engine is an efficient HCCI combustion engine at a high compression ratio. A maximum output can attain 2MPa(s) by IMEP in combination with a supercharging system. Thus, in an HCCI engine, auto-ignition of the fuel and the characteristic of combustion are closely related to the design and performance of the HCCI engine. A natural gas and DME can be said to be outstanding as fuels of HCCI engines.

16.9 References

1. Shinichi Suzuki, 'The Present Conditions of DME Technology Development (first)', *Natural Gas*, No. 6 (2002), (in Japanese).
2. Takashi Koyama, Ibaraki Yasshimitsl and Iida Sei, 'Elementary reaction numerical value calculation of compression ignition combustion process of dimethyl ether air mixture nature', Japan Society of Mechanical Engineers thesis collection (chapter B), and Vol. 67, No. 657 (2001).
3. Susumu Sato and Norimasa Iida, 'Analysis of DME Homogeneous Charge Compression Ignition Combustion', SAE Paper 2003-01-1825 (2003).
4. H. J. Curran, W. J. Pitz, C. K. Westbrook, P. Dagaut, J-C Boettner and M. Cathonnet; 'A Wide Range Modeling Study of Dimethyl Ether Oxidation', *International Journal Chemical Kinetics*, 30–3, pp. 229–241 (1998).
5. Philippe Dagaut, Jean-Claude Boettner and Michel Cathonnet, 'Chemical Kinetic Study of Dimethylether Oxidation in a Jet Stirred Reactor from 1 to 10 atm: Experiments

and Kinetic Modeling', 26th Symposium (International) on Combustion, The Combustion Institute, pp. 627–632 (1996).
6. Takashi Koyama, Yasumitsu Ibaragi and Norimasa Iida, 'Numerical Analysis of Auto-ignition and Combustion Process of Dimethyl Ether/Air Mixtures in a Homogeneous Charge Compression Ignition Engine by using Elementary Reaction Model', International Symposium on Alcohol Fuels XIII (2000).
7. Robert J., Kee Fran M. Rupley and James A. Miller, 'CHEMKIN-II: A FORTRAN Chemical Kinetics Package for the Analysis of Gas-Phase Chemical Kinetics', Sandia National Laboratories Report, SAND89-8009B (1989).
8. Andrew E. Luz, Robert J. Kee and James A. Miller, 'SENKIN: A FORTRAN Program for Predicting Homogeneous Gas Phase Chemical Kinetics With Sensitivity Analysis', Sandia National Laboratories Report, SAND87-8248 (1988).
9. Tetsuo Ohmura, Masato Ikemoto and Norimasa Iida, 'A Study on Combustion Control by Using Internal and External EGR for HCCI Engines Fuelled with DME', SAE Paper 2006-32-0045 (2006).
10. Masato Ikemoto, Yuichiro Kojima and Norimasa Iida, 'Development of the Control System Using EGR for the HCCI Engine Running on DME', SAE Paper 2005-32-0062 (2005).
11. Yuichiro Kojima and Norimasa Iida, 'A Study of the Combustion Completion on the 2-Stroke HCCI Engine with n-Butane/Air Mixture – Investigation of the Composition and the Exhaust Mechanism of the Exhaust Gas', SAE Paper 2004-01-1978 (2004).
12. Daesu Jun, Kazuaki Ishii and Norimasa Iida, 'Autoignition and Combustion of Natural Gas in a 4 Stroke HCCI Engine', *JSME International Journal*, Vol. 46–1, P. 60–69 (2003).
13. Norimasa Iida and Tetsuya Igarashi, 'Auto-ignition and Combustion of n-Butane and DME /Air Mixtures in a Homogeneous Charge Compression Ignition Engine' SAE Paper 2000-01-1832 (2000).
14. Susumu Sato, Daesu Jun, Soonpyo Kweon, Daisuke Yamashita and Norimasa Iida, 'Basic Research on the Suitable Fuel for HCCI Engine from the Viewpoint of Chemical Reaction', SAE Paper 2005-01-0149 (2005).
15. Mitsuru Konno and Zhili Chen, 'Ignition Mechanisms of HCCI Compression Process Fueled with Methane/DME Composite Fuel', SAE Paper 2005-01-0182 (2005).
16. Takuya Muto, Hideo Shoji and Kazunori Yoshida, 'A Study of Ignition Timing Control in an HCCI Engine Effects of Compression Ratio Changes and Methane Additive', The 13th International Pacific Conference on Automotive Engineering, pp. 647–652 (2005).
17. Hideyuki Ogawa, Naoya Kaneko, Hirokazu Ando and Noboru Miyamoto, 'Combustion Control and Operating Range Expansion with Direct Injection of Reaction Suppressors in a Premixed DME HCCI Engine', SAE Paper 2003-01-0746 (2003).
18. Toshio Shudo, Yoshitaka Ono and Takehiro Takahashi, 'Ignition Control by DME-Reformed Gas in HCCI Combustion of DME', SAE Paper 2003-01-1824 (2003).
19. Magnus Sjöberg, John E. Dec and Nicholas P. Cernansky, 'Potential of Thermal Stratification and Combustion Retard for Reducing Pressure-Rise Rates in HCCI Engines, Based on Multi-Zone Modeling and Experiments', SAE Paper 2005-01-0113 (2005).
20. Kengo Kumano and Norimasa Iida, 'Analysis of the Effect of Charge Inhomogeneity on HCCI Combustion by Chemiluminescence Measurement', SAE Paper 2004-01-1902 (2004).

Part V

Advanced modelling and experimental techniques

17

Auto-ignition and chemical kinetic mechanisms of HCCI combustion

C K WESTBROOK and W J PITZ, Lawrence Livermore National Laboratory, USA and H J CURRAN, National University of Ireland, Galway

17.1 Introduction

The homogeneous charge, compression ignition (HCCI) engine has the potential to provide high efficiency combustion with very low oxides of nitrogen (NOx) and particulate emissions. However, HCCI combustion has been found to be difficult to control, its emissions of unburned hydrocarbons and CO are considerable, and heat release rates at high loads can be quite high. In many ways, HCCI can be characterized as a controlled chemical auto-ignition process, and an important feature is the unusually large role that fuel chemistry plays in determining its combustion characteristics, when compared with spark-ignition (SI) and diesel engine combustion. For these reasons, considerable attention has been directed recently towards developing a thorough understanding of the combustion chemistry of hydrocarbon fuels under HCCI conditions.

An important factor that influences virtually all current HCCI engine design is the ignition quality of the fuel. HCCI operation has been demonstrated for a variety of fuels with auto-ignition properties that cover a broad range, and it has been observed that some fuels ignite in a single step while others experience a two-stage auto-ignition. This distinction can be seen in Fig. 17.1 (Sjöberg and Dec, 2007), showing the heat release rate (HRR) for two different fuels, one consisting of iso-octane and the other of PRF80 (80% iso-octane, 20% n-heptane). While both fuels ignite at about the same time, the PRF80 mixture shows a distinct region with a small amount of heat release at about 28 degrees before the main ignition, while no such region of early heat release is observed for iso-octane. Some other fuels, including diesel fuel, n-heptane, dimethyl ether (DME), and others with low octane and high cetane numbers, show the same type of early heat release, followed by the major ignition step (e.g., Peng *et al*., 2005), while other fuels such as gasoline, ethanol, natural gas (Christensen *et al*., 1997; Christensen and Johansson, 1998b; Christensen *et al*., 1998a) and other high octane, low cetane number fuels do not have this early heat release feature. Sjöberg and

Dec (2007) have shown that this early heat release can be affected by changes in engine operating conditions and fuel properties, and they have found ways to exploit these effects to better control HCCI combustion. For the example shown in Fig. 17.1, the early, first stage heat release makes it necessary to lower the intake temperature in the PRF80 case to retard ignition so that the two cases both ignite at the same time, close to TDC.

A general understanding of HCCI combustion kinetics must be able to explain the two types of ignition shown in Fig. 17.1, along with a wide variety of other phenomena that have been discovered in HCCI combustion systems. This degree of understanding can then be used to develop better combustion controls and determine the best types of fuels to use for HCCI systems in different situations.

17.2 Kinetics of auto-ignition

Combustion of hydrocarbon fuels takes place via a classical chain reaction mechanism, converting fuel to products, primarily water and carbon dioxide, and releasing energy in the form of heat. The chain carriers are free radicals including H and O atoms, as well as OH, HO_2, CH_3, CH, CH_2, C_2H, C_2H_5, C_2H_3, and many others. As in other types of chain reactions, under certain conditions the population of chain carriers can grow exponentially, and in a combustion system this leads to auto-ignition (Westbrook, 2000). Combustion system auto-ignition can be harmful, as in accidental chemical explosions or as a cause of end gas knocking in SI engines, but auto-ignition is also desirable as the onset of normal combustion in an HCCI or diesel engine. In

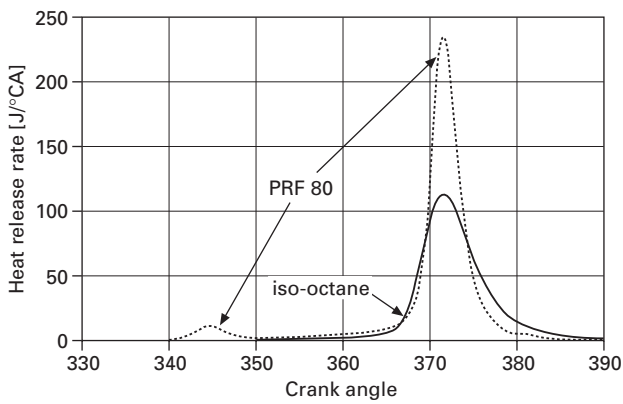

17.1 Experimental values of heat release rate in HCCI engine combustion, using two different fuels. The fuel labeled PRF80 is 80% iso-octane and 20% n-heptane, which shows a marked two-stage ignition, while the pure iso-octane fuel has no first stage heat release. Data are from Sjöberg and Dec (2007).

the context of HCCI combustion, most of the combustion in the engine consists of an array of auto-ignition events throughout the combustion chamber, often at very nearly the same instant in time. Prediction and control of the timing of this auto-ignition in an HCCI engine therefore require a thorough understanding of the detailed chemistry of auto-ignition of the hydrocarbon fuels being used. Once the process is understood, strategies for optimization of that engine combustion become possible.

Fuel oxidation is accomplished for typical hydrocarbons by networks of elementary chemical reactions; for automotive fuels, there can be many hundreds or even thousands of distinct chemical species and many thousands of elementary chemical reactions (Westbrook *et al.*, 2005) that are coupled together to describe collectively the overall combustion process. Chemical kinetic models solve the resulting coupled rate equations, subject to the relevant initial and boundary conditions.

17.3 Reaction types

It is convenient to group elementary reactions into four general classes which describe their effects on the combustion chain reaction and the population of radical species. These include initiation, propagation, branching and termination reactions. Using heptane (C_7H_{16}) for illustration, initiation reactions generate radicals from stable species via decomposition reactions, such as

$$C_7H_{16} \rightarrow C_3H_7 + C_4H_9 \qquad 17.1$$

producing propyl and butyl radicals, or by bimolecular reactions such as

$$C_7H_{16} + O_2 \rightarrow C_7H_{15} + HO_2 \qquad 17.2$$

where C_7H_{15} is the heptyl radical. Both of these initiation reactions produce two radical species from stable reactants. Because the rates of most initiation reactions are quite small and have high activation energies, they usually contribute little to the later rate of the chain reaction, but their major role of initiating the overall chain reaction is essential.

Propagation reactions produce the same number of radicals as they consume, as in

$$C_7H_{16} + OH \rightarrow C_7H_{15} + H_2O \qquad 17.3$$

or

$$C_7H_{16} + HO_2 \rightarrow C_7H_{15} + H_2O_2 \qquad 17.4$$

which consume one OH or HO_2 radical and produce the C_7H_{15} radical and a stable product, water or hydrogen peroxide in these examples. We will return to Reaction 17.4 and others like it that produce H_2O_2, because H_2O_2 does not remain stable as the reaction temperature increases, eventually decomposing thermally into two OH radicals

$$H_2O_2 \rightarrow OH + OH \qquad 17.5$$

This reaction illustrates some of the hazards of classifying elementary reactions in this rather simplified manner, since Reaction 17.5 is in some ways an initiation reaction since it produces two radicals from a stable species, but its eventual function in HCCI auto-ignition is actually to contribute to chain branching. In effect, H_2O_2 represents a temporary storage system or reservoir for OH radicals which are released at a later stage in the overall reaction. This process is termed *degenerate branching* (Griffiths and Barnard, 1995) and it is a major feature of auto-ignition in internal combustion engines of all types (Westbrook, 2000).

Chain branching reactions produce more radical species than they consume, thereby increasing the concentrations of radicals, such as

$$H + O_2 \rightarrow O + OH \qquad 17.6$$

or

$$C_7H_{16} + O \rightarrow C_7H_{15} + OH \qquad 17.7$$

Reaction 17.6 is the most important chain branching reaction at high temperatures and controls such combustion systems as flame propagation (Warnatz, 1980), flame inhibition (Westbrook, 1982a), and shock tube ignition and propagation of detonations (Westbrook, 1982b). However, this branching reaction has a minimal role in determining auto-ignition under HCCI conditions because, in most cases, auto-ignition in HCCI has already occurred before the reactants reach the elevated temperatures of 1200K and above where Reaction 17.6 is dominant.

Finally, termination reactions reduce the concentration of radicals via recombination reactions that combine two radicals into a stable product, such as

$$C_7H_{15} + H \rightarrow C_7H_{16} \qquad 17.8$$

$$C_7H_{15} + CH_3 \rightarrow C_8H_{18} \qquad 17.9$$

This simple classification of elementary reactions into initiation, propagation, branching and termination steps is not always unambiguous, primarily because not all radical species have the same effect on the overall rate of auto-ignition and combustion. For example, the decomposition of ethyl radicals via

$$C_2H_5 \rightarrow C_2H_4 + H \qquad 17.10$$

is formally a propagation reaction because the number of radical species does not change, but H atoms are much more reactive than ethyl radicals and contribute directly to chain branching at high temperatures via Reaction 17.6. Conversely, production of methyl radicals actually decreases the overall rate of ignition at high temperatures because they recombine rapidly via the termination reaction

$$CH_3 + CH_3 \rightarrow C_2H_6 \qquad 17.11$$

and do not lead to either chain propagation or branching.

Once begun, chain branching will continue and grow exponentially until the conditions producing that branching no longer exist. In the final stages of HCCI engine combustion, those conditions do not stop until virtually all of the fuel is consumed and the total heat of reaction is released. In fact, the 'hot' ignition in HCCI begins with Reaction 17.5 when the temperature is high enough for H_2O_2 to decompose, and the temperature rises rapidly until the auto-ignition transitions smoothly into a true high temperature ignition driven by Reaction 17.6. However, for some types of hydrocarbon fuels, the conditions necessary for chain branching can appear briefly and last for only a short time, early in the compression stroke of the piston when the temperature is quite low, and ending when the reactant temperature becomes too high to sustain the branching chain reaction; this is the case for PRF80 fuel shown in Fig. 17.1. Such early and brief auto-ignition-like events usually consume only a small fraction of the available fuel, but they can still be very critical for determining the later onset of significant reaction and heat release. The central parameter of these different types of auto-ignition events is the reactant temperature.

17.4 Temperature regimes of auto-ignition

Reactants in HCCI combustion begin at room temperature and are steadily heated during the compression stroke by piston motion. As the reactant temperature increases, the specific elementary reactions that contribute to fuel consumption in general and chain branching and auto-ignition in particular also change. The reactants pass through three distinct temperature ranges, each with its own unique chain branching reaction pathways that contribute to the eventual auto-ignition.

17.4.1 Low temperature kinetics

Virtually no significant reaction takes place until the reactant temperatures reach about 550K. Eventually the first initiation steps (e.g., Reactions 17.1 and 17.2) produce small amounts of radical species, which then abstract H atoms from the fuel via reactions such as

$$C_7H_{16} + OH \rightarrow C_7H_{15} + H_2O \qquad 17.12a$$

again using heptane as a representative alkane fuel molecule and producing heptyl radicals. Most of the examples below will assume that the hydrocarbon fuel is an alkane, or saturated hydrocarbon species, and employ the notation of the fuel as RH, where R represents an alkyl radical. Reaction 17.12a can then be rewritten more generally as

$$RH + OH \rightarrow R + H_2O \qquad 17.12$$

At high temperatures, alkyl radicals decompose into smaller species, most often into a smaller alkyl radical and a small olefin, such as

$$C_7H_{15} \rightarrow C_3H_7 + C_4H_8 \qquad 17.13$$

but at temperatures below about 1000K, alkyl radicals R primarily add to molecular oxygen via reactions

$$R + O_2 \rightarrow RO_2 \qquad 17.14$$

or specifically $C_7H_{15} + O_2 \rightarrow C_7H_{15}O_2$ 17.14a

that produce alkylperoxy (RO_2) radicals. Reaction 17.14 has several key features that are very important in the auto-ignition process. In particular, the reaction is reversible, with quite different rates in the forward and reverse directions, and both rates are important because the reaction reaches a dynamic equilibrium early in the compression stroke. In the forward (addition) direction, the reaction has little or no activation energy barrier, so its rate is influenced only by the concentrations of the radical R and molecular oxygen. The reverse reaction has a high activation energy barrier (approximately 30 kcal/mol) because the bond between the alkyl radical and the oxygen molecule must be broken. In addition, because the number of chemical species changes in this reaction, the forward reaction rate depends more on the pressure than does the reverse reaction. For these reasons, the equilibrium of the reaction depends sensitively on both temperature and presssure, shifting to the RO_2 side as pressure increases and to the $R + O_2$ side as the temperature increases. As explained below, the main chain branching reaction pathway at low temperatures is initiated by production of RO_2 in Reaction 17.14, so when the temperature increases to the point where the reverse direction is faster than the forward reaction, the concentrations of RO_2 radicals decrease sharply, the low temperature chain branching is extinguished, and the overall rate of combustion slows significantly. This feature of low temperature hydrocarbon oxidation is so fundamental and important that Benson (1976) coined the term 'ceiling temperature' for the temperature at which this reversal occurs and $[R] \cong [RO_2]$. This phenomenon is the basis of the 'negative temperature coefficient' (NTC) of reaction that is a somewhat counter-intuitive feature of the low temperature range, where the rate of overall fuel consumption can decrease with increasing temperature for temperatures in the range of about 700–850K.

The next reaction step is 'alkylperoxy radical isomerization' of the RO_2 radical, which involves a transfer of a H atom from a location within the RO_2 species to the free end of the O_2 species which is now bonded to the alkyl radical. This can be illustrated, with the heptyl radical, as shown in Fig. 17.2. This is a fairly 'floppy' species, and its motion brings the free electron site

on the terminal O atom close to the H atoms located at other positions in the RO_2 radical, pulling off that H atom and transferring it to make an OOH group. Figure 17.2 shows only one example of H atom transfer within the radical, but every other H atom within this RO_2 species can also be transferred to the O—O site by the same type of process. The rates of these H atom transfer reactions depend rather sensitively on several factors, including the number of atoms between the O—O group and the H atom that is moved (the 'ring strain energy'), on the type of C—H bond that must be broken (primary, secondary or tertiary), and the number of equivalent H atoms at the same type of site. In the example shown in Fig. 17.2, the transition state (TS) ring has 6 atoms (3 C atoms, 2 O atoms and 1 H atom), the H atom is abstracted from a secondary site and there are 2 equivalent H atoms that have the same characteristics. All these factors make the rates of these RO_2 isomerization reactions strongly dependent on the size and structure of the parent fuel molecule (Westbrook *et al*., 1991). The overall isomerization reactions of the alkylperoxy radicals are usually written

$$RO_2 \rightarrow QOOH. \qquad 17.15$$

There are many important details, however, concealed within the apparent simplicity of Reaction 17.15, and these details determine all of the subsequent fuel reactivity and the time at which auto-ignition occurs. A more thorough discussion of the alkylperoxy radical isomerization reactions can be found in Pollard (1977).

The subsequent reactions of the QOOH then depend on the structure of the QOOH and therefore on the rates of the RO_2 isomerization reactions (Reaction 17.15). The forms of QOOH included in current models are illustrated in Fig. 17.3; each form is distinguished by the number of atoms (from 5 to 8) that were contained in the transition state ring which transferred the H atom from one location to the location shown in the figure. The example shown in Fig. 17.2 can be seen to correspond to case b in Fig. 17.3.

The QOOH produced by the 5-membered transition state ring (the smallest ring possible and having only 2 C atoms in the ring) decomposes primarily by the reaction

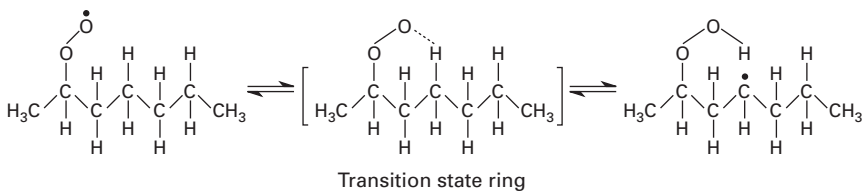

17.2 Schematic diagram of an RO_2 isomerization reaction in n-heptane. This specific reaction uses a 6-membered transition state ring structure in going from RO_2 to QOOH.

(a)

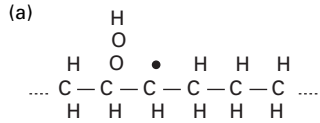

5-membered transition state ring

(b)

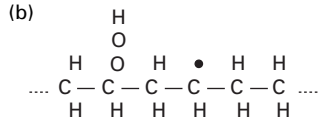

6-membered transition state ring

(c)

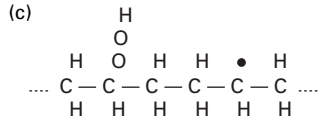

7-membered transition state ring

(d)

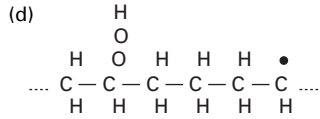

8-membered transition state ring

17.3 Diagrams of products of possible RO_2 isomerization reactions in a straight-chain hydrocarbon species. The products of isomerization reactions in 5-membered, 6-membered, 7-membered and 8-membered transition state ring structures are demonstrated.

$$QOOH \rightarrow Q + HO_2 \qquad 17.16a$$

This reaction can occur only because removal of the HO_2 leaves two adjacent C atoms that can bond together to make the olefin Q. This is not the case for the RO_2 formed in Fig. 17.2 or for cases b, c, or d in Fig. 17.3, so the QOOH product of the 6-membered transition state ring, shown in Fig. 17.2 cannot react via Reaction 17.16a. Reaction 17.16a is a chain propagation pathway, producing one HO_2 radical from the radical QOOH.

All of the possible QOOH species can decompose by breaking the O—O bond to produce OH and a cyclic ether species QO, with a size and structure that depend on the geometry of the transition state ring. For the example shown in Fig. 17.2, the cyclic ether would have 3 C atoms and 1 O atom in the stable ring. All of these reactions are denoted collectively by the general reaction

$$QOOH \rightarrow QO + OH \qquad 17.16b$$

where the QO is the relatively stable cyclic ether product. It is important to note that this reaction pathway is a chain propagation sequence.

In addition to formation of cyclic ethers, any of the QOOH species can also react by adding another O_2 species to produce a larger radical species denoted as O_2QOOH. This adduct is shown as the first component in Fig. 17.4, showing an O_2QOOH formed from the QOOH corresponding to type c in Fig. 17.3. This reaction is fundamentally the same as Reaction 17.14,

$$QOOH + O_2 \rightarrow O_2QOOH \qquad 17.16c$$

consisting of the addition of O_2 to a carbon atom, and the nature of the equilibrium and its variation with temperature and pressure are the same as for Reaction 17.14. All of the reactions of QOOH, including Reactions 17.16a, 17.16b and 17.16c, are essentially chain propagation reactions. Only Reaction 17.16c offers any possibility of eventual chain branching, depending on the fate of the O_2QOOH product.

The O_2QOOH species formed in Reaction 17.16c isomerize in the same ways as the RO_2 reactions described above in Reaction 17.15, depending on the ring strain energies, the C—H bond strengths and degeneracies involved, and the result is a complex ketohydroperoxide species and an OH radical. This is illustrated as the reaction shown in Fig. 17.4. Although the ketohydroperoxide species is fairly stable, as temperature continues to increase the O—O bond breaks, producing a second OH radical and another radical oxygenated hydrocarbon radical which also decomposes rapidly. The net reaction can be written as

$$O_2QOOH \rightarrow OPO + OH + OH \qquad 17.17$$

in which P represents a hydrocarbon radical with one less H atom than the corresponding olefin species. There are many forms for the OPO radical, depending on the details of the O_2QOOH isomerization pathways, but the most important thing to note is that at least 3 radicals are produced in the overall Reaction 17.17, which makes this step extremely effective as a chain branching process. This decomposition pathway is the only low temperature reaction sequence that produces chain branching. It cannot be called a chain branching *reaction* because it really represents an overall step that includes

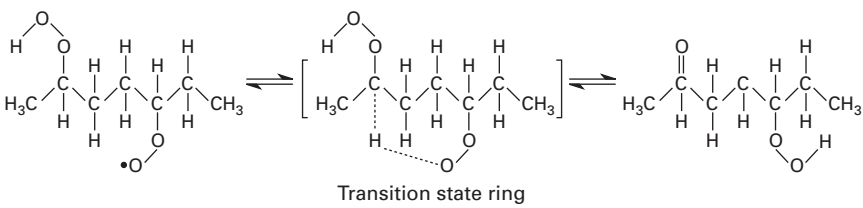

17.4 An example of a reaction of O_2QOOH species via a 7-membered transition state ring. In this example, the C—H bond being broken is a secondary bond.

several elementary reactions that occur in sequence, with some intermediate species that are stable for a period of time until the temperature increases.

We can collect these low temperature reaction sequences:

$$RH + OH \rightarrow R + H_2O \quad 17.12$$

$$R + O_2 \rightarrow RO_2 \quad 17.14$$

$$RO_2 \rightarrow QOOH \quad 17.15$$

$$QOOH \rightarrow Q + HO_2 \quad 17.16a$$

$$QOOH \rightarrow QO + OH \quad 17.16b$$

$$QOOH + O_2 \rightarrow O_2QOOH \quad 17.16c$$

$$O_2QOOH \rightarrow OPO + OH + OH \quad 17.17$$

This sequence of reactions is shown graphically in Fig. 17.5. Almost every alkyl radical produced from the fuel by H atom abstraction at low temperatures below about 850K follows the sequence of Reactions 17.12, 17.14 and 17.15. Note that only one radical is consumed by this sequence, namely the original radical that abstracted the H atom from the fuel in Reaction 17.12. The QOOH produced from the 5-membered transition state rings then react primarily via Reaction 17.16a, and the QOOH produced via the 7- and 8-membered transition state rings then react primarily via Reaction 17.16b. Only the

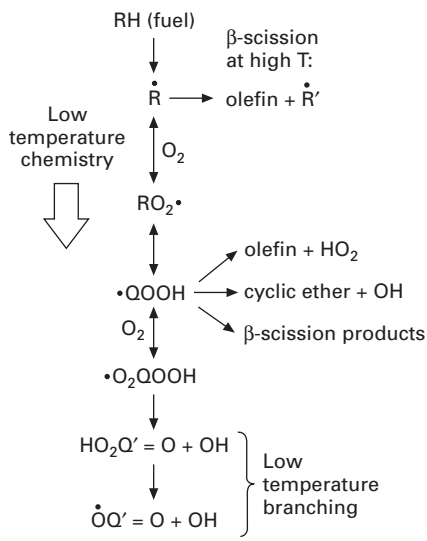

17.5 Schematic diagram of general paraffin hydrocarbon oxidation pathways over the entire temperature range of conventional combustors.

QOOH species produced from the 6-membered transition state rings react significantly via Reaction 17.16c and then Reaction 17.17. Since Reactions 17.16a and 17.16b each produce only one radical (i.e., the HO_2 in Reaction 17.16a and the OH in Reaction 17.16b), these chain propagation reaction pathways have no net influence on the concentration of radicals and therefore provide no chain branching. Therefore the only chain branching pathway is through the 6-membered transition state QOOH species which add a second O_2 molecule via Reaction 17.16c and then produce two OH radicals and at least one more from the OPO species in Reaction 17.17 (Cox *et al.*, 1996; Curran *et al.*, 1996a, 1998, 2002). Thus a low temperature auto-ignition can be produced from Reactions 17.16c and 17.17 which is quite vigorous and leads to a period of auto-ignition, accompanied by rapid reactant consumption and heat release.

It was noted above that two key reactions, Reaction 17.14 and Reaction 17.16c, involved the temperature- and pressure-dependent equilibrium of radicals with molecular oxygen. As the temperature increases to values above 700–750K, caused both by gradual chemical heat release and by continuing piston compression, the equilibria shift towards the reactant, or dissociation, sides. This shift begins slowly, then more abruptly, and by about 800–850K the net addition reactions of O_2 to these radicals are completely stopped. The same increases in temperature also accelerate the chain propagation reactions, particularly the pathway producing HO_2 (Reaction 17.16a), providing additional competition for the chain branching pathways (Cox *et al.*, 1996; Ribaucour *et al.*, 2000). Therefore, increasing temperature eventually terminates the low temperature ignition stage by drastically reducing the chain branching from these low temperature reaction pathways. It is important to note that the low temperature reactions rarely consume more than a small fraction of the fuel and result in a temperature increase of about 10–20 K. As will be shown below, this additional temperature increase, while rather modest in magnitude, can be very important in accelerating the onset of the later, main ignition event.

Once the low temperature chain branching reaction pathways have been extinguished by the increasing temperature, the rate of chemical reaction decreases and most of the reactant heating occurs by compressional heating from piston motion, combined with slow chemical reactions. This temperature regime, in which the more rapid low temperature reaction rate has been replaced by a slower rate of reaction because Reactions 17.14 and 17.16c are no longer important, is known generally as the region of negative temperature coefficient (NTC) of reaction, where the rate of reaction actually decreases with increasing temperature. Note that the reaction sequence initiated by Reaction 17.14, the low temperature oxidation pathway, is eventually replaced by the much simpler alkyl radical decomposition Reaction 17.13 when the temperature reaches about 1000K or higher.

17.4.2 Intermediate and high temperature chain branching

As the temperature increases above about 850K, where the equilibria of Reactions 17.14 and 17.16c have effectively extinguished the low temperature chain branching pathways, the main reaction sequences involve consumption of fuel RH, primarily by H atom abstraction by OH and HO_2, and the temperature increases gradually, accompanied by a steady increase in the level of hydrogen peroxide (H_2O_2). The rate of heat release grows steadily, until at about 1000K, four important events occur. The H_2O_2, which has been relatively stable due to the strength of its O—O bond and the correspondingly large value of the activation energy of its decomposition Reaction 17.5, begins to decompose at ever-increasing rates. This decomposition causes the concentration of OH to grow very quickly. As a result, the fuel is very rapidly consumed by reacting with this sudden source of OH radicals, and the temperature increases very rapidly, due to the production of significant amounts of water in Reaction 17.12, further accelerating the rate of H_2O_2 decomposition. All of these events occurring together create an auto-ignition event.

The 'trigger' for this event can be found in the kinetics of the decomposition reaction of hydrogen peroxide. This reaction has a critical temperature for ignition that is also a function of the pressure of the reactive system. H_2O_2 decomposition can be written, ignoring for the moment all other reactions of H_2O_2, by the simple differential equation

$$\frac{d[H_2O_2]}{dt} = -k_5[H_2O_2][M] \qquad 17.18$$

where M is the total molar concentration and k_5 is the rate of Reaction 17.5. This equation can be rearranged to define a characteristic decomposition time

$$\tau = [H_2O_2]/(d[H_2O_2]/dt) = 1/(k_5\,[M]) \qquad 17.19$$

The rate expression for this reaction is

$$k_5 = 1.2 \times 10^{17} \times \exp(-45500/RT) \qquad 17.20$$

so the characteristic time τ becomes

$$\tau = 8.3 \times 10^{-18} \times \exp(+22750/T) * [M]^{-1} \qquad 17.21$$

As the temperature increases, τ becomes smaller, and when it is 'short' compared with the residence time, rapid consumption of hydrogen peroxide occurs and results in auto-ignition that begins as an intermediate temperature process and is completed by the high temperature kinetics pathways that are dominated by Reaction 17.6. Characteristic decomposition time also decreases with increasing total concentration [M] or, equivalently, with increasing pressure

at constant temperature. This also means that, as pressure increases, the critical temperature for ignition decreases gradually.

The total post-compression concentrations [*M*] in a representative rapid compression machine (RCM) experiment are about 10^{-4} mol/cm^3, so τ is approximately 7.8 ms at T = 900K, 640 μs at T = 1000K and 80 μs at T = 1100K. With total reaction times in the RCM of tens of milliseconds, rapid decomposition or auto-ignition is observed at 950–1000K, with characteristic times for ignition less than a millisecond. At the higher pressures of internal combustion engines, including spark ignition, diesel and HCCI engines, the same calculations show that this simple mechanism predicts ignition at temperatures between 900 and 950K (Westbrook *et al.*, 1991; Westbrook, 2000). Another very important implication of the central role of Reaction 17.5 in auto-ignition under HCCI conditions is the fact that this reaction is not related to any particular type of fuel. It is part of the H_2-O_2 submechanism, which is the basis for all hydrocarbon kinetics (Westbrook and Dryer, 1984), and one outcome of its importance is that the temperature at which auto-ignition is observed is largely independent of the hydrocarbon fuel being used.

All of these effects are functions of the size and structure of the fuel molecules, which determine octane and cetane numbers. Different fuels proceed through the low and intermediate temperature regimes at different rates, which strongly influences the auto-ignition event and octane and cetane numbers (Midgley, 1925, Lovell, 1948; Westbrook *et al.*, 1991).

The above discussion emphasizes the importance of H_2O_2 decomposition and its sensitivity to temperature in the range from about 900–1000K. Heat release and temperature increases in the low temperature, alkylperoxy radical isomerization range are quite small, often only of the order of 20K increase in the reactant mixture, but these very modest increases can still have a significant impact on the timing of the full auto-ignition in the HCCI engine. Most HCCI engines are intended to have auto-ignition occur close to TDC for maximum efficiency, and the piston speed and compressional heating are very slow as the piston approaches TDC. Therefore, a reactant mixture with 20K higher temperature due to this early reactive period will ignite much earlier than a mixture with a lower temperature. The combination of reactivity at low temperatures and the temperature sensitivity of the onset of auto-ignition due to Reaction 17.5 are responsible for the ignition timing advance that is seen with diesel and lower octane fuels under HCCI conditions and is illustrated in Fig. 17.1 (Sjöberg and Dec, 2007).

17.5 Illustrations of auto-ignition in the rapid compression machine

The kinetic principles described above can be shown by using experimental and computed kinetic modeling studies of hydrocarbon auto-ignition in the

rapid compression machine (RCM), a laboratory-scale device that in many ways is the academic equivalent of the HCCI engine (Griffiths *et al*., 1997; Minetti *et al*., 1995; Silke *et al*., 2005). In this system, a reactive mixture is placed into a combustion chamber, usually at room temperature and sub-atmospheric pressure. The reactive mixture is then rapidly compressed by a piston in single stroke with a stroke duration of 20–50 ms. The resulting pressures are in the range of 5–10 atmospheres, and the gas mixture composition can be adjusted to produce compressed gas temperatures over a range from 600K to about 950K. The piston stops at the end of the compression stroke, so there is no expansion stroke, and the most common diagnostic used is a measurement of the ignition delay time, usually using a pressure gauge. For the present study, the most important feature of the RCM is that the reactant mixtures are compressively heated to the same temperature range where early combustion occurs in HCCI and other engines.

In a very illustrative study (Ribaucour *et al*., 2000), three isomeric forms of pentane were used as fuels in the RCM. In each case, the same set of initial conditions led to the same end-of-compression temperature of 757K and about 10 bar pressure for all three fuels, n-pentane (research octane number, RON = 62), neo-pentane (2,2-dimethyl propane, RON = 85) and iso-pentane (2-methyl butane, RON = 92). The subsequent temperatures for the three fuel mixtures are shown in Fig. 17.6. The time zero is taken as the end of the compression stroke.

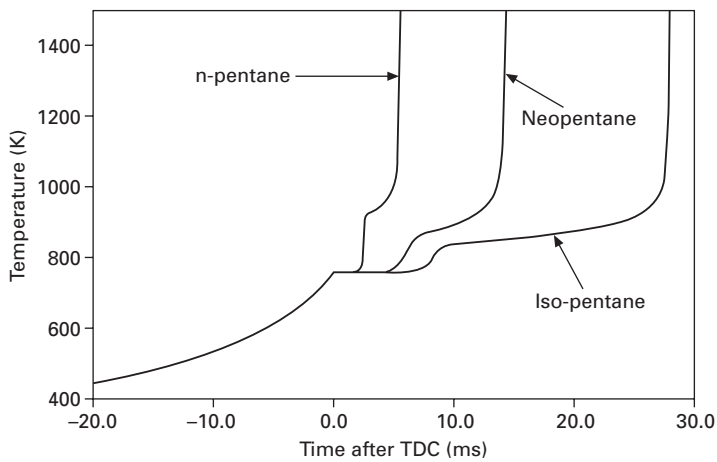

17.6 Temperature histories in rapid compression machine (RCM) ignition of the three isomers of pentane at the same compressed gas temperature. The n-pentane isomer ignites first, followed by the neo-pentane and then the iso-pentane isomers. This ordering, which is consistent with the octane numbers for these species, demonstrates the influence of fuel molecular structure on auto-ignition rates under combustion conditions.

The compression histories of the three fuels are virtually identical, but the constant-volume ignitions are quite different. All three show a distinct first-stage ignition, but the time delays for that first ignition are very short (2.4 ms) for n-pentane, longer for neopentane (6 ms) and even longer for iso-pentane (7.5 ms). Temperature increases (ΔT = 163K, 106K and 70K, respectively) and fuel consumption (Δfuel = 41%, 21% and 20%, respectively, taken from model simulations and not shown in Fig. 17.6) during the first-stage ignition for n-pentane, neopentane and iso-pentane are quite different, as is the duration of the first-stage ignition (0.7 ms, 3 ms, 2.6 ms, respectively). Onset of the second stage occurs in the same order as expected from octane ratings for these fuels.

For each pentane isomer, low-temperature oxidation occurs via alkylperoxy radical isomerization as described above. The main reactions are H-atom abstraction from the fuel, primarily by OH described by Reaction 17.13 above, with R being a different pentyl radical for each isomer of pentane. Processes leading to the first-stage ignition begin by addition of molecular oxygen to the pentyl radicals (Reaction 17.14), and the pentylperoxy radicals then isomerize via internal abstraction of H atoms. As explained earlier, the rates of these isomerization reactions depend on the type of C—H bond being broken and the number of atoms in the transition state ring through which the H atom is abstracted.

The most reactive pentane isomer, n-pentane, can be visualized as:

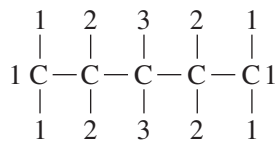

17.22

where the numbers indicate logically distinguishable H atoms, with the '1' H atoms bonded at primary sites in the molecule and the '2' and '3' H atoms bonded to secondary sites in n-pentane. H atom abstraction rates by OH radicals are nearly equal for primary, secondary and tertiary H atoms, so the two major pentyl radicals formed will be the 1-pentyl and 2-pentyl radicals, and the two RO_2 radicals produced by O_2 addition will be:

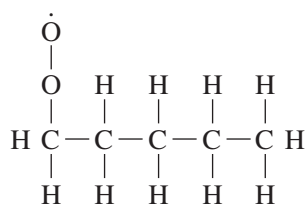

1-pentylperoxy

17.23

and

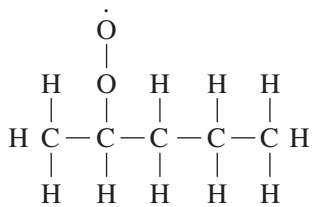

2-pentylperoxy 17.24

The key to the extended low-temperature reactivity of n-pentane is that both of these $C_5H_{11}O_2$ radicals have H atoms which can be internally abstracted with the lowest possible activation energy barriers. Recalling from above that the activation energy for these RO_2 isomerizations is the sum of contributions from the ring strain, the bond being broken and the endothermicity of the reaction, and that the smallest values for ring strain energy are from 6-membered and 7-membered transition state rings, and the smallest bond energy values are for secondary and tertiary C—H bonds, it can be seen that the 1-pentylperoxy radical has 4 such easily-abstracted H atoms and the 2-pentylperoxy radical has 2 such H atoms. For example, the product of internal abstraction of a secondary H atom in the 1-pentylperoxy radical via a 6-membered transition state ring is:

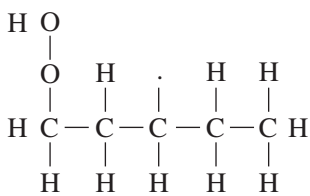

17.25

These isomerization reactions then initiate the series of Reactions 17.16 and 17.17, and Reaction 17.16c in particular, there is a considerable amount of chain branching that occurs in low-temperature oxidation of n-pentane. Because its molecular structure offers so many H atoms that are easily transferred via RO_2 isomerization, n-pentane has a particularly vigorous first-stage ignition phase. One of the major factors is that n-pentane has a large fraction of its H atoms at secondary sites.

In contrast, neopentane has no H atoms at either secondary or tertiary sites, and 9 of the H atoms in iso-pentane are at primary sites. In the case of neopentane, the neopentylperoxy radical has 9 H atoms which can be abstracted via 6-membered transition state rings, but all 9 are bonded at primary sites, which are difficult to abstract. In iso-pentane, there is a single easily abstracted H atom at a tertiary site, but the resulting RO_2 radical has only 3 primary H atoms available for abstraction via a 6-membered transition state ring, so the possible reaction pathways leading to low-temperature chain branching are even more limited in iso-pentane than the other isomers.

The first-stage ignition ends when the temperature has increased enough to reverse the addition reactions of molecular oxygen to alkyl (Reaction 17.14) and hydroperoxyalkyl (Reaction 17.16c) radicals. The alkylperoxy radicals then decompose via lower activation energy chain propagation pathways to produce olefin + HO_2 and epoxide + OH species, effectively shutting off the chain-branching reaction pathways, and reaction remains slow until higher temperatures activate new, alternative reaction pathways.

For all three isomers of pentane, the second stage or hot ignition has exactly the same kinetic source. As shown in Fig. 17.6, all three fuels ignite at approximately the same temperature of about 950K. For the pressures of this study, this is the temperature at which hydrogen peroxide (H_2O_2) begins to decompose at a significant rate. The low-temperature reactions produce considerable amounts of H_2O_2 that is stable until its decomposition temperature is reached; since this reaction is common to the kinetic oxidation mechanism of all hydrocarbons, this ignition mechanism is common to all hydrocarbon fuels. Past modeling studies have shown that the same decomposition reaction and its temperature dependence is responsible for the onset of knock in spark-ignition engines, ignition in diesel engines, and ignition in HCCI engines (Westbrook, 2000).

The lowest octane isomer, n-pentane, therefore ignites first in Fig. 17.6 because it is the first to reach 950K; it reaches this 'trigger' temperature first because it had the greatest amount of temperature increase from the low-temperature reactions. The greater amount of low-temperature reactivity is a result of its molecular structure, giving it the largest number of easily abstracted H atoms with secondary C—H bonds and 6- and 7-membered transition state rings.

This reasoning can be extended to explain a number of trends that are important for HCCI combustion. Figure 17.1 shows the rate of heat release in HCCI engines with high octane and low octane fuels. The high octane fuel (iso-octane) shows a negligible rate of heat release until ignition occurs close to Top Dead Center (TDC), while the second case with the lower octane fuel PRF80 from the study of Sjöberg and Dec (2007) shows a clear region of heat release about 15 degrees before TDC. At the same crank angle where the smaller region of heat release begins, the reactive mixture is at a temperature of about 750K, and this early heat release ends at a temperature of about 875K, so it is clear that this first-stage heat release region is caused by the same alkylperoxy radical isomerization kinetics as that responsible for the first-stage ignition shown in Fig. 17.6. This is consistent with observations of the effect of fuel octane number on HCCI ignition, since fuels with lower octane numbers produce greater amounts of low-temperature reactivity and ignite more quickly under HCCI conditions. Higher engine speeds reduce the differences in time of ignition between fuels with different octane numbers because the reactive mixture, being heated by piston motion,

passes through the low-temperature regime more rapidly than at lower engine speeds, giving it less time to react before the temperature has reached the high end of the low-temperature regime. Dilution by EGR or excess air slows the onset of ignition simply by reducing the rate of heating, so the reactive mixture takes longer to reach the H_2O_2 decomposition temperature. The effects of changes in boost pressure are somewhat more complex, because increased pressure increases the effects of oxygen addition to alkyl and hydroperoxyalkyl radicals (Reactions 17.14 and 17.16c), which increases the amount of low-temperature heat release, but it also moves the decomposition of H_2O_2 (Reaction 17.5) to slightly higher temperatures, which would retard ignition.

Experiments in the RCM illustrate another complication associated with the use of familiar auto-ignition metrics to describe HCCI ignition. The most common metric of hydrocarbon auto-ignition under engine combustion conditions is the octane number. Fuels with low octane numbers tend to auto-ignite easily and are therefore more likely to produce engine knock, while fuels with high octane numbers resist knocking. The analysis described above can explain the influences of fuel molecule size and structure on octane numbers (Westbrook *et al.*, 1991). However, the influence of the time-dependent engine environment on octane number is often overlooked. In particular, the engine test for research octane number (RON) involves stoichiometric fuel/air mixtures in an engine running at 600 rpm in an engine with a great deal of wall heat losses. Comparable engine conditions in an HCCI engine running under normal conditions (e.g., 1500 rpm, little heat loss by the core reacting gas, high dilution or low equivalence ratio) are much different, and the relative contributions of low-temperature kinetics and many other factors are therefore not likely to be the same in the two types of engines. As a result, the octane number cannot be expected to give realistic measures of relative auto-ignition rates under HCCI conditions.

An illustration of this is given by Fig. 17.7, showing ignition delay times for n-pentane, n-heptane, and PRF60 (60% iso-octane, 40% n-heptane) in the Leeds University RCM (Curran *et al.*, 1996b). The RON for n-heptane is zero (by definition), the RON for PRF60 is 60 (again by definition), and that of n-pentane is 62. The experimental results in Fig. 17.7 show that, consistent with the relative values of RON, n-heptane ignites much more quickly than n-pentane. However, the results for n-pentane and PRF60, with very nearly equal values of RON, show very different behavior, igniting much more rapidly than PRF60 and more like n-heptane at lower temperatures, and more slowly than PRF at higher temperatures. The variations with temperature of n-pentane and PRF60 are also qualitatively much different. The point is that the RCM, much like the HCCI engine, is a combustion environment that is quite different from the test engine used to determine RON, and the auto-ignition behavior of a fuel/air mixture depends on the path the mixture

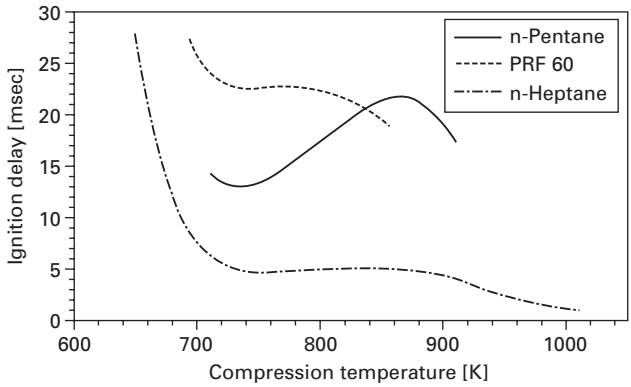

17.7 Experimentally measured ignition delay times in a rapid compression machine for stoichiometric fuel/oxygen mixtures diluted by argon, nitrogen and carbon dioxide to vary the compressed gas temperature. Fuels are n-pentane, n-heptane and PRF60 (60% iso-octane, 40% n-heptane).

travels in temperature and pressure and the speed of the compression. Figure 17.7 is a warning that metrics such as octane number should not be used with confidence in evaluating relative ignition qualities of fuels under HCCI conditions.

17.6 Kinetic models for HCCI ignition

Computational models of HCCI combustion have the same limitations as those for other complex engine systems. The demands of full 3-dimensional spatial models, including fluid dynamics and turbulence models, with detailed multicomponent chemical kinetics are too great for current computers, so some model simplification is necessary. This has been done in both possible ways, with significant simplifications of the fluid mechanics or significant reductions in the chemical kinetics. A good review of the options available that have been used for chemical kinetic simulations of HCCI auto-ignition with different degrees of spatial simplification is provided by the thesis of Ogink (2004).

Fully detailed chemical kinetic mechanisms have been used extensively in many simulations of HCCI combustion. The simplest assumption for HCCI is that the combustion is truly homogeneous, and single-zone spatial models have been used frequently (e.g., Kelly-Zion and Dec, 2000). Single-zone models with detailed chemical kinetics generally give good predictions of the start of ignition, since the details of the low temperature, alkylperoxy radical isomerization reaction pathways and the hydrogen peroxide decomposition can all be included. Effects of different fuels, engine speed,

and other factors can all be properly simulated. However, while the start of ignition can be accurately predicted, the computed rate of pressure rise, burn duration, and emissions of unburned hydrocarbons and carbon monoxide are poorly reproduced in a single-zone, purely homogeneous model. It is quite simple to see that the rate of pressure rise, burn duration and emissions from HCCI engines must be influenced by departures from spatial homogeneity in real engines that are not included in the single-zone approximation.

To deal with these effects, Aceves *et al.* (1999, 2000) developed a multizone spatial model, linking complex 3-dimensional fluid dynamics with a fully detailed chemical kinetics mechanism, into a hybrid model. In their calculations, originally designed to reproduce the effects of wall heat transfer on HCCI combustion, a very detailed fluid dynamics model is used during the time period from intake valve closing to the time when low-temperature reaction begins. During this period, no chemical model is used, and special attention is given to heat transfer to engine walls and flow into crevice volumes. Once reaction begins, the complex 3-dimensional fluid dynamics are abandoned, and all of the spatial zones are collected into a few conceptual zones to proceed with the fully detailed kinetic model. Only the inhomogeneities in temperature produced during the pre-reactive time period are retained into the few (~10) zones, and the progress of each conceptual zone towards ignition are computed, with each zone reacting independently. Since each of these remaining conceptual zones begin at different temperatures (from the 3-D fluid dynamics model), they ignite at different times, and some do not ignite at all. The result is that this approach is able to retain the ability to predict the start of ignition, and the multiple zones are able to reproduce the major features of a realistic burn duration and residual or unburned hydrocarbons and carbon monoxide.

Practical transportation fuels such as diesel fuel and gasoline usually contain many hundreds of different chemical species, and as a result, it is impossible to include all of these species in a usable kinetic mechanism. An approach currently being pursued is to create a computational model that includes some number of distinct species that can reproduce the effects of the many real components in the fuel. Thus a 4- or 5-component numerical mechanism might have submodels for one or two n-alkane and branched-alkane species such as n-heptane and iso-octane, another submodel with an aromatic compound such as toluene or o-xylene, and another for a cyclic paraffin such as methyl cyclohexane. Varying the fractions of these components to optimize the degree to which the model can reproduce a given set of experimental results in HCCI engines is the computational equivalent of varying composition in order to match an observed 'blending' octane number for engine knock tendency. The current status of these efforts to produce reliable surrogate mixtures is summarized in a group of papers which will appear shortly, for gasoline (Pitz *et al.*, 2007), diesel fuel (Farrell *et al.*, 2007), and for jet fuel (Edwards *et al.*, 2007).

A wide variety of reduced chemical kinetic models have also been used in fully-resolved, 3-D fluid dynamics. These kinetic mechanisms can be produced in the same ways that reduced kinetics are included for other applications, including simulations of spark-ignition or diesel engine combustion. Reduced mechanisms can be developed by sequential removal of unnecessary reactions or chemical species, or skeletal mechanisms that do not look at all like chemical reactions but can still reproduce the onset of ignition.

From the kinetic discussions above, it seems clear that the most important features that must be included are the effects of the low-temperature alkylperoxy radical isomerizations, and the decomposition of hydrogen peroxide. Early reduced mechanisms for engine knock, such as the Shell Model (Halstead *et al*., 1975) and the model of Hu and Keck (1987), both of which include these important reaction sequences in one form or another, have been adapted successfully for HCCI simulations.

17.7 Summary

Chemical kinetic analysis of engine auto-ignition has been developed over the past 15 years and has been able to explain, in fundamental chemical terms, the origin of the low-temperature reactivity and its relation to such factors as octane number and cetane number. In simple terms, long, straight chain molecules and n-alkanes in particular, with lots of secondary C—H bonds, have much lower octane numbers, higher cetane numbers, and more extensive low-temperature reactivity, than highly branched, compact fuel molecules. The same factors determine the amounts of low-temperature reactivity under HCCI conditions and strongly affect the timing of the eventual real ignition. However, auto-ignition under HCCI conditions is related to, but not identical with auto-ignition in SI or diesel engines, and the metrics such as octane number and cetane number do not translate successfully to HCCI engine operation. Sjöberg and Dec (2007) have shown recently how it is possible to exploit these effects by using variations in low temperature reactivity with variables like exhaust gas recirculation, intake boost, octane number and engine speed to control the timing of ignition, burn duration, and rate of pressure rise in HCCI engines.

17.8 References

Aceves, S.M., Smith, J.R., Westbrook, C.K., and Pitz, W.J., (1999), 'Compression Ratio Effect on Methane HCCI Combustion', *J Engin Gas Turb Power* 121, 569–574.

Aceves, S.M., Flowers, D.L., Westbrook, C.K., Smith, J.R., Pitz, W.J., Dibble, R., Christensen, M., and Johansson, B., (2000), 'A Multi-Zone Model for Prediction of HCCI Combustions and Emissions', *SAE Trans*, Section 3, Volume 109, 431–441.

Benson, S.W., (1976), '*Thermochemical Kinetics*', Wiley, New York.

Christensen, M., Johansson, B., and Einewall, P., (1997), 'Homogeneous Charge

Compression Ignition (HCCI) Using Isooctane, Ethanol and Natural Gas – A Comparison with Spark Ignition Operation', SAE 972874.

Christensen, M., Johansson, B., Amneus, P., and Mauss, F., (1998a), 'Supercharged Homogeneous Charge Compression Ignition', SAE 980787.

Christensen, M., and Johansson, B., (1998b), 'Influence of Mixture Quality on Homogeneous Charge Compression Ignition', SAE 982454.

Cox, A., Griffiths, J., Mohamed, C., Curran, H.J., Pitz, W., and Westbrook, C.K., (1996), 'Extents of Alkane Combustion During Rapid Compression Leading to Single- and Two-Stage Ignition', *Proc Combust Inst* 26, 2685–2692.

Curran, H.J., Gaffuri, P., Pitz, W.J., Westbrook, C. K., and Leppard, W.R., (1996a), 'Auto-ignition Chemistry in a Motored Engine: An Experimental and Kinetic Modeling Study', *Proc Combust Inst* 26, 2669–2677.

Curran, H.J., Pitz, W.J., Westbrook, C.K., Griffiths, J.F., and Mohamed, C., (1996b), 'Kinetic Modeling of Hydrocarbon Auto-ignition at Low and Intermediate Temperatures in a Rapid Compression Machine', Proc 3rd Workshop *Modelling of Chemical Reaction Systems*, Heidelberg, Germany, ISBN 3-932217-00-4.

Curran, H.J., Gaffuri, P., Pitz, W.J., and Westbrook, C.K., (1998), 'A Comprehensive Modeling Study of n-Heptane Oxidation', *Combust Flame* 114, 149–177.

Curran, H.J., Gaffuri, P., Pitz, W.J., and Westbrook, C.K., (2002), 'A Comprehensive Modeling Study of iso-Octane Oxidation', *Combust Flame* 129, 253–280.

Edwards, T., Coket, M., Cernansky, N., Dryer, F.L., Egolfopoulos, F., Friend, D., Lenhert, D., Lindstedt, P., Pitsch, H., Sarofim, A., Seshadri, K., Smooke, M., Tsang, W., and Williams, S. (2007), Development of an Experimental Database and Kinetic Models for Surrogate Jet Fuels', manuscript in preparation for Society of Automotive Engineers.

Farrell, J.T., Cernansky, N.P., Dryer, F.L., Friend, D., Hergart, C.A., Law, C.K., McDavid, R.M., Mueller, C.J., Patel, A.K., and Pitsch, H., (2007), 'Development of an Experimental Database and Kinetic Models for Surrogate Diesel Fuels', manuscript in preparation for Society of Automotive Engineers.

Griffiths, J.F., Halford-Maw, P.A., and Mohamed, C., (1997), 'Spontaneous ignition delays as a diagnostic of the propensity of alkanes to cause engine knock', *Combust Flame* 111, 327–337.

Griffiths, J.F., and Barnard, J.A., (1995), *Flame and Combustion*, Oxford, Chapman and Hall.

Halstead, M.P., Kirsch, L.J., Prothero, A., and Quinn, C.P., (1975), 'Mathematical-model for Hydrocarbon Auto-ignition at High-Pressures', *Proc Roy Soc A* 346, 515–538.

Hu, H., and Keck, J.C., (1987), 'Auto-ignition of Adiabatically Compressed Combustible Gas Mixtures', SAE 872110, Trans.

Kelly-Zion, P.L., and Dec, J.E., (2000), 'A Computational Study of the Effect of Fuel-Type on Ignition Time in Homogeneous Charge Compression Ignition Engines', *Proc Combust Inst* 28, 1187–1194.

Lovell, W.G., (1948), 'Knocking Characteristics of Hydrocarbons", *Ind Eng Chem* 40, 2388–2438.

Midgley, T.A., (1925), 'How we found ethyl gas', *Motor* 43, 92.

Minetti, R., Carlier, M., Ribaucour, M., Therssen, E., and Sochet, L.R., (1995), 'Rapid Compression Machine Investigation of Oxidation and Auto-ignition of n-heptane – Measurements and Modeling', *Combust Flame* 102, 298–309.

Ogink, R., (2004), *Computer Modeling of HCCI Combustion*, Ph.D. Thesis, Chalmers University of Technology, Division of Thermo and Fluid Dynamics, Göteborg, Sweden.

Peng, Z., Zhao, H., Ma, T., and Ladommatos, N., (2005), 'Characteristics of Homogeneous

Charge Compression Ignition (HCCI) Combustion and Emissions of n-Heptane', *Combust Sci Technol* 177, 2113–2150.

Pitz, W.J., Cernansky, N.P., Dryer, F.L., Egolfopoulos, F.N., Farrell, J.T., Friend, D.G., and Pitsch, H., (2007), 'Development of an Experimental Database and Kinetic Models for Surrogate Gasoline Fuels', manuscript in preparation for Society of Automotive Engineers.

Pollard, R.T., (1977), 'Hydrocarbons', Chapter 2, *Comprehensive Chemical Kinetics*, vol. 17, Gas-Phase Combustion (C. H. Bamford and C. F. H. Tipper, eds.), Elsevier, New York.

Ribaucour, M., Minetti, R., Sochet, L.R., Curran, H.J., Pitz, W.J., and Westbrook, C.K., (2000), 'Ignition of Isomers of Pentane: An Experimental and Kinetic Modeling Study', *Proc Combust Inst* 28, 1671–1678.

Silke, E., Curran, H.J., and Simmie, J.M., (2005), 'The influence of fuel structure on combustion as demonstrated by the isomers of heptane: a rapid compression machine study', *Proc Combust Inst* 30, 2639–2647.

Sjöberg, M., and Dec, J.E., (2007), 'Comparing Late-Cycle Auto-ignition Stability for Single- and Two-Stage Ignition Fuels in HCCI Engines', *Proc Comb Inst,* 31, 2895–2902.

Warnatz, J., (1980), The structure of laminar alkane-, alkene-, and acetylene flames', *Proc Combust Inst* 18, 369–384.

Westbrook, C.K., (1982a), 'Inhibition of Hydrocarbon Oxidation in Laminar Flames and Detonations by Halogenated Compounds', *Proc Combust Inst* 19, 127–141.

Westbrook, C.K., (1982b), 'Chemical Kinetics of Hydrocarbon Oxidation in Gaseous Detonations', *Combust Flame* 46, 191–210.

Westbrook, C.K., and Dryer, F.L., (1984), 'Chemical Kinetics Modeling of Hydrocarbon Combustion', *Prog Energy Combust Sci* 10, 1–57.

Westbrook, C.K., Pitz, W.J., and Leppard, W.R., (1991), 'The Auto-ignition Chemistry of Paraffinic Fuels and Pro-Knock and Anti-Knock Additives: A Detailed Chemical Kinetic Study', *SAE Trans*, Section 4, Volume 100, 605–622.

Westbrook, C.K., (2000), 'Chemical Kinetics of Hydrocarbon Ignition in Practical Combustion Systems', *Proc Combust Inst* 28, 1563–1577.

Westbrook, C.K., Mizobuchi, Y., Poinsot, T., Smith, P.A., and Warnatz, J., (2005), 'Computational Combustion', *Proc Combust Inst* 30, 125–157.

18

Overview of modeling techniques and their application to HCCI/CAI engines

S M ACEVES, D L FLOWERS, R W DIBBLE and A BABAJIMOPOULOS, Lawrence Livermore National Laboratory, USA

18.1 Introduction

Growing concern over local environmental pollution and climate destabilization has moved governments to enact laws mandating increased fuel efficiency and reduced emissions. These laws have targeted combustion processes, including internal combustion engines, both for transportation and for stationary applications.

HCCI (homogeneous charge compression ignition) has recently emerged as an alternative combustion mode for internal combustion engines with efficiency and emission advantages over conventional (spark ignited, SI; and diesel) engines. While HCCI engines are not a new concept (Erlandsson, 2002), only recently have advances in microprocessor-based control and combustion technologies made HCCI possible.

Different HCCI approaches are being researched for meeting existing and upcoming emissions legislation. Some of these approaches deviate from pure 'homogeneous' combustion into 'partially stratified' combustion – for example, premixed charge compression ignition (PCCI; Nakagome and Niimura, 1997) and controlled auto-ignition (CAI; Oakley *et al.*, 2001a). The HCCI label is typically used for partially stratified regimes so long as the engine charge is reasonably well mixed and thus the combustion phenomenon remains HCCI-like in nature.

There are some fundamental differences between combustion in HCCI, SI and diesel engines. HCCI combustion is clean and efficient, but difficult to control. In addition, HCCI works best at low to medium loads; extension to full power is a research topic. Obtaining the greatest benefit from HCCI requires advanced engines with fast sensors and actuators that permit *both* controlled HCCI combustion and transition to SI or diesel modes when the load cannot be satisfied in HCCI mode. This flexibility enables optimum engine performance at every combination of load and speed, maximizing efficiency with minimum emissions.

Computer modeling is increasingly part of the engine discovery and design

process. This trend will expand in the future as computers become more powerful. The unique properties of HCCI engines demand new analysis tools to characterize operation. In this chapter, we describe modeling approaches for homogeneous and partially stratified HCCI.

18.2 Fundamentals of HCCI ignition and combustion

HCCI is a thermal auto-ignition process that initiates simultaneously at numerous sites before rapidly spreading throughout the combustion chamber (Onishi *et al*., 1979; Noguchi *et al*., 1979). HCCI auto-ignition contrasts sharply with the turbulent flame propagation of SI engines and the mixing controlled combustion of diesel engines. This contrast has important consequences. Auto-ignition can be sustained even at very lean (equivalence ratio, $\phi < 0.2$; Dec and Sjöberg, 2003), or very dilute (exhaust gas recirculation, EGR > 0.6; Oakley *et al*., 2001a) conditions, with the result that the final flame temperatures are low, say 1900K; sufficiently cold to keep nitrogen oxide (NOx) emissions at remarkably low levels (a few parts per million). If the HCCI combustion charge is lean and well mixed, little particulate matter (PM) is produced. Furthermore, HCCI engines can approach the high efficiency of diesel engines because they can operate unthrottled and at a high compression ratio.

The basic nature of the thermal auto-ignition in HCCI also creates two engineering challenges for practical engines: control and power. Control of HCCI ignition timing cannot be directly determined by an external event such as fuel injection in diesel engines or spark plug firing in SI engines. Control of HCCI ignition is therefore 'one step removed' and thus is a greater challenge. Many control approaches have been explored, these approaches typically requiring fast sensors and flexible actuators such as variable valve timing. HCCI auto-ignition releases heat very rapidly, potentially damaging the engine if run at high equivalence ratios ($\phi > 0.5$) and no dilution where strong pressure oscillations are generated (higher equivalence ratios are possible with EGR). Sudden heat release limits the operational range of satisfactory HCCI combustion, in turn limiting the engine specific power.

Spectroscopy experiments (Onishi *et al*., 1979) and computer models (Aceves *et al*., 2000) suggest that chemical kinetics dominates thermal auto-ignition in HCCI. Ignition begins in slightly hotter spots formed due to non-uniformities in temperature or concentration (Warnatz *et al*., 2006). Combustion then propagates as a pressure wave from these initial ignition points. The expansion of hot reaction products compresses and heats the unburned fuel and air that is adjacent to the initial ignition points. As adjacent fuel is near ignition, slight compression is all that is required to 'push it over the top' to ignition.

Compression typically generates temperatures hot enough to combust the fuel, except in the boundary layer and in the crevices, which are too cold to ignite (Aceves *et al*., 2002; Aceves *et al*., 2004). Compression heating is the main mechanism for spreading combustion in HCCI engines, and flame propagation (diffusion of energy and radicals from the burned zone to the unburned zone; Turns, 2000) plays a secondary role. This vision is supported by experimental results (Hultqvist *et al*., 2002) that indicate that the speed of propagation of the combustion front in HCCI is far faster than deflagration in SI engines.

It is generally thought that turbulence plays an indirect role in HCCI combustion. Turbulence controls heat transfer to the cylinder walls, thereby establishing the temperature distribution in the cylinder. The temperature distribution determines the heat release rate. If the engine charge is isothermal, all the fuel auto-ignites simultaneously; such an event would be too rapid, causing a damaging sudden increase in pressure. A broad temperature distribution has the desirable effect of distributing the combustion event over a longer time period.

The chemical kinetic description of the combustion process is also applicable to partially stratified combustion (PCCI) if the degree of stratification is relatively small. Recent modeling work (Sankaran and Im, 2004) studied the influence of inhomogeneity on the auto-ignition of mixtures of a premixed fuel/air stream and hot exhaust gases. It was found that dissipation rate and mixture inhomogeneity can have a significant effect on auto-ignition. However, at low mixing rates and high pressures, chemical kinetics dominates the auto-ignition process and diffusion has little effect in the propagation of the reaction front. As the level of fuel-air mixture stratification increases, turbulence plays a more direct role in combustion (Zhang *et al*., 2004; Benkenida and Angelberger, 2004). Further research is needed to determine the level of stratification that still allows a chemical kinetic description of the combustion process.

The chemical kinetic nature of HCCI foretells a bright future for HCCI engine analysis. Fortunately, the computational expense of highly resolved turbulence calculations is not needed, enabling detailed and accurate HCCI modeling with reduced computational expense relative to SI or diesel modeling. This computational advantage may ultimately become an important practical advantage of HCCI engines, enabling extensive computer-based engine design with reduced reliance on empirical validation.

18.3 The chemistry of HCCI

Auto-ignition in internal combustion engines has been studied for many years, initially for prediction of knock in SI engines (Smith *et al*., 1985), and more recently for HCCI analysis. The chemical reactions that play a role in

the process are classified as low temperature reactions, intermediate temperature reactions, and high temperature reactions.

18.3.1 Low temperature chemistry

As the engine charge heats up during the compression stroke, chemistry becomes increasingly active at temperatures above 600 K. At these conditions, fuel dissociation is described by the following 'low temperature' mechanism (Warnatz *et al.*, 2006; Eng, 2003).

$RH + O_2$	$\rightarrow R\bullet + HO_2$	initiation	18.1
$R\bullet + O_2$	$\leftrightarrow RO_2\bullet$	first O_2 addition	18.2
$RO_2\bullet$	$\rightarrow \bullet R'OOH$	internal H-atom abstraction	18.3
$\bullet R'OOH$	$\rightarrow R'O + OH\bullet$	chain propagation	18.4
$\bullet R'OOH + O_2$	$\leftrightarrow HO_2R'O_2\bullet$	second O_2 addition	18.5
$HO_2R'O_2\bullet + RH$	$\rightarrow HO_2R'O_2H + R\bullet$	external H-atom abstraction	18.6
$HO_2R'O_2H$	$\rightarrow HO_2R'O\bullet + OH\bullet$	chain branching	18.7
$HO_2R'O\bullet$	$\rightarrow OR'O + OH\bullet$	chain propagation	18.8
$HO_2R'O_2\bullet$	$\rightarrow HO_2R''O_2H$	internal H-atom abstraction	18.9
$HO_2R''O_2H\bullet$	$\rightarrow HO_2R''O + OH\bullet$	chain propagation	18.10
$HO_2R''O$	$\rightarrow OR''O\bullet + OH\bullet$	chain branching	18.11

In the initiation step, a hydrocarbon (RH) reacts with oxygen to make a hydrocarbon radical (R•), which reacts with oxygen to make a peroxy radical ($RO_2\bullet$). Next, an internal hydrogen-atom abstraction takes place (i.e., the abstraction of a hydrogen atom from the molecule itself; Fig. 18.1). Following

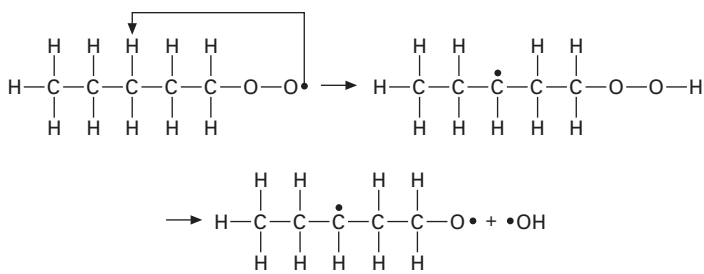

18.1 Internal hydrogen abstraction in a heptyl peroxy radical via an intermediate 6-membered ring structure. The biradical in the right-hand side will immediately isomerize to form a stable aldehyde C_4H_9-CHO (Warnatz *et al.*, 2006).

the internal abstraction, the radical •R′OOH reacts internally to eliminate (eject) OH and form a compound without free valences (unpaired electrons) such as an aldehyde or ketone (Equation 18.4). The mechanism continues with a second O_2 addition to the peroxy radical initially formed (Equation 18.5; Chevalier *et al.*, 1990a, b). After a few steps, ketohydroperoxide ($HO_2R''O$) is formed (Equation 18.10). Ketohydroperoxide decomposes at ~800 K, producing further OH• radicals that consume the fuel (Equation 18.11).

In the hydrogen abstraction reaction (Equation 18.3) the molecule isomerizes by 'reaching around' and abstracting a hydrogen atom from somewhere on the hydrocarbon chain. Straight chain molecules such as n-heptane (C_7H_{16}) are long enough for flexible internal abstraction of hydrogen (Fig. 18.1). In addition to this, H atoms in n-heptane are bound to 'secondary sites' (the $–CH_2–$ backbone), which makes them easier to abstract than H atoms in primary sites, where the hydrogen is attached to the end of a chain (the $–CH_3$ group). Iso-octane (C_8H_{18}) is actually a short pentane chain with 3 methyl groups attached to the chain. The short chain has difficulty 'reaching around' to abstract a hydrogen atom and furthermore, most of the H atoms in iso-octane are primary, thus harder to abstract. This flexibility and abstraction theory explains the higher reactivity and lower octane number of n-heptane (octane number = 0) with respect to iso-octane (octane number = 100). The theory further explains the high octane number of methane (CH_4; octane number = 120), and similarly ethane (C_2H_6 or $(CH_3)_2$; octane number = 115) where no internal abstraction is possible.

The mechanism [18.1] to [18.11] listed above also explains the observation of so-called *two-stage ignition,* also called the *negative temperature coefficient* (NTC) zone. At low temperature, the oxygen addition (reactions [18.2] and [18.5]) leads to a product 'P' that then undergoes reactions that lead to chain branching ([18.7] and [18.11]). These chain branching reactions lead to a rapid increase in the temperature of the mixture. As the temperature increases, the NTC zone is reached where the newly formed product P can now either continue toward chain branching or decompose back to the reactants (i.e. reverse reaction, see the bi-directional arrow on reactions [18.2] and [18.5]). The increase in the reverse rate results in a lower concentration of products P which in turn leads to a reduction of chain branching, causing a reduction in the rate of temperature increase; the ignition delay is prolonged. As a consequence, one observes what is called a 'two-stage ignition.' At low temperatures, the reactions are proceeding at a slow, but observable rate. Starting at temperatures below the NTC zone, the energy released by these reactions slowly increases the temperature. With this increased temperature, the reaction rates increase, the temperature is increasing faster and faster. This is the 'first stage' of ignition. The temperature increases until the NTC zone is reached. At this temperature, the concentration of P decreases, and

thus the rate of increase in temperature slows down, but is never zero. In time, the slowly increasing temperature reaches a point where low concentration of product P is more than compensated by the increased chain branching reaction rate and then, the system explodes; this is the 'second stage' of ignition. Surprisingly, if one starts the system in the NTC zone, the concentration of P is extremely low and the ignition delay can be longer than if one started the system at a temperature below the NTC zone. This is why it is called 'negative temperature coefficient' zone.

18.3.2 Intermediate and high temperature combustion

Heating the engine charge beyond ~850 K activates a new set of chemical reactions, called the intermediate temperature reactions:

$RH + O_2$	$\rightarrow R\bullet + HO_2$	initiation	18.12
$HO_2\bullet + RH$	$\rightarrow H_2O_2 + R\bullet$	propagation	18.13
$H_2O_2 + M$	$\rightarrow OH\bullet + OH\bullet + M$	chain branching	18.14

HCCI ignition occurs when the chain branching reaction [18.14] becomes active, decomposing the hydrogen peroxide (H_2O_2) that has been accumulating in the reactive mixture, producing two hydroxyl (OH•) radicals for each H_2O_2 that decomposes. The importance of reaction [18.14] is clearly seen in Fig. 18.2, where the concentration of H_2O_2 decreases rapidly during HCCI

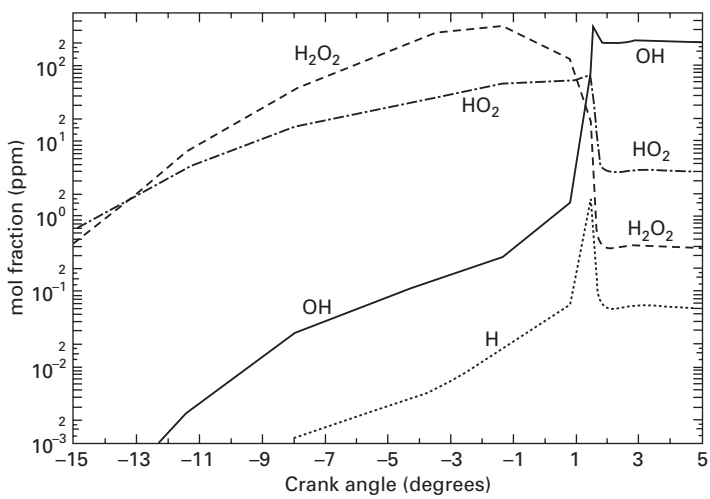

18.2 Calculation of chemical composition during HCCI ignition (Aceves *et al.*, 2000). At ignition (at 2° after top dead center), the concentration of H_2O_2 drops rapidly due to decomposition into two OH radicals.

ignition as OH• radicals are being formed, increasing the temperature of the reacting mixture and setting in motion an effective chain branching sequence. This reaction sequence proceeds until the temperature has increased sufficiently that the *high-temperature* chain branching sequence takes over, controlled by $H\bullet + O_2 \rightarrow O\bullet + OH\bullet$ which dominates the remainder of the overall HCCI combustion process. Low temperature reactivity does not directly affect the chemistry of HCCI ignition, which is dominated by Equations 18.12–18.14 for all fuels. However, low temperature reactivity accelerates ignition by providing heat release early in the process. Early heat release is amplified by the compression process, so the reactive mixture arrives sooner at the ignition temperature where reaction [18.14] proceeds (Westbrook, 2000).

The decomposition of hydrogen peroxide [18.14] 'triggers' ignition in HCCI engines. This decomposition occurs when the kinetic energy of the reactive molecules, as measured by the gas temperature, becomes comparable to the bond energy of the bond being broken, namely the HO–OH bond. Ignition occurs at temperatures between 1050 K and 1100 K. The consistency of this temperature is a recognized feature of HCCI combustion. Not surprisingly, this temperature is comparable to the ignition temperature that is observed during engine knock in spark-ignition engines (Smith *et al.*, 1985).

18.4 Prediction of ignition in HCCI engines

When using models for investigating control in HCCI engines it is often enough to determine ignition timing. Analysis of ignition often uses lumped (single zone) thermodynamic models, which assume uniform temperature, pressure and composition throughout a cylinder with changing volume. Single zone models predict ignition with good accuracy because they are representative of the hottest gases in the combustion chamber, the 'central core' gases where ignition occurs. The central core is nearly adiabatic and according to basic combustion theory it would always ignite if given enough time, which may not be available in an engine. Processes sensitive to the core conditions, such as combustion timing, NOx emissions, and trends in peak cylinder pressure and indicated work, can be well predicted with single zone models. Processes sensitive to boundary layer effects, such as combustion duration and HC and CO emissions, are not well predicted by single zone methods. Different methods can be used to predict ignition, such as auto-ignition integrals and detailed chemical kinetics.

18.4.1 The auto-ignition integral

Auto-ignition integral methods were introduced in a classic paper by Livengood and Wu (1955), who developed an expression to determine the instantaneous ignition delay (τ) of the mixture within the cylinder:

$$\tau = cP^n \exp\left(-\frac{b}{T}\right) \quad 18.15$$

where P and T are the instantaneous pressure and temperature within the cylinder, and b, c, and n are empirical constants. To determine the onset of ignition, the instantaneous ignition delay is integrated for the gases within the cylinder as a function of time, producing the auto-ignition integral, AI:

$$\text{AI} = \int \frac{1}{\tau} dt \quad 18.16$$

Auto-ignition is said to occur when AI = 1.0. Thus, the Livengood-Wu model accounts for the thermochemical path dependency of the auto-ignition process, considering the contributions to the ignition from chemical processes occurring throughout the compression stroke. The constants c, n, and b are fuel specific, and were determined in the 1955 paper from several experiments: rapid compression machine, motoring engine, and firing engine experiment.

The AI approach has been applied to modeling ignition in HCCI engines. For example, Agrell *et al.* (2003a, b) successfully predicted ignition in an HCCI engine with variable valve timing by applying an AI model in combination with a cycle simulation code. The AI can be used to very rapidly estimate start of combustion in HCCI engines, however it has limitations. One limitation is that AI methods do not account for low temperature heat release, integrating instead over motored temperature and pressure. AI methods are therefore best suited for high-octane fuels that exhibit little low temperature heat release. Another limitation of AI methods is that the c, n, and b constants must be determined experimentally or computationally by comparison with more accurate chemical kinetic calculations.

It is possible to improve the accuracy of the auto-ignition integral model with more detailed expressions for the ignition delay (Equation 18.16). Recent work (Choi and Chen, 2005) predicted ignition delay with an artificial neural network. A neural network is a universal approximator for non-linear functions that predicts an output value (or values) based on a set of input parameters and a training procedure. The neural network was trained with tens of thousands of detailed chemical kinetic simulations (that required 3 months of computer time) to determine ignition delay based on instantaneous pressure, temperature, equivalence ratio, and residual gas fraction. Once the computationally intensive training procedure is completed, the neural network can conduct very fast computations (less than a second) of ignition delay and ignition timing. Model validation demonstrated good agreement with experimental results.

18.4.2 Chemical kinetics

Detailed chemical kinetics approaches have the advantage of directly simulating all the chemical processes leading to auto-ignition in HCCI engines. Detailed

chemical kinetic mechanisms have been developed for a wide variety of fuels, including natural gas (Frenklach *et al*., 1995), di-methyl ether (Curran *et al*., 1998), isooctane (Curran *et al*., 2002), n-heptane (Westbrook *et al*., 2002), and many others. These mechanisms capture reaction rate information for elementary reaction steps. In other words, they capture the collisions that convert one molecule to another. The advantage of detailed chemical kinetics is that the processes leading to ignition are directly modeled and processes such as cool flame chemistry can be resolved. The disadvantage is that mechanisms for practical hydrocarbon fuels can contain hundreds or even thousands of species, resulting in large and stiff systems of differential equations (Kee *et al*., 2003), which can be computationally intensive to solve.

HCCI ignition calculations are often conducted with lumped (single zone) chemical kinetics models, which assume spatially uniform temperature, pressure, and composition in a fixed-mass, variable volume reactor. These models have been applied to predicting engine performance over a wide range of operating conditions assuming different control strategies, such as thermal control (Yang *et al*., 2002) or EGR based control (Martinez-Frias *et al*., 2001). Figure 18.3 shows performance maps (engine torque versus speed) for HCCI operation with natural gas based on single zone simulations (Martinez-Frias *et al*., 2001). The single zone model was used with an optimizer to select the control inputs (equivalence ratio, EGR) that gave the highest engine efficiency for each operating condition.

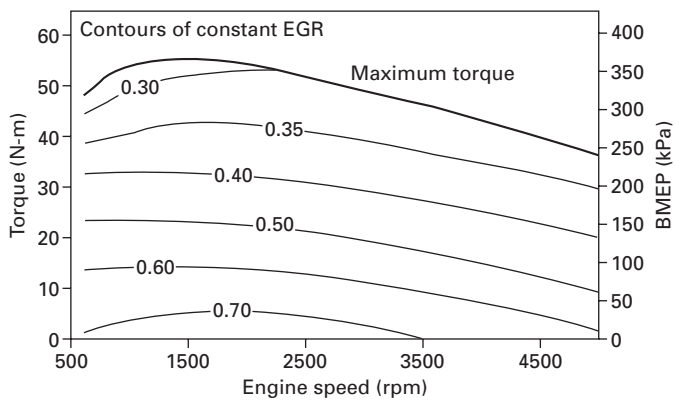

18.3 HCCI engine performance map calculated by linking a single zone chemical kinetics code with an optimizer (Martinez-Frias *et al.,* 2001). The figure shows contours of constant EGR that maximize engine efficiency as a function of rpm and torque (and BMEP in the right scale). The figure also shows the line of maximum engine torque.

18.5 Detailed calculation of HCCI combustion and emissions

Detailed HCCI analysis requires distributed models that go beyond the single zone approach and consider the interaction between the non-homogeneous temperature field and the auto-ignition chemistry. Two main approaches have been used for detailed HCCI analysis: fully integrated models and multi-zone models.

18.5.1 Full integration of fluid mechanics and chemical kinetics codes

In this approach, the fluid mechanics and chemical kinetics codes are directly linked. The fluid mechanics code calculates the temperature distribution, and the chemical kinetics code calculates composition and chemical heat release in each cell of the grid. In principle, this procedure can solve any engine combustion problem, as long as appropriate grid resolution and detailed chemical kinetic mechanisms are used. In practice, applicability of the fully integrated method is limited by the computer resources necessary to solve the problem. A three-dimensional engine mesh with good boundary layer resolution (necessary for accurate HCCI analysis) often requires 10^5–10^6 computational cells, and an appropriate mechanism for long chain hydrocarbons (n-heptane, iso-octane) requires at least 200 species. A problem of this magnitude takes years of running time in today's (~2 GHz) single processor computers. The fully integrated approach may become the preferred method for HCCI analysis in the future, when faster processors and widespread availability of massively parallel computers considerably reduce the computational cost. However, at this time, the fully integrated approach has been restricted to small chemical kinetic mechanisms (~100 species) and coarse grids (~1000 cells) (Agarwal and Assanis, 2000; Kusaka *et al*., 2002; Kong *et al*., 2003).

Much research has been directed at reducing the computational requirements of the fully integrated approach (Assanis *et al*., 2003). The most common technique for speeding up the computations is developing reduced chemical kinetic mechanisms (Montgomery *et al*., 2002; Chen and Chen, 2005) that eliminate chemical species that have little effect on the combustion process (ignition time, burn duration, combustion efficiency). Detailed mechanisms (~800 species for iso-octane) are too large for most practical computations, and therefore reduced mechanisms are necessary for reasonable computational times. However, these reduced mechanisms are applicable only to a restricted set of conditions and moving outside the regime of applicability may produce erroneous results.

It is possible to reduce the computational time without simplifying the

chemical kinetic mechanism by improving the equation solvers. The set of differential equations that result from the chemical kinetic mechanism is quite sparse, because cells are weakly coupled to one another (Yelvington and Green, 2003). Much reduction in computational time can be obtained by using numerical methods especially developed for sparse systems of equations (Schwer *et al*., 2002).

In typical HCCI runs, many computational cells are at similar conditions (pressure, temperature and composition), and therefore it is not necessary to run a chemical kinetic integration for all cells. Instead, the chemical kinetic results can be stored in a *lookup table* for later reuse in other cells with similar conditions, thereby reducing the computational time (Embouazza *et al*., 2002). The method produces accurate results and considerable speedup (a factor of 10 or more) for typical HCCI combustion. The computational advantage of the lookup table approach decreases for stratified mixtures. Mass stratification increases the variability in cell composition and reduces the probability of reusing lookup table results. Little computational advantage was obtained in direct injected engines, where composition varies broadly between cells.

A recent publication (Aceves *et al*., 2006) describes the application of a neural network-based combustion model for HCCI analysis. The neural network is first trained with a detailed chemical kinetics code to predict ignition in the individual cells of the grid. Ignited cells react according to a very simplified two-step chemical kinetic mechanism (Westbrook and Dryer, 1981). The procedure produces good estimates of HCCI combustion and emissions and the computational time is only 10% longer than required for a motored (no combustion) run in a fluid mechanics code. The neural network approach is appropriate for evaluating performance maps and other tasks that require multiple individual runs. When more accuracy is required, a more physically representative multi-zone model is necessary.

18.5.2 Multi-zone models

Multi-zone models (Aceves *et al*., 2000, 2002; Babajimopoulos *et al*., 2003) are an alternative to full integration of a fluid mechanics code and a chemical kinetics code that yields accurate HCCI results while greatly reducing the computational time (by a factor of 100 or more). In a multi-zone HCCI analysis, cells that have similar temperature, pressure, and composition histories are grouped into a relatively small number of zones. The chemical kinetics solver is then applied to this small number of zones (10–100) instead of the large number of cells typically used in fluid mechanics (10^4–10^6). Considering that chemical kinetics is the most computationally intensive part of the problem, the multi-zone model offers great computational advantage with respect to a fully integrated calculation. Multi-zone models produce solutions within a

reasonable time (~1 day) in today's single processor computers, even when using fine meshes (~10^5 cells) and detailed chemical kinetic mechanisms (800 species).

The multi-zone model works best for homogeneous combustion where composition in the combustion chamber is (nearly) uniform. The first step in the process consists of running a fluid mechanics code under motored (no combustion) conditions. Mass in the cylinder is distributed in a few zones (10–100) according to temperature. The fluid mechanics code calculates zone temperature histories during the compression stroke. The chemical kinetics code is run for the multiple zones, with the zone temperatures prescribed by the temperature histories calculated in the motored run using detailed fluid mechanics and heat transfer. Pressure is assumed equal for all zones, and the mass of each zone is conserved. Motored temperature histories fall behind when chemical heat release is significant. At this point, the motored temperatures are abandoned and the chemical kinetics code continues the analysis of the combustion process using an empirical correlation for wall heat transfer and neglecting mixing between zones. The only interaction between zones is the compression work that a zone exerts on the remaining zones when it ignites and expands due to chemical heat release.

The multi-zone model (10 to 100 zones) has proven successful in predicting many details of the HCCI combustion process. The model has been used for multiple fuels and multiple operating conditions, consistently producing results that closely capture the experimental pressure traces (Fig. 18.4; Aceves *et al*., 2004), heat release rate, and hydrocarbon emissions. The multi-zone model is also capable of indicating the locations in the combustion chamber that produce different chemical species (unburned fuel, oxygenated hydrocarbons, carbon monoxide; Plate 18 (between pages 268 and 269); Aceves *et al*., 2004). The multi-zone model is less accurate at predicting carbon monoxide, because the model neglects diffusion between zones after ignition. In an engine, some CO is produced when unburned fuel from the crevices partially oxidizes as it diffuses into the hot cylinder core during the expansion stroke. As the piston further expands, the temperature plummets causing the OH population to drop, leaving nothing to oxidize CO to CO_2.

Flowers *et al*. (2003) modified the multi-zone model to include mixing effects by introducing a coupled CFD/multi-zone model. Instead of a one-way mapping of the CFD temperature distribution onto the multi-zone chemical kinetics solver, the temperature, pressure and composition are mapped back and forth between the chemical kinetics and the CFD code throughout the cycle. The advantage is that the fluid mechanical processes are still calculated on a high-resolution grid, while the computationally intensive chemical kinetics processes can be solved for a small number of zones. The goal of the study was to investigate the mixing of cold gases from the crevices and the boundary layer with the hot gases in the core after the main heat release event. It was

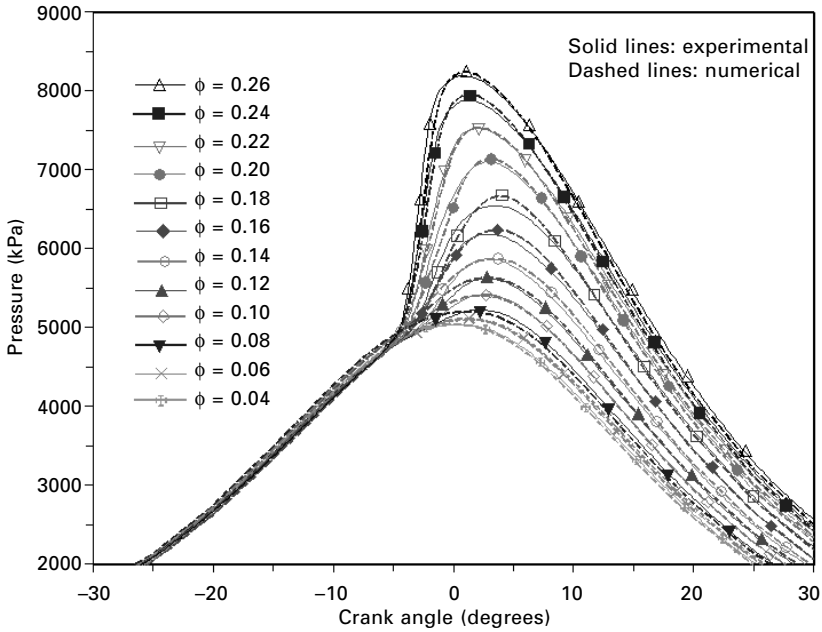

18.4 Comparison between experimental and multi-zone numerical pressure traces for an HCCI experiment at low equivalence ratio and load (Aceves *et al.,* 2004). In the experiment, the equivalence ratio was varied between $\phi = 0.04$ and $\phi = 0.26$ while keeping the ignition timing a few degrees before TDC by adjusting the intake temperature. The figure shows experimental results with solid lines and numerical results with dashed lines.

found that there is diffusion of CO and fuel from the lowest temperature regions into the hotter gases in the core and that the fuel continues to react during the expansion stroke. In addition, the prediction of HC and CO emissions was improved compared to the multi-zone model.

In addition to improving CO predictions in HCCI combustion, the method of Flowers *et al*. (2003) has applicability to analyze partially stratified (PCCI) combustion. In a recent publication (Flowers *et al*., 2006), the model was applied to an engine with a fuel concentration distribution that varies radially from a maximum at the cylinder center to a minimum at the cylinder liner. The model produced accurate predictions that match the results obtained with a fully integrated approach. Future application of the model will focus on early direct injected PCCI engines.

18.6 Prediction of operating range

One of the fundamental limitations of HCCI engines is their reduced load and speed range of operation. At high load, HCCI combustion is very fast,

potentially resulting in knock that may damage the engine. Low load is limited by partial or intermittent combustion that produces high emissions of HC and CO (Koopmans and Denbratt, 2002). Dual mode engines (HCCI-SI or HCCI-diesel) may provide the appropriate operating range while benefiting from clean and efficient HCCI combustion at low to mid loads. However, full load HCCI engines are important for applications that demand very low emissions at high load (heavy trucks or stationary engines). Analysis tools described in this section can predict the HCCI operating range and evaluate techniques aimed at extending it.

18.6.1 High load limit

Maximum load in HCCI engines is limited by very fast combustion leading to knock. During knocking combustion, ignition of hot spots is too fast for the pressure to equilibrate. Consequently, pressure waves are generated, which can produce detonation waves and potentially damage the engine (Warnatz *et al*., 2006).

The knock limit in HCCI engines is often correlated to the rate of pressure rise. The maximum allowable rate of pressure rise is often set at 5–10 bar per crank angle degree (Yap *et al*., 2005), although it is more appropriate to express the rate of pressure rise as a *time* derivative (in bar per second instead of bar per crank angle degree) for accurately predicting knock over a wide range of engine speeds (Yoshizawa *et al*., 2003). A fundamental study of HCCI engine knock (Eng, 2002) indicated that maximum rate of pressure rise is a function of operating parameters such as intake pressure and is therefore inappropriate as knock criterion. Instead, ringing intensity is recommended, and limiting values are set at 2 MW/m^2 for automotive engines and 6 MW/m^2 for truck engines.

Another HCCI modeling effort (Yelvington and Green, 2003) used a multi-zone model to predict knock. The model calculates ignition and the subsequent expansion of the multiple zones. Knock occurs whenever the expansion speed of a zone is faster than the speed of sound and therefore too fast for pressure equilibration. The model was successful in predicting experimental operating ranges for a controlled auto-ignition (CAI) engine with high residual gas fraction (Oakley *et al*., 2001a).

18.6.2 Low load limit

Low power HCCI combustion is limited by partial misfire or intermittent combustion producing high HC and CO emissions. Partial misfire is often defined in terms of a minimum acceptable level of combustion efficiency (85–90%, Oakley *et al*., 2001b). Experiments by Yoshizawa *et al*. (2003) show that the misfire limit can be correlated to the crank angle where 50%

of the chemical energy is released (θ_{50}). They proposed $\theta_{50} \geq 18$ degrees after top dead center as a criterion for misfire. While this criterion is very easy to use, its applicability to other engines or operating conditions has not been established.

Accurate prediction of combustion efficiency requires a distributed HCCI combustion model (a fully integrated or a multi-zone model), and these are appropriate tools to predict partial misfire (Yelvington and Green, 2003). For faster analysis, a lumped (single zone) model can be used at the expense of some accuracy. Single zone models are representative of conditions in the hottest part of the cylinder (the adiabatic core), and they may predict appropriate ignition at conditions where much of the boundary layer fails to ignite, resulting in low combustion efficiency. Therefore, single zone models predict an extended region of satisfactory combustion with respect to more physically representative distributed combustion models.

Intermittent combustion is caused by cycle-to-cycle variations in cylinder conditions. Marginal HCCI combustion is very sensitive to variations in temperature or composition of the engine charge, and small changes may cause misfire in a fraction of the cycles. According to Yoshizawa *et al.* (2003), cycle stability (expressed as the coefficient of variance of the indicated mean effective pressure, COV of IMEP), correlates with θ_{10-50} (the crank angle interval between the points at which 10% and 50% of the chemical energy is released). The criterion for intermittent combustion was set at $\theta_{10-50} \geq 6$ crank angle degrees.

A fundamentals-based prediction of intermittent combustion requires analysis of multiple consecutive engine cycles including both the gas exchange and the closed parts of the cycle. This is typically too computationally intensive to be analyzed with fully integrated or multi-zone models, and simpler models (single zone or stochastic partially stirred reactor; Bhave *et al.*, 2005) are necessary.

18.7 Summary and future trends

HCCI is an alternative engine combustion process with potential for efficiencies as high as diesel engines while producing ultra-low oxides of nitrogen (NOx) and particulate matter (PM) emissions. HCCI engines operate on the principle of having a dilute, premixed charge that reacts and burns volumetrically throughout the cylinder as it is compressed by the piston. In some regards, HCCI incorporates the best features of both spark ignition (SI) and diesel engines. As in SI engines, the charge is well mixed, which minimizes particulate emissions, and as in diesel engines, the charge is compression ignited and has no throttling losses, which leads to high efficiency. However, unlike either of these conventional engines, the combustion occurs simultaneously throughout the volume rather than in a flame front. This important attribute

of HCCI allows combustion to occur at much lower temperatures (e.g. 1800K as opposed to 2500K), dramatically reducing engine-out NOx emissions.

Experiments and analysis to date suggest that chemical kinetics dominates thermal auto-ignition in HCCI. Ignition begins in hot spots formed due to non-uniformities in temperature or concentration, and combustion propagates as a compression wave from the initial ignition points. Turbulence plays an indirect role in HCCI combustion by controlling heat transfer to the cylinder walls and determining the temperature distribution in the cylinder. This secondary influence of the fluid mechanics allows one to devote most of the computational effort on the chemical kinetics. The chemical kinetic nature of HCCI foretells a bright future for HCCI engine analysis. Detailed chemical kinetics enables accurate HCCI modeling that is not possible with SI or diesel modeling.

The promise of computationally efficient and accurate HCCI analysis is increasingly being fulfilled. This chapter has described fast ignition models that can successfully predict the start of combustion, enabling efficient model-based control systems. Operating limits for low and high power can also be well predicted with a variety of analytical methods described in this chapter. Multi-zone models efficiently analyze HCCI combustion and emissions. Fully integrated fluid mechanics and chemical kinetics models are too computationally intensive for today's computers, but may become the preferred choice in the future due to widespread availability of fast, massively parallel computers. Engine manufacturers can take advantage of these analytical tools, enabling extensive computer-based engine design with reduced reliance on empirical validation.

Partially stratified (PCCI) combustion remains a more difficult problem. It is often considered that PCCI combustion is controlled by chemical kinetics if the degree of stratification is relatively small. If combustion is controlled by chemical kinetics, it is possible to apply computationally efficient multi-zone models to predict combustion and emissions. Fully integrated models can be applied even beyond the chemistry controlled range, but they may require very high resolution if discontinuities (flame fronts) exist due to the stratified nature of the problem. Further research is required for determining ranges of operation that allow a chemical kinetic description of the model.

18.8 References

Aceves S M, Flowers D L, Westbrook CK, Smith J R, Pitz WJ, Dibble R, Christensen M and Johansson B (2000) 'A Multi-Zone Model for Prediction of HCCI Combustion and Emissions', SAE Paper 2000-01-0327.

Aceves S M, Flowers D L, Espinosa-Loza F, Martinez-Frias J, Dibble R W, Christensen M, Johansson B and Hessel R P (2002) 'Piston-Liner Crevice Geometry Effect on HCCI Combustion by Multi-Zone Analysis', SAE Paper 2002-01-2869.

Aceves S M, Flowers D L, Espinosa-Loza F, Martinez-Frias J, Dec J E, Sjöberg M,

Dibble R W and Hessel R P (2004) 'Spatial Analysis of Emissions Sources for HCCI Combustion at Low Loads Using a Multi-Zone Model', SAE Paper 2004-01-1910.

Aceves S M, Flowers D L, Chen J Y and Babajimopoulos A (2006) 'Fast Prediction of HCCI Combustion with an Artificial Neural Network Linked to a Fluid Mechanics Code', SAE Paper 2006-01-3298.

Agarwal A and Assanis D N (2000) 'Multi-Dimensional Modeling of Ignition, Combustion and Nitric Oxide Formation in Direct Injection Natural Gas Engines', SAE Paper 2000-01-1839.

Agrell F, Angstrom H E, Eriksson B and Wikander J (2003a) 'Transient Control of HCCI Through Combined Intake and Exhaust Valve Actuation', SAE Paper 2003-01-3172.

Agrell F, Eriksson B, Angstrom H E, Wikander J and Linderyd J (2003b) 'Integrated Simulation and Engine Test of Closed-Loop HCCI Control By Aid of Variable Valve Timings', SAE Paper 2003-01-0748.

Assanis, D N, Lavoie G A and Fiveland S B (2003) 'HCCI Modeling Approaches', in H Zhao, Ed. *Homogeneous Charge Compression Ignition (HCCI) Engines: Key Research and Development Issues,* SAE Special Publication PT-94.

Babajimopoulos A, Lavoie G A and Assanis D N (2003) 'Modeling HCCI Combustion With High Levels of Residual Gas Fraction – A Comparison of Two VVA Strategies', SAE Paper 2003-01-3220.

Benkenida A and Angelberger C (2004) 'Toward a Three-Dimensional CFD Model for HCCI Combustion in Diesel Engines', *Combustion Science and Technology*, 176, 667–683.

Bhave A N, Kraft M, Mauss F, Oakley A J and Zhao H (2005) 'Evaluating the EGR-AFR Operating Range of a HCCI Engine', SAE Paper 2005-01-0161.

Chen Y H and Chen J Y (2005) 'Development of Isooctane Skeletal Mechanisms for Fast and Accurate Predictions of SOC and Emissions of HCCI Engines based on LLNL Detailed Mechanism', Paper WSS/CI 05F-44, Proceedings of the Fall Meeting of the Western States Section of the Combustion Institute, Palo Alto, California.

Chevalier C, Louessard P, Müller UC and Warnatz J (1990a) 'A detailed low-temperature reaction mechanism of n-heptane auto-ignition', Proceedings of the 2nd International Symposium on Diagnostics and Modeling of Combustion in Reciprocating Engines, p 93. Japanese Society Mechanical Engineers, Tokyo.

Chevalier C, Warnatz J and Melenk H (1990b) 'Automatic generation of reaction mechanisms for description of oxidation of higher hydrocarbons', *Ber Bunsenges Phys Chem* 94, 1362.

Choi Y and Chen J Y (2005) 'Fast Prediction of Start of Combustion in HCCI with Combined Artificial Neural Networks and Ignition Delay Model', *Proceedings of the Combustion Institute*, 30, 2711–2718.

Curran H J, Pitz W J, Westbrook C K, Dagaut P, Boettner J C and Cathonnet M (1998) 'Wide range modeling study of dimethyl ether oxidation', *International Journal of Chemical Kinetics*, 30, 229–241.

Curran H J, Gaffuri P, Pitz W J and Westbrook C K (2002) 'Comprehensive modeling study of isooctane oxidation' *Combustion and Flame*, 129, 253.

Dec, J E and Sjöberg M (2003) 'A Parametric Study of HCCI Combustion – the Sources of Emissions at Low Loads and the Effects of GDI Fuel Injection', SAE Paper 2003-01-0752.

Embouazza M, Haworth D C and Darabiha N (2002) 'Implementation of Detailed Chemical Mechanisms into Multidimensional CFD Using in Situ Adaptive Tabulation: Application to HCCI Engines', SAE Paper 2002-01-2773.

Eng J A (2002) 'Characterization of Pressure Waves in HCCI Combustion', SAE Paper 2002-01-2859.

Eng, J A (2003) 'Kinetics of HCCI Combustion', in H Zhao, Ed. *Homogeneous Charge Compression Ignition (HCCI) Engines: Key Research and Development Issues*, SAE Special Publication PT-94.

Erlandsson O (2002) 'Early Swedish Hot-Bulb Engines – Efficiency and Performance Compared to Contemporary Gasoline and Diesel Engines', SAE Paper 2002-01-0115.

Flowers D L, Aceves S M, Martinez-Frias J, Hessel R P and Dibble R W (2003) 'Effects of Mixing on Hydrocarbon and Carbon Monoxide Emissions, Predictions for Iso-octane HCCI Engine Combustion Using a Multi-Zone Detailed Kinetics Solver', SAE Paper 2003-01-1821.

Flowers D L, Aceves S M and Babajimopoulos A (2006) 'Effect of Charge Non-uniformity on Heat Release and Emissions in PCCI Engine Combustion', SAE Paper 2006-01-1363.

Frenklach M, Wang H, Goldenberg M, Smith G P, Golden D M, Bowman C T, Hanson R K, Gardiner W C and Lissianski V (1995) 'GRI-Mech – An Optimized Detailed Chemical Reaction Mechanism for Methane Combustion', GRI Topical Report No. GRI-95/0058.

Hultqvist A, Christensen M, Johansson B, Richter M, Nygren J, Hult J and Alden M (2002) 'The HCCI Combustion Process in a Single Cycle-High-Speed Fuel Tracer LIF and Chemiluminescence Imaging, SAE Paper 2002-01-0424.

Kee R J Coltrin M E and Glarborg P (2003) *Chemically Reacting Flow: Theory and Practice*, John Wiley, New York.

Kong S C, Reitz R D, Christensen M and Johansson B (2003) 'Modeling the Effects of Geometry-Generated Turbulence on HCCI Engine Combustion', SAE Paper 2003-01-1088.

Koopmans L and Denbratt I (2002) 'A Four-stroke Camless Engine, Operated in Homogeneous Charge Compression Ignition Mode with Commercial Gasoline', SAE Paper 2001-01-3610.

Kusaka J, Tsuzuki K and Daisho Y (2002) 'A Numerical Study on Combustion and Exhaust Gas Emissions Characteristics of a Dual-Fuel Natural Gas Engine Using a Multi-Dimensional Model Combined With Detailed Kinetics', SAE Paper 2002-01-1750.

Livengood J C and Wu P C (1955) 'Correlation of Autoignition Phenomenon in Internal Combustion Engines and Rapid Compression Machines', *Proceedings of the Combustion Institute*, 5, 347–356.

Martinez-Frias J, Aceves S M, Flowers D, Smith J R and Dibble R (2001) 'Equivalence Ratio-EGR Control of HCCI Engine Operation and the Potential for Transition to Spark-Ignited Operation', SAE Paper 2001-01-3613.

Montgomery C J, Cremer M A, Chen J-Y, Westbrook C K and Maurice L Q (2002) 'Reduced chemical kinetic mechanisms for hydrocarbon fuels', *Journal of Propulsion and Power*, 18, 192–198.

Nakagome K and Niimura (1997) 'Combustion and Emission Characteristics of Premixed Lean Diesel Combustion Engine', SAE Paper 970898.

Noguchi M, Tanaka Y, Tanaka T and Takeuchi Y (1979) 'A Study on Gasoline Engine Combustion by Observation of Intermediate Reactive Products during Combustion', SAE Paper 790840.

Oakley A, Zhao H, Ma T and Ladommatos N (2001a) 'Experimental Studies on Controlled Auto-ignition (CAI) Combustion of Gasoline in a 4-Stroke Engine', SAE Paper 2001-01-1030.

Oakley A, Zhao H, Ma T and Ladommatos N (2001b) 'Dilution Effects on the Controlled Auto-Ignition (CAI) Combustion of Hydrocarbon and Alcohol Fuels' SAE Paper 2001-01-3606.

Onishi S, Jo S H, Shoda K, Jo P D and Kato S (1979) 'Active Thermo-Atmosphere Combustion (ATAC) – A New Combustion Process for Internal Combustion Engines' SAE Paper 790501.

Sankaran R and Im H G (2004) 'Effects of Mixture Inhomogeneity on the Auto-ignition of Reactants under HCCI Environment' AIAA Paper 2004-1328, Proceedings of the 42nd AIAA Aerospace Sciences Meeting and Exhibit, Reno, Nevada.

Schwer D A, Tolsma J E, Green W H and Barton P I (2002) 'On upgrading the numerics in combustion chemistry codes', *Combustion and Flame*, 128, 270–291.

Smith J R, Green R M, Westbrook C K and Pitz W J (1985) 'An Experimental and Modeling Study of Engine Knock', *Proceedings of the Combustion Institute*, 20, 91–100.

Turns S R (2000) *An Introduction to Combustion, Concepts and Applications*, McGraw-Hill, New York.

Warnatz J, Maas U and Dibble R W (2006) *Combustion*, 4th Edition, Springer-Verlag, Berlin.

Westbrook C K and Dryer F L (1981) 'Simplified Mechanisms for the Oxidation of Hydrocarbon Fuels in Flames', *Combustion Science and Technology*, 27, 31–43.

Westbrook C K (2000) 'Chemical kinetics of hydrocarbon ignition in practical combustion systems', *Proceedings of the Combustion Institute*, 28, 1563.

Westbrook C K, Pitz W J, Boercker J E, Curran H J, Griffiths J F, Mohamed C and Ribaucour M (2002) 'Detailed chemical kinetic reaction mechanisms for autoignition of isomers of heptane under rapid compression' *Proceedings of the Combustion Institute*, 29, 1311–1318.

Yang J, Culp T and Kenney T (2002) 'Development of a Gasoline Engine System Using HCCI Technology – The Concept and the Test Results' SAE Paper 2002-01-2832.

Yap D, Karlovsky J, Megaritis A, Wyszynski M L and Xu H (2005) 'An investigation into propane homogeneous charge compression ignition (HCCI) engine operation with residual gas trapping', *Fuel*, 84, 2372–2379.

Yelvington P E and Green W H (2003) 'Prediction of the Knock Limit and Viable Operating Range for a Homogeneous-Charge, Compression-Ignition (HCCI) Engine', SAE Paper 2003-01-1092.

Yoshizawa K, Teraji A, Miyakubo H, Yamaguchi K and Urushihara T (2003) 'Study of high load operation limit expansion for gasoline compression ignition engines' American Society of Mechanical Engineers, Internal Combustion Engine Division ICE, *Design, Application, Performance and Emissions of Modern Internal Combustion Engine Systems and Components*, 40, 3–17.

Zhang Y Z, Kung E H and Haworth D C (2004) 'A PDF Method for Multidimensional Modeling of HCCI Engine Combustion: Effects of Turbulence/Chemistry Interactions on Ignition Timing and Emissions', Proceedings of the International Multidimensional Engine Modeling Users' Group Meeting, Detroit, MI.

19

Overview of advanced optical techniques and their applications to HCCI/CAI engines

M RICHTER, Lund University, Sweden

19.1 Introduction

Various laser-based measurement techniques have been developed during the past decades and today many of them have become well-accepted tools for combustion diagnostics. Typical combustion-related properties that can be successfully probed by the use of laser diagnostics are, for example, temperature, velocity, droplet size, evaporation characteristics and species distribution/concentration.

Many of these properties can also be measured by means of physical probing with equipment, such as, for example, thermocouples and gas chromatographs. However, the optical techniques are superior in several respects compared to physical probing. They are non-intrusive, if wisely performed, which means that the measurement object is not affected by the actual act of measuring, in terms of chemical or physical properties. The remote probing capability of optical techniques can be utilized for *in situ* measurements in hostile environments such as a combustion chamber in an engine. Furthermore, laser techniques feature high spatial and temporal resolution. Typical pulse duration, i.e. probing time, for lasers commonly used in combustion research is around 10 ns. On this time scale, the flow and the chemical reactions studied can be considered frozen. Hence, it is possible to measure short-lived intermediate species such as radicals. Regarding the spatial resolution, for point measurements, laser beams can be focused to a spot with a diameter <70 μm. This will then be the width of the probe volume. The corresponding length will be determined by the signal collection apparatus, except for coherent techniques where the probe volume is the volume common to the intersecting laser beams.

Another major advantage is that laser diagnostics can be species specific. Every atom or molecule has a unique spectral pattern, which can be probed with a spectrally tuneable laser source. For molecules consisting of multiple atoms, this spectral pattern gets more complicated as the molecules grow.

Hence, true species-specific detection is, in most cases, only feasible for small molecules.

Not surprisingly there are also distinct drawbacks with these laser-based techniques. One of the most obvious is the requirement for optical access to the measurement region. In open flame environments this is perhaps easily achievable, but in internal combustion engines it is not as trivial. Another area in which the optical techniques are not favoured is the ease of operation and maintenance. Although turnkey systems for some applications, such as velocimetry and temperature measurements have appeared on the commercial market, most techniques are still quite complicated and require a skilful operator. As with most highly specialized equipment, lasers have to be considered as 'expensive'. However, there are certain areas where no other measurement technique can compete and where the costs can be justified.

Optical diagnostics is a huge research area and this chapter can only provide a very brief introduction to the field. A few examples of optical techniques applicable to HCCI/CAI engine research will be given, but please keep in mind that this is only a fraction of what is available. Two books (Eckbreth, 1996; Kohse-Höinghaus *et al.*, 2002) can be recommended to the reader who would like to gain more general knowledge on this subject. Then there is also an extensive amount of technical papers with more detailed content available.

19.2 Diagnostic approaches

Today there exists an extensive range of highly specialized equipment for applying optical measurements. This section aims to provide only a brief introduction to the most essential experimental apparatus, such as lasers, image intensified cameras, photomultiplier tub, as well as different approaches to provide optical access to engines.

19.2.1 Optical access

For any kind of optical measurement technique to be feasible, it is necessary to have some sort of optical access to the measurement region. In the field of combustion engines there are quite a few solutions to this. In general there is a trade-off between achieving engine-like conditions and providing a high level of access. Since glass is not a great construction material for engines, the task of putting windows in engines is far from trivial. The most widely used window material in this type of application is quartz or fused silica. Along with suitable mechanical properties, it is also transparent in the UV spectral region. The more expensive sapphire is also frequently used in optical engines. The benefits with sapphire are mainly very high wear resistance and transparency ranging from the UV to the infra-red region.

In principle it is possible to have multi-cylinder optical engines but due to the complexity involved most of them are based on single cylinder engines. On two-stroke engines it is often convenient to just put a window in the cylinder head. One straightforward strategy, applicable to four-stroke engines, is to replace one of the valves with a window (Espey and Dec, 1993). Another approach is to perform the measurements in a secondary chamber, similar to a pre-chamber in a diesel engine but larger. This usually results in good optical access, but also in conditions that are not exactly engine-like. Examples of this configuration can be found in Meier *et al*., (1996) and Martinez *et al*., (2003). The use of a square-piston provides a minor improvement to the latter issue while good optical access is maintained. An example from Daimler can be seen in Lawrenz *et al*. (1992). Other popular designs are briefly described below.

Optical spacer

A quite common approach to achieve optical access is to fit a steel spacer, equipped with windows, between the cylinder head and the engine block. See Fig. 19.1. The standard wet piston rings can be used, but the height of the piston needs to be increased to maintain the compression ratio. This modification will increase the crevice volume compared to the standard geometry. The number and size of windows can be altered depending on the application. By keeping the glass surface small, the deviation from the properties of the steel engine can be minimized. With this design it is possible to run higher load compared to when a full 360 degree quartz liner (see next section) is used.

Elongated piston

The use of an elongated piston was introduced by F. W. Bowditch in 1961 (Bowditch, 1961) and today this is probably the most common design for optical engines. Optical access to the combustion chamber is provided through a transparent piston via a 45 degree mirror placed in the hollow piston extension, see Fig. 19.2. For flat pistons it is convenient to fit a large window in the piston crown providing access to almost the entire combustion chamber. For more complex piston geometries, e.g. in diesel engines, even smaller windows cannot be fitted arbitrarily. Although it might be possible to fit a window at some location, there will be restrictions to the field of view. One solution to this is to use a piston crown that has been machined from a single piece of fused silica. The obvious benefit is that a high level of access can be achieved while the full geometry of the metal piston can be maintained. The drawback is the optical distortions, which can be severe, introduced by the curved surfaces. This might lead to certain areas

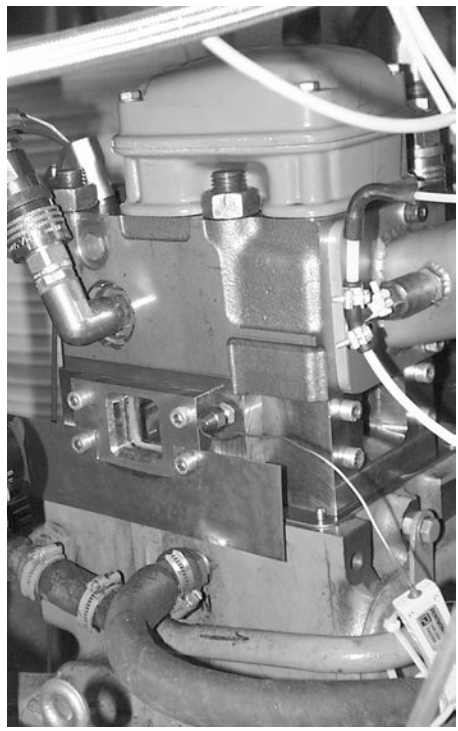

19.1 A Volvo TD100 truck engine modified for optical access. A spacer equipped with four square quartz windows is mounted between the engine block and the cylinder head. (Photo: M. Richter, Lund University).

being non-accessible even thought the entire piston is made of transparent material.

The optical access through the piston is most often used for signal detection. When applying techniques that also require light to be delivered to the combustion chamber, the elongated piston is often complemented with a transparent cylinder liner, see Fig. 19.2. The height of the liner is selected so that the desired amount of access is achieved. By using special dry piston rings an oil-free environment can be certified in the chamber. This is important since lubricants can introduce severe background signals. The dry piston rings can actually run in a full height transparent liner which makes it feasible to have optical access during the entire stroke. The major drawbacks with this setup, apart from having a large glass surface, are large crevice volumes and limited load capacity. The latter can be improved by using an optical spacer, as described earlier, in combination with the elongated piston.

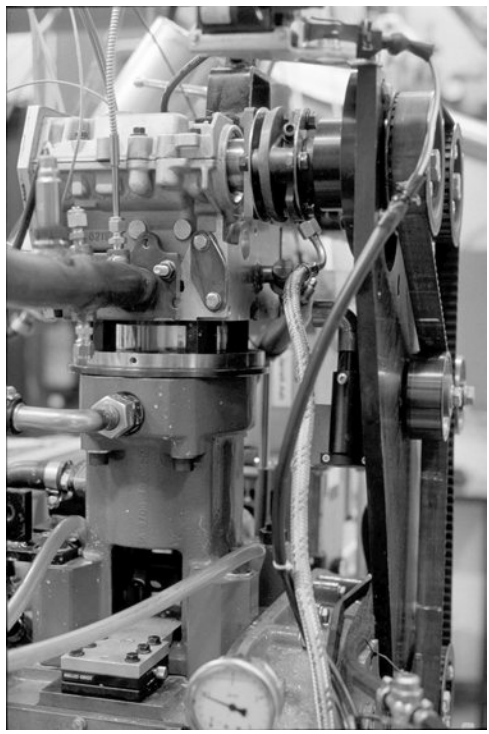

19.2 A Volvo car cylinder head fitted to an AVL single cylinder engine. The Boditch style elongated piston allows for optical access to the combustion chamber through the transparent piston. The upper part of the cylinder liner is replaced by a quartz ring for additional access. (Photo: M. Richter, Lund University).

Endoscopic detection system

An endoscope can be either flexible or rigid. A conventional endoscope is a flexible tube-shaped device that relays the image through an optical fibre bundle. The rigid type, which is most commonly found in engine applications, is referred to as a boroscope. Basically a boroscope consists of a collection lens assembly, a few rod-lenses and an ocular. In general, a wide-angle collection lens is mounted at the tip of a metal tube. The collected light is then relayed, through the tube, via the rod-lenses to the ocular. The image can be viewed through the ocular, either with a naked eye or with a camera device. As an additional feature, boroscopes can be equipped with a fibre optic light guide for illumination of the imaged object. This will, of course, increase the diameter of the tube or result in smaller lenses and thereby a decreased transmission of light from the object. Other options are internal cooling by water or by compressed air. The obvious advantage with the use of boroscopes is the reduced dimensions of the optics. This can be utilized

to insert endoscopes in squeezed areas where conventional optics simply don't fit. The small size also makes it possible to leave most of the original materials and geometry of the investigated engine unaltered. Hence, the optical measurements can be performed under more realistic conditions. Today endoscopes are primarily used for video recordings, but detection of laser induced fluorescence signals is also feasible as demonstrated in Richter *et al.* (1998, 1999). Unfortunately boroscopes with quartz optics are not readily available, which makes detection in the UV unfeasible. Lately a few examples of tailor made UV-boroscopes have been shown but they are still quite costly. In the future the development will most probably go towards optical access with minimal intrusion and the use of boroscopes will definitely increase.

19.2.2 Signal collection and light sources

Measurement techniques in general and optical diagnostics in particular require systems for signal collection and detection. Most of the applications described in this chapter are focused on two- and three-dimensional visualization, but there are also examples of spectrally resolved measurements.

For point measurements a photomultiplier tube (PMT) can be used for achieving an extremely high sensitivity and fast response. For 2D-imaging a charge coupled device (CCD) chip is often used. The chip is placed in the image plane of a digital camera. The photosensitive surface of the CCD chip is divided into small sub-areas referred to as pixels. When imaging weak or short-lived signals, a multi channel plate (MCP), serving as an image intensifier, can be attached in front of the CCD-chip. In an image intensifier the incoming photons are first converted to electrons by a photocathode. Amplification is then achieved by sending the electrons through the MCP, which acts as a high-voltage electron multiplier. The gain level is governed by controlling the applied voltage. Thereafter, the electrons are back converted to photons by letting them impinge on a phosphor screen. These photons can then be detected by the CCD-chip in a conventional manner. The MCP is also used as an electronic shutter, by rapid switching of the high-voltage, when high temporal resolution is desired. Exposure times down to about 1 ns are then achievable. These short exposure times are highly useful for detecting, for example, short lived laser induced fluorescence while discriminating against background light originating from a luminous flame.

When performing high-speed laser diagnostics (see later in this chapter) a framing camera can be used for signal collection in combination with a high repetition rate laser system. Different designs are available but in general an extremely high frame rate is achieved by sequential exposure of several individual CCD-detectors mounted in a cluster.

For all techniques that requires excitation or utilize the absorption of

light, it is necessary to have some sort of light source. This chapter will be focused on laser-based techniques but under certain conditions it is also possible to use various lamps, especially when broadband low intensity radiation is required.

In general a laser consists of an active medium enclosed in a reflective cavity. In short, the laser medium is excited in a process referred to as pumping. When the atoms in the medium relax, photons are emitted. These photons induce stimulated emission, which results in a strong amplification in the cavity. Some of the photons are out-coupled to form a laser beam. A more detailed description of lasers and their working principles can be fond in Silfvast, (1996) and Siegman, (1986). Laser types that are often used for engine diagnostics are, e.g. Nd:YAG-, Excimer- and dye-lasers. The first two are examples of high power, fixed wavelength lasers, while the dye-lasers produce tuneable radiation suitable for species specific excitation. When it is crucial to capture single-cycle events, such as in HCCI combustion research, a cluster of lasers can be fired in sequence to obtain a rapid burst of pulses.

19.3 Spectroscopic environment

The HCCI/CAI combustion process is very different from SI and diesel combustion. In order to select the most feasible measurement technique, it is necessary to know how the spectral properties vary during the cycle. This is highly dependent on the fuel and on the pressure and temperature history. Therefore these investigations need to be performed for each specific running condition.

19.3.1 Absorption measurements

Spectrally resolved absorption measurement is a useful tool for characterizing the spectral environment of the investigated apparatus. Absorption, or transmission, measurement is a line-of-sight technique. Usually light from a broadband source is collimated and guided through the measurement region. The transmitted light is thereafter focused onto the slit of a spectrometer. By making recordings of the transmission with and without the light absorbing medium, the absorption can be calculated. When performing absorption measurements in rapidly changing environments such as engines, it is necessary to have a detector with high temporal resolution, e.g. an intensified CCD-detector.

Deuterium and xenon lamps are frequently used as broadband light sources. Together they cover the wavelength region between 200 and 360 nm.

An example can be seen in Figs 19.3–19.6. where the spectrally and crank angle resolved absorption of light passing through the combustion chamber

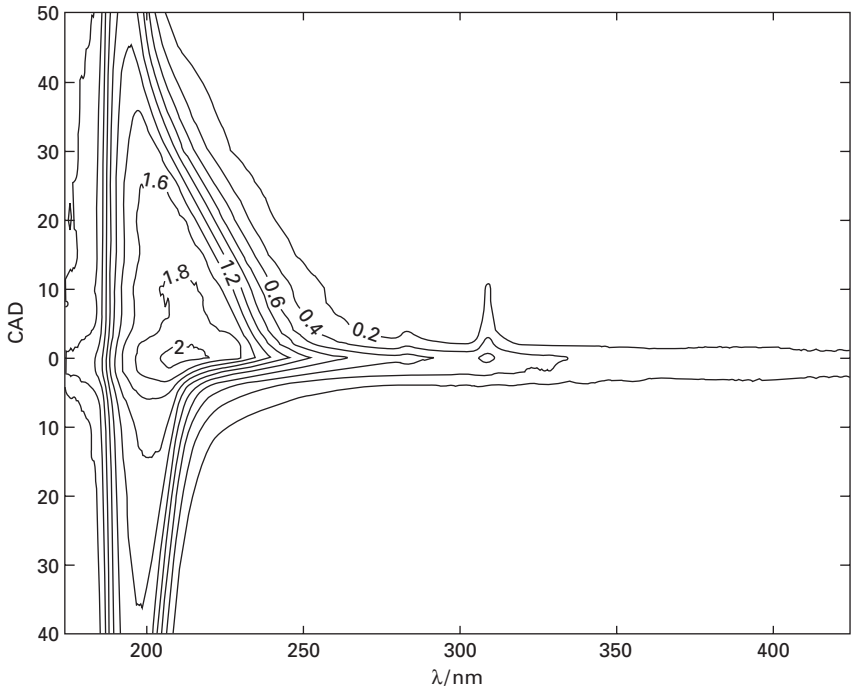

19.3 Spectrally resolved data showing the absorption of light through the combustion chamber during compression and combustion in a port-injected HCCI engine running on methanol (Dept. of Physics, Lund University).

of an HCCI engine running on four different fuels, ethanol, methanol, iso-octane and a mixture of iso-octane and n-heptane was investigated. The absorbance is plotted as iso-curves and the number that can be found on the curves corresponds to the absorbance given by

$$-\log_{10}\left(\frac{I_T}{I_0}\right) \qquad 19.1$$

It should be noted how the occurrence of cool flame reactions has a dramatic influence on the absorption profile prior to auto-ignition. More information on this topic can be found in Knapp *et al*., (1996) and Richter *et al*. (1999b).

19.4 Chemiluminescence imaging

Quite a lot of information can be retrieved by analyzing the natural flame emission. Chemiluminescence arises from electronic states that are excited during chemical reactions. Spectrally the luminosity contains a mix of lines from atoms and broader bands from molecules. Each emitting species has a

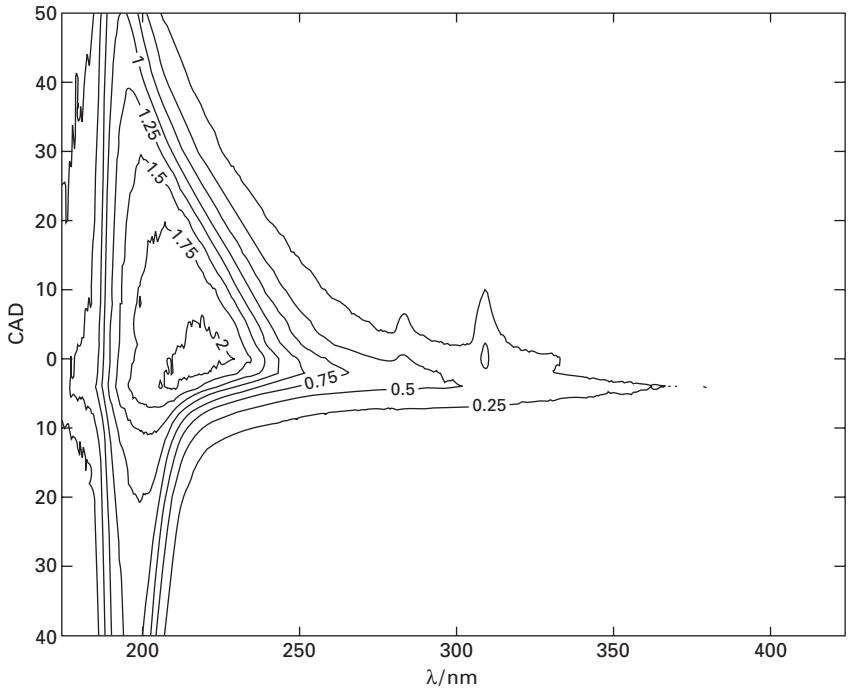

19.4 Spectrally resolved data showing the absorption of light through the combustion chamber during compression and combustion in a port-injected HCCI engine running on ethanol. The absorption characteristics are very similar to those found for methanol. (Dept. of Physics, Lund University).

specific spectral profile. In premixed, non-sooting flames these emissions are the dominant source of luminosity (Eckbreth, 1996). Species with strong characteristic emissions are, for example, CH at 430 nm, OH at 308 nm and C_2 at 516 nm. If the spectral profiles of the emitting species don't severely overlap, spectral filtering of the collected signal can be used for species specific detection. Dec and Espey (1998) presented a study of the auto-ignition phenomena in a diesel engine. Results from spectrally resolved detection of chemiluminescence indicated that the main contributors to the chemiluminescence signal were formaldehyde (CH_2O) and CH. This was also found to be in good agreement with known spectra from 'cool flames'. An example of spectrally resolved chemiluminescence detection showing the cool flame emission in an HCCI engine can be seen in Fig. 19.7.

Two-dimensional recording of this natural emission of light is referred to as chemiluminescence imaging. The most common application of chemiluminescence imaging is probably broadband detection, e.g. for high-speed video recordings. Although being a line of sight technique this approach

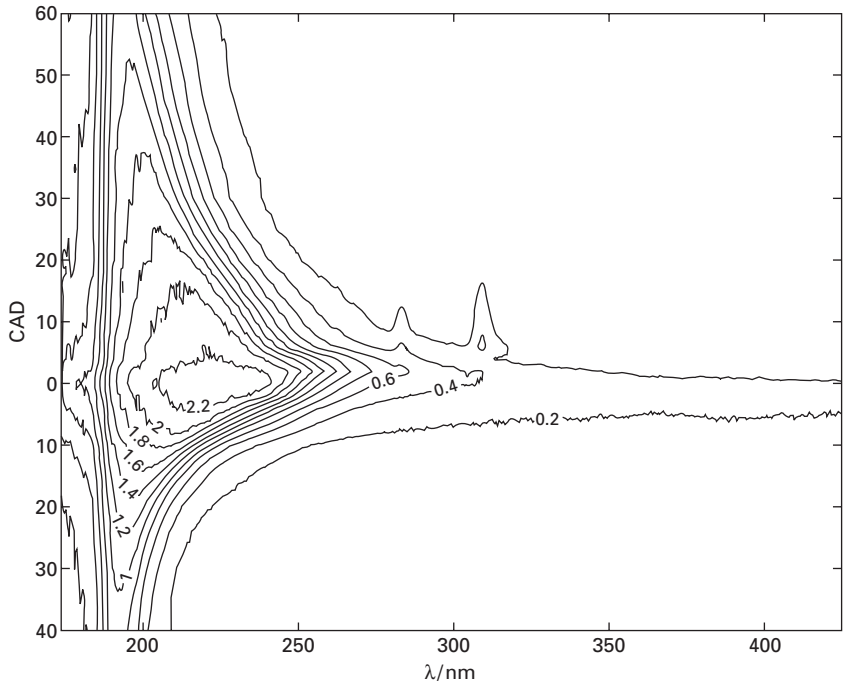

19.5 Spectrally resolved data showing the absorption of light through the combustion chamber during compression and combustion in a port-injected HCCI engine running on iso-octane. Note a slightly stronger absorption during the compression stroke, compared to what was found for the alcohols. (Dept. of Physics, Lund University).

allows for time-resolved studies of combustion development which can be highly useful. It has also been shown that the integrated intensity of the chemiluminescence correlates very well with the rate of heat release in HCCI engines (Hultqvist *et al.*, 1999).

19.5 Laser induced fluorescence

Laser-induced fluorescence (LIF) is the emission of light resulting from relaxation in a molecule that has been excited to higher energy levels by absorption of laser radiation. For molecules that can be excited, LIF provides species-specific excitation. The main advantage of fluorescence measurements is the high sensitivity achievable.

Thanks to high signal intensity, LIF can be used for two-dimensional imaging by forming the laser beam into a thin sheet and then passing it through the measurement volume. This technique is usually referred to as Planar Laser Induced Fluorescence (PLIF). By placing a camera device at

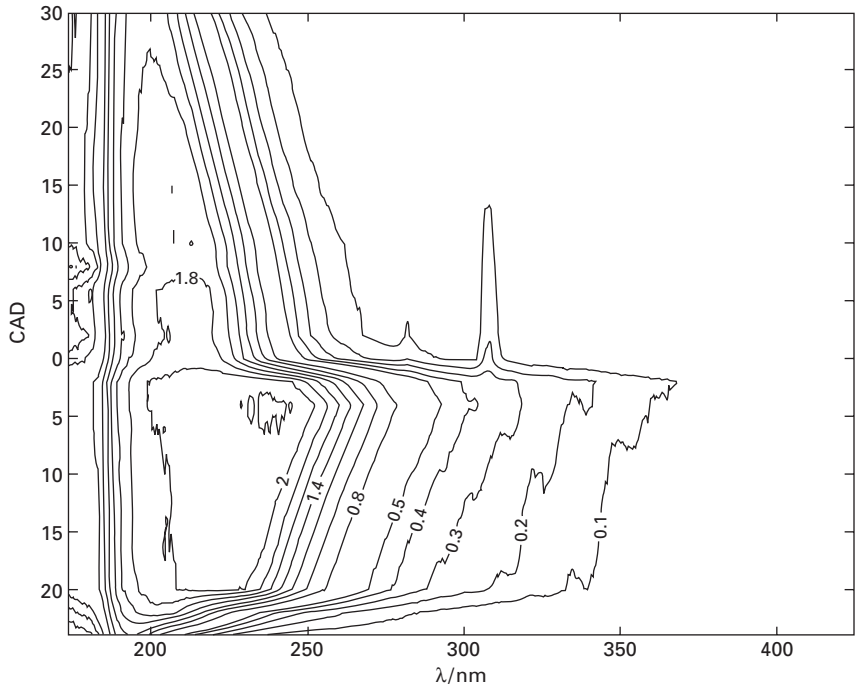

19.6 Spectrally resolved data showing the absorption of light through the combustion chamber during compression and combustion in a port-injected HCCI engine running on a mixture of 50% iso-octane and 50% n-hepthane. Note the strong absorption introduced by intermediates formed in the cool-flame reactions (Dept. of Physics, Lund University).

right angles to the sheet, a two-dimensional image can be obtained. The collected signal is related to the distribution of the probed species. The image recorded is not integrated across the entire volume but results only from fluorescence in the thin light sheet. In combination with a short laser pulse duration this results in high spatial and temporal resolution. In principle it is possible to obtain quantitative concentration data from PLIF measurements, but in practice this is usually very hard, since the generated signal varies with pressure, temperature and composition of surrounding species. However, the qualitative time-resolved information on species distributions revealed by PLIF imaging can provide a good understanding of the investigated process.

19.5.1 Fuel distribution

Mixture preparation is of major importance in all types of combustion engines. Especially in direct injected engines, both Otto and Diesel, mixture preparation

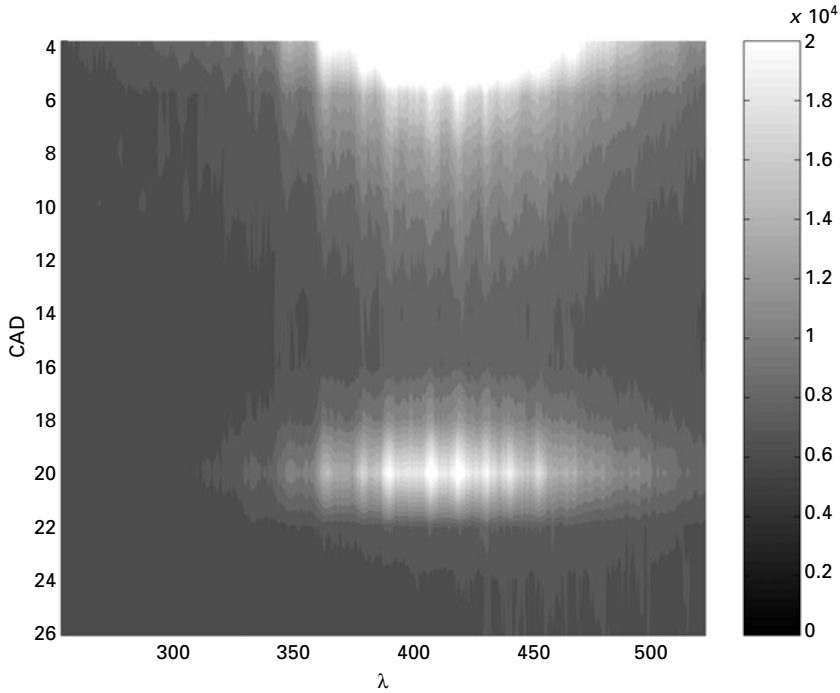

19.7 Temporally and spectrally resolved detection of chemiluminescence from the cool-flame in an HCCI engine running on a mixture of iso-octane and n-hepthane. The detected wavelength peaks correspond to the spectra known from aldehydes. (Dept. of Physics, Lund University).

has a greater impact on engine performance. In engine concepts featuring stratified charge there is a self-evident demand for having good control of the charge motion and timing.

During the last two decades Planar Laser Induced Fluorescence (PLIF) techniques for measurement of fuel distributions have undergone continuous development. Today PLIF is no longer limited to academic use, but is considered a valuable tool and is used on a regular basis by many of the leading engine manufacturers.

Two different strategies can be identified. The most straightforward method is to use a commercial fuel such as diesel or gasoline. These multi-component fuels show strong LIF signals when excited with UV laser light. Examples of this technique can be found in Fansler *et al*. (1995) and Arnold *et al*. (2000). The advantage with this approach, except the ease of use, is that the studied combustion device is operated with a fully realistic fuel. However, there are also several drawbacks associated with LIF from commercial fuels. The species contributing to the fluorescence signal are not known. In a work by Fansler *et al*., (1995) polycyclic aromatics, benzenes, aldehydes and ketones

are pointed out as likely candidates. As a consequence of this uncertainty, the dependence of pressure, temperature and surrounding species are also unknown. Furthermore, the fluorescent species in gasoline represent fractions with different boiling points, which makes it hard to interpret what is actually measured. In a study by Le Coz *et al.*, (1994) naphthalene is stated as the dominating contributor to the LIF signal. Since naphthalene has a boiling point located at 217°C it does not make a good representation of the 50%-evaporated point of standard gasoline which is around 100°C.

The most common strategy to avoid these types of problems is to use a non-fluorescent, single-component model-fuel and then add a fluorescent tracer.

Fuel tracers

When using tracers it is, by definition, not the fuel itself but the tracer species that is being monitored. Therefore, great care must be taken when selecting the tracer. Both optical and physical properties of the tracer must be matched to the specific experiment. The most crucial parameters that should be taken into consideration can be summarized as:

- The tracer species must generate a strong fluorescence when excited with radiation from commercially available pulsed laser systems.
- The fluorescence signal must be sufficiently red-shifted with respect to the excitation wavelength to allow for spectral filtering in order to suppress scattered light. Well-separated emission and excitation regions also minimize fluorescence trapping, i.e. when an emitted fluorescence photon is being reabsorbed by the medium before reaching the detector.
- The mixture of tracer, fuel and oxidizing medium must show a moderate absorption of the excitation radiation so that it can be considered optically thin over characteristic distances, e.g. the size of the investigated combustion chamber.
- Since it is the tracer distribution that is being visualized, it is of major importance that the tracer actually follows the fuel during injection and evaporation. Hence, boiling points and diffusion rates for fuel and tracer should be in the same range. For port-injection engines running homogeneous charge this requirement is less critical.
- Ideally the fluorescence signal should be insensitive to collisional quenching. In other words, the fluorescence should be independent of temperature and pressure as well as ambient gas composition.
- If measurements are to be performed after the onset of combustion, it is important that the tracer and the fuel are consumed in a similar manner. The tracer must be chemically stable under high pressure and high temperature conditions. Especially when CI-engines are studied it is important that the tracer does not suffer from low temperature pyrolysis.

- Even when the mixture formation is investigated only prior to ignition, it is important that the tracer is consumed during combustion in order to prevent tracer buildup.

As indicated above, the choice of suitable tracer species is highly dependent on the specific experimental conditions. The aim of the investigation along with the chosen fuel and type of engine result in different requirements on the tracer. Consequently a huge number of fuel/tracer combinations have been proposed by different research groups. Ketones and aldehydes are dominating among the proposed tracers. It is the carbonyl group, i.e. a carbon and an oxygen atom connected with a double bond (C=O), that is responsible for the favourable fluorescence properties. It is beyond the scope of this section to review the field of fuel tracers, and only a short summary of promising substances can be given. For more extensive information on fuel tracers, see Schulz and Sick (2005).

Beside the ketones and aldehydes aromatic substances have also been proposed as fuel tracers. For example, toluene and xylene have been used together with acetone and 3-pentanone to mark different fuel volatility classes. Toluene and xylene have boiling points at 110°C and 138°C respectively. The fluorescence from these aromatics is spectrally separated from the fluorescence from acetone and 3-pentanone. Hence, it is possible to perform simultaneous visualization of different volatility classes.

Acetone and 3-pentanone

The use of 3-pentanone as a fluorescent marker of iso-octane was first presented by Neij *et al*. (1992a). Today acetone and 3-pentanone are commonly used as fuel tracers in engine experiments. Both have been studied thoroughly by several researchers. Important properties that have been investigated are, for example, the influence of pressure and temperature on the fluorescence signal, absorption and emission characteristics, influences from different excitation wavelengths, etc. The chemical formulas of acetone and 3-pentanone are ($[CH_3]_2CO$) and ($[CH_3CH_2]_2CO$) respectively. They are both ketones with one carbonyl group. Since it is this carbonyl group that is responsible for the fluorescence characteristics, the spectral profiles for absorption and emission are very similar for these two species. The fluorescence emission spectrum for acetone excited at 266 nm can be seen in Fig. 19.8.

Both species have very short lifetimes (<2ns) as reported by Ossler and Aldén (1997). This will minimize the influence from collisional quenching. In a work by Grossmann *et al*. (1996) the fluorescence intensity from both acetone and 3-pentanone in air environment, is shown to increase slightly with pressure, at low pressures, i.e. up to a few bar. At higher pressures, relevant to engine conditions, the influence from pressure decreases.

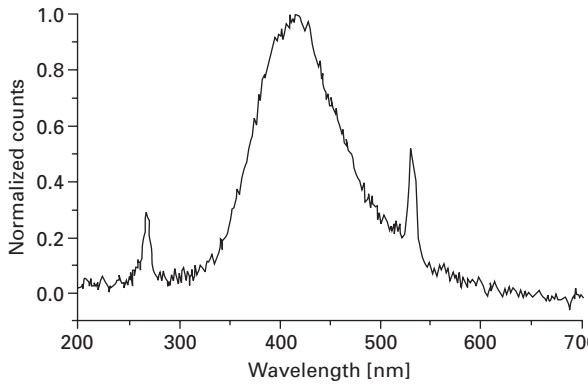

19.8 The fluorescence spectrum from acetone when excited by 266 nm UV radiation from a YAG-laser. Note the broadband characteristics of the emission ranging from 350 nm to about 550 nm, with a peak close to 420 nm. The peaks at 266 nm and 532 nm correspond to residuals from the light source (Dept. of Physics, Lund University).

Experiments performed on acetone by Yuen *et al*. (1997) and Thurber and Hanson (1999) revealed similar trends. The latter duo also showed that the fluorescence signal is linear with laser energy when excited at 248, 266 and 308 nm.

An extensive investigation of the temperature dependence of fluorescence from acetone, excited at several wavelengths, can be found in Thurber *et al*. (1998). They indicate that the influence from temperature is minimized for experiments below 800 K if excitation near 289 nm is used. The absorption profile is slightly red-shifted at elevated temperatures (Grossmann *et al*., 1996). This fact has been utilized for performing temperature measurements. Einecke *et al*. (1998, 2000) have performed two-dimensional temperature measurements in engines using two-line fluorescence from 3-pentanone dissolved in iso-octane. In the latter report they also suggest excitation close to the absorption peak, i.e. 276–280 nm, to minimize the temperature dependence in measurements of A/F-ratio.

Fujikawa *et al*. (1997) investigated the temperature and pressure dependence for acetone, 3-pentanone, toluene, and three other tracer species, excited at 248 nm and 266 nm. They concluded that the optimum combination, for experiments in fired engines, was acetone excited at 266 nm.

Fuel PLIF in HCCI-engines

As indicated in Fig. 19.6, the UV absorption, when running on fuels with cool-flame behaviour, increases dramatically from the start of the cool-flame

reactions. To be able to perform PLIF imaging after the onset of these low temperature reactions, the excitation wavelength must be long enough to avoid the absorption introduced by the generated intermediate species. From the absorption measurements it can be concluded that the recommendation by Thurber *et al.* (1998) to use 289 nm, to minimize the temperature dependence, could be a reasonable choice. This wavelength is also close to the absorption peak of 3-pentanon and acetone. Hence, an efficient utilization of the excitation light could be expected.

In a brief comparison performed by the author it was noted that acetone showed a higher signal intensity compared to 3-pentanone, late in the compression stroke and after the onset of combustion in an HCCI engine. This result is in consistence with Fujikawa *et al.* (1997) who reported a decreased fluorescence signal for 3-pentanone at the end of the compression stroke in a motored SI-engine. In the same investigation, acetone was reported not to show this signal decrease. In addition, the auto-ignition characteristics of HCCI combustion makes it extra important to have a stable tracer species if diagnostics are to be performed after the cool-chemistry has started. Yip *et al.* (1994) reported that there was no significant pyrolysis of acetone below 1000 K.

19.5.2 OH distribution

The OH-radical is one of the most important chemical intermediates formed during combustion. In general OH marks regions where combustion has occurred and are formed in high concentrations in a propagating flame front. There is a strong coupling between the maximum temperature and maximum OH concentration in flames (Norton *et al.*, 1993). The concept of using OH visualization for flame studies in engine environments is well proven.

It is common to excite the $Q_1(8)$ transition near 283 nm in the $v'' = 0$, $v' = 1$ band of the $A^2\Sigma \leftarrow X^2\Pi$ system. This is a fairly strong line with little temperature dependence of the population (less than 5% over the range 1400 to 2100 K (Puri *et al.* 1992). Detection of the resulting fluorescence is usually around 308 nm. To isolate this OH emission from background fluorescence and scattered laser light different filtering strategies can be applied. It should be noted that, if a dye-laser is used, scattered light appears both at 283 nm and around 566 nm (residual light from the dye-laser). A straightforward approach is to use a narrowband interference filter with the transmission wavelength centred on 308 nm.

Although there is no flame front in HCCI combustion the OH-radicals can be used as a marker of burnt areas. Although this type of imaging obviously can be done in other engine types, it is not easy to achieve an acceptable signal to noise ratio in HCCI engines. Due to the very low peak temperature, characteristic to the highly diluted HCCI combustion, the amount

of generated OH-radicals is small compared to what is known from diesel or SI-engines.

For this to be feasible it is crucial to have a powerful excitation source. A possible way to further increase the LIF intensity could be to excite another transition with a higher population at typical HCCI temperatures, i.e. around 1500 K. Excitation and detection at 308 nm would certainly improve the LIF signal, but then the scattered laser radiation could not be filtered out.

19.5.3 Formaldehyde distribution

The formaldehyde molecule is formed as an intermediate species when combusting hydrocarbons. The formation occurs through low temperature oxidation in an early phase of the combustion process. Formaldehyde is then being consumed later in the combustion process. Formaldehyde is also associated with the low temperature reactions (LTR) that occur in cool-flames. Spectrally resolved chemiluminescence recordings performed during the LTR-phase of HCCI combustion have shown that aldehydes are being formed. Modelling of the chemical kinetics gives that formaldehyde is the major constituent. Hence, formaldehyde is an indicator of the first stage of combustion and a marker for zones with low temperature reactions. PLIF from formaldehyde has been used for characterization of the controlled auto-ignition (CAI) combustion concept (Graf *et al*., 2001).

Since formaldehyde is formed as an intermediate species in the low temperature combustion it can also, under certain conditions, be used as a marker of areas where fuel has been present. The strong temperature dependence of the formaldehyde LIF signal allows no quantification without further information about local temperature. However, if imaged after the onset of LTR, the spatial distribution of the formaldehyde can be assumed to reflect the fuel distribution before the onset of main combustion. This approach has been used to investigate the degree of mixing for different injection timings, see Fig. 19.9. As can be seen, for early injection timing there is enough time to create a smooth formaldehyde distribution covering the entire imaged area. For late injection the time available before ignition is too short for this, resulting in a highly stratified formaldehyde distribution covering only part of the corresponding area. If the surface fraction containing formaldehyde is plotted versus NOx emission, the correlation between mixture homogeneity and the transition from low temperature/low NOx HCCI combustion to more diesel-like combustion is evident. See Fig. 19.10.

The formaldehyde molecule has several absorption bands suitable for laser excitation in the wavelength range from 270 to 360 nm. The third harmonic from an Nd:YAG laser can been used. Although this transition is not among the strongest, the approach is feasible since radiation at 355 nm is easily available at high energy levels. The resulting broadband fluorescence

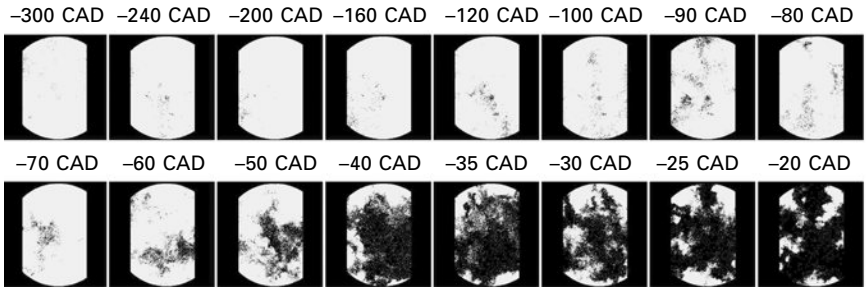

19.9 Two-dimensional LIF images of formaldehyde distributions acquired after the cool-flame reactions but before the onset of the main combustion for different injection timings. The light grey fields indicate the distributions of formaldehyde and the number above each image indicates the start of injection in crank angles degrees BTDC for that frame (Dept. of Physics, Lund University).

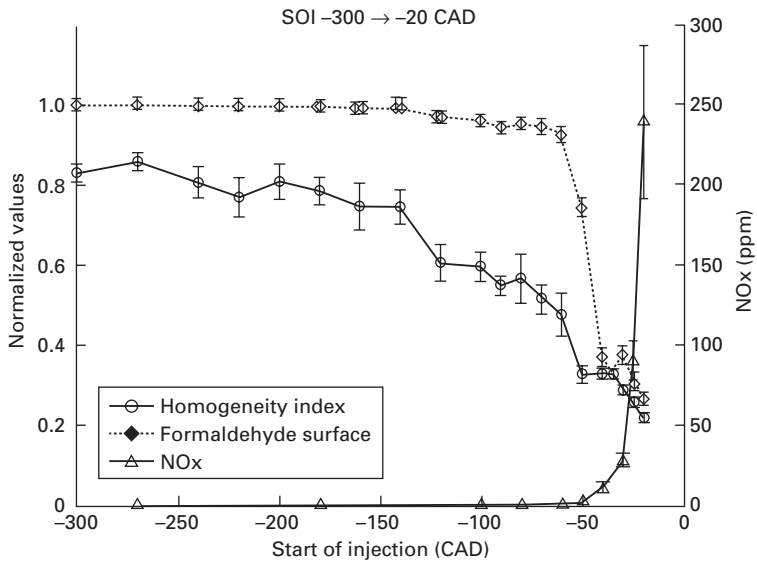

19.10 The NOx emissions and surface fractions covered with formaldehyde from the measurements in Fig. 19.9, are plotted versus the crank angle degree for start of injection. Note the strong coupling between the heterogeneity of the formaldehyde distribution and the NOx emissions (Dept. of Physics, Lund University).

ranges from 350–500 nm with the peak centred around 420 nm. More information about the use of the third harmonic of an Nd:YAG laser for performing formaldehyde LIF can be found in Brackmann *et al*. (2003) and Metz *et al.* (2004). As mentioned earlier, in HCCI combustion, a number of other aldehydes and ketones are also formed during the LTR reactions, but

in much lower concentrations than formaldehyde. These other intermediates, that might make a minor contribution to the collected signal when using 355 nm excitation, are, however, formed and consumed at the same time and location as formaldehyde. Therefore, possible interference from these molecules would not cause any effect on the measurement results when visualizing the spatial distribution.

19.5.4 Simultaneous measurements

If the spectral properties allow, PLIF visualization of more than one species can be performed simultaneously. A feasible example that is useful for HCCI/CAI diagnostics is simultaneous visualization of formaldehyde and OH. As indicated earlier, formaldehyde can be used as a marker of regions with low temperature reactions and OH as a marker of regions with a high rate of heat release (high temperature reactions). Given that a fuel featuring LTR is used, the formaldehyde PLIF will reflect the spatial distribution of the early LTR. In the time span after the end of LTR but before the beginning of formaldehyde consumption, the formaldehyde distribution is assumed to indicate the distribution of fuel. At the onset of the main heat release, the formaldehyde will be consumed in the hot areas where OH is formed. A typical result can be seen in Fig. 19.11. The simultaneous visualization of these two species is very useful when studying how the LTR and main combustion is affected by changes in engine operating conditions. More information can be found in Collin *et al*. (2003, 2004) and Hildingsson *et al*. (2005a).

Other examples of simultaneous probing of multiple species are found in Hildingsson *et al*. (2005b) and Särner *et al*. (2005b) where formaldehyde and fuel distributions are imaged simultaneously in a diesel engine and in a

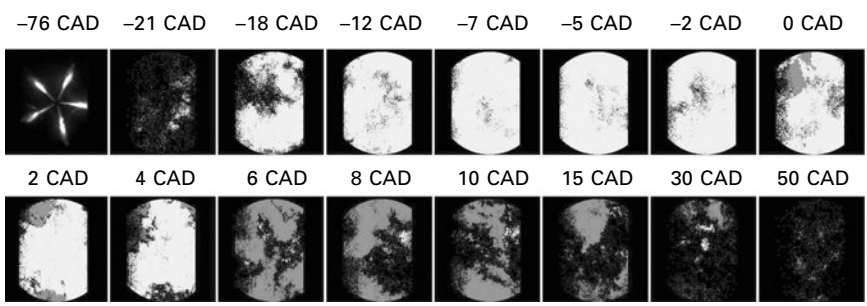

19.11 Simultaneous two-dimensional LIF imaging of formaldehyde and OH. The numbers above each frame indicate the crank angle for which that frame was recorded. The signal seen in the first frame, recorded at 76 BTDC, represent Mie scattering from the spray during injection. Formaldehyde distribution is shown in light grey and OH distribution in dark grey (Dept. of Physics, Lund University).

HCCI engine respectively. The purpose of these studies was to verify the assumption, mentioned earlier, that the presence of formaldehyde can be used as a marker of fuel under certain conditions. An example from HCCI combustion is shown in Fig. 19.12. Initially there are LIF signals from the fuel tracer only. Then during the LTR formaldehyde is being formed as can be seen at 17 CAD BTDC. After the LTR but before the onset of main heat release formaldehyde and fuel show similar spatial distributions as expected. More remarkably, also during the main combustion phase the two species show quite similar distributions. Hence, after the LTR, for fuels with LTR characteristics, is feasible to use the intermediate species formaldehyde as a naturally occurring marker of fuel.

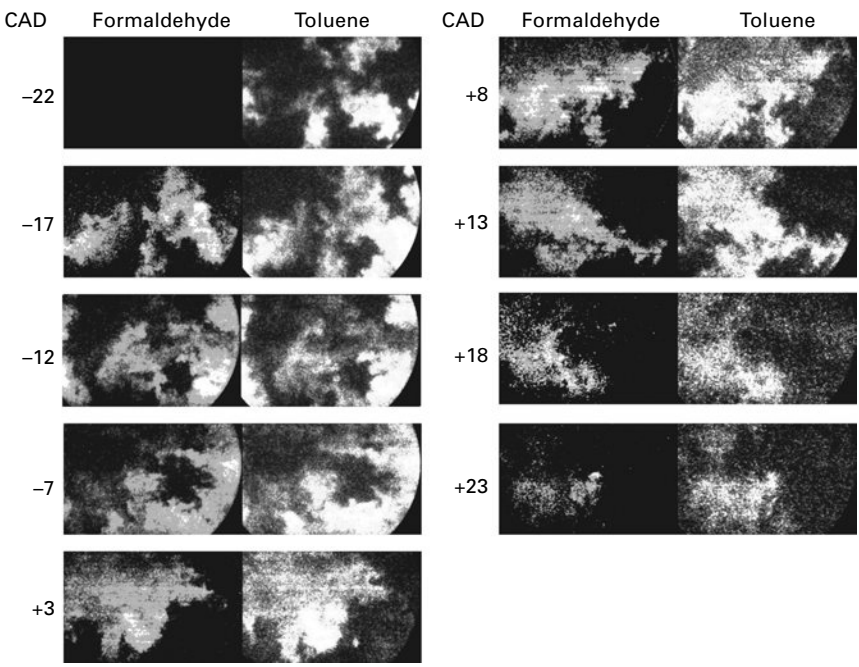

19.12 Simultaneous two-dimensional LIF imaging of formaldehyde and fuel tracer (toluene). Before the onset of low temperature reactions (LTR) only LIF signals from toluene are present. Around 20 CAD BTDC the LTR occurs resulting in formation of intermediate species such as formaldehyde. During this formation phase the distribution of formaldehyde does not necessarily represent the distribution of unburnt fuel. However, at the stage after the completion of LTR the distributions of formaldehyde and fuel tracer show remarkably similar structure. Hence, under these conditions the formaldehyde can be used as a marker of unburnt fuel (Dept. of Physics, Lund University).

19.5.5 High-speed diagnostics

Most laser sources have a repetition rate that limits the number of measurements to one per engine cycle. To follow, for example spray or flame propagation, data from many cycles must be used when a statistical material is captured at different crank angles. If only averaged information on spray penetration or flame behaviour is of interest, the limitation of one image per cycle can be accepted. However, if the stability of the process is low, the assembled average technique suffers significantly. High repetition rate laser diagnostics allow for cycle-resolved engine measurements where single combustion events can be followed in time. Cycle-to-cycle variations of complex events can be studied, which is impossible when single shot images are captured in different cycles. Time scales of such phenomena can be estimated from the time-resolved data. An example where true cycle-resolved imaging can provide unique information is in HCCI/CAI engines, which are known to have a high rate of heat release and large spatial variations of the combustion process.

High-speed fuel visualization in HCCI engines

From single-shot experiments it is known that the HCCI/CAI combustion features a heterogeneous structure. Since the spatial pattern of the combustion varies from cycle to cycle, it would not be meaningful to use the conventional technique where one image per cycle is recorded. In order to follow the evolution of the combustion event in time it is more or less necessary to utilize a high-speed laser/camera system.

When working with a pulse burst system, such as the multi-YAG, it is no longer trivial to use wavelengths around 289 nm, to avoid absorption, as suggested earlier. It is of course no problem to generate this wavelength with dye-laser but in practice the pulse energy would decrease at high repetition rates. Instead 266 nm is the more favoured alternative. To minimize the absorption it is desired to reduce the appearance of cool flame chemistry. From the absorption measurements shown earlier it was concluded that the alcohol fuels showed virtually no cool flames. For this reason high-speed imaging in the HCCI engine, such as the series presented in Fig. 19.13, were performed with either pure iso-octane or pure ethanol as fuel and acetone as fluorescent tracer. The results show the multiple ignition sites and how combustion progresses through distributed reactions. As can be seen, the spatial variations in the combustion process can vary significantly from cycle to cycle. This is the case even if there are only minor deviations in terms of IMEP. Without the use of optical diagnostics such characteristics would not be detected. More details from these experiments are presented in Hult *et al.* (2002) and Hultqvist *et al.* (2002). In order to verify the applicability of using acetone as a tracer for ethanol, quasi-simultaneous detection of

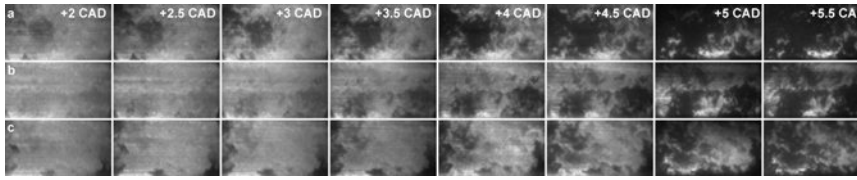

19.13 Example of high-speed fuel tracer LIF imaging. The three series are single-cycle resolved; hence each series shows the combustion process during one engine cycle. As can be seen, the combustion occurs through distributed reactions. Note the large spatial variations of the combustion process in the three cycles (Dept. of Physics, Lund University).

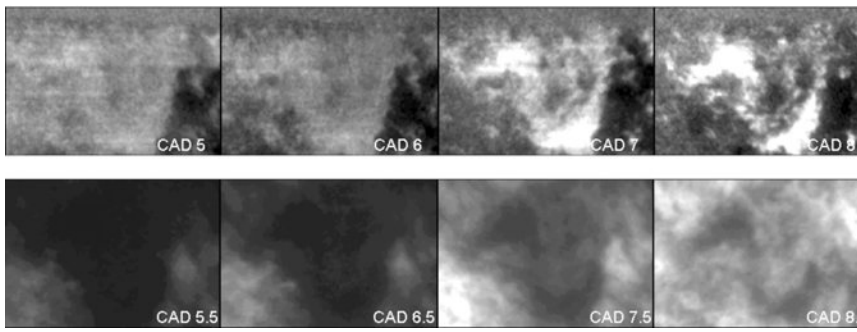

19.14 The upper row shows high-speed fuel tracer LIF images similar to the ones shown in Fig. 19.13. The lower row shows chemiluminescence images recorded 0.5 crank angle degrees after each LIF image in the same cycle. Bright areas in the LIF images indicate a higher concentration of fuel, and a corresponding high intensity in the chemiluminescence images indicates a high rate of heat release. Although the chemiluminescence imaging suffers from being a line of sight technique, the good correlation between the two image series is evident. Areas where the fuel has been consumed according to the LIF image show a corresponding high intensity in the chemiluminescence image. Later in the cycle it can be seen how areas with remaining fuel appear dark in the chemiluminescence image. Altogether this is a good indication that the fuel tracer (acetone) does behave properly (Dept. of Physics, Lund University).

chemiluminescence and LIF from acetone added to ethanol was performed in a single cycle. These tests were performed in a port-injected engine, thus the differences in boiling temperature and diffusion rate were less critical since significant time was available for evaporation and mixing before the onset of combustion. A typical result can be seen in Fig. 19.14. It should be noted that the chemiluminescence signal is integrated along the line of sight. However, the use of a pancake combustion chamber limited the integration length to about 1 cm, which makes the comparison with the 2D PLIF images

feasible. In the image series it can be seen that brighter areas in the chemiluminescence images, representing ongoing heat release, corresponds spatially to darker areas in the PLIF images, indicating fuel break-up. Knowing that the chemiluminescence intensity correlates well with rate of heat release, this example of simultaneous imaging indicates that acetone is reasonable marker, at least for these running conditions.

19.5.6 3-D measurements

Three-dimensional imaging

Reacting flows, like combustion, are truly three-dimensional phenomena. A lot of information regarding flame spread and species distributions can be retrieved from two-dimensional data. However, to resolve the complete structure of, for example flame surface topology, 3-D imaging is necessary. Other examples of properties that can be accessed through 3-D measurements are the surface to volume ratio of mixing layers and their gradients in all directions.

A problem associated with conventional 2-D imaging is to distinguish if isolated islands in a fluorescence image really are isolated or if it is an effect from wrinkling in and out of the laser sheet. By employing 3-D imaging such uncertainties will diminish. 2-D imaging techniques can be applied to obtain 3-D information by rapidly recording a set of closely spaced planar images. In order to freeze the investigated phenomena the event must be imaged at repetition rates higher than the characteristic time scales of the studied system.

The first application of this approach, in engines, is reported by Mantzaras *et al.* (1988). They used four closely spaced laser sheets at different wavelengths to visualize Mie scattering from seeding particles. The sheet separation was achieved by utilizing the wavelength dispersion in a prism, i.e. the four planes were imaged simultaneously. The burnt and unburnt regions could be distinguished through the difference in scattering cross-section of the seeding material.

A slightly different approach is to record multiple images with a short exposure time, as the laser sheet is swept through the measurement volume. Yip *et al.* (1988) and Patrie *et al.* (1994) have utilized the long pulse duration of a flash-lamp pumped dye-laser in combination with a rotating mirror to accomplish this. With this technique it is possible to have multiple sheets with the same wavelength and the measurements are no longer limited to scattering, i.e. fluorescence imaging is feasible.

3-D visualization of the HCCI combustion

In HCCI/CAI combustion the fuel is consumed through distributed reactions throughout the combustion chamber. The temporal evolution of the rapidly

changing structure could be captured by the 2-D high-speed imaging technique described earlier. To visualize the three-dimensional topology of the HCCI combustion, a 3-D fuel visualization experiment was set up. The multiple-YAG and framing camera system were used for this purpose, but now in a slightly different configuration. The eight laser beams from the Nd:YAG laser cluster, fired with 10 μs time separation, were spatially separated by a rapidly scanning mirror. This resulted in a spatial separation of 0.5 mm between the individual laser sheets within the combustion chamber. All data was collected in 70 μs, corresponding to 0.5 CAD. During this acquisition time the combustion event is nearly frozen.

By combining the resulting eight PLIF images the 3-D structure could be revealed. From the 3-D fuel distribution, iso-concentration surfaces like the one in Fig. 19.15 could be generated. More details concerning this technique can be found in Nygren *et. al.* (2002).

19.6 Thermographic phosphors

This technique has been developed for performing surface temperature measurements with very high temporal and spatial resolution. By utilizing

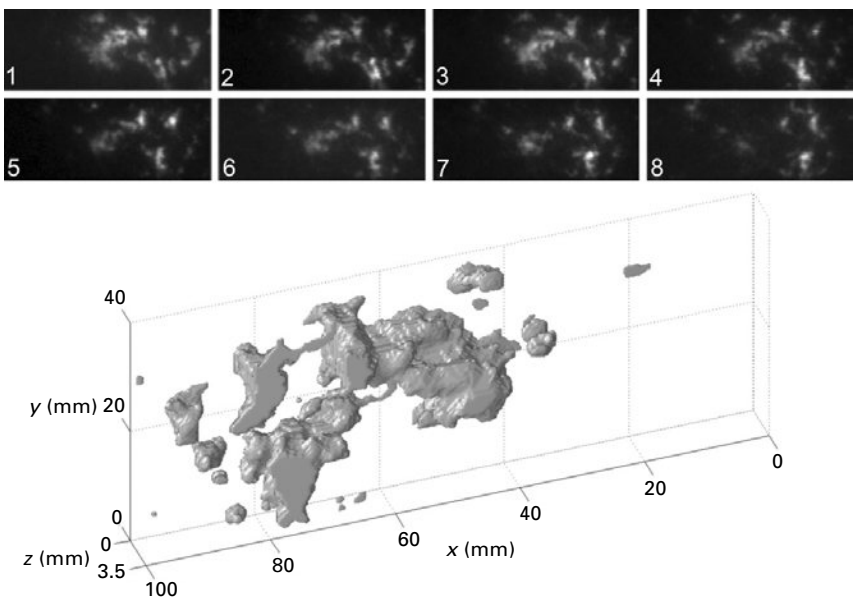

19.15 This is an example of 3-D iso-concentration fuel visualization. Eight, closely spaced, 2-D images of the fuel distribution have been recorded with a very short time separation. These eight images have then been used to reconstruct a three-dimensional iso-concentration surface (Dept. of Physics, Lund University).

the well known long-lived phosphorescence from thermographic phosphors, temperatures can be measured remotely and non-intrusively with high accuracy in the range between room temperature and 2000°C. An appropriate phosphor is applied on the surface area of investigation using a non-fluorescent binder. The surface is then illuminated with UV laser radiation for excitation of the phosphor material. The resulting emission intensity will decay exponentially according to

$$I = I_0 e^{-\frac{t}{\tau}} \tag{19.2}$$

where I_0 is the initial emission intensity, t is time and τ is the characteristic lifetime of the phosphorescence. This is defined as the amount of time to which the intensity has decreased to $1/e$ of the initial emission I_0. This phosphorescence lifetime changes in time with the temperature of the thermo-sensitive phosphor. The temperature can thus be determined by calculating the phosphorescence lifetime from the measured intensity decay and then retrieve the corresponding temperature from a calibration data set. This is normally done by fitting the intensity decay to the theoretical model (Eq. 19.2). The error in such a temperature measurement can ideally be less than 1% (Omrane *et al*., 2004) There exist several phosphorescent materials which are sensitive in different temperature intervals.

For the temperature range expected in an HCCI/CAI engine the phosphor La_2O_2S:Eu can be a suitable choice. In this case the light emitting substance is the Eu^{3+} ion doped in the host La_2O_2S. The Eu^{3+} ion has a broad absorption spectrum in the UV-region and both 266 nm and 355 nm radiation can be used for excitation. Several of the phosphorescence spectral peaks have temperature dependent lifetime. For HCCI/CAI applications the transition producing emission at 538 nm is suitable due to its very high sensitivity in the range 100–300 °C. An interference filter centred at this wavelength is preferably used to suppress against emission wavelengths other than the phosphorescence peak of interest.

The calibration of the themographic phosphor must be made in a controlled environment. Typically the lifetime is measured for a number of temperatures in the expected temperature range, in this case 100–300°C. Lifetime versus temperature can then be plotted, see Fig. 19.16. With such calibration data available phosphorescence decay curves recorded from an engine can be converted to surface temperature. This technique has, for example, been used in engine control research when studying the wall temperature during load transients in HCCI/CAI engines. In Fig. 19.17b the cylinder head surface temperature response after a step increase in load according to Fig. 19.17a is shown. More information on this topic is found in Särner *et al.* (2005a) and Husberg *et al*. (2005).

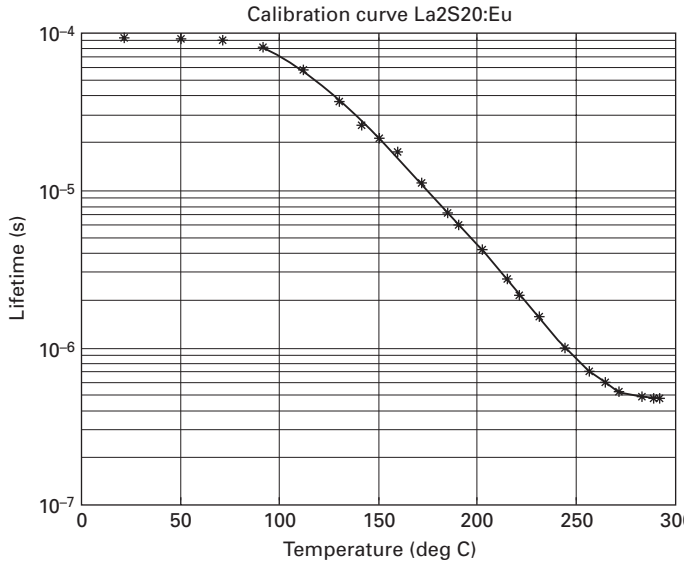

19.16 Example of calibration curve for the thermographic phosphor used for the load transient surface thermometry experiment. The calibration chart is created by measuring the phosphorescence decay time under controlled conditions for different temperatures. With this data available a measured decay can be linked to the surface temperature (Dept. of Physics, Lund University).

19.7 Future trends

Already today there is an extensive range of optical measurement techniques available. The few examples mentioned in this chapter represent only a fraction of what is on offer. In addition, the development is still ongoing and new techniques are emerging. The present techniques are being refined to provide improved accuracy and precision and also facilitate measurement of 'new' species. To mention a few examples, there is ongoing work on measuring very close to surfaces, with the aim of resolving the boundary layer in engines. Many of the present techniques use excitation in the UV- and the visible part of the spectrum. By moving into the infra-red, new species will become accessible. The excessive use of EGR calls for a measurement technique suitable for visualizing such distributions. A general trend towards simultaneous measurements of multiple species can be seen. High frame rate techniques are under development to resolve the rapid combustion process in one cycle, and thereby avoid the averaging effect introduced by the cycle-to-cycle variations.

When it comes to the optical engines the development will go towards experiments under higher and more realistic load conditions. The use of

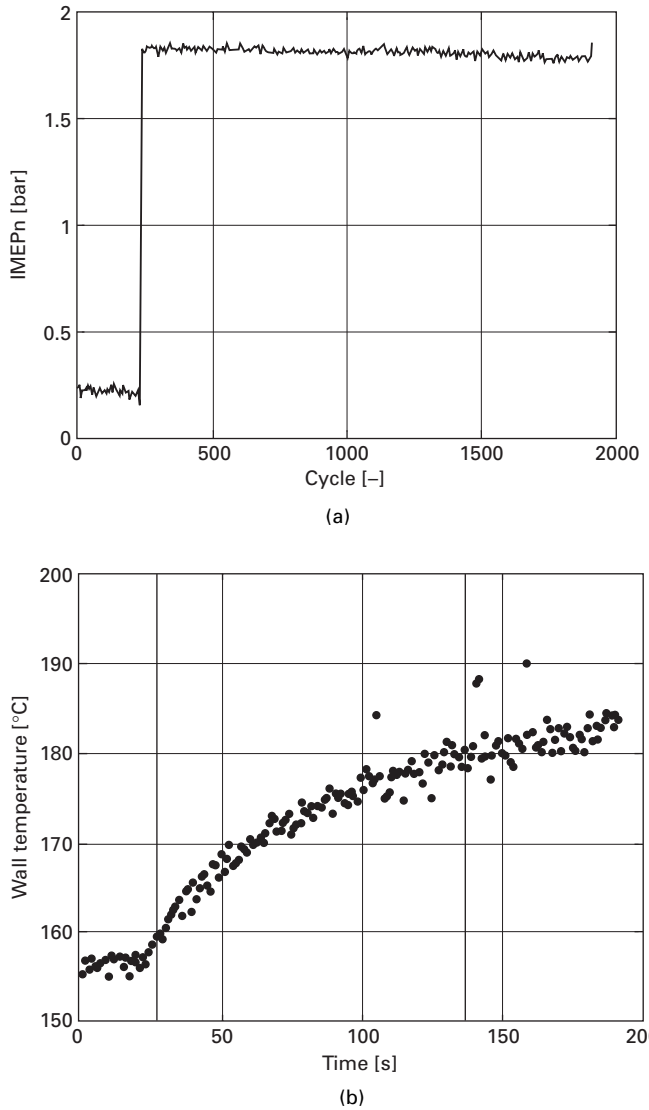

19.17 (a) The load-step in IMEP for which the surface temperature should be measured (Dept. of Energy Science, Lund University). (b) The response in surface temperature, during the load-step shown in Fig. 19.17(a), measured by the thermographic phosphors (Dept. of Physics, Lund University).

elongated pistons and quartz liners will probably persist for a while but in parallel we will see a development towards minimal intrusion optical access where the use of boroscopes and optical fibres play a major role.

19.8 References

Arnold A, Bombach R, Hubschmid W, Inauen A and Käppeli B (2000), 'Fuel-oil concentratiom in a gas turbine burner measured with laser-induced fluorescence', *Experiments in Fluids* 29, pp. 468–477.

Bowditch F W (1961), 'A new tool for combustion research – A quartz piston engine', SAE technical paper 610002.

Brackmann C, Nygren J, Bai X, Li Z, Bladh H, Axelsson B, Denbratt I, Koopmans L, Bengtsson P-E, and Alden M (2003), 'Laser-induced fluorescence of formaldehyde in combustion using third harmonic Nd:YAG laser excitation', *Spectrochim. Acta A*, 59: 3347–3356.

Collin R, Nygren J, Richter M, Aldén M, Hildingsson L and Johansson B (2003), 'Simultaneous OH- and formaldehyde-LIF measurements in an HCCI engine', SAE technical paper 2003-01-3218.

Collin R, Nygren J, Richter M, Aldén M, Hildingsson L and Johansson B (2004), 'Studies of the Combustion Process with Simultaneous Formaldehyde and OH PLIF in a Direct-Injected HCCI Engine', Proceedings of the COMODIA 2004.

Dec J E and Espey C (1998), 'Chemiluminescence imaging of autoignition in a D1 diesel engine', SAE Technical Paper 982685.

Eckbreth A C (1996), *Laser Diagnostics for Temperature and Species*, Amsterdam, Overseas Publisher Association, ISBN 90-5699-532-4.

Einecke S, Schultz C, Sick V, Dreizler A, Schiessl R and Maas U (1998), 'Two-dimensional temperature measurements in an SI engine using two-line tracer LIF', SAE technical paper 982468.

Einecke S, Schultz C and Sick V (2000), 'Measurement of temperature, fuel concentration and equivalence ratio fields using tracer LIF in IC engine combustion', *Applied Physics B*, Vol. 71, pp. 717–723.

Espey C and Dec J (1993), 'Diesel Engine Combustion Studies in a Newly Designed Optical-Access Engine Using High-Speed Visualization and 2-D Laser Imaging', SAE paper 930971.

Fansler T D, French D T and Drake M C (1995), 'Fuel Distributions in a Firing Direct-Injection Spark-Ignition Engine Using Laser-Induced Fluorescence Imaging', SAE technical paper 950110.

Fujikawa T, Hattori Y and Akihama, K (1997), 'Quantitative 2-D Fuel Distribution Measurements in an SI Engine Usin Laser-Induced Fluorescence with Suitable Combination of Fluorescence Tracer and Excitation Wavelength', SAE technical paper 972944.

Graf N, Gronki J, Schulz C, Baritaud T, Cherel J, Duret P and Lavy J (2001), 'In-Cylinder Combustion Visualization in an Auto-igniting Gasoline Engine Using Fuel Tracer- and Formaldehyde-LIF Imaging', SAE Technical paper: 2001-01-1924.

Grossmann F, Monkhouse P B, Ridder M, Sick V and Wolfrum J (1996), 'Temperature and pressure dependencies of laser-induced fluorescence of gasphase acetone and 3-pentanone', *Applied Physics B*, Vol. 62, pp. 249–253.

Hildingsson L, Persson H, Johansson B, Collin R, Nygren J, Richter M, Aldén M, Hasegawa R and Yanagihara H (2005a), 'Optical diagnostics of HCCI and UNIBUS using 2-D PLIF of OH and formaldehyde', SAE technical paper 2005-01-0175.

Hildingsson L, Johansson B, Hultqvist A, Särner G, Richter M and Aldén M (2005b), 'Simultaneous Formaldehyde and Fuel-Tracer LIF Imaging in a High-Speed Diesel

Engine With Optically Accessible Realistic Combustion Chamber', Proceedings of the International Conference on Engines, SAE 2005-24-008.

Hult J, Richter M, Nygren J, Aldén M, Hultqvist A, Christensen M and Johansson B (2002), 'Application of a high-speed laser diagnostic system for single-cycle resolved imaging in IC engines', *Applied Optics*, Vol. 41, No. 24.

Hultqvist A, Christensen M, Johansson B, Franke A, Richter M and Aldén M (1999), 'A Study of the Homogeneous Charge Compression Ignition Combustion Process by Chemiluminescence Imaging' SAE technical paper 1999-01-3680.

Hultqvist A, Christensen M, Johansson B, Richter M, Nygren J, Hult J and Aldén M (2002), 'The HCCI Combustion Process in a Single Cycle – High-Speed Fuel Tracer LIF and Chemiluminescence Imaging', SAE technical paper 2002-01-0424.

Husberg T, Gjirja S, Denbratt I, Omrane A, Aldén M and Engström J (2005), 'Piston temperature measurement by use of thermographic phosphors and thermocouples in a heavy-duty Diesel engine run under partly premixed conditions', SAE technical paper 2005-01-1646.

Knapp M, Luczak A, Schlüter H, Beushausen V, Hentschel W and Andresen P (1996), 'Crank-angel-resolved laser-induced fluorescence imaging of NO in a spark ignition engine at 248 nm and correlations to the flame front propagation and pressure release', *Applied Optics*, Vol. 35, No. 21, pp. 4009–4017.

Kohse-Höinghaus K and Jeffries J B (2002), *Applied combustion diagnostics*, New York, Taylor & Francis, ISBN 1-56032-938-6.

Le Coz J F, Catalano C and Baritaud T (1994), 'Application of Laser Induced Fluorescence for Measuring the Thickness of Liquid Films on Transparent Walls', Seventh International Symposium on Applications of Laser Techniques to Fluid Mechanics, II 29.3.1–29.3.8.

Lawrenz W, Köhler J, Meier F, Stolz W, Wirth R, Bloss W H, Maly R, Wagner E and Zahn M (1992), 'Quantitative 2D LIF Measurements of Air/Fuel Ratios During the Intake Stroke in a Transparent SI Engine', SAE technical paper 922320.

Mantzaras J, Felton P G and Bracco F V (1988), 'Three-Dimensional Visualization of Premixed-Charge Engine Flames: Islands of Reactants and Products; Fractal Dimensions; and Homogeneity', SAE technical paper 881635.

Martinez S, Bermudez V, Garcia J M and Julia E (2003), 'Engine with Optically Accessible Cylinder Head: a Research Tool for Injection and Combustion Processes', SAE technical paper 2003-01-1110.

Meier F, Wiltafsky G, Köhler G and Stolz W (1996), 'Quantitative Time Resolved 2-D Fuel-Air Ratio Measurements in an Hydrogen Direct Injection SI Engine Using Spontaneous Raman Scattering', SAE paper 961101.

Metz T, Bai, Ossler F and Alden M (2004), 'Fluorescence lifetimes of formaldehyde (H2CO) in the ˜A1A2 → ˜X 1A1 band system at elevated temperatures and pressures', *Spectrochim. Acta A*, 60: 1043–1053.

Neij H, Aldén M and Magnusson I (1992), 'Investigation of the influences of inhomogeneities in the air/fuel/exhaust mixture on cyclic variations in spark ignition engines', Contract JOUE CT-90-0066, 3rd Periodic Progress Report, July–December.

Norton T, Smyth K, Miller J and Smooke M (1993), 'Comparison of Experimental and Computed Species Concentration and Temperature Profiles in Laminar Two-Dimensional Methane/Air Diffusion Flames', *Combustion Science and Technology*, Vol. 90, pp. 1–34.

Nygren J, Hult J, Richter M, Aldén M, Hultqvist A, Christensen M and Johansson B (2002), 'Three-Dimensional Laser Induced Fluorescence Imaging of Fuel Distributions in an HCCI Engine', Proceedings of the 29th International Symposium on Combustion, The Combustion Institute.

Omrane A, Juhlin G, Ossler F and Aldén M (2004), 'Temperature measurements of single droplets by use of laser-induced phosphorescence', *Applied Optics*, Vol. 43, No. 17.

Ossler F and Aldén M (1997), 'Measurements of picosecond laser induced fluorescence from gas phase 3-pentanone and acetone: Implications to combustion diagnostics', *Applied Physics B*, Vol. 64, pp. 493–502.

Patrie B, Seitzman J and Hanson R (1994), 'Instantaneous three-dimensional flow visualization by rapid acquisition of multiple planar flow images', *Optical Engineering*, Vol. 33, No. 3, pp. 975–980.

Puri R, Moser M, Santoro R and Smyth K (1992), 'Laser-induced Fluorescence of OH Concentrations in the Oxidation Region of Laminar, Hydrocarbon Diffusion Flames', Twenty-Fourth International Symposium on Combustion/The Combustion Institute, pp. 1015–1022.

Richter M, Axelsson B and Aldén M (1998), 'Engine Diagnostics Using Laser Induced Fluorescence Signals Collected Through an Endoscopic Detection System', SAE paper 982465.

Richter M, Axelsson B and Aldén M (1999), 'Investigation of the Fuel Distribution and the In-Cylinder Flow Field in a Stratified Charge Engine Using Laser Techniques and Comparison with CFD-Modelling', SAE paper 1999-01-3540.

Richter M, Franke A, Aldén M, Hultqvist A and Johansson B (1999b), 'Optical Diagnostics Applied to a Naturally Aspirated Homogeneous Charge Compression Ignition Engine', SAE paper 1999-01-3649.

Siegman A E (1986), *Lasers*, New York: University Science Books, ISBN 0-935702-11-3.

Silfvast, W T (1996), *Laser Fundamentals*, Cambridge, University Press, ISBN 0-521-55424.

Schulz C and Sick V (2005), 'Tracer-LIF diagnostics: quantitative measurement of fuel concentration, temperature and fuel/air ratio in practical combustion systems', *Progress in Energy and Combustion Science*, 31, pp. 75–121.

Särner G, Richter M, Aldén M, Vressner A and Johansson B (2005a), 'Cycle Resolved Wall Temperature Measurements using Laser-Induced Phosphorescence in an HCCI Engine', SAE technical paper 2005-01-3870.

Särner G, Richter M, Aldén M, Hildingsson L, Hultqvist A and Johansson B (2005b), 'Simultaneous PLIF Measurements for Visualization of Formaldehyde- and Fuel-Distributions in a DI HCCI Engine', SAE Technical paper 2005-01-3869.

Thurber M C, Grisch F, Kirby B J, Votsmeier M and Hanson R K (1998), 'Measurements and modeling of acetone laser-induced fluorescence with implications for temperature-imaging diagnostics', *Applied Optics*, Vol. 37, No. 21, pp. 4963–4978.

Thurber M C and Hanson R K (1999), 'Pressure and composition dependence of acetone laser-induced fluorescence with excitation at 248, 266, and 308 nm', *Applied Physics B*, Vol. 69, Issue 3, pp. 229–240.

Yip B, Schmitt R and Long M (1988), 'Instantaneous three-dimensional concentration measurements in turbulent jets and flames', *Optics Letters*, Vol. 13, No. 2, pp. 96–98.

Yip B, Miller M F, Lozano A and Hanson R K (1994), 'A combined OH/acetone planar laser-induced fluorescence imaging technique for visualizing combustion flows', *Experiments in Fluids*, Vol. 17, pp. 330–336.

Yuen L S, Peters J E and Lucht R P (1997). 'Pressure dependence of laser-induced fluorescence from acetone', *Applied Optics*, Vol. 36, No. 15, pp. 3271–3277.

Part VI

Future directions for CAI/HCCI engines

20

Outlook and future directions in HCCI/CAI engines

H ZHAO, Brunel University West London, UK

Before reaching for the crystal ball regarding the future of CAI/HCCI engines, the Editor would like to share with the reader his personal experience on his involvement in this field. When he first submitted a grant application for funding in 1997, it was considered by the referees to be unrealistic to achieve CAI/HCCI combustion in the four-stroke gasoline engine without substantial modification to the engine and its auxiliaries. Fortunately, the same proposal was approved the second time around, one year later, although it was still considered to be a very risky project. Three years later, when the project was completed in 2002, CAI combustion was achieved for the first time in a four-stroke production engine with only modification to the camshafts, together with much better understanding with respect to the effects of engine operating parameters, fuel properties, and EGR. As a result, the project was given the highest rating by a panel comprising some of the original referees and assessors.

During this same period of time, some most successful approaches to achieving CAI/HCCI combustion in automotive engines were proposed and demonstrated. These include, for gasoline engines: (i) the residual gas trapping method by negative valve overlap; (ii) the rebreathing method by secondary opening of the exhaust valve; (iii) a mechanically variable compression ratio engine with intake charge thermal management; and (iv) internal EGR by positive valve overlap together with increased compression ratio and intake charge thermal management. In addition, research has shown that the operational range of CAI/HCCI combustion can be enlarged or better controlled by the introduction of boost, direct injection, rapid control of coolant temperature, fuel blending or reforming, spark assistance, and the implementation of closed-loop control using ion or pressure sensors. In the case of diesel engines, the research and development of HCCI combustion have been dominated by two main approaches: (i) early injection well before TDC to prepare for a homogeneous fuel and air mixture; (ii) retarded injection after TDC. The first approach is normally accomplished through two or more injections with a normal or a narrow cone high-pressure fuel injector

to avoid cylinder wall wetting, whereas the second approach requires the use of high EGR and high swirl for extended ignition delay and rapid mixing. Additional measures, such as a lower compression ratio and hot EGR, have helped to expand the high- and low-load HCCI operation limits in diesel engines.

CAI/HCCI engines have not yet reached the level of development and cost that would make a market introduction possible at the moment. The technical challenges facing both gasoline and diesel HCCI combustion are their limited operational range and less optimised combustion phasing, owing to the lack of direct control over the start of ignition and the rate of heat release. For both engines, the high load limit is imposed by the very early ignition and too rapid heat release, causing noisy combustion which is potentially damaging for the engine components. The moment of ignition is determined by the conditions in the cylinder during the compression stroke, so in order to influence the combustion phasing, the conditions of the compressed gas must be altered. Therefore, a lowered compression ratio and the use of large fractions of cooled EGR, which acts as an inert gas and absorbs heat during combustion, are necessary to extend the high load limit of CAI/HCCI operation. The low load limit in a gasoline engine is imposed by the failure of repeatable auto-ignition of combustible mixtures, whereas the diesel HCCI combustion is limited at low load by the increased CO and uHC emissions and cyclic variations due to the sensitivity to pressure and temperature. It is therefore critical to provide within the cylinder a thermal zone that is sufficiently hot to ignite the mixture, by increased compression ratio, higher charge temperature, and possibly thermal stratification.

The feasibility of a full HCCI engine has been demonstrated in a single cylinder heavy-duty diesel engine at Caterpillar, in which HCCI combustion can be achieved at imep values as high as 20 bar, provided that various engine and air management technologies can be implemented at the same time. However, in the short and medium terms, it is certain that partial HCCI or hybrid combustion operation will be first implemented in both gasoline and diesel automotive engines, owing to their wide range of speed and load operations. For gasoline engines, spark ignited flame propagation and CAI/HCCI combustion would not only be employed separately but they could also contribute to the heat release process in the same cycle as a hybrid combustion process with initial spark ignited flame propagation and multiple auto-ignited combustion later in the cycle. In the case of diesel engines, pure HCCI combustion does not exist in reality, as some form of inhomogeneity will always be present owing to the nature of diesel fuels and the limited time available for complete mixing to take place. Even for gasoline engines, some forms of thermal and charge stratifications, in particular between the combustible charge (air/fuel mixture) and diluents (recycled or trapped burned

gases), will often be present and they can be beneficial to extending the upper and lower limit of CAI/HCCI combustion regions.

One major concern with this new technology is the assumed inherent complexity and high cost of engine hardware necessary to CAI/HCCI engine operations. However, this should be viewed in the context of current and future engine developments and the increasing flexibility associated with future SI and CI engines. For example, the next generation of gasoline engines will be turbocharged direct injection with variable valve timing, cam profile switching or even infinite variable valve lift. In such an engine, it would be straightforward to incorporate CAI/HCCI combustion as well as the conventional SI combustion. Furthermore, the availability of low-cost in-cylinder pressure transducers has opened up the opportunity for real-time control over in-cylinder conditions for optimised SI and CI combustion as well as CAI/HCCI combustion.

Finally, it should be pointed out that CAI/HCCI combustion represents a step change in combustion technology and its future research and application should be considered as part of an effort to achieve low-temperature combustion in a wide range of operating conditions in an IC engine, rather than as the hot pursuit of pure CAI or HCCI for the sake of it. For both future gasoline and diesel engines, their combustion process converges towards premixed auto-ignited compression ignition combustion, while turbocharging and direct injection become a norm on such engines: it therefore may not remain futuristic but become a realistic possibility that, with more flexible engine hardware and their real-time control, a fully flexible engine could be developed to convert the chemical energy from any type of fuel into mechanical work through premixed auto-ignited low-temperature combustion.

Index

absorbance 482
absorption measurements 481–2, 483, 484, 485
acetone 488–9, 490, 495–7
air-fuel ratio (AFR) 15
  internal EGR 146, 147
  mode transition in 'mixed mode' engine 198–9, 201–2
  two-stroke engine 59–61
  see also equivalence ratio
air loop 307, 318–19
  control 319–20
aldehydes 488, 492–3
alkyl radicals 437–8, 442, 443
alkylperoxy radicals 438
  isomerisation 438–40, 442–3, 447–8, 449
ARC exhaust control valve 66, 68, 69
aromatic compounds 360, 361
Arrhenius equation 212, 411
Arrhenius rate threshold model 175
artificial neural networks 463, 466
ATAC generator engine 35, 43, 44, 63–4, 68
atomisation 244–5, 254
auto-ignition 15–16, 433–55, 457–8
  diesel engines 248–9
  in four-stroke engines 77
  kinetic models for HCCI ignition 451–3
  kinetics of 434–5
  multiple auto-ignition sites 49
  in the rapid compression machine 445–51
  reaction types 435–7
  temperature regimes of 437–45
    intermediate and high temperature chain branching 444–5, 461–2
    low temperature kinetics 437–43, 459–61
  timing *see* combustion timing
auto-ignition integral (Livengood-Wu integral) 211–14, 462–3
auto-ignition quality of fuels 210–24, 350–4, 355, 433–4
  chemical kinetic modelling 210–11
  empirical approaches to defining 214–17
  ignition delay and Livengood–Wu integral 211–14
  octane index and *K* value 217–22
  requirement of a CAI/HCCI engine 222–4
  and volatility 231–2
AVL-CSI valve train 141–62
AVT system 141
  mode switching 189, 191–2, 203
    experimental results 193–6
    mode transition 199–202, 203

backflow intake re-breathing 138–40
bio-fuels 208
black-box combustion timing models 175–8
  PRBS excitation for identification of state space models 177–8
  sensitivity estimation from stationary map 176
boosted intake pressure 89–90, 93–4, 388–91
boroscopes 479–80
Bosch smoke number 345, 346
bottom dead centre (BDC) 168
brake mean effective pressure (BMEP)
  premixed compression ignition 280–2
  supercharged natural gas engines 385, 386, 388, 389–91
burned gases

as diluents 29–35
cooled burned gases 30–2
effects on CAI combustion 34–5
hot burned gases 33–4
thermal energy in 78
n-butane 366, 367, 393, 394
influence on auto-ignition and combustion in natural gas 376–83
main chemical reaction path 378–9
by-pass valve 56

CA50 165, 166, 172
auto-ignition quality of fuel 217–18, 219
estimation of 224, 238
predicting 360, 361
sensitivity to changes in octane index 222–4
sensitivity estimation from stationary map 176
California Air Resources Board (CARB) permitted emission levels 3–5
cam profile switching 80–1
cam profile switching and phaser VVT system (CPS-P) 189–91, 203
experimental results 194–9
mode transition 196–9, 203
carbon dioxide emissions 3, 4–5, 289
DME engine 399–400, 401, 417, 418
high combustion efficiency and low emissions 403–6, 407
natural gas engine 374–6, 380–3
carbon monoxide emissions 3–4, 15
DME engine 399–400, 401, 402–3, 417, 418
high combustion efficiency and low emissions 403–6, 407
gasoline engines 24–6
MK combustion 331, 332
NADI 294, 295, 300, 304, 310, 314, 317
natural gas engines 374–6, 380–3
supercharged 386, 387
OKP engine 86
expanding operating range 87–8
premixed compression ignition combustion 273, 274, 283–5
residual gas trapping 112–13, 114
spark assisted CAI combustion 131, 133
carbon monoxide freezing problem 426–9
catalytic converters 5–6
Caterpillar 508
ceiling temperature 438
cetane number (*CN*) 214–15, 216–17, 343, 349, 351–2, 360
MK combustion and hydrocarbon emissions 337–9
chain branching reactions 435–7
temperature regimes of auto-ignition 437–45
charge coupled device (CCD) chips 480
charge dilution 139–40, 147–8, 149, 150, 152
charge heating effect 29, 33–5
injection timing 121, 124, 126
charge stratification 15, 38–9, 97
injection timing 121–4, 126
OKP engine 87–8
two-stroke engine 57
chemical effect 29, 30–2
injection timing 119–21, 124, 126
chemical kinetics 433–55, 458–62
auto-ignition in the rapid compression machine 445–51
kinetics of auto-ignition 434–5
modelling *see* modelling
reaction types 435–7
temperature regimes of auto-ignition 437–45
intermediate and high temperature 444–5, 461–2
low temperature kinetics 437–43, 459–61
chemical kinetics codes 465–6
chemical species concentration profile 402–3, 404, 405
chemiluminescence imaging 173, 482–4, 486
closed-loop control 40, 156–7, 164–84
combustion timing sensors 171–4
control means 165–71
future trends 182
experimental results 178–81
internal EGR and 156–7
methods 174–81
timing control problem 164, 165, 166
co-axial bucket tappets 189–91
cold start 96–7, 195
MK combustion and SULEV compliance 337–40
combined mechanical electro-hydraulic valve train 141–6
combined variable valve lift and timing devices 115

combustion chamber walls, thermal energy in 78, 79
combustion characteristics 10–13, Plate 1
  DME engine 396–407, 417–18, 424, 425, 426, 427, 428, 429
  gasoline engines 27–9
  MK 324–30
  premixed compression ignition combustion 278–80, 281
  residual gas trapping 107–12
combustion control *see* control
combustion duration
  gasoline engine 27–9
    effect of cooled burned gases 31, 32
    effect of hot burned gases 34
    residual gas trapping 111–12
  natural gas engines 371–2
combustion efficiency 13–15
  DME engine 396–407, 411–12, 421, 422
    high combustion efficiency and low emissions 403–6, 407
  natural gas engines 374–6
    influence of n-butane in methane/n-butane/air mixtures 380–3
    supercharged engines 385–6, 388
combustion kinetics *see* chemical kinetics
combustion limits 23–4
  gasoline fuel effects 224–6
  OKP engine 87–91, 93–6
  see also operating range
combustion reaction speed 416, 418–20
combustion stability 50, 51, 52–3
combustion timing/phasing 206, 508
  control problem 164, 165, 166
  diesel fuel HCCI 345–50
  gasoline engine 27, 28
    effect of cooled burned gases 31–2
    effect of hot burned gases 33–4
    effect of injection timing 124, 126
    fuel effects 222–4
  ignition timing control for DME engine 410–11
  natural gas engines 371–2, 380, 381
  OKP engine 87–8, 90
    operating range 93–4
    quick adjustment capability 96
    thermal efficiency 91, 92
  residual gas trapping 110–11
  sensors 171–4, 182
compressed natural gas (CNG) *see* natural gas
compression heat 77–8, 79, 95, 458
compression ignition (CI) combustion 5, 7, 10–11, Plate 1
  heat release characteristics 12–13
  performance and emission characteristics 14
compression ratio (CR) 35–6, 59, 91–2, 93–4
  effective compression ratio control using VVA 168–70, 179–80
  MK combustion and hydrocarbon emissions 334, 337–9
  NADI 301–2
  supercharged natural gas engines 385–9
    performance and exhaust gas characteristics at CR of 17 385–8
    performance and exhaust gas characteristics at CR of 21 388–9, 390
computational fluid dynamics (CFD) 467–8
control 39–40, 289, 457
  closed-loop control *see* closed-loop control
  DME engine 408–22
  HCCI diesel combustion 249–52
  NADI 320
  problems in 185–8
  re-breathing 139–40, 155–9
  timing problem 164, 165, 166
  two-stroke engines 56–67
controlled auto-ignition (CAI) *see* homogeneous charge compression ignition (HCCI)/controlled auto-ignition (CAI)
controlled auto-ignition number (CAN) 228–9
cool flame magnitude 353–4, 355, 358, 359, 360
coolant, thermal energy in 78, 79, 95, 99–100
coolant temperature 38, 62–3
  control of 99–100
  MK combustion and hydrocarbon emissions 334
cooled burned gases 30–2, 34–5
  effect on auto-ignition timing 31–2
  effect on combustion duration 32
  effect on rate of pressure rise 32
cooling effect (charge cooling effect) 124, 126, 128–9

crank shaft torque fluctuations 173–4
cross scavenged two-stroke engines 65, 66
crude oil 208
cycle-resolved LIF imaging 495–7
cyclic ethers 440
cyclic hydrocarbons 360, 361
cylinder liner, transparent 478, 479
cylinder wall wetting problem 10

degenerate branching 436
derived cetane number (*DCN*) 215
diesel engines 7, 9–10, 12–13, 241–66, 507–8 509
  compression ignition combustion *see* compression ignition (CI) combustion
  convention diesel combustion 242–6
  fuels for *see* fuels
  HCCI combustion 247–52
    heat release and combustion control 249–52
    mixture auto-ignition 248–9
    mixture formation 248
  HCCI diesel engines 252–61
    early injections *see* early injections
    late injections 251–2, 253, 259–61, 263, 297
    port fuel injection 252–4, 262
  historical background of HCCI 9–10
  HSDI 6
  modulated kinetics *see* modulated kinetics (MK)
  NADI 258, 289–321, Plate 10
  premixed compression ignition combustion 9–10, 257, 267–88
  thermal efficiency 91–3
diesel fumigation 9–10
diesel particulate trap (DPF) 339–40
diffusion controlled combustion 242–4, 245
diffusion flame 243–4, 245
dilution effect 29, 30–2, 35
dimethyl ether (DME) 36, 393–430
  carbon monoxide freezing problem 426–9
  characterisation of 393–4
  chemical reaction model 394–5
  combining DME and other fuels 422–3, 424
  combustion completeness in DME engine 396–407
    chemical species concentration profile 402–3, 404, 405
    equivalence ratio 396–400, 401
    initial temperature 400–1, 402, 403
    LTR and HTR appearance conditions 401–2, 404
    necessary factor for high combustion efficiency and low emissions 403–6
  combustion control system for small HCCI engine 408–22
    calculation and experimental conditions 415–16
    calculation and experimental results 416–22
    control method 410–12
    control system 412–14
    engine specifications 408–10
    two-stage exhaust cam system 414
  DME reforming system 423, 424
  HCCI engine 394
  reducing pressure rise rate with inhomogeneous DME/air mixture 423–5, Plate 16
direct injection 10, 37–8
  residual gas trapping 115–29, 134
    early injections 116–21, 122, 123, 124, 126
    mid and late injections 121–4, 125–6
    split fuel injections 124–9
  two-stroke engine 45, 52–4
displacement volume, effective 168–70
distillation 208
distributed models 465–8, 470
DoE (design of experiments) 149
dual fuel control 171, 178–9, 182, 186
dual mode engines
  diesel *see* narrow angle direct injection (NADI)
  fuel requirements 230–1
  see also mode switching
Duret, P. 45

early backflow 107
early injections
  diesel engines 251–2, 253, 255–8, 262–3, 267–88
    low cetane fuel 271–4
    NADI 297
  gasoline engines
    residual gas trapping 116–21, 122, 123, 124, 126, Plate 5, Plate 6
    two-stroke engine 62

early re-breathing 138–40
ECO-Engine Network of Excellence 16
effective compression ratio control using VVA 168–70, 179–80
effective displacement volume 168–70
electro-hydraulic valve actuation (EHVA) 141–6, 181
electro-hydraulic variable valve train (AVT) system (Pro AVT) *see* AVT system
electro-magnetic valve actuation systems 141
electromechanical valve actuation system 181
elevated pressure auto-ignition temperature (EPAIT) 358–9, 360
  diesel HCCI 351–4
  gasoline HCCI 354–6
elongated piston 477–9
elongated transfer duct 63–4
emissions
  characteristics of conventional combustion and CAI/HCCI combustion 13–15
  DME engine 399–400, 401, 417–18
    high combustion efficiency and low emissions 403–6, 407
  legislation 3–5, 6
    MK and meeting SULEV standard 337–40
  MK combustion 323–4, 326, 327
    future trends 337–40
    performance improvement of second generation 334–7
    second generation 331, 332–4
  NADI 294–5, 298, 299, 300, 301, 302, 304–7, 309–18
  natural gas engines 374–6
    influence of n-butane in methane/n-butane/air mixture 380–3
    supercharged 386, 387, 388–9
  OKP engine 84–6
  PFI diesel engines 252
  premixed compression ignition combustion 273, 274, 275–6
    varying injection timing 283–5
  re-breathing 150–4, 160, 161
  residual gas trapping 112–14
  spark assisted CAI combustion 131, 133
  two-stroke engines 49, 50–2
    IAPAC engine 71–2
  see also carbon dioxide emissions; carbon monoxide emissions; hydrocarbon emissions; nitrogen oxides (NO_x) emissions; particulate emissions
endoscopes 479–80
energy balance analysis 154–5, 156
engine speed
  and auto-ignition temperature in natural gas engines 372–4
  fluctuations and control 174
  two-stroke engine 54, 57–8
engine torque 198–9, 201–2
equivalence ratio
  DME engine 396–400, 401
  natural gas engines 369–71, 376, 377
  see also air-fuel ratio
ethane 366, 367, 460
ethanol 208, 482, 483
ethers 208
ethyl hexyl nitrate (EHN) blends with FTN 350–3, 356
European driving cycle 159–62
European Union permitted emission levels 3–5
evaporation 253
exhaust blow down supercharging 140
exhaust control valve 45
exhaust gas recirculation (EGR) 36, 78, 95, 99–100, 185–6, 187, 203
  changing EGR ratios and premixed compression ignition combustion 278–80, 281, 283–5
  diesel engines 253–4
  DME engine 410–11, 412–14, 418–21
  external *see* external EGR
  internal *see* internal EGR; re-breathing
  low pressure EGR 319
  mass fraction 222
  tolerance and spark assisted CAI combustion 132, 134
exhaust gases 36–7
  as diluents 29–35
  thermal energy in 78, 79, 95
exhaust throttling 55, 58, 59, 60, 66, 67, 68
  combined with transfer throttling 66–7
external EGR 78
  DME engine 411, 412–14, 418–21

fast thermal management (FTM) *see* thermal management

finger-follower valve train 162
first-stage heat release 213
Fischer Tropsch naphtha (FTN) 346–50
  blends with ethyl hexyl nitrate (EHN) 350–3, 356
Fischer-Tropsch process 208
five-way catalyst 336–7
flame front 11, 13, 48–9
flame lift-off length 243–4
flame propagation 458
fleet-averaged system 4–5
flow velocities, control of 58–9
formaldehyde 483
  distribution 491–3
  simultaneous measurements 493–4
4-SPACE Project 73
four-stroke engines 8–9, 35
  auto-ignition in 77
  with internal EGR 136–63
  with residual gas trapping 103–35
  with thermal management 77–102
fuel burned prior to compression, thermal energy in 78, 79, 95
fuel cell vehicles 5
fuel consumption
  fleet average 4–5
  indicated specific fuel consumption 227–8
  NADI 293–4, 300, 301, 302, 304, 305, 306, 309, 313, 317
  premixed compression ignition combustion 273, 274, 275–6, 280–2
  re-breathing 150, 153, 159–2
  residual gas trapping 112, 113
  two-stroke engines 47–8, 50–2, 53
    high-performance motorcycles 69–70
fuel control 320
fuel distribution 485–90
fuel energy per cycle (*FEN*) 226–8
fuel injection system (NADI) 299–301
fuel injection timing *see* injection timing
fuel spray guiding effect 291–2, 296
fuel tracers 487–9
  high-speed imaging 495–7
  simultaneous visualisation of formaldehyde and 493–4
fuel/wall interaction 292, 297
fuels 206–38, 252, 342–62
  auto-ignition quality 219–24, 350–4, 355, 433–4
  auto-ignition requirement and fuel effects in combustion phasing 222–4
  CAN 228–9
  cetane number *see* cetane number
  combustion limits 224–6
  diesel fuel HCCI 345–50
  DME *see* dimethyl ether
  formulation and two-stroke engines 63
  fundamental factors 360–1
  future trends 361–2
  gasoline HCCI 354–8
  IMEP and indicated efficiency 226–8, 238
  IQT 215–16, 229–30, 350–4, 355, 359
  K value 217–22
  MK and SULEV compliance 337–9
  natural gas *see* natural gas engines
  octane index 217–4, 230
  octane number 63, 214–17, 343, 351–3, 360, 450–1
  practical transport fuels 207–10
  requirements of gasoline HCCI engines 230–2
    full HCCI engines 231–2
    practual dual-mode engines 230–1
  specification 342–3
    for HCCI 358–60
  variation in fuel blend 36
full engine simulation programme
  early ignition 119–21, 122, Plate 7
  mid and late injection 123–4, Plate 8
  split fuel injection 124–8
fully integrated models 465–6
fused silica 476

gas dissociation 91, 92
gas to liquid (GTL) fuels 208, 231–2
gas specific heat ratio 91–2
gasoline direct injection (GDI) engines 6
gasoline/electric hybrids 5
gasoline engines 7–9, 11–12, 21–42, 507, 508–9
  approaches to CAI/HCCI operation 35–40
    approaches to CAI/HCCI gasoline engines 35–7
    challenges facing CAI/HCCI combustion 37–9
    combustion control 39–40
  closed-loop control 40, 156–7, 164–84
  four-stroke 77–163

with internal EGR 136–65
with residual gas trapping 103–35
with thermal management 77–102
fuels for *see* fuels
fundamentals 21–9
combustion characteristics 27–9
NO_x emissions 26–7
operating region for CAI 22–4
unburned hydrocarbon and carbon monoxide emissions 24–6
historical background of CAI/HCCI 7–9
mode switching *see* mode switching
spark ignition *see* spark ignition (SI) combustion
use of exhaust gases as diluents 29–35
cooled burned gases 30–2
effects of burned gases on CAI/HCCI combustion 34–5
hot burned gases 33–4
two-stroke *see* two-stroke CAI engines
generators, small 35, 43, 44, 67–8
Grenada-Dakar Rally 44, 45, 69

HCLI (homogeneous charge late injection) 260–1
heat capacity effect 29, 30–2, 35
heat exchangers 79–80
heat flux measurement 326–30, Plate 14
heat release
characteristics of CAI/HCCI combustion 11–13
combustion timing control problem 165, 166
diagrams at various loads 344–5, Plate 15
DME engine 397–9, 416, 417, 425, 426, 427, 428, 429
intial temperature 401, 403
fuel ignition quality 353–4, 355, 433–4, Plate 17
gasoline engines 22, 217, 218
early injection 117, 118, 119–21, Plate 6
mid and late injection 121, 123
split fuel injection 126–8
HCCI diesel combustion 249–52, 347–9
IQT and heat release rates 359
MK combustion 325–6, 327–8, 330, Plate 14
natural gas engines 370
influence of n-butane in methane/n-butane/air mixtures 377–8, 379, 380
supercharged 386–8
premixed compression ignition combustion 278–80, 281
spark assisted CAI combustion 129–31
two types of ignition 433–4
heat transfer losses 91, 92
heptamethylnonane-hexadecane blends 350–3, 356
n-heptane 211–13, 249, 360, 361, 450–1, 460
iso-octane/n-heptane mixtures 350–3, 356, 433, 434, 449, 450–1, 482, 485
hexadecane-heptamethylnonane blends 350–3, 356
high speed direct injection (HSDI) diesel engines 6
high-speed LIF diagnostics 495–7
high temperature reactions (HTR) 344–5, 444–5, 461–2
in the DME 393, 394, 395, 397–9
appearance conditions 401–2, 404
highly premixed combustion (HPC) mode of NADI 293, 317
improved concept at part load 304–7
initial results at part load 293–5
HiMICS concept 256–7
homogeneous charge compression ignition (HCCI)/controlled auto-ignition (CAI) 6–16
CAI gasoline engines 7–9
combustion 22, Plate 2
definition of HCCI and CAI combustion engines 15–16
HCCI diesel engines 9–10
performance and emission characteristics 13–15
principle and combustion characteristics 10–13
Honda 5
AR combustion motorcycles 8, 35, 44, 45, 56, 68–9
Pantheon scooters 44, 45, 69
hot burned gases 33–5
HPLI (highly premixed late injection) combustion concept 260–1
hybrid operation 39, 508
see also mode switching

hybrid vehicles 5
hydrocarbon emissions 4, 15
DME engine 399–400, 401, 403
high combustion efficiency and low emissions 403–6, 407
gasoline engines 24–6
internal EGR 160, 161
'mixed mode' engine 198–9, 201–2
MK combustion 326, 327
effect of cetane number and compression ratio 337–9
low compression ratio in cold condition 334
second generation 331, 332
NADI 294, 295, 300, 304, 306, 310, 314, 317
natural gas engines 374–5, 380–3
supercharged 386, 387
OKP engine 85–6
premixed compression ignition combustion 273, 274, 275–6, 283–5
residual gas trapping 112, 114
spark assisted CAI combustion 131, 133
two-stroke engines 50–2, 53
hydrogen peroxide 435–6, 444–5, 449, 450, 461–2
hydroxyl radicals
distribution 490–1
simultaneous visualisation of formaldehyde and 493

IAPAC engine 44, 45, 56, 65–6, 70–2
idle operation 55, 96
ignition delay
n-butane 393, 394
diesel combustion 242
DME 393, 394
fuel auto-ignition quality 211–14, 215–16, 350–4
methane 393, 394
MK combustion and prolonged 324, 330–2
combined with shortened injection duration 332–3
in rapid compression machine 450–1
ignition quality test (IQT) 215–16, 229–30, 350–4, 355, 359
ignition timing *see* combustion timing
indicated fuel conversion efficiency 227–8, 238
indicated mean effective pressure (IMEP) 24, 238
coefficient of variation of 225, 226
and indicated efficiency 226–8
indicated specific fuel consumption 227–8
inhomogeneity of mixture 423–5, 458, Plate 16
initiation reactions 435–7
injection duration, shortened 330, 332–3
injection timing
early injections *see* early injections
formaldehyde distribution 491, 492
gasoline engines 115–29
late injections *see* late injections
mid-injections 121–4, 125–6
NADI 296–9
two-stroke engine 62
varying and premixed compression ignition combustion 280–5
injector layout 272
Institut Français du Pétrole (IFP)
approach and NADI 289–1
IAPAC engine 44, 45, 56, 65–6, 70–2
intake charge heating *see* thermal management
intake ports, thermal energy in 78, 79
intake valve closing (IVC) angle 168–70
intermediate temperature combustion 444–5, 461–2
internal EGR 36–7, 78, 79, 136–63, 356–8, 507
DME engine 410–11, 412–14, 418–20
re-breathing *see* re-breathing
two-stroke engine 56–7
internal hydrogen abstraction 459–60
ion current sensing 172–3, 182
irregular combustion 54–5
Ishibashi, Y. 45
iso-octane 209–10, 433, 434, 449, 460
absorption measurements 482, 484
mixtures of heptane and 350–3, 356, 433, 434, 449, 450–1, 482, 485
iso-pentane 209–10, 446–9

K value 217–22
kerosene 208, 231–2
ketohydroperoxide 441, 459
ketones 488, 492–3
knock integral model 174–5
knock limit 23–4, 224
knocking 27, 247

avoidance in DME engine 411
diesel engines 250
natural gas engines 366–9
OKP engine 89
prediction of operating range 469

LAG system (avalanche activated combustion) 7–8
laser-induced fluorescence (LIF) 484–98
formaldehyde distribution 491–3
fuel distribution 485–90
fuel PLIF in HCCI engines 489–90
fuel tracers 487–9, 493–4, 495–7
high-speed diagnostics 495–7
hydroxyl radical distribution 490–1
simultaneous measurements 493–4
three-dimensional measurements 497–8
lasers 481
see also optical techniques
late backflow 107
late diffusion combustion 242–3
late injections
diesel engines 251–2, 253, 259–61, 263
NADI 297
residual gas trapping 121–4, 125–6
two-stroke engine 62
late re-breathing 138–40
light sources 480–1
linear time-invariant (LTI) systems 177–8
liquid petroleum gas (LPG) 208
Livengood-Wu integral (auto-ignition integral) 211–14, 462–3
load limits 49–50, 54–5
location of peak pressure (LPP) 199, 201–2
lookup table approach 466
loop scavenged two-stroke engines 64–5
Lotus 8–9
low cetane fuel 271–6
low pressure EGR 319
low temperature and premixed combustion *see* modulated kinetics (MK)
low temperature reactions (LTR) 11, 229–30, 344–5, 459–61
DME engine 393, 394, 395, 397–9
appearance conditions 401–2, 404
kinetics 437–43
luminescence 424–5, Plate 16

mass fraction burned curves 22, Plate 3
maximum pressure rise rate (MPRR) 199, 201–2, 224–5, 238
residual gas trapping 109–11
maximum temperature
DME engine 411–12, 418–20
high combustion efficiency and low emissions 403–6, 407
natural gas engines 374–6, 380–3
mechanical friction 91, 92–3
methane 366, 367, 393, 394, 460
influence of n-butane in methane/n-butane/air mixtures 376–83
mixing with DME 422, 423
methanol 63, 482
methyl tertiary butyl ether (MTBE) 208
mid-injections 121–4, 125–6
misfire limit 23–4, 224
misfiring 15, 23–4, 46–7
natural gas engines 366–9
prediction of operating range 469–70
two-stroke engines 54–5
'mixed mode' engine *see* mode switching
mixture formation/preparation
control of two-stroke gasoline engine 61–2
diesel engines 244, 248, 289
DME engine 412–14
optical techniques for fuel distribution 485–90
mode switching (CAI/SI switching) 39, 180–1, 185–205
control problems 185–8
internal EGR 156–9
switching algorithm 157–9
'mixed mode' engine in operation 192–202
experimental apparatus and set up 192–5
mode transition using fully variable VVT system 199–202, 203
mode transition using simulated CPS-P VVT system 196–9, 203
OKP engine 96
transition between operating modes 188–92
cam profile switching and phasing device VVT system 189–91
research grade AVT system 191–2
valve train requirements 188–9
two-stroke engine 55–6
model aeroplane engine 9

model-based control methods 174–8, 182
  black-box models 175–8
  physically-based models 174–5
model predictive control (MPC) 179–80
modelling 210–11, 451–3, 456–74
  chemistry of HCCI 458–61
  detailed HCCI analysis 465–8
    fully integrated models 465–6
    multi-zone models 452, 466–8, 469, Plate 18
  fundamentals of ignition and combustion 457–8
  future trends 470–1
  prediction of ignition 462–4
    auto-ignition integral 462–3
    chemical kinetics 463–4
  prediction of operating range 468–70
    high load limit 469
    low load limit 469–70
  single zone models 451–2, 462, 464, 470
modulated kinetics (MK) 10, 260, 322–41
  basic concept 323–4
  challenges for MK combustion 330
  combustion photographs 324–6
  emission performance improvement of second generation 334–7
    performance compared with conventional combustion 335, 336
    possibility of clean diesel 335–7
    smoke 334–5, 336–7
  experimental measurement of transient heat flux 326–30
  future trends 337–40
    future fuel 337–9
    possibility of meeting SULEV standard 339–40
  performance characteristics 326, 327
  second generation 330–4
    combining prolonged ignition delay and shortened injection duration 332–3
    hydrocarbon emission in cold condition 334
    prolonged ignition delay 330–2
mole fraction histories 402–3, 404, 405
Motor Octane Number (*MON*) 214–17
motorcycles 8, 35, 44, 45, 56, 68–70
MULDIC 255–6, 274–6
multi channel plate (MCP) 480
multiple auto-ignition sites 49
multiple injections 10
  diesel engines 267–88
  NADI 297, 298
multi-zone models 452, 466–8, 469, Plate 18

naphtha 208, 232, 346–50
naphthalene 487
narrow angle direct injection (NADI) 258, 289–321, Plate 10
  concept overview 290–2
    combustion system 291–2, Plate 11, Plate 12
    IFP approach 290–1
  evaluation in a multi-cylinder engine 307–18
    engine configuration 307
    full load tests 308
    part load tests 308–18
  first results and limitations 292–5
    full load using conventional combustion 295
    part load using HPC combustion 293–5
  future trends 318–20
    air loop circuit 318–19
    engine control 319–20
  improving the concept 296–307
    fuel injection system 299–301
    fuel injection timing 296–9
    results of improved concept 303–7
    ways of improvement 296–302
natural gas engines 365–92, 427–9
  auto-ignition temperature and auto-ignition pressure 372–4
  auto-ignition timing and combustion duration 371–2
  emissions, maximum cycle temperature and combustion efficiency 374–6
  equivalence ratio 369–71, 376, 377
  experiment and calculation conditions 365–6
  gas composition 366–9
  influence of n-butane on auto-ignition and combustion in natural gas 376–83
  supercharged engine 383–91
    performance and exhaust gas characteristics at CR of 17 385–8
    performance and exhaust gas characteristics at CR of 21 388–9, 390

potential of 389–91
set-up and experiments 383–5
negative temperature coefficient (NTC) zone 212–13, 438, 443, 460–1
negative valve overlap (NVO) *see* residual gas trapping
neo-pentane 446–9
net heat release analysis 172
neural networks 463, 466
Nippon Clean Engine (NiCE) 43
ATAC generator 35, 43, 44, 63–4, 68
Nissan Motor Company 10
nitrogen oxides (NO_x) emissions 6, 13, 289, 322
diesel combustion 14, 246
DME engine 417–18
formaldehyde distribution and 491, 492
gasoline engines 26–7
internal EGR 146, 148, 149, 150–4, 160, 161
'mixed mode' engine 198–9, 201–2
MK combustion 323–4, 326, 327
performance improvement of second generation 335–7
second generation 331, 332–3
NADI 294–5, 300, 301, 302, 304, 305, 306, 309, 313, 317, 318
OKP engine 84–5, 89
premixed compression ignition combustion 273, 274, 275–6, 283–5
regulation levels 3–4, 322–3
residual gas trapping 112, 113
spark assisted CAI combustion 131, 133
supercharged natural gas engines 386, 387
two-stroke engines 49, 53–4
CAI-IAPAC engine 72
Noguchi, M. 8, 43
noise 295, 300, 301, 302, 304–5, 306, 311, 315, 317, 318

octane index (*OI*) 217–22, 230
engine's requirement 222–4
octane number 63, 214–17, 343, 351–3, 360, 450–1
Onishi, S. 8, 43, 64–5
operating range 100, 186–8, 289, 508
gasoline engine 22–4, 38
NADI 295, 317
natural gas engines 366–9
OKP engine 82–3
expanding 87–91
lower boundary 87–8, 94–6
upper boundary 89–91, 93–4
wide 93–6
prediction of 468–70
high load limit 469
low load limit 469–70
residual gas trapping 108–9
two-stroke engines 46–8
high load limit 55
IAPAC engine 71
low load limit 54–5
optical spacer 477, 478
optical techniques 475–504
chemiluminescence imaging 173, 482–4, 486
diagnostic approaches 476–81
optical access 476–80
signal collection and light sources 480–1
future trends 500–1
laser-induced fluorescence 484–98
spectroscopic absorption measurements 481–2, 483, 484, 485
thermographic phosphors 498–500, 501
optimised kinetic process (OKP) engine 78–97
concept 79–81
expanding HCCI operating range 87–91
lower boundary 87–8
upper boundary 89–91
single-cylinder 82–6
emissions 84–6
operating range 82–3
thermal efficiency 83–4
strengths and weaknesses 91–7
cold start and warm-up 96–7
combustion mode transition 96
combustion timing control 96
concerns 97
conventional hardware 97
high thermal efficiency 91–3
wide operating range 93–6
oxygenates 208

Pantheon scooters 44, 45, 69
paraffins 208–10, 360, 361
partial burn region 23–4
partially stratified (PCCI) combustion 458, 468, 471

particulate emissions 6, 13, 14, 322
diesel combustion 246
intake air temperature and 345–6
MK combustion 323–4, 326, 327
performance improvement of second generation 334–5, 336–7
second generation 331, 332–3
NADI 294–5, 300, 301, 302, 305, 307, 312, 316, 317
premixed compression ignition combustion 274, 275–6, 283–5
n-pentane 446–9, 450–1
3-pentanone 488–9, 490
peroxy radicals 459–60
phosphors, thermographic 498–500, 501
photomultiplier tube (PMT) 480
physically based auto-ignition models 174–5
planar laser-induced fluorescence (PLIF) *see* laser-induced fluorescence
pneumatic direct injection (PDI) 69–70
port fuel injection (PFI) engines
diesel HCCI engines 252–4, 262
gasoline engines 83–6, 107–15
combined variable valve lift and variable valve timing 115
fuel consumption and emission characteristics 112–14
performance and combustion characteristics 107–12
practical transport fuels 207–10
PREDIC system 255–6, 267, 271–4
premixed combustion 242–3, 244, 245
modulated kinetics *see* modulated kinetics
premixed compression ignition (PCI) combustion 9–10, 257, 267–88
experimental apparatus 268–71
HCCI for normal cetane fuel 277–85
combustion experiment 277–8
exhaust emissions 283–5
pressure diagram and heat release process 278–80, 281
thermal efficiency and brake mean effective pressure 280–2
low cetane fuel 271–6
MULDIC 274–6
PREDIC 271–4
pressure 22
boosted intake pressure 89–90, 93–4, 388–91
brake mean effective pressure *see* brake mean effective pressure (BMEP)
combustion timing sensor 172, 182
DME engine 396–7, 425, 426, 427, 428
reducing pressure rise rate by introducing ‘unmixed-ness’ of DME/air mixture 423–5, Plate 16
effect of cooled burned gases on pressure rise rate 31, 32
indicated mean effective pressure *see* indicated mean effective pressure (IMEP)
maximum pressure rise rate *see* maximum pressure rise rate (MPRR)
mode transition in ‘mixed mode’ engine 196–8, 199–201
naphtha fuelled HCCI 347
natural gas engines 370
auto-ignition pressure 372–4, 379–80, 381
influence of n-butane in methane/n-butane/air mixtures 376–7, 378, 379–80, 381
intake pressure and operating region 366–9
supercharged engines 386, 387, 391
premixed compression ignition combustion 278–80, 281
re-breathing methods 137–8, 139–40
residual gas trapping 104, 105, 137–8
early injections 116–17, 118, 119–21, Plate 5
mid and late injections 121, 123
spark assisted CAI combustion 129, 130
two-stroke engines 59, 60
primary reference fuels (PRF) 210
Pro AVT system *see* AVT system
Progress Aero Works (PAW) 9
propagation reactions 435–7
propane 366, 367
pseudo-random binary sequence (PRBS) excitation for identification of state space models 176, 177–8
pumping loop 105, 106
pumping losses 91–2
early fuel injection 116, 117
re-breathing methods 139–40

quartz 476

radical reactions 248–9
rapid compression machine (RCM) 211
  modelling auto-ignition in 445–51
re-breathing 8–9, 36–7, 136–63, 167–8, 185–6, 187, 203, 507
  compared with trapping method 137–8
  comparison of re-breathing methods 138–40
  engine concepts and layout 141–6
    approaches to CAI combustion 141
    operation strategies with a combined mechanical electro-hydraulic valve train 144–6
    re-breathing with a combined mechanical electro-hydraulic valve train 141–4, 145
  future trends 162
  thermodynamic results and analysis 146–55
    energy balance analysis 154–5, 156
    four-cylinder engine 148–54
    single-cylinder research engine 146–8
  transient operation 155–62
    combustion control 155–9
    real driving transient operation of four-cylinder engine 159–62
  see also internal EGR
recompression *see* residual gas trapping
reduced chemical kinetic models 453
Research Octane Number (*RON*) 214–17
residual gas 49–50, 78, 79, 95
  control using VVA 166–8, 179
  expanding the operating range of the OKP engine 89–90
residual gas trapping (negative valve overlap) 8–9, 36–7, 80–1, 103–35, 185–6, 203, 507, Plate 4, Plate 5, Plate 6
  compared with re-breathing 137–8
  control using VVA 166–7
  direct injection 115–29, 134
    early injections during valve overlap period 116–21, 122, 123, 124, 126
    mid and late injections during intake and compression strokes 121–4, 125–6
    split fuel injections 124–9
  port fuel injection (PFI) engine 107–15
    combined variable valve lift and variable valve timing 115
    fuel consumption and emission characteristics 112–14
    performance and combustion characteristics 107–12
  principle of 103–7
  sequential phases 115–16
  spark assisted CAI combustion 129–32, 133, 134, Plate 8, Plate 9
road load curve 46–7
'run-on' ('after-run') 7

sapphire 476
scooters 44, 45, 69
Semenov, Nikolai 7–8
sensitivity
  auto-ignition quality 214
  estimation from stationary maps 176
sensors, combustion timing 171–4, 182
Shell auto-ignition model 119–21, 122, 175
Shell middle distillate synthesis (SMDS) 208, 232
signal collection devices 480
simultaneous LIF measurements 493–4
single zone models 451–2, 462, 464, 470
Souk Hong Jo 43
spark assisted CAI combustion 38, 97–9, 129–32, 133, 134, Plate 8, Plate 9
spark ignition (SI) combustion 5–6, 7, 10–11, 428, Plate 1
  compared with CAI combustion 48–9
  heat release characteristics 11, 12
  performance and emission characteristics 13
  SI/CAI switching *see* mode switching
  thermal efficiency of SI engines 91
  two-stroke engines 49–50
    management of transition between SI and CAI combustion 55–6
spectrally resolved absorption measurement 481–2, 483, 484, 485
split fuel injections
  NADI 297, 298, Plate 13
  residual gas trapping 124–9
stratification

charge *see* charge stratification
partially stratified combustion 458, 468, 471
thermal 38–9, 90–1, 93–4, 425
stratified-charge direct-injection spark-ignition (SC-DISI) engine 83–6
thermal efficiency 83–4, 91–2
super clean diesel engine 267–8
super ultra low emission vehicle (SULEV) target 4, 322–3
MK and meeting SULEV standard 337–40
supercharged natural gas engines 383–91
performance and exhaust gas characteristics
CR of 17 385–8
CR of 21 388–9, 390
potential of 389–91
set-up and experiments 383–5
surging range 46–7
surrogate fuel mixture models 211, 452
switching between modes *see* mode switching
system identification control methods 175–8

taxation 3, 4
TDC split injection 297, 298, Plate 13
temperature
auto-ignition temperature 372–4, 379–80, 382
ceiling temperature 438
compression temperature and auto-ignition quality of fuel 220–2, 349–50, 355, 356, 357
coolant temperature 38, 62–3, 334
DME engine 396–7, 425, 426, 427, 428
calculation 415–16, 417
initial temperature 400–1, 402, 403
maximum temperature 403–6, 407, 411–12, 418–20
effect of hot burned gases 33
intake temperature and BSN for fuel blends 345–6
measurement with thermographic phosphors 498–500, 501
natural gas engines 370–1, 372–4
auto-ignition temperature 372–4, 379–80, 382
influence of n-butane in methane/n-butane/air mixtures 379–80, 380–3
maximum temperature 374–6, 380–3
operating region and intake temperature 366–7, 368
premixed compression ignition combustion 278–80, 281
re-breathing and charge temperature 139–40, 146–7
regimes of auto-ignition 437–45
intermediate and high temperature chain branching 444–5, 461–2
low temperature kinetics 437–43, 459–61
spark assisted auto-ignition 98–9
two-stroke engines 49–50
effect of overall temperature 62–3
termination reactions 435–7
thermal efficiency 100
diesel engines 91–3
DME engine 421, 422
MK combustion 326, 327
OKP engine 83–4, 91–3
premixed compression ignition combustion 280–2
supercharged natural gas engines 385, 386, 388, 389–91
thermal management 35, 37, 77–102, 186
available thermal energy sources 77–8
utilisation of 78–9
combustion control 96, 170–1, 180, 181, 182
direction of research 100
EGR and coolant temperature control 99–100
future trends 97–9
OKP engine *see* optimised kinetic process (OKP) engine
strengths and weaknesses 91–7
VCR-HCCI engine 79, 91–6, 100
thermal stratification 38–9, 93–4
DME engine 425
OKP engine 90–1
two-stroke engine 57
thin-film thermocouple 326–7, 328
thermographic phosphors 498–500, 501
three-dimensional fuel visualisation 497–8
three-dimensional LIF imaging 497

Thring, R.H. 8
throttle valve 13
toluene 210, 360, 361, 488, 494
top dead centre (TDC) 165
  TDC split injection 297, 298, Plate 13
total heating value 367–8, 369
Toyota 5
tracers, fuel *see* fuel tracers
transfer throttling 45, 52–4
  two-stroke engines 54–5, 57, 64–6
    combined with exhaust throttling 66–7
transient operation 155–62
transition state ring 439–40
TS (Toyota-Soken) process 43
turbochargers 319
  natural gas engines 383–91
turbulence 458
two-stage exhaust cam system 414
two-stage ignition 212–13, 438, 443, 460–1
two-stroke CAI engines 8, 35, 43–76, 77
  combustion control 56–67
    associated technologies and control devices 63–7
    relevant control parameters 56–63
  early research on CAI 43–5
  future of 72–3
  potential application 67–72
    automotive engines 70–2
    small generators 67–8
    two-wheeler engines 68–70
  principles of 46–56
    advantages and benefits of CAI/SI 50–4
    basic principles and in-cylinder conditions 48–50
    combustion modes 46–8
    drawbacks and difficulties 54–6
  transferring knowledge to development of four-stroke engines 73
two-stroke diesel model aeroplane engine 9
two-stroke operation in two-stroke/four-stroke switching engines 38

unburned hydrocarbon emissions *see* hydrocarbon emissions
uncontrolled combustion 55
UNIBUS system 257–8
United States permitted emission levels 3–5

valve lift curves
  EHVA system 144
  'mixed mode' engine 194–5
  residual gas trapping 104–5, 106
  two-stage exhaust cam system for DME engine 414
variable cam timing (VCT) 80–1, 104–6
  see also cam profile switching and phaser VVT system (CPS-P)
variable compression ratio (VCR) 36, 81, 180, 182, 186, 507
  VCR-HCCI engine 79, 100
    operating range 93–6
    thermal efficiency 91–3
variable geometry compressor 319
variable valve actuation (VVA) 37, 80–1, 104–5, 166–70, 182, 203
  combined continuous variable lift and timing devices 115
  combined mechanical electro-hydraulic valve train 141–6
  effective compression ratio control 168–70
  'mixed mode' engine
    AVT system 189, 191–2, 193–6, 199–202, 203
    cam profile switching and phasing device VVT system 189–91, 194–9, 203
    in operation 193–202
    valve train requirements 188–9
  residual gas control 166–8, 179
vehicle speed 159–62
volatility characteristics of fuels 208, 209
Volvo 8–9

wall wetting problem 10
warm-up 96–7
windows 476–7

xylene 210, 488

zero emissions vehicles (ZEVs) 5

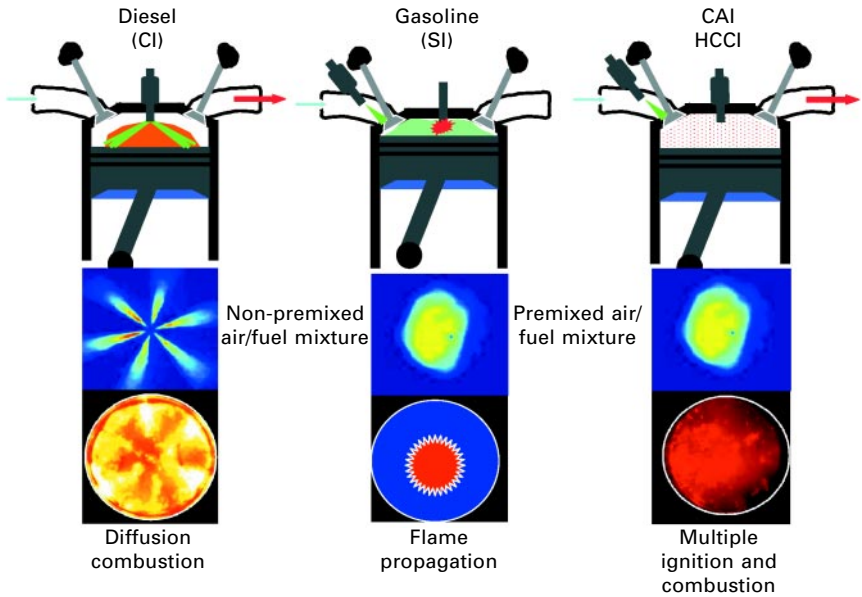

Plate 1 Salient features of three combustion modes.

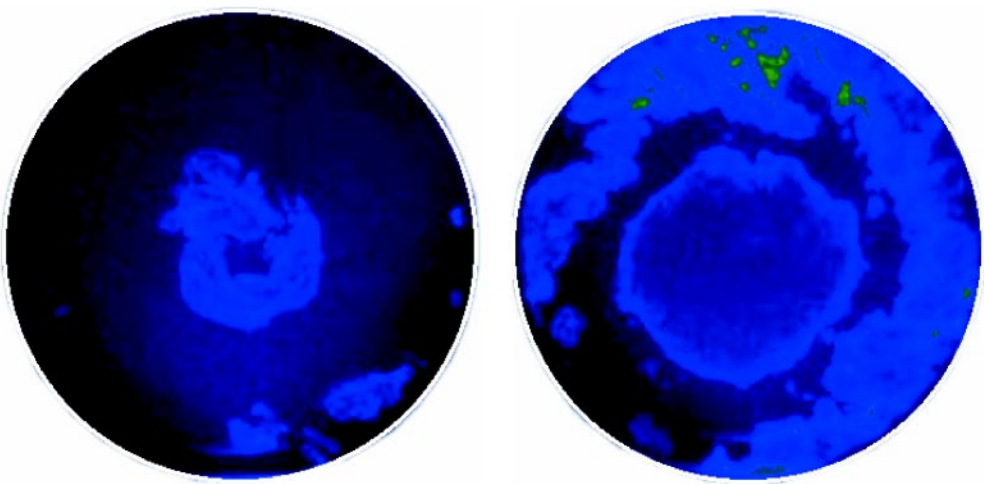

Plate 2 Direct visualisation of controlled auto-ignition combustion in a gasoline engine.

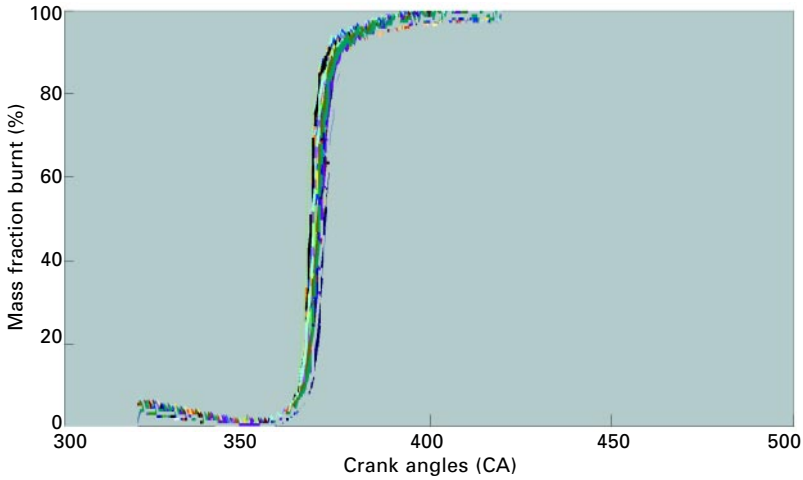

Plate 3 Mass fraction burnt curves of 100 CAI combustion cycles.

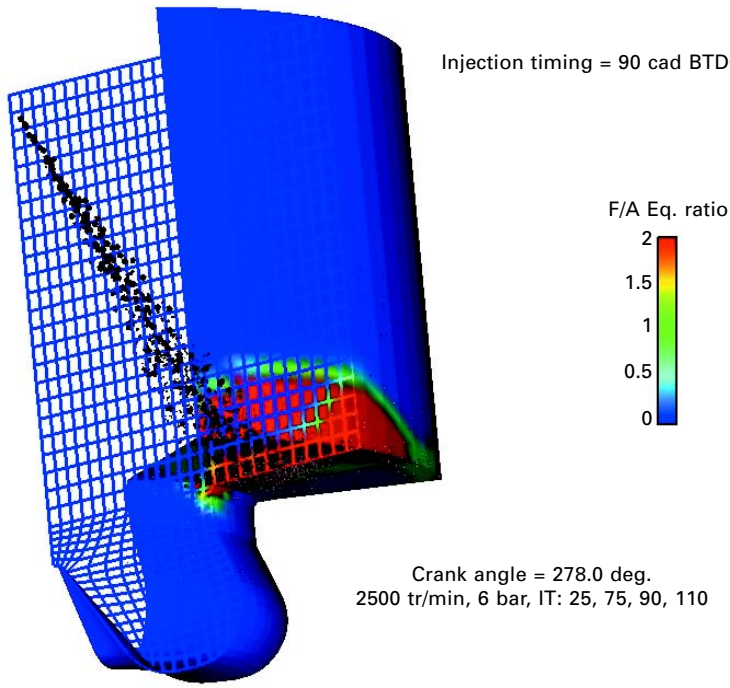

Plate 4 Injection calculation in HPC mode, Start of injection 90 crank angle before top dead centre.

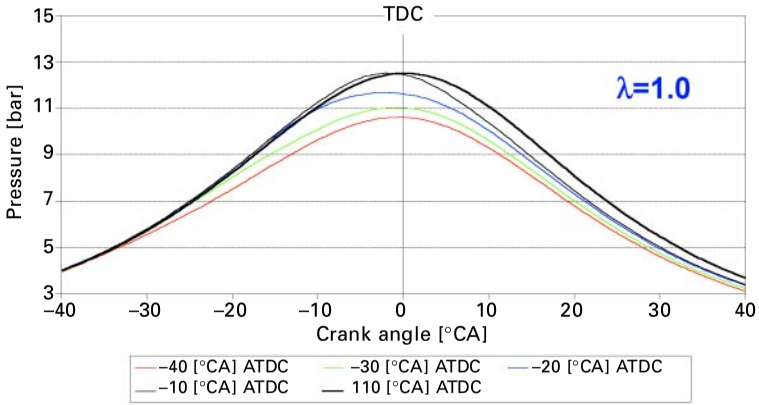

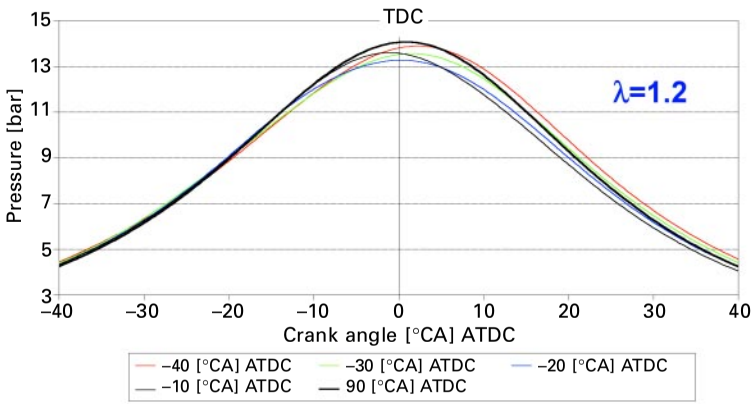

Plate 5 In-cylinder pressure traces during the negative valve overlap period.

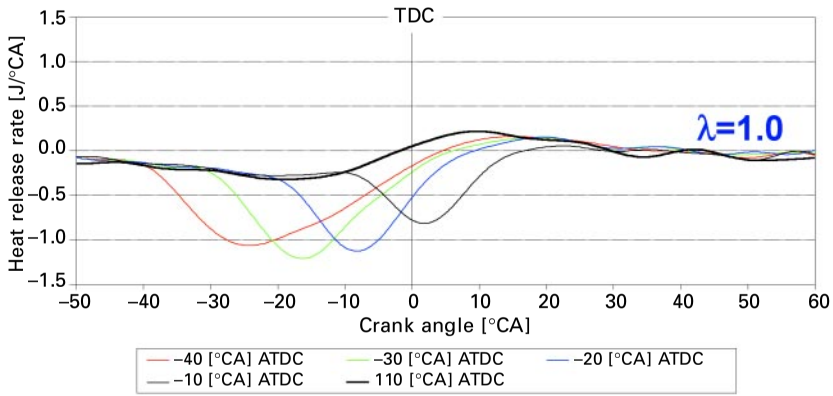

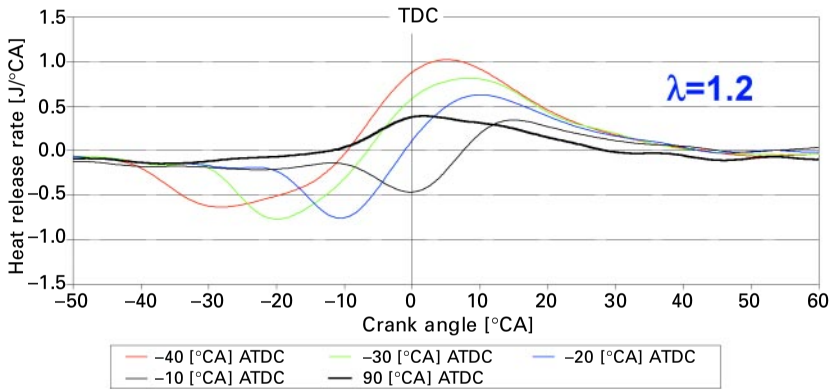

Plate 6 In-cylinder thermal process during the negative valve overlap period.

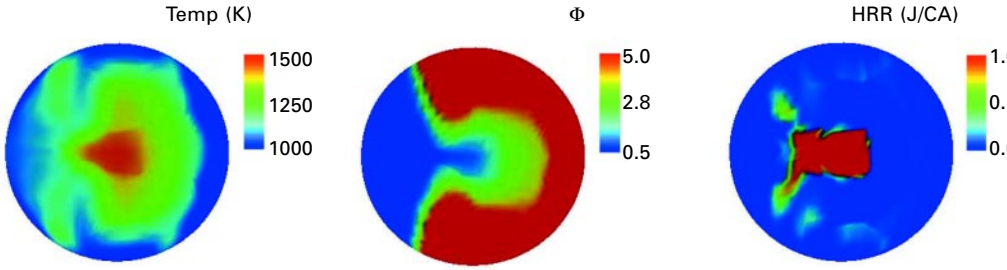

(a) $TDC_{overlap}$ (Case of SOI at –75°ATDC)

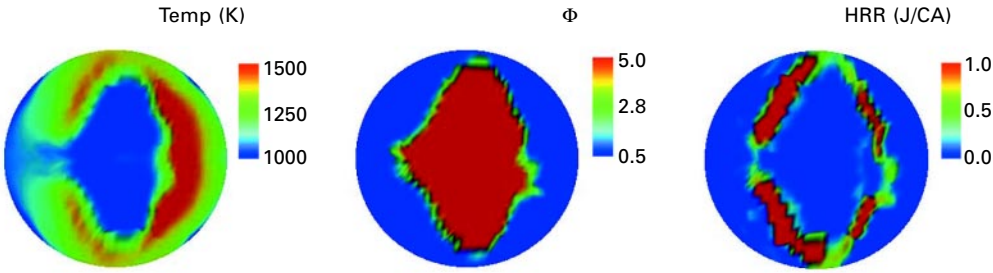

(b) $TDC_{overlap}$ (Case of SOI at –40°ATDC)

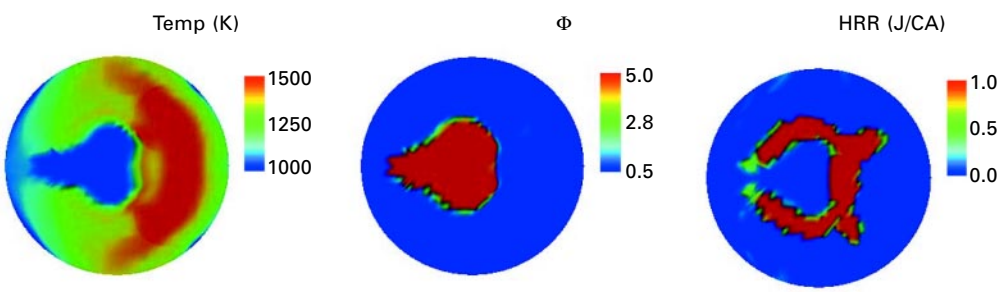

(c) $TDC_{overlap}$ (Case of SOI at –20°ATDC)

Plate 7 Distributions of temperature, equivalence ratio and heat release rate at $TDC_{overlap}$ for three injection timings at λ = 1.2.

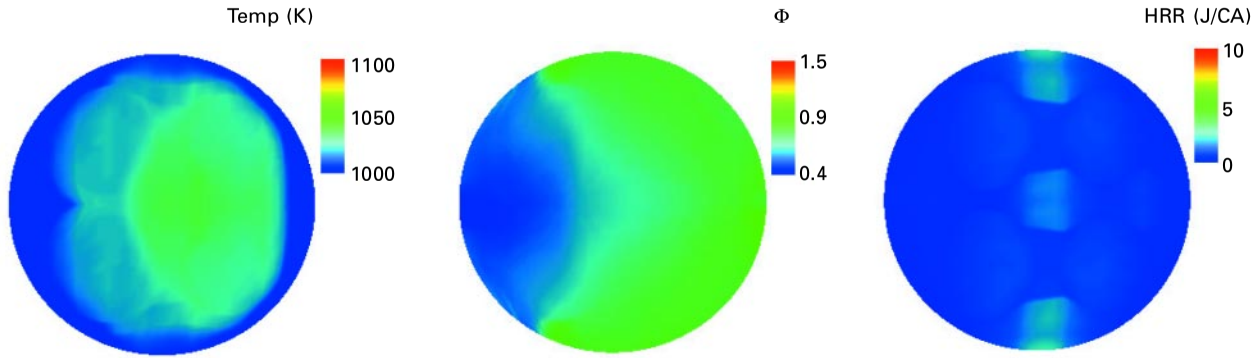

(a) SOI at 98° $ATDC_{overlap}$

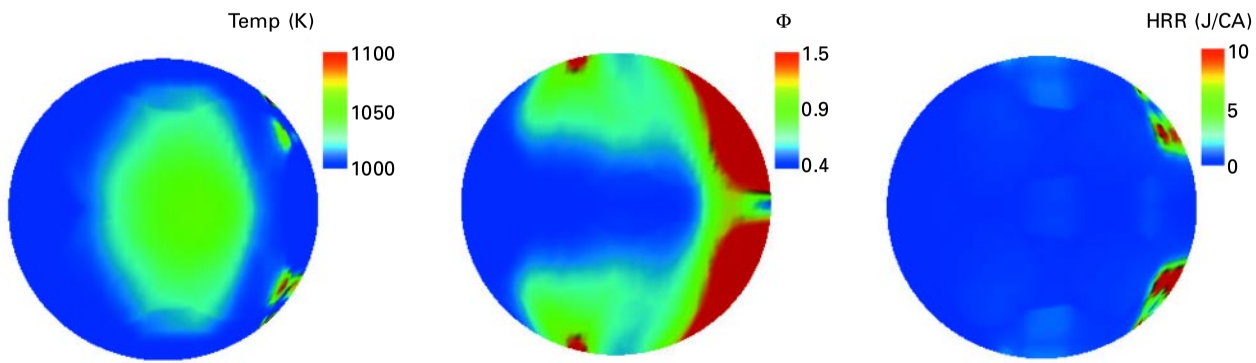

(b) SOI at 218° $ATDC_{overlap}$

Plate 8 In-cylinder spatial distributions of temperature, equivalence ratio and heat release rate at 10°CA BTDC with injections at 98° and 218° ATDC.

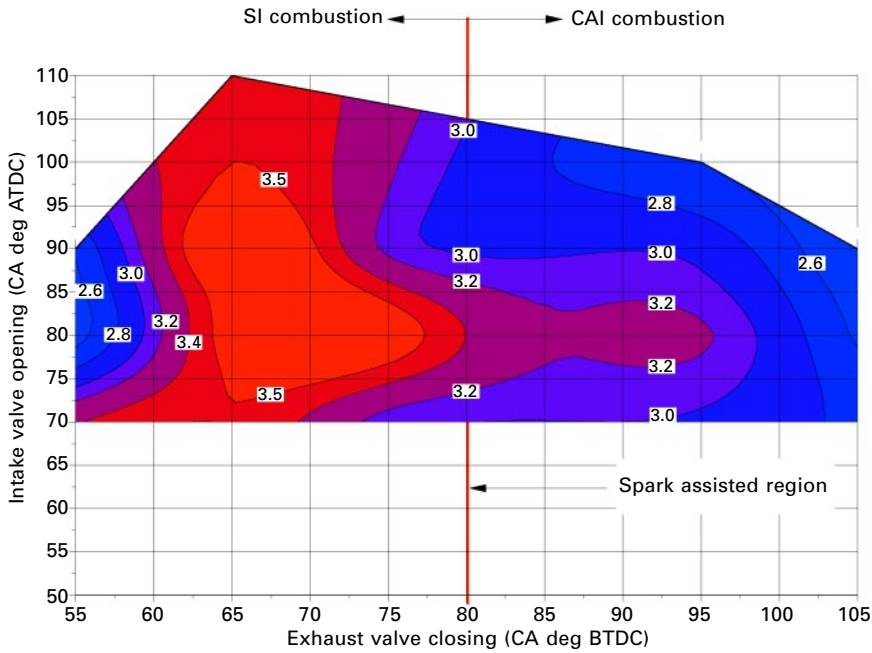

Plate 9 Combustion modes in a DI gasoline engine with negative valve overlap with SOI @30 CA deg ATDC, lambda 1.2 and 1500 rpm.

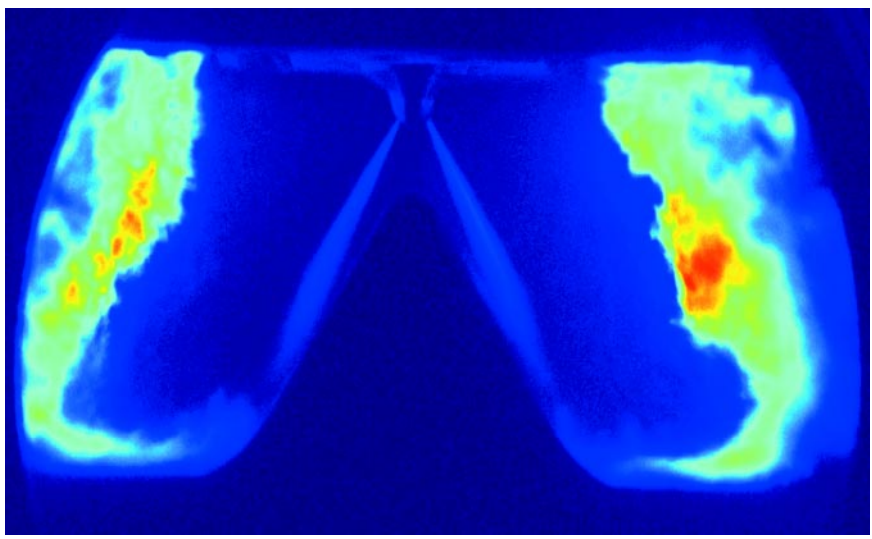

Plate 10 Image of a flame with a NADI-type combustion chamber and narrow angle injection nozzle.

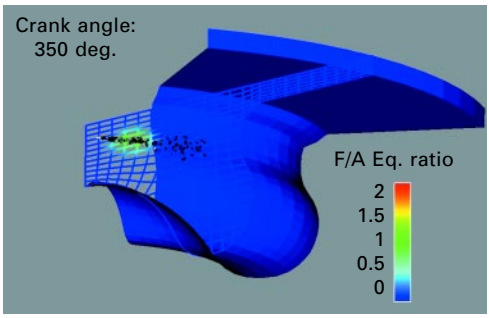

(a)

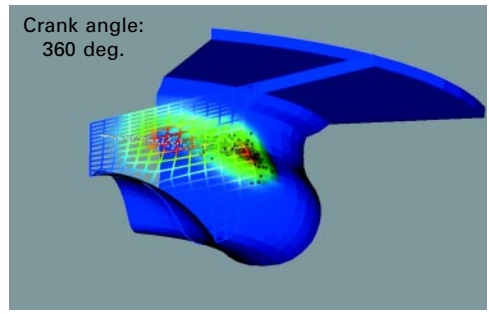

(b)

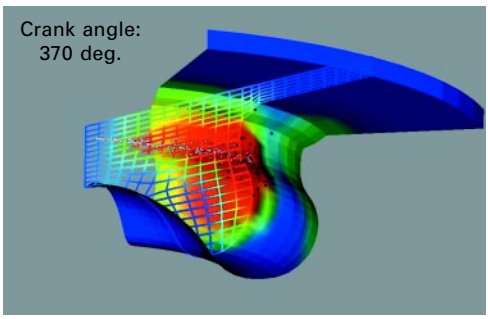

(c)

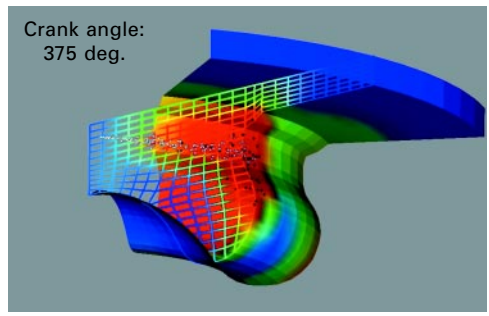

(d)

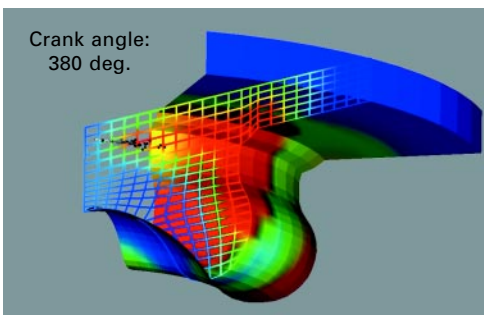

(e)

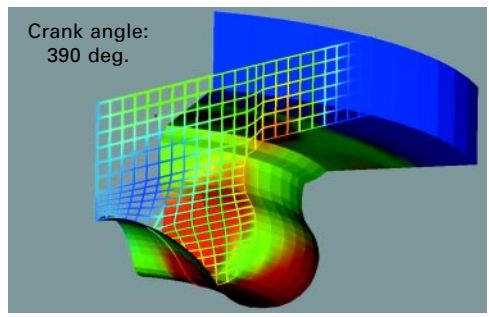

(f)

Plate 11 Computed combustion process at 4000 rpm, full load – conventional combustion chamber (a–f).

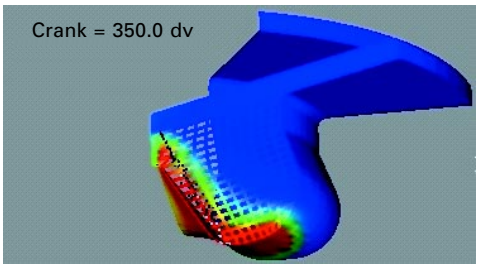

(a)

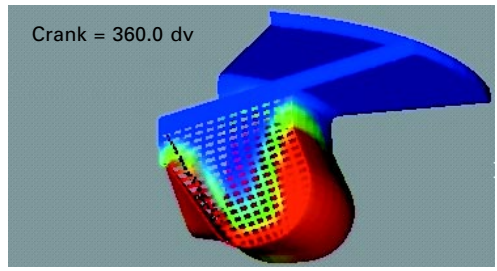

(b)

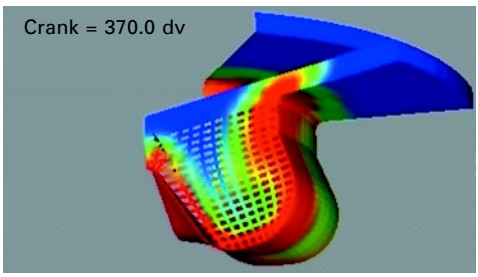

(c)

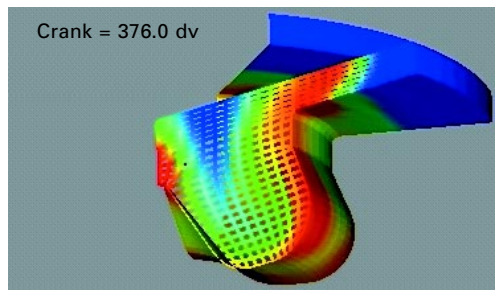

(d)

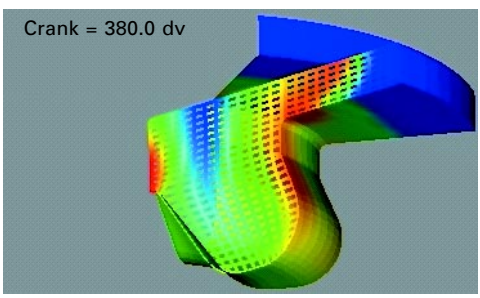

(e)

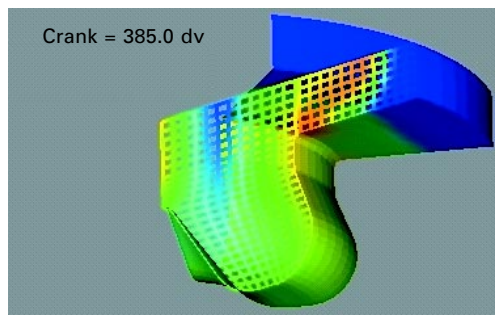

(f)

Plate 12 Computed combustion process at 4000 rpm, full load – NADI™ combustion chamber.

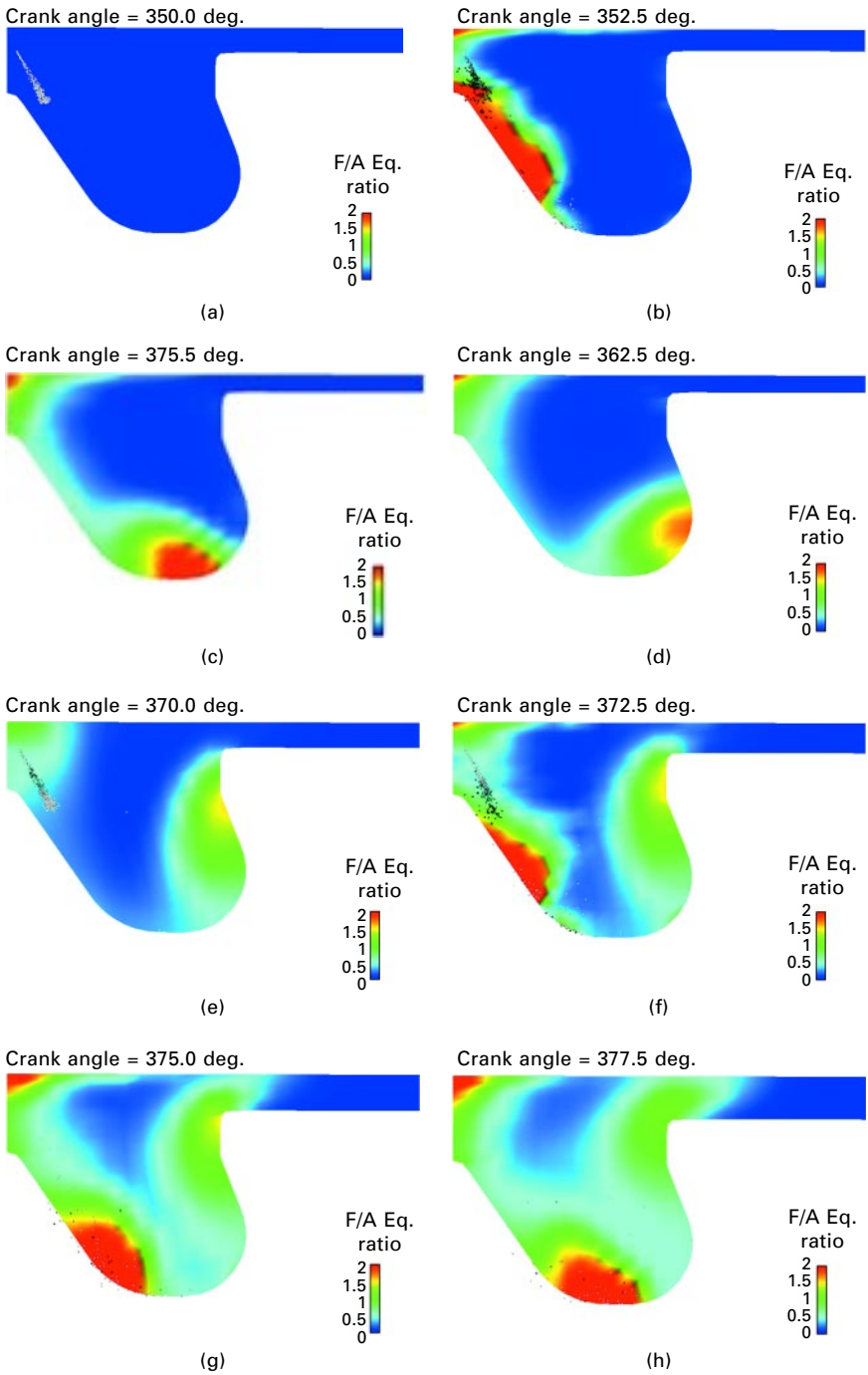

Plate 13 CFD of a split injection strategy.

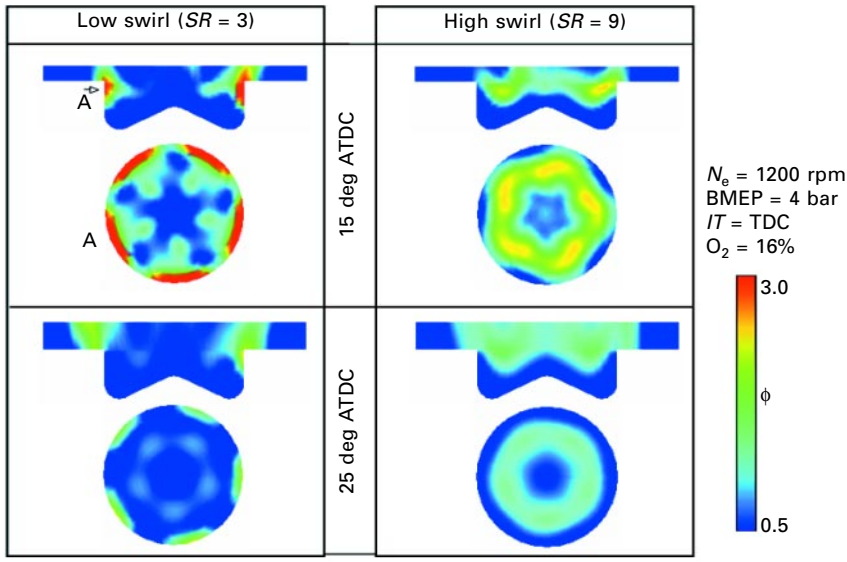

Plate 14 Distribution of equivalent ratio of low and high swirl.

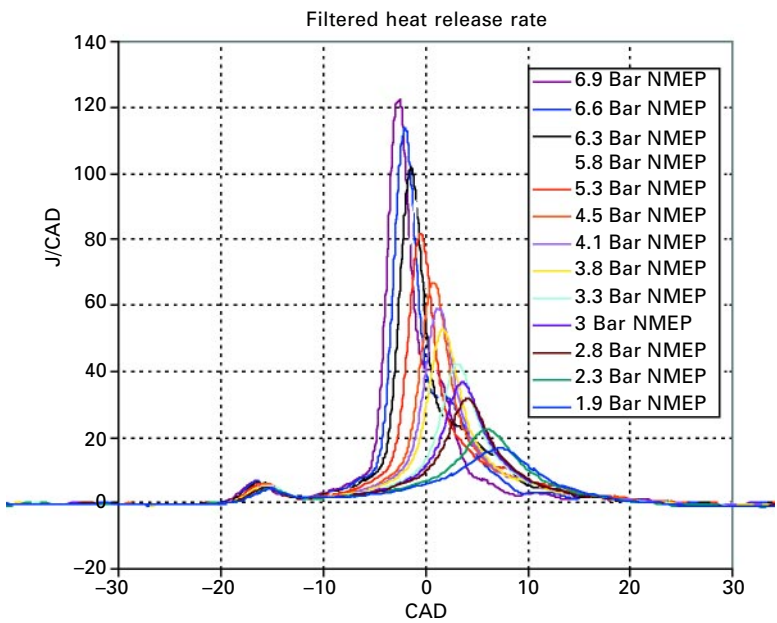

Plate 15 Heat release rate diagrams at various loads (SwRI).

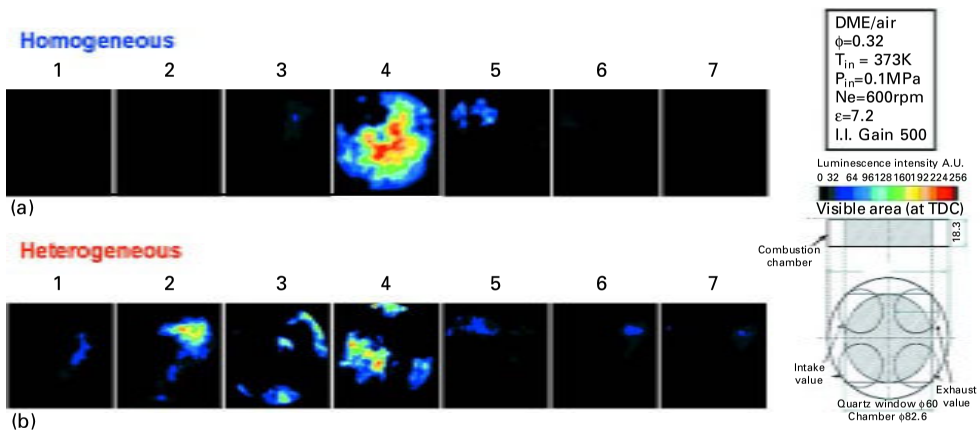

Plate 16 Luminescence images in the combustion chamber (comparison for case of homogeneous mixture and inhomogeneous mixture) [20].

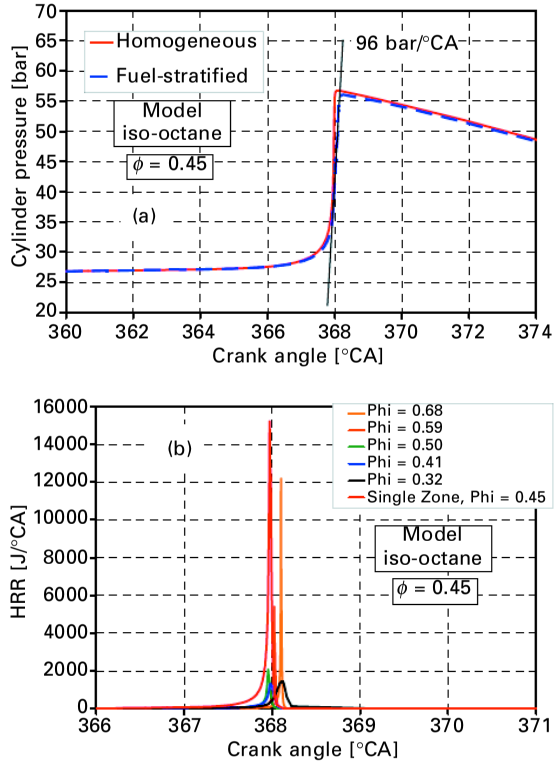

Plate 17 Predicted heat release rate diagrams for a fuel with no low temperature reactions at various loads.

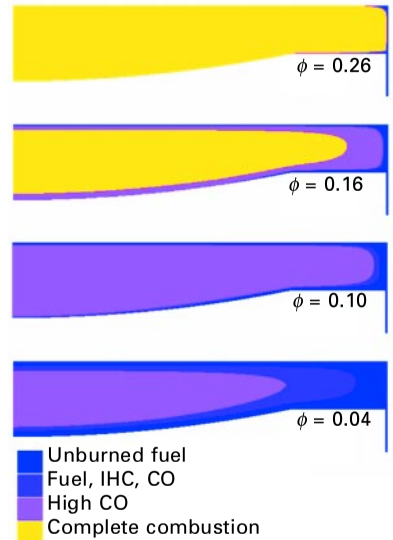

Plate 18 Geometrical distribution of the mass that burns to completion, the mass that reacts partially into CO, the mass that reacts partly into intermediate hydrocarbons and fuel, and the mass that does not react at all and remains as unburned fuel (Aceves *et al.*, 2004). The geometrical distribution is shown at 6°BTDC for four values of equivalence ratio ϕ = 0.26, 0.16, 0.10 and 0.04. The figure shows that the case with ϕ = 0.26 burns to completion, and HC and CO are only produced at the crevices and boundary layer. As the equivalence ratio is reduced, the fraction of fuel that does not burn to completion increases rapidly. At ϕ = 0.10, most of the fuel partially oxidizes into CO. At ϕ = 0.04, much of the fuel remains unreacted or partially reacted into intermediate hydrocarbons.